Aspects of the Mechanisms of Alkaline Hydrolysis of Amino Acid Esters

A thesis
submitted in partial fulfilment
of the requirements for the degree
of
Doctor of Philosophy in Chemistry
at the
University of Waikato
by
Lusha Anjalika Kodikara

THE UNIVERSITY OF
WAIKATO
Te Whare Wānanga o Waikato

2005

Abstract

Thermodynamic proton dissociation constants (K_a^T) of the hydrochlorides of some α-amino acid methyl, ethyl and benzyl esters have been determined by potentiometric titration at 25, 37.1 and 50.2°C, and at I = 0.1 mol l^{-1}. From this temperature dependence, the energetics of the reactions (ΔG°, ΔH°, ΔS° values) were determined and examined.

The ester hydrochlorides of the 2-amino acids have pK_a^T values that are about 2 units lower than the corresponding *n*-alkylammoniums. The major contributors to this large ΔG° lowering (acid strengthening) are the strong -**I** effect of the adjacent alkoxy/benzyloxy carbonyl group which produces a large decrease in ΔH° and a reduction in the nett solvent (H_2O) bonding for the free base form of the ester (E) which increases ΔS°.

pK_a^T values rise sharply from 2-aminoethanoic acid methyl ester hydrochloride (2-AE Me·HCl) to 3-aminopropanoic acid methyl ester hydrochloride (3-AP Me·HCl). There are much smaller rises with further increases in the chain length to the 4-, 5- and 6-amino acid methyl ester hydrochlorides. Similar trends occur for the corresponding ethyl and benzyl ester hydrochlorides. However, this simple increase in pK_a^T (ΔG°) hides a complicated interplay between ΔH° and ΔS°. There is a rapid increase in ΔH° from 2-AE Me·HCl to 4-aminobutanoic acid methyl ester hydrochloride (4-AB Me·HCl), but a dramaticrise to 5-aminopentanoic acid methyl ester hydrochloride (5-APe Me·HCl). These large fluctuations in ΔH° are moderated by ΔS° changes to produce the observed overall increase in ΔG° with increasing chain length. This behaviour is probably due to intramolecular H-bonding between the ammonium and methoxycarbonyl groups in 5-APe Me·HCl which results in an 8-membered ring and stabilisation of the protonated form (EH^+) relative to the E form, with consequent changes in solvation and ΔS°.

The results of N-methylation reinforce the need for ΔH° and ΔS° values if structural effects on pK_a^T values are to be understood. In going from 4-AB Me·HCl to its N, N-dimethyl analogue, pK_a^T falls. Inductive effects predict pK_a^T should rise as the weak +**I** effect of the two methyl groups is acid weakening and so makes a positive

contribution to $\Delta H°$. However, solvent bonding changes produce a much larger negative contribution to $\Delta H°$. This makes the overall $\Delta H°$ (and $\Delta G°$) lower than for 4-dimethylaminobutanoic acid methyl ester hydrochloride (4-DMAB Me·HCl), however the $\Delta S°$ value is also compensatingly low.

Stepwise methylation at C-3 in 4-AB Me·HCl produces stepwise decreases in pK_a^T. This decrease in $\Delta G°$ is mainly due to a fall in $\Delta H°$, which apparently arises from the protonated form of 4-amino-3,3-dimethylbutanoic acid methyl ester (4-A-3,3-DMB Me) existing predominantly in the gauche conformation. Consequently, the ammonium and methoxycarbonyl groups can intramolecularly H-bond which produces the observed changes in $\Delta G°$ and $\Delta H°$, however $\Delta S°$ are abnormally large and negative since this interaction is lost on deprotonation.

Changes in the ester function alone have little effect on the pK_a^T value; the methyl, ethyl and benzyl ester hydrochlorides of 4-AB have almost identical pK_a^T values.

The rate constants for the alkaline hydrolysis of the ω-amino acid esters have been measured at 25, 37.1 and 50.2 °C, and at I = 0.1 mol l^{-1}, using the pH-Stat method. All the reactions are pseudo first order at constant pH with a rate constant, k_{obs}. Values of $k_{obs}/[OH^-]$ vary with pH so the reaction is not simple second order. However, the data is consistent with a reaction scheme involving both forms of the ester, E and EH^+, reacting in two parallel, second order, pathways with rate constants k_E and k_{EH^+}. The two forms of the ester are connected by a pH dependent equilibrium governed by K_a^T. Values for k_E and k_{EH^+} were separated using plots of $k_{obs}/[OH^-](K_a^T + [H^+])$ vs. $[H^+]$ which were linear. For some esters, the E form undergoes lactamisation with a large rate constant, k_L, which replaces the negligibly small k_E.

The k_E values for the methyl, ethyl and benzyl esters of 2-AE, 3-AP, 6-AH and 4-DMAB, and the k_{EH^+} values for all of the esters, are consistent with a simple $B_{Ac}2$ reaction mechanism. This predicts changes in the reaction energetics ($\Delta H^‡$, $\Delta S^‡$ values), and hence changes in the rate constants, with changes in structure, that agree with those observed. These rate constant changes cannot be explained simply by the contribution made by inductive effect changes to the reaction energetics. This again emphasises the need for temperature dependence studies if a complete understanding is to be gained.

For the 2-amino acid esters, k_{EH^+} is much larger than k_E. This is due entirely to an increase in $\Delta S^{\ddagger}$ associated with solvation effects. Since little difference in $\Delta H^{\ddagger}$ between the E and EH^+ forms of the ester The differences in k_{EH^+} and k_E become smaller as the amino group is removed from the carbonyl reaction centre, as expected.

The E forms of 4-AB Me and 5-APe Me undergo intramolecular aminolysis rather than simple $B_{Ac}2$ hydrolysis. This is because the potential 5- and 6-membered rings are energetically the optimum size for ring closure. The resulting lactams are stable under the reaction conditions. Lactamisation also occurred for the E form of the ethyl and benzyl esters of 4-AB, the ethyl ester of 5-APe, the methyl and ethyl esters of 4-(methylamino)-butanoic acid (4-MAB), 4-amino-3-methylbutanoic acid (4-A-3-MB) and 4-A-3,3-DMB. However, lactamisation was blocked for the methyl and ethyl esters of 4-DMAB because of the lack of an amino hydrogen.

The rate constant for 6-membered lactam ring formation (k_{L6}) is about 23 times larger than for the corresponding 5-membered lactam (k_{L5}). The origin of this difference is mainly the smaller $\Delta H^{\ddagger}$ for k_{L6}, reflecting the smaller strain in the 6-membered ring transition state.

Single N-methylation produces a small (about 5 times) increase in k_{L5}, with 4-MAB Me hydrolysing more rapidly than 4-AB Me. This is due to a decrease in $\Delta H^{\ddagger}$ associated with the increased nucleophilicity of the amino nitrogen.

Stepwise methylation at C-3 in 4-AB Me produced moderate increases in k_{L5} with the largest effect (about 6 times) for the gem-dimethyl case, associated with an increase in $\Delta S^{\ddagger}$ due a smaller loss of internal freedom in the transition state.

The simplest reaction mechanism for the lactamisation that is consistent with all of the observations involves an initial, rate determining step, consisting of OH^- deprotonating the amino nitrogen which simultaneously attacks the ester carbonyl C. The cyclic tetrahedral intermediate formed then rapidly decomposes to form the lactam, parent alcohol and OH^-, probably in several steps. This mechanism can be described as "hydroxide assisted intramolecular nucleophilic catalysis."

Acknowledgements

My especial thanks go to my supervisor, Dr Peter Morris, for his guidance, interest and assistance throughout both the research and writing-up of this work.

A debt of gratitude is owed to my friends, Guy Billet, Stefan Hill and Natalie Curnow, who kept me sane and happy over the years. To Natalie my thanks for the illustration in Chapter Three. Dr Bruce Morris at the University of North Dakota, thanks for taking time to assist with my thesis write-up. I am grateful to Dr Ralph Thomson for his assistance with some of the NMR assignments (and for the coffee mornings at the Station). I must also thank Mrs Pat Gread, who always had the ESMS ready for me to run my samples.

I am deeply indebted to Tissa and Mahima Senanayake for their help in organising my thesis in final days. Thank you to Jannine Sims for all the practical help that she has shown me ever since my 203 lab days. A bouquet must also go out to Mr Renat Radosinsky for his assistance with the computer.

Last but not least I must thank my parents, Herbert and Pushpa for their patience and understanding over all these years. To Tusshara and Chalika, I appreciate all the love you have given me.

Table of Contents

List of Tables

Table Page

List of Figures

List of Schemes

List of Symbols and Abbreviations

β	Bronsted parameter
δ	chemical shift
σ^*	substituent constant of the Taft equation
ρ^*	reaction constant of the Taft equation
A^-	(AH) amino acid and protonated form
A	Debye-Huckel parameter
A	pre-expotential parameter (Arrhenius theory)
$B_{Ac}2$	Base catalysed bimolecular and acyl-oxygen fission
d	doublet
DW	degassed doubly distilled water
E	(EH^+) amino acid and protonated form
E_a	activation energy
EM	effective molarity
GB	general base
ΔG°	standard Gibbs free energy change
$\Delta G^\ddagger$	standard Gibbs free energy of activation
h	Planck constant
ΔH°	standard enthalpy change
$\Delta H^\ddagger$	standard enthalpy of activation
I	ionic strength
I	inductive effect
IGBC	intramolecular general base catalysis
INC	intramolecular nucleophilic catalysis
J	Joule
k_B	Boltzmann constant (R/N)
k_X	rate constant x = numeral, denotes the order of the rate constant x = species, e.g. k_E, denotes rate constant of species E
K	Kelvin
K_a^T	thermodynamic (activity) acid dissociation constant
K_w^T	thermodynamic (activity) water dissociation constant
N	Avogardo constant
NBS	National Bureau of Standards
NGP	neighbouring group participation
Nu:	nucleophile
q	quartet
rds	rate determining step
R	gas constant
s	singlet
ΔS°	standard entropy change

$\Delta S^{\ddagger}$	standard entropy of acctivation
t	triplet
$t_{1/2}$	half-life of first order reaction
T	temperature
TS	transition state
V	volume
{X}	activity of species X
[X]	concentration of species X
y_n	molar activity coefficient, n = charge on the species
z_i	Charge on species, i

Amino Acids and Esters

Are referred to in the following manner:

x-Name.zHCl. for monoamino cases

x,y-Name Me.zHCl for diamino cases

where:

Me refers to the type of ester i.e. methyl ester. Et refers to ethyl ester Bz benzyl ester. If there is nothing, then the compound is the corresponding parent amino acid.

x and y denote the position(s) of the amino groups.

zHCl refers to the number of HCl incorporated into the compound in the solid

state.

L refers to the laevorotatory optical isomer. D is the dextrorotatory isomer.

Name refers to the abbreviation to four letters or less of the systematic name, i.e.

2-AE	2-aminoethanoic acid (glycine)
3-AP	3-aminopropanoic acid (β-alanine)
4-AB	4-aminobutanoic acid (γ-aminobutyric) acid
4-MAB	4-(methylamino)butanoic acid
4-DMAB	4-(diamino)butanoic acid
4-A-3-MB	4-amino-3-methylbutanoic acid
4-A-3,3-DMB	4-amino-3,3-dimethylbutanoic acid
5-APe	5-aminopentanoic acid
6-AH	6-aminohexanoic acid
Ser	2-amino-3-hydoxypropanoic acid (serine)
2,3-DAP	2,3-diaminopropanoic acid
2,4-DAB	2,4-diaminobutanoic acid
2,5-DAPe	2,5-diaminopentanoic acid
4,5-DAPe	4,5-diaminopentanoic acid
Glu	2-aminopentanedioic acid (glutamic acid)
P-5-CA	2-pyrrolidone-5-carboxylic acid

Synthetic Precursors

The following compounds were used to prepare some amino acids that were not available commercially.

1,5-PDA	1,5-pentanedioic acid
3-M-1,5-PDA	3-methyl-1,5-pentanedioic acid
3,3-DM-1,5-PDA	3,3-dimethyl-pentanedioic acid
DPD	dihydro-pyrano-2,6-dione
4-M-DPD	4-methyl-dihydro-pyrano-2,6-dione
4,4-DM-DPD	4,4-dimethyl-dihydro-pyrano-2,6-dione
5-CPA	5-carbamyl- pentanedioic acid
3-M-5-CPA	3-methyl-5-carbamyl- pentanedioic acid
3,3-DM-5-CPA	3,3-dimethyl-5-carbamyl- pentanedioic acid

Chapter One

Introduction

1.1 Enzymes

Enzymes are remarkable molecules. These biologic pathway catalysts exert extraordinary control over reactions,[1-6] by altering the only aspects of reactions that can be changed: their kinetics and mechanisms. The thermodynamic properties of a reaction are immutable. Each enzyme is usually "reaction class specific", e.g. Carboxypeptidase A is a hydrolytic enzyme, cleaving peptide and ester bonds. However, by controlling the relative heights of the $\Delta G^{\ddagger}$ barriers for what is usually a set of potentially parallel reactions, the enzyme directs the formation of the desired single product at a greatly increased rate, and often with elegant stereochemical control, e.g. Carboxypeptidase A preferentially cleaves the C-terminal L-amino acid from a peptide. The catalytic power of an enzyme can be enormous, with rate increases of up to 10^{15} times having been reported.

Generally, enzymes are protein macromolecules with their chains of amino acids arranged in complex three dimensional structures - although recently, some ribonucleic acid (RNA) molecules have also been shown to possess enzyme activity.[7] Enzyme activity is usually centred at one or more small regions on the surface of the enzyme, the active site(s). Here are present various functional groups originating from the side chains of amino acid residues in an environment determined by the remainder of the enzyme. There may also be a metal ion present.

Kinetic and mechanistic studies of enzymes are complicated by many factors: the active site is only a small part of a large molecule; such molecules are difficult to isolate and purify as they readily denature. While losing the "enzyme environment", small molecule model systems can be used to overcome many of these problems. These model systems can be constructed to mimic what are thought to be the key features of the particular enzyme active site. The results of kinetic and mechanistic studies on these systems can be used to provide suggestions, but not proof, of how the enzyme active site functions.

The chemical literature shows that the complete elucidation of an enzyme mechanism is a long and evolving process.[2-7] Many of the concepts that are incorporated into a suggested mechanism have originated from the results of many studies on model systems. In this review, some of these model systems will be discussed.

1.2 Modelling Enzyme Active Sites

There are two main features of enzymes that have been investigated using enzyme models:

(i) Coordinated Metal Ion at the Active Site. This occurs for a significant proportion of enzymes.[8] Of these metalloenzymes, one of the most important classes are the hydrolytic enzymes such as the peptidases and esterases. These include Carboxypeptidase (A, B), Leucine aminopeptidase, Alkaline phosphatase, and Thermolysin.

Generally, the correct functioning of the enzyme is critically dependent on the presence of the particular metal ion involved. Its removal usually results in complete deactivation of the enzyme and its substitution by another metal ion can result in either a loss or reduction in activity.[8]

The nature of the role played by the metal ion has been investigated using a variety of model systems, e.g the metal ion catalysed hydrolysis of amino acid esters.[9-13] These studies have shown that the presence of a metal ion facilitates hydrolytic reactions via three main properties of the metal ion:

- **Positive charge.** The addition of this increases the ease of nucleophilic attack, particularly by negatively charged nucleophiles, on the substrate.

- **Electron Withdrawal.** The strong **–I** inductive effect decreases the electron density at the reaction centre (e.g. the carbonyl C of an ester or amide), hence promoting nucleophilic attack at that centre.

- **Ligand Collection.** By collecting the substrate and reactant together, the reaction molecularity is reduced which leads to an increase in $\Delta S^{\ddagger}$ and hence an increase in the rate constant.

This metal ion aspect of the enzyme active site has been extensively reviewed.[8-13]

(ii) Neighbouring Groups at the Active Site. There are five main functional groups that are associated with the catalytic activity of most enzymes. These are imidazolyl (from a histidine residue), amino (from the residues of diamino acids such as lysine and from the enzyme's N-terminus), carboxylate (from the residues of dicarboxylic acids such as aspartic acid), hydroxyl (from serine and tyrosine residues), and thiol (from a cysteine residue). Suitably positioned, these neighbouring groups can act as nucleophilic, electrophilic, general acid or general base catalysts. Again, studies on small molecule model systems have shown that these groups can provide very large rate increases by replacing an intermolecular (multimolecular) pathway by an intramolecular (unimolecular) one. These studies are far from complete and one of the main aims of this thesis is to help increase our understanding of the mechanistic details of neighbouring group participation in hydrolytic reactions.

1.3 Neighbouring Group Model Systems

1.3(a) General

For hydrolytic enzymes such as peptidases and esterases, the role of neighbouring groups in catalysing the cleavage of acyl or phosphoryl linkages has been examined. Suitable model systems have involved a simple carboxylic acid ester with an appropriately positioned neighbouring imidazolyl, amino, carboxylate or hydroxyl group. The results of kinetic and mechanistic studies on such systems have been useful in helping to interpret what is occurring in the enzyme catalysed reaction.

In particular, the role of neighbouring groups in catalysing the hydrolysis of esters have been widely studied as possible enzyme models for esterase and peptidase activity.[14-17] For neighbouring group catalysis (NGC) to occur, the NG must fulfil two criteria; it must be a nucleophile and it must be suitably positioned relative to the ester group. The optimum positions are those that produce a 5- or 6-membered ring involving the nucleophilic group and reaction centre. Smaller rings are disfavoured by ring strain (despite being favoured entropically); larger rings while being unstrained are disfavoured entropically because of the low likelihood of the chain ends meeting.

Suitable nucleophiles that meet the nucleophilicity criterion (and these occur at the enzyme active sites) are:

Figure 1.1 Suitable Nucleophilic Groups for NGC in Ester/Amide hydrolysis.

These NG's can act as a nucleophile or as a general base. Which of these processes dominate has been the subject of many investigations.[14-17]

Two general type of mechanisms have been proposed (Schemes 1.1 and 1.2):

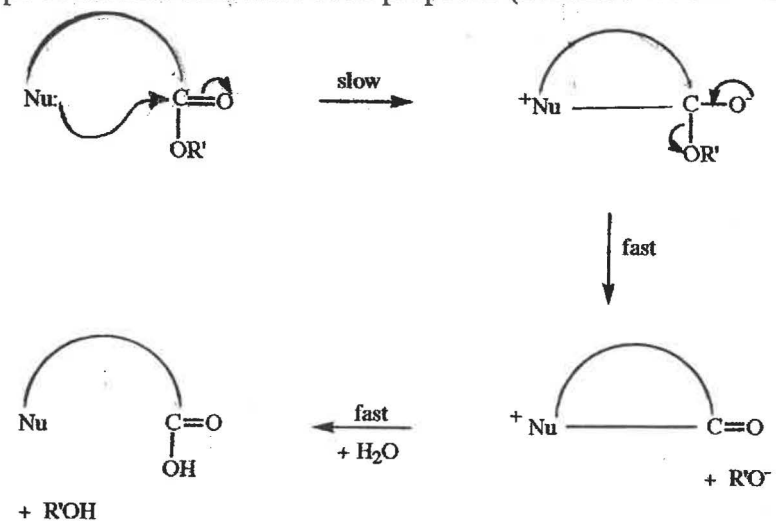

Scheme 1.1 Intramolecular Nucleophilic Catalysis (INC) Mechanism.

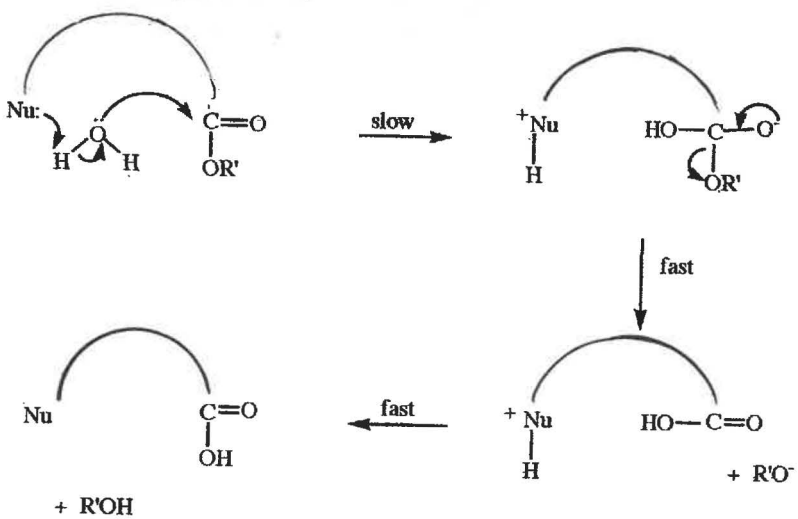

Scheme 1.2 Intramolecular General Base Catalysis (IGBC) Mechanism.

INC needs a strong nucleophile and a good leaving group, e.g. RO- = *p*-nitrophenolate.

IGBC is favoured by weak nucleophiles and poor leaving groups such as $-OCH_3$.

The IGBC and INC mechanisms are kinetically indistinguishable, since the two rate equations are:

(1) $$-\frac{d[E]}{dt} = k_1[E]$$

(2) $$-\frac{d[E]}{dt} = k_2[E][H_2O] = k_1'[E] \text{ since } [H_2O] = \text{const.}$$

This has often led to considerable confusion in the literature (e.g. see 1.3(b)). Fersht and Kirby have clearly established the following criteria for distinguishing between INC and IGBC:[14-17]

- INC forms a cyclic intermediate, which can usually be identified spectroscopically or by the use of trapping agents. This intermediate may be a reaction product.

- IGBC, which involves O-H bond breaking in the rate determining step (rds), shows a kinetic isotope effect, i.e. $k_{H_2O} \neq k_{D_2O}$.

- IGBC, in the presence of ^{18}O enriched water, leads to ^{18}O enrichment in the -COOH group of the product.

- INC being unimolecular will usually have a low (~ 0) $\Delta S^{\ddagger}$ value, whereas the bimolecular IGBC usually has a $\Delta S^{\ddagger}$ which is significantly negative.

- IGBC would be expected to occur when the pK_a of the conjugate acid of the leaving group is much higher than that of the nucleophile. Therefore the leaving group is unlikely to be displaced by a direct nucleophilic attack.

The INC mechanism is the more efficient with rate constant increases of up to 10^{15} times those of the analogous uncatalysed (intermolecular) reactions. In contrast, the IGBC rate increases are generally $< 10^2$ times.

The results of kinetic and mechanistic studies should be useful in helping to interpret what is occurring in the enzyme catalysed reaction. This is discussed in Section 1.5.

1.3(b) Carboxylate Group

This is a weak nucleophile and weak base ($pK_b = 9 - 11$ depending on the environment),[18] and has been the subject of many investigations.[14-17, 19-22]

(i) Acetyl Salicylic Acid

Fersht and Kirby demonstrated in their studies on the hydrolysis of the acetoxy group in acetyl salicylic acid (aspirin) that the reaction involves IGBC. The reaction occurs in acidic, neutral and basic conditions:

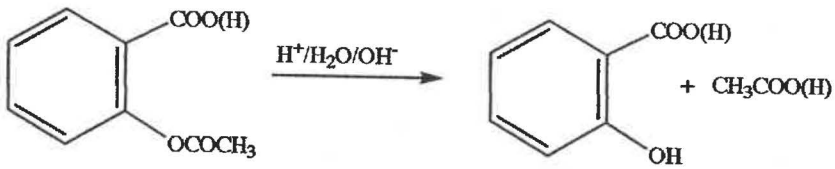

Scheme 1.3 Hydrolysis of Acetyl Salicylic Acid in Acidic, Neutral and Basic Solutions

At a given pH, 1st order kinetics are observed, but the pH/rate profile is anomalous. There is a plateau between pH 5 and 9, and the rise to the plateau begins at pH ~ 2, which strongly suggests NGC by carboxylate since the -COOH → -COO^- ionisation begins this pH. The mechanism of the reaction has been the subject of many studies. [11,12 14-17, 19-23] The initial work concluded INC occurred, but Fersht and Kirby[1617] clearly showed that the reaction involved IGBC by the carboxylate. INC requires the formation of an anhydride intermediate and in ^{18}O enriched H_2O there would be ^{18}O enrichment in both reaction products, which was not observed, Scheme 1.4:

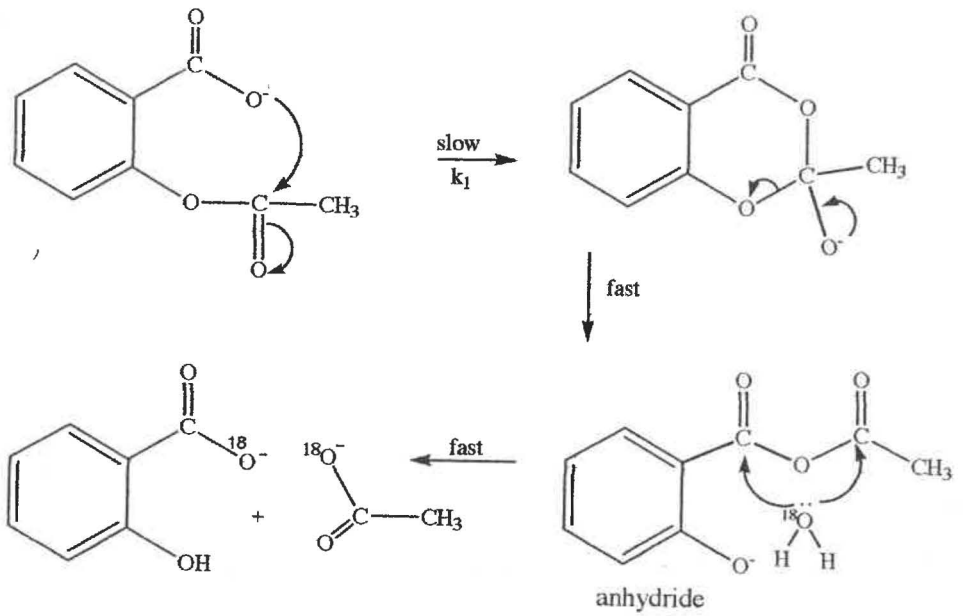

Scheme1.4 Incorrect (INC) Mechanism for NGC by Carboxylate in Acetyl Salicylic Acid Hydrolysis.

The IGBC mechanism does not involve the formation of an anhydride and ^{18}O enrichment only occurs in the acetic acid product, as observed:

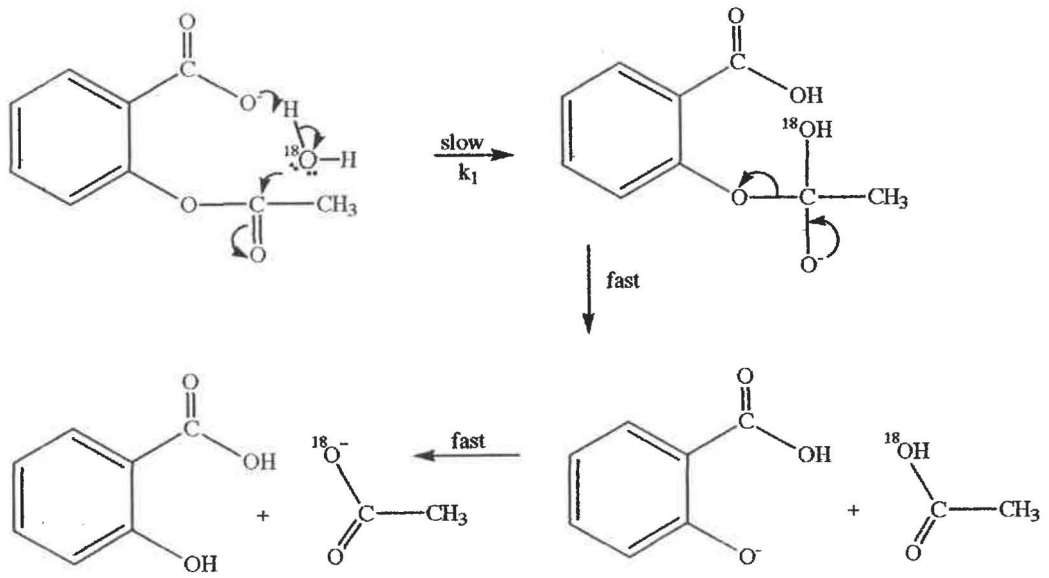

Scheme 1.5 Correct (IGBC) Mechanism for NGC by Carboxylate in Acetyl Salicylic Acid Hydrolysis.

The presence of the IGBC mechanism demonstrates the weakly nucleophilic nature of -COO^- which cannot directly displace the poor leaving group, CH_3CO-.

Fersht and Kirby also showed that greatly lowering the electron density at the acetoxyl carbonyl by placing the strongly electron withdrawing -NO_2 group both *o*- and *p*- to the -$OCOCH_3$ (i.e. 3,5-dinitrosalicylic acid), changes the mechanism to INC.[16,17] The decreased electron density at the carbonyl C facilitates attack by the weakly nucleophilic –COO^-. However, one -NO_2 group was found to be insufficient, with both the 3- and 5-nitrosalicylic acids hydrolysing via the IGBC pathway. This has implications for the role of carboxylate at an enzyme active site, e.g in Carboxypeptidase A.

The INC mechanism for the dinitro case is the fastest although perhaps surprisingly, the rate constant is only ~40 times that of the mononitro IGBC reaction, at 30°C and I = 0.1 mol l^{-1}.

In the analogous intermolecular reaction only the GB mechanism is observed:

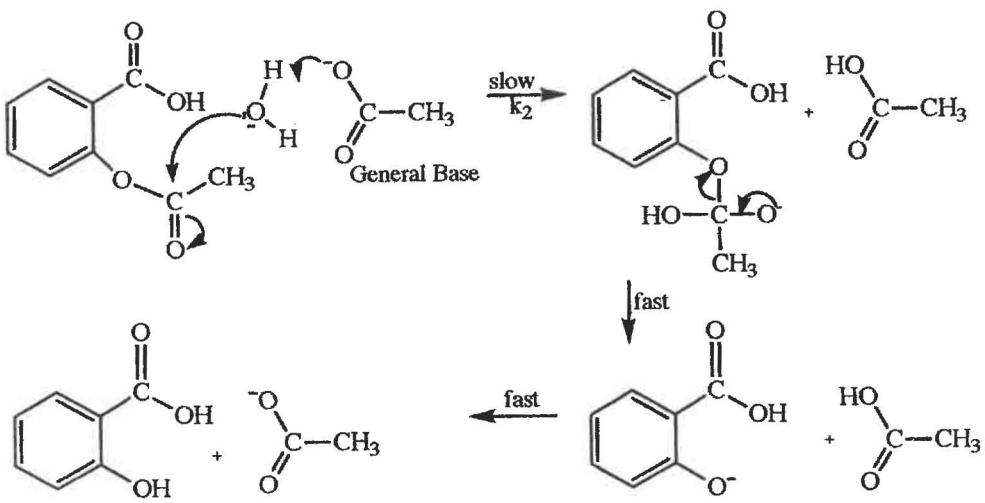

Scheme 1.6 Mechanism for Intermolecular GB Catalysis by the Carboxylate

Effective Molarity[23-26]

The effective molarity (EM) of a NG is an index of its catalytic strength. It has units of concentration because it is the ratio of k_1 for an intramolecular reaction to k_2 for the corresponding intermolecular process.

Values for EM's have been reported to range up to 1 x 10^{12} mol l^{-1}. Many explanations that have been proposed to account for the large efficiency of intramolcular catalysis, e.g. orbital steering, rotamer distribution and stereo-population control.[23] However, currently the most accepted theory appears to be that

that proposed by Jencks and Page.[26] This explains EM's (for both rate and equilibrium constants), using free energy differences between the reactants and transition state (for rate constants, $\Delta G^{\ddagger}$) or between reactants and products (for equilibrium constant, ΔG). For rate constants, the transition state theory[27-29] entropy of activation ($\Delta S^{\ddagger}$) is used to predict the effect of changes in ordering on the $\Delta G^{\ddagger}$ for the two pathways. The maximum entropic favouring of an intramolecular reaction is calculated to be ~ 180 J K^{-1} mol^{-1}.[26] This is equivalent to an EM of ~ 10^8 mol l^{-1}, which is considered to be the maximum possible EM.

Most intramolecular reactions have smaller EM's; the largest are seen for INC reactions because the corresponding intermolecular reactions have "tighter" transition states, i.e. there is a larger loss of entropy than for the IGBC reaction pathway.

For carboxylate in acetyl salicyclic acid, the EM of $-COO^-$ is the ratio of k_1 for intramolecular IGBC hydrolysis (Scheme 1.5) to the k_2 for intermolecular GB hydrolysis (Scheme 1.6). A correction is usually made to compensate for the differences in pK_a between the intermolecular and intramolecular mechanism. CH_3COO^- (pK_a ~ 4.76)[18] is more basic than the carboxylate group of salicyclic acid (pK_a ~ 3.69).[18] This results in an EM of ~13 mol l^{-1} (at 39°C) for carboxylate in acetyl salicylic acid, a moderate value which reflects the greater efficiency of the intra- over the intermolecular processes.

(ii) Mono-phenyl Esters of ω-Dicarboxylic Acids

Phenyl esters of the type shown in Figure 1.2, also undergo intramolecular hydrolysis:

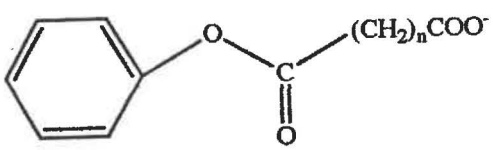

Figure 1.2 General Structure of Mono -phenyl Esters of ω-Dicarboxylic Acids.

INC is possible because the phenolate is a good leaving group. Hence there is an interplay between INC and IGBC mechanisms, but in this case, changing the distance between the $-COO^-$ and the carbonyl carbon atom (i.e. changing the value of n) controls which mechanism operates, because this determines the potential anhydride ring size needed for INC. The results are summarised Table 1.1.[30]

Table 1.1 Summary of the Relative Rates of Hydrolysis for a Series of Mono-phenyl Esters of Some ω-Dicarboxylic Acids.

Ester	Relative Rate 25 °C, pH 7	Mechanism	Potential Anhydride Ring Size for INC	Effective Molarity [COO^-]
n = 0	1	No NGC	3	-
n = 1	50	IGBC	4	10 mol l^{-1}
n = 2	23,000	INC	5	4,000 mol l^{-1}
n = 3	150	INC	6	25 mol l^{-1}

For n = 0 and n = 1, the potential anhydride ring sizes are 3 and 4 respectively, which are too strained to allow INC. n = 2 results in rapid, INC, hydrolysis because of the unstrained 5-membered ring involved which is not too disfavoured entropically. The n = 3, the 6-membered ring, is more disfavored entropically, but has low strain, so the reaction still involves INC but is slower.

1.3(c) Imidazolyl Group

Intramolecular catalysis by this group has been widely studied.[31-39] It is a stronger nucleophile and base ($pK_b \sim 7$)[18] than carboxylate. Of the five neighbouring groups considered (Figure 1.1), imidazolyl is uniquely placed. It is a stronger base than carboxylate but not too strong; ~ 50% of imidazolyl is present in the nucleophilic free base form at biological pH (~ 7.2). This is in contrast to the more basic amino group which is largely protonated ($-NH_3^+$) at this pH (see 1.3(h)).

Consequently, the unprotonated imidazolyl group has been implicated in several enzyme mechanisms. It has been widely used in model systems, several of which have reaction rates which match those of the analogous enzymatic processes.[25-30] As for carboxylate, competition between IGBC and INC reaction mechanisms has been observed, with the dominant mechanism being dependent on the structure of the ester. Provided the potential ring size is 5 or 6, esters with good leaving groups generally hydrolyse via the INC pathway but poor leaving groups generally result in the IGBC mechanism taking over. This has been shown in studies on esters of 2-(4'-imidazoyl)phenol (Scheme 1.7):[37]

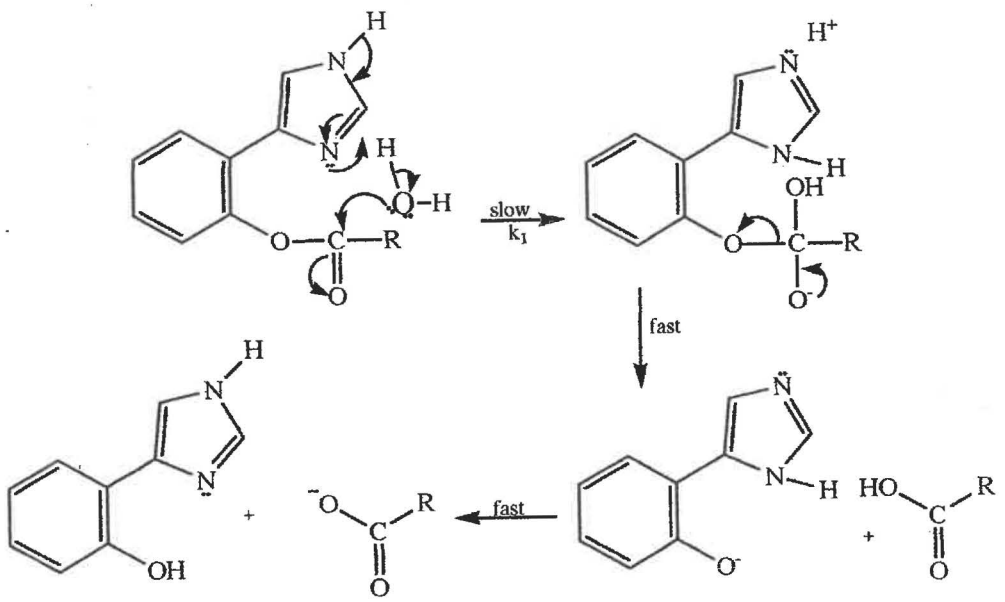

Scheme 1.7 Mechanism for IGBC by the Imidazolyl for Esters of 2-(4'-imidazoyl)phenol.

Some of the results on the studies of 2-(4'-imidazolyl)phenol esters are summarised in Table 1.2.[35]

Table 1.2 Rate Constants for Hydrolysis of Esters of 2-(4'-Imidazolyl)phenol.

R	k_1 (s^{-1} at 30 °C)	Mechanism
p-NO_2-C_6H_4	137 x 10^{-6}	INC
CH_3	35 x 10^{-6}	IGBC?
p-Br-C_6H_4	13 x 10^{-6}	IGBC
C_6H_5	9 x 10^{-6}	IGBC
o-Br-C_6H_4	4 x 10^{-6}	IGBC
p-CH_3O-C_6H_4	2 x 10^{-6}	IGBC

Despite arguments that the mechanism changeover occurs when the leaving group becomes poorer than benzoyl (R = C_6H_5), it seems clear that only the R = *p*-NO_2-C_6H_4 compound undergoes INC. Reaction of the R = CH_3 compound has a significant deuterium isotope effect (k_{H_2O} / k_{D_2O} = 3.20) and $\Delta S^{\ddagger}$ = - 37 J K^{-1} mol^{-1}, which suggests a bimolecular rds involving H_2O.[23] This type of IGBC reaction is of interest because of its similarity to what occurs at the active site of esterases and proteases such as chymotrypsin. In chymotrypsin, the imidazolyl group of His-57 acts as a general base and assists attack of the acyl-serine intermediate. The INC reaction mechanism requires the formation of an N-acyl imidazolyl intermediate which should be observable for R = *p*-NO_2-C_6H_4.

1.3(d) Hydroxyl Group

Biological interest[40,41] in the role of -OH as an intramolecular catalyst arises from its presence at the active site of several enzymes. In the serine esterases, such as chymotrypsin and acetylcholine esterase, there is an alcoholic hydroxyl associated with the hydroxymethylene of a serine residue. A phenolic hydroxyl group from a tyrosine residue is present at the active site of some metalloproteases/esterases such as the Carboxypeptidases. Therefore, it is important that reactions in which $-O^-$ participates as a nucleophile are properly understood.

In an aliphatic (alcohol) environment, the -OH group is generally a very poor nucleophile; it shows little basic character being a very weak acid (pK_a = 13 to 16)[18] Consequently, the conjugate base, alkoxide $-O^-$, is an extremely powerful base (pK_b = 1 to -2)[18]. Clearly, for an alcoholic-OH to function as an IN or IGB catalyst, it must be in a very special environment, i.e. highly electron rich and/or sterically correctly oriented. The presence of a general base neighbouring group able to convert the -OH to a transistent $-O^-$ would be even more desirable. In contrast, the phenolic -OH is more acidic and the phenolate ion (pK_b = 4 to 6)[18] can exist in aqueous solution, and can act as a nucleophile. It is difficult to construct simple model systems where alcoholic -OH acts as an NGC in ester amide/peptide hydrolysis. However, one such system involved is the hydrolysis of 4-hydroxybutanamide.[41] The reaction pathways are outlined in Scheme 1.8:[41]

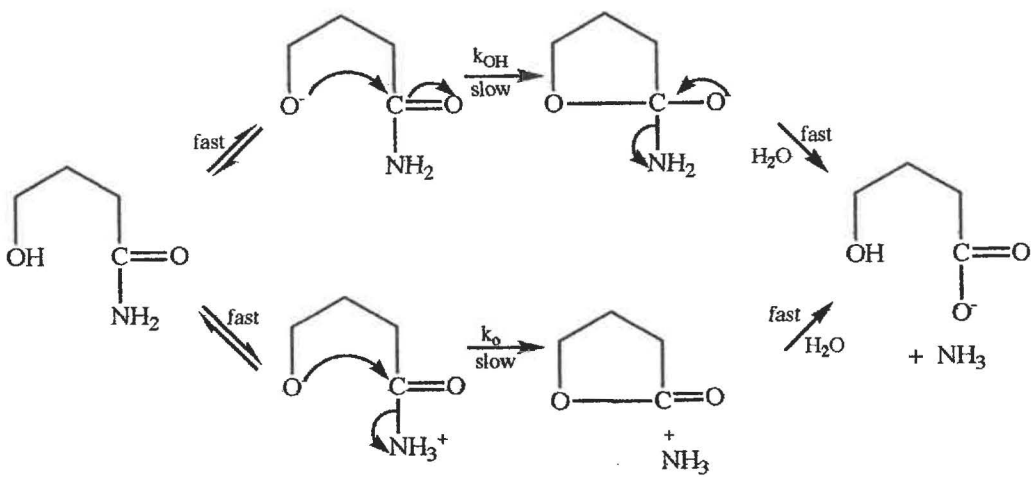

Scheme 1.8 Alternative Pathways for the Hydrolysis of 4-Hydroxybutanamide.

The observed kinetics were explained in terms of two parallel pathways with:

$$-\frac{d[amide]}{dt} = (k_0 + k_{OH}[OH^-])[amide],$$

where k_0 was ~ 800 times the uncatalysed rate constant and k_{OH} ~ 20 times. However, it is difficult to understand the proposed mechanism; the equilibrium concentrations of the two alkoxide intermediates would be very small in aqueous solution (unless $[OH^-]$ was very high) although they will be extremely reactive. A similar type of reaction has not yet been observed for esters with a better leaving group than $-NH_2$.

1.3(e) Hydroxymethyl Group[42-49]

(i) Imidazole Assisted INC by Alkoxide

Fife and Benjamin investigated the presence of GB catalysis by inidazole (Im) in the cyclisation of the ethyl esters of 2-hydroxymethylbenzoate and 2-hydroxymethyl-4-nitrobenzoate (Scheme 1.9):[44]

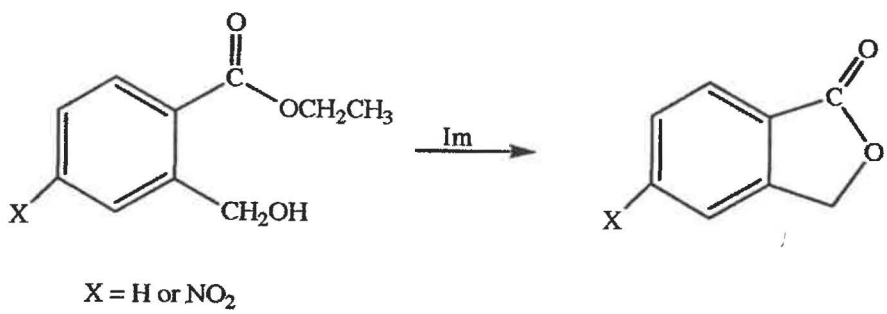

X = H or NO_2

Scheme 1.9 Cyclisation of the Ethyl Esters of 2-Hydroxymethylbenzoate and 2-Hydroxymethyl-4-Nitrobenzoate to form Phthalide and 5-Nitrophthalide.

Both reactions showed a significant D_2O solvent isotope effect for the imidazole catalysed reaction ($k_{Im}^{H_2O}/k_{Im}^{D_2O}$ = 3.46 for the methyl ester and 3.15 for the 4-nitrobenzoate ester). These results strongly suggest that proton transfer occurs during the rate determining step, Figure 1.3:[42]

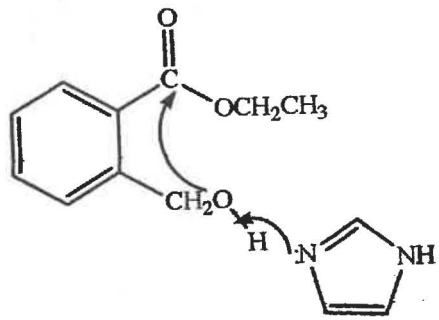

Figure 1.3 GB Catalysis by the Imidazolyl Group in the Cyclisation of the Ethyl Ester of 2-Hydroxymethylbenzoate.

Fife[43] proposed that this system could represent a reasonable model system for the process that occurs in chymotrypsin (Section 1.5(a)). However, the results from the Brønsted plot for the GB catalysed cyclisation contradict the proposed mechanism shown in Figure 1.3, since the graph shows good linearity with $\beta = 0.97$. This suggests that proton transfer is diffusion controlled, and is unlikely to be rate determining.[40] In contrast, for X = $-NO_2$ (Scheme 1.9), $\beta = 0.87$ which suggests a concerted mechanism involving GB catalysed proton removal and nucleophilic attack. These results seem a little surprising, since the electron withdrawing effect of the $-NO_2$ group on $-COOC_2H_5$ group would be expected to activate it toward nucleophilic attack, but deactivate it toward leaving group departure, as compared to 2-hydroxymethylbenzoate. Clearly, nitro substitution produces a complex effect on the reaction mechanism. More work needs to be done on the NG catalysed reaction, e.g. investigate the effect of a variety of other leaving groups, to get a better understanding of the mechanism.

(ii) Unassisted INC by Alkoxide

There are few reactions where a mechanism for INC by alkoxide at an ester carbonyl has been proposed, e.g. the lactonisation of ethyl and *p*-nitrophenyl esters of 2-hyroxymethyl-N-methylcarbanillic acid.[46] Hutchins and Fife obtained pH/rate profile plots for both esters that had slopes of 1, but were unable to spectrometrically detect the presence of the intermediate required by their proposed mechanism (Scheme 1.10):

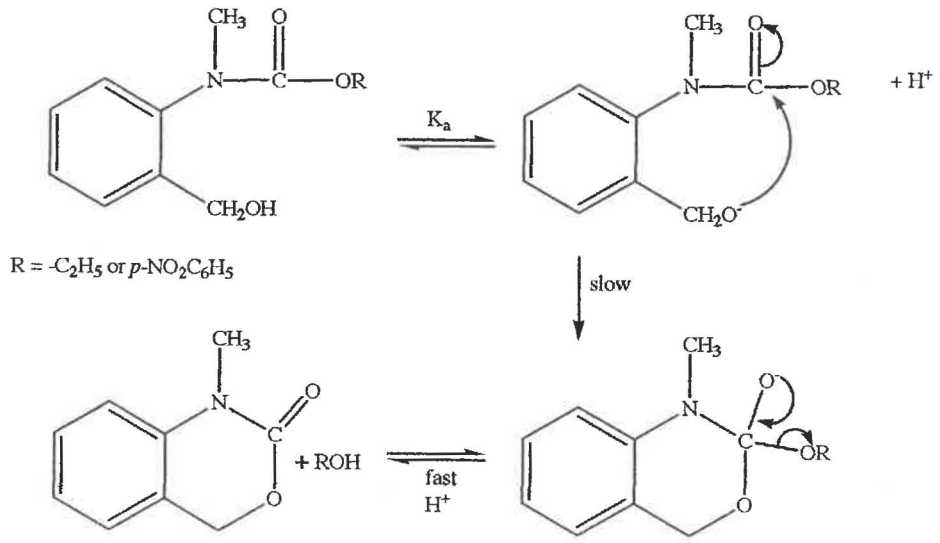

Scheme 1.10 Cyclisation of Esters of 2-Hydroxymethyl-N-methylcarbanilic Acid.

Hence, it is possible that the reaction mechanism involves OH^- catalysis. Subsequently, these authors obtained values for the second order rate constant, k_{OH}, which they defined as:

$$k_{OH} = \frac{k_r K_a}{K_w}$$

where,

k_r is the rate constant for the rate determining step

K_w is the ionic product of water

K_a is the dissociation constant of the hydroxymethyl group.

The NG effect of $-CH_2OH$ on the reaction can clearly be seen in the values of the second order rate constants, e.g., k_{OH} for the cyclisation of the *p*-nitrophenyl ester of 2-hydromethyl-N-methylcarbanilic acid is 3×10^5 times greater than the OH^- ion catalysed hydrolysis of *p*–nitrophenyl N-methyl N-phenylcarbamate (where the NG effect is absent).[49] Surprisingly, the cyclisation of the corresponding ethyl ester was found to give a rate enhancement of 1×10^6 for k_{OH} over that for the uncatalysed reaction even though the *p*-nitrophenyl is a better leaving group than ethyl. These impressive rate enhancements demonstrate the powerful catalytic effect of a neighbouring group alkoxide ion.

(iii) Intramolecular Amino GB Catalysis of Cyclisation Involving $-CH_2OH$

The cyclisation of 6-amino-2-hydroxymethylbenzamide has shown to be subject to GB catalysis by a 6-amino group (Scheme 1.11).[47] It has been proposed that $-NH_2$ group assists with the decomposition of the tetrahedral intermediate rather than with the attack of the -OH on the carbonyl C.

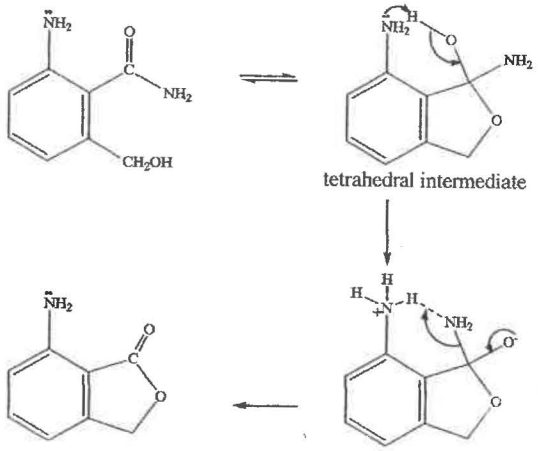

Scheme 1.11 The GB Catalysed Cyclisation of 6-Amino-2-hydroxymethylbenzamide.

(iv) Amino Assisted Hydroxymethyl Catalysis

The pH/rate profile for the lactonisation of 3-amino-2-hydroxymethylbenzamide is complicated, since it shows an inflection point at ~ pH 3.5. This is likely to correspond to the conversion of $-NH_3^+ \rightarrow -NH_2$.[48] The reaction rate is independent of pH in the region 3.5 – 10. This compound has a rate constant that is ~ 1 x 10^3 times larger than for the reaction for 2-hydromethylbenzamide which lacks the $-NH_2$ group. This seems to suggest that the $-NH_2$ group acts as an intramolecular catalyst. The position of the $-NH_2$ substitution on the benzene ring is critical for catalysis, since none occurs for the corresponding 4-, 5- and 6-amino isomers. This suggests that here the $-NH_2$ group is too remote to act as a GB catalyst. Furthermore, the 3-amino isomer uniquely shows no evidence of external buffer catalysis,[48] whereas this is found for the other amino isomers and the parent 2-hydroxymethylbenzamide. Presumably, the 3-amino group acts as an internal GB in the lactonisation of 3-amino-2-hydroxymethylbenzamide. Studies on its D_2O solvent isotope effect show the value of $k_{H_2O} / k_{D_2O} = 2.82$, in the pH-independent reaction. This suggests that there is some degree of proton transfer occurring in the rds. Consequently, two possible mechanisms have been proposed for the role of the 3-NH_2 group as a GB catalyst:[48]

(i). -NH_2 GB assisted direct attack by an alcoholic -OH (Figure 1.4).

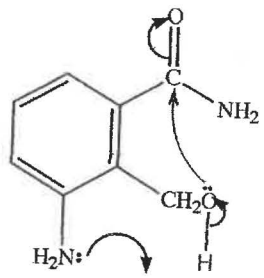

Figure 1.4 Internal GB Catalysis by the –NH_2 Group in the Lactonisation of 3-Amino-2-hydroxymethylbenzamide.

(ii). -NH_2 assisted direct attack by an alcoholic –O^-, where -NH_2 removes H^+ from a H_2O molecule. (Figure 1.5)

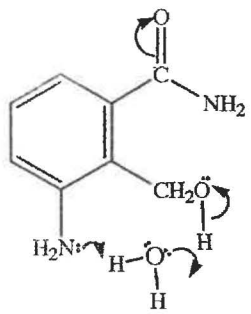

Figure 1.5 Internal GB Catalysis by the –NH_2 Group in the Lactonisation of 3-Amino-2-hydroxymethylbenzamide Involving H_2O.

The $\Delta S^{\ddagger}$ value (-96 J K^{-1} mol^{-1}) suggests that that the transition state for the lactamisation is highly ordered and the rds is probably bimolecular. This is consistent with the mechanism in Figure 1.5. The Figure 1.4 mechanism is unimolecular and would be expected to have a $\Delta S^{\ddagger}$ value ~ 0.[48] Additionally if the unimolecular mechanism occurred, it would involve an unfavourable, highly strained transition state (TS). This reaction has low EM of 15 mol l^{-1}.[48] However, such an EM value seems meaningless, since it is very difficult to set up a small molecule system that involves bifunctional catalysis. This rds would be trimolecular, involving the simultaneous participation of an amine, a molecule of H_2O and the substrate which would be entropically disfavoured. The low magnitude of the EM of this reaction means that it is of little use as an enzyme model for Chymotypsin.

1.3(f) Phenolate Group

There have been many reports of neighbouring phenolate groups acting as intramolecular catalysts in ester hydrolysis,[50,51] in contrast to the uncommon alkoxide case. Carbamate esters are generally resistant to hydrolysis since the partial positive charge on the carbonyl group is reduced by resonance delocalisation from the adjacent N. However these compounds undergo very rapid hydrolysis in the presence of a suitably positioned phenolic -OH. The pH-rate constant profile is sigmoidal, with a pK_{app} ~ 9.0. This suggests that the reaction involves INC by phenolate (Scheme 1.12):[50]

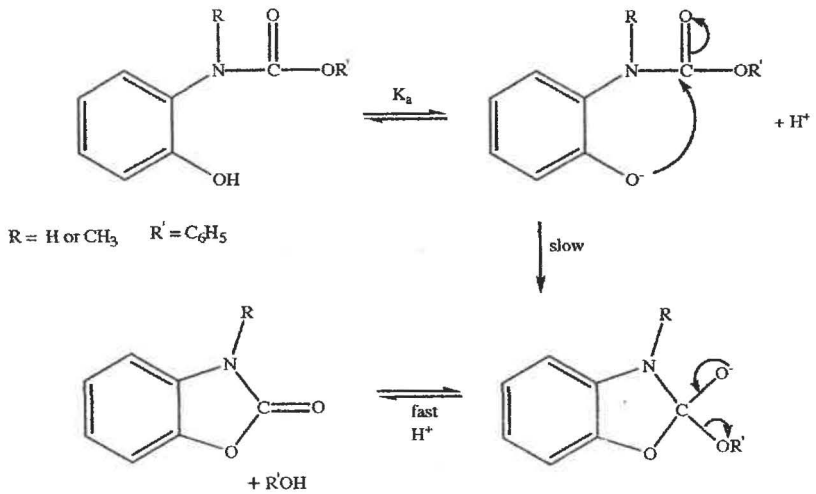

Scheme 1.12 INC by Phenolate in Lactamisation of Carbamate Esters.

The EM of the phenoxide is 3 x 10^8 mol l^{-1} for the N-methyl derivative, which is ~ 10 times greater than that for (2-hydroxyphenyl)-carbamic acid phenyl ester.

IGBC by phenolate has been reported in the hydrolysis of *o*-hydroxybenzamide (Figure 1.6):[51]

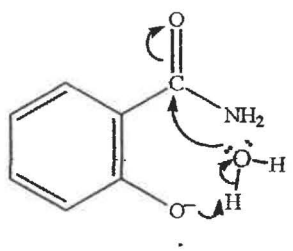

Figure 1.6 IGBC by Phenolate in the Hydrolysis of o-Hydroxybenzamide.

1.3(g) Sulfhydryl Group

This group plays an important role at the active site of thiol protease enzymes such as papain. These enzymes are analogous to the Chymotrypsin class with the cysteine – CH_2SH group replacing the serine $-CH_2OH$ in the reaction mechanism.

The -SH group is a weak acid ($pK_a \sim 8.5$)[18], which is likely to be partially ionised under biological conditions. However the conjugate base ($-S^-$, $pK_b \sim 5.5$) would be expected to be only a moderately good nucleophile cf. to an alkoxide (Section 1.3(d)). Some reactions involving the -SH group as models for the enzyme Papain, have been investigated, e.g. Fife et al. investigated the *p*–nitrophenyl ester of (2-mercapto-phenyl)-N-methyl-carbamic acid.[52] This compound undergoes cyclisation involving INC attack by $-S^-$ of the conjugate base to form 3-methyl-3H-benzathiazol-2-one (Scheme 1.13):[52]

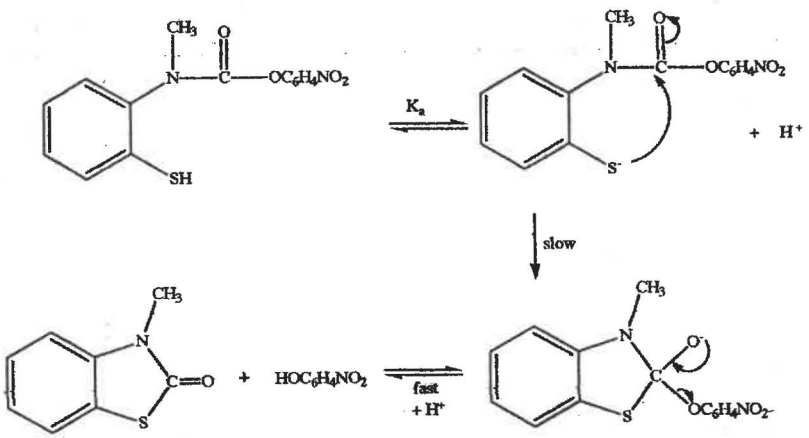

Scheme 1.13 Cyclisation of the *p*–Nitrophenyl Ester of (2-Mercapto-phenyl)-N-methyl-carbamic Acid.

Experimental support for this mechanism includes UV detection of the cyclic product and a sigmoidal pH rate constant profile ($pK_{app} \sim 8.7$),[52] which suggests the participation of the anionic form, $-S^-$. No buffer catalysis was observed. The EM for the reaction is 1.4×10^5 mol l^{-1}.[52] Interestingly, the largest catalytic rate constant seen for the thiol group in this reaction was 24 s^{-1} cf. the phenyl ester of N-(2-hydrophenyl)-N-methylcarbamate which was 2.2 s^{-1} (Section 1.3(f)). *p*–nitrophenol is expected to be a more effective leaving group than phenoxide, and would be expected to result in a 10 – 100 times larger rate constant. It appears that $-S^-$ is a better nucleophile than $-O^-$, possibly due to the greater hydration of $-O^-$ than $-S^-$, in the rds.

1.3(h) Amino Group, Intramolecular Catalysis

The $-NH_2$ group is similar to imidazolyl, but is a stronger base and nucleophile (pK_b = 3 - 5)[18]. Like imidazolyl, it is a moderately common functional group present in enzymes and so its role as a neighbouring group catalyst has been the subject of several investigations.[54-61] Most have focussed on catalysis in the alkaline hydrolysis of the ester function in amino acid esters. These studies have involved poor leaving groups, such as $-OCH_3$ (i.e. methyl esters).

However unlike the imidazolyl and carboxylate groups, amino group catalysis does not appear to involve competition between INC and IGBC mechanisms. In fact, it appears that a simple INC mechanism (expected to be dominant because of the amino group's high basicity) is impossible. Paradoxically, this is because of this high basicity – the amino group remains protonated to high pH; no INC is possible until the free $-NH_2$ begins to be formed and the $[OH^-]$ required for this is sufficiently high that an OH^- assisted type of INC mechanism apparently results. The reaction kinetics are now second order, first order in both the amino compound **and** OH^-. This has been observed in the studies on the alkaline hydrolysis of three classes of amino acid esters:

(i) ω - Monoamino Acid Methyl Esters

These esters undergo alkaline hydrolysis with the following rate equation:[55,57,58,60]

$$-\frac{d[E]_T}{dt} = k_2[E]_T[OH^-]$$

where $[E]_T$ = total ester concentration = $[E] + [EH^+]$

Two parallel reactions involving $E + OH^-$ and $EH^+ + OH^-$ occur, with rate constants k_E and k_{EH^+} respectively. E and EH^+ are interconnected by a pH dependent equilibrium so the alkaline hydrolysis reaction must be studied at constant pH, commonly by using a pH-stat.[48,53] Values of k_E for some ω-amino acid methyl esters ($T = 25°C$, $I = 0.1$ mol l^{-1}) are summarised in Table 1.3:

Table 1.3 Relative Rates for Alkaline Hydrolysis of a Series of Some ω - Monoamino Acid Methyl Esters, $H_2N(CH_2)_nCOOCH_3$.

n	Methyl Ester of:	k_E^* ($l\ mol^{-1}\ min^{-1}$)	Mechanism
1	2-aminoethanoic acid (2-AE Me)	$72^{(60)}$	$B_{AC}2$
2	3-aminopropanoic acid (3-AP Me)	$11^{(60)}$	$B_{AC}2$
3	4-aminobutanoic acid (4-AB Me)	$1674^{(57)}$	OH^-/INC
4	5-aminopentanoic acid (5-APe Me)	$28260^{(57)}$	OH-/INC
5	6-aminohexanoic acid (6-AH Me)	$9^{(57)}$	$B_{AC}2$

* at T = 25°C, I = 0.1 mol l^{-1}.

It is generally accepted that the simple base hydrolysis of ω-monoamino acid methyl esters involves a reaction mechanism with bimolecular acyl-oxygen fission ester hydrolysis ($B_{AC}2$).[55] The rds is the first step, nucleophilic attack of the OH^- on the electron deficient carbonyl C of the ester (Scheme 1.14).[62]

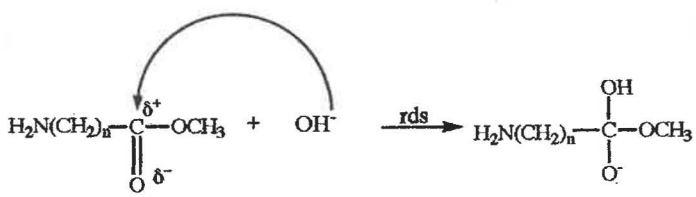

Scheme 1.14 Rate Determining Step for the $B_{AC}2$ Mechanism.

Subsequent steps involve acyl-O bond cleavage and the ejection of the alkoxide; its conversion into an alcohol and the formation of the amino acid.

There is a rapid decrease in k_E from 2-AE Me (n = 1) to 3-AP Me (n = 2), with little further fall to 6-AH Me (n = 5) (ignoring the n = 3 and 4 cases). This behaviour is in agreement with inductive effects predicted by the $B_{AC}2$ mechanism. The $-NH_2$ group exerts an indirect **-I** effect through the carbon chain to the ester carbonyl C. This raises the positive charge on this C, hence increasing the rate of nucleophilic attack by OH^-. Insertion of one methylene causes a rapid (~ exponential) decrease in this indirect **-I** effect. Hence, k_E for 3-AP Me is much smaller than for 2-AE Me. However for n = 3 and n = 4, the k_E value is anomalously large, suggesting NGC. Further evidence for this is that a lactam (rather than the parent amino acid) is formed

in both cases. These are stable under the reaction conditions, pH ~ 9 and 25°C. The size of the potential lactam ring controls whether or not NGC occurs: only the 5-membered (n = 3) and 6-membered (n = 4) rings are unstrained and can be formed readily (see 1.3(a)).

(ii) α,ω-Diamino Acid Methyl Esters

The alkaline hydrolysis of methyl esters α, ω-diamino acids, $NH_2(CH_2)_nCH(NH_2)COOCH_3$, shows the same characteristics as the monoamino acid esters. Again, for the neutral (E) form of the ester, NGC occurs when 5- and 6-membered lactams can be formed (Table 1.4):

Table 1.4 Rate Constants for the Alkaline Hydrolysis of α, ω - Diamino Acid Methyl Esters, $H_2N(CH_2)_nCH(NH_2)COOCH_3$.

n	Methyl Ester of:	k_E^* (l mol-1 min^{-1})	Mechanism
1	2,3-diaminopropanoic acid (2,3 DAP Me)	44[55]	$B_{AC}2$
2	2, 4-diaminobutanoic acid (2, 4 DAB Me)	25320[55]	OH^-/INC
3	2,5-diaminopentanoic acid (2, 5 DAPe Me)	190200[57]	OH^-/INC
4	2,6-diaminohexanoic acid (2, 6 DAH Me)	28[55]	$B_{AC}2$

* at T = 25°C, I = 0.1 mol l^{-1}

From the results for both the monoamino and diamino acid esters, an estimate can be made for the optimum potential ring size for intramolecular catalysis. For 5-membered ring formation, $k_E = k_{L5}$ (5-membered ring lactam) and for 6-membered, $k_E = k_{L6}$. (In both cases, the contribution to k_E from the uncatalysed $B_{Ac}2$ reaction is negligible). For the monoamino acids, k_{L6}/k_{L5} = 16.9 at 25°C, indicating an amino group positioned such as to produce a 6-membered ring provides the best catalysis. The same conclusion can be drawn for diamino acid esters, but the preference for a 6-membered ring (k_{L6}/k_{L5}) is now 7.2. As expected, these ratios are different because each involves a comparison of the rate constants for two different compounds. Each of the compounds in a pair may have different electronic, steric and solvation effects which contribute to the k_L value. These complications were overcome by combining the two reactions into one molecule, i.e. by studying the competitive intramolecular aminolysis in the following compound.

(iii) 4,5-Diaminopentanoic Acid Methyl Ester (4,5-DAPe Me)

The neutral (E) form, present alone at sufficiently high pH, undergoes competitive 5- and 6-membered ring closure (Scheme 1.15):[61]

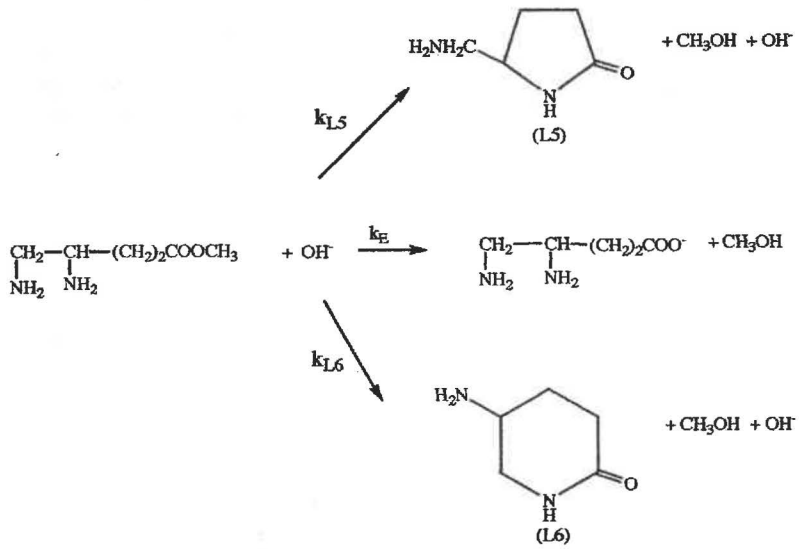

Scheme 1.15 Parallel Pathways for the Alkaline Hydrolysis and Lactamisation of 4,5 -DAPe Me.[61]

The rate constant for the $B_{Ac}2$ reaction is negligibly small. At 25°C k_{L6}/k_{L5} was found to be 4.5[(61)] which is a best estimate for the catalytic efficiency of $-NH_2$ in these systems. The preference for a potential 6-membered ring position is small, much smaller than might be mistakenly deduced from the monoamino and diamino acid ester studies.

1.3(i) Amino Group, Intermolecular Catalysis

Reactions involving the intermolecular aminolysis of alkyl esters have been the subject of several investigations.[63-70] The proposed mechanism is very complicated because the rds changes depending on several factors including pH, strength of the leaving group and the type of the amino group.[63] However, in all cases, intermolecular aminolysis involves initial attack by the amine at the ester carbonyl. This results in the formation of an unstable zwitterion intermediate (Scheme 1.16):

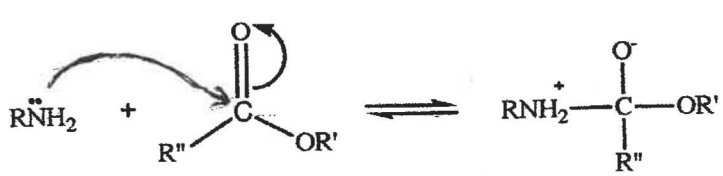

Scheme 1.16 Formation of Zwitterion Intermediate in Intermolecular Aminolysis.

The ultimate fate of this intermediate depends on the nature of the leaving group. It will revert back to the reactants in the absence of suitable stabilisation. Three cases arise depending on the leaving group (Scheme 1.16):

(i) Poor Leaving Groups

The $-NH_2$ group is unable to directly displace the poor alkoxide leaving groups (OR' = OCH_3, C_2H_5 etc.) from the zwitterion intermediate, because these are a stronger base than $-NH_2$ (pK_a = 9-11).[18] Instead, at high pH, the proposed rds involves an internal proton transfer mediated by either one or more molecules of H_2O, giving a neutral intermediate. This rapidly breaks down to generate the hydrolysis products, which is assisted by a proton transfer agent, B (Scheme 1.17):

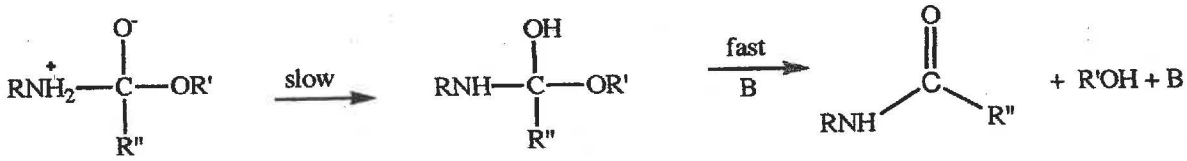

Scheme 1.17 Internal Proton Transfer During the Intermolecular Aminolysis of Esters with Poor Leaving Groups.

Alternatively, the $-NH_3^+$ group of the zwitterion can donate a proton to an external general base. B. The resulting anionic intermediate formed, then rapidly expels the leaving group (Scheme 1.18):

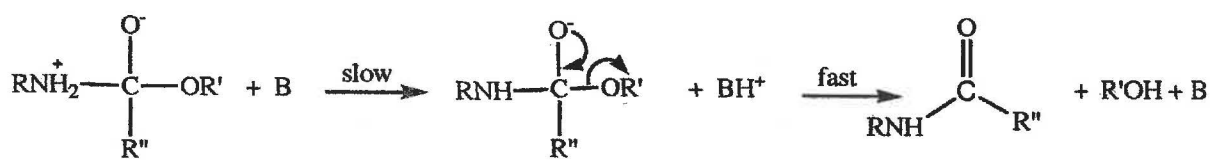

Scheme 1.18 Intermolecular Proton Transfer to a GB During Intermolecular Aminolysis of Esters with Poor Leaving Groups.

Clearly, such proton transfers (Schemes 1.17 and 1.18) are only possible for primary and secondary amines. Consequently, tertiary amine intermolecular aminolysis of esters with poor leaving groups is not observed. Interestingly, both primary and secondary amines have similar rates of reaction. This may suggest that there is little

or no bond breaking taking place during the rds. However, as the pH is lowered the rds changes (shown by negative deviations in the pH/rate profile), and at low pH, the rds may involve the breakdown of the tetrahedral intermediate.[63]

(ii) Moderately Good Leaving Groups

When esters with moderately good leaving groups, e.g. *p*-nitrophenolate (pK_b = 5 –7)[18] are used, the rds appears to involve breakdown of the tetrahedral intermediate and expulsion of the leaving group (Scheme 1.19):

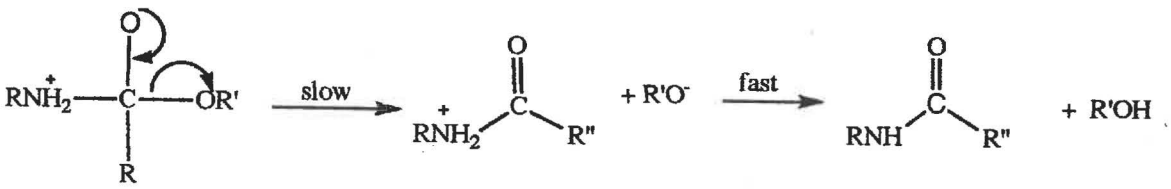

Scheme 1.19 Generalised rds for the Intermolecular Aminolysis for Esters with Good Leaving Groups.

Support for this conclusion, comes from the increase in the reaction rate as the pK_b of the leaving group decreases, which suggest that leaving group is lost in the rds. Primary, secondary and tertiary amines were all found to have similar rates of aminolysis, which implies that proton transfer does not occur in the rds.

(iii) Extremely Good Leaving Groups

When extremely good leaving groups, e.g. 1-acetoxy-4-methoxypyridium and acetyl-pyridium are used, the rds appears to involve nucleophilic attack by the amine at the ester carbonyl C (Scheme 1.16), to generate a tetrahedral intermediate, followed by rapid departure of the leaving group. Again the reaction rate is independent of the type of amine.

1.3(j) (Phenyl Aromatic) Amino Intramolecular Nucleophilic Catalysis

Aniline amino groups have some properties that are different to those of aliphatic amino groups and are not involved in enzyme active sites. However, their intramolecular catalytic reactions have been extensively studied and the results throw some light on the corresponding aliphatic amino reactions.

Anilines are extremely weak bases (pK_b 9 – 13)[18] and consequently are usually poor nucleophiles. As a result, **intermolecular** aniline catalysed hydrolysis of carboxylic acid alkyl esters involves GB rather than nucleophilic attack by aniline.[49,52,71-73]

However, **intramolecular** aromatic amino catalysis often involves direct nucleophilic attack, with some large rate enhancements (up to 10^5 times) reported.[52,71-73]

(i) Cyclisation of 2-(Aminophenyl)-N-methylcarbamic Acid Phenyl Ester.

Fife et al.[52] investigated the kinetics of this reaction (determined at 50°C and I = 0.5 mol^{-1}), (Scheme 1.20):

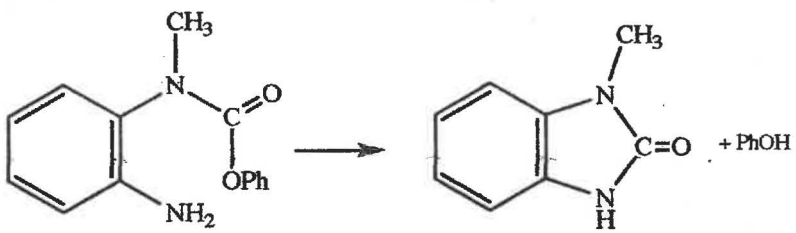

Scheme 1.20 Cyclisation of 2-(Aminophenyl)-N-methyl-carbamic Acid Phenyl Ester.

They obtained a sigmoidal curve for the pH/rate profile with pK_{app} = 2.7, which suggests that the free base form is the reactive species. The proposed rds involves a concerted nucleophilic attack by the $-NH_2$ at the ester carbonyl-C coupled to the expulsion of the phenolate ion. Evidence for this unimolecular rds included the value of the deuterium solvent isotope ratio, k_{H_2O} / k_{D_2O} = ~ 1.2, (which implies that an INC type mechanism operates). Also, no intermediate(s) could be detected, suggesting that the rds involves synchronous bond breaking and making. However, it is difficult to rationalise how the mechanism for the aminolysis of this ester could be concerted. The aniline–NH_2 group is expected to be a poor nucleophile and the carbamate carbonyl centre is essentially deactivated, factors that should discourage the proposed

INC type mechanism from occurring. Clearly, more work needs to be done on this reaction, especially regarding the effect of varying the leaving group strength on the reaction rate.

(ii) Cyclisation of Esters of (2-Aminophenyl)acetic and Propanoic Acids.

The intramolecular aminolysis of a series methyl and trifluoroethyl esters of (2-aminophenyl)acetic acid (n = 1), at 50°C and I = 0.5 mol l^{-1} [71] and 3-(2-aminophenyl)propanoic acid (n =2), at 39°C and I = 1.0 mol l^{-1} [72] has been studied to investigate the effect of ring size upon the rate of lactamisation (Scheme 1.21):

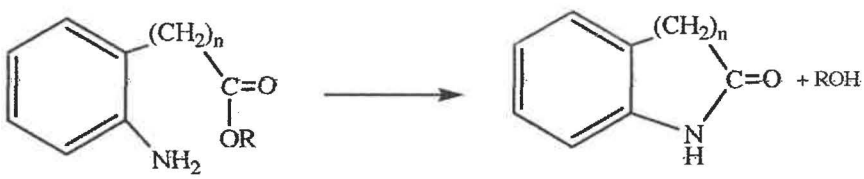

where,
n = 1, R = -CH_3 or -CH_2CF_3

n = 2, R = -CH_3

Scheme 1.21 Cyclisation of Methyl and Trifluoroethyl Esters of (2-Aminophenyl)acetic and (2-Aminophenyl)propanoic Acid.

Intramolecular nucleophilic aminolysis occurs only when stable 5- and 6-membered lactams can be formed, i.e. n = 1 and n = 2. Although the n = 1 and n = 2 systems are very similar, the mechanisms for the external GB catalysed formation of their lactams are different; there are differences in the shape of the pH/rate profiles and they have different Brønsted plot β values. This is difficult to rationalise, as the methyl esters of the n = 1 and n = 2 systems have the same nucleophile and leaving group. In contrast, changing the R-group has no effect on the mechanism: methyl and trifluoroethyl esters of (2-aminophenyl)acetic acid (n = 1) undergo external GB catalysed lactamisation via the **same** mechanism.

The initial step in all the lactamisation mechanisms (for n = 1 and n = 2) appears to involve the rapid formation of a zwitterion intermediate (similar to that proposed for intermolecular aminolysis, Scheme 1.16).[71,72] Due to the poor nucleophilicity of the

aniline-amino group, the concentration of this intermediate will presumably be low, (Scheme 1.22):

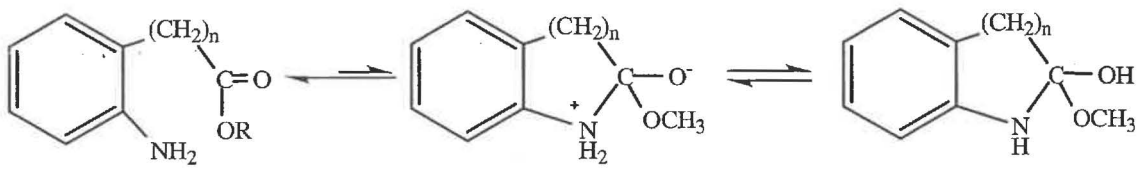

Scheme 1.22 Formation of Zwitterion and Neutral Intermediates During the Cyclisation of Esters of 3-(2-Aminophenyl)acetic Acid (n =1) and 3-(2-Aminophenyl)propanoic Acid (n =2).

The subsequent steps in this mechanism depend on the value of n:

n = 1. The rds for the intramolecular cyclisation of methyl 3-(2-aminophenyl)acetate is dependent on the buffer concentration. At low buffer concentration, it involves a buffer GB catalysed formation of a tetrahedral intermediate, whereas at high buffer concentration, a buffer GB catalysed breakdown of this intermediate is the rds.
The mechanism at high buffer concentration involves rapid internal proton transfer within the zwitterion intermediate (from $-NH_3^+$ to $-O^-$), generating a neutral intermediate, followed by a rds involving a concerted proton transfer to the buffer GB coupled to leaving group departure (Scheme 1.23):

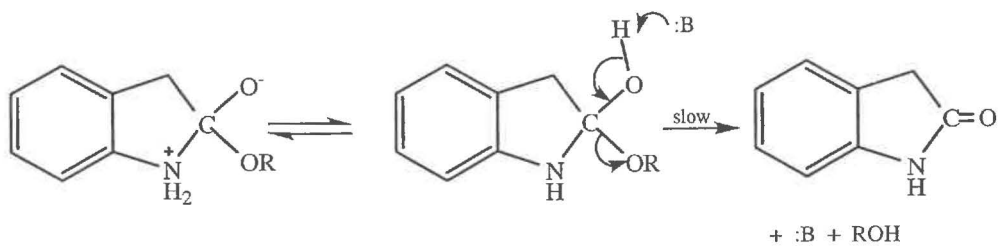

Scheme 1.23 Aminolysis of Methyl and Trifluoroethyl Esters of 3-(2-Aminophenyl)acetic Acid.

This mechanism is supported by the value of the Brønsted parameter, β, changing from 0.5 to 0.2 as the leaving group changed from $-OCH_3$ to the more favourable $-OCH_2CF_3$, suggesting that the breaking of the –C-OR bond is rate determining.

n = 2. In contrast, the cyclisation of methyl 3-(2-aminophenyl)propanoate has no change in the rds with changing buffer concentration.[72] The proposed mechanism involves rate determining proton transfer from the zwitterion to a GB followed by a series of fast steps involving the expulsion of the leaving group and the formation of products,(Scheme 1.24):

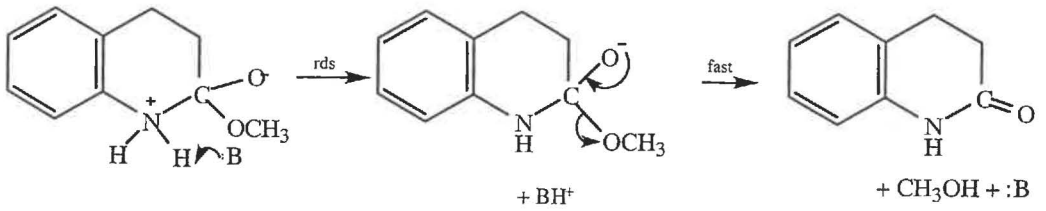

Scheme 1.24 Mechanism for the Cyclisation of the Methyl Ester of 3-(2-Aminophenyl)propanoic Acid.

There are two possible factors contributing towards the change in the rate determining step from n = 1 to n = 2:[71] For n = 1 (5-membered lactam), the zwitterion is stabilised by –**I** effect of the adjacent phenyl group. This **-I** effect will be much smaller (due to attenuation) for the n = 2 system.

It is likely that the 6-membered zwitterion is more strained than its 5-membered analogue because Fife et al.[71] have suggested that the 6-membered lactam is more strained than its 5-membered equivalent.

Unfortunately, it is difficult to compare the results of these n =1 and n = 2 systems, as they were studied at two different temperatures and ionic strengths. Any conclusions are somewhat tentative.

(iii) IGBC by Aniline –NH_2 in 2-Aminobenzoic Acid Ester Hydrolysis

This has recently been reported in the hydrolysis of a series of 2-aminobenzoate esters at 50 °C.[73] The low basicity of the aniline-NH_2 group ensures that at pH ~ 7, it almost completely in the free base form and can be involved in IGBC.

Support for this comes from the pH/rate profiles. All of the ester reactions have a distinctive plateau region between pH 4 and 9, suggesting that the free base is the reactive form. The proposed mechanism for the reaction is depicted in Scheme 1.25:

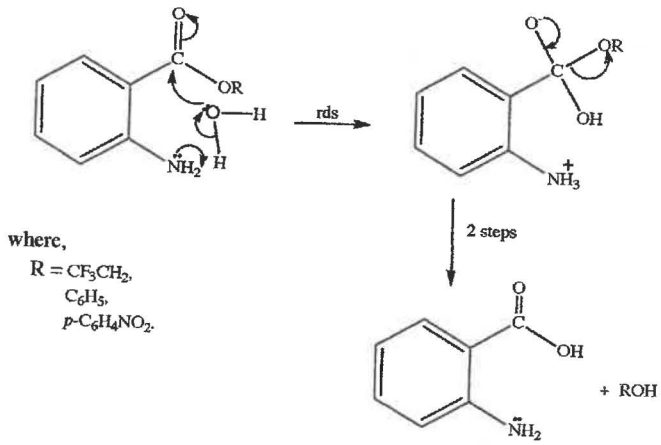

Scheme 1.25 IGBC Mechanism for Esters of 2-Aminobenzoic Acid.

Evidence supporting the IGBC mechanism includes:

- The value of k_{H_2O}/k_{D_2O} = ~ 2.0 for the phenyl ester. This is consistent with proton transfer during the rds.

- The rate of hydrolysis is almost unaffected by changing the leaving group from trifluoroethyl (pK_a = 12.4) to *p*-nitrophenyl (pK_a = 4.4). This indicates that there is no C-OR bond breaking occurring during the rds.

- No evidence could be found for the unstable 4-membered cyclic zwitterion intermediate required by the alternative, INC, mechanism.

In contrast, esters of 4-aminobenzoic acid show no evidence of IGBC. Such catalysis is impossible because the -NH_2 group is too remote from the -COOR group.

1.3(k) Benzylamino Group Intramolecular Catalysis

Inserting a methylene between the amino and benzene ring results in a more aliphatic type of behavior by the amino group.[74,75] The Ph-CH_2NH_2 group is a stronger base (pK_a 8 - 9)[18] than the aniline –NH_2. Consequently, it is expected to be a better nucleophile and there has been a lot of interest in the lactamisation reactions of the

and a parent alcohol. NGC is clearly involved because the reactions have large rate constants cf. methyl benzoate (Table 1.5):

Table 1.5 Rate Constants for Hydrolysis of Some 2-(Aminomethyl)benzoic Acid Esters.

Esters	k_2^* $l\ mol^{-1}\ s^{-1}$	Relative Rate
methyl benzoate	0.125[74]	1
methyl (2-aminomethyl) benzoate	7.2×10^3[75]	5.76×10^4
cyclohexyl(2-aminomethyl) benzoate	1.7×10^3 [75]	1.36×10^4
trifluoroethyl(2-aminomethyl) benzoate	1.7×10^5[75]	1.36×10^6
phenyl(2-aminomethyl) benzoate	5.7×10^7[75]	4.56×10^8

* at 30 °C and I = 0.5 mol l^{-1}

The mechanism of lactamisation for these esters is very complicated. Their pH/rate profiles lack a pH-independent region (in contrast to intermolecular bimolecular aminolysis) and their shape is dependent on the strength of the leaving group. For the methyl ester, the pH/rate profile at low pH has a slope = +1. However at pH ~ 8.6, there is an inflection, and the slope changes to +2.[74] This is probably associated with the ionisation, $-CH_2NH_3^+ \rightarrow -CH_2NH_2$, and suggests that the free base form of the ester is the active species. In contrast, the pH/rate profiles for the trifluoro and phenyl esters have plots that have a constant slope of + 1 from pH 3 - 11. This difference in pH/rate profiles with changing the strength of the leaving groups suggests a change in mechanism.

Methyl Ester

It has been suggested that the aminolysis proceeds by a stepwise mechanism. Proton transfer to a GB is rate determining, followed by either a bond breaking or bond forming reaction. The two proposed mechanisms are:

(1) GB catalysed deprotonation of $-CH_2NH_2$ followed by nucleophilic attack at the ester carbonyl group (Scheme 1.26):

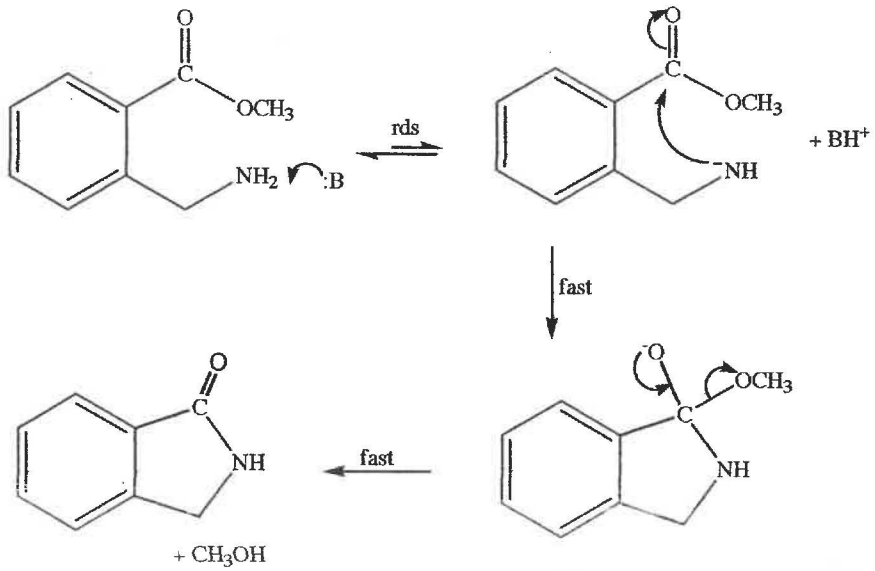

Scheme 1.26 Mechanism (1) for the Intramolecular Aminolysis of 2-(Methylamino)benzoic Acid Methyl Ester.

(2) GB catalysed proton removal from a neutral intermediate in the rds, followed by the expulsion of the $-OCH_3$ leaving group from the anionic intermediate (Scheme 1.27):

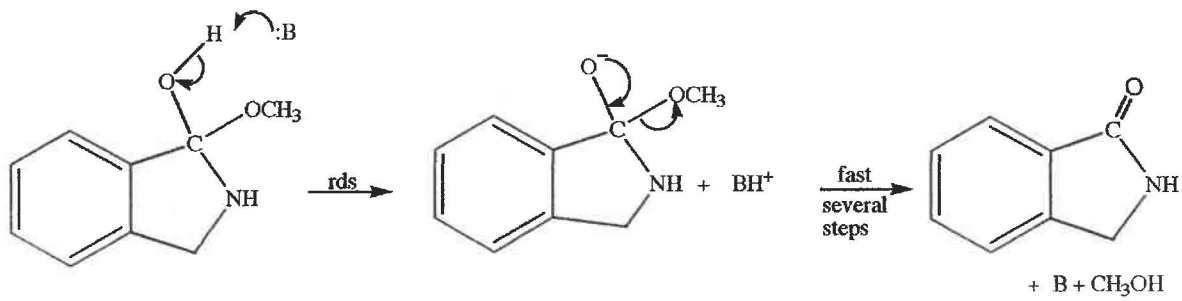

Scheme 1.27 Mechanism (2) for the Intramolecular Aminolysis of 2-(Methylamino)benzoic Acid Methyl Ester.

However, it seems unlikely that the rds would involve the stepwise formation of a $-CH_2NH^-$ species, (Mechanism (1) Scheme 1.26) as this species is extremely reactive and its concentration in aqueous solution would be very low. Mechanism 2, (Scheme 1.27) appears more likely as a stepwise proton removal apparently occurs in the cyclisation of esters of 2-(aminophenyl)acetic acid (Scheme 1.23):

Trifluoroethyl and Phenyl Esters

The values of the Brønsted parameters for $-CH_2CF_3$ ($\beta = 0.7$)[75] and $-C_6H_5$ ($\beta = 0.5$)[75] suggest that for these better leaving groups, the rds is different from the methyl. This evidence supports a mechanism which involves a concerted GB catalysed proton transfer from a neutral intermediate and leaving group departure, (Scheme 1.28):

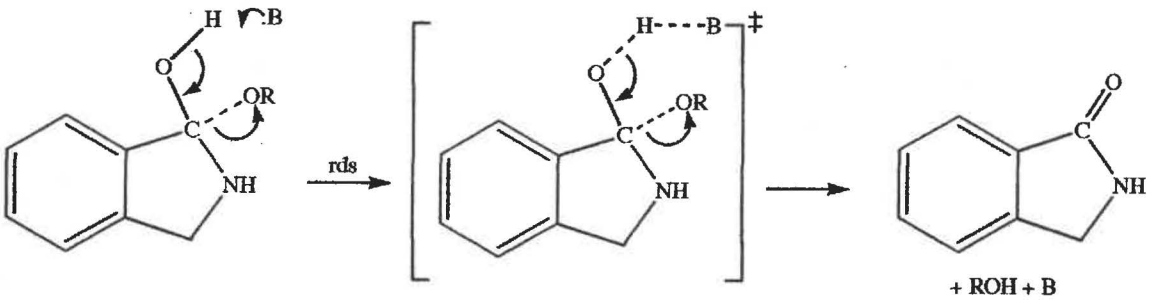

Scheme 1.28 Mechanism for the Aminolysis of Phenyl and Trifluoroethyl Esters of 2-(Methylamino)benzoic Acid.

It is suggested that the reason for the change in the aminolysis mechanism as the leaving group is strengthened could be the increasingly favourable cleavage of the acyl bond in the neutral intermediate. This is energetically impossible for the poor leaving group $-OCH_3$. Consequently, this group requires a stepwise GB catalysed proton removal to generate an anionic intermediate. This contains a $-O^-$ group which assists in the rapid departure of the $-OCH_3$. For better leaving groups, this assistance from $-O^-$ is not needed and a concerted rds step occurs.

1.4 Conclusions on Value of Model Systems

From the wide range of results summarised in 1.3, it is clear that neighbouring groups can produce large increases in the rates of hydrolysis of esters and other substrates. These rate increases in small molecule systems can approach, and in some cases exceed, those seen in enzyme catalysis. As a consequence, many of the ideas regarding the origins of NGC in small molecule systems have been used in attempts at developing mechanisms for analogous enzyme catalysed reactions. Many enzymes have been studied and the possible mechanisms for two of these are discussed in 1.5.

1.5 Enzyme Reaction Mechanisms

1.5(a) Chymotrypsin

This is probably the most well studied of all the enzymes. It is part of a major class of proteins which also includes the serine proteases, trypsin, elastase, and thrombin. α–Chymotrypsin is the most thoroughly studied member; it selectively cleaves peptides (and esters) on the carboxyl side of both aromatic side chains (tyrosine, tryptophan, phenylalanine) and large hydrophobic residues such as methionine.

The mechanism has proved difficult to elucidate completely despite many investigations .[76-100] A wide variety of techniques has been used in these studies including, classical techniques such as functional group analysis, identification of reaction intermediates, and the determining specificity of the reaction. However, X-ray[78-81] and model system studies have provided incisive details about the most likely reaction mechanism.

Classical techniques were initially used to identify the type and nature of the functional groups present at the active site. Using pH/rate profiles, it was observed that maximum activity occurred at pH ~ 7. Kinetic studies of *p*-nitrophenyl acetate,[84] revealed that α–Chymotrypsin catalyses the hydrolysis of peptides (and esters) in two distinct stages. When large amounts of enzyme are used, there is initially a rapid burst of *p*-nitrophenolate; this is followed by the formation of more product but at a much slower steady rate.

Organic fluorophosphates, such as di-isopropyl phosphofluoridate were used to identify an unusually reactive serine-195 (Ser-195) residue.[40] The importance of a second residue, histidine-57 (His-57), in catalysis was shown by affinity labelling.[91] Tosyl-L-phenylalanine chloromethylketone, a pseudo-substrate, specifically alkylates the 3-nitrogen of the imidazoyl ring of His-57, and this was used to demonstrate its importance at the active site.

X-ray crystal structures of α–Chymotrypsin have confirmed that Ser-195 and His-57 are in close proximity,[78-81] as required if they are part of the active site. A third group,

the carboxylate of aspartate-102 (Asp-102) was revealed to be buried in the protein, near to His-57. These three residues form a catalytic triad.

Model system studies have greatly helped explain why the positioning of these groups is so critical to the catalytic efficiency of the enzyme. Such studies were also instrumental in assisting the interpretation of complicated X-ray electron density maps which showed the positions of the residues at the active site.

The currently accepted mechanism for α–Chymotrypsin, deduced from the data available (X-ray crystallographic, chemical data, NMR (^{1}H. ^{13}C, ^{15}N, ^{31}P)[88,94-97] studies, and model system studies) involves initial acylation of the enzyme, (Scheme 1.29):

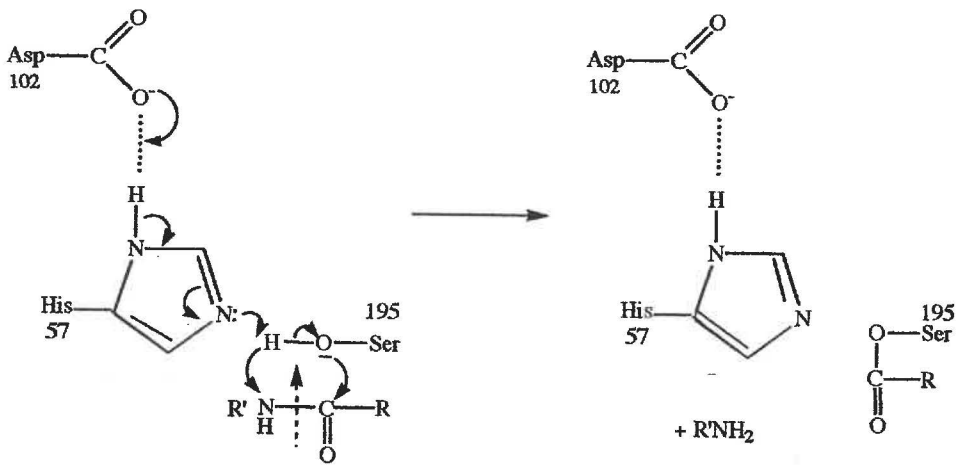

Scheme 1.29 Stage 1 in the α-Chymotrypsin Peptide Hydrolysis Mechanism: Acylation of the Enzyme.

The cleavage of the substrate is accomplished by an intramolecular $B_{Ac}2$ type of hydrolysis in which the nucleophile is the "activated" hydroxyl group of Ser-195. This is achieved by a remarkable "charge relay" system. The hydroxyl proton is abstracted by the pyridine nitrogen on the imidazolyl ring of His-57 and the imidazolyl ring in turn passes on its pyrrole N proton to a deeply hidden Asp-102. The histidine residue acts as a proton relay acting as both a general base and a general acid, while the more remote aspartate is an intramolecular general base catalyst. Substrate cleavage produces a shortened peptide chain, $R'NH_2$, and the enzyme acylated at Ser-195.

The overall reaction pathway probably occurs in two steps, as seen in the hydrolysis of esters and amides.[93,94] There is a rate determining formation of a tetrahedral intermediate followed by its rapid breakdown to an acylated adduct probably via proton donation from His-57:

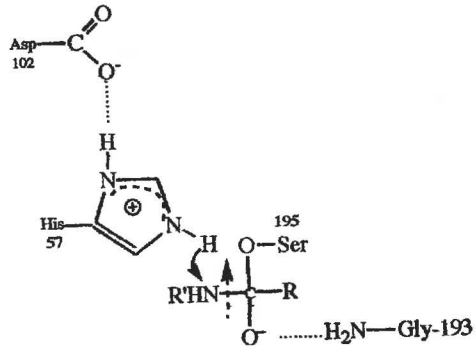

Figure 1.7 Step 2 in Stage 1 of the α-Chymotrypsin Peptide Hydrolysis Mechanism: Breakdown of the Tetrahedral Intermediate.

However, it is also possible that the reaction is concerted (and does not involve a tetrahedral intermediate) as proposed by Bender and Kormiyama[99] for amide hydrolysis. If this is the case, then the proton abstracted from the hydroxyl group of Ser-195 by the imidazolyl of His-57 is donated to the N-atom adjacent to the carbonyl carbon atom of the substrate, prior to the formation of the bond between the carbonyl carbon and the attacking $-O^-$ (i.e. an S_N2 type mechanism occurs).

The deacylation of the enzyme is the slowest step (Scheme 1.30):

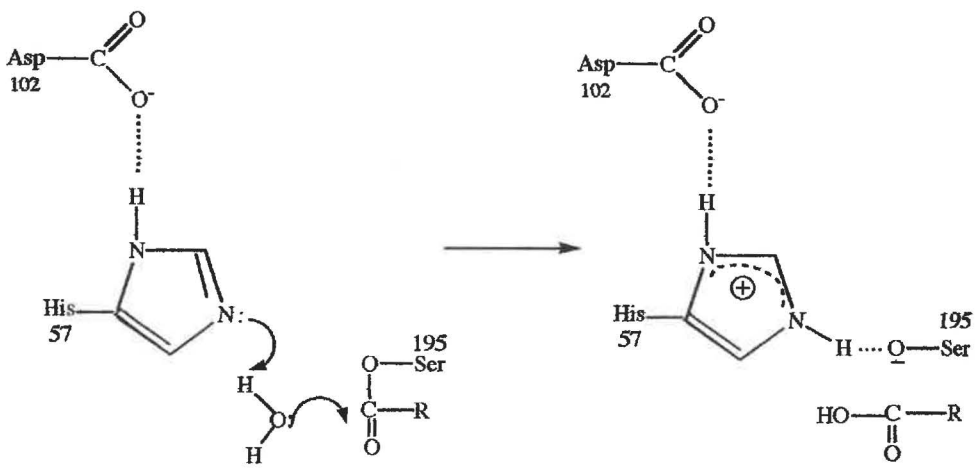

Scheme 1.30 Stage 2 in the α-Chymotrypsin Peptide Hydrolysis Mechanism: Deacylation of the Enzyme.

The deacylation begins when the His-57 residue (once again acting as proton relay) deprotonates an incoming water molecule. The resulting OH^- ion immediately attacks

the carbonyl carbon atom of the acyl group that is attached to Ser-195. His-57 donates a proton to the oxygen of Ser-195, which releases the acid component of the substrate. This diffuses away and the enzyme is regenerated for another round of catalysis.

1.5(b) Ribonuclease A

This enzyme specifically hydrolyses ribonucleic acid (RNA), the carrier of genetic information from deoxyribonucleic acid. Ribonuclease A (RNAase) is a relatively small protein, consisting of a single polypeptide chain of 124 amino acid residues.[101,102]

The active site of RNAase is a cleft containing the amino acid residues His-12, His-119 and the side chains Lys-7, Lys-41 and Lys-66. The structure of the enzyme-RNA complex has been deduced from X-ray studies on the enzyme-Upc A complex.[103,104] Upc A is a good substrate analogue because it differs from RNA only by the replacement of an oxygen by a methylene group. Consequently, the structure of the enzyme-Upc A complex is expected to be almost identical to that of the productively bound enzyme-substrate complex. The crystal structure shows that His-119 is within H-bonding distance of the leaving group, while His-12 is within H-bonding distance of 2'-OH of the pyrimidine ribose sugar. The lysine side chains are not in contact with the substrate, but are essential to the enzyme's activity since this is lost when they are acetylated.[105] It is thought that the positive charges on these side chains stabilise the 5-coordinate P intermediate involved in the reaction mechanism.[106]

The currently accepted reaction mechanism was first deduced by classical experiments (pH/rate profile; pK_a's of groups required for activity)[107] and confirmed by X-ray studies.[103,104] The enzyme's activity shows a bell shaped pH/rate profile with optimum activity at pH ~ 7. Kinetic studies also showed that for the free enzyme, the reaction rate depended on the ionisation of a base with pK_a 5.22 and an acid of pK_a 6.78, but in the enzyme substrate complex these pK_a's became 6.3 and 8.1 respectively.[105] It was proposed that concerted general acid and general base catalysis by two histidine residues occurred and these were identified by the X-ray and ^{1}H NMR studies as His-12 and His-119.[108-118]

The first step of the mechanism involves the imidazolyl of His-12 acting as a GB and abstracting a proton from the 2'-OH of the RNA substrate. This generates a powerful alkoxide nucleophile which attacks the neighbouring phosphoryl centre,[108,109] (Scheme 1.31):

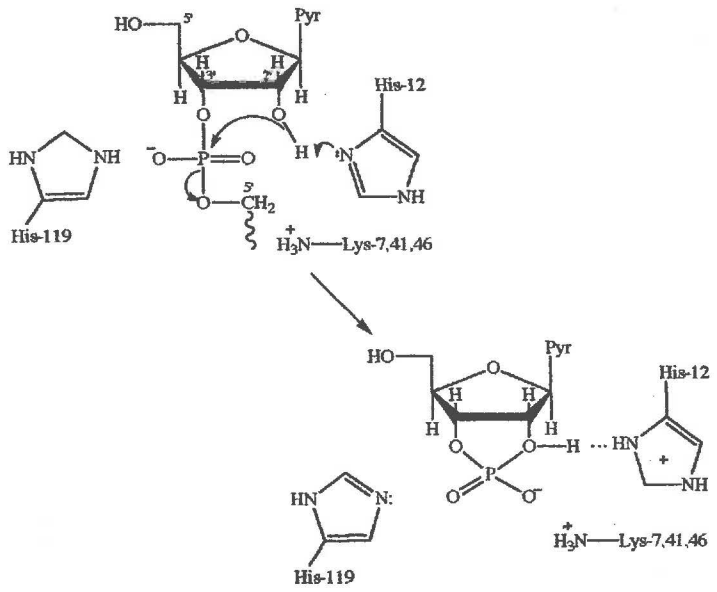

Scheme 1.31 Step 1 in Ribonuclease A Catalysed Hydrolysis of RNA: Formation of a Cyclic Intermediate.

The reaction thus involves GB assisted INC, which is similar to what is seen in the Chymotypsin mechanism. The stereochemistry of this step can occur in two possible ways: an "in-line" mechanism in which the nucleophile attacks the P centre on the side opposite to the leaving group,[116] or an "adjacent" mechanism in which nucleophilic attack occurs from the same side as the leaving group.[117] In the latter case, the pentavalent, trigonal bipyramidal P must pseudorotate so that the leaving group moves to the apical position. This is required by the Principle of Microscopic Reversibility: the entry point of the nucleophile is apical so the leaving group must depart apically because in the reverse reaction it must enter apically.

An elegant series of experiments were performed on model compounds to confirm the in-line mechanism, [108,109] with the reaction proceeding through the transition state stabilised by GA catalysis by His-119 (Figure 1.8):

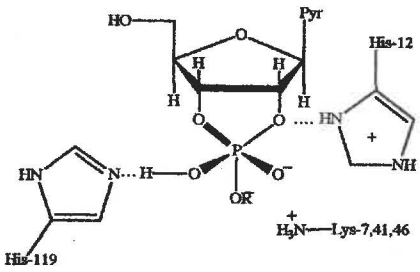

Figure 1.8 Transition State in Step 1 of Ribonuclease A Catalysed Hydrolysis of RNA Involving Pentavalent Phosphorus.

Breslow et al. have proposed and alternative mechanism, in which an intermediate species is formed by a sequence of proton transfers. [110,114,118] Initially, His-12 functions a GB, resulting in nucleophilic attack by the 2' alkoxide ion. However, the protonated His-12 (imidazolium) then behaves as a general acid and donates its proton to the equatorial P-O^-. The resulting intermediate is stabilised by lysine residues. His-119 proceeds to donate a proton to the leaving group, which departs. The equatorial P-OH donates the proton back on to the imidazolyl group of His-12.

In the second step in the reaction, hydrolysis of the cyclic intermediate occurs via His-119 acting as the GB. It deprotonates an incoming molecule of H_2O, which forms a transient OH^- species that attacks the cyclic phosphate via another pentavalent transition state. Evidence for this part of the mechanism was provided by neutron and X-ray diffraction studies, (Scheme 1.32):

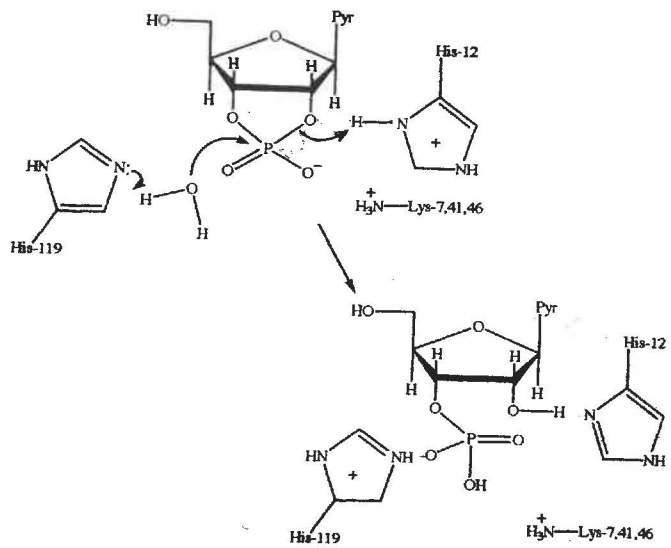

Scheme 1.32 Step 2 in Ribonuclease A Catalysed Hydrolysis of RNA: Hydrolysis of Cyclic Intermediate.

In the second step, the catalytic role of His-12 and His-119 are reversed compared to the cyclisation step.

Interestingly, this mechanism of hydrolysis is similar to that of the OH^- catalysed hydrolysis of RNA. In this reaction (OH^- acts as a GB abstracting a proton from the 2'-hydroxyl. The difference between the two reactions is that for the OH^- catalysed reaction, a mixture of both the 2'-phosphate and 3'-phosphate products are formed.

1.6 Aims of this Investigation

The preceding review of peptidase/esterase reaction mechanisms has shown that one of the major sources of an enzyme's catalytic power is its use of intramolecular reactions. Small molecule model systems provide an excellent way of gaining a more complete understanding of the huge efficiency of such processes, without the confusion associated with the complexities of enzyme structures.

One model system which has been investigated is the intramolecular catalysis by the amino group in the alkaline hydrolysis of amino acid esters.[54-61] Some of the factors responsible for the catalytic effects observed have been elucidated, but much remains to be uncovered. It was these gaps that the present investigation helped to partially fill. A major gap is the effect of structural changes on the rate constants for amino group catalysis in the simplest ω-amino acid ester cases: 4-aminobutanoic acid methyl ester (4-AB Me) and 5-aminopentanoic acid methyl ester (5-APe Me). Hence investigations were made on the effect of the alkaline hydrolysis rate constant of changing the nature of the leaving group (methyl → ethyl → benzyl ester), the effect of $-CH_3$ substitution in the alkyl chain (in particular is there a "gem-dimethyl effect" in the reaction?) and the effect of N-CH_3 substitution. These kinetic studies needed to be done at three temperatures to establish the enthalpy and entropy of activation values required for a thorough understanding of the factors responsible for any observed changes in the catalytic effect.

As an essential to these kinetic studies, pK_a^T measurements also had to be made because there are two forms of the reactant ester (the neutral E, and protonated EH^+ forms) which are interconnected by a pH dependent equilibrium. Hence two parallel hydrolysis reactions occur, with rate constants k_E and k_{EH^+} ; their separation from k_{obs} is critically dependent on the accuracy of the pK_a^T value, so considerable care was taken in its measurement.

Chapter 2 describes the synthesis and characterisation of the amino acid esters and reagents needed to determine their pK_a^T, k_E and k_{EH^+} values. An outline of the instruments needed for these determinations is contained in Chapter 3, while Chapters 4 and 5 describe the procedures used in these determinations. At the end of each chapter is a discussion of the results. Chapter 6 summarises the most important results and conclusions gained in this investigation.

References

1. F. H. Westheimer, *Adv. Phys. Org. Chem.*, **1985**, *21*, 1.
2. A. J. Kirby, *Angew. Int.* , **1996**, *35*, 707.
3. A. J. Kirby, Comprehensive Organic Chemistry, D. H. R. Barton and W. D. Ollis, Eds., Vol 5, Pergaman, Oxford, **1979**.
4. A. L. Lehninger, Biochemistry, Worth Publishers Inc., New York, **1975**.
5. L. Stryer, Biochemistry, W. H. Freeman and Co., New York, **1988**.
6. G Zurby, Biochemistry, W. M. C. Brown Publishers, Melbourne, **1993**.
7. T. R. Cech, *Science*, **1987**, *236*, 1532.
8. R. W. Hay and P. J. Morris, Metal Ions in Biological Systems, Marcel Dekkar, New York, **1976**.
9. R. Breslow and C. McAllister, *J. Am. Chem. Soc.*, **1971**, *93*, 7096.
10. N. C. Li, E. Doody and M. White, *J. Am. Chem. Soc.*, **1957**, *79*, 5859.
11. D. A. Buckingham and J. P. Collman, *J. Am. Chem. Soc.*, **1967**, *89*, 1082.
12. D. A. Buckingham, F. R. Keen and A. M. Sargeson, *J. Am. Chem. Soc.*, **1974**, *96*, 4981.
13. E. Kimura, *Inorg. Chem.*, **1974**, *13*, 951.
14. A. R. Fersht and A. J. Kirby, *J. Am. Chem. Soc.*, **1967**, *89*, 4853.
15. A. R. Fersht and A. J. Kirby, *J. Am. Chem. Soc.*, **1967**, *89*, 4857.
16. A. R. Fersht and A. J. Kirby, *J. Am. Chem. Soc.*, **1968**, *90*, 5818.
17. A. R. Fersht and A. J. Kirby, *J. Am. Chem. Soc.*, **1967**, *90*, 5826.
18. D. D. Perrin, B Dempsey and E. P. Serjeant, pK_a Predictions for Organic Acids and Bases, Chapman Hill, London and New York, **1981**.
19. M. L. Bender, *J. Am. Chem. Soc.*, **1957**, *78*, 1258.
20. M. L. Bender, F. Chloupek and M. C. Neveu, *J. Am. Chem. Soc.*, **1958**, *80*, 5384.
21. A. R. Fersht and A. J. Kirby, *Chem. Brit*, **1980**, 136.
22. J. W. Thanassi and T. C. Bruice, *J. Am. Chem. Soc.*, **1966**, *88*, 747.
23. M. I. Page, *Phil. Trans. R. Soc. Lond. B.*, **1991**, *332*, 149.
24. M. I. Page, *Chem. Soc. Rev.*, **1973**, *2*, 295.
25. M. I. Page, *Angew. Int.*, **1977**, *16*, 449.
26. M. J. Page and W. P. Jencks, *Proc. Nat. Acad. Sci. USA.*, **1971**, *68*, 1678.
27. J. H. Erying, *J. Chem. Phys.*, **1935**, *3*, 107.

28. W. F. Jones and J. H. Eyring, *J. Chem. Phys.*, **1935**, *3*, 492.
29. M. G. Evans and M. Polanyi, *Trans. Faraday Soc.*, **1935**, *31*, 875.
30. A. J. Kirby and G. J. Lloyd, J. *Chem. Soc., Perkin Trans. 2*, **1976**, 1753.
31. F. Schneider, *Angew. Int.*, **1978**, *17*, 583.
32. T. C. Bruice and G. L. Schmir, *J. Am. Chem. Soc.*, **1957**, *79*, 1663.
33. T.C. Bruice and S. J. Benkovic, *J. Am. Chem. Soc.*, **1964**, *86*, 418.
34. T. C. Bruice and U. K. Pandit, *J. Am. Chem. Soc.*, **1960**, *82*, 3396.
35. T.C. Bruice and S. J. Benkovic, Biorganic Mechanisms, W.A. Benajamin, New York, **1966**.
36. W. P. Jencks, Catalysis in Chemistry and Enzymology, Dover Publication Inc., New York, **1986**.
37. T. C. Bruice, *J. Am. Chem. Soc.*, **1959**, *81*, 5444.
38. W. P. Jencks and J. Carriuolo, *J Biol. Chem.*, **1959**, *234*, 1272.
39. J. F. Kirsch and W. P. Jencks, *J. Am. Chem. Soc.*, **1964**, *86*, 837.
40. J. Kraut, *Ann. Rev. Biochem*, **1977**, *46*, 331.
41. T. C. Bruice and J. Marquardt, *J. Am. Chem. Soc.*, **1962**, *84*, 365.
42. C. J. Belke, C. K. Su and A. Schafer, *J. Am. Chem. Soc.*, **1971**, *93*, 4553.
43. T. H. Fife, *Adv. Phys. Org. Chem.*, **1975**, *11*, 1.
44. T. H. Fife and B. M. Benjamin, *J. Am. Chem. Soc.*, **1973**, *95*, 2059.
45. T. H. Fife and B. M. Benjamin, *Biorg. Chem.*, **1976**, *5*, 37.
46. J. E. C. Hutchins and T. H. Fife, *J. Am. Chem. Soc.*, **1973**, *95*, 3786.
47. T. H. Fife and B. M. Benjamin, unpublished results.
48. T. H. Fife and B. M. Benjamin, *Chem. Commum.*, **1974**, 525.
49. T. H. Fife, Biorganic Chemistry, E. E. van Tamelan Ed., Vol 1., Academic Press, New York, **1977**.
50. J. E. C. Hutchins and T. H. Fife, *J. Am. Chem. Soc.*, **1973**, *95*, 2282.
51. T. C. Bruice and W. Tanner, *J. Org. Chem.*, **1965**, *30*, 1668.
52. J. E. C. Hutchins and T. H. Fife, *J. Am. Chem. Soc.*, **1973**, *95*, 5878.
53. T. H. Fife and B. R. DeMark, unpublished results.
54. B. Martin, A Purcell and R. I. Hendrik, *J. Am. Chem. Soc.*, **1963**, *85*, 2406.
55. R. W. Hay and P. J. Morris, *J. Chem. Soc., Perkin II*, **1972**, 1022.
56. B. Capon, *Quart. Rev.*, **1964**, 45.
57. J. A. Zender, M Sc. Thesis, University of Waikato, **1989**.

58. G. J. Depree, M Sc. Thesis, University of Waikato, **1992**.

59. K. H. Patterson, M Sc. Thesis, University of Waikato, **1985**.

60. L. A.. Kodikara, M Sc. Thesis, University of Waikato, **1996**.

61. K. H. Patterson, G. J. Depree, J. A. Zender and P. J. Morris, *Tetrahedron Lett,* **1994**, *35*, 281.

62. M. L. Bender, *Chem. Rev.*, **1960**, 53.

63. A. C. Satterthwait and W. P. Jencks, *J. Am. Chem. Soc.*, **1974**, *96*, 7018.

64. A. R. Fersht and W. P. Jencks, *J. Am. Chem. Soc.*, **1970**, *92*, 5442.

65. F. M. Menger and J. H. Smith, *J. Am. Chem. Soc.*, **1972**, *94*, 3824.

66. F. M. Menger and A. C. Vitale, *J. Am. Chem. Soc.*, **1968**, *90*, 2622.

67. W. P. Jencks and M. Gilchrist, *J. Am. Chem. Soc.*, **1968**, *90*, 2622.

68. J. P. Fox, M. I. Page, A. C. Satterthwait and W. P. Jencks, *J. Am. Chem. Soc.*, **1972**, *94*, 4729.

69. M. I. Page and W. P. Jencks, *J. Am. Chem. Soc.,* **1972**, *94*, 8828.

70. J. P. Fox and W. P. Jencks, *J. Am. Chem. Soc.*, **1974**, *96*, 1436.

71. T. H. Fife and N. W. Duddy, *J. Am. Chem. Soc.*, **1983**, *105*, 74.

72. A. J. Kirby, T. G. Mujahid and P. Camilleri, *J. Chem. Soc., Perkin II*, **1979**, 1610.

73. T. H. Fife, R. Singh and R. Bembi, *J. Org. Chem.*, **2002**, *67*, 3179.

74. T. H. Fife and B. R. DeMark, *J. Am. Chem. Soc.*, **1976**, *98*, 6978.

75. T. H. Fife and L. Chauffe, *J. Org. Chem.*, **2000**, *65*, 3579.

76. D. M. Blow, *Acc. Chem. Res.*, **1976**, *9*, 145.

77. B. W. Matthews, P. B. Sigler, R. Henderson and D. Blow, *Nature*, **1967**, *214*, 652.

78. B. S. Hartley, *Nature*, **1964**, *201*, 1284.

79. T. A. Steitz, R. Henderson and D. M. Blow, *J. Mol. Biol.*, **1969**, *46*, 348.

80. B. S. Hartley and D. M. Shotten, The Enzymes, Vol. III, 323, Academic Press, New York, **1971,** .

81. D. M. Blow, The Enzymes, Vol. III, 185, Academic Press, New York, **1971**.

82. B. S. Hartley and B. A. Kilby, *Biochem. J.*, **1952**, *50*, 672.

83. A. K. Balls and J. H. Wood, *J. Biol. Chem.*, **1956**, *219*, 245.

84. J. Fastrez and N. Houyet, *Eur. J. Biochem.*, **1977**, *81*, 515.

85. R. Henderson, *J. Mol. Biol.*, **1970**, *54*, 341.

86. J. L. Markley and I. B. Ibanez, *Biochem*, **1978**, *17*, 627.

87. J. Fastrez, *J. Chem. Soc., Perkin II*, **1980**, 1067.

88. R. M. Gravito, G. Rossman, P. Argos and W. Eventoff, *Biochem.*, **1977**, *16*, 5065.

89. S. Makimoto, K. Suzuki and Y. Taniguchi, *J. Phys. Chem.*, **1984**, *80*, 6021.

90. W. W. Bachovchin, *Biochem.*, **1986**, *25*, 7751.

91. E. L. Smith, R. L. Hill, I. R. Lehman, R. J. Lefkowitz, P. Handler and R. White, Principles of Biochemistry, Vol. I, McGraw-Hill, New York, **1983**.

92. M. W. Hunkpeiller, S.H. Smallcombe, D. R. Whittaker and J. H. Richards, *Biochem.*, **1973**, *12*, 4732.

93. G. Robillard and R. G. Shulman, *J. Mol. Biol.*, **1972**, *71*, 507.

94. W. W. Bachovchin and J. D. Roberts, *J. Chem. Saoc.*, **1978**, *100*, 8041.

95. M. A. Porubcan, W. M. Westler, B. Ibañez and J. L. Markley, *Biochem.*, **1979**, *18*, 4108.

96. W. P. Jencks, *Acc. Chem. Res.*, **1980**, *13*, 161.

97. R. A. McClelland and L. J. Santry, *Acc. Chem. Res*, **1983**, *16*, 394.

98. L. Fink and P. Meehan, *Proc. Nat. Acad. Sci. USA.*, **1979**, *76*, 1556.

99. M. Komiyana and M. L. Bender, *Proc. Nat. Acad. Sci. USA.*, **1979**, *76*, 557.

100. A. Zaks and M. J. Kilbanov, *J. Am. Chem. Soc.*, **1986**, *108*, 2767.

101. H. Dugas, Bioorganic Chemistry, Springer-Verlag, New York, **1996**.

102. H. W. Hirs, S. Moore and W. H. Stein, *J. Biol. Chem*, **1960**, *235*, 633.

103. F. M. Richards and H. W. Wyckoff, The Enzymes, Vol. IV, 647, Academic Press, New York, **1971**

104. F. M. Richards, H. W. Wyckoff, W. D. Carlson, N. M. Allewell, B. lee and Y. Mitsui, *Cold Spring Harb. Symp. Quant. Biol.*, **1971**,*36*, 35.

105. B. Walter and F. Wold, *Biochem.*, **1976**, *125* 304.

106. L. Markley, *Biochem.*, **1975**, *14*, 3546.

107. D. Findlay, D. G. Herries, A. P. Mathais, R. Rabin and C. A. Ross, *Nature*, **1961**, *190*, 781.

108. D. A. Usher, E. Erenrich and D. F. Eckstein, *Proc. Nat. Acad. Sci. USA*, **1972**, *69*, 115.

109. D. A. Usher and D. J. Richardson, *Nature*, **1970**, *228*, 663.

110. R. Breslow and W. Chapman, *Proc. Nat. Acad. Sci. USA.*, **1996**, *93*, 10018.

111. C. A. Deakyne and L. C. Allen, *J. Am. Chem. Soc.*, **1979**, *101*, 3951.

112. D. K. Lavallee and B. M. Myers, *J. Am. Chem. Soc.*, **1978**, *100*, 3907.

113. A. J. Kirby and R. Marriot, *J. Chem. Soc., Perkin II*, **2002**, 422.

114. R. Breslow and R. Xu, *Proc. Nat. Acad. Sci. USA.*, **1993**, *90*, 201.

115. V. Saenger, D. Suck and D. F. Eckstein, *Eur. J. Biochem.*, **1974**, *46*, 559.

116. F. H. Westheimer, *Acc. Chem. Res.*, **1968**, *1*, 70.

117. S. J. Benkovic and K. J. Schray, The Enzymes, Vol. VIII, 201, Academic Press, New York, **1973**

118. R. Breslow and M. Labelle, *J. Am. Chem. Soc.*, **1986**, *108*, 2655.

Chapter Two

Reactants and Reagents

2.1 Reactants

2.1(a) Introduction

The amino acid esters required for the kinetic and pK_a^T studies were synthesised from their parent amino acids by either the Fischer Speier[1] or thionyl chloride[1] methods.

Most of the amino acids used were commercial samples (Sigma-Aldrich, Aldrich or BDH). However, some of them had to be synthesised.

All of the amino acids, synthetic intermediates, and amino acid ester hydrochlorides used were characterised by a variety of methods:

Melting Points

These were determined using Reichert-Thompson melting microscope apparatus (accuracy ± 0.05°C). However, m.p.'s were of limited use as purity criteria since they were often accompanied by decomposition.

Infra-red Spectroscopy

IR spectra were run on a Perkin-Elmer 1600 ETIR spectrometer, as KBr discs, with 16 scans and at a resolution of 8 cm^{-1}. For the amino acids and esters, the carbonyl stretch (1600 – 2200 cm^{-1}) and ester C-O stretch (~ 1250 cm^{-1}) regions were used to characterise the compounds.

Nuclear Magnetic Resonance Spectroscopy

For the synthesised C-3 methylated amino acid acids and their precursors, ^{13}C and ^{1}H NMR spectra were aquired using a Bruker Advance DRX 400 FT NMR spectrometer. Samples were run in either $CDCl_3$ or D_2O for 2000 - 3000 scans. Signal assignment was assisted by "Distortion Enhancement by Polarisation Transfer" (DEPT-^{13}C) experiments, usually run for 1000 scans. Spectra were processed using Bruker software.

For all other compounds, ^{1}H-NMR spectra were run on a Bruker Advance 300 FT NMR spectrometer usually in D_2O solvent. 16 scans were used and the spectrum was processed using Bruker software.

Electrospray Mass Spectrometry

ESMS spectra were determined using a VG Platform II (Fisons Mircomass) spectrometer. Typically, spectra were run in 100% aqueous (de-ionised water) solutions using a cone voltage of + 30V, and 25 scans.

2.1(b) Amino Acids

Commercial

The purity of the commercial amino acids used was stated to be be ">99% pure" or chromatographically pure. This was checked using some of the methods outlined in 2.1(a) and by pK_a^T titration. Before use, all amino acid (hydrochlorides) had to be titrimetrically pure (endpoint within ± 0.1% of the theoretical endpoint) and were recrystallised (H_2O, hot H_2O/EtOH) if necessary (see 4.2(b)).

The data resulting from the purity checks using methods in 2.1(a) is summarised in the following Tables. Also included is data for the corresponding amino acid ester hydrochlorides to show the differences between them and their parent amino acids. These differences are discussed in 2.1(c).

Table 2.1 lists the m.p. data and Table 2.2 gives the characteristic IR stretch frequencies.

In Tables 2.3 and 2.4, ^{13}C and ^{1}H NMR chemical shifts are listed for all of the amino acids and the ester hydrochlorides. For this, the compounds were divided into five different structural types and the atoms numbered as outlined in Figure 2.1.

No ESMS spectra were run for the commercial amino acids. All characterisations showed no sign of any impurities.

Table 2.1 Melting Points of Amino Acid (Hydrochlorides) and Amino Acid Ester Hydrochlorides.

Amino Acid (Hydrochloride)	m.p.*/°C	(Lit)	Amino Acid Ester Hydrochloride	m.p.*/°C	(Lit)
2-AE	240	(228)[2]	2-AE Me.HCl	175-178	(175)[1]
			2-AE Bz.HCl	138	(139)[3]
3-AP	205	(207)[4]	3-AP Bz.HCl	106 -107	(none)
4-AB	194	(193)[2]	4-AB Me.HCl	120	(120 -121)[1]
			4-AB Et.HCl	70-72	(65–72)[1], (66-70)[5]
			4-AB Bz.HCl	114-116	(none)
4-MAB.HCl	122-126	(125)[2]	4-MAB Me.HCl	48-49	(46-48)[6]
			4-MAB Et.HCl	75-76	(74-76)[6]
4-DMAB.HCl	142-145	(145 -147)[2]	4-DMAB Me.HCl	88-89	(8-90)[7]
			4-DMAB Et.HCl	111-112	(none)
4-A-3-MB.HCl†	124	(none)	4-A-3-MB Me.HCl†	94-95	(none)
4-A-3,3-DMB.HCl	140-141	(none)	4-A-3,3-DMB Me.HCl		
5-APe.HCl	96-98	(95 –97)[2]	5-APe Me.HCl	145	(145)[8]
			5-APe Et.HCl	92-94	(84–86)
6-AH	204-206	(202–203)[2]	6-AH Et.HCl	104-106	(none)
L-Glu	205	(205)[2]	L-Glu-5-Me.HCl	166	(167)[1]
			L-Glu DMe.HCl	149	(149)[1]
Ser.HCl†	240	(228)[2]	Ser Me.HCl†	135	(134 -136)[1]

* Usually accompanied by decomposition.
† Racemic D,L.

Table 2.2 Characteristic IR Stretch Frequencies of Amino Acid (Hydrochlorides) and Amino Acid Ester Hydrochlorides.

Amino Acid (Hydrochloride)	$\upsilon_{C=O}$ cm^{-1}	Amino Acid Ester Hydrochloride	$\upsilon_{C=O}$ cm^{-1}	υ_{C-O} cm^{-1}
2-AE	1608	2-AE Me.HCl	1745	1265
		2-AE Bz.HCl	1745	1219
3-AP	1632	3-AP Bz.HCl	1732	1211
4-AB	1650	4-AB Me.HCl	1730	1215
		4-AB Et.HCl	1734	1210
		4-AB Bz.HCl	1722	1209
4-MAB.HCl	1724	4-MAB Me.HCl	1732	1208
		4-MAB Et.HCl	1738	1206
4-DMAB.HCl	1728	4-DMAB Me.HCl	1735	1210
		4-DMAB Et.HCl	1741	1212
4-A-3-MB.HCl†	1737	4-A-3-MB Me.HCl†	1728	1206
4-A-3,3-DMB.HCl	1745	4-A-3,3-DMB Me.HCl	1732	1208
5-APe.HCl	1725	5-APe Me.HCl	1731	1211
		5-APe Et.HCl	1738	1206
6-AH	1625	6-AH Et.HCl	1730	1208
L-Glu	α-1630	l-Glu-5-Me.HCl	α-1635	-
	γ-1650		γ-1723	1224
		L-Glu DMe.HCl	α-1750	1270
			γ-1723	1224
Ser.HCl†	1635	Ser Me.HCl†	1733	1244

† Racemic D,L.

Structure Type 1

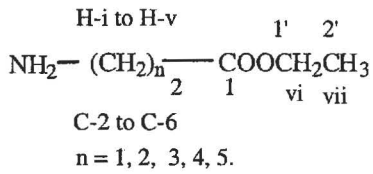

ω-amino acids nd (m)ethyl esters

(2-AE, 3-AP, 4-AB, 5-APe, 6-AH)

Structure Type 2

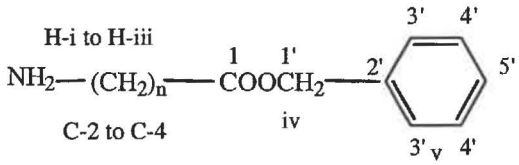

ω-amino acid benzyl esters

(2-AE, 3-AP, 4-AB)

Structure Type 3

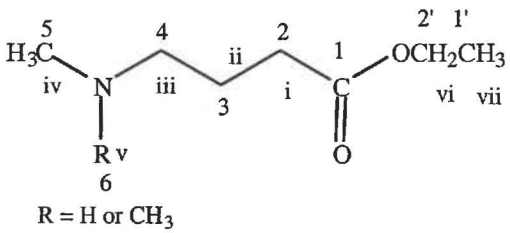

R = H or CH_3

4-(di)-methylaminobutanoic 4acids and (m)ethyl esters

(4-MAB, 4-DMAB)

Structure Type 4

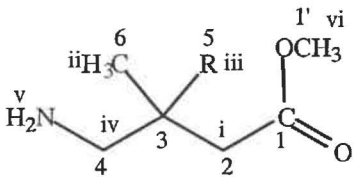

R = H or CH_3

4-amino-3, (3-di)-methylbutanoic acid and methyl ester

(4-A-3-MB, 4-A-3,3-DMB)

Structure Type 5

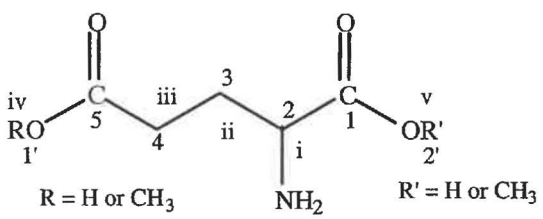

glutamic acid and (di)methyl esters

(Glu)

Note no numbers for -COOH and -NH_2 protons in instances because signals were broad or indistinct.

Figure 2.1 Atom Numbering Assignments for NMR Spectra of Amino Acids and Esters.

Table 2.3 ^{13}C Chemical Shifts

(a) Structure Type 1 Compounds.

Compound	Chemical Shifts, δ (ppm)							
	C-1	C-2	C-3	C-4	C-5	C-6	C-1'	C-2'
2-AE	172.7	41.6	-	-	-	-	-	-
2-AE Me	169.1	40.4	-	-	-	-	53.7	-
4-AB	176.5	34.4	25.7	41.4	-	-	-	-
4-AB	177.6	32.7	24.2	41.0	-	-	54.9	-
4-AB Et	175.4	31.1	22.3	39.1		-	62.2	13.6
5-APe	178.4	33.4	21.4	26.4	39.5	-	-	-
5-APe Me	176.9	33.3	21.2	26.4	39.4	-	52.3	-
5-APe Et	176.5	33.8	21.7	26.6	39.7	-	62.1	13.8
6-AH Et	178.8	35.5	25.6	26.9	28.2	41.2	63.5	15.2

(b) Structure Type 2 Compounds.

Compound	Chemical Shifts, δ (ppm)								
	C-1	C-2	C-3	C-4	C-1'	C-2'	C-3'	C-4'	C-5'
2-AE Bz	169.8	42.1	-	-	70.2	136.6	130.8	130.7	130.4
3-AP	178.4	34.4	36.6	-	-	-	-	-	-
3-AP Bz	172.3	31.1	34.9	-	67.5	135.2	128.8	128.7	128.5
4-AB Bz	176.5	32.6	23.8	40.5	69.0	137.4	130.7	130.5	130.2

(c) Structure Type 3 Compounds.

Compound	Chemical Shifts δ (ppm)							
	C-1	C-2	C-3	C-4	C-5	C-6	C-1'	C-2'
4-MAB	176.9	33.3	21.0	33.0	48.6	-	-	-
4-MAB Me	175.8	33.4	21.2	33.3	48.7	-	51.8	-
4-MAB Et	175.7	33.3	21.2	32.7	48.5	-	60.8	14.2
4-DMAB	176.8	30.7	19.7	57.1	43.0	43.0	-	-
4-DMAB Me	175.6	30.6	19.7	57.0	43.1	-	52.7	-
4-DMAB Et	175.0	30.7	15.1	56.9	42.8	42.8	60.9	14.1

(d) Structure Type 4 Compounds.

Compound	Chemical Shifts, δ (ppm)						
	C-1	C-2	C-3	C-4	C-5	C-6	C-1'
4-A-3-MB*	178.2	40.3	30.3	46.3	18.4	-	-
4-A-3-MB Me*	175.2	38.7	34.9	44.7	18.4	-	52.7
4-A-3,3-DMB	174.0	44.8	33.4	49.6	16.4	16.4	-
4-A-3,3-DMB Me	172.1	40.1	31.2	46.8	16.3	16.3	51.6

* D, L Racemic

(e) Structure Type 5 Compounds.

Compound	Chemical Shifts, δ (ppm)						
	C-1	C-5	C-2	C-3	C-4	C-1'	C-2'
Glu*	175.6	178.9	55.7	31.9	27.4	-	-
Glu-5-Me*	178.1	176.2	57.1	32.2	27.2	55.1	54.5
Glu-DMe*	172.2	176.8	55.7	31.3	26.8	54.1	54.5

* D, L Racemic

Table 2.4 ^{1}H Chemical Shifts

(a) Structure Type 1 Compounds.

Compound	Chemical Shifts, δ (ppm)						
	H-i	H-ii	H-iii	H-iv	H-v	H-vi	H-vii
2-AE	3.59(s)	-	-	-	-	-	-
2-AE Me	3.68(s)	-	-	-	-	3.60(s)	-
4-AB	2.21(t)	1.81(m)	2.71(m)	-	-		-
4-AB Me	2.48(t)	1.94(m)	2.99(t)	-	-	3.66(s)	-
4-AB Et	2.72(t)	2.18(m)	3.26 (t)	-	-	4.38 (q)	1.46(t)
5-APe	2.38(t)	1.68(m)	1.63(m)	2.95(t)	-	-	
5-APe Me	2.29(t)	1.61(m)	1.64(m)	2.84(t)	-	3.55 (s)	1.43(t)
5-APe Et	2.62(t)	1.82(m)	1.88(m)	3.2(t)	-	4.32 (q)	1.46(t)
6-AH	2.15(t)	1.52(m)	1.30(m)	1.58(m)	2.94(t)	-	-
6-AH Et	2.35(t)	1.56(m)	1.31(m)	1.62(m)	2.94(t)	4.14(q)	1.21(t)

(b) Structure Type 2 Compounds.

Compound	Chemical Shifts δ (ppm)				
	H-i	H-ii	H-iii	H-iv	H-v
2-AE Bz	3.90(s)	-	-	5.25(s)	7.41(s)
3-AP	2.61(t)	3.25(t)	-	-	-
3-AP Bz	2.71(t)	3.15(t)	-	5.07(s)	7.31(m)
4-AB Bz	2.40(t)	1.81(m)	2.86(t)	5.03 (s)	7.29 (s)

(c) Structure Type 3 Compounds.

Compound	Chemical Shifts δ (ppm)						
	H-i	H-ii	H-iii	H-iv	H-v	H-vi	H-vii
4-MAB	2.45(t)	1.91(m)	3.03(t)	2.67(s)	-	-	-
4-MAB Me	2.50(t)	1.96(m)	3.04(t)	2.71(s)	-	3.68(s)	-
4-MAB Et	2.46(t)	1.93(m)	3.02(t)	2.67(s)	-	4.12(q)	1.20(t)
4-DMAB	2.69(t)	2.13(m)	3.31(m)	3.09(s)	3.09(s)	-	-
4-DMAB Me	2.63(t)	2.13(m)	3.31(m)	3.02(s)	3.02(s)	3.82(s)	-
4-DMAB Et	2.46(t)	2.16(m)	3.08(m)	2.81(s)	2.81(s)	4.11(q)	1.23(t)

(d) Structure Type 4 Compounds.

Compound	Chemical Shifts, δ (ppm)					
	H-i	H-ii	H-iii	H-iv	H-v	H-vi
4-A-MB*	2.33(d.q.)	0.94(d)	2.26(m)	2.92(d.q.)	-	-
4-A-3-MB Me*	2.27(m)	1.01(d)	2.41(m)	2.92(d.q.)	2.17(s)	2.66(s)
4-A-3-DMB	2.59(s)	1.03(s)	1.03(s)	2.84(s)	2.32(s)	-
4-A-3,3-DMB Me	2.41(s)	1.07(s)	1.07(s)	2.97(s)	2.17(s)	3.67(s)

* D, L Racemic

(e) Structure Type 5 Compounds.

Compound	Chemical Shifts, δ (ppm)					
	H-i	H-ii	H-iii	H-iv	H-v	H-vi
Glu*	3.75(t)	2.09(m)	2.49(t)	-	-	-
Glu-5-Me*	3.99(m)	2.16(m)	2.23(m)	3.65(s)	-	-
Glu- DMe.*	4.15(t)	2.22(m)	2.58(t)	3.66(s)	3.79(s)	-

* D, L Racemic

Synthetic

The amino acids that were required but not available commercially, 4-A-3-MB.HCl and 4-A-3,3-DMB.HCl, were synthesised using the reaction scheme in Figure 2.2. The parent amino acid, 4-AB.HCl was also synthesised to trial the procedure.

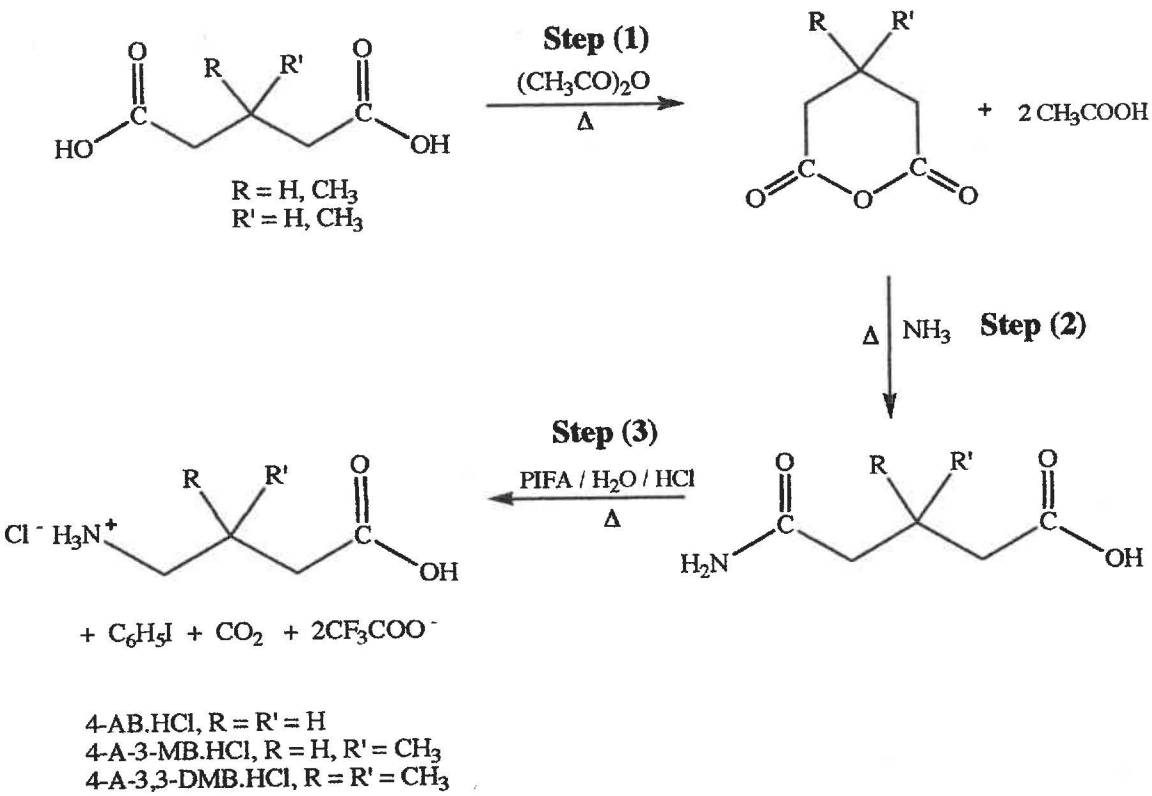

Figure 2.2 Synthetic Scheme for 4-AB.HCl, 4-A-3-MB.HCl and 4-A-3,3-DMB.HCl.

Step(1) Synthesis of Dihydro-pyrano-2, 6-dione Derivatives

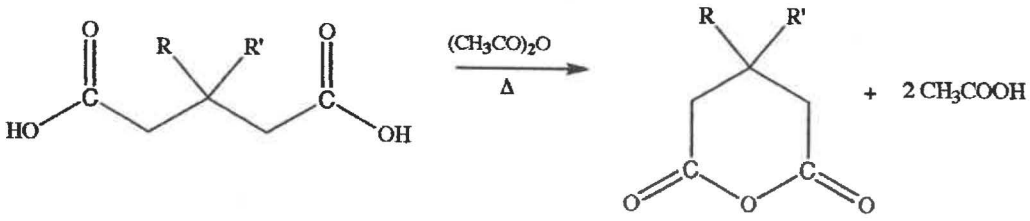

R	R'	Reactant
H	H	1,5-pentanedioic acid (1, 5 -PDA)
CH_3	H	3-methyl-1,5-pentanedioic acid (3-M-1,5-PDA)
CH_3	CH_3	3,3-dimethyl-pentanedioic acid (3,3-DM-1,5-PDA)

Procedure

This was a modification of that described by Vogel.[9]

The appropriate dicarboxylic acid (0.1 mole, Note 1) and redistilled acetic anhydride (0.2 mole, 85 g, 96 ml) (Note 2) were placed in a dry, 250 ml 3-necked round bottom flask equipped with a double walled condenser protected by a $CaCl_2$ drying tube. The mixture was gently refluxed (~ 1 hour) then allowed to slowly cool and was eventually chilled in an ice bath. The resulting precipitate was filtered off on a sintered frit (Type 2), washed with dry ether (2 x 50 ml), rigorously dried (vacuum pump) to ensure that all traces of any residual acetic anhydride were removed, and stored in a desiccator over silica gel. The crude solid was recrystallised from redistilled AR chloroform (Note 3).

Note 1

The following dicarboxylic acids were purchased as reactants for Step (1):

(i) 1, 5-pentanedioic acid (1,5-PDA) (BDH).

(ii) 3-methyl-1, 5-pentanedioic acid (3-M-1,5-PDA) (Aldrich).

(iii) 3, 3-dimethyl-1,5-pentanedioic acid (3,3-DM-1,5-PDA) (Aldrich).

Note 2

Sufficiently pure acetic anhydride (b.p. 138°C)[2] was obtained by the method outlined in Armarego and Perrin.[10]

Note 3

All dione products (anhydrides) were recrystallised from chloroform by dissolving the crude material in the proportion of 1g of solid in ~ 3 ml of hot AR chloroform. The solution was then allowed to cool, then refrigerated overnight. The desired products all crystallised as white solids. These were:

(i) dihydro-pyrano-2, 6-dione (DPD).

(ii) 4-methyl- dihydro-pyrano-2, 6-dione (4-M-DPD).

(iii) 4, 4-dimethyl- dihydro-pyrano-2,6-dione (4,4-DM-DPD).

The percentage yields of these three diones and details of their characterisation by m.p., IR and ^{13}C NMR (together with a comparison with the starting dicarboxylic acids) are summarised in Table 2.5. The IR and ^{13}C NMR showed no sign of peaks associated with impurities, particularly the starting materials.

Table 2.5(a) Yields, m.p.'s, Characteristic IR Frequencies and NMR Assignments of Dihydro-pyrano-2, 6-diones.

Compound	Yield	m.p./°C (Lit.)	Characteristic Frequencies (cm^{-1}) $\upsilon_{C=O}$ (1)	$\upsilon_{C=O}$ (2)
DPD	88%	55 – 56 (56)[2]	1803	1725
cf. 1,5-PDA		95 –96 (95 – 98)[2]	1708	1665
4-M- DPD	84%	41 (41-42)[2]	1805	1745
cf. 3-M-1,5-PDA		87 (85 – 87)[11]	1716	1676
4,4-DM-DPD	86%	124 (124)[2]	1811	1775
cf. 3,3-DM-1,5-PDA		103-104 (100 - 102)[12]	1725	1680

(b) ^{13}C NMR chemical shifts, based on the following numbering assignments:

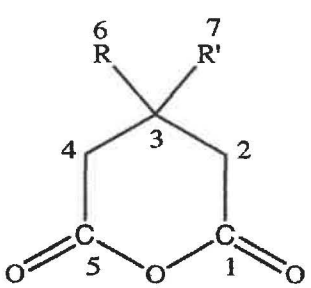

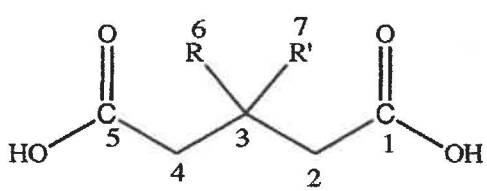

Table 2.5 cont.

Compound	Chemical Shifts, δ (ppm)						
	C-1	C-5	C-2	C-3	C-4	C-6	C-7
DPD*	169.3	169.3	36.3	17.2	36.3	-	-
cf. 1,5-PDA†	177.6	177.6	36.1	19.9	36.1	-	-
4-M- DPD*	168.3	168.3	42.2	20.6	42.2	19.4	-
cf. 3-M-1,5-PDA†	177.2	177.2	42.6	21.7	42.6	18.7	-
4, 4-DM-DPD*	167.4	167.4	48.1	17.3	48.1	22.4	22.4
cf. 3,3-DM-1,5-PDA†	178.1	178.1	48.6	19.1	48.6	26.1	26.1

*In $CDCl_3$.

† In D_2O.

Step(2) Synthesis of 5-Carbamyl-pentanoic Acid Derivatives

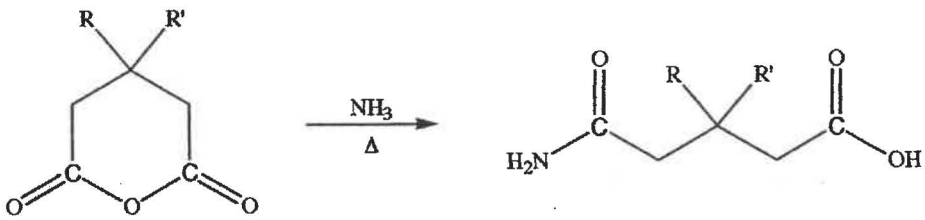

R	R'	Reactant
H	H	dihydro-pyrano-2, 6-dione (DPD)
CH_3	H	4-methyl- dihydro-pyrano-2, 6-dione (4-M-DPD)
CH_3	CH_3	4, 4-dimethyl- dihydro-pyrano-2,6-dione (4,4-DM- DPD)

Procedure

The procedure is a modification of the method of Arrizabalaga and Laurent.[13]

The appropriate dihydro-pyran-2,6-dione (0.1 mole), 180 ml of redistilled AR diethyl ketone (Fluka) (Note 1) and some anti-bumping chips were placed into a clean, dry 3-necked round bottom flask attached to a two necked still-head equipped with thermometer placed long enough to reach the reaction mixture, and a double walled condenser connected to a $CaCl_2$ drying tube. The reaction mixture was heated and refluxed at 115°C. Once all the solid material had dissolved (~ 20 minutes), a steady stream of NH_3 gas (BOC, Note 2) was gently bubbled into the reaction mixture via a side arm ~ 40 minutes. Considerable heating was required to keep the reaction

mixture under reflux at all times during reaction, since the passage of the NH_3 gas into the flask tended to cause the contents of the flask to cool down and solidify.

After refluxing, the reaction mixture was rotary evaporated to dryness (water bath <50°C, to prevent decomposition). The crude product was recrystallised by dissolving it in warm AR acetone, (~1g solid in 3 ml solvent), and then AR sodium dried ether was added dropwise until the solution just went cloudy. Refrigeration completed crystallisation (Note 3).

Note 1

The diethyl ketone that was used in these preparations was initially dried using anhydrous $CaSO_4$, then distilled at atmospheric pressure (b.p. 102°C, Lit. b.p. 102°C).[10] Diethyl ketone was chosen as the reaction solvent after trialling several solvents including chloroform, dichloromethane and acetone. It was found that the reactant diones were most readily soluble in this solvent and the products could be recovered in good yield from it.

Note 2

The NH_3 gas was initially passed through a protecting scrubber containing redistilled diethyl ketone prior to bubbling into the test solution, in order to minimise traces of moisture.

Note 3

The following products were obtained:

(i) 5-carbamyl-pentanoic acid (5-CPA)

(ii) 3-methyl-5-carbamyl-pentanoic acid (3-M-5-CPA)

(iii) 3,3-dimethyl-5-carbamyl-pentanoic acid (3,3-DM-5-CPA)

The percentage yields of these three 5-carbamyl-pentanoic acids and details of the characterisation by m.p., IR and ^{13}C NMR (together with the starting diones) are summarised in Table 2.6. The characterisations showed no evidence for the presence of any impurities, particularly starting materials.

Table 2.6(a) Yields, m.p.'s, Characteristic IR Frequencies and NMR Assignments of 5-Carbamyl-pentanoic Acids.

Compound	Yield	m.p. /°C (Lit.)	Characteristic Frequencies (cm^{-1})* $\upsilon_{C=O}$ (1)	$\upsilon_{C=O}$ (2)
5-CPA	88%	93 (93-94)[2]	1698 (amide)	1637 (acid)
cf. DPD		55-56	1803	1725
3-M-5-CPA*	84%	88-89 (none)†	1672 (amide)	1616 (acid)
cf. 4-M-DPD		41	1805	1745
3,3-D-5-CPA	86%	145-146 (146)[2]	1662 (amide)	1623 (acid)
4,4-DM-DPD		124	1811	1775

*Racemic R,S forms.

† No m.p. reported in original preparation.[13]

(b) ^{13}C NMR Chemical Shifts based on the following atom numbering assignments:

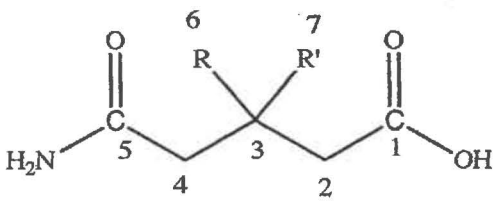

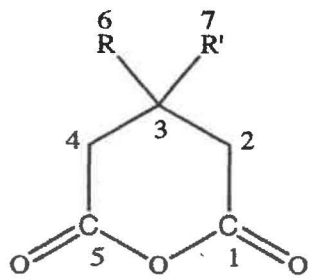

Compound	Chemical Shift, δ (ppm) C-1	C-5	C-2	C-3	C-4	C-6	C-7
5-CPA*	178.6	176.8	35.2	19.6	36.2	-	-
cf. DPD†	169.3	169.3	36.3	17.2	36.3	-	-
3-M-5-CPA*	180.9	178.5	42.4	20.3	13.8	18.3	-
cf. 4-M_DPD†	168.3	168.3	42.2	20.6	42.2	19.4	-
3,3-D-5-CPA*	181.8	179.4	48.6	19.9	48.1	24.5	24.7
cf. 4,4-DM-DPD†	167.4	167.4	48.1	17.3	48.1	22.4	22.4

*In D_2O.

† In $CDCl_3$.

Step (3) Synthesis of ω-Amino Acid Hydrochlorides

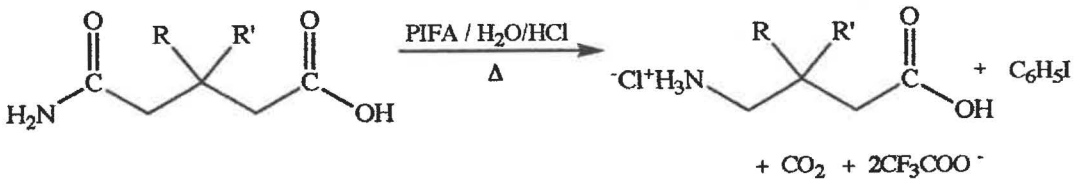

R	R'	Reactant
H	H	5-carbamyl-pentanoic acid (5-CPA)
CH_3	H	3-methyl-5-carbamyl-pentanoic acid (3-M-5-CPA)*
CH_3	CH_3	3,3-dimethyl-5-carbamyl-pentanoic acid (3,3-DM-5-CPA)

*Racemic R, S form.

Procedure

A modification of that described in references.[14,15,16]

I,I--bis(trifluoroacetoxy)iodo]benzene (PIFA) (1.73g, 4.0 mmol) (Note 1) was placed in a dry 250 ml round bottom flask wrapped in aluminum foil (to prevent photolysis) and protected by a $CaCl_2$ drying tube. A mixture of 6 ml AR acetonitrile and 6 ml of de-ionised water (Note 2) was added. The flask was gently stirred and heated on a hotplate at ~ 50°C. Once the mixture had equilibrated and the PIFA had dissolved, an equimolar amount (~1.0 g) of the appropriate 5-carbamyl-pentanoic acid derivative was added to the flask. The reaction mixture was stirred at ~ 50°C for 5 hours. At the end of this period, 8 ml of conc. HCl was added and after cooling to room temperature, 75 ml of distilled water was added.

The reaction mixture was transferred into a 250 ml separating funnel, 75 ml of diethyl ether added, and the mixture was vigorously shaken. The aqueous layer was removed and kept. 10 ml of HCl (~ 2 mol l^{-1}) was added to the ether layer, the contents shaken and the aqueous layer removed (Note 3). This procedure was repeated twice. All the aqueous layers were combined and rotary evaporated to dryness. Care was taken to ensure that the temperature of the rotary evaporator water-bath did not exceed 45°C, as this can lead to the decomposition of the product. The crude product was recrystallised by dissolving it in hot redistilled AR acetone (~ 1.5 g to 3 ml). Sodium dried ether was then carefully added until the solution went slightly cloudy. The flask

was stoppered and refrigerated until crystallisation was complete. This usually took ~ 2 days.

Note 1

This reagent was prepared by the method outlined in Loudon et al.[15,16]

Note 2

De-ionised H_2O must be used as anionic contaminants hinder the reduction reaction

Note 3

The following products were obtained

(i) 4-aminobutanoic acid.HCl (4-AB.HCl)

(ii) 4-amino-3-methyl-butanoic acid.HCl (4-A-3-MB.HCl)

(iii) 4-amino-3,3-dimethyl-butanoic acid.HCl (4-A-3,3-DMB.HCl)

The percentage yields of these three 4-aminobutanoic acid hydrochlorides and details of their characterisation (together with a comparison with the starting 5-carbamyl pentanoic acids) are given in Table 2.7. In all cases, there was no evidence for the presence of any impurities (particularly reactants) in the products.

Table 2.7(a) Yields, m.p.'s Characteristic IR Frequencies and NMR Assignments of 4-Aminobutanoic Acid Hydrochlorides

Compound	Yield	m.p. /°C (Lit.)	Characteristic Frequencies (cm^{-1}) $\upsilon_{C=O}$ (acid)	$\upsilon_{C=O}$ (amide)
4-AB.HCl	82%	119 (119-120)[2]	1730	-
cf. 5-CPA		93	1698	1637
4-A-3-MB.HCl*	77%	124 (none)†	1737	-
cf. 3-M-5-CPA*		88-89	1672	1616
4-A-3,3-DMB.HCl	76%	140-141 (none)†	1745	-
cf. 3,3-D-5-CPA		145-146	1662	1623

*Racemic D,L forms.

** Note absence of amide $\upsilon_{C=O}$ in the amino acid.HCl products.

† No m.p. reported in original preparation.

(b) ^{13}C NMR Chemical shifts based on the following atom numbering assignments:

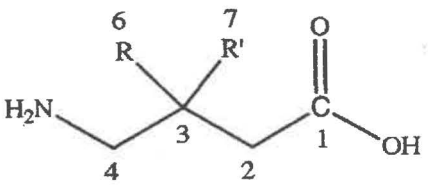

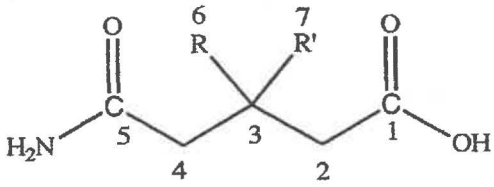

Table 2.7 cont.

Compound*	Chemical Shift, δ (ppm)						
	C-1	C-5**	C-2	C-3	C-4	C-6	C-7
4-AB	176.3	-	34.9	24.4	41.4	-	-
cf. 5-CPA*	178.6	176.8	35.2	19.6	36.1	-	-
4-A-3-MB†	178.2	-	40.3	30.3	46.3	18.4	-
cf. 3-M-5-CPA†	180.9	178.5	42.4	20.3	13.8	18.3	-
4-A-3,3-DMB	174.0	-	44.8	33.4	49.6	16.4	16.4
cf. 3,3-D-5-CPA*	181.8	179.4	48.6	19.9	48.1	24.5	24.7

*All run in D_2O.

† Racemic R,S forms.

** Note the absence of any amide C=O signal in the products.

^1H NMR chemical shifts for the product amino acid hydrochlorides only, based on the following atom numbering assignments:

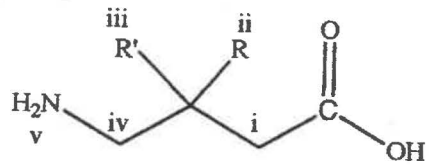

Amino Acid*	Chemical Shifts, δ (ppm)				
	H-i	H-ii	H-iii	H-iv	H-v
4-AB	2.21 (t)	1.81 (m)**	1.81 (m)**	2.71(m)	-
4-A-3-MB†	2.33 (d.q.)	0.94 (d)	2.26 (m)	2.93 (d.q.)	-
4-3,3-DMB	2.59 (s)	1.03 (s)**	1.03 (s)**	2.84(s)	2.32(s)

*All run in D_2O.

† Racemic D,L forms.

** Protons equivalent.

Notes; The broad H signal of the –COOH group is not listed.

The multiplicity of the shifts is listed with the chemical shift.

2.1(c) Amino Acid Methyl and Ethyl Esters

These were prepared as their hydrochlorides from the parent amino acid by both the Fischer Speier and thionyl chloride methods. The procedures used were modifications of those outlined by Greenstein and Wintz.[1]

However, Glu DMe.HCl was a commercial sample (Sigma-Aldrich).

Fischer Speier Method

This involves the dry hydrogen chloride gas catalysed esterification of of amino acids using a large excess of "super-dry" (m)ethanol. (Note 1):

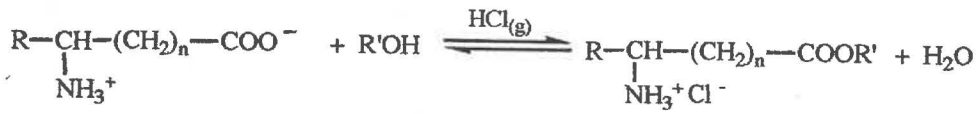

Procedure

About 20 g (0.1- 0.2 mole) of the appropriate amino acid, ~ 400 ml of "super-dry" (m)ethanol and some anti-bumping chips, were placed in a 3-necked 1 litre flask, equipped with a double walled reflux condenser topped with a $CaCl_2$ drying tube. The reaction mixture was refluxed for approximately 2 hours (the amino acid usually dissolved after ~ 30 minutes) while a steady stream of dry HCl gas passed through it (Note 2). The HCl gas was generated by dropping concentrated H_2SO_4 into concentrated HCl using a closed system consisting of a 3-necked 500 ml flask and a 250 ml side arm dropping funnel. The HCl gas evolved was dried by passing it through a concentrated H_2SO_4 scrubber. Suck back protection traps separated the HCl generator/scrubber and the scrubber/reaction vessel.

Once the reflux had been completed, the reaction mixture was evaporated to dryness (rotary evaporator). The temperature of the water bath was kept below ~ 50°C to prevent product decomposition. The crude ester hydrochloride (Note 3) was dissolved in "super-dry" (m)ethanol (~ 100 ml) and reduced to dryness to help remove any water present. This was repeated twice.

The thoroughly dried (P_4O_{10}, vacuum desiccator) crude ester hydrochloride was then re-esterified to remove traces of the parent amino acid, and the rotary evaporation and drying procedures were repeated. The final dissolving in (m)ethanol also assists in removing excess (interstitial) HCl.

The solid ester hydrochloride was recrystallised by dissolving it in a minimum volume of warm "super-dry" (m)ethanol (~ 50°C). This solution was filtered through a sintered frit, then sodium dried ether was added to the warm solution until the solution became just cloudy. After refrigeration, the ester hydrochloride was filtered off and stored in a desiccator over silica gel.

Note 1

"Super-dry" methanol and ethanol were prepared by the magnesium (m)ethylate method outlined by Vogel.[9] They were prepared in 2 litre batches and stored over Type 4A molecular sieves in a Flask capped by a $CaCl_2$ drying tube.

Note 2

The inlet tube to the reaction mixture needed continuous monitoring to ensure that it did not become blocked by the build-up of reaction product.

Note 3

Some amino acid ester hydrochlorides did not recrystallise. The oils involved were shaken several times with "super-dry" (m)ethanol and dry benzene, then rotary evaporated to dryness in an attempt to azeotrope off any water present. If this failed to induce crystallisation, the oil was dried under vacuum over P_4O_{10} until solidification occurred. This type of problem often indicated the final purified ester hydrochloride was hygroscopic. In some cases (notably the N-methylated esters), the Fischer Speier method produced products that could not be crystallised. However, the alternative thionyl chloride method was usually more successful.

Thionyl Chloride Method

Here the amino acid is converted to the acid chloride which then undergoes alcoholysis. The method used was essentially that outlined by Greenstein and Wintz[1] for the preparation of 4-methyl L-glutamate.HCl, except that the cooled reaction mixture was stirred continuously, and the product solution was reduced to dryness (rotary evaporator) before recrystallisation. The crude solid was dissolved in ~ 50 ml of warm (~ 40 °C), dry AR acetone, filtered, then sodium dried ether was added until the solution was just cloudy. Acetone was a better recrystallising medium than

(m)ethanol because many of the ester hydrochlorides prepared by this method were hygroscopic and difficult to recover from alcohol solvents. After the solution had been refrigerated overnight, the solid ester hydrochloride was filtered off, washed with sodium dried ether, and stored under vacuum over P_4O_{10}.

Comparison of Fischer Speier and Thionyl Chloride Methods

Small traces of acidic contaminants are a major problem in pK_a^T measurements of amino acid ester hydrochlorides. The Fischer Speier method tends to produce products contaminated by excess HCl; the thionyl chloride method contaminants are various S-acids; in both methods there may also be traces of the parent amino acid. pK_a^T titration is extremely sensitive to traces of acidic contaminants, and while repeated recrystallisations will eventually reduce them to below detectable levels, the process can be laborious. It was worthwhile to find out how many recrystallisations were needed in each method to generally produce a product for "simple" (non-hygroscopic) cases. The comparison was made using the preparation of L-Ser Me.HCl, which had well established properties.[1,17,18] Purity criteria used included m.p., IR, ^{13}C and ^1H NMR, ESMS and pK_a^T titration.

It was found that two Fischer Speier esterifications followed by two recrystallisations (methanol/ether) were sufficient to produce a product that contained no detectable impurities. For the thionyl chloride method, its single esterification had to be followed by three recrystallisations (acetone/ether) before a sufficiently pure product could be produced. Interestingly, while the m.p. criterion required the above number of recrystallisations before the correct value was obtained (see Table 2.1), IR, ^{13}C and ^1H NMR, and ESMS of the **unrecrystallised** products showed no detectable impurities. Figure 2.3 shows one of the two identical ^{13}C NMR spectra obtained from the products of the two methods , while Figure 2.4 is the ^1H equivalent.

The ESMS spectra of unrecrystallised Ser Me.HCl also showed the absence of any detectable impurities. A typical spectrum (Figure 2.5) shows a single parent ion at m/z = 121 which matches EH^+, i.e. $HOCH_2CH^+NH_3COOCH_3$ with no peak matching the parent amino acid, $HOCH_2CH^+NH_3COOH$, m/z = 106.

Figure 2.3 ^{13}C NMR (bottom) and DEPT (top) of Unrecrystallised Ser Me.HCl Obtained by both Fischer Speier and Thionyl Chloride Methods.

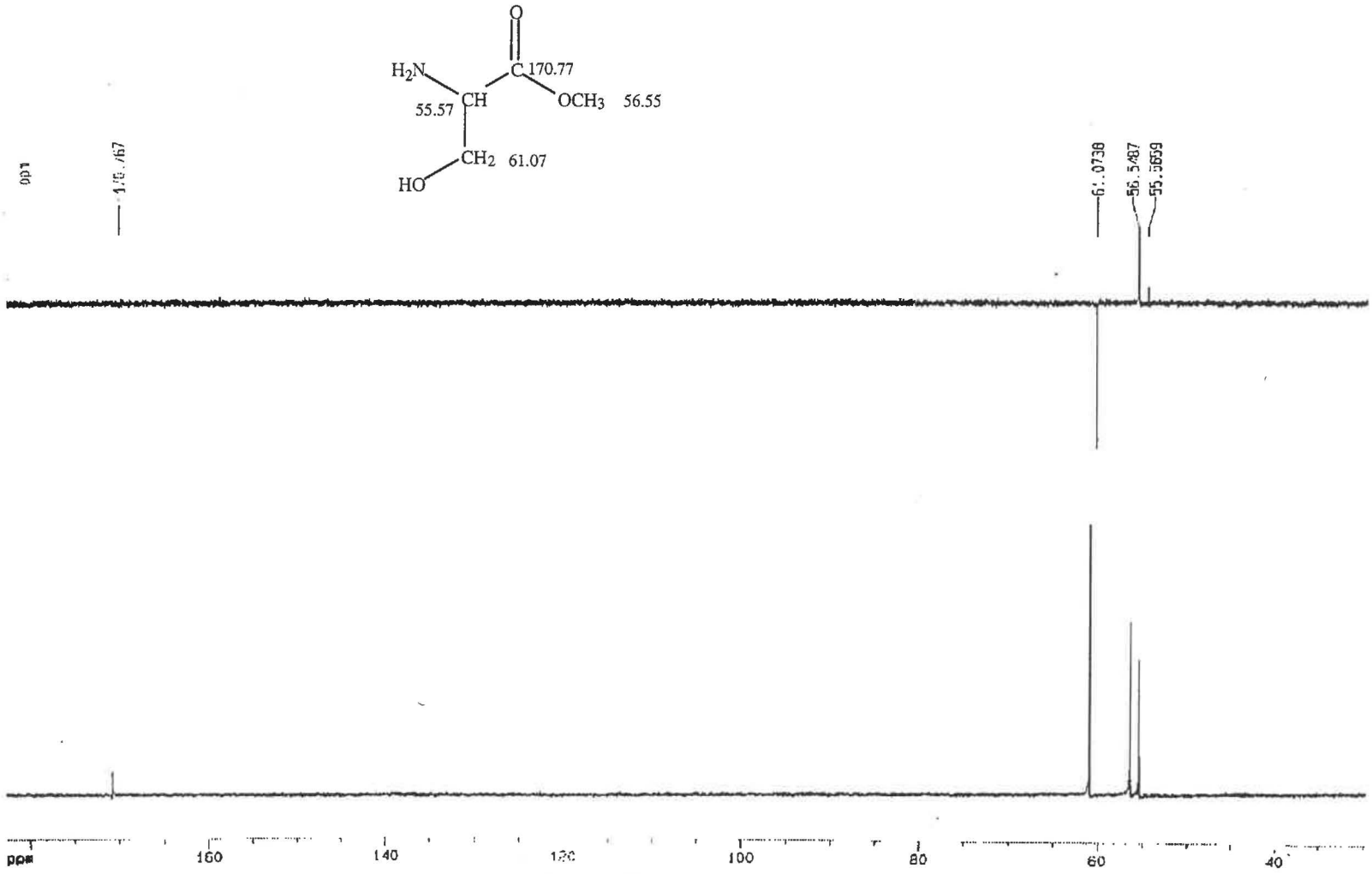

Figure 2.4 ^{1}H NMR of Unrecrystallised Ser Me.HCl Obtained by both Fischer Speier and Thionyl Chloride Methods.

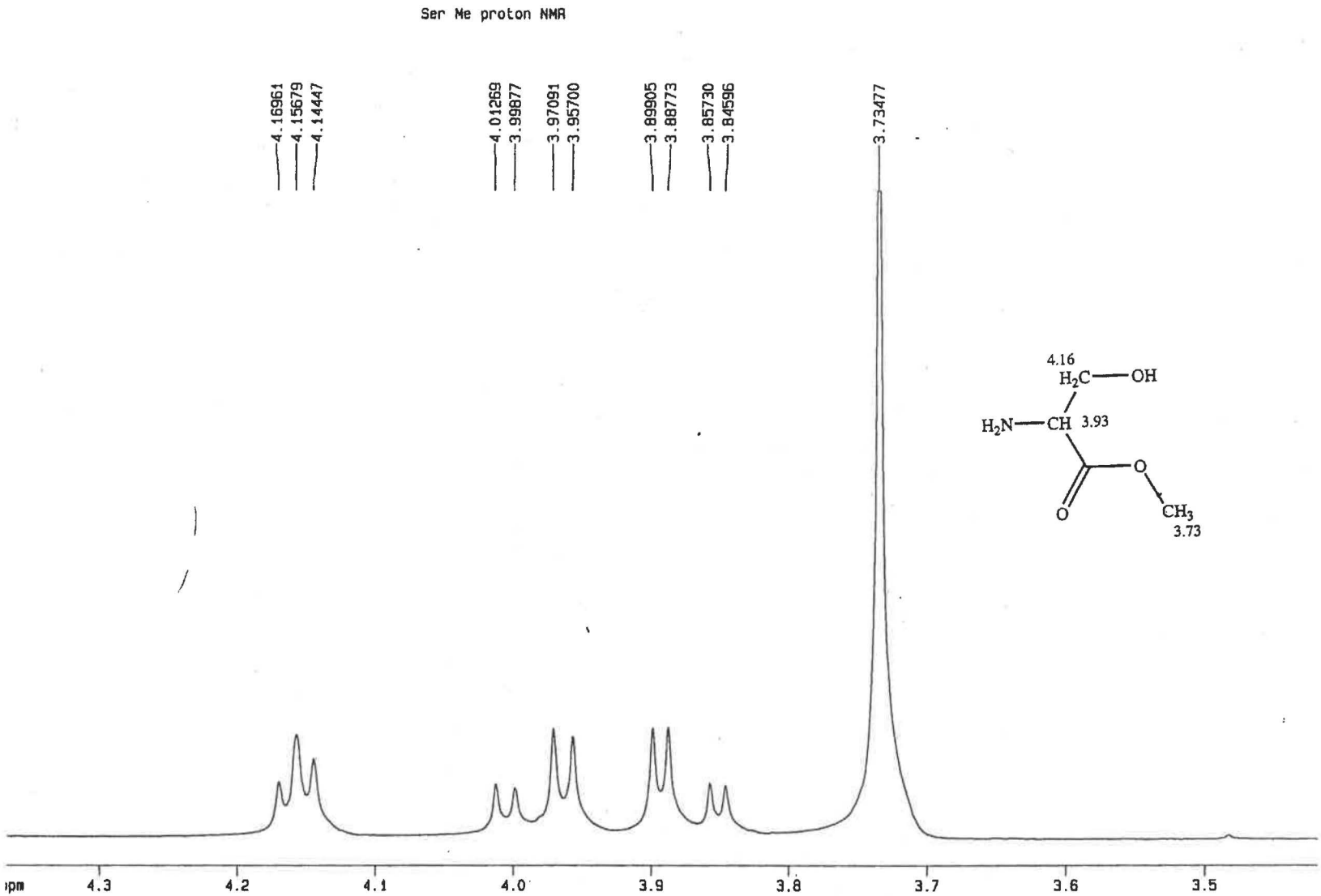

Figure 2.5 ESMS of Unrecrystallised Ser Me,HCl Obtained by both Fischer Speier and Thionyl Chloride Methods.

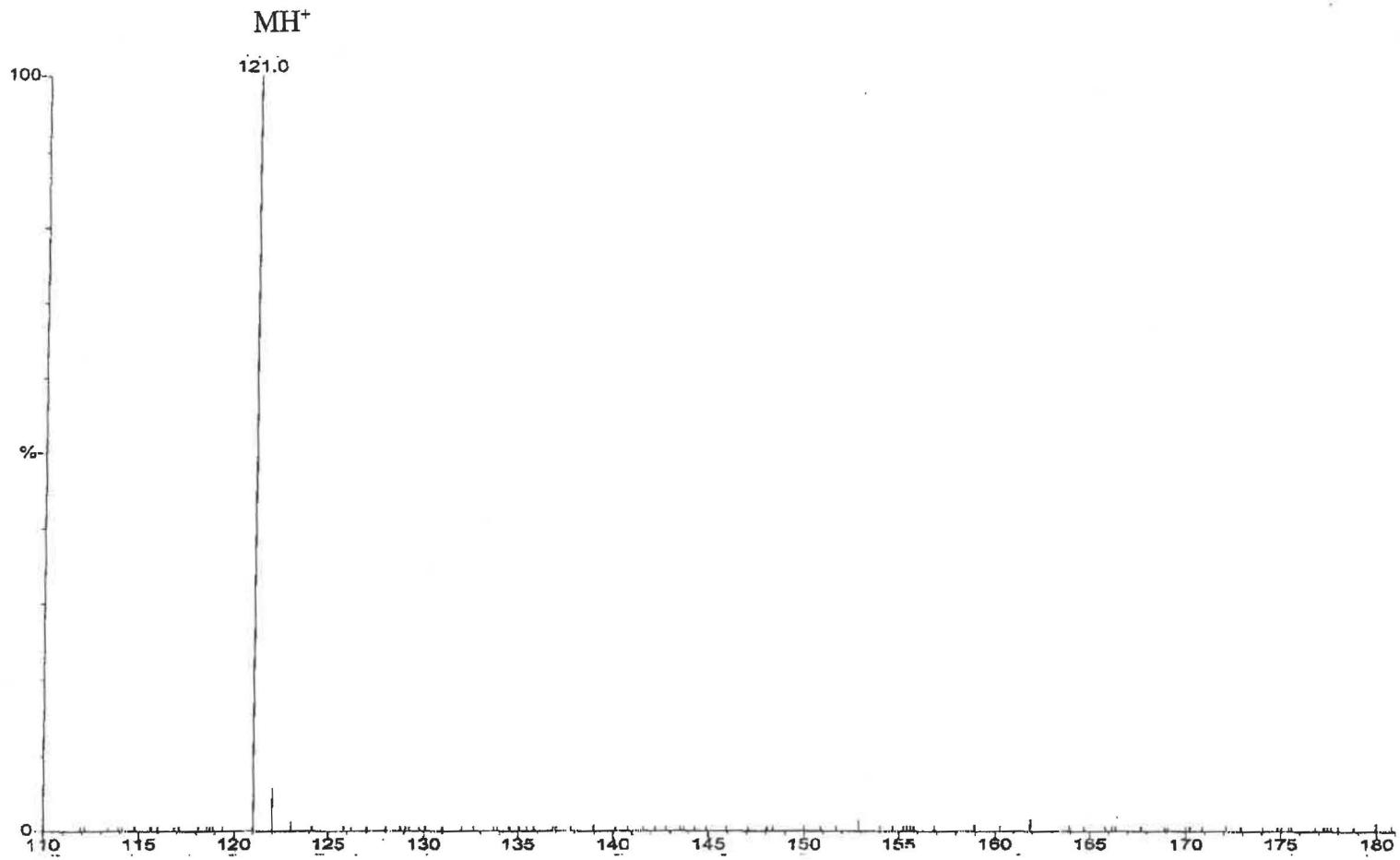

However, unrecrystallised material from both methods, was unsatisfactory for pK_a^T titrations. The set of pK_a^T's showed considerable change with the volume of 0.1000 mol l^{-1} NaOH added, and the average pK_a^T and its range did not agree with the accepted literature value of 7.03 ± 0.01 (see Table 4.9).

Two recrystallisations of the Fischer Speier Ser Me.HCl and three recrystallisations of that from the thionyl chloride method were required to produce satisfactory pK_a^T sets (Table 4.1 and 4.2).

It was concluded that the time taken to get potentiometrically pure ester hydrochlorides, for simple cases like Ser Me.HCl was similar for the Fischer Speier and thionyl chloride methods. The overall yields for the two methods were also similar (~ 70%). However the thionyl chloride method is better for very hygroscopic ester hydrochlorides (such as 4-MAB Me.HCl and 4-DMAB Me.HCl) presumably because the water produced in the reaction is consumed by the slight excess of $SOCl_2$ present. Consequently, the crude material crystallises readily rather than forming an oil.

In general, because of all of the above of all the above considerations, the Fischer Speier method was used to prepare the hydrochlorides of 2-AE Me, 4-AB Me and Et, 5-APe Me and Et. The thionyl chloride method was found best for the preparation of the hydrochlorides of 4-MAB Me and Et, 4-DMAB Me and Et, D,L-4-A-3-MB Me, 4-A-3,3-DMB Me, L-Glu-5-Me and 6-AH Et.

2.1(d) Amino Acid Benzyl Esters

The benzyl ester hydrochlorides of 3-aminopropanoic and 4-aminobutanoic acids were prepared by the oxalyl chloride method[19] since Fischer Speier esterification produces poor yields:[1]

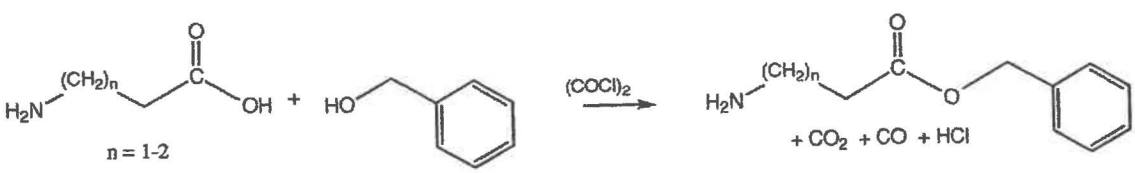

Procedure

0.1 mole of the appropriate amino acid (Note 1), 0.5 ml DMF (Note 2) and 100 ml of dry CH_2Cl_2 (Note 3) were placed in a 250 ml 2-necked round bottom flask. One arm was capped by a $CaCl_2$ drying tube, and in the other arm there was a 100 ml side arm dropping funnel which contained 60 ml of dry CH_2Cl_2, 16 ml of 98% oxalyl chloride (0.18 moles, Aldrich), protected by a $CaCl_2$ drying tube. The flask was placed in an ice bath (~ 4°C) and stirred magnetically while the contents of the dropping funnel was slowly added to the reaction mixture over a period of about twenty minutes. After the addition, the dropping funnel was removed and replaced with a $CaCl_2$ drying tube, and the stirred contents of the reaction vessel were allowed to come to room temperature followed by stirring for a further 5 hours.

At the end of this period, the reaction mixture was quickly transferred into a 250 ml round bottom flask, and the mixture rotary evaporated to dryness. The flask containing the crude reaction product was then fitted with a 250 ml sidearm dropping funnel containing 120 ml of redistilled benzyl alcohol (Note 4) protected by a $CaCl_2$ drying tube. The flask was placed in an ice bath, and it contents stirred, while the benzyl alcohol was slowly added. After the addition, the reaction mixture was further stirred until it developed a pale yellow colour (~ 45 minutes). At this point, diethyl ether (Na dried) was added, until the reaction mixture became slightly turbid. It was then refrigerated overnight. The crude amino acid benzyl ester hydrochloride was filtered off, and thoroughly dried in a desiccator over silica gel, before recrystallisation. from a minimum volume of "super-dry" methanol and diethyl ether.

Note 1

It was found that that this method produced excellent yields for some ω-amino acids (viz. 3-AP and 4-AB), but attempts to prepare the benzyl ester of 2-AE (glycine) by this method were unsuccessful. This may have been due to the insolubility of the parent amino acid in CH_2Cl_2. Consequently, the 2-aminoethanoic acid (glycine) benzyl ester hydrochloride used was a commercial sample (Bachem).

Note 2

N, *N*-dimethylformamide (DMF) was used fresh from the bottle.

Note 3

Dichloromethane (CH_2Cl_2) was distilled over sodium hydride.

Note 4

AR benzyl alcohol (Technico), was purified and redistilled according to the method of Armarrego and Perrin,[10] then stored over 4A molecular sieve.

The overall percentage yields for all the amino acid ester hydrochlorides were between 60 – 70%. Characterisation and purity checks are summarised in Tables 2.1 (m.p.'s), 2.2 (IR), 2.3 (^{13}C NMR), 2.4 (^{1}H NMR) except for Ser Me.HCl (Figures 2.3 (^{13}C NMR), 2.4 (^{1}H NMR) and 2.5 (ESMS)). All other ESMS details are given in Table 2.8. ESMS is a sensitive test for impurities, particularly traces of starting material. Operated in the positive ion mode, with cone voltage ~ +30 V, it will give parent ions MH^+. However, ESMS preferentially detects species that are initially charged over those that are neutral and cannot be used to identify species with m/z < 90. Also, at high cone voltages, extensive fragmentation can occur.

2.1(e) Discussion of Purity Criteria

As can be seen from the above Tables (2.1 – 2.8) and Figures (2.3 – 2.5), there is no sign of any impurities in all of the amino acid hydrochlorides. However, as discussed in the comparison of the Fischer Speier and thionyl chloride methods (p. 66), the most sensitive technique for product purity is pK_a^T determination by potentiometric titration. Consistency (within ±0.01) of the calculated pK_a^T throughout the titration, unless hydrolysis produces a fall in pK_a^T, is a good indicator of purity (see also 4.2(b)).

Table 2.8 Summary of ESMS Results for Amino Acid Ester Hydrochlorides.

Amino Acid Ester HCl	Molecular Formula of Parent Ion (M^+)	Calculated Mass of M^+	ESMS Mass of M^{+*}
2-AE Me.HCl	$C_3H_8NO_2^+$	90.06	90.2
4-AB Me.HCl	$C_5H_{12}NO_2^+$	118.09	118.2
4-AB Et.HCl	$C_6H_{14}NO_2^+$	132.10	132.3
5-APe Me.HCl	$C_6H_{14}NO_2^+$	132.10	132.2
5-APe Et.HCl	$C_7H_{16}NO_2^+$	146.12	146.4
4-MAB Me.HCl	$C_6H_{14}NO_2^+$	132.10	132.3
4-MAB Et.HCl	$C_7H_{16}NO_2^+$	146.12	146.3
4-DMAB Me.HCl	$C_7H_{16}NO_2^+$	146.12	146.2
4-DMAB Et.HCl	$C_8H_{18}NO_2^+$	160.10	160.3
4-A-3-MAB Me.HCl	$C_6H_{14}NO_2^+$	132.10	132.2
4-A-3,3-DMAB Me.HCl	$C_7H_{16}NO_2^+$	146.12	146.3
Glu-5 Me.HCl	$C_6H_{12}NO_4^+$	162.08	162.3
6-AH Et.HCl	$C_8H_{18}NO_2^+$	160.13	160.3
Glu DMe.HCl	$C_7H_{14}NO_4^+$	176.09	176.3
2-AE Bz.HCl	$C_9H_{12}NO_2^+$	166.09	166.3
3-AP Bz..HCl	$C_{10}H_{14}NO_2^+$	180.10	190.3
4-AB Bz..HCl	$C_{11}H_{16}NO_2^+$	194.12	194.3

* Abundance 100% in all cases.

2.1(f) 2-Pyrrolidone-5-carboxylic Acid (M)ethyl Esters

These two compounds were required for kinetic study, as they were considered to be formed as intermediates in the alkaline hydrolysis of L-Glu DMe. They were synthesised from the parent acid by the modified thionyl chloride procedure.[20]

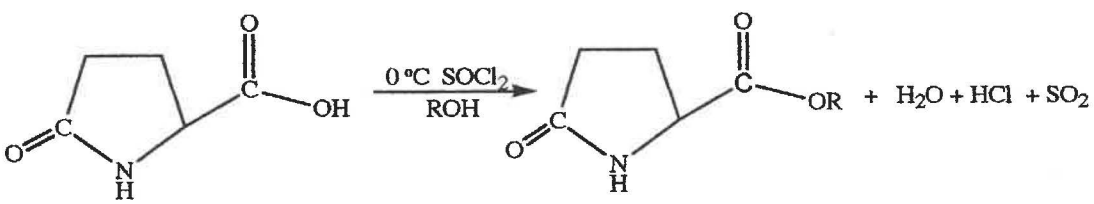

Procedure

14.7 g (0.1 mol) of D,L-2-pyrrolidone-5-carboxylic acid (P-5-CA) (Aldrich) was placed in a 250 ml flask containing 75 ml of "super dry" (m)ethanol. The flask was chilled to 0°C and 8.0 ml (0.11 mol) of thionyl chloride (Univar) was added dropwise to the reaction mixture while stirring. After the addition, the reaction mixture was allowed to stand at 0°C for another 30 minutes. The pH was then raised to ~ 5 by the addition of a ~ 40 ml of a solution of 50 % KOH in (m)ethanol.(Note 1). The reaction mixture was rotary evaporated to dryness and the crude solid that formed was rinsed with dry, freshly distilled, AR CH_2Cl_2. the precipitated solid (KCl) was filtered off and washed with CH_2Cl_2. The filtrate and the washings were collected and rotary evaporated to dryess (Note 2).

Note 1

This was prepared by dissolving 50 g AR KOH pellets in 100 ml (m)ethanol.

Note 2

2-pyrrolidone-5-carboxylic acid methyl ester (P-5-CA Me) was found to form an oil and was used in the kinetic studies without further purification (since it appeared to be sufficiently pure. Yield was 75%.

2-pyrrolidone-5-carboxylic acid ethyl ester P-5-CA Et) initially formed an oil but later solidified after it was dried under vacuum over P_4O_{10}. m.p. 52°C, lit 53°C.[21] It was used without any purification in the kinetic studies. Yield was 70%.

Both esters were characterised as follows:

IR of both P-5-CA Me and Et esters (as neat liquid and KBr disc, respectively) showed the absence of any parent acid (Table 2.9).

Table 2.9 Characteristic IR Frequencies of 2-Pyrrolidone-5-carboxylic Acid Esters

Compound	$\upsilon_{C=O}$ amide (cm^{-1})	$\upsilon_{C=O}$ ester (cm^{-1})
P-5-CA	1700	1690
P-5-CA Me	1697	1742
P-5-CA Et	1695	1738

^{13}C NMR showed the absence of any parent acid (Table 2.10); signal assignments are based on:

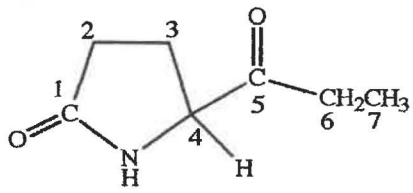

Table 2.10 ^{13}C NMR Chemical Shift and Assignments for 2-Pyrrolidone-5-carboxylic Acid Esters

Compound	Chemical Shifts, δ (ppm)						
	C-1	C-5	C-2	C-3	C-4	C-6	C-7
P-5-CA*	178.3	183.7	31.1	26.3	57.8	-	-
P-5-CA Me†	178.9	172.9	29.7	25.0	55.8	52.7	-
P-5-CA Et†	180.6	171.8	29.8	24.8	56.9	62.2	14.4

*Sample run in D_2O.

†Sample run in $CDCl_3$.

2.2 Reagents

2.2(a) Degassed Doubly Distilled Water (DW)

Doubly distilled water was degassed (by water pump vacuum) prior to use to remove any dissolved CO_2. This yielded water with a specific conductance of ~ 3 x 10^{-6} $\Omega^{-1}cm^{-1}$, which was considered sufficiently pure for the present studies. Test solutions were kept under a N_2 atmosphere to prevent the re-absorption of CO_2.

2.2(b) pH Buffers

National Bureau of Standards (NBS) Primary Standard Buffers used to calibrate the pH assembly were:[22]

(1) 0.01 mol l^{-1} sodium tetraborate (Borax).

This was prepared by dissolving 7.62745 g of AR $Na_2B_4O_7.10H_2O$ in 2 litres of DW.

(2) 0.05 mol l^{-1} potassium hydrogen phthalate,

This was prepared by dissolving 20.4230 g of AR $KOOC.C_6H_4COOH$ (oven dried at 120 °C for 2 hours) in 2 litres of DW.

Great care was taken in preparing these buffers since they underpin the accuracy of all the pK_a^T and kinetic measurements. Buffers were replaced about monthly or when sediment growth became visible.

2.2(c) Potassium Chloride Solution

1 mol l^{-1} KCl solution was made by dissolving 0.5 mole (37.2775 g) of oven dried (120°C overnight) AR KCl (Univar) in 500 ml of DW. This was used to maintain a constant ionic strength of 0.1 mol l^{-1} in the titrations and kinetic reactions.

2.2(d) Sodium Hydroxide Solution

Approximately (but slightly >) 0.1 mol l^{-1} NaOH solution was prepared by dissolving ~ 8.1 g of fresh (carbonate free) AR sodium hydroxide (BDH) pellets in 2 litres of DW. Care was taken to to minimise CO_2 adsorption by weighting directly into the 2 litre volumetric flask as quickly as possible. NaOH solutions were protected by Carbosorb® (BDH) filled tubes. This solution was standardised by two methods:

(i) By titration (50 ml A-grade 50 ml ±0.05 ml burette) against 25 ml proportions of the 0.05 mol l^{-1} potassium hydrogen phthalate buffer using phenolphthalein indicator. The concentration of the NaOH was then adjusted to exactly 0.1000 mol l^{-1} by appropriate dilution, and re-titrated to check the final concentration.

(ii) By pH-Stat titration, the NaOH solution was placed in the 2.5 ml burette (Section 3.1 (b)) and the standardisation was checked by titration against 50 ml portions of the 0.05 mol l^{-1} potassium hydrogen phthalate buffer at 25°C. Initially, the titration curve was plotted to determine that the endpoint pH was 8.450.

Considerable care was taken in this procedure since the accuracy of the [NaOH] is critical to the accuracy of the pK_a^T values. Initially there was a significant disagreement between the results of the two titration methods and this was traced to an inaccurate A-grade 25 ml pipette. The final [NaOH] = (0.1000 ± 0.0001) mol l^{-1}.

References

1. J. P. Greenstein and M. Wintz, Chemistry of the Amino Acids, John Wiley and Sons, New York, **1961**.
2. Dictionary of Organic Compounds, 5th ed., Chapman and Hall, New York, **1982**.
3. R. P. Patel and S. Price, *J. Org. Chem*, **1965**, *30*, 3575.
4. The Merek Index, 11th ed , Rathway, NJ, **1989**.
5. R. W. Hay and R. Bennett, *J. Chem Soc. (Dalton)*, **1972**, 1524.
6. T. Hidehiko and K. Misao, Jap. Patent, JP 37017960, **1962**.
7. L. A. Kodikara, M Sc. Thesis, University of Waikato, **1996**.
8. J. A. Zender, MSc. Thesis, University of Waikato, **1989**.
9. Vogel's Textbook of Practical Organic Chemistry, 5th ed., Longmans, London, **1988**.
10. W. L. F. Armarego and D. D. Perrin, Purification of Laboratory Chemicals, 4th ed, Butterworth-Heinemann, **1998**.
11. Beil., *2*, 659.
12. Ibid., *2*, 684.
13. P. C. P. Arrizabalaga and J. P. Laurent, *J. Am. Chem. Soc.*, **1984**, *106*, 4814.
14. R. Andruszkiewicz, A. G. Barrett and R. B. Silverman, *Syn. Commun.*, **1990**, *20*, 159.
15. G. M. Loudon, S. Radhakrishna, R. Almond, J. K. Blodgett and R. H. Boutin, *J. Org. Chem.*, **1984**, *49*, 4272.
16. R. H. Boutin and G. M. Loudon, *J. Org. Chem.*, **1984**, *49*, 4277.
17. R. W. Hay and P. J. Morris, *J. Chem. Soc. (B)*, **1970**, 1577.
18. R. W. Hay and L. J. Porter, *J. Chem. Soc. (B)*, **1970**, 1261.
19. R. J. Devita, A. J.Frontier, W. R. Schoen, M. J. Wyvratt, M. H. Fischer, K. Cheng, W. S. Chen, B. S. Butler and R. G. Smith, *Helv.*, **1997**, *80*, 1244
20. T. Gillan, G. Moir, F. W. Pepper and S. G. Cohen, *Bioorg. Chem.*, **1977**, *6*, 329.
21. M. Caswell, R. K. Chaturvedi, S. M. Lane, B. Zvilichovsky and G. L. Schmir, *J. Org. Chem.*, **1981**, *46*, 1585.
22. R. G. Bates, Determination of pH, Theory and Practice, John Wiley and Sons, New York, **1971**.

Chapter Three

pH Assemblies and pH, [H^+] Measurement

3.1 pH Assemblies

3.1(a) General

All monoamino acid esters exist in two forms, E and EH^+ interconnected by a pH-dependent equilibrium. Because of this, their alkaline hydrolysis must be studied at constant pH to keep the conjugate acid/base ratio constant. This is best achieved using a **pH-Stat** since this not only keeps the pH constant, but the volume of standard NaOH consumed is a measure of reaction extent. Other techniques can be used but often involve complications: **buffers and U.V. spectrophotometry** involve general base catalysis and lack of sensitivity due to small spectral changes that occur;[1] **Conductance** fails to control pH and consequent changes in the [E]:[EH^+] ratio make the value of the "rate constant" obtained meaningless;[2,3,4] **Stopped Flow U.V. spectrophotometry** at high pH (>12) where only the E form of the ester exists and no buffer is needed, suffers again from smallness of the spectral changes involved in the reaction and has produced some spurious results.[1]

Separation of the values of the rate constants for the two forms requires a value for the thermodynamic acid dissociation constant, K_a^T, of the amino acid hydrochloride.

Two different electrochemical assemblies were used in the present studies, one as a pH-Stat and the other to carry out the titrations required for the K_a^T determination. The assemblies used the same electrochemical cell:

Glass Electrode // Test Solution / Reference Electrode

i.e. $Ag_{(s)}$, $AgCl_{(s)}$/ HCl // Test Solution / $KCl_{(sat.)}$/ $AgCl_{(s)}$, $Ag_{(s)}$

Radiometer equipment was used throughout and details of the pH assemblies are given in 3.1(b) and 3.1(c).

3.1(b) pK_a^T Assembly

This consisted of:

- pH meter type PHM 26c
- Titrator TTT11b
- Autoburette, type ABU 11
- Combined Electrode, type GK2401B

This equipment was used because it allowed manual control of the volume of titrant (NaOH solution) added in each aliquot to the test solution; these volumes needed to be adjusted carefully depending on the pH change observed for the previous aliquot. Also with a 10x scale expansion, pH could be measured to 3 d.p. which ensured that the reading error, ± 0.001pH, was trivial and far less than the measurement error .

3.1(c) pH-Stat Assembly

This consisted of:

- pH meter type PHM-290
- Autoburette, type ABU 11
- Glass electrode, type pHG211†
- Reference electrode, type REF201†

†This electrode pair was replaced by the combination electrode GK2401B towards the end of the pH-Stat studies, because of the problems with the pH response accuracy of the pHG211 glass electrode (see 5.3(a)).

With this apparatus, highly accurate control of pH (±0.002 pH) was possible. The kinetic results (volume of NaOH consumed, time, pH) were able to be monitored and recorded on a spreadsheet (see 5.2(a)).

3.1(d) Instrumental Tests

Routine checks were carried out on the pK_a^T and pH-Stat Assemblies as described in the Radiometer Instruction Manuals, pHM26c (pE2)[5] and PHM290,[6] and adjustments were made as necessary.

3.1(e) Reaction Vessel

All pK_a^T and pH-Stat measurements were carried out in a double-walled glass vessel (Figure 3.1). This was capped by a polyurethane sealed cork carrying the electrode(s), thermometer, burette delivery tube and N_2 gas inlet. The N_2 gas was used to exclude other gases (particularly CO_2) from the test solution. It was presaturated with water vapour (to prevent evaporation of the test solution) by passage through a scrubber containing DW.

3.1(f) Temperature: Control and Measurement

Correct temperature control and measurement is essential in determining accurate values for equilibrium and rate constants since both quantities are significantly temperature dependent.

Temperature control of the test solution was achieved by cycling water from a thermostatted bath through the jacket of the reaction vessel (Figure 3.1). Control in the test solution was to ± 0.05°C at 25 and 37°C and ± 0.1°C at 50°C.

Temperature measurement in the reaction vessel was via a 0-50°C Zeal "total immersion" thermometer. However, only 30 mm of the thermometer could be immersed in the test solution (i.e. there was an emergent column error) and the thermometer was of unknown accuracy. Because of this, the thermometer was calibrated at 30 mm immersion against a series of certified, small range, Zeal thermometers, at 25, 37 and 50°C. The results are in Table 3.1.

Table 3.1 Calibration of 0-50°C Reaction Vessel Thermometer.

Reaction Vessel Thermometer Reading (°C)†	Calibrated Thermometer Reading(°C) †/Specified Immersion	Correction(°C)
25.00 ± 0.05	25.02 ± 0.02/Total	zero
37.00 ± 0.05	37.10 ± 0.05/70mm	+0.10
50.00 ± 0.05	50.2 ± 0.1/ 70mm	+0.2

†Errors are reading errors.

Figure 3.1 Reaction Vessel

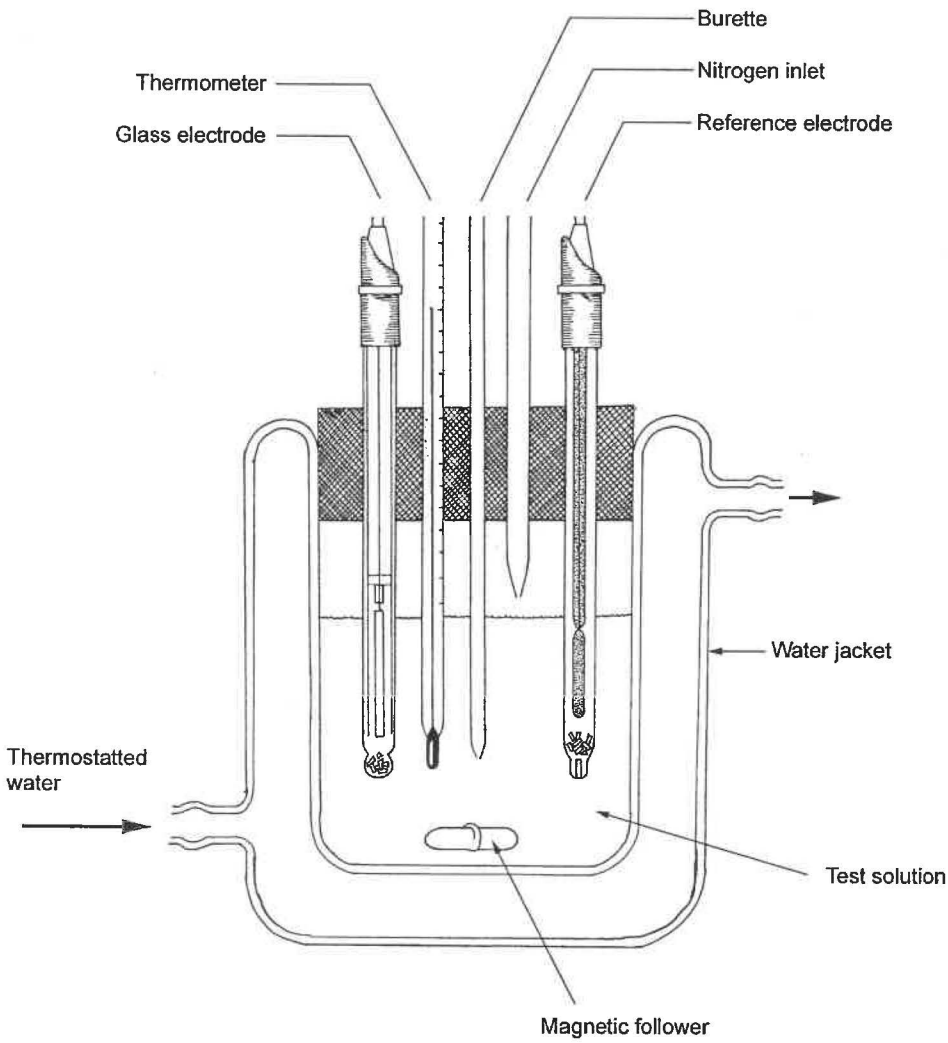

3.2 pH, [H^+] Measurement

3.2(a) Electrode Standardisation

Two Buffers

Each pH assembly was standardised initially on two standard buffers (see 3.2(b)). This was repeated at about monthly intervals (to check the electrode response) and when a new electrode was used.

Considerable case was taken in this standardising because it is critical to the accuracy of all of the pH's measured.

The procedure for the "two standard buffer" standardisation on the pK_a^T Assembly was:

The reaction vessel was thoroughly rinsed with Buffer 1 (0.01 mol l^{-1} Borax, see 3.2(b)), filled with this buffer and capped with the cork carrying the electrode, thermometer and N_2 inlet (see Figure 3.1). The buffer was stirred for about 30 minutes to allow electrode and thermal equilibration at the test temperature. The stirrer was stopped (to eliminate the "stirrer effect", see 3.2(c)), and the "Buffer Adjustment" set so the pH meter read the correct pH at the test temperature; the "isopH" was also set to this pH. The set pH was then monitored for about 30 minutes to check that the electrode drift rate was satisfactorily small (<0.005 pH). Monitoring was continued until the drift rate was satisfactory; any pH drift was corrected by re-setting the "Buffer Adjustment".

Buffer 2 (0.05 mol l^{-1} KHphthalate) then replaced Buffer 1 after the reaction vessel had been throughly rinsed with DW and dried. This buffer was again stirred for about 30 minutes, the stirrer was stopped and the pH adjusted to read the correct value using the "Electrode Sensitivity %" dial. This was usually 97-99% and must be between 95 and 100% if the glass electrode is functioning satisfactorily.

The "two standard buffer" standardisation for the pH-Stat Assembly was the same as above, except that the instrument was automatically calibrated on two buffers in the "Fixed" mode at 25°C and in the "Free" mode at 37 and 50°C.

One Buffer

After initial standardisation on two buffers, each pH assembly was than standardised at least once a day on the single "standard buffer" of pH nearest to the pH, or pH range, of interest. The same procedure was used as for Buffer 1 in the two buffer

calibration. The daily changes required to the "Buffer Adjustment" setting were carefully monitored; small changes suggest that the glass electrode is performing satisfactorily; sudden large changes often indicate a problem.

3.2(b) Standard Buffers

The pH's of the two National Bureau of Standards (NBS) buffers used to standardise the electrode(s) are listed in Table 3.2. These buffers were prepared in 2 litre batches as described by Bates.[7] Great care was taken with this (see 2.2(b)) since the accuracy of all the experimental results depends on the accuracy of the buffer pH. The buffer solutions were stored in tightly stopped flasks and were replaced at least monthly.

Table 3.2 Standard pH (pH_s) of NBS Buffers Used. [8]

Temperature °C	pH_s 0.05 mol l^{-1} potassium hydrogen phthalate	pH_s 0.01 mol l^{-1} Borax (sodium tetraborate)
25.0	4.005	9.180
37.1	4.022	9.088
50.2	4.050	9.011

3.2(c) Stirrer Effect

The test solution was stirred using a magnetic follower and rotating magnet. Stirring was needed for thermal equilibration and to mix the NaOH solution added during titrations and pH-Stat kinetic runs. However, the consequent turbulence affects the pH reading; it has been suggested[8] that this is due to a change in the liquid junction potential, E_j, associated with the movement of the ions in the diffusion zone around the reference electrode. The result is usually a lowering of the pH and the size of this depends on the nature of the test solution. The largest lowering was found for the NBS Borax buffer (up to 0.06 pH); other alkaline solutions showed significant but smaller pH lowering on stirring; acid solutions generally showed insignificant changes.

Because of the variable and often significant stirrer effect, all pH readings were taken with the stirrer stopped. At the end of pH-Stat kinetic runs, the stirrer was stopped and the run pH corrected to the "stopped stirrer" value. Ignoring this can lead to very large errors in $[OH^-]$ since $\pm$ 0.01pH is equivalent to $\pm$ 2.3% in $[OH^-]$.

3.2(d) Activity Coefficients: Calculation of $[H^+]$ $[OH^-]$

Calculation of $[H^+]$ and $[OH^-]$ from the pH reading requires a value for the activity coefficient of a univalent ion, y_1, under the test solution conditions. This cannot be determined experimentally; only mean activity activity coefficients for cation/anion pairs $y_\pm$, can be measured.

However, there are several theoretical methods for calculating individual activity coefficients, y_i's; these include Debye-Huckel,[9] extended Debye-Huckel,[10] Guntelberg[11] and Davies.[12] All apply only to dilute aqueous solutions with ionic strengths, $I \leq \sim 0.1$ mol l^{-1}. The Davis equation[12] was used because it gives y_1 values which agree more closely (to within ±2%)[13] with the average experimental $y_\pm$ values for 1:1 electrolytes under the test solution conditions (I = 0.1 mol l^{-1}).[14] The form of the Davies equation used was:

$$-\log_{10} y_i = A z_i^2 \left(\frac{\sqrt{I}}{(1+\sqrt{I})} - 0.2\, I \right) \qquad \text{....(3.1)}$$

where,

A = Debye- Huckel parameter (temperature dependent),[15]

z_i = charge on species i,

I = ionic strength.

Calculated values for y_1(and y_2 needed for some pK_a^T calculations), along with the A value used, are listed in Table 3.3 at the three experimental temperatures.

Table 3.3 Davies Equation Values for Activity Coefficients.

T°C	A Value[15]	y_1	y_2
25.0	0.5115	0.7715	0.3545
37.1	0.5231†	0.7670	0.3461
50.2	0.5373	0.7615	0.3363

† Obtained by interpolation

Values for $[H^+]$ and $[OH^-]$ were calculated using these y_1 values and the equations:

$$pH = -\log_{10}\{H^+\} \qquad \text{....(3.2)}$$

$$= -\log_{10}\left([H^+]\cdot y_1\right)$$

$$\therefore \quad [H^+] = \frac{10^{-pH}}{y_i} \qquad \text{....(3.3)}$$

$$pK_w^T = -\log_{10}\{H^+\}\{OH^-\} \qquad \text{....(3.4)}$$

$$K_w^T = \{H^+\}\{OH^-\} = 10^{-pK_w^T}$$

$$= 10^{-pH}[OH^-]\cdot y_1 \qquad \text{....(3.5)}$$

$$\therefore \quad [OH^-] = \frac{K_w^T}{10^{-pH}\cdot y_1} = \frac{10^{pH-\,pK_w^T}}{y_1} \qquad \text{....(3.6)}$$

Table 3.4 Thermodynamic Ionisation Constants of Water[16]

T°C	K_w^T	pK_w^T
25.0	1.008×10^{-14}	13.9965
37.1	2.388×10^{-14} †	13.6220 †
50.2	5.474×10^{-14}	13.2617

†Obtained by interpolation

The calculated values for $[OH^-]$ at all pH's and at the three experimental temperatures, are listed in Table 3.5.

Table 3.5 Hydroxide Ion Concentration.

pH	$[OH^-] \times 10^{14-x}$ mol l^{-1}		
	25.0°C	37.1°C	50.2°C
x.00	1.307*	3.113	7.188
x.10	1.645	3.920	9.041
x.20	2.071	4.934	11.39
x.30	2.607	6.212	14.34
x.40	3.282	7.821	18.06
x.50	4.132	9.846	22.73
x.60	5.201	12.39	28.61
x.70	6.549	15.61	36.03
x.80	8.243	19.64	45.34
x.90	10.38	24.73	57.10

*e.g. if pH =10.00, $[OH^-] = 1.307 \times 10^{-4}$ mol l^{-1}

3.2(e) Temperature Effect on Concentration

While $[H^+]$ and $[OH^-]$ were calculated from the measured pH at a given temperature, the concentrations of other species will decrease with increasing temperature, due to the expansion of water. This must be allowed for using the density of water, ρ_{H_2O}, at each temperature. All solution volumes were measured out at 20°C, since volumetric glassware is generally calibrated at this temperature.

For the work at 25.0°C, the change in the water volume resulting from the increase in temperature from 20 to 25°C was negligible.[17]

At 37.1°C, this change was significant and was corrected for using:

$$V_{37} = V_{20} \times \frac{(\rho_{H_2O})_{20}}{(\rho_{H_2O})_{37.1}} = V_{20} \times 1.0053 \qquad \text{....(3.7)}$$

Similarly, at 50.2 °C:

$$V_{50} = V_{20} \times \frac{(\rho_{H_2O})_{20}}{(\rho_{H_2O})_{50.2}} = V_{20} \times 1.0103 \qquad \text{....(3.8)}$$

where,

V_x = Volume at temperature X(°C)

$(\rho_{H_2O})_X$ = Density of H_2O at temperature X.[17]

References

1. J. A. Zender, M Sc. Thesis, University of Waikato, **1989**.
2. J. M. White, R. A. Manning and N. C. Li, *J. Am. Chem. Soc.*, **1957**, *79*, 5859.
3. N. C. Li and R. A. Manning, *J. Am. Chem. Soc.*, **1955**, *77*, 5225.
4. J. M. White, R. A. Manning and N. C. Li, *J. Am. Chem. Soc.*, **1956**, *78*, 2367.
5. Radiometer, Copenhagen, Instruction Manuel for PHM 26c, Titrator Type TTT11b, Autoburette Type ABU111.
6. Radiometer, Copenhagen, Operating Instructions for PHM290 pH-Stat Controller.
7. R. G. Bates, Determination of pH, Theory and Practice, John Wiley and Sons, New York, **1971**.
8. H. Galster, pH Measurement, Fundamentals, Methods, Applications and Instrumentation, VCH Publishers, Inc., New York, **1991**.
9. P. Debye and E. Huckel, *Z. Physik*, **1923**, *24*, 305.
10. H. M. Spencer, *J. Am. Chem. Soc.*, **1932**, *54*, 4490.
11. E. Guntelberg, *Kem. Maanedablad*, **1938**, *19*, 85.
12. C. W. Davis, *J .Chem. Soc.*, **1938**, 2093.
13. C. W. Davis, Ion Association, Butterworths, London, **1962**.
14. R. A. Robinson and R. H. Stokes, Electrolyte Solutions, Butterworths, 2nd ed, **1965**, Appendix 8.10, Tables 9, 10, 11.
15. ibid., Appendix 7.1.
16. ibid., Appendix 12.2 (Water K_w's).
17. ibid., Appendix 1.1 (ρ_{H_2O}'s).

Chapter Four

Proton Dissociation Constants

4.1 Introduction

Values for the thermodynamic proton dissociation constants, K_a^T's, of the amino acid ester hydrochlorides were needed in the analysis of their alkaline hydrolysis kinetics. This is because a pH dependent equilibrium connects the two forms of the ester (the free base E, and its conjugate acid, EH^+) and both forms undergo alkaline hydrolysis, i.e. there are two parallel reactions. In addition, for a series of structurally related esters, any anomalous K_a^T value will provide information about the nature of unusual interactions in the E or EH^+ forms; e.g. evidence for intramolecular H-bonding. Such structural information about the nature of the reactant may help interpret the value of its alkaline hydrolysis rate constant.

4.2 pK_a^T of Monoamino Acid Ester Hydrochlorides

4.2(a) Equilibra

These ester hydrochlorides behave as monobasic acids in aqueous solution, e.g. serine methyl ester.HCl, Ser Me.HCl, Scheme 4.1:

$$\overset{+}{N}H_3\text{–}CH(CH_2OH)\text{–}COOCH_3\,(aq) \underset{}{\overset{K_a^T}{\rightleftharpoons}} NH_2\text{–}CH(CH_2OH)\text{–}COOCH_3\,(aq) + H^+_{(aq)}$$

$$\text{i.e.}\quad EH^+ \rightleftharpoons E + H^+$$

$$\therefore K_a^T = \frac{\{E\}\{H^+\}}{\{EH^+\}}$$

Scheme 4.1 Dissociation of the $-NH_3^+$ Group of Ser Me.HCl

However, for dicarboxylic acid half esters such as glutamic acid 5-methyl ester.HCl, Glu-5-Me.HCl, the free base is E^- and its conjugate acid is EH, Scheme 4.2:

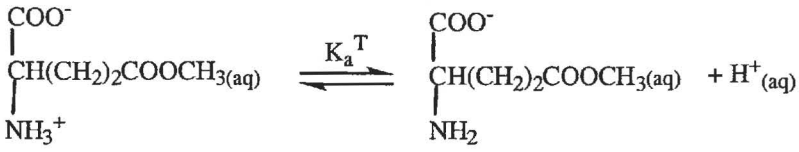

i.e. $EH \rightleftharpoons E^- + H^+$

$$\therefore K_a^T = \frac{\{E^-\}\{H^+\}}{\{EH\}}$$

Scheme 4.2 Dissociation of the $-NH_3^+$ Group of Glu-5-Me.HCl

4.2(b) Experimental Procedure

Values for K_a^T were determined by potentiometric titration using the pH assembly (pHM 26c see 3.1(b)) at 25.0°C, and for selected ester hydrochlorides, at 37.1°C and 50.2 °C.

10^{-4} moles of EH^+Cl^- were weighted out (porcelain crucible; 5-place balance), washed carefully into the reaction vessel using the required volume of degassed doubly distilled water (DW); the appropriate volume of 1.0 mol l^{-1} KCl was added such that at half-neutralisation (0.500 ml 0.1000 mol l^{-1} NaOH) the I = 0.1 mol l^{-1} and the total volume = 100.00 ml. Total concentration of the ester = 10^{-3} mol l^{-1}. For very hygroscopic EH^+Cl^-, a 4-place balance and dry N_2 atmosphere were used. The reaction vessel was assembled (Figure 3.1), the stirrer started and the reaction mixture equilibrated and brought up to the required temperature (at least 30 minutes). While this was happening, the alkali inlet tube was thoroughly flushed with the titrant (at least 3 x 2.5 ml), and any bubbles present were carefully removed before insertion into the reaction mixture. For all the EH^+Cl^-, at 25°C, the composition of the test solution was:

10^{-4} moles EH^+Cl^-
9.90 ml 1.0 mol l^{-1} KCl
89.60 ml DW

At half-neutralisation (0.500 ml of 0.1000 mol l^{-1} NaOH), the total volume = 100.00 ml, I = 0.1 mol l^{-1} and $[ester]_{total}$ = 10^{-3} mol l^{-1}. For Glu-5-Me.HCl ($EH_2^+Cl^-$), 9.85 ml 1.0 mol l^{-1} KCl and 88.65 ml DW were used since half-neutralisation is 1.500 ml of 0.1000 mol l^{-1} NaOH.

Due allowance was made for water expansion at higher temperatures (see 3.2(e)). Temperature control was ± 0.05°C at 25 and 37°C, and ± 0.1°C at 50°C. The titration method depended on the rate of alkaline hydrolysis in the pH range defined by the pK_a^T:

Method 1 (Group 1, slowly hydrolysing esters), Method 2 (Group 2, moderately hydrolysing esters) and Method 3 (Group 3, rapidly hydrolysing esters).

The objective was to obtain a set of pK_a^T values which showed:

1. Good **internal consistency**; range of ± 0.01 or better.
2. Good **reproducibility**; titrations were done at least twice with agreement to ± 0.01 or better being considered satisfactory.

Data was checked using the computer program PKAESTERS1 (Appendix A1.2(a)) which calculated the pK_a^T value at each titre volume. All computer programs used were checked by doing hand calculations.

(i) Method 1. Group 1, Slowly Hydrolysing Esters

Hydrochlorides of Ser Me, 2-aminoethanoic benzyl ester (2-AE Bz), 3-aminopropanoic acid benzyl ester (3-AP Bz), 4-dimethylaminobutanoic acid ethyl ester (4-DMAB Et), 6-aminohexanoic acid ethyl ester (6-AH Et) and glutamic acid methyl ester (Glu DMe).

Small aliquots (0.050 or 0.100 ml) of 0.1000 mol l^{-1} NaOH were added to the test solution, with the stirrer going to ensure rapid mixing and minimal hydrolysis due to locally high [OH^-]. After each addition, when the solution had equilibrated (steady pH reading; correct temperature), the stirrer was stopped and the steady pH reading noted. Stirring tends to lower the pH reading (see 3.2(c)). When hydrolysis became noticeable (falling pH), the titration was completed quickly to get the best possible endpoint estimate. However, pK_a^T values calculated in this region were increasingly low, so that they were not included in the average. Titration endpoints could only be seen for compounds with low pK_a^T's; for higher pK_a^T's, endpoints were masked by the high pH's and buffer capacities involved.

For this group of esters, the objectives of good internal pK_a^T consistency and reproducibility were readily achieved, provided the compounds were highly pure. Potentiometric titration is a searching test for acidic impurities (such as excess HCl or S-acids and traces of parent acid) from the Fischer Speier and thionyl chloride preparation methods. Such impurities were often undetectable by other analytical methods (NMR, IR, and ESMS), but showed up in upward trends within the pK_a^T set (see 2.1(c)). Repeated (up to 5 times in some cases) recrystallisation was needed to achieve potentiometrically pure ester hydrochlorides. Generally, it was more difficult to remove the acid impurities from the products of thionyl chloride preparation.

Ser Me.HCl Standard

This compound provides an excellent check on the accuracy of the experimental technique and equipment. Because its pK_a^T is low (~ 7 cf. other α-amino acid ester hydrochlorides , ~ 7.6, at 25°C), and its alkaline hydrolysis rate constant is "normal", there is insignificant hydrolysis at the pH's involved in almost the whole titration. Consequently, Ser Me.HCl has well-established literature values for pK_a^T at various temperatures. Hence, Ser Me.HCl was the first compound investigated. Samples prepared by the Fischer-Speier and thionyl chloride methods were subjected to repeated titrations and recrystallisations until consistent sets of pK_a^T's were obtained (Tables 4.1 and 4.2). This provided a guide as to the number of recrystallisations likely to be needed for ester hydrochlorides where hydrolysis prevented purity estimation from pK_a^T; for such compounds, only a few pK_a^T values could be calculated before they were affected by hydrolysis.

In Tables 4.1 and 4.2 (and in subsequent pK_a^T Tables), average pK_a^T values were calculated from the K_a^T values involved, rather than averaging the $-\log_{10}K_a^T$'s. Some initial values were ignored in the average because they had larger errors associated with the higher value of d(pH)/dV. Values near the endpoint were also rejected because of hydrolysis.

Table 4.1 pK_a^T for Ser Me.HCl (2 x recryst.) (Fischer Speier).

Test solution contained: 10^{-4} moles EH^+Cl^- 9.90 ml 1.0 mol l^{-1} KCl 89.60 ml DW			T = (25.00 ± 0.05)°C I = 0.1 mol l^{-1} $[ester]_{total} = 10^{-3}$ mol l^{-1}	
Vol. 0.1000 mol l^{-1} NaOH (ml)	Titration 1		Titration 2	
	pH	pK_a^T	pH	pK_a^T
0.000	5.123	(7.019) †	5.125	(7.023) †
0.100	6.183	(7.021) †	5.180	(7.018) †
0.150	6.389	7.028	6.388	7.027
0.200	6.544	7.033	6.542	7.031
0.250	6.672	7.036	6.670	7.034
0.300	6.782	7.037	6.780	7.035
0.350	6.882	7.038	6.880	7.036
0.400	6.974	7.037	6.972	7.035
0.450	7.065	7.040	7.062	7.037
0.500	7.153	7.041	7.151	7.038
0.550	7.240	7.040	7.239	7.039
0.600	7.327	7.039	7.325	7.037
0.650	7.419	7.039	7.417	7.036
0.700	7.516	7.038	7.513	7.033
0.750	7.622	7.036	7.620	7.031
0.800	7.738*	(7.033) †	7.736*	(7.023) †
0.850	7.872*	(7.025) †	7.870*	(7.007) †
Average pK_a^T =		7.037 ± 0.009		7.035 ± 0.008

Overall, average pK_a^T = 7.03 ± 0.01

† Values in parentheses were excluded from the average.

* Hydrolysis noticeable

Table 4.2 pK_a^T for Ser Me HCl (3 x recryst.) (Thionyl Chloride).

Test solution contained: 10^{-4} moles EH^+Cl^- 9.90 ml 1.0 mol l^{-1} KCl 89.60 ml DW			$T = (25.00 \pm 0.05)°C$ $I = 0.1$ mol l^{-1} $[ester]_{total} = 10^{-3}$ mol l^{-1}	
Vol. 0.1000 mol l^{-1} NaOH (ml)	Titration 1		Titration 2	
	pH	pK_a^T	pH	pK_a^T
0.000	5.109	(6.991)†	5.118	(7.009)†
0.100	6.182	(7.020)†	6.175	(7.013)†
0.150	6.382	7.021	6.380	(7.019)†
0.200	6.540	7.029	6.535	7.023
0.250	6.668	7.032	6.662	7.026
0.300	6.778	7.033	6.772	7.027
0.350	6.875	7.034	6.872	7.028
0.400	6.970	7.033	6.963	7.026
0.450	7.060	7.034	7.055	7.030
0.500	7.149	7.035	7.142	7.029
0.550	7.236	7.036	7.228	7.028
0.600	7.325	7.036	7.316	7.027
0.650	7.418	7.036	7.408	7.027
0.700	7.515	7.035	7.503	7.023
0.750	7.626	7.037	7.609	7.020
0.800	7.742	7.029	7.722*	(7.010)†
0.850	7.889*	(7.026)†	7.860*	(6.997)†
Average pK_a^T =		7.033 ± 0.009		7.026 ± 0.006

Overall, average $pK_a^T = 7.03 \pm 0.01$

† Values in parentheses were excluded from the average.

* Hydrolysis noticeable

The error given with the average pK_a^T covers the range of results; however, the real error is probably ± 0.01.

The two preparation methods produced satisfactorily consistent pK_a^T sets with the same overall average, 7.03 ± 0.01. This is in excellent agreement with the literature value 7.03 ± 0.01.[1,2] The Fischer Speier prepared compound required fewer recrystallisations than the thionyl chloride one, to achieve a consistent set of pK_a^T's. These results show that the accuracy of the experimental technique and equipment (see 3.2(b)) is satisfactory, so studies were continued using the remaining Class 1 ester hydrochlorides: 2AE Bz.HCl, 4-DMAB Et.HCl and 3-AP Bz.HCl were straight forward (Table 4.9 and Appendix 1), but there were some problems with 6-AH Et.HCl and Glu DMe.HCl.

6-AH Et.HCl

This has a high pK_a^T (> 10) which results in the high pH's during the titration. Consequently, there is considerable buffering from the water equilibrium which results in reduced accuracy and sensitivity of the glass electrode. Small changes in pH represent large [OH^-] changes and so any error in calibration or response of the glass electrode is greatly magnified. One method of increasing the accuracy in such cases is to increase the concentration of ester.HCl, e.g. from 10^{-3} to 10^{-2} mol l^{-1}. However, this would require either a very large volume of 0.1000 mol l^{-1} NaOH (with consequently increased total hydrolysis) or an increased [NaOH] (e.g. from 0.1 to 1.0 mol l^{-1}). Increasing the [NaOH] is not an option since this produces rapid etching of the glass delivery burette. Titrations were done at [NaOH] = 0.1000 mol l^{-1} and [6-AH Et.HCl] = 10^{-3} mol l^{-1}, realising the accuracy would be limited. The results (Table 4.3) show a much larger range (± 0.03) than usual, as expected. While there is good reproducibility, there is a small trend in pK_a^T with increasing pH. This may reflect a small response error in the glass electrode, magnified by the high buffering.

Glu DMe.HCl

This has a low pK_a^T (~7) and hydrolyses only slowly at the titration pH's (~5 – 8). Consequently, like Ser Me.HCl, it is one of the few ester hydrochlorides where an

Table 4.3 pK_a^T of 6-AH Et.HCl (2 x recryst.).

Test solution contained: 10^{-4} moles EH^+Cl^- 9.90 ml 1.0 mol l^{-1} KCl 89.60 ml DW			T = (25.00 ± 0.05)°C I = 0.1 mol l^{-1} $[ester]_{total} = 10^{-3}$ mol l^{-1}	
Vol. 0.1000 mol l^{-1} NaOH (ml)	Titration 1		Titration 2	
	pH	pK_a^T	pH	pK_a^T
0.000	6.780	-	6.720	-
0.050	8.910	(10.316)†	8.910	(10.316)†
0.100	9.383	10.476	9.380	10.475
0.200	9.719	10.462	9.717	10.461
0.300	9.922	10.464	9.929	10.477
0.400	10.080	10.484	10.085	10.490
0.500	10.202	10.496	10.208	10.507
0.600	10.302	10.501	10.308	10.514
0.700	10.388	10.506	10.392	10.516
0.800	10.464	10.512	10.468	10.522
0.900	10.533	10.520	10.536	10.529
Average pK_a^T =		10.490 ± 0.03		10.499 ± 0.03

Overall, average pK_a^T = 10.49 ± 0.03

† Values in parentheses were excluded from the average.

accurate endpoint can be obtained so its titrimetric purity can be checked. The results obtained for the two titrations are summarised in Table 4.4. The endpoint for Titration 1 was slightly low (0.998 ml cf. expected 1.000 ml 0.1000 mol l^{-1} NaOH), so a + 0.002 ml correction was made to all the titres (Figure 4.1) before pK_a^T's were calculated. The titration 2 endpoint was exactly 1.000 ml, showing that either this sample was slightly purer than for titration 1, or that there was a small amount of hydrolysis in titration 1. The results (Table 4.4) show excellent agreement, suggesting that the correction to titration 1 was needed and was not due to hydrolysis. The overall average, 7.04 ± 0.01 agrees with the single literature value, 7.03 ± 0.01,[2] obtained under the same conditions. Results for all the compounds are summarised in Table 4.9.

(ii) Method 2. Group 2, Moderately Hydrolysing Esters

Hydrochlorides of 4-aminobutanoic acid ethyl and benzyl esters (4-AB Et, 4-AB Bz), 4-methylaminobutanoic acid methyl and ethyl esters (4-MAB Me, 4-MAB Et), 4-amino-3-methylbutanoic acid methyl ester (4-A-3-MBMe), 4-amino-3,3-dimethylbutanoic acid methyl ester (4-A-3,3-DMB Me) and glutamic acid 5-methyl ester (Glu 5-Me).

The same procedure was used as for Method 1 except that the more rapid hydrolysis meant that the titration was stopped at ~ 0.500 ml 0.1000 mol l^{-1} NaOH added. Hence, pK_a^T averages were determined from usually about six points and the reproducibility and accuracy were usually somewhat poorer than for Method 1. The titration data and results are given in Appendix A1.3(b); two compounds produced unique problems:

Glu-5-Me.HCl

Because this is the half-ester of a dicarboxylic acid, a purity estimate can be made from the endpoint for the titration of the α–COOH group (pK_a ~ 4.3). Two titrations (Table 4.5) showed slightly high endpoints (1.005 and 1.010 ml 0.1000 mol l^{-1} NaOH for Titrations 1 and 2 respectively). Hence, corrections of - 0.005 ml and - 0.010 ml were applied in calculating the respective sets of pK_a^T's, using the computer program

Table 4.4 pK_a^T of Glu DMe.HCl (1 x recryst.)

Test solution conditions same as in Table 4.3.			T = (25.00 ± 0.05)°C I = 0.1 mol l^{-1} $[ester]_{total}$ = 10^{-3} mol l^{-1}	
Vol. 0.1000 mol l^{-1} NaOH (ml)	Titration 1§		Titration 2	
	pH	pK_a^T	pH	pK_a^T
0.000	5.128	-	5.119	-
0.100	6.186	(7.023)†	6.181	(7.019)†
0.150	6.392	(7.024)†	6.385	(7.024)†
0.200	6.543	(7.026)†	6.539	7.028
0.250	6.672	7.032	6.663	7.027
0.300	6.782	7.033	6.775	7.030
0.350	6.881	7.034	6.872	7.028
0.400	6.975	7.035	6.965	7.029
0.450	7.068	7.040	7.058	7.033
0.500	7.157	7.042	7.148	7.036
0.550	7.243	7.040	7.235	7.036
0.600	7.334	7.043	7.325	7.037
0.650	7.429	7.045	7.419	7.039
0.700	7.531	7.048	7.521	7.042
0.750	7.640	7.048	7.632	7.044
0.800	7.769	7.052	7.758	7.046
0.850	7.922*	(7.054)†	7.912*	(7.050)†
0.900	8.132*	(7.065)†	8.120*	(7.062)†
0.920	8.239	-	8.227	-
0.940	8.370	-	8.359	-
0.960	8.535	-	8.520	-
0.980	8.752	-	8.738	-
0.990	8.878	-	8.863	-
1.000	9.010	-	8.988	-
1.010	9.141	-	9.116	-
1.020	9.249	-	9.223	-
1.040	9.445	-	9.426	-
1.060	9.598	-	9.576	-
1.080	9.712	-	9.692	-
1.100	9.812	-	9.788	-
1.150	9.998	-	9.971	-
Average pK_a^T =		7.041 ± 0.011		7.035 ± 0.011

Overall, average pK_a^T = 7.03 ± 0.01

§ pK_a^T values calculated using a + 0.002 ml correction.

† Values in parentheses were excluded from the average.

* Hydrolysis noticeable.

Figure 4.1 Titration 1 Curve for Glu DMe.HCl

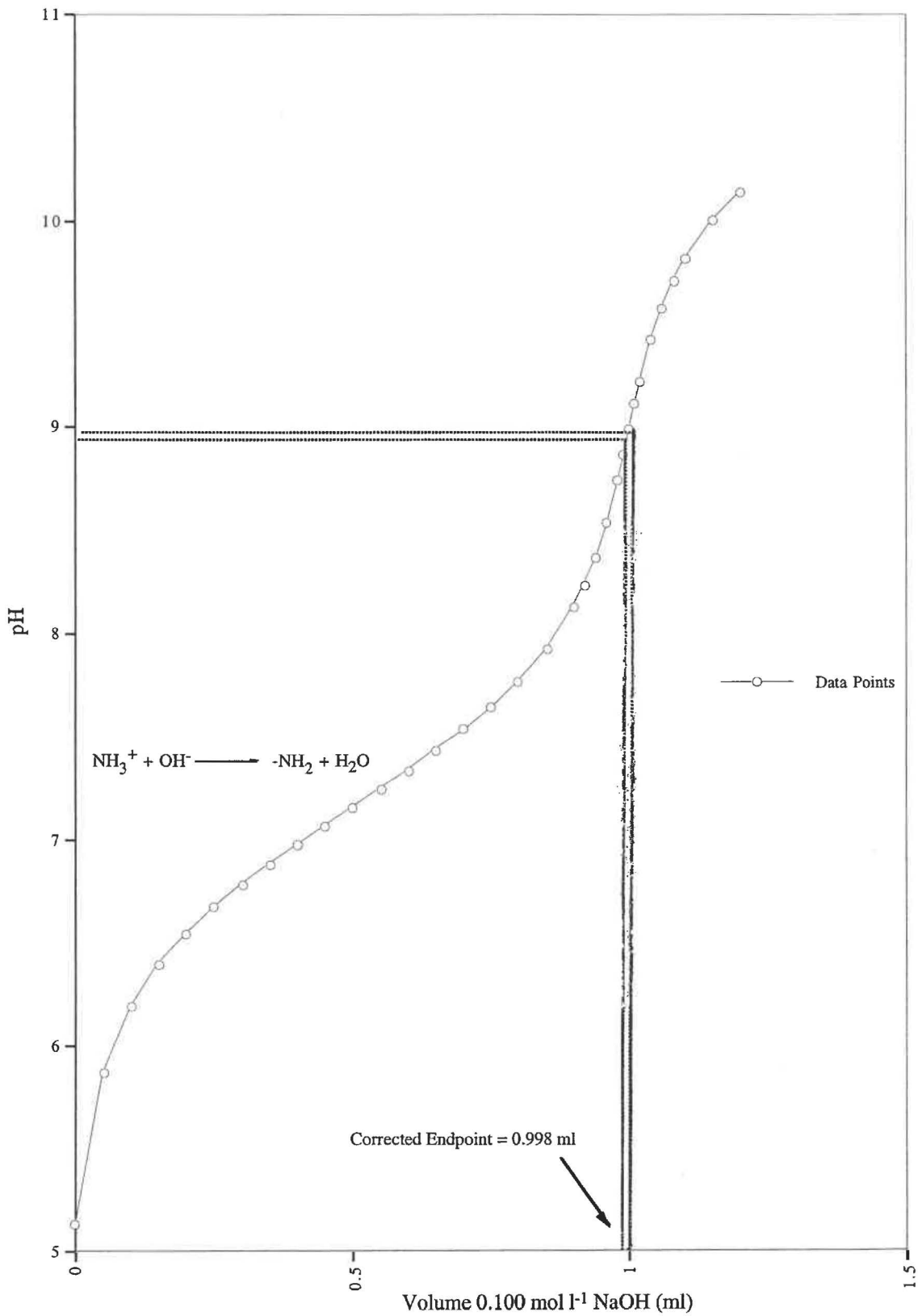

Table 4.5 pK_a^T for Glu 5-Me.HCl (2 x recryst.)

Test solution contained:			T = (25.00 ± 0.05)°C	
10^{-4} moles EH^+Cl^-			I = 0.1 mol l^{-1}	
9.90 ml 1.0 mol l^{-1} KCl			$[ester]_{total} = 10^{-3}$ mol l^{-1}	
89.60 ml DW				
Vol. 0.1000 mol l^{-1} NaOH (ml)	Titration 1§		Titration 2§§	
	pH	$pK_a^{T\,\S}$	pH	$pK_a^{T\,\S\S}$
0.000	3.147	-	3.134	-
0.200	3.249	-	3.236	-
0.400	3.380	-	3.368	-
0.600	3.570	-	3.554	-
0.800	3.899	-	3.877	-
0.900	4.242	-	4.208	-
0.920	4.352	-	4.311	-
0.940	4.499	-	4.451	-
0.960	4.702	-	4.642	-
0.980	5.059	-	4.941	-
1.000	5.700	-	5.590	-
1.020	6.740	-	6.705	-
1.040	7.290	-	7.275	-
1.060	7.598	-	7.603	-
1.080	7.806	-	7.802	-
1.100	7.989	(8.862)†	7.977	(8.876)†
1.200	8.422	8.935	8.415	8.942
1.300	8.673	8.952	8.660	8.949
1.400	8.870	8.961	8.859	8.958
1.500	9.042	8.964	9.030	8.960
1.600	9.200	8.958	9.189	8.955
1.700*	9.358	8.948	9.345	8.943
Average pK_a^T =		8.95 ± 0.01*		8.950 ± 0.01*

Overall, average pK_a^T = 8.95 ± 0.01

§ pK_a^T values calculated using a - 0.005 ml volume correction.

§§ pK_a^T values calculated using a - 0.010 ml volume correction.

† Values in parentheses were excluded from the average.

* Hydrolysis noticeable.

PKAESTERS2 (Appendix A1.2(b)). Both titrations showed good internal consistency and gave exactly the same average $pK_a^T = 8.95 \pm 0.01$.

4-AB Bz.HCl

This ester had acidic impurities which could not be removed with repeated recrystallisations. The titration (Figure 4.2) showed a starting pH of ~ 4.8 which was far too low for a compound with a $pK_a^T \sim 10$. Similar compounds had starting pH's ~ 6. To estimate the "starting volume correction" needed, only small aliquots of NaOH were added until the pH was well past 6. The titration was completed as usual. The graph suggested a starting ("endpoint") volume of between 0.030 and 0.045 ml. Sets of pK_a^T's were than calculated (PKAESTERS1) using the series of starting volume corrections - 0.030, - 0.031, - 0.032....- 0.042 ml as well as for no correction. Some of these results are given in Table 4.6. The results for no correction are clearly nonsensical. The best "starting volume correction" was chosen to be that value (-0.040 ml) which gave the most internally consistent set of pK_a^T's and with "sensible" pK_a^T values (i.e. similar to related, but pure compounds). As can be seen from Table 4.6, the effect of small changes in the "starting volume correction" on the pK_a^T value is insignificant near the best value and $pK_a^T = 9.80 \pm 0.01$. A second titration yielded a best "starting volume correction" of – 0.041 ml. The results of both titrations are given in Appendix 1, Table A1.15.

(iii) Method 3. Group 3, Rapidly Hydrolysing Esters

Only two esters, the hydrochlorides of 5-aminopentanoic acid methyl ester (5-APe Me.HCl) and the corresponding ethyl ester (5-APe Et.HCl) were in this group. For both, the rate of alkaline hydrolysis was too fast to record reliable pH values beyond 0.1 ml (5-APe Me.HCl) and 0.2 ml (5-APe Et.HCl) 0.1000 mol l^{-1} NaOH added, i.e. only the first 10 or 20% of the titration curve was usable. However, the lower buffer capacities (high d(pH)/dV values) involved meant that great care had to be taken to obtain meaningful pH values. The ester hydrochlorides were carefully recrystallised at least three times to ensure potentiometric purity. For each titration, a maximum of two adjacent titres/pH's were recorded, to minimise accumulated hydrolysis. The

Figure 4.2 Titration Curve for 4-AB Bz.HCl (3 x recryst.)

$T = (25.00 \pm 0.05)\ °C$

$I = 0.1\ mol\ l^{-1}$

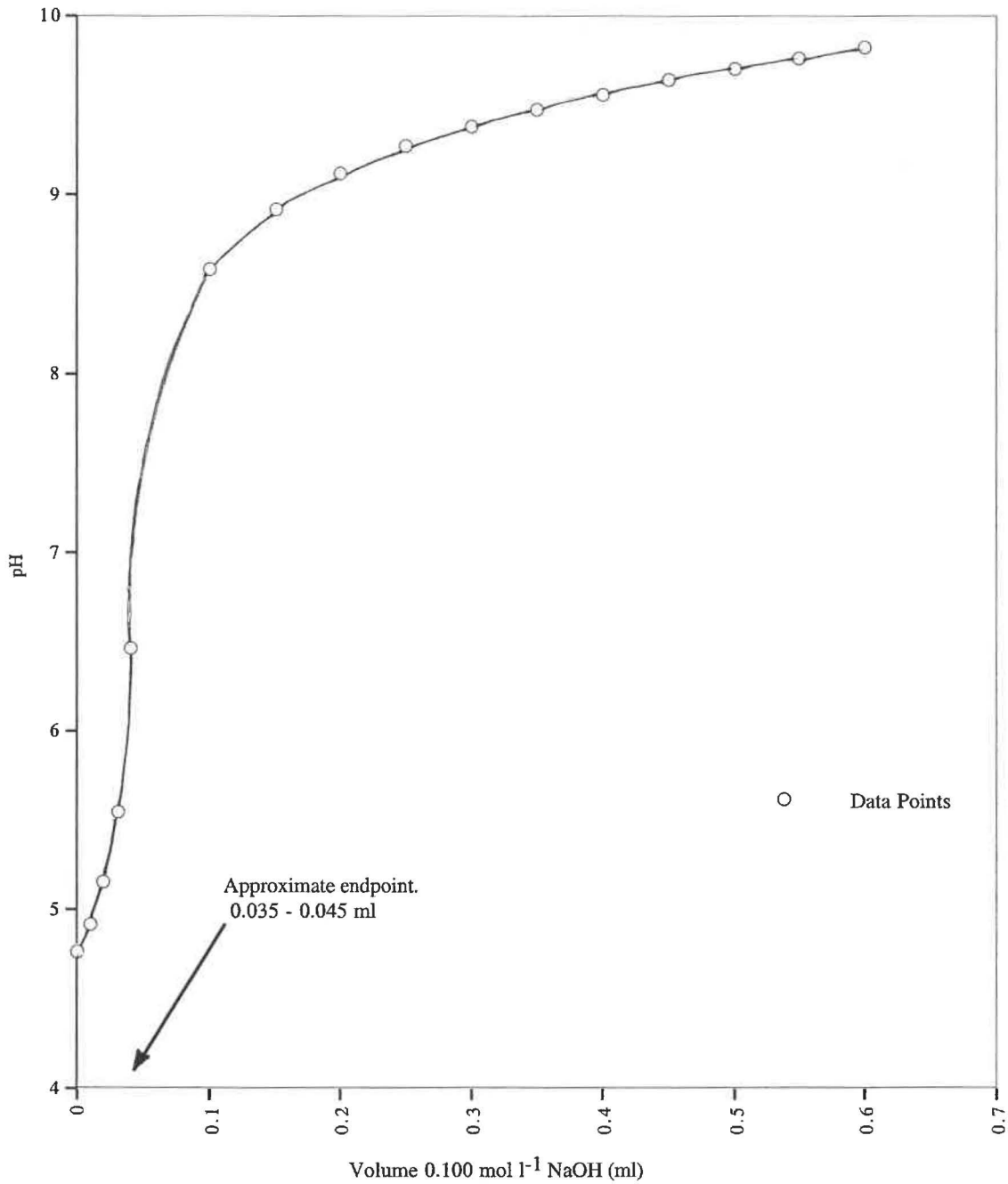

Table 4.6 Effect of "Starting Volume Correction" on the pK_a^T Values of 4-AB Bz.HCl (3 x recryst.)

Test solution contained: 10^{-4} moles EH^+Cl^-; 9.90 ml 1.0 mol l^{-1} KCl; 89.60 ml DW		T = (25.00 ± 0.05) °C; I = 0.1 mol l^{-1}; $[ester]_{total} = 10^{-3}$ mol l^{-1}					
Uncorrected Vol. 0.1000 mol l^{-1} NaOH (ml)	pH	pK_a^T calculated with the following volume corrections (ml): 0.000	- 0.030	- 0.038	- 0.039	- 0.040	- 0.042
0.000	4.762						
0.010	4.924						
0.020	5.164						
0.030	5.548						
0.040	6.475	(7.738)†					
0.100	8.589	9.455	(9.635)†	(9.695)†	(9.703)†	(9.712)†	(9.729)†
0.150	8.923	9.602	(9.722)†	(9.759)†	(9.764)†	(9.769)†	(9.779)†
0.200	9.130	9.669	9.766	9.790	9.793	9.797	9.804
0.250	9.276	9.669	9.778	9.800	9.803	9.806	9.812
0.300	9.390	9.714	9.783	9.802	9.805	9.807	9.812
0.350	9.486	9.721	9.783	9.801	9.803	9.805	9.810
0.400	9.570	9.723	9.782	9.798	9.800	9.802	9.806
0.450	9.644			9.792	9.794	9.795	9.799
0.500*				(9.785)†	(9.787)†	(9.789)†	(9.792)†
Average pK_a^T			9.778± 0.012	9.797 ± 0.008	9.799 ± 0.006	9.799 ± 0.006	9.807 ± 0.008
Rounded Average pK_a^T			9.78 ± 0.01	9.80 ± 0.01	9.80 ± 0.01	9.80 ± 0.01	9.81 ± 0.01

† Values in parentheses not included in averaging of pK_a^T values.

* Hydrolysis noticeable.

overall titration was built up in a series of steps, e.g. Titration 1: 0.100, 0.110 ml; Titration 2: 0.120, 0.130 ml, etc.

5-APe Me.HCl

This hydrolysed very rapidly and only titre points below 0.100 ml were accessible. Here, any CO_2 contamination must be minimised, so after degassing, the doubly distilled water was purged with O_2 free N_2 gas for ~ 30 minutes before use. To remove traces of CO_2 introduced during the preparation of the test solution, it was stirred under O_2 free N_2 for about an hour before the titration commenced. This raised the pH by ~ 0.02. Despite all these precautions, traces of CO_2 were still present; these were neutralised by adding about 0.002 ml 0.1000 mol l^{-1} NaOH (to take the starting pH to 6.6) before the titration was begun. During the titration, the stirrer was not stopped. Stopped stirrer values are usually ~ 0.005 pH above the stirrer value, but this error was considered to be much smaller than that resulting from hydrolysis during the time required to stop the stirrer. Six titrations were done, using the pairs of values: 0.060, 0.070 ml; 0.080, 0.090 ml. Values below 0.060 ml were too erratic to be useful. These six titrations were condensed into 3 overall titrations (Table 4.7). As can be seen, each "overall titration" showed a small decrease in pK_a^T from 0.060 to 0.070 ml, followed by much larger falls to 0.090ml. Values at 0.060 and 0.070 ml were considered to be the best estimates, with an overall average of 10.15 ± 0.02. Later kinetic studies (Chapter 5.3(d)) showed that the $t_{1/2}$ was ~ 9 minutes at the pH ~9.1 of the 0.090 ml reading, which explains the great difficulty in getting an accurate pK_a^T value.

5-APe Et.HCl

Slower hydrolysis meant that reliable titration data could be obtained up to 0.200 ml. The exhaustive removal of CO_2 was unnecessary and the stirrer was stopped for each of the pair of points for each titration. Sets of 6 titrations were condensed into "overall titrations" using titres between 0.100 and 0.200 ml. pK_a^T values were calculated from the averaged pH's (Table 4.8). There was no trend in pK_a^T with increasing titre. The overall average, 10.10 ± 0.02, is probably more reliable than for the methyl ester, despite the same error range, because of the larger data set.

Table 4.7 pK_a^T of 5-APe Me.HCl (2 x recryst.)

Test solution contained:					T = (25.00 ± 0.05)°C	
10^{-4} moles EH^+Cl^-					I = 0.1 mol l^{-1}	
9.90 ml 1.0 mol l^{-1} KCl					$[ester]_{total} = 10^{-3}$ mol l^{-1}	
89.60 ml DW						
Vol 0.1000 mol l^{-1} NaOH	Overall "Titration 1"		Overall "Titration 2"		Overall "Titration 3"	
	pH	pK_a^T	pH	pK_a^T	pH	pK_a^T
0.000	6.6		6.53		6.58	
0.060	8.972	10.159	8.960	10.143	8.972	10.159
0.070	9.032	10.146	9.013	10.122	9.020	10.131
0.080	9.063*	(10.108)†	9.049*	(10.091)†	9.059	(10.104)†
0.090	9.096*	(10.092)†	9.085*	(10.069)†	9.090	(10.075)†
Averaged pK_a^T Values =		10.153 ± 0.007		10.133 ± 0.010		10.145 ± 0.014

Overall, average pK_a^T = 10.15 ± 0.02

* Hydrolysis noticeable.

† Values in parentheses were excluded from the average.

Table 4.8 pK_a^T of 5-APe Et.HCl (2 x recryst.)

Test solution contained: 10^{-4} moles EH^+Cl^- 9.90 ml 1.0 mol l^{-1} KCl 89.60 ml DW				T = (25.00 ± 0.05)°C I = 0.1 mol l^{-1} $[ester]_{total} = 10^{-3}$ mol l^{-1}	
Vol. 0.1000 mol l^{-1} NaOH	Overall "Titration 1" pH	Overall "Titration 2" pH	Overall "Titration 3" pH	Averaged pH	pK_a^T
0.100	9.134	9.135	-	9.134 ± 0.001	(10.072)†
0.110	9.188	9.180	9.180	9.183 ± 0.005	10.077
0.120	9.231	9.217	9.222	9.223 ± 0.008	10.076
0.130	9.280	9.273	9.272	9.275 ± 0.005	10.091
0.140	9.305	9.296	9.296	9.299 ± 0.006	10.077
0.150	9.352	9.355	-	9.354 ± 0.002	10.104
0.160	9.396	9.399	9.390	9.395 ± 0.004	10.117
0.170	9.418	9.433	9.412	9.421 ± 0.012	10.112
0.180	9.440	9.435	9.430	9.435 ± 0.005	10.095
0.190	9.475	9.471	9.490	9.479 ± 0.011	10.117
0.200*	9.483	9.479	9.497	9.486 ± 0.011	10.095
				Average pK_a^T = 10.096 ± 0.021	

Average pK_a^T = 10.10 ± 0.02

† Value in parenthesis excluded from the average.

*.Hydrolysis noticeable.

Table 4.9 summaries the pK_a^T values for the amino acid ester hydrochlorides studied at 25.0 °C and I = 0.1 mol l^{-1}. Also included are the available literature values.

4.3 Monoamino Acids

Introduction

pK_a^T values for the $-NH_3^+$ group of the parent amino acids were measured because they provided useful information about unusual interactions present in the E and EH^+ forms of the esters, e.g. for the α-amino acids, there is normally a 2 unit difference between the pK_a^T of an acid and its methyl ester.[1] Interactions, such as intramolecular H-bonding in say the ester only, can change this relationship. In addition, the pK_a^T value of the amino acid is needed to calculate the expected V_∞ value for the alkaline hydrolysis of the ester (5.2(d)); deviation from the expected values suggests unusual hydrolysis pathways.

The prepared and commercially sourced amino acids used were in one of three possible forms: zwitterion (AH), monoamino hydrochloride ($AH_2^+Cl^-$) and monoamino dicarboxylic acid (AH_2). Hence, three different equilibria exist; the experimental procedure and the program needed to calculate pK_a^T, are different for the three cases.

4.3(a) Zwitterions

(i) Equilibrium

Most of the simple ω-amino acids studied were zwitterionic: i.e. 2-aminoethanoic acid (2-AE), 3-aminopropanoic (3-AP), 4-aminobutanoic acid (4-AB) and 6-aminohexanoic acid (6-AH). These behave as monobasic acids in aqueous solution, Scheme 4.3:

$$H_3N^+\text{-}(CH_2)_n\text{-}COO^-_{(aq)} \overset{K_a^T}{\rightleftharpoons} H_2N\text{-}(CH_2)_n\text{-}COO^-_{(aq)} + H^+_{(aq)}$$

$$\text{i.e. } AH \rightleftharpoons A^- + H^+$$

$$\text{i.e. } K_a^T = \frac{\{A^-\}\{H^+\}}{\{AH\}}$$

Scheme 4.3 Dissociation of $-NH_3^+$ Group of Zwitterion ω-Amino Acids.

Table 4.9 Summary of pK_a^T Values for Monoamino Acid Ester Hydrochlorides.

		T = (25.00 ± 0.05) °C I = 0.1 mol l^{-1}
Amino Acid Ester.HCl	Thesis pK_a^T	Literature pK_a^T
Ser Me.HCl	7.03 ± 0.01	7.03 ± 0.01[1], 7.04 ± 0.01[2]
2-AE Me.HCl†		7.674 ± 0.004[3], 7.63 ± 0.01[4] 7.624 ± 0.004[3], 7.66[5], 7.59 ± 0.04[6]
3-AP Me.HCl*		9.176 ± 0.003[3], 9.170 ± 0.004[1] 9.16 ± 0.01[4]
4-AB Me.HCl†		9.83 ± 0.01[3], 9.84 ± 0.01[1] 9.85 ± 0.01[4]
4-MAB Me.HCl	10.00 ± 0.01	
4-DMAB Me.HCl†		9.31 ± 0.01[3]
4-A-3-MB Me.HCl	9.45 ± 0.01	
4-A-3,3-DMB Me.HCl	9.23 ± 0.01	
5-APe Me.HCl	10.15 ± 0.02	10.02 ± 0.03[4], 10.15 ± 0.03[6]
Glu-5-Me.HCl	8.95 ± 0.01	9.06[7]**
Glu DMe.HCl	7.03 ± 0.01	7.03 ± 0.03[5]
6-AH Me.HCl*		10.474 ± 0.006[4]
4-AB Et.HCl	9.86 ± 0.01	9.91[7]**, 9.71[8]***
4-MAB Et.HCl	10.08 ± 0.01	
4-DMAB Et.HCl	9.29 ± 0.02	
5-APe Et.HCl	10.10 ± 0.02	10.11[7]**, 10.15[8]***
6-AH Et.HCl	10.49 ± 0.03	
2-AE Bz.HCl	7.52 ± 0.01	
3-AP Bz.HCl	9.06 ± 0.01	
4-AB Bz.HCl	9.81 ± 0.02	

† pK_a^T was only determined at 37°C and 50°C in this thesis.

* pK_a^T not determined in this thesis.

** Estimated pK_a^T at I = 0.2 mol l^{-1}.

*** Ionic strength conditions not given.

(ii) Experimental Procedure

At 25°C, the test solution used was:

10^{-4} moles AH

9.95 ml 1.0 mol l^{-1} KCl

89.55 ml DW

At half-neutralisation (0.500 ml of 0.1000 mol l^{-1} NaOH), total volume = 100.00 ml, $[acid]_{total} = 10^{-3}$ mol l^{-1} and I = 0.1 mol l^{-1}.

Due allowance was made for water expansion at higher temperatures (see 3.2(e)).

The titration procedure was the same as described for the ester hydrochlorides (4.2(b)) but without the complication of falling pH due to ester hydrolysis. However, endpoints were not generally observable because of the high pH's involved with the high pK_a^T's (9 – 10), e.g. for 2-AE, pK_a^T's were calculated using program PKAACIDS1 (Appendix 2.2(a)). At least two titrations were done for each acid with the aim of an internal consistency and reproducibility of ± 0.01 pK_a^T or better.

2-AE

For this typical case, pK_a^T values calculated below ~0.250 ml and above 0.900 ml were ignored as they were more error weighted. The most accurate pK_a^T's are those near the titration midpoint (0.500 ml) where the conjugate acid: base ratio is near 1. Two titrations gave acceptable internal consistency and reproducibility, with $pK_a^T = 9.79 \pm 0.01$ (Appendix 2.3(a), Table A2.1). No trend was evident in the pK_a^T sets which indicates good purity and lack of any glass electrode response problems.

3-AP was similar to 2-AE, but with a higher $pK_a^T = 10.28 \pm 0.01$, Appendix 2.3(a), Table A2.2.

4-AB

This and 6-AH (along with 5-APe, see 4.3(b)) had increasingly high pK_a^T's. The pH's were so high that the resulting high buffer capacity tended to magnify any small response error in the glass electrode, resulting in some drift in pK_a^T's values (e.g. for 4-AB, Appendix 2.3(a), Table A2.3). Repeated recrystallisation did not remove this

problem but it could be overcome by increasing the total amino acid concentration to 5 x 10^{-3} mol l^{-1} using the test solution (at 25 °C):

5 x 10^{-4} moles 4-AB

9.75 ml 1.0 mol l^{-1} KCl

87.75 ml DW

The results (Appendix 2.3(a), Table A2.4 cf. Table A2.3 at 10^{-3} mol l^{-1}) gave pK_a^T = 10.60 ± 0.02 (cf. 10.58 ± 0.04), a considerable improvement in the drift and internal consistency.

6-AH

Because of the very high pK_a^T, titrations were done at a total amino acid concentrations of 5 x 10^{-3} and 10^{-2} mol l^{-1}. The results (Appendix 2.3(a), Table A2.5,) show excellent agreement with very little trend (pK_a^T = 10.95 ± 0.01).

4.3(b) Monoamino Acid Hydrochlorides

(i) Equilibria

These compounds, 5-APe.HCl, 4-MAB.HCl, 4-DMAB.HCl, 4-A-3-MB.HCl and 4-A-3,3-DMB.HCl, behave as dibasic acids in aqueous solution, Scheme 4.4:

$$H_3N^+\text{-}(CH_2)_n\text{-}COOH_{(aq)} \xrightleftharpoons{K_a^T(\text{-}COOH)} H_3N^+\text{-}(CH_2)_n\text{-}COO^-_{(aq)} + H^+_{(aq)}$$

$$H_3N^+\text{-}(CH_2)_n\text{-}COO^-_{(aq)} \xrightleftharpoons{K_a^T(\text{-}NH_3^+)} H_2N\text{-}(CH_2)_n\text{-}COO^-_{(aq)} + H^+_{(aq)}$$

Scheme 4.4 Dissociation of Monoamino Acid Hydrochlorides.

Only the $-NH_3^+$ dissociation was of interest, i.e.

$$\text{i.e. } AH \rightleftharpoons A^- + H^+$$

Hence, the definition of pK_a^T is the same as for the zwitterion case (4.3(a)) and the same program (PKAACIDS1) can be used to calculate the pK_a^T using the titration data starting from the endpoint for the –COOH neutralisation.

(ii) Experimental Procedure

At 25°C, the test solution was:

10^{-4} moles $AH_2^+Cl^-$

9.85 ml 1.0 mol l^{-1} KCl

88.65 ml DW

At half-neutralisation (1.500 ml of 0.1000 mol l^{-1} NaOH), total volume = 100.00 ml, $[acid]_{total}$ = 10^{-3} mol l^{-1} and I = 0.1 mol l^{-1}. Due allowance was made for water expansion at higher temperatures (see 3.2(e)).

1.000 ml of 0.1000 mol l^{-1} NaOH was added before the data on the $-NH_3^+$ ionisation was collected. The first endpoint was clearly identifiable (pH ~ 8 since pK_a^T ~ 4.3) and was used to check the purity of the amino acid hydrochloride; in particular, that the stoichiometric amount of HCl was present.

5-APe.HCl

Initial titrations showed variable and high endpoints (1.020 and 1.030 ml). Recrystallisation (from redistilled t-butyl alcohol) removed the excess HCl but the endpoint was still variable (1.008 and 0.990 ml, Appendix 2.3(a), Figure A2.1). Starting volume corrections were made and the results (Appendix 2.2(c), Table A2.6) showed good reproducibility, but some trend which resulted in a wide error range: $pK_a^T = 10.76 \pm 0.04$. As was found later (see 4-AB and 6-AH, (p. 108), this problem could have been eliminated by increasing the amino acid concentration. However, the change is mostly in a reduced trend with little change in the average pK_a^T (see 4-AB, p. A54) and so this compound was not re-investigated.

4-A-3-MB.HCl

Despite being spectroscopically pure (NMR, IR, Table 2.7), initial titrations resulted in –COOH endpoints of 0.760 and 0.770 ml 0.1000 mol l^{-1} NaOH (Appendix 2.3(a), Figure A2.2). Intensive drying (P_4O_{10}/vacuum) did not improve the endpoint.

Chloride gravimetric analysis[9] yielded an average Cl = (17.6 ± 0.1)% cf. theoretical 23.1%. The compound is thus deficient in HCl and appears to be a mixture of 75% $AH_2^+Cl^-$ and 25% AH. The weight of the compound and the volume of reagents were consequently modified:

10^{-4} moles $AH_2^+Cl^-$/AH

9.93 ml 1.0 mol l^{-1} KCl

88.82 ml DW

At half-neutralisation (1.250 ml of 0.1000 mol l^{-1} NaOH), total volume = 100.00 ml, $[acid]_{total}$ = 10^{-3} mol l^{-1} and I = 0.1 mol l^{-1}. This adjustment resulted in a satisfactory set of pK_a^T's (Appendix 2.3(c), Table A2.7)

4.3(c) Monoamino Dicarboxylic Acid

(i) Equilibrium

The only compound studied was glutamic acid, Glu (2-aminopentandioic acid). Its $-NH_3^+$ pK_a^T was needed to complete the effect of structure on $pK_a^T(-NH_3^+)$ in the series: Glu-5-Me.HCl, Glu DMe.HCl and Glu. The equilibrium involved for Glu is:

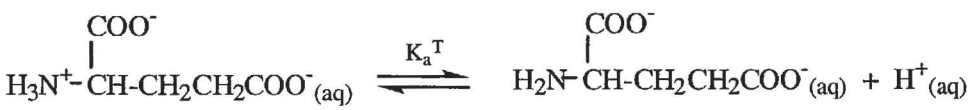

$$H_3N^+\text{-}CH(COO^-)\text{-}CH_2CH_2COO^-_{(aq)} \overset{K_a^T}{\rightleftharpoons} H_2N\text{-}CH(COO^-)\text{-}CH_2CH_2COO^-_{(aq)} + H^+_{(aq)}$$

$$\text{i.e. } AH^- \rightleftharpoons A^{2-} + H^+$$

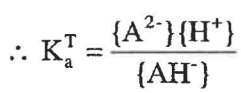

$$\therefore K_a^T = \frac{\{A^{2-}\}\{H^+\}}{\{AH^-\}}$$

Scheme 4.5 Dissociation of Glu-NH_3^+ Group.

(ii) Experimental Procedure

At 25°C, the test solution was:

10^{-4} moles AH_2

9.80 ml 1.0 mol l^{-1} KCl

88.90 ml DW

1.000 ml 0.1000 mol l^{-1} NaOH was required to neutralise the –COOH group before titrating the $-NH_3^+$ group. At half-neutralisation (1.500 ml of 0.10000 mol l^{-1} NaOH), total volume = 100.00 ml, $[acid]_{total} = 10^{-3}$ mol l^{-1} and I = 0.1 mol l^{-1}.

pK_a^T values were calculated using the program PKAACIDS2 (Appendix 2.2(b)). The results (Appendix 2.3(c), Table A2.9) showed good internal consistency with little spread ($pK_a^T = 10.01 \pm 0.01$). However, the accuracy is less than usual because y_2 at I = 0.1 mol l^{-1} has to be calculated using the Debye-Huckel equation (see 3.2(d)). This equation is considered to yield satisfactory y_1 values up to I = 0.1 mol l^{-1}, but activity coefficients for multiply charged ions are usually considered to have an ionic strength limit of 0.01 mol l^{-1} for reliable values.[10]

Table 4.10 summarises pK_a^T values for the three classes of amino acids, along with available literature values.

4.4 Temperature Dependence

4.4(a) Introduction

The effect of temperature on the K_a^T value for a particular compound, gives a more complete picture of the factors controlling the dissociation, than can be obtained from a single temperature K_a^T value. From the temperature dependence, values for ΔG°, ΔH° and ΔS° for the dissociation can be calculated. Hence, the relative values of K_a^T's (i.e. relative acidities) in a set of related compounds can be discussed in terms of not only inductive effects (+**I** acid weakening; -**I** acid strengthening) but more importantly in terms of enthalpy and entropy changes. The latter, dominated by solvation effects, has been shown to play a major role in determining the relative pK_a^T values for substituted ammonium ion systems,[19] e.g. NH_4^+, $CH_3NH_3^+$, $(CH_3)_2NH_2^+$, $(CH_3)_3NH^+$. It was hoped that such an insight might yield structural information such as the presence of intramolecular H-bonding, which would be helpful in interepting the ester hydrolysis kinetics. The ester hydrochlorides (and their parent acids) chosen for pK_a^T temperature dependence were those whose kinetics were going to be examined at three temperatures, for the reasons to be discussed in Section 5.4.

Table 4.10 Summary of pK_a^T ($-NH_3^+$) Values for Monoamino Acids

		T = (25 .00 ± 0.05)°C I = 0.1 mol l^{-1}
Amino Acid*	Thesis pK_a^T	Literature pK_a^T
2-AE†	9.79 ± 0.01	9.62[10] †† 9.78[11] 9.78[12] 9.780 ± 0.005[13] 9.78[14]
3-AP†	10.28 ± 0.01	10.333 ± 0.004[1] 10.08[10] 10.238[15]
4-AB†	10.60 ± 0.01	10.565 ± 0.004[1] 10.556 ± 0.005[16]
4-MAB**		10.88 ± 0.05[3]
4-DMAB**		10.138 ± 0.003[3]
4-A-3-MB**	9.67 ± 0.02	
4-A-3,3-DMB**	10.48 ± 0.01	
5-APe**	10.76 ± 0.03	10.852 ± 0.005[4] 10.766 ± 0.005[13]
Glu§	10.01 ± 0.01	9.95 ± 0.01[8]
6-AH†	10.95 ± 0.01	10.936[4] 10.804[17] 10.912[18]

*Starting form:

†Zwitterion.

**Monohydrochloride.

§Monoamino dicarboxylic acid.

†† pK_a^T's measured at I = 0.1 mol l^{-1} but used $y_1 = 0.83$.

Accuracy Check

As at 25°C, the pK_a^T values of Ser Me.HCl were used to check the accuracy of the equipment (3.1(b)) and experimental procedure (4.2(b)) at 37.1°C and 50.2°C. The results (Appendix 1.4(a), 1.5(a), Tables A1.10, A1.24) show excellent agreement with well established literature values.

4.4(b) Monoamino Acid Ester Hydrochlorides

Essentially the same experimental procedure was used as at 25°C, with due allowance being made for water expansion. The increased temperature results in increased hydrolysis rates (2-4 times per 12°C rise) and this was only partly compensated for by decreased pK_a^T values (~ 0.3 pK_a^T units per 12°C rise). Consequently, it became increasingly difficult to obtain reliable titration data.

Group 1 ester hydrochlorides studied were: 2-AE Me.HCl (previous study at 25°C),[3] 3-AP Bz.HCl, 4-DMAB Me.HCl, (previous study at 25°C)[3] and 4-DMAB Et.HCl. Their titrations yielded reliable pK_a^T values until near the midpoint of the titration curve when hydrolysis became significant. Because of decomposition, 4-DMAB Me.HCl was re-synthesised; traces of acidic impurities could not be removed so an endpoint correction was made (see 4-AB Bz.HCl, p. 100)

Group 2 ester hydrochlorides studied were: 4-AB Me.HCl, (previous study at 25°C),[3] 4-AB Et.HCl, 4-AB Bz.HCl, 4-MAB Me.HCl, 4-MAB Et.HCl, 4-A-3-MB Me.HCl and 4-A-3,3-DMB Me.HCl. Fast hydrolysis rates meant that the 25°C procedure had to be modified. Increasing temperature resulted in a decreasing % (10-20 maximum) of the titration that could be used to calculate reliable pK_a^T values. To minimise hydrolysis, the stirrer was not stopped; this results in a small pH error (-0.005) but this was considered to be less important than the pH lowering caused by the additional ester hydrolysis with the time taken to stop the stirrer and allow the pH meter reading to stabilise. While ester hydrolysis is slow, its effect on pH is magnified by the low buffer capacity of the test solution. Thus the reproducibility and accuracy became poorer as the temperature was raised. To improve the quality of the pK_a^T value, titrations were performed many times (at least 10).

Group 3 compounds were the hydrochlorides of the methyl and ethyl esters of 5-APe. Very rapid hydrolysis rates meant that less than 10% of the titration could be used. Great care was taken to ensure the highest possible accuracy of the pH values in this steep region of the titration curve. More rigorous procedures were used than for 5-APe Me.HCl at 25°C (see p. 103): CO_2 was removed by N_2 purging of the DW for at least 1 hour; the test solution was held under a N_2 atmosphere for at least 30 minutes. Despite this, a small endpoint correction was still necessary. Again, the stirrer was not stopped for readings and the titration was repeated at least 15 times to improve the quality of the pK_a^T value.

All the results for the temperature dependence of the pK_a^T's for the ester hydrochlorides are summarised in Table 4.11, along with available literature values. As can be seen there is generally excellent agreement between the literature and present study values.

4.4(c) Monoamino Acids

The $-NH_3^+$ pK_a^T's of the parent amino acids are of much less use than those of their ester hydrochlorides, in interpreting the ester hydrolysis kinetics. Hence, only a few acids were studied and these were ones where there were gaps or conflicts in the literature values: 2-AE, 4-MAB.HCl, 4-DMAB Me.HCl, 4-A-3-MB.HCl, 4-A-3,3-DMB.HCl and 5-APe.HCl. The titration procedure was the same as at 25°C (see 4.3), with none of the increasing hydrolysis problems of the esters. The only problem with increasing temperature was the increasing water buffering (due to decreasing pK_w^T) at the high pH's involved. This was only partially offset by the decrease in pK_a^T. Consequently, there was a decrease in sensitivity and any pH response error of the glass electrode was increasingly magnified with increasing temperature. While the results for 2-AE and 4-DMAB (Appendices A2.4 and A2.5) showed excellent reproducibility and little trend (< 0.01 pK_a^T), those for 4-MAB, 4-A-3,3-DMB and 5-APe (Appendices A2.4 and A2.5) all showed some trend, despite a correct –COOH titration endpoint.

Table 4.11 Temperature Dependence of pK_a^T's of Selected Amino Acid Ester Hydrochlorides*

Amino Acid Ester.HCl	25.0 °C	37.1 °C	50.2 °C
Ser Me.HCl	7.03 ± 0.01	6.72 ± 0.01	6.42 ± 0.01
(Lit. Value)[1]	7.030	6.724	6.412
2-AE Me.HCl	7.67 ± 0.01	7.33 ± 0.01	7.02 ± 0.01
(Lit Value)[5]	7.66	7.33	7.00
3-AP Bz.HCl	9.06 ± 0.01	8.69 ± 0.01	8.34 ± 0.01
4-AB Me.HCl	9.83 ± 0.01	9.46 ± 0.01	9.09 ± 0.01
(Lit. Value)[1]	9.839	9.461	9.091
4-AB Et.HCl	9.86 ± 0.01	9.48 ± 0.01	9.10 ± 0.01
4-AB Bz.HCl	9.81 ± 0.02	9.42 ± 0.01	9.05 ± 0.02
4-MAB Me.HCl	10.00 ± 0.01	9.73 ± 0.01	9.44 ± 0.01
4-MAB Et.HCl	10.08 ± 0.01	9.68 ± 0.01	9.30 ± 0.01
4-DMAB Me.HCl	9.31 ± 0.01	9.10 ± 0.01	8.87 ± 0.01
4-DMAB Et.HCl	9.29 ± 0.01	9.02 ± 0.01	8.76 ± 0.01
4-A-3-MB Me.HCl	9.45 ± 0.01	9.08 ± 0.01	8.73 ± 0.01
4-A-3,3-DMB Me.HCl	9.23 ± 0.01	8.96 ± 0.01	8.68 ± 0.01
5-APe Me.HCl	10.15 ± 0.02	9.71 ± 0.02	9.29 ± 0.02
5-APe Et.HCl	10.10 ± 0.02	9.74 ± 0.02	9.39 ± 0.02

* All pK_a^T values measured at at I = 0.1 mol l^{-1}

All values are summarised in Table 4.12 along with the literature values for 2-AE. For this acid, the 25°C literature result agrees well that in this study, but there is a small but significant disagreement at 50°C.

Table 4.12 Temperature Dependence of pK_a^T ($-NH_3^+$) Values of Selected Amino Acids

Amino Acid	25.0 °C	37.1 °C	50.2 °C
2-AE	9.79 ± 0.01	9.50 ± 0.01	9.23 ± 0.01
(Lit. Values)[12]	9.78	**	9.19
4-MAB	10.88 ± 0.04[3]	10.58 ± 0.02	10.29 ± 0.02
4-DMAB	10.14 ± 0.01[93]	9.89 ± 0.01	9.67 ± 0.01
4-A-3-MB	9.67 ± 0.02	9.31 ± 0.02	8.95 ± 0.01
4-A-3,3DMB	10.48 ± 0.03	10.17 ± 0.02	9.86 ± 0.02
5-APe	10.76 ± 0.03	10.54 ± 0.02	10.30 ± 0.02

** None available.

4.4(d) Thermodynamic Constants

Values for the standard, Gibbs free energy change, ΔG°, enthalpy change, ΔH° and entropy change, ΔS°, were calculated from the temperature dependence of pK_a^T using the equations:

$$\Delta G^\circ = -RT\ln K_a^T = 2.3026RTpK_a^T \quad \ldots.(4.1)$$

$$\Delta G^\circ = \Delta H^\circ - T\cdot\Delta S^\circ \quad \ldots.(4.2)$$

$$pK_a^T = \frac{\Delta H^\circ}{2.3026RT} - \frac{\Delta S^\circ}{2.3026R}$$

$$= \frac{\Delta H^\circ}{19.1450}\cdot\frac{1}{T} - \frac{\Delta S^\circ}{19.1450} \quad \ldots.(4.3),$$

using $R = 8.3145\ J\ K^{-1}\ mol^{-1}$.

Therefore, the plot of pK_a^T (y-axis) vs. 1/T (x-axis) is linear, slope = $\Delta H^\circ/19.1450$ and y-axis intercept = $-\Delta S^\circ/19.1450$, assuming ΔH° and ΔS° are independent of temperature.

However, since there are only three experimental points, the accuracy of the line of best fit will be poor if there is any non-linearity. This accuracy can be improved by calculations using the coordinates of the three points.

ΔH°

Eqn. (4.3), ΔH° = (graph slope, $\Delta pK_a^T/\Delta(1/T)$ (K)) x 19.1450 J mol^{-1}.

Three values for the graph slope (and, thus ΔH°) can be calculated by using the coordinates of the three points in pairs, with $\Delta(1/T)$ in K^{-1}:

25.0 and 37.1°C: $\Delta H^\circ = \Delta pK_a^T$ x 1.4636 x 10^5 J mol^{-1}

25.0 and 50.2°C: $\Delta H^\circ = \Delta pK_a^T$ x 7.3242 x 10^4 J mol^{-1}

37.1 and 50.2°C: $\Delta H^\circ = \Delta pK_a^T$ x 1.4661 x 10^5 J mol^{-1}

Generally, there was good agreement between the three values, reflecting the good linearity of the pK_a^T vs. 1/T plots. e.g. for Ser Me.HCl, the three values were 45.37, 44.68 and 43.98, with an average $\Delta H^\circ \pm$ range = (44.7 ± 0.7) kJ mol^{-1}.

ΔS°_{298}

From eqn. (4.3), $\Delta S^\circ = \Delta H^\circ/T - 19.1450pK_a^T$ J K^{-1} mol^{-1}, with ΔH° in J mol^{-1}. While ΔS° is assumed to be independent of temperature, it has to be calculated at a given temperature (usually 298 K) using the pK_a^T at that temperature. Calculations at three temperatures usually yielded identical results, e.g. for Ser Me.HCl, ΔS°_{298} = 15.3 J K^{-1} mol^{-1} = ΔS°_{310} = ΔS°_{323}. Any variation is the result of non-linearity of the pK_a^T vs. 1/T plot.

ΔG°_{298}

Eqn. 4.2, $\Delta G^\circ_{298} = \Delta H^\circ - 298.15 \cdot \Delta S^\circ_{298}$ kJ mol^{-1}, where ΔH° is in kJ mol^{-1} and ΔS°_{298} is in kJ K^{-1} mol^{-1}.

Table 4.13 summarises the ΔG°, ΔH° and ΔS° values for the monoamino acid ester hydrochlorides, while values for some of their parent amino acids are in Table 4.14.

These were calculated using pK_a^T values rounded to 2 d.p., the experimental error.

Table 4.13 Values for pK_a^T, ΔG°, ΔH°, ΔS° and $T \cdot \Delta S^\circ$ for the Proton Dissociation of Some Monoamino Acid Ester Hydrochlorides.

Amino Acid Ester.HCl	pK_a^T (298 K)	ΔG°_{298} * kJ mol^{-1}	ΔH° § kJ mol^{-1}	ΔS°_{298} J K^{-1} mol^{-1}	$298 \cdot \Delta S^\circ_{298}$ kJ mol^{-1}
Ser Me.HCl	7.03	40.2	44.7 ± 0.7	15.3	4.5
Lit. Values[1]	7.03	40.1	45.6 ± 0.5	18.4	5.5
2-AE Me.HCl	7.67(I)	43.7	47.6 ± 2.1	12.8	3.8
Lit. Values[5]	7.66	43.7	48.1	14.6	4.4
2-AP Me.HCl[1]	7.743	44.1	48.1 ± 0.6	13.4	4.0
2-AB Me.HCl[1]	7.640	43.4	47.9 ± 1.9	15.1	4.5
3-AP Me.HCl[1]	9.170	52.3	52.8 ± 1.2	1.7	0.5
3-AP Bz.HCl	9.06	51.7	52.7 ± 1.4	3.4	1.0
4-AB Me.HCl	9.83	56.1	53.5 ± 0.8	-8.7	-2.6
Lit. Values[1]	9.84	56.2	55.2 ± 0.6	-3.3	-1.0
4-AB Et.HCl	9.86	56.3	55.7 ± 0.1	-2.1	-0.6
4-AB Bz.HCl	9.81	56.0	55.7 ± 1.4	-1.1	-0.3
4-MAB Me.HCl	10.00	57.1	41.0 ± 1.5	-53.9	-16.1
4-MAB Et.HCl	10.08	57.5	57.1 ± 1.4	-1.3	-0.4
4-DMAB Me.HCl	9.31(I)	53.0	32.1 ± 0.8	-70.2	-20.9
4-DMAB Et.HCl	9.29	53.1	38.9 ± 0.7	-47.7	-14.2
4-A-3-MB Me.HCl	9.45	53.4	52.2 ± 1.4	-4.1	-1.2
4-A-3,3 DMB Me.HCl	9.23	52.7	40.3 ± 0.8	-41.6	-12.4
5-APe Me.HCl	10.15	57.9	63.0 ± 1.4	16.9	5.1
5-APe Et.HCl	10.10	57.6	52.0 ± 0.7	-19.0	- 5.6

*Note: This has been calculated from: $\Delta G^\circ_{298} = \Delta H^\circ - 298.15 \cdot \Delta S^\circ_{298}$

These values sometimes differ very slightly (by 0.1 kJ mol^{-1}) from those calculated using:

$\Delta G^\circ_{298} = 2.3026RTpK_a^T(298) = 5.7081pK_a^T(298)$ kJ mol^{-1} because of rounding. The same procedure has been used in similar Tables which follow, e.g. 4.14, 4.15.

§Errors are spread of 3 calculated values.

Table 4.14 Values for pK_a^T, ΔG°, ΔH°, ΔS° and $T \cdot \Delta S^\circ$ for the Proton Dissociation of Some Monoamino Acids.

Amino Acid	pK_a^T (298 K)	ΔG°_{298} * kJ mol^{-1}	ΔH° § kJ mol^{-1}	ΔS°_{298} J K^{-1} mol^{-1}	$298 \cdot \Delta S^\circ_{298}$ kJ mol^{-1}
Ser Lit. Values [1]	9.260	52.9	42.4 ± 0.7	-35.1	-10.5
[17]	9.208	52.6	43.6	-30.1	-9.0
2-AE	9.79	55.8	41.0 ± 1.4	-49.8	-14.8
Lit. Values [12]	9.78	55.7	43.9	-39.7	-11.8
[14]	9.78	55.9	45.0	-36.6	-10.9
2–AP Lit. Values [1]	9.916	56.6	43.5 ± 1.0	-43.9	-13.1
[17]	9.87	56.4	45.7	-35.9	-10.7
2–AB Lit. Values [1]	9.852	56.3	44.2 ± 1.4	-40.6	-12.1
[17]	9.830	56.1	45.4 ± 0.3	-36.0	-10.7
3–AP Lit. Values [1]	10.333	59.1	47.2 ± 0.4	-39.8	-11.9
[17]	10.238	58.5	47.3 ± 0.2	-37.7	-11.2
4-AB Lit. Values [1]	10.565	60.2	49.0 ± 1.7	-37.6	-11.2
[17]	10.556	60.2	52.1 ± 0.4	-27.2	-8.1
4–MAB	10.88	62.1	43.2 ± 0.7	-63.4	-18.9
4–DMAB	10.133	57.8	34.4 ± 2.2	-78.6	-23.4
4-A-3-MB	9.67	55.1	51.3 ± 1.2	-12.8	-3.8
4-A-3,3-DMB	10.48	59.8	44.7 ± 0.7	-50.6	-15.1
5-APe	10.76	61.4	33.7 ± 1.5	-93.0	-27.7
6-AH Lit. Values[17]	10.804	61.7	56.7	-16.7	-5.0

* ΔG°_{298} values calculated using same procedure as for Table 4.13.

§Errors are spread of 3 calculated values.

4.5 Discussion

4.5(a) Literature Values

As can be seen from Tables 4.9, 4.10, 4.11 and 4.12, pK_a^T values obtained in this study generally agree with the available literature values, within the experimental error limits. The errors quoted in this study, and usually in the literature, are the range of the set of results, but where this is less than 0.01 pK_a^T, the "real" error is probably at least ±0.01. If no literature range is given, this can be taken to be least ±0.01. Disagreements beyond ± 0.01 are probably due to different conditions (sometimes unstated), e.g. I > 0.1 mol l^{-1}.

4.5(b) Substituent Effects

The effect of structural changes on the pK_a^T of the $-NH_3^+$ ionisation in H_2O for aliphatic systems, arises mainly from the following factors:

1. Changes in electronic effects (mainly ±**I**). These are quantitatively correlated by the Taft equation.[20]

$$\log_{10}\left(\frac{K}{K_\circ}\right) = \sigma^*\rho^* \qquad \ldots.(4.4)$$

   Such effects change bond energies and are only one of the many contributors to ΔH° for the ionisation.

2. Changes in nett solvent bonding. This is the other major contributor to ΔH° and arises, in aqueous solution, from changes in number of H-bonds between $-NH_3^+$ and H_2O's. Solvation effects are expected to be large for these ionisations in the highly polar H_2O solvent.

3. Changes in ΔS°. This reflects the change in disorder and is likely to be dominated by the large solvation effects.

Clearly, all factors must be considered in explanations for the relative pK_a^T values across a set of structurally related compounds. As a consequence, arguments based on data at a single temperature (i.e. lacking ΔH°, ΔS° values) are of very limited validity, e.g. the order of decreasing acid strength of methyl substituted ammonium ions in water at 25°C (Table 4.15) is: $NH_4^+ > (CH_3)_3NH^+ > CH_3NH_3^+$ sl.> $(CH_3)_2NH_3^+$.

Clearly, this order cannot be rationalised solely on the basis of the **+I** effect of $-CH_3$ group. Such an effect decreases the ease of proton loss (increase pK_a^T) and predicts the order of decreasing acid strength should be the order of increasing number of CH_3's (increasing total **+I**): $NH_4^+ > CH_3NH_3^+ > (CH_3)_2NH_2^+ > (CH_3)_3NH^+$. Interestingly, this is exactly the order observed in the gas phase,[19] indicating that solvent effects are very important for the aqueous solutions as expected. Because the overall value of ΔH° is a balance between mainly inductive and nett solvent bonding effects, it can be seen (Table 4.15) that the values of ΔH° fluctuate along the series of methyl substituted ammonium ions. Accompanying this are the increasingly negative ΔS°_{298} values. As a result ΔG°_{298} (and hence pK_a^T (298 K)) varies erratically along the series.

(i) Monoamino Acid Ester Hydrochlorides

These can be treated as substituted *n*-alkyl ammonium ions, $R–NH_3^+$, which have a typical $pK_a^T \sim 10.6$ at 25°C (bottom half of Table 4.15). The thermodynamics for the ionisation of protonated amines has been discussed by Christensen et al.[17] This paper is mainly concerned with trends in ΔH°, ΔS° with structural change; little is mentioned about the origins of the general values for these parameters, e.g. why is ΔH° large and positive, while ΔS° is negative for the *n*-alkylammoniums? These are defined from the reactions (with the analogous ester hydrochloride ionisation given for comparison):

n-alkylammonium: $RNH_3^+{}_{(aq)} \rightleftharpoons RNH_{2(aq)} + H^+_{(aq)}$

ester.HCl: $\underset{(EH^+_{(aq)})}{RCH(NH_3^+)COOCH_{3(aq)}} \rightleftharpoons \underset{(E_{(aq)})}{RCH(NH_2)COOCH_{3(aq)}} + H^+_{(aq)}$

ΔH° is defined by:

$$\Delta H^\circ (n\text{-alkylammonium}) = H^\circ(R–NH_{2(aq)}) + H^\circ(H^+_{(aq)}) - H^\circ(R\text{-}NH_3^+{}_{(aq)}) \quad \ldots.(4.5)^\dagger$$

$$\Delta H^\circ (\text{ester.HCl}) = H^\circ(E_{(aq)}) + H^\circ(H^+_{(aq)}) - H^\circ(EH^+_{(aq)}) \quad \ldots.(4.6),$$

with similar definitions for ΔS°.

Table 4.15 Literature Values for pK_a^T, ΔG°, ΔH°, ΔS° and $T \cdot \Delta S^\circ$ for the Proton Dissociation of Some Alkylammonium Compounds.

Alkylammonium Ref.	pK_a^T (298K)	ΔG°_{298} kJ mol^{-1}	ΔH° kJ mol^{-1}	ΔS° J K^{-1} mol^{-1}	$298 \cdot \Delta S^\circ_{298}$ kJ mol^{-1}
NH_4^+ [17]	9.25	52.8	52.3	-1.8	-0.5
[19]	9.24	52.7	52.3	-1.3	-0.4
$CH_3NH_3^+$ [17]	10.65	60.9	55.2	-19.0	-5.7
[19]	10.64	60.7	55.6	-17.2	-5.1
$(CH_3)_2NH_2^+$ [17]	10.78	61.5	50.4	-37.4	-11.1
[19]	10.73	61.3	50.4	-36.4	-10.9
$(CH_3)_3NH^+$ [17]	9.80	55.9	36.9	-63.8	-19.0
[19]	9.75	55.6	36.8	-63.2	-18.8
$CH_3CH_2NH_3^+$ [17]	10.67	61.0	57.4	-12.1	-3.6
[19]	10.63	60.8	57.4	-11.3	-3.4
$CH_3(CH_2)_2NH_3^+$ [17]	10.56	60.3	57.9	-8.1	-2.4
[19]	10.57	60.4	57.9	-8.4	-2.5
$CH_3(CH_2)_3NH_3^+$ [19]	10.64	60.7	58.5	-7.5	-2.2
$CH_3(CH_2)_4NH_3^+$ [17]	10.63	60.7	58.5	-7.3	-2.2
[19]	10.64	60.8	58.5	-7.5	-2.3
$CH_3(CH_2)_5NH_3^+$ [17]	10.64	60.7*	**	**	**

*Calculated from $\Delta G^\circ_{298} = 5.7081 pK_a^T(298)$.

**None available.

†Footnote

It can be argued that such ionization should involve one H_2O molecule on the LHS and consequently there is a 2 particles to 2 particles reaction i.e no nett change in the number of particles. However, it can also be argued that the departing proton is already hydrated and so there is no need for the additional H_2O on the LHS. However, which argument is the more valid is of little consequence in determining ΔH° and ΔS° since the major contributor is the change in the number of h-bonded H_2O's.

The value for ΔH° for ionisations in aqueous solution arise mainly from changes in bond energies which usually include some contribution from solvation, chiefly intermolecular H-bonding changes.

For the *n*-alkylammonium ionisation, the large positive, ΔH° values (~ +58 kJ mol^{-1}) mean that the H° sum for $R–NH_{2(aq)}$ and $H^+_{(aq)}$ is much larger than H° for $R–NH_3^+{}_{(aq)}$. This is mainly due to the loss of one of the ammonium N-H bonds in the ionisation; bond breaking is endothermic. Smaller contributions to ΔH° will arise from the change in the R-N bond energies from $R–NH_3^+$ (σ^* ($-NH_3^+$) = +3.76,[20] strong –**I**) to $R–NH_2$ (σ^* ($-NH_2$) = +0.62,[20] moderate –**I**); overall a negative contribution to ΔH°. There is also a contribution from the change in the extent of the weak, intermolecular H-bonding. This will be extensive for $H^+_{(aq)}$, moderate for $R–NH_3^+{}_{(aq)}$ but much smaller for $R–NH_{2(aq)}$ (because of the loss of the positive charge and one of the N-H's). Therefore, there is probably a small increase in nett H-bonding giving a small negative contribution to ΔH°. Overall, these two negative contributions are far outweighed by the large positive enthalpy change for the N-H bond breaking, which results in ΔH° being ~ +58 kJ mol^{-1}.

The ΔS° can give some indication of the change in hydration extent. Simplistically, this measures the nett change in disorder on ionisation. This is controlled partly by a combination of a change in the number of particles (1 to 2 in these reactions, a positive contribution to ΔS°, see also footnote on p. 123) and the change in the number of H-bonded H_2O's. For the *n*-alkylammoniums, ΔS° is typically -9 J K^{-1} mol^{-1} (although $CH_3NH_3^+$ is ~ -18 J K^{-1} mol^{-1}), Table 4.15. This increase in order supports the suggestion from the ΔH° discussion above, that there is a nett increase in the number of H-bonded H_2O's. Such a negative contribution to ΔS° is expected to outweigh the negligible contribution from the 1 to 2 particle change (because of the large number of H-bonded H_2O's involved), resulting in small negative values for ΔS°.

2-Amino Acid Methyl Ester Hydrochlorides $RCH(NH_3^+)COOCH_3.Cl^-$

Here, the strongly –**I**, $-COOCH_3$ group ($\sigma^* = 2.00$)[20,21] close to the $-NH_3^+$ greatly increases its ease of proton loss (increases acidity, decreases pK_a^T) by weakening the $-NH_2^+$ to H bond. These compounds typically have $pK_a^T \sim 7.7$ at 25°C (Table 4.13). The same argument applies to the ethyl and benzyl ester hydrochlorides. Thus the introduction of the methoxycarbonyl group has increased the acidity over that for the *n*-alkylammoniums by ~10^3 times. Ser Me.HCl is even more acidic (pK_a^T ~7.0), because of its additional –**I**, CH_2OH, group.

Again, as for the *n*-alkylammoniums, a more complete picture of the factors controlling the pK_a^T values can be obtained by examining the ΔH° and ΔS° values for the deprotonation reactions.

ΔH° decreases from ~58 kJ mol^{-1} for the *n*-alkylammoniums (Table 4.15) to ~ 48 kJ mol^{-1} for the 2-amino acid ester hydrochlorides (Table 4.13). As before, the two main factors which control changes in ΔH° values for the ionisation in aqueous solution (changes in bond energies arising from the changes in inductive effects, and changes in nett solvent bonding) must be considered. Introduction of the strongly –**I**, $-COOCH_3$, substituent facilitates deprotonation by lowering the $^+$N-H bond energy and decreasing ΔH°.

The sign of the other factor contributing to the overall ΔH° value, changes in nett solvent bonding, can be gauged from the ΔS° value. For the 2-amino acid ester hydrochlorides this is typically ~ +14 J K^{-1} mol^{-1} (Table 4.13) whereas for the *n*-alkylammoniums it is ~ -9 J K^{-1} mol^{-1} (Table 4.15). This ~ 23 J K^{-1} mol^{-1} increase in ΔS° (increase in disorder) suggests that introducing the methoxycarbonyl group has decreased the extent of hydration on ionisation; the number of particles change (1 to 2) is the same for the two reactions. This decrease in solvent bonding for the $EH^+_{(aq)} \rightarrow E_{(aq)} + H^+_{(aq)}$ reaction relative to $R\text{–}NH_3^+{}_{(aq)} \rightarrow R\text{–}NH_{2(aq)} + H^+_{(aq)}$ will result in a positive contribution to ΔH°.

Hence, the overall decrease in ΔH° is due solely to the –I effect of the $-COOCH_3$ and would have been larger in the absence of solvation effects. The relative decrease in solvation could be due to decreased solvation in the E cf. $R-NH_2$ and/or increased solvation in EH^+ cf. $R-NH_3^+$. Both are likely to occur: in E, the –I effect of the $-COOCH_3$ group will reduce the electron density on the tertiary N (delocalises the lone pair) and this will hinder H-bond formation by making the N–H bond less polar For the reactant, EH^+, the –I effect will remove electron density away from the quarternary N^+ resulting in strengthening H-bonding by increasing the positive charge on the nitrogen H's.

Table 4.13 also shows the relative contributions made by ΔH° and $T \cdot \Delta S^\circ$ to ΔG° (i.e. pK_a^T). For 2-amino acid ester hydrochlorides, ΔH° (~ +48 kJ mol^{-1}) dominates $298 \cdot \Delta S^\circ_{298}$ (~ +4 kJ mol^{-1}). Thus the two terms work against each other resulting in $\Delta G^\circ_{298} \sim +44$ kJ mol^{-1}.

Christiensen et al.[17] assume that these "compensating" (because $\Delta G^\circ = \Delta H^\circ - T \cdot \Delta S^\circ$) changes in ΔH° and ΔS° with increasing hydrocarbon chain length are due to "hydrocarbon chain stiffening". The hydrocarbon chain "loses both rotational enthalpy and entropy under the influence of an ionic charge". Thus ΔH° and ΔS° would be expected to become more positive with increasing chain length for "isoelectric reactions" such as $EH^+_{(aq)} \rightarrow E_{(aq)} + H^+_{(aq)}$. These authors observed this effect for proton ionisations for *n*-alkylammoniums and 2-amino acids ($-NH_3^+$ group). The –COOH ionisation for the 2-amino acids showed the reverse trend (ΔH° and ΔS° become more negative with increasing chain length "as expected for an iongenic reaction").

This "hydrocarbon chain stiffening with increasing chain length" is another factor contributing to the trends in ΔH° and ΔS°. Changes in bond energies raising from changes in inductive effects and changes in nett solvent bonding are also important. The relative contributions of all these factors are such that overall both ΔH° and ΔS° increase with increasing chain length.

ω-Amino Acid Ester Hydrochlorides

Many of the ester hydrochlorides studied are members of the homologous series:

$$H_3N^+(CH_2)_nCOOCH_3.Cl^- \qquad n = 1, 2,.....5$$

As can be seen (Table 4.16), the pK_a^T rises sharply from 2-AE Me.HCl (n = 1) to 3-AP Me.HCl (n = 2) with progressively smaller increases to the 4-, 5- and 6-amino acid ester hydrochlorides. This is usually explained just in terms of inductive effects: the strong –**I** of the $-COOCH_3$ decreases rapidly (~ exponentially) with increasing number of CH_2's resulting in a rapid fall off in its acid strengthening (pK_a^T lowering) effect. By 6-AH Me.HCl, pK_a^T has risen to almost that of a typical *n*-alkylammonium (Table 4.15).

Table 4.16 Summary of the Changes in pK_a^T, ΔG°, ΔH°, ΔS° and $T\cdot\Delta S^\circ$ as a Function of ω-Amino Acid Ester Hydrochloride Chain Length.

Amino Acid Ester.HCl	pK_a^T (298 K)	ΔG°_{298} kJ mol^{-1}	ΔH° kJ mol^{-1}	ΔS°_{298} J K^{-1} mol^{-1}	$298\cdot\Delta S^\circ_{298}$ kJ mol^{-1}
2-AE Me.HCl	7.67	43.8	47.6	12.9	4.0
3-AP Me.HCl	9.17[1]	52.4	52.8	1.7	0.5
4-AB Me.HCl	9.83	56.1	53.5	-8.7	-2.6
5-APe Me.HCl	10.15	57.9	63.0	17.0	5.1
5-APe Et.HCl	10.10	57.7	51.3	-21.4	-6.4
6-AH Me.HCl	10.47[4]	59.8*	**	**	**

*Calculated from $\Delta G^\circ_{298} = 5.7081 pK_a^T(298)$.

** None available.

However, this pK_a^T (ΔG°) behaviour hides a complicated interplay between ΔH° and $T\cdot\Delta S^\circ$ (Table 4.16 and Figure 4.3). This Figure also gives a comparison with the behaviour of the parent amino acids and *n*-alkylammoniums .

For the methyl ester hydrochlorides, withdrawal of the –**I**, $-COOCH_3$, group from $-NH_3^+$ reduces the weakening of the NH_2^+ to H bond. This reduction in $H^\circ(EH^+_{(aq)})$

Figure 4.3 (a) ΔG°, ΔH° and ΔS° vs. No. of Carbons in Alkyl Chain for; Amino Acid Ester Hydrochlorides, Their Parent Amino Acids and Corresponding Straight Chain Alkylammoniums.

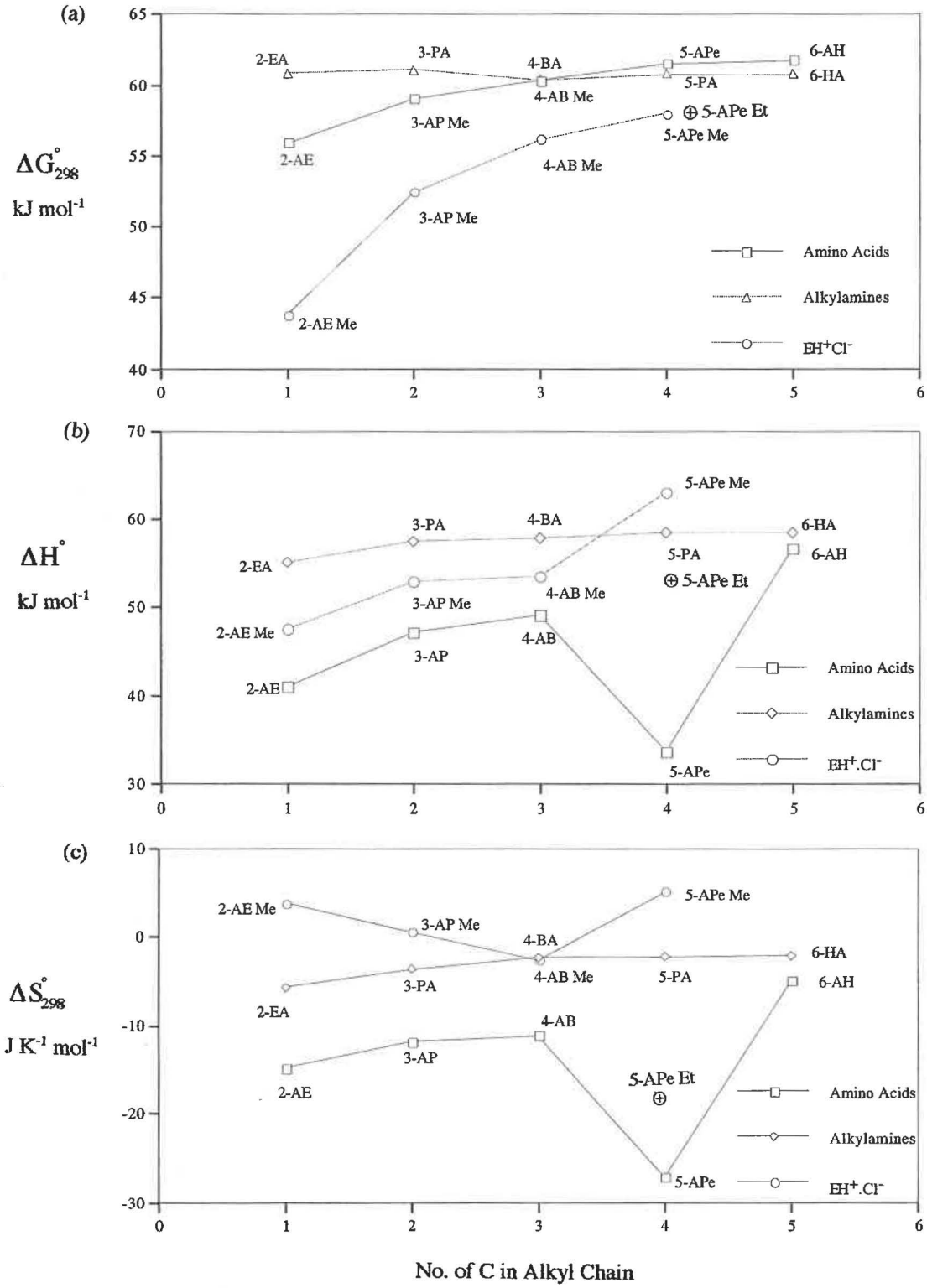

(2-EA = 2-ethylamine, 3-PA = 3-propylamine, 4-BA = 4-butylamine, 5-PA = 5-pentylamine and 6-HA = 6-hexylamine)

will give a positive contribution to ΔH° (see eqn. 4.6). Changes in the other main factor controlling ΔH°, the nett solvent bonding change, can be estimated from ΔS°. This steadily decreases (Table 4.16) from 2-AE Me.HCl to 4-AB Me.HCl; at 5-APe Me.HCl there is a dramatic increase, but in contrast the analogous ethyl ester continues the steady decrease. No data is available for 6-AH Me.HCl. Ignoring the 5-APe esters, the steady decrease in ΔS° suggests that the decrease in the extent of hydration in the ionisation gets smaller with increasing chain length, i.e. the high solvation of EH^+ cf. E disappears by 4-AB Me.HCl which has a ΔS° that is similar to that for a typical *n*-alkylammonium (Table 4.15). This is what would be expected from the decrease in the **–I** effect of the $-COOCH_3$ group on the N electron densities in the $-NH_3^+$ group (hence a decrease in H-bonding to H_2O) and the $-NH_2$ group (hence an increase in H-bonding to H_2O). The result will be a negative contribution to ΔH° with increasing chain length.

The overall balance between these two opposing contributions is a small increase in ΔH° from 2-AE Me.HCl to 3-AP Me.HCl (by ~ 5 kJ mol^{-1}) with little change from the 3- to 4-amino acid ester hydrochlorides.

The values of ΔH° and ΔS° for 5-APe Me.HCl and its parent acid are clearly anomalous, but $\Delta G^\circ (pK_a^T)$ values are not (Figure 4.3). It is obviously very important to separate out the ΔH° and ΔS° contributions to ΔG° in order to understand what is happening in these ionisations. For 5-APe Me.HCl, ΔH° and ΔS° are both anomalously high. The ΔH° value indicates either an abnormally large value for $H^\circ(E_{(aq)})$ or a low value for $H^\circ(EH^+_{(aq)})$ (eqn. 4.6) associated with the four CH_2's between the $-COOCH_3$ and $-NH_3^+$ groups. The most likely explanation for this is that intramolecular H-bonding becomes important at n = 4 (Figure 4.4). Such an interaction is favoured by this large 8-membered ring.[22]

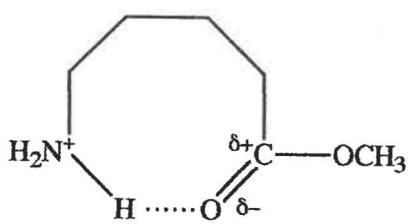

Figure 4.4 Intramolecular H-Bonding in the EH^+ Form of 5-APe Me

This intramolecular H-bonding will stabilise (lower the H°) of the $EH^+_{(aq)}$ form , thus increasing ΔH° (eqn. 4.6). Its ionisation to $E_{(aq)}$ plus $H^+_{(aq)}$ will disrupt a highly ordered structure, resulting in an abnormal increase in disorder (ΔS°), as observed (Table 4.16). In contrast, ionisation of other amino acid ester hydrochlorides, and the *n*-alkylammoniums, involves no such increase in internal freedom and their ΔS°'s are lower. This argument assumes that change in the contribution to ΔS° from intermolecular H-bonding is small compared to that for the H-bonding, Scheme 4.6, and that any intramolecular H-bonding in $E_{(aq)}$ is relatively insignificant.

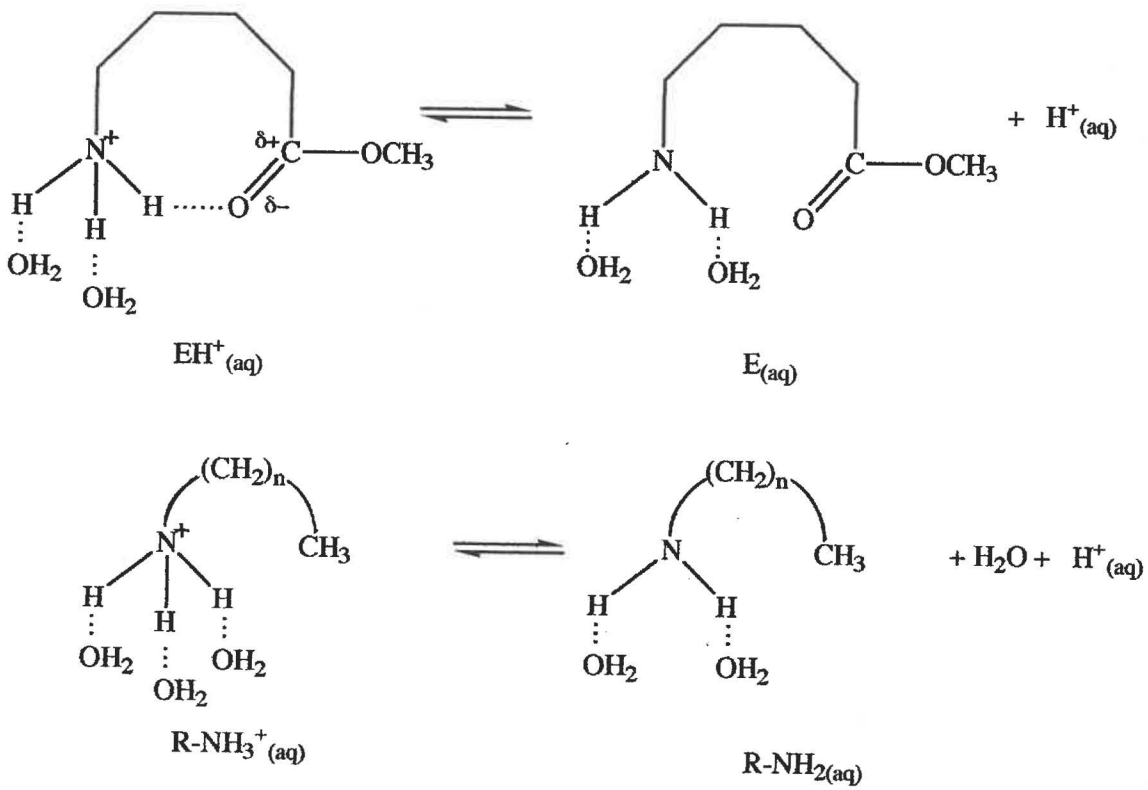

Scheme 4.6 Comparison of H-bonding of Proton Ionisations for 5-APe Me.HCl and *n*-Alkylammoniums.

Oddly, this intramolecular H-bonding does not effect the $pK_a^T(\Delta G^\circ)$ value for 5-APe Me.HCl. It is commonly argued that such bonding, by "stabilising" the EH^+ form, will make H^+ loss more difficult and hence raise the pK_a^T. In this particular case there appears to be a balance in the ΔH° and $T\cdot\Delta S^\circ$ effects produced by intramolecular

H-bonding, which results in a neutral effect on ΔG°; again, the importance of looking at the effect of temperature on pK_a^T is clear.

Further evidence supporting intramolecular H-bonding in the EH^+ form of 5-APe Me comes from the kinetics results (Chapter 5). The rate constant for the alkaline hydrolysis of EH^+ is abnormally large (Table 5.11), which can be explained by intramolecular H-bonding assistance.

Unexpectedly, the ethyl ester of 5-APe lacks the abnormal behaviour of the methyl ester. While its pK_a^T is similar, the ΔH° value is much lower and similar to that for 4-AB Me.HCl and 3-AP Me.HCl (Table 4.16). The ΔS° value is much lower; while it continues the expected falling trend with increasing chain length (Figure 4.3 (c)), it is anomalously low because it is more negative than for the corresponding *n*-alkylammonium. The simplest explanation is that there is no intramolecular H-bonding in the EH^+ form of 5-APe Et. Support for this comes from the kinetic results: the rate constant for the alkaline hydrolysis of the EH^+ form of 5-APe Et is "normal" and shows no sign of catalysis by intramolecular H-bonding.

It is difficult to explain how replacing $-OCH_3$ by $-OC_2H_5$ could produce such a dramatic change. Electronic effects seem unlikely to be responsible since the two groups have similar, moderate –I effects (σ^* ($-OCH_3$ = +1.81);[21] (σ^* ($-OC_2H_5$ = +1.68).[21] Sterically, the $-OC_2H_5$ is more bulky than $-OCH_3$ but it is hard to understand how increased bulk at the carbonyl C could prevent intramolecular H-bonding. It has been suggested[22] that the reverse occurs at the amino N; increased bulk here is responsible for increased intramolecular H-bonding and hence anomalous properties of $^+NH(CH_3)_2(CH_2)_nCOOCH_3$ (n = 2, 3). The effect of changing the ester group on the properties of the EH^+ form of 5-APe esters clearly needs further investigation.

A hint that the answer may lie in the unusual solvation effects is that ionisation of the protonated ethyl ester ($EH^+_{(aq)}$ to $E_{(aq)} + H^+_{(aq)}$) has an abnormally low value for ΔS°, -21.4 J K^{-1} mol^{-1}. This is much more negative than for the corresponding *n*-alkylammonium (-7.4 J K^{-1} mol^{-1}), i.e. there is an abnormal decrease in disorder) in

forming $E_{(aq)}$. The simple explanation would be a highly ordered $E_{(aq)}$ due to intramolecular H-bonding, but this would then be expected in EH^+ as well and why is the methyl ester so different?. Unfortunately, kinetic results are of no help. The E form of 5-APe esters undergoes intramolecular aminolysis (not the $B_{Ac}2$ hydrolysis of the EH^+ form), the rds of which is not expected to be affected by intramolecular H-bonding. Rate constant values, k_L, appear "normal" (Table 5.11).

One possible explanation for the anomalous behavior of the EH^+ form of 5-APe Me is that it is an artifact caused by rapid alkaline hydrolysis. This problem makes it difficult to obtain accurate values for pK_a^T (4.2(b), Method 3 p. 100). Considerable effort was put into obtaining the best possible values and 5-APe Me.HCl and 5-APe Et.HCl behaved consistently differently at the three temperatures (Table 4.11). However, there remains the possibility that the 5-APe ester hydrochloride pK_a^T's are too low because of hydrolysis, particularly for the faster hydrolysing methyl ester. If this is the case, then the kinetic analysis used to separate and evaluate k_{EH^+} and (k_E + k_L) (5.3(c)) will be affected because it uses K_a^T. Changes in this will change the value of k_{EH^+} and this may compromise the kinetic support for intramolecular H-bonding. Examination of the effect of raising the pK_a^T (5-APe Me.HCl), at 25°C, from the experimental value, 10.15, to 10.20, 10.25 and 10.30 showed that k_{EH^+} rises from 546 to 551, 556 and 560 l mol^{-1} min^{-1}; (k_E + k_L) also rises from 36,380 to 40,360, 44,855 and 49,885 l mol^{-1} min^{-1}. Analysis plots (Table 5.10) remained linear throughout (r ~ 0.995). The effect of this large increase in K_a^T (~29%) is only a small increase (~2.6%) in k_{EH^+}. A similar result was obtained for the ethyl ester. It can be concluded that the values for k_{EH^+} are "real" and the anomalously large k_{EH^+} (5-APe Me) is good kinetic support for intramolecular H-bonding in the EH^+ form of 5-APe Me.
This conclusion is further supported by the kinetics result for the alkaline hydrolysis of 2,5 diaminopentanoic acid methyl ester (2,5-DAPe Me) . Again, the EH^+ form (2-NH_2, 5-NH_3^+) is anomalously reactive; at 25°C, the value of k_{EH^+}/k_E is ~ 2000[4] in contrast to ~2.8[1] for 2,6-diaminohexanoic acid methyl ester (2,6-DAH Me). It has been argued[23] that this is mainly due to the direct –I effect of an intramolecular H-bond between the 5-NH_3^+ and the C=O groups which involves an 8-membered ring. No such acceleration occurs for 2,6-DAH Me because the required 9-membered

ring is too large. Only 7 and 8-membered rings show rate accelerations. Oddly, the $pK_a^T(\Delta G^\circ)$ (5-NH_3^+) for 2,5-DAPe Me is abnormally low which is the reverse of what would be expected on the basis of the simple argument: "intramolecular H-bonding stabilises the EH^+ form so inhibiting deprotonation". Remembering that for 5-APe Me, intramolecular H-bonding in the EH^+ form produces no change in $pK_a^T(\Delta G^\circ)$, it is clear that ΔH° and ΔS° values are needed before drawing any conclusions. **Trends in pK_a^T values at a single temperature are often misleading.**

For 6-AH Me.HCl, the pK_a^T (10.47)[4] is still slightly less than that for a typical *n*-alkylammonium (~10.6) despite the **–I** effect of the $-NH_3^+$ having become negligible. This lowering of pK_a^T is probably due to small solvation effects associated with the weakly polar $-COOCH_3$ group, but no ΔH°, ΔS° values are available to check this. The kinetics results support the lack of any **–I** effect by the 6–NH_2 group on $-COOCH_3$; at 25°C, the values of k_E for 6-AH Me and 2,6-DAH Me are ~9[(4)] and ~28[(1)] l mol^{-1} min^{-1}, respectively. The value for 6-AH Me is similar to that for methyl acetate (~9 l mol^{-1} min^{-1})[24] while the value for 2,6-DAH Me is increased by the **–I** effect of the 2-NH_2 group, and is similar to that for most 2-amino acid methyl esters (~23 l mol^{-1} min^{-1}, except for 2-AE Me (~72 l mol^{-1} min^{-1})).[3]

N-methylated Amino Acid Ester Hydrochlorides

The effect of N-methylation was examined only for the 4-AB methyl and ethyl esters so data is limited and any conclusions are tentative. Simplistically, inductive effects predict that replacing nitrogen-H's by the **+I** $-CH_3$ group should increase the nitrogen's basicity (decrease its acidity; decrease K_a^T and increase pK_a^T). Consequently, the predicted order of decreasing acid strength (increasing pK_a^T) for the 4-AB methyl (or ethyl) ester hydrochlorides, at a given temperature, should be:

4-AB Me.HCl > 4-MAB Me.HCl > 4-DMAB Me.HCl

1° 2° 3°

In fact (Table 4.11), 4-DMAB Me.HCl is the strongest acid (has the lowest pK_a^T) and the order at 25°C is:

4-DMAB Me.HCl > 4-AB Me.HCl > 4-MAB Me.HCl

	3°	1°	2°
pK_a^T	9.31	9.82	10.00

This order is the same at 37 and 50°C, and is the same for the ethyl esters at all three temperatures.

Clearly, inductive effect arguments are again inadequate. Such simple arguments ignore ΔH° and ΔS° contributions arising from solvation effects. For alkylammonium ions in aqueous solution, N-methylation produces erratic changes in pK_a^T because of a delicate balance between ΔH° and ΔS° (Table 4.15 and previous discussion, p. 124); this results in the order of decreasing acid strengths:

$(CH_3)_3NH^+ > CH_3NH_3^+ > (CH_3)_2NH_2^+$

	3°	1°	2°
pK_a^T	9.80	10.65	10.75

which is the same as for the N-methylated amino acid ester hydrochlorides and for the parent amino acids (see p. 144). It has been suggested[3] that ammonium ions have unusual pK_a^T's because of the presence of two opposing effects of N-methylation: stabilisation of the cation by delocalisation of the N's positive charge ($-CH_3$'s +I effect) and destabilisation of the cation by reducing intermolecular H-bonding to the solvent. The balance between these two effects should be reflected in the ΔH° and ΔS° values. These have been extracted from Tables 4.13 (monoamino acid ester hydrochlorides) 4.14 (monoamino acids) and 4.15 (alkylammoniums) into Table 4.17 for ease of comparison. While the pattern of ΔG°'s (pK_a^T) is obviously going to be the same for all three classes of compounds, there are interesting variations within the sets of contributing ΔH° and ΔS° values:

For the ***n*-alkylammoniums**, the origin of the values for ΔH° and ΔS° have been discussed (p. 124). The trend with increasing N-methylation is that both ΔH° and ΔS° decrease (Table 4.17). N-methylation, by pushing electron density onto the

Table 4.17 Effect of N-Methylation on Balance Between ΔH° and $T \cdot \Delta S^\circ$ for 4-AB Ester Hydrochloride 4-AB Acid and Alkylammonium Proton Dissociations.

Amino Acid Ester.HCl	pK_a^T (298 K)	ΔG°_{298} kJ mol^{-1}	ΔH° kJ mol^{-1}	ΔS°_{298} J K^{-1} mol^{-1}	$298 \cdot \Delta S^\circ_{298}$ kJ mol^{-1}
4-AB Me	9.83	56.1	53.5	-8.7	-2.6
4-MAB Me	10.00	57.1	41.0	-53.9	-16.1
4-DMAB Me	9.31	53.0	32.1	-70.2	-20.9
4-AB Et	9.86	56.3	55.7	-2.1	-0.6
4-MAB Et	10.08	57.5	57.1	-1.3	-0.4
4-DMAB Et	9.29	53.1	38.9	-47.7	-14.2

Amino Acid	pK_a^T (298 K)	ΔG°_{298} kJ mol^{-1}	ΔH° kJ mol^{-1}	ΔS°_{298} J K^{-1} mol^{-1}	$298 \cdot \Delta S^\circ_{298}$ kJ mol^{-1}
4-AB [1]	10.57	60.2	49.0	-37.6	-11.2
4-MAB	10.88[3]	62.1	43.2	-63.4	-18.9
4-DMAB	10.14[3]	57.8	34.4	-78.6	-23.4

Alkylammonium	pK_a^T (298 K)	ΔG°_{298} kJ mol^{-1}	ΔH° kJ mol^{-1}	ΔS°_{298} J K^{-1} mol^{-1}	$298 \cdot \Delta S^\circ_{298}$ kJ mol^{-1}
$CH_3NH_3^+$ [17]	10.65	60.9	55.2	-19.0	-5.7
$(CH_3)_2NH_2^+$ [17]	10.78	61.5	50.4	-37.4	-11.1
$(CH_3)_3NH^+$ [17]	9.80	55.9	36.9	-63.8	-19.0

ammonium N^+ will stabilise its positive charge and hence lower $H^\circ(R\text{-}NH_3^+{}_{(aq)})$ relative to $H^\circ(R\text{-}NH_{2(aq)})$, so giving a positive contribution to ΔH°. At the same time, nett intermolecular H-bonding to H_2O's is reduced (as indicated by a steady fall in ΔS° values) raising $H^\circ(R\text{-}NH_3^+{}_{(aq)})$ relative to $H^\circ(R\text{-}NH_{2(aq)})$, and giving a negative contribution to ΔH°. Overall, this solvent effect dominates, so the originally large positive ΔH° decreases on N-methylation.

The abnormally low ΔG° (high acid strength) for the 3° ammonium, $(CH_3)_3NH^+$, appears to be mainly due to a low ΔH° value. This means that either $H^\circ(R\text{-}NH_{2(aq)})$ is lower than expected or that $H^\circ(R\text{-}NH_3^+{}_{(aq)})$ is high. Nett changes in solvation appear not to be responsible for this since ΔS° decreases regularly with increasing N-methylation. One possible explanation is that for 3° ammoniums, the addition of the last $-CH_3$ group produces proportionally more delocalisation of the N's positive charge than for the previous $-CH_3$. This would result in a larger stabilisation of the $R\text{-}NH_3^+{}_{(aq)}$ and a higher ΔH°.

With the **amino acids,** N-methylation produces a pattern that is similar (Table 4.17) to that for *n*-alkylammoniums, suggesting that the $-COO^-$ group is having little nett effect. Again, the main reason for the anomalously high acidity of the 3° compound, 4-DMAB, is an abnormally low ΔH°, with the $T\cdot\Delta S^\circ$ changes being fairly regular (Table 4.17). The cause of the low ΔH° is presumably the same as for the alkylammoniums.

However, N-methylation of the **protonated amino acid esters** produces a more complex pattern of ΔH° and ΔS° values (Table 4.17). The anomalously high acidities of 4-DMAB Me.H^+ and 4-DMAB Et.H^+ are again due to anomalously low ΔH°'s, but there are irregular changes in both ΔH° and ΔS° with increasing methylation. The 4-MAB esters are unusual; for the methyl ester, ΔH° is low while ΔS° is compensatingly also low. In contrast, the values for ΔH° and ΔS° are both high for the ethyl ester. The explanation most likely lies in solvation effects associated with the ester function hence ΔS° is affected which in turn affects ΔH°. More studies need to be made using a wider range of ester groups is needed before a firm conclusion can be drawn.

C-methylated Amino Acid Ester Hydrochlorides

As for N-methylation, only the 4-AB system was investigated. The effect of C-methylation was examined only at C-3 and only for the methyl esters, so the conclusions drawn are clearly just indicative.

Based on inductive effects, progressive replacement of H's at C-3 by the weak +I CH_3 group should produce a small base strengthening (pK_a^T increasing) effect on the 4-NH_3^+ group. The predicted order of decreasing acid strength (increasing pK_a^T), at a given temperature, is:

4-AB Me.HCl > 4-A-3-MB Me.HCl > 4-A-3,3-DMB Me.HCl

However, experimentally it was found that the order was the reverse of this at all temperatures, with 4-A-3,3-DMB Me.HCl being the strongest acid by up to ~ 0.6 pK_a^T units. For ease of comparison, Table 4.18 contains the relevant pK_a^T data extracted from Table 4.11 and the ΔH°, ΔS° data from Table 4.13.

Table 4.18 Effect of C-3 Methylation on pK_a^T, ΔG°, ΔH°, ΔS° and $T \cdot \Delta S^\circ$ for 4-AB Me.HCl.

Amino Acid Ester.HCl	pK_a^T (298 K)	ΔG°_{298}	$\Delta H^{\circ\,\S}$ kJ mol^{-1}	ΔS°_{298} J K^{-1} mol^{-1}	$298 \cdot \Delta S^\circ_{298}$ kJ mol^{-1}
4-AB Me.HCl	9.83[(1)]	56.1	53.5	-8.7	-2.6
4-A-3-MB Me.HCl	9.45	53.4	52.2	-4.1	-1.2
4-A-3,3-DMB Me.HCl	9.23	52.7	40.3	-41.6	-12.4

Again, inductive effect arguments are inadequate: an examination of ΔH° and ΔS° should be more informative. Table 4.18 shows that the high acidity (low pK_a^T, low ΔG°) of the EH^+ form of 4-A-3,3-DMB Me is due to a low ΔH° (~ 13 kJ mol^{-1} less than for the other two compounds) but this is partly counterbalanced by a low ΔS°. The latter suggests that there is an unusually large decrease in disorder (increase in order) on forming $E_{(aq)} + H^+_{(aq)}$ from $EH^+_{(aq)}$; i.e. that either $E_{(aq)}$ has an unusually high degree of order or that $EH^+_{(aq)}$ is much less ordered for 4-A-3,3-DMB Me than for the other two compounds.

One possible explanation is that $EH^+_{(aq)}$ is abnormally disordered because of low solvation due to intramolecular H-bonding between $-NH_3^+$ and $-COOCH_3$ forced by the two gem-methyl groups. This would require a 7-membered intramolecular H-bond and a gauche conformation along the C2-C3 bond (Figure 4.5, Structure I).

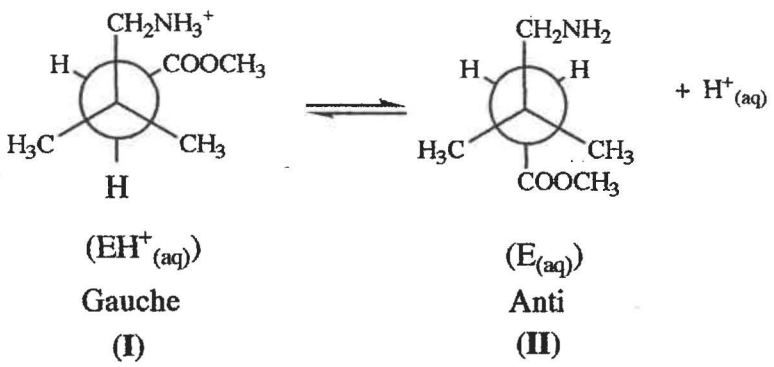

Figure 4.5 Newman Projection Along C2-C3 Bond for 4-A-3,3-DMB Me.H$^+$ Ionisation.

Such conformations are generally energetically disfavoured for steric reasons, but intramolecular H-bonding between the $-NH_3^+$ and carbonyl of the $-COOCH_3$ group may outweigh their steric repulsion (the Gauche Effect).[25,26] Evidence supporting this comes from ^{13}C and ^1H NMR spectra (Table 2.7). In the ^{13}C spectrum of 4-A-3,3-DMB Me.HCl, the gem-methyl C's are a singlet (at 16.3 ppm) which means they are equivalent. Also, all 6 H's attached to the gem-methyl C's are equivalent as they appear as a singlet (at 1.07 ppm) in the ^1H spectrum. Such a pair of results indicate that either there is an internal plane of symmetry in EH^+ (i.e. an interaction between $-NH_3^+$ and $-COOCH_3$ and the gauche conformation) or that there is simply free rotation about the C2-C3 bond (unlikely in view of the bulk of the $-CH_2NH_3^+$ and $-COOCH_3$ groups, Figure 4.5, Structure I). There is also strong kinetic evidence for intramolecular H-bonding in $EH^+_{(aq)}$ (Section 5.5).

Deprotonation of $EH^+_{(aq)}$ will result in the collapse of the intramolecular H-bond, so that $E_{(aq)}$ can adopt the anti conformation (Figure 4.5, Structure II) and there will be "normal" extensive intermolecular H-bonding to the solvent. The resulting "normal" $S^\circ(E_{(aq)})$ combined with the large positive $S^\circ(EH^+_{(aq)})$, results in ΔS° for the ionisation of 4-A-3,3-DMB Me.H$^+$ being abnormally large and negative. As a consequence of

the intramolecular H-bonding in $EH^+_{(aq)}$, it will lack the usual extensive intermolecular H-bonding to H_2O's and so $H^\circ(EH^+_{(aq)})$ would be expected to be abnormally low, resulting in a low ΔH° for the ionisation and a low ΔG°, i.e. enhanced acidity.

Interestingly, this increase in the acidity due to "intramolecular H-bonding in $EH^+_{(aq)}$ is the reverse of what might be expected intuitively, i.e. "intramolecular H-bonding makes proton loss more difficult and so decreases acidity". The enhancement of the NH_3^+'s acidity is driven by solvation effects which outweigh the energy change associated with the intramolecular H-bonding; again the importance of determining the total energy balance, as reflected in the ΔH° and ΔS° values, must be emphasised.

Nature of the Ester (Leaving) Group

Table 4.11 shows that the pK_a^T values for 4-AB Me.HCl, 4-AB Et.HCl and 4-AB Bz.HCl are very similar at all three temperatures. At 25°C, the values range from 9.81 to 9.86, at 37.1°C, 9.42 to 9.48 and at 50.2°C, 9.05 to 9.10. Hence, the nature of the ester group has little effect on $pK_a^T(\Delta G^\circ)$. Examining the components of ΔG°, Table 4.13 shows that there is little variation in both ΔH° (range 53.5 to 55.7 kJ mol^{-1}) and ΔS° (-8.7 to –1.1 J K^{-1} mol^{-1}). Of the factors that contribute to ΔH° and ΔS°, the inductive effect experienced by the $-NH_3^+$ group from the –COOR group is expected to undergo very little change as R changes from $-CH_3$ ($\sigma^* = 0.00$)[21] to $-C_2H_5$ ($\sigma^* = -0.10$)[21] to $-CH_2C_6H_5$ ($\sigma^* = +0.27$)[21] because of the small variation in σ^* and attenuation by the intervening three methylene groups. The major factor contributing to the energy balance, solvation effects, would be expected to be fairly constant because such effects are associated with the weakly polar –COOR group. Its intermolecular H-bonding to the water will be little affected by the small changes in polarity as R changes from $-CH_3$ to to $-C_2H_5$ to $-CH_2C_6H_5$.

Similar results and conclusions can be drawn from the more limited data (one temperature, less R variation in –COOR) for the various ester hydrochlorides of 2-AE, 3-AP, 4-MAB and 4-DMAB (Table 4.11). The 5-APe system shows more pK_a^T variation because of changes in intramolecular H-bonding (see p. 13).

(ii) Glutamic Acid Esters

The pK_a^T values for Glu DMe.HCl and Glu-5-Me.HCl were measured only at one temperature (25°C). Consequently, any explanation for the relative magnitudes of the pK_a^T values is limited to a discussion of the changes in inductive effects provided by structural changes. Glu DMe.HCl can be considered as part of the ester HCl series $RCH(NH_3^+)COOCH_3.Cl^-$, where R = $(CH_2)_2COOCH_3$. Table 4.19 lists the pK_a^T and σ^* values for some members of this series.

Table 4.19 The Effect of Structural (σ^*) Changes on pK_a^T for Series $RCH(NH_3^+)COOCH_3.Cl^-$ §

Ester.HCl	2-AB Me.HCl	2-AP Me.HCl	Glu DMe.HCl	2-AE Me.HCl	Ser Me.HCl
R	CH_2CH_3	CH_3	$(CH_2)_2COOCH_3$	H	CH_2OH
$\sigma^{*\,20,21}$	-0.10	0.00	+0.26	+0.49	+0.62
pK_a^T	7.66[(1)]	7.64[(1)]	7.03†	7.67[(3)]	7.03

§Measured at 25°C and I = 0.1 mol l^{-1}.
†This thesis.

Inductive effects predict that as the electron withdrawing effect experienced by the $-NH_3^+$ increases (i.e. σ^* increases), the acidity (K_a^T) should increase and pK_a^T should fall. In addition to the σ^* in Table 4.19 there is the added, but constant and larger, $\sigma^* = +2.00$ from $-COOCH_3$. Overall, there is clearly no relationship between the total σ^* and the pK_a^T values. Clearly, the simple inductive effect argument is again inadequate, presumably because of larger contribution to ΔH° and ΔS° from solvation effects. A similar treatment for Glu-5-Me.HCl as a member of the amino acid series $RCH(NH_3^+)COO^-$, produces the same type of result (Table 4.20).

Table 4.20 The Effect of Structural (σ^*) Changes on pK_a^T for Series $RCH(NH_3^+)COO^-$. §

Amino Acid	2-AB	2-AP	Glu -5-Me	2-AE	Ser
R	CH_2CH_3	CH_3	$(CH_2)_2COOCH_3$	H	CH_2OH
$\sigma^{*20,21}$	-0.10	0.00	+0.26	+0.49	+0.62
pK_a^T	9.85[(1)]	9.92[(1)]	8.95†	9.79	9.26[(1)]

§Measured at 25°C and I = 0.1 mol l^{-1}.
†This thesis.

Again, it can be concluded that inductive effect explanations for changes in the pK_a^T values for ammonium systems, are of little value.

(iii) Monoamino Acids

ω-Amino Acids

Many of the amino acids studied are members of the ω-amino acid homologous series:

$$H_3N^+(CH_2)_nCOO^- \qquad n = 1, 2, \ldots\ldots 5$$

As can be seen, pK_a^T rises rapidly from 2-AE (n = 1) to 3-AP (n = 2) with smaller rises to the 4-, 5- and 6-amino acids, Table 4.21, ex. Table 4.12 for ease of comparison.

Table 4.21 Summary of the Changes in pK_a^T, ΔG°, ΔH°, ΔS° and $T \cdot \Delta S^\circ$ as a Function of ω-Amino Acid Chain Length.

Amino Acid	pK_a^T (298 K)	ΔG°_{298} kJ mol^{-1}	$\Delta H^{\circ\,\S}$ kJ mol^{-1}	ΔS°_{298} J K^{-1} mol^{-1}	$298 \cdot \Delta S^\circ_{298}$ kJ mol^{-1}
2-AE	9.79	55.8	41.0	-49.8	-14.8
3-AP [1]	10.33	59.1	47.2	-39.8	-11.9
4-AB[1]	10.57	60.2	49.0	-37.6	-11.2
5-APe	10.76	61.4	33.7	-93.1	-27.7
6-AH[17]	10.80	61.7	56.7	-16.7	-5.0

This parallels the trend observed for the ω-amino acid ester hydrochlorides, and is usually explained simplistically in terms of the decreasing –I effect of the -COO^- group. This is described as a weaker –I group than $-COOCH_3$ ($\sigma^* = +2.00$)[21] and so the pK_a^T's of the amino acids are higher than their protonated esters[27]. This difference is ~2 pK_a^T units for the 2-amino case and falls to ~0.4 pK_a^T units by 6-AH (Tables 4.9 and 4.10), in line with the attenuation of inductive effects with increasing chain length. However, the electronic effect exerted by the $-COO^-$ group is controversial; Perrin[14] states that it has $\sigma^* = -1.06$, i.e. is electron donating, but that $-\Delta pK_a^T$ (the acid

strengthening effect) is +0.8 for attachment at the α-carbon, but –0.2 for attachment at the β-carbon, in aliphatic ammoniums. This fails to explain why both 2-AE (pK_a^T = 9.79) and 3-AP (pK_a^T = 10.33) are both stronger acids (lower pK_a^T's, ΔG°'s) than the corresponding *n*-alkylammoinums at 25°C (2-EA = 10.65, 3-PA = 10.56)[17] (Figure 4.3(a)). The $pK_a^T(\Delta G^\circ)$ of the amino acid and its corresponding *n*-alkylammonium become almost equal for the 4-amino case, then as the alkyl chain lengthens further, pK_a^T for the amino acid rises slightly above that for *n*-alkylammoniums.

Again, it is clear that simple inductive effect arguments are inadequate, the ±**I** effect of a neighbouring group is only one of the many energy terms that affect pK_a^T values. Separating ΔG° into its ΔH° and ΔS° components (Figure 4.3 (b),(c)) is revealing; ignoring the anomaly at 5-APe, increasing chain length results in increases in both ΔH° and ΔS°. Again, as for the protonated esters, these are "compensating increases"[17] and result in $pK_a^T(\Delta G^\circ)$ increasing by only a small amount with increasing chain length. This contrasts with the very large ΔG° increases seen for the protonated esters.

Christensen et al.[17] conclude that if the charges on a zwitterion (e.g. an amino acid) "have a larger chain stiffening effect than a single ionic charge", then it is expected that ΔH° and ΔS° would become more positive with increasing hydrocarbon chain length. As for the protonated ester, the other important factors are changes in bond energies due to changes in inductive effects and changes in nett solvent bonding. An additional factor in these zwitterions, $H_3N^+(CH_2)_nCOO^-$, is changes in the electrostatic effect of the $-COO^-$ on the ease of $-^+NH_2$ to H bond breaking with changes in chain length.

Ignoring the uncertain inductive effect of the $-COO^-$ group, the decreasing electrostatic effect of the $-COO^-$ on NH_3^+ with increasing chain length will increase the ease of deprotonation, i.e. the strength of $-^+NH_2$ to H bond energy will fall, raising $H^\circ(AH^\pm_{(aq)})$ and hence lowering ΔH°. The contribution from changes in nett solvent bonding can be found from the ΔS° value. This will have a small positive contribution from the particle change (1 to 2) and a large negative contribution from the large increase in solvation (decrease in disorder) associated with the ion forming reaction, $AH^\pm_{(aq)} \rightarrow A^-_{(aq)} + H^+_{(aq)}$. Hence, overall ΔS°'s for the ω-amino acids are negative and

are smaller than for their protonated methyl esters ($EH^+_{(aq)} \rightarrow E_{(aq)} + H^+_{(aq)}$) (Figure 4.3(c)).

This nett increase in solvent bonding will contribute an increase to the total bond energy (decrease in H°) for the reaction product and hence a decrease to ΔH°. Overall, the balance between the lowering of ΔH° (produced by the decreasing electrostatic effect and the nett increase in solvent bonding) and the raising of ΔH° (produced by chain stiffening) is that ΔH° increases with increasing chain length (Figure 4.3(b)). For the overall value of ΔS°, increasing chain length decreases the "neutralising effect" of the $-NH_3^+$ and $-COO^-$, i.e. the solvation of $AH^\pm_{(aq)}$ increases (a positive contribution to ΔS°), while the "chain stiffening effect" also increases ΔS°. Consequently, ΔS° must increase with increasing chain length, as observed (Figure 4.3(c)).

Again, as for the protonated esters, there is an anomaly at 5-amino. While the pK_a^T of 5-APe is "normal", ΔH° and ΔS° are both anomalously low, in contrast to the abnormally high values for 5-APe Me.HCl. The most likely explanation is again intramolecular H-bonding, with the major difference in behaviour being associated with the replacement of the neutral $-COOCH_3$ group by the negatively charged $-COO^-$ group.

The key to understanding the origin of this abnormal behavior by 5-APe is the value of ΔS°. This is extremely low, -93 J K^{-1} mol^{-1} (typically ~ -40 to –50 J K^{-1} mol^{-1} for the 2-, 3- and 4-amino acids, but ~ -17 for 6-AH) and such low ΔS° values are only seen for the N-methylated 4-amino acids, 4-MAB (-63 J K^{-1} mol^{-1}) and 4-DMAB (-79 J K^{-1} mol^{-1}, Table 4.14). Values for the N-methylated 5-amino acids would be very interesting. These low ΔS° indicate that either $S^\circ(A^-_{(aq)})$ is abnormally small ($A^-_{(aq)}$ is highly ordered) or that $S^\circ(AH^\pm_{(aq)})$ is abnormally large ($AH^\pm_{(aq)}$ is highly disordered) or that both phenomena occur. Such unusual ordering can be due to intramolecular H-bonding and intermolecular H-bonding to H_2O. A high level of disorder in the $AH^\pm_{(aq)}$ form of 5-APe could indicate abnormally low intermolecular H-bonding associated with the "neutralising effect" of the $-COO^-$ on the $-NH_3^+$ involved in an intramolecular H-bond. This would involve the stable, 8-membered H-bond ring (as in 5-APe Me.HCl) but the ordering effect of this is presumably

outweighed by the disordering associated with the lack of intermolecular H-bonding resulting in an abnormally disordered $AH^{\pm}_{(aq)}$. In $A^{-}_{(aq)}$, a high degree of order could arise from extensive intermolecular H-bonding from the negatively charged carboxylate (in contrast to the ester) as well as from the $-NH_2$. The balance is a large increase in order (large negative ΔS°) on forming $AH^{\pm}_{(aq)}$ (Scheme 4.7(a)).

In contrast, the 2-, 3- and 4-amino acids lack intramolecular H-bonding in their $AH^{\pm}_{(aq)}$ forms because the ring sizes required are too small. This results in "normal" (more extensive) intermolecular H-bonding, less disorder, and hence a smaller decrease in disorder (less negative ΔS°) on forming the extensively H-bonded, highly ordered, $A^{-}_{(aq)}$ (Scheme 4.7(b)). 6-AH follows the trend for the 2-, 3- and 4-amino acids; small increases in ΔH° and ΔS° with increasing chain length in line with "increased chain stiffening with increasing chain length"[17] superimposed on the other effects discussed (Figure 4.3(b), (c)). The similarity to the results for the higher alkylammoniums, such 6-HA, suggests that no 9-membered intramolecular H-bond is formed.

N-methylated Amino Acids

N-methylation of the 4-amino acid (4-MAB, 4-DMAB) also results in abnormally low ΔS° values (Table 4.14). As for 5-APe, the reasons for this are probably an abnormally disordered $AH^{\pm}_{(aq)}$ (but without an intramolecular H-bond) as compared to the "normal" order in $A^{-}_{(aq)}$. In $AH^{\pm}_{(aq)}$, N-methylation removes some of the H's needed for intermolecular H-bonding to H_2O (ΔS° is more negative for **di**methylation); the **+I** effect of the $N\text{-}CH_3$, combined with the negative charge of the $-COO^{-}$, results in considerable charge neutralisation and there may be little or no intermolecular H-bonding as a result. Contrastingly, the $A^{-}_{(aq)}$ form has no charge neutralisation; this allows extensive intermolecular H-bonding via the $-COO^{-}$. Despite no such bonding through the tertiary N, $A^{-}_{(aq)}$ is much more ordered than $AH^{\pm}_{(aq)}$, resulting in a large negative ΔS° value (Scheme 4.7(c)).

These large negative ΔS° values suggest that the H° of the $A^{-}_{(aq)}$ forms (which involve considerable H-bonding) will be low while the H° of the $AH^{\pm}_{(aq)}$ forms (little H-bonding) will be abnormally high. This will result in abnormally low ΔH° values, as observed (Figure 4.3(b), Table 4.17).

(a) 5-APe

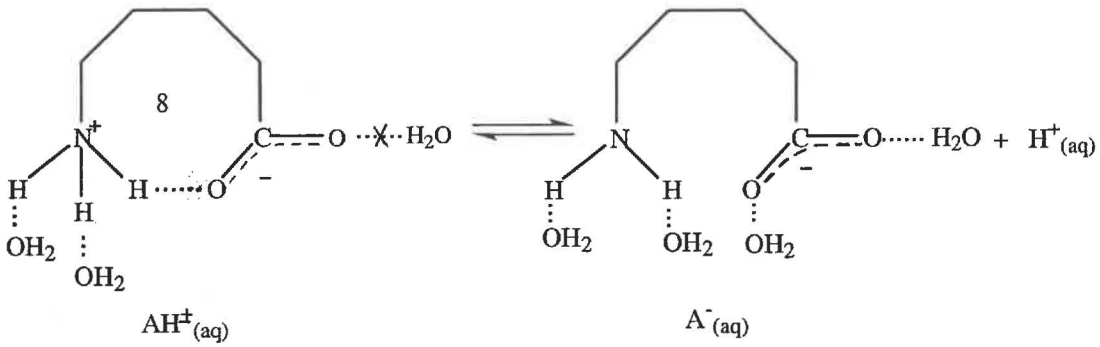

$AH^{\pm}_{(aq)}$ $A^{-}_{(aq)}$

Intramolecular H-bonding causes almost complete charge neutralisation and prevents intermolecular H-bonding to H_2O. **(high disorder)**

Extensive intermolecular H-bonding now possible. **(low disorder)**

(b) 4-AB

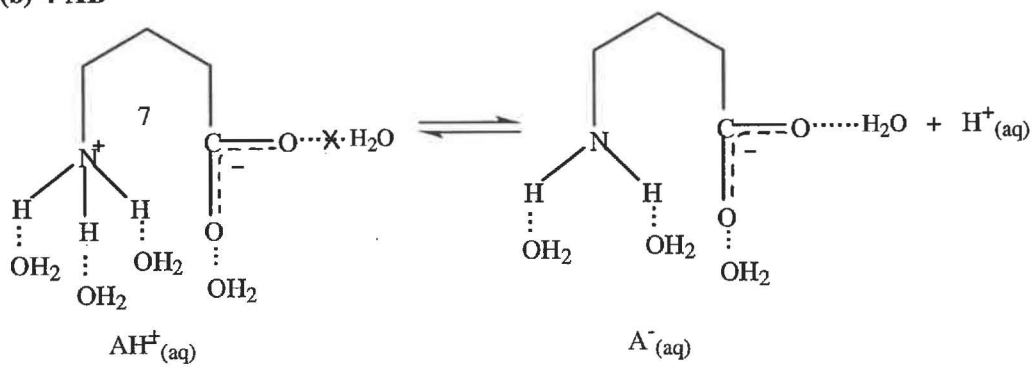

$AH^{\pm}_{(aq)}$ $A^{-}_{(aq)}$

No intramolecular H-bond. Some intermolecular H-bondingbut limited by charge neutralisation of shorter chain. **(moderate disorder)**

Extensive intermolecular H-bonding. **(low disorder)**

(c) 4-DMAB

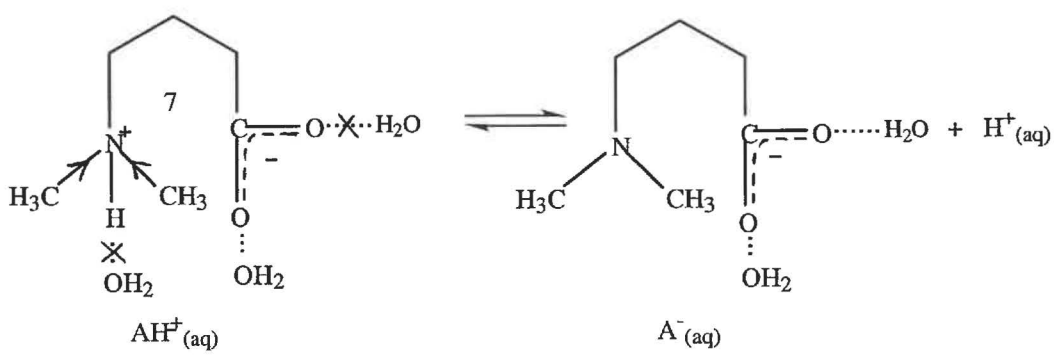

$AH^{\pm}_{(aq)}$ $A^{-}_{(aq)}$

No intramolecular H-bond. Charge neutralisation and N-CH_3's prevent? intermolecular H-bonding. **(high disorder)**

No charge neutralisation. Intermolecular H-bonding possible. **(low disorder)**

Scheme 4.7 H-bonding in Proton Ionisation for 5-APe, 4-AB and 4-DMAB.

Support for the proposed intramolecular H-bonding in 5-APe comes from *ab initio* calculations on ω-amino acids.[28,29] Ramek[28] found that the strongest intramolecular H-bond in the 5-amino acid with an 8-membered ring (Figure 4.6). This zwitterion has a geometry like the chair form of cyclohexane, with the atoms of the –COOH group, C-2 and N in one plane and the other atoms C-3, C-4 and C-5 in another, with the two planes being almost parallel. The favoured intramolecular H-bonded ring size is eight; smaller and larger rings are less stable. However, these calculations take no account of interaction with the solvent.

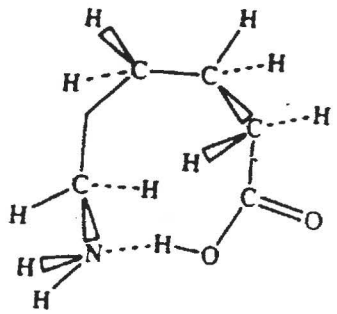

Figure 4.6 Intramolecular H-bonding in 5-APe (modified from Ramek).[27]

C-methylated Amino Acids

As for the amino acid ester hydrochlorides (p. 137), the data is limited to the effect of C-3 methylation for the 4-AB system, and so it is difficult to draw firm conclusions. Based on the discussion for the ester hydrochlorides, inductive effects predict that the order of decreasing acid strengths (increasing $pK_a^T(\text{-}NH_3^+)$ at a given temperature should be:

$$\text{4-AB} > \text{4-A-3-MB} > \text{4-A-3,3-DMB}$$

However, experimentally, the order at all three temperatures, is:

$$\text{4-A-3-MB} > \text{4-A-3,3-DMB} > \text{4-AB},$$

with 4-AB being the weakest (rather than the strongest) acid, and 4-A-3-MB being a much stronger acid (by $\sim 0.9\,pK_a^T$ units) than the other two. Again, inductive effect arguments are inadequate. For ease of comparison, Table 4.22 contains the relevant pK_a^T data and ΔG°, ΔH°, ΔS° and $T \cdot \Delta S^\circ$ values (ex. Table 4.14).

Table 4.22 Effect of C-3 Methylation on pK_a^T, ΔH°, ΔS° and $T \cdot \Delta S^\circ$ for 4-AB.

Amino Acid	$pK_a^T(-NH_3^+)$ (298 K)	ΔG°_{298} kJ mol^{-1}	ΔH° kJ mol^{-1}	ΔS°_{298} J K^{-1} mol^{-1}	$298 \cdot \Delta S^\circ_{298}$ kJ mol^{-1}
4-AB[1]	10.57	60.2	49.0	-37.6	-11.2
4-A-3-MB	9.67	55.1	51.3	-12.8	-3.8
4-A-3,3-DMB	10.48	59.8	44.7	-50.6	-15.1

The patterns of relative acidities and ΔH°, ΔS° values are quite different to those for the corresponding methyl ester hydrochlorides. (Compare Tables 4.18 and 4.22). Replacement of the $-COOCH_3$ by $-COO^-$ will strengthen the interaction between the $-CH_2NH_3^+$ and the –COOX groups (Figure 4.5) which would make 4-A-3,3-DMB the strongest acid due to a low ΔH°, ΔS° combination. $\Delta H^\circ$and ΔS° for 4-A-3,3-DMB are indeed the lowest in Table 4.22, suggesting that the intramolecular H-bonding argument is indeed correct. However, ΔS° is extremely low, presumably due to the increased strength of the intramolecular H-bond and less intermolcular H-bonding than for the analogous ester hydrochloride, i.e. increased disorder in the $AH^{\pm}_{(aq)}$ form of 4-A-3,3-DMB cf. its $A^-_{(aq)}$ form. This allows 4-A-3-MB, with its much larger ΔS°, despite its also much larger ΔH°, to have the smaller ΔG°_{298} (55.1 cf. 59.8 kJ mol^{-1}) and hence it is the stronger acid. The reason for the large ΔS° for 4-A-3-MB is obscure. The introduction of a single $-CH_3$ at C-3 has resulted in little change in ΔH° but a large increase in ΔS°. This is presumably associated with changes in solvation about the $-COO^-$ (such a ΔS° change was not seen for the esters) but if this was the case, then ΔH° would also be expected to change.

Clearly, solvation effects combined with intramolecular H-bonding, result in a delicate energy balance in the 4-AB system, but as for the ester hydrochlorides C-3 methylation increases the acidity of the $-NH_3^+$ group.

In conclusion, these studies have shown the importance of determining the effect of temperature on pK_a^T values, i.e. of determining ΔH° and ΔS° values for proton dissociation from $-NH_3^+$ groups in aqueous solution. Explanations for trends in pK_a^T values with changes in structure, at a single temperature, using arguments such inductive and intramolecular H-bonding, are superficial because these effects represent only a part of the energy change that makes up the total ΔH° and ΔS° values. It is these totals, and the balance between them ($\Delta H^\circ - T\Delta S^\circ = \Delta G^\circ$) that determine the value of pK_a^T ($\Delta G^\circ = 2.3026RTpK_a^T$). It appears that the dominant energy term in many cases arises from the solvation effects associated with intermolecular H-bonds to H_2O, a factor which is ignored by concepts such as inductive effects.

References

1. R. W. Hay and P. J. Morris, *J. Chem. Soc. (B)*, **1970**, 1577.
2. R. W. Hay, L. J. Porter and P. J. Morris, *Aust. J. Chem*, **1966**, *19*, 1197.
3. L. A. Kodikara, M Sc. Thesis, University of Waikato, **1996**.
4. J. A. Zender, M Sc. Thesis, University of Waikato, **1989**.
5. R. W. Hay and L. J. Porter, *J. Chem. Soc. (B)*, **1967**, 1261.
6. A. Albert and E. P. Sergeant, The Determination of Ionisation Constants, Chapman and Hall, London, **1971**.
7. R. B. Martin, A Purcell and R. I. Hedrick, *J. Am. Chem. Soc.*, **1964**, *86*, 2406.
8. A. E. Martell and R. M. Smith, Critical Stability Constants, Vol. 1: Amino Acids, Plenum Press, New York, **1974**.
9. A. I. Vogel, Textbook of Quantitive Inorganic Analysis, Longmans, London, **1951.**
10. R. A. Robinson and R. H. Stokes, Electrolyte Solutions, Butterworths, 2nd ed, **1965**.
11. S. Takat, E. Kyuno and R. Tsuchiya, *Bull. Chem. Soc. Jpn.*, **1968**, *41*, 3416.
12. R. M. Izatt, H. D. Johnson and J. J. Christensen, *J. Chem,. Soc. (Dalton),* **1972**, 1152.
13. E. J. King, *J. Am. Chem. Soc.*, **1951**, *73*, 155.
14. D. D. Perrin, Dissociation Constants of Organic Bases in Aqueous Solution, Butterworths, London, **1969.**
15. B. B. Owen, J. *Am. Chem. Soc.*, **1934**, *56*, 24.
16. M. May and W. A. Felsing, J. *Am. Chem. Soc.*, **1951**, *73*, 406.
17. J. J. Christensen, R. M. Izatt, R. P. Wrathall and L. D. Hansen, *J. Chem. Soc.(A)*, **1969**, 1212.
18. G. Kortum, W. Vogel and K. Andrussow, Dissociation of Organic Acids in Aqueous Solution, Butterworths, London. **1961.**
19. F. M. Jones and E. M. Arnett, *Prog. Phys. Org.*, **1976**, *11*, 263.
20. R. W. Taft, Steric Effects in Organic Chemistry, ed. M. S. Newman, John Wiley and Sons, New York, **1956**.
21. G. B. Barlin and D. D. Perrin, *Quart. Rev.*, **1966**, *20*, 75.
22. G. Arksnes and P. Froyen, *Acta. Chem. Scand.*, **1966**, *20*, 1451.

23. K. H. Patterson, M Sc. Thesis, University of Waikato, **1985**.

24. R. A. Fairclough and N. Hinshelwood, *J. Chem. Soc.*, 538, **1937**.

25. S. Wolfe, *Acc. Chem. Res.*, **1972**, *5*, 102.

26. C. A. Kingsbury, *J. Chem. Ed.*, **1979**, *56*, 431.

27. R. W. Hay and P. J. Morris, Metal Ions in Biological Systems, Marcel Dekkar, New York, **1970**.

28. M. Ramek, *Int. J. Quantum Chem Biol. Symp.*, **1990**, *17*, 45.

29. M. Ramek and P. I. Nagy, *J. Phys. Chem, (A),* **2000**, *104*, 6844.

Chapter Five

Alkaline Hydrolysis Kinetics and Mechanisms

5.1 Introduction

It has been proposed that the alkaline hydrolysis of ω-amino acid esters involves the following pathways (Scheme 5.1):[1]

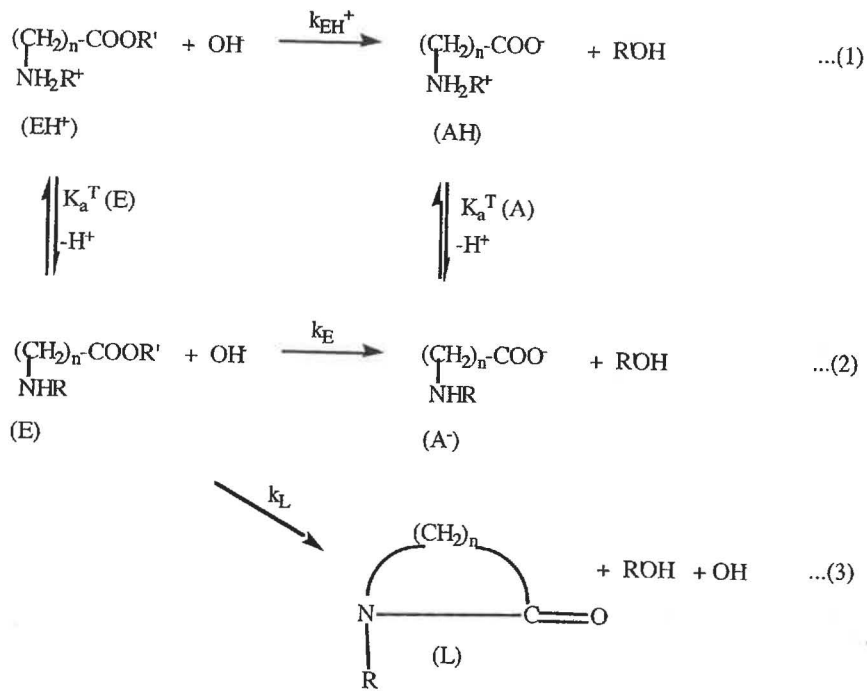

Scheme 5.1 Equilibria and Alkaline Hydrolysis Pathways for ω-Monoamino Acid Esters.

Using the pH-Stat assembly, (see 3.1(c)), the alkaline hydrolysis of the following esters was studied for the reasons given:

3-Hydroxy-2-aminopropanoic acid (serine) methyl ester (Ser Me) was used to pilot the experimental technique and check the accuracy of the pH-Stat assembly.

2-Aminoethanoic acid (glycine) methyl ester (2-AE Me) was used to examine the structural effect of placing an $-NH_2$ ($-NH_3^+$) group α to the $-COOCH_3$ on the value of the alkaline hydrolysis rate constant k_E (or k_{EH^+}) in the absence of intramolecular aminolysis.

4-Aminobutanoic acid methyl ester (4-AB Me) and 5-aminopentanoic acid methyl ester (5-APe Me), because their E forms undergo intramolecular aminolysis, resulting in five or six membered lactam rings under alkaline conditions. One aspect of the current research was to investigate the factors that influence the magnitude of the intramolecular aminolysis rate constant k_L. Hence various systematic structural changes were made to 4-AB Me and 5-APe Me, to investigate factors that affect k_L and also k_{EH^+}, the rate constant for the alkaline hydrolysis of the protonated form. The compounds involved are listed below; it was anticipated that the results from these studies would provide a better understanding of the mechanisms by which amino acid esters undergo alkaline hydrolysis. The structural changes consisted of the following:

N-methylation.

The effect on the rate constant of replacing one or both of the nitrogen-H's on 4-AB Me by a $-CH_3$ group, allowed the effect of N-methylation on the rate of intramolecular aminolysis to be examined. N-methylation effects were investigated using the esters; 4-(methylamino)butanoic acid methyl ester (4-MAB Me) and 4-(dimethylamino)butanoic acid methyl ester (4-DMAB Me). However, 4-DMAB Me did not undergo intramolecular aminolysis and was therefore used to determine a value k_E in the absence of the lactamisation.

C-methylation

The effect on the reaction rate of progressive methylation at C-3 of 4-AB Me was studied by using 4-amino-3-methyl butanoic acid methyl ester (4-A-3-MAB Me) and 4-amino-3,3'-dimethyl butanoic acid methyl ester (4-A-3,3-DMB Me).

Leaving Group

The effect of changing the nature of the leaving group on the rates of alkaline hydrolysis and intramolecular aminolysis were investigated using the following:

For $-OCH_3$ to $-OC_2H_5$:

4-Aminobutanoic acid ethyl ester (4-AB Et), 4-(methylamino)butanoic acid ethyl ester (4-MAB Et), 5-aminopentanoic acid ethyl ester (5-APe Et),

4-(dimethylamino)butanoic acid ethyl ester (4-DMAB Et) and 6-aminohexanoic acid ethyl ester (6-AH Et).

For $-OCH_3$ to $-OCH_2C_6H_5$:

4-Aminobutanoic acid benzyl ester (4-AB Bz), 2-aminoethanoic acid benzyl ester (2-AE Bz), 3-aminopropanoic acid benzyl ester (3-AP Bz), was studied to investigate the effect of removing the $-NH_2$ (or $-NH_3^+$) group from the $-COCH_2OC_6H_5$ group, on the value of the alkaline hydrolysis rate constant k_E (or k_{EH^+}), in the absence of intramolecular aminolysis.

Glutamic Acid Esters

The alkaline hydrolysis of 2-aminopentanedioic acid dimethyl ester (Glu DMe) is complicated, as it involves a pair of parallel reactions, which are both followed by a consecutive reaction (Scheme 5.2):

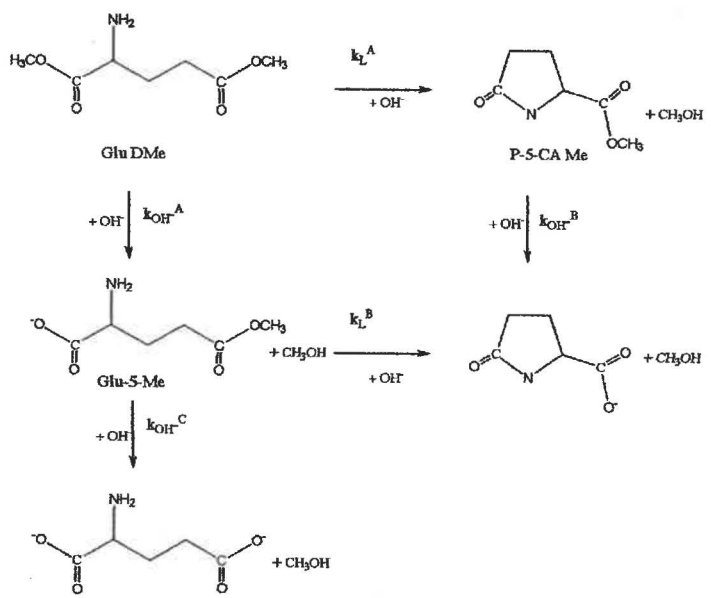

Scheme 5.2 Alkaline Hydrolysis Pathways for Glu DMe (Modifed from Schnir et al.).[2]

Glu DMe and 2-aminopentanoic acid 5-methyl ester (Glu-5-Me) can be considered to be substituted forms of 4-AB Me, where the C-4 H-atom has been replaced by a $-COOCH_3$ or $-COO^-$ group. These esters allowed examination of the effect of these substitutions on the rate of alkaline hydrolysis or intramolecular aminolysis.

The alkaline hydrolysis of 2-pyrolidone-5-carboxylic acid methyl ester (P-5-CA Me), an intermediate in the hydrolysis of Glu DMe, was investigated to compare its rate of alkaline hydrolysis to that for simple aliphatic (non-cyclic) amino acid esters. 2-pyrrolidone-5-carboxylic acid ethyl ester (P-5-CA Et) was also studied to examine the effect of changing the leaving group on the value of the rate constant for the alkaline hydrolysis of pyrrolidone-5-carboxylic acid esters

The rate constants of a selected number of these ω–amino acid esters were also measured at 37.1°C and 50.2°C, in order to obtain the values of the Transition State Theory activation parameters; $\Delta H^{\ddagger}$ (the enthalpy of activation) and $\Delta S^{\ddagger}$ (the entropy of activation).

The changes in $\Delta H^{\ddagger}$ and $\Delta S^{\ddagger}$ which accompany systematic structural modifications should reveal details about the nature of the rate determining step and reaction mechanism. Values for the Arrhenius Theory E_a (activation energy) and A (pre-exponential factor) were also determined.

Since the kinetics are complicated by the presence of two parallel reactions (or three if lactamisation also occurs), considerable care was taken in measuring the value of the rate constant for the overall reaction at a given pH. The highest accuracy possible is essential if reliable values are to be calculated for the separated rate constants (Section 5.2(c)).

5.2 pH-Stat Method

5.2(a) General

The alkaline hydrolysis of amino acids esters consumes OH^-. Hence a pH-Stat which keeps the pH of the reaction mixture stationary by adding OH^- from a burette, can be used to follow the reaction progress at a given (constant) pH. At any time t, the volume of the NaOH added is proportional to the reaction extent.

All pH-Stat kinetic runs were performed using a Radiometer PHM-290 (outlined in 3.2(c)), at 25.0°C and at 37.1°C and 50.2°C for selected amino acid esters. The progress of the reaction was monitored electronically and the data recorded and stored on a computer connected to the pH-Stat system.

In order to achieve the most accurate and reproducible results, the pH-Stat was optimised prior to performing a kinetic investigation. This optimisation procedure involved selecting and adjusting the various settings located in the built-in modes of the PHM-290 controller. The Proportional Integral Derivative (PID) regulation mode was used to control the pH-Stat system for all kinetic investigations in this thesis. The PID mode contained several built-in settings. The most important of these were the gain and time constant, since they controlled the addition of the alkali into the test solution. However, they were the most difficult settings to adjust and had to be systematically optimised to suit the reaction rate and solution buffer capacity at the reaction pH for each individual ester. This was carried out using several pilot runs. Failure to set the gain and time constant correctly resulted in overshoot of the desired pH at the beginning of a kinetic run. Consequently, reaction time is lost as the pH of the test solution "falls back" to the set value. This "dead time" results in the loss of kinetic data and if it is too long, the reaction has to be aborted. Overshooting is a particular problem at high pH where d(pH)/dV is small and a modest change in pH corresponds to a large volume change. This problem is minimised by using a low gain (0.01 – 0.26) and a small time constant setting (0.1 – 2.0) An automated 2.000 ml burette was used for the addition of the 0.1000 mol l^{-1} NaOH to the test solution. This was used in preference to larger sized burettes (i.e. 5.000 and 10.000 ml) as it enabled a more controlled addition of alkali into the reaction mixture, and helped minimize pH overshooting.

5.2(b) Experimental Procedure

Electrode standardization was carried out as discussed for the pK_a^T studies (see 3.2(b)). Single buffer calibration used 0.01 mol l^{-1} sodium tetraborate since the kinetic run pH's were all >7. After standardization, the reaction mixture was placed in the reaction vessel (Figure 3.1). Details of the reaction mixture are discussed later in Section 5.3. The cork carrying the electrodes was replaced and the reaction mixture stirred until thermal equilibrium was reached (about 10 minutes). Due allowance was made for water expansion at higher temperatures. Air bubbles were removed from the burette delivery system and the alkali inlet inserted into the reaction mixture with the delivery tip placed as close to the stirrer as possible.

The method used to raise the reaction mixture pH to the desired value was limited by the 2.000 ml capacity of the burette. There must be enough NaOH to bring the pH and the solution up to the set pH and to hydrolyse all the ester, without having to refill the burette. Refilling the burette in the PID mode disrupts the monitoring of the kinetic run with the loss of data. Whether or not refilling the burette was needed depended on the pH and buffer capacity of the reaction involved, so two methods were used:

Method 1

For reactions at low pH (< 10) or low buffer capacity (i.e. pH well removed from the pK_a^T of the $-NH_3^+$ group), the alkali could be added until the desired pH was reached, and the subsequent reaction followed in the PID mode without needing to refill the burette. Hence, the kinetic investigation was initated in the PID mode, by pressing the Sample key followed by the Enter or √ key (3 times). The collection of volume of NaOH vs. time data from the pH-Stat run was recorded automatically on a Microsoft Excel spreadsheet program stored on the computer.

Method 2

For reactions at high pH (> 10) or those in highly buffered test solutions (i.e. pH's close to the pK_a^T of the $-NH_3^+$ group), a total of more than 2.000 ml of NaOH was needed. Refilling the burette was avoided by first performing an endpoint titration in the pH-Titration mode (PHM-290), where the pH of the test solution was raised to just below the desired value. The burette was refilled in this mode prior to switching to the PID mode to commence the kinetic run. A small percentage of the reaction was missed due to alkaline hydrolysis at the raised pH while the burette was being refilled, but this approach is probably more accurate than "pH jumping", where the NaOH is pipetted into the test solution, because of the difficulty in controlling the pH.

5.2(c) Limitations of the pH-Stat Method

pH Value Accuracy

In general, pH could be controlled to ± 0.002 (PHM-290). This was easier to achieve in more highly buffered systems, e.g. runs at pH > ~ 10.5 or where pH ~ pK_a^T for the ester concerned. However, for these solutions, very accurate pH control was essential, since even a small pH drift represents a large volume of NaOH solution. Despite the pH control to ± 0.002, the overall accuracy of the method is probably ~ ± 0.01 pH

(± 2.3%). This is made up of a combination of electrode calibration drift and uncertainty in the buffer pH_S value. The "stirrer effect" (Section 3.2(c)) produces a lowering of the pH (typically ~ 0.005 pH, 1.2% in $[OH^-]$), but this was corrected for by stopping the stirrer at the end of the reaction and recording the run pH as the "stopped stirrer" pH.

Maximum and Minimum Reaction Half-lives

The calibration drift rate of the glass electrode limits the maximum reaction time which can be studied to about 6 hours, while the maximum reaction half-life is ~ 3 hours since at least two half-lives must be observed. There is also a minimum reaction time limit of ~10 minutes with a minimum reaction half-life ~ 5 minutes, due to the time taken to add and mix the NaOH solution, and the rate of electrode response. These half-life limits control the range of pH over which a given reaction can be studied. There is also an upper pH limit for all reactions of pH ~ 11.4 due to the increasing electrode drift with the increasing $[OH^-]$ etching the glass electrode. High buffer capacity necessitates very accurate pH control and "Na^+ ion error" also begins to occur, i.e. the glass electrode begins to respond to Na^+ as well as H^+ since when $[Na^+]$ is ~ 10^{-3} mol l^{-1}, $[H^+]$ becomes > ~10^{-11} mol l^{-1}.

5.2(d) Data Collection Timescales

Data collection for reactions with $t_{1/2} > 25$ minutes concentrated on the first 3 - 4 half-lives of the reaction, since electrode drift may make readings at longer times inaccurate. For reactions with $t_{1/2} < 15$ minutes the entire reaction could be followed accurately, and a V_∞ value could be recorded at 10 half-lives.

5.2(e) Data Analysis

If all the reactions studied (Scheme 5.1, paths (1), (2) and (3)) have second order kinetics overall, first order in OH^- and first order in the form of the ester involved, then:

$$\frac{-d[E]_T}{dt} = k_E [E][OH^-] + k_{EH^+} [EH^+][OH^-] + k_L [E][OH^-] \qquad ....(5.1)$$

where,

$$= k_{obs}[E]_T \qquad \text{at a given, constant pH} \qquad ...(5.2)$$

$$[E]_T = [E] + [EH^+] = \text{total ester concentration} \qquad ....(5.3)$$

and k_{obs} is the observed pseudo first order rate constant at constant pH.

The kinetic data was analysed primarily by using Guggenheim plots (see Appendix 3, A3.1(b)). Infinity plots were used to confirm the results from the Guggenheim analysis; it is possible to get linear Guggenheim plots from non-first order reactions. A linear Infinity plot, covering at least three reaction half-lives, proves that the reaction is first order. However, the accuracy of the k_{obs} obtained depends on the value of a single reading, V_∞, which may be inaccurate because of electrode drift. Graphs were plotted using the Cricket Graph 3 program, version 3.11 (Computer Associates Inc.).

Hence, for each ester, an Infinity plot was made for a run at a given pH. Having established that this was linear (i.e. linear regression coefficient, $r \geq 0.9995$) for a particular ester, the data was re-analyzed using a Guggenheim plot. The data for runs at other pH's was also analysed using the Guggenheim method. This does not depend on a single reading and the resulting k_{obs} values were found to be internally more consistent than for the Infinity plots. Guggenheim plot calculations were done using a spreadsheet program (Appendix 3). Infinity and Guggenheim k_{obs} values were generally in good agreement (to ± 3% or better). As a check on the Guggenheim method, values for the Δt (Appendix 3.1(c)) were varied between one and three half-lives. Any variation in k_{obs} beyond ~ 3% suggests some problem in the run and the results were discarded. This was also done if the r value for a run was < ~ 0.9995. The k_{obs} value used was the average for the various Δt values for the satisfactory runs.

5.2(f) Evaluation of Rate Constants k_E and k_{EH^+}

The alkaline hydrolysis of ω-monoamino acid esters generally involves two parallel pathways (ignoring a possible lactamisation reaction), and the two reactants are interconnected by a pH-dependent equilibrium (Scheme 5.1). Consequently, not only

do the pH-Stat k_{obs} values vary with pH, but $k_{obs}/[OH^-]$ is also usually pH dependent. $k_{obs}/[OH^-]$ will only be constant if only one form of the ester is present.

Hence from equation 5.1, at high pH , where $[E] >> [EH^+]$, and if $k_L = 0$

$$\frac{-d[E]_T}{dt} = \frac{-d[E]}{dt} = k_E [E][OH^-]$$

$$= k_{obs} [E] \text{ at constant pH}$$

$$\therefore \quad k_E = \frac{k_{obs}}{[OH^-]} = \text{a constant}$$

Similarly at low pH, if $k_L = 0$, and since $[EH^+] >> [E]$,

$$\frac{-d[E]_T}{dt} = \frac{-d[EH^+]}{dt} = k_{EH^+} [EH^+][OH^-]$$

$$= k_{obs} [EH^+] \text{ at constant pH}$$

$$\therefore \quad k_{EH^+} = \frac{k_{obs}}{[OH^-]} = \text{a constant}$$

Such high and low pH's are generally inaccessible because the reaction is either too fast or too slow; an exception is Ser Me, Section 5.3.

In general k_E and k_{EH^+} can be separated as follows:

Substituting (5.1), (5.2) in (5.3) and assuming no lactamisation occurs, gives:

$$\therefore \quad k_{obs} ([E] + [EH^+]) = k_E [E] [OH^-] + k_{EH^+} [EH^+] [OH^-] \qquad ...(5.4)$$

By definition:

$$K_a^T = \frac{[E] [H^+]}{[EH^+]} \cdot \frac{y_o \cdot y_1}{y_1} = \frac{[E] [H^+]}{[EH^+]} \qquad ....(5.5)$$

Substituting (5.5) into (5.4):

$$k_{obs}\left(K_a^T\frac{[EH^+]}{[H^+]}+[EH^+]\right)=k_{EH^+}[EH^+][OH^-]+k_E\frac{[EH^+]}{[H^+]}.K_a^T[OH^-] \qquad ....(5.6)$$

$$\therefore\ \frac{k_{obs}}{[OH^-]}(K_a^T+[H^+])=k_{EH^+}[H^+]+k_EK_a^T \qquad ....(5.7)$$

Therefore, by plotting $\frac{k_{obs}}{[OH^-]}(K_a^T+[H^+])$ versus $[H^+]$ a straight line is obtained.

The slope = k_{EH^+} and the y-axis intercept = $k_EK_a^T$, which yields k_E provided K_a^T for the ester is known.

If lactamisation occurs in addition to simple alkaline hydrolysis of E, it follows that:

$$\frac{k_{obs}}{[OH^-]}(K_a^T+[H^+])=k_{EH^+}[H^+]+(k_E+k_L)K_a^T \qquad ....(5.8)$$

The slope is still equal to k_{EH^+} but the y-axis intercept is now $(k_E+k_L)K_a^T \approx K_a^Tk_L$, since $k_L >>> k_E$ (by usually at least 10^3 times).

5.2(g) Total Alkali Consumption, V_∞

In general it was found that less then one mole of OH^- per mole of ester was required for complete hydrolysis (V_∞) of a given ester at constant pH. Also the value of V_∞ usually increased as the pH was raised except for 4-AB Me where lactamisation, favoured by higher pH's, consumes no OH^- overall (Scheme 5.1). The reason for the lowered V_∞ values are differences in the pK_a^T values for the amino acid ester and its amino acid hydrolysis product ($pK_a^T(E) < pK_a^T(A)$), and the difference in the rate constants for the hydrolysis of the E and EH^+ forms ($k_E < k_{EH^+}$). As a consequence of the continuous adjustment of the two equilibria as the reaction proceeds, OH^- is generated overall, e.g. by the net reaction:

$$E \xrightarrow{-OH^-} EH^+ \xrightarrow{+OH^-} AH + CH_3OH \xrightarrow{+OH^-} A^- + CH_3OH$$

It has been shown that the moles of OH^- consumed for each mole of ester hydrolysed (assuming no lactamisation) is given by:[1]

$$\alpha = 1 + \left(\frac{1}{1 + A\,[OH^-]}\right) - \left(\frac{1}{1 + B\,[OH^-]}\right) \qquad \text{....(5.9)}$$

where,

$$A = K_a^T\,(E) \;/\; K_w^c$$

$$B = K_a^T\,(A) \;/\; K_w^c$$

$K_w^c = 1.678 \times 10^{-14}$ at I = 0.1 mol l^{-1}, 25°C

Terms involving k_E and k_{EH^+} cancel out in the algebra. However, if lactamisation occurs the expression becomes more complicated:

$$\alpha = 1 + \left(\frac{1}{1 + \frac{A}{C}}\right)\left(1 + \frac{\frac{1}{C} - [OH^-]}{\frac{1}{A} + [OH^-]} + \frac{[OH^-]}{\frac{1}{B} + [OH^-]}\right) \qquad \text{...(5.10)}$$

where, $C = k_{EH^+} \;/\; k_L$

Calculated values for V_∞ using the value of α provide a useful check on the validity of the alkaline hydrolysis reaction scheme proposed for a given ester. Values for V_∞ are also slightly reduced at higher pH because an increasing % of the reaction is missed as the reaction becomes faster.

5.2(h) Accuracy Check: Ser Me Ester

This ester is unique among the α-amino acid esters. Because of the **–I** effect of its 3-OH group, Ser Me has a low pK_a^T value (see 4.2(b), p. 91). Consequently, at high pH(> ~ 10.3) the usually complicated alkaline hydrolysis reaction (Scheme 5.1) is greatly simplifed; only one reaction is significant, viz. the alkaline hydrolysis of the E form. No lactamisation occurs and the $[EH^+]$ is too small for the $k_{EH^+}[EH^+][OH^-]$ term to be significant cf. $k_E[E][OH^-]$. This results in $k_{obs}/[OH^-]$ = constant = k_E at pH > ~ 10.3. Also, the value for k_E at 25°C (and at 37°C and 50°C) can be readily measured by pH-Stat (the reaction is not too fast or too slow) and it has been clearly established by several previous studies.[1,3-6] Thus **the rate constant for Ser Me provides a check for the correct functioning of a pH-Stat.** In carrying out this Ser

Me k_E check, the pH-Stat electrodes were standardized using two buffers as described in the pK_a Section 3.2. This was done very carefully because pH's much higher than that of the higher of the two NBS buffers (Borax, pH = 9.180 at 25°C) were needed for the kinetic runs, i.e. the electrode calibration had to be extrapolated to a higher pH. Once the particular glass electrode's response had been corrected to exactly that of a H-electrode (0.0591 V/pH at 25°C), single buffer (Borax, pH = 9.180 at 25°C) calibrations were made for subsequent kinetic runs.

The reaction mixture contained:

10^{-4} moles Ser Me

89.10 ml DW

9.90 ml 1.0 mol l^{-1} KCl

Hence, at complete neutralisation (1.000 ml 0.1000 mol l^{-1} NaOH),

total volume = 100.00 ml

$[Ester]_T = 10^{-3}$ mol l^{-1}

$I = 0.1$ mol l^{-1}

Initially at 25°C, three runs were done at pH 11.000 (the stopped stirrer value was 11.006) to check both the reproducibility and accuracy. The Infinity results for the first run are summarised in Table 5.1 These were used to construct a plot of $\log_{10}(V_\infty - V_t)$ versus time (Figure 5.1). The Guggenheim plot data for this run is in Table 5.2, where λ_1 and λ_1' become V_2 and V_1 since volume is the variable monitored. Figure 5.2 shows the resulting Guggenheim plot, with $\log_{10}(V_2 - V_1)$ versus time.

The Infinity plot showed good linearity (r = 0.9999), confirming that the reaction has first order kinetics for the entire 20 minutes (~ 2 half lives).

For each plot, the slope = $-\frac{k_{obs}}{2.303}$.

Table 5.1 Data for Infinity Plot for Alkaline Hydrolysis for Ser Me

pH = 11.006

T = (25.00 ±0.05)°C

I = 0.1 mol l^{-1}

Time, t (min)	V_t ml	$(V_\infty - V_t)$ ml $V_\infty = 0.891$ ml	$\log_{10} (V_\infty - V_t)$
0	0.000	0.891	-0.05012
1	0.055	0.836	-.0.07778
2	0.109	0.782	-0.10679
3	0.165	0.726	-0.13906
4	0.220	0.671	-0.17328
5	0.265	0.626	-0.20343
6	0.315	0.576	-0.23958
7	0.360	0.531	-0.27491
8	0.400	0.491	-0.30892
9	0.437	0.454	-0.34294
10	0.472	0.419	-0.37779
11	0.506	0.385	-0.41454
12	0.533	0.358	-0.44612
13	0.560	0.331	-0.48017
14	0.586	0.305	-0.51570
15	0.609	0.282	-0.54975
16	0.630	0.261	-0.58336
17	0.650	0.241	-0.61798
18	0.668	0.223	-0.65170
19	0.685	0.206	-0..68613
20	0.700	0.191	-0.71897

Figure 5.1 Infinity Plot for the Alkaline Hydrolysis of Ser Me at pH = 11.006

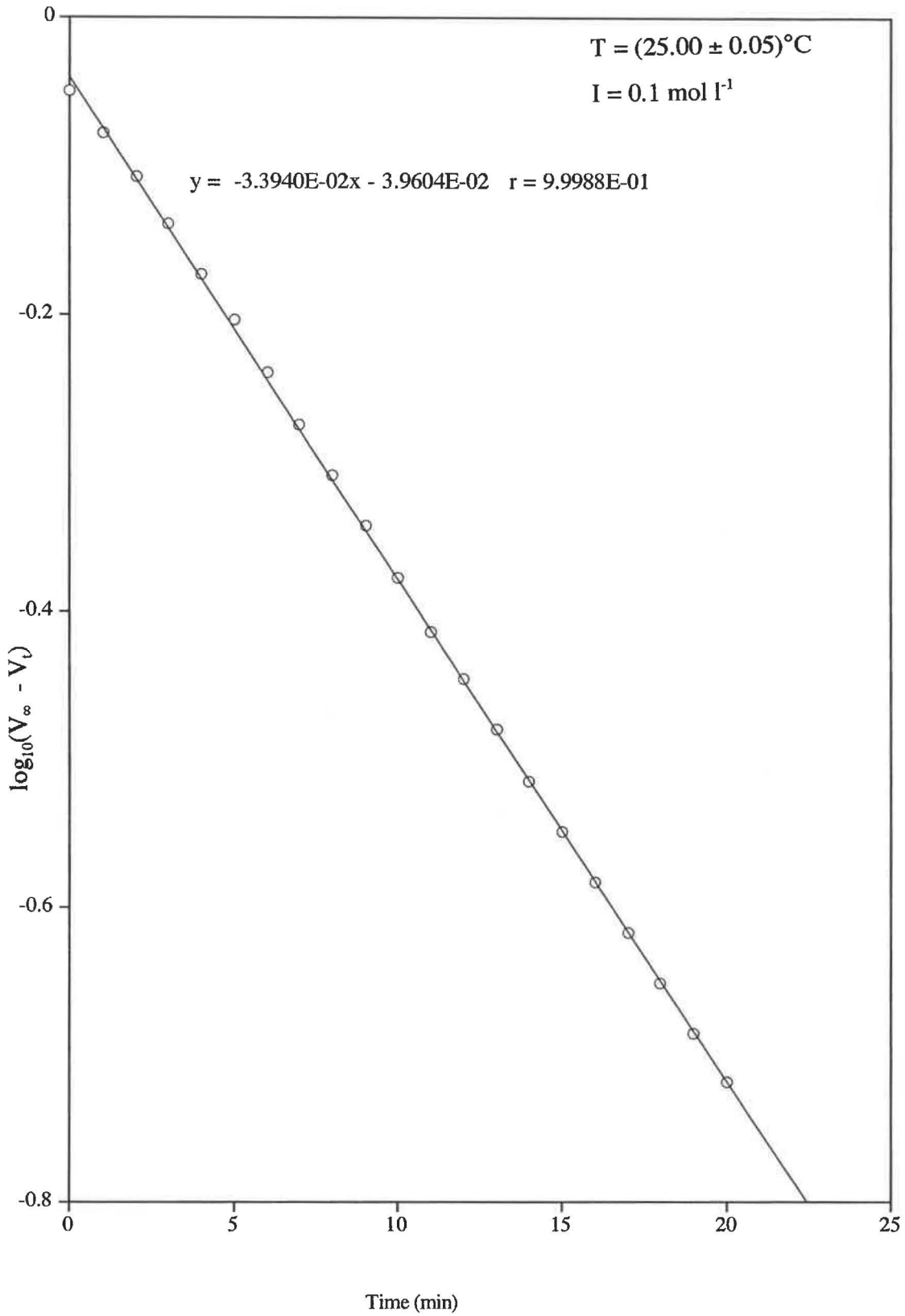

Table 5.2 Data for Guggenheim Plot for Alkaline Hydrolysis for Ser Me

pH = 11.006

T = (25.00 ±0.05)°C

I = 0.1 mol l^{-1}

Time, t (min)	Volume V_1 (ml)	Time, Δt + t (min)	Volume V_2 (ml)	$(V_2 - V_1)$ (ml)	$\log_{10}(V_2 - V_1)$
0	0.000	20	0.701	0.701	-0.15428
1	0.055	21	0.715	0.660	-0.18046
2	0.109	22	0.729	0.620	-0.20761
3	0.165	23	0.742	0.577	-0.23882
4	0.220	24	0.753	0.533	-0.27327
5	0.265	25	0.764	0.499	-0.30189
6	0.315	26	0.774	0.459	-0.33819
7	0.360	27	0.783	0.423	-0.37366
8	0.400	28	0.791	0.391	-0.40782
9	0.437	29	0.799	0.362	-0.44129
10	0.472	30	0.805	0.333	-0.47755
11	0.506	31	0.811	0.305	-0.51570
12	0.533	32	0.817	0.284	-0.54668
13	0.560	33	0.823	0.263	-0.58005
14	0.586	34	0.828	0.242	-0.61618
15	0.609	35	0.833	0.224	-0.64976
16	0.630	36	0.837	0.207	-0.68403
17	0.650	37	0.840	0.190	-0.72125
18	0.668	38	0.844	0.176	-0.75449
19	0.685	39	0.847	0.162	-0.79049
20	0.701	40	0.850	0.149	-0.82681

Figure 5.2 Guggenheim Plot for the Alkaline Hydrolysis of Ser Me at pH = 11.006

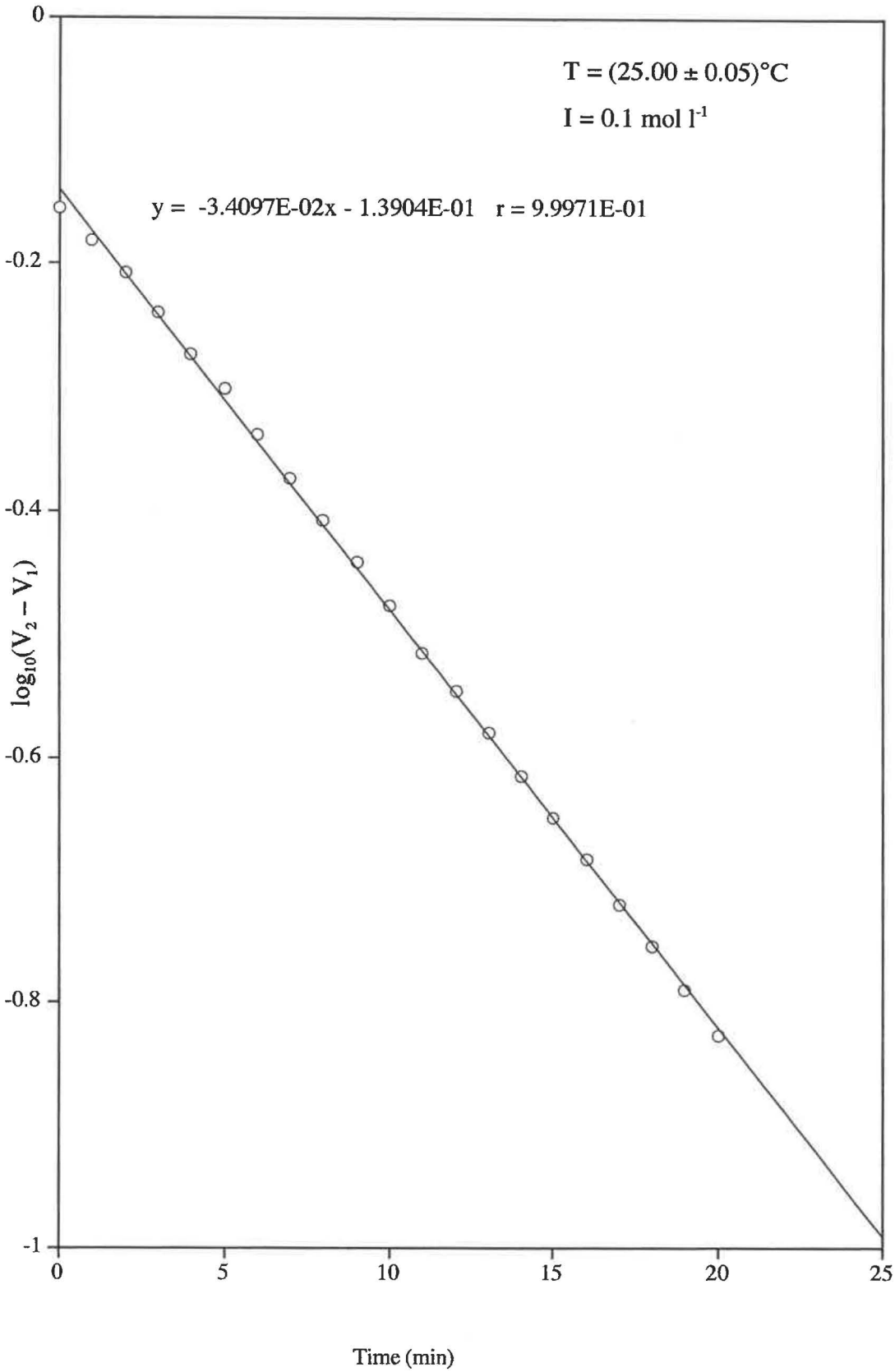

Therefore the following values for the first-order rate constants , k_{obs}, were obtained:

Infinity Plot, $k_{obs} = 0.07815\ min^{-1}$

Guggenheim Plot, $k_{obs} = 0.07853\ min^{-1}$

The results agree well (within ± 0.2%), confirming that Guggenheim plots can be used for other runs. Errors were not calculated for each run; measurement errors (pH, volumes, weights) were trivial. The major source of error is the uncertain one from electrode drift. During the run this will usually show up as non-linearity in the plot, but clearly this did not happen in the present runs. However, drift can occur during the process of wiping the glass electrode in changing from the calibrating buffer to the reaction solution. Drift during the run may also not show up as a non-linear plot. The total drift can be estimated by recalibrating the electrodes after the run. However, one way of estimating the experimental error is using the variation in k_{obs} with replicate runs at a given pH. This was generally < ± 1%, but added on to this is the uncertainty in the calibrating buffer pH_S values. Overall, the experimental error in the rate constants is probably ~ ± 2.3 % which covers the pH uncertainty of ± 0.01.

Table 5.3 Summary of Pilot Guggenheim Plot Results for the Alkaline Hydrolysis of Ser Me.

Run*	Slope (min^{-1})	r	k_{obs} (min^{-1})	$\frac{k_{obs}}{[OH^-]}$ ($l\ mol^{-1}\ min^{-1}$)
1	3.376×10^{-2}	0.99993	7.775×10^{-2}	58.4
2	3.362×10^{-2}	0.99985	7.743×10^{-2}	58.1
3	3.410×10^{-2}	0.99971	7.8530×10^{-2}	59.0

* pH = 11.006.

Initial results were obtained using a Radiometer pHG-211 glass electrode in conjunction with a REF 201 reference electrode. These produced a rate constant, k_E of (58.5 ± 0.5 1 $mol^{-1}\ min^{-1}$), at pH = 11.006, which is in excellent agreement with the accepted literature value of 59.0 ± 1.0 1 $mol^{-1}\ min^{-1}$.[1,3-6]

This confirmed that the electrodes were responding correctly at pH 11.006, and presumably at other values > the calibrating buffer pH of 9.180. Therefore, determination of the unknown rate constants for other amino acid esters could be made with confidence using this equipment. As a routine check on the accuracy of the equipment at high pH, a kinetic run on Ser Me, at pH = 11.000 was done weekly, throughout the kinetic investigations. Appendix 3, Table A3.1, shows the results that were obtained, at 25°C, I = 0.1 mol l^{-1}.

Several Radiometer glass electrodes of the type pHG-211 (with a reference electrode REF-201, see Section 3.2) were used for kinetic studies on various amino acid esters, without any complications. However, towards the end of the work at 25°C, it was found replacement pHG-211 electrodes were producing erratically low values for k_E for Ser Me (~ 48 l mol min^{-1}, i.e. ~ 25% low). Numerous attempts were made to determine the cause this problem (and improve the value of k_E) but these were unsuccessful. It was concluded that the new electrodes had a high pH response error. Eventually it was decided, in consultation with the manufacturer, to switch to a GK 2401B combination glass, reference electrode to complete the remaining pH-Stat investigations at 25°C and for the temperature dependence studies. This electrode type produced satisfactory values for k_E for Ser Me at pH ~ 11, at all temperatures.

5.2(i) Reaction Conditions Needed for Accurate Separation of Rate Constants

For all amino acids except Ser Me, values were required for both k_E (or k_L) and k_{EH^+}. Accurate separation of these using the effect of pH on the value of k_{obs} requires the following:

(i) Measure k_{obs} Over as Large as Possible a pH Range.

This minimizes the errors involved in the separation because these are large at "high" and "low" pH's where the concentrations of E and EH^+, respectively are low so they make little contribution to k_{obs}. The values of these "high" and "low" pH's depend on the pK_a^T of the ester concerned and the values of k_E and k_{EH^+}, but are skewed towards higher pH because $k_{EH^+} > k_E$, e.g. for 2-AE Me, $pK_a^T = 7.67$ at 25°C[6] and "high" pH's are > ~10.4 (about 3 units above pK_a^T) whereas the "low" pH's are < ~9.79 which is still above pK_a^T (see Appendix 4, Table A 4.1).

The **maximum pH** at which k_{obs} can be measured depends on the value of k_{obs} (minimum $t_{1/2} \sim 5$ minutes for a pH-Stat), but cannot be $> \sim 11.4$ because of rapid glass electrode drift due to alkali etching of glass bulb. The **minimum pH** for a run is controlled by the accumulated electrode drift over long reaction times (maximum $t_{1/2} \sim 3$ hours) and decreasing V_∞ values (see 5.2(g)) which lead to increasing errors in $(V_2 - V_1)$.

Little can be done to reduce the electrode drift, but it can be monitored from the linearity of the plot and the effect of changing the Δt on the calculated k_{obs} value. Runs involving plots which showed significant curvature ($r < 0.9995$), or runs where changing Δt from 1 to 3 half-lives which resulted in a change in k_{obs} of $> 3\%$ were rejected. Also, if recalibration of the electrodes after the run showed a reading that was $> \pm 0.01$ pH from the correct value, then the run was rejected.

Falling V_∞ values with decrease in the run pH were countered by increasing the concentration of ester, but only if it undergoes alkaline hydrolysis via a $B_{Ac}2$ type mechanism alone. Reactions involving lactamisation may be subject to "self catalysis" at higher concentrations of ester, so this cannot be raised.[7] Hence four different reaction mixtures were used depending on the reaction half-life. At 25.0 °C, these were:

(1) For half-lives < 60 minutes:

10^{-4} moles EH^+Cl^-

89.10 ml DW

9.90 ml 1.0 mol l^{-1} KCl

Hence, at complete neutralisation (1.000 ml 0.1000 mol l^{-1} NaOH),

total volume = 100.00 ml

$[Ester]_T = 10^{-3}$ mol l^{-1}

(2) For Half-lives 60 -100 minutes:

2×10^{-4} moles EH^+Cl^-

88.20 ml DW

9.80 ml 1.0 mol l^{-1} KCl

Hence, at complete neutralisation (2.000 ml 0.1000 mol l^{-1} NaOH),

total volume = 100.00 ml

$[Ester]_T = 2 \times 10^{-3}$ mol l^{-1}

(3) For Half-lives 100 -150 minutes:

4×10^{-4} moles EH^+Cl^-

86.40 ml DW

9.60 ml 1.0 mol l^{-1} KCl

Hence, at complete neutralisation (4.000 ml 0.1000 mol l^{-1} NaOH),

total volume = 100.00 ml

$[Ester]_T = 4 \times 10^{-3}$ mol l^{-1}

(4) For Half-lives >150 minutes:

1×10^{-3} moles EH^+Cl^-

81.00 ml DW

9.00 ml 1.0 mol l^{-1} KCl

Hence, at complete neutralisation (10.000 ml 0.1000 mol l^{-1} NaOH),

total volume = 100.00 ml

$[Ester]_T = 1 \times 10^{-2}$ mol l^{-1}

Due allowance was made for the expansion of water at higher temperatures.

(ii) Measure K_a^T as Accurately as Possible.

Why the accuracy of the separation of the rate constants k_{EH^+} and $(k_E + k_L)$ depends on the accuracy of the K_a^T value can be seen from equ. 5.7. This accuracy decreases from Group 1 (slowly hydrolysing esters) to Group 2 (moderately hydrolysing esters) to Group 3 (rapidly hydrolysing esters), for the reasons discussed in 4.2(b).

5.3 Studies on Individual Amino Acid Esters.

These were divided into three groups depending on their rates of alkaline hydrolysis.

5.3(a) Group 1, Slowly Hydrolysing Esters

This group included the following esters: 2-AE Me, 2-AE Bz, 3-AP Bz, 4-DMAB Me, 4-DMAB Et, Glu DMe and 6-AH Et. Their volume of NaOH vs. time data was

analysed using the Guggenheim method, which produced plots that had r values of 0.999 or better. In general, the separation of k_{EH^+} and k_E was straightforward: lactamisation was absent; this group of esters had pK_a^T's that had high accuracy, and their reaction rates could be measured over a wide range of pH.

Typical of this group is 2-AE Me. Its alkaline hydrolysis is discussed in detail below, to show the usual type on results obtained for this group of esters. Results are given at 37 °C because the 25 °C investigation had been made earlier.[6]

2-AE Me

At 37 °C, the accessible pH-range was ~ 8 – 10.5.

Declining V_∞ values meant that higher concentrations of ester had to be used at lower pH's (see 5.2(i)). Table 5.4 summarises the effect of pH on the value of $k_{obs}/[OH^-]$ and Table 5.5 lists the data needed to separate the rate constants k_{EH^+} and k_E. Using eqn. 5.7, the data from Table 5.5 was used to construct a separation plot for 2-AE Me (Figure 5.3). This data was graphed as a scatter plot using a software package (Cricket Graph 3, version 1.5.3), with a computer generated line of best fit being drawn through the points, and values for the slope, intercept and correlation (r-value) were obtained. No error bars are displayed in Figure 5.3; details of the rate constant error calculations for Group 1 esters are outlined in Appendix 5, Section A5.2(a).

As can be seen from Figure 5.3, the value of r = 0.9998 indicates good linearity for the plot needed to separate the rate constants across the large pH range of 8.013 – 10.510. The rate constants k_{EH^+} and k_E were evaluated using equ. 5.7 as follows:

$$\text{y-axis intercept} = 7.0684 \times 10^{-6}\ \text{min}^{-1}$$

$$= k_E \cdot K_a^T$$

$$\therefore \quad k_E = 7.0684 \times 10^{-6} / 4.677 \times 10^{-8}$$

$$= 151.1\ \text{l mol min}^{-1}$$

$$\text{slope} = 5596.1\ \text{l mol}^{-1}\ \text{min}^{-1} = k_{EH^+}$$

Table 5.4 Effect of pH on the Value of $k_{obs}/[OH^-]$ for 2-AE Me.

$T = (37.10 \pm 0.05)°C$

$I = 0.1$ mol l^{-1}

pH†	k_{obs} (min^{-1})	$t_{1/2}$ (min)	$[OH^-]^*$ (mol l^{-1})	$\frac{k_{obs}}{[OH^-]}$ (l mol^{-1} min^{-1})
8.013	4.191×10^{-3}	165.4	3.208×10^{-6}	1306.5
8.208	4.757×10^{-3}	145.7	5.026×10^{-6}	946.5
8.210	4.821×10^{-3}	143.8	5.049×10^{-6}	954.8
8.411	5.605×10^{-3}	123.7	8.021×10^{-6}	698.8
8.610	6.322×10^{-3}	109.6	1.268×10^{-5}	498.5
8.611	6.300×10^{-3}	110.0	1.271×10^{-5}	495.6
8.809	7.733×10^{-3}	89.6	2.005×10^{-5}	385.6
9.009	9.487×10^{-3}	73.1	3.178×10^{-5}	298.5
9.010	9.627×10^{-3}	72.0	3.186×10^{-5}	302.2
9.208	1.113×10^{-2}	62.3	5.026×10^{-5}	221.5
9.208	1.145×10^{-2}	60.5	5.026×10^{-5}	227.9
9.409	1.598×10^{-2}	43.4	7.984×10^{-5}	200.1
9.810	3.514×10^{-2}	19.7	2.010×10^{-4}	174.8
10.010	5.454×10^{-2}	12.7	3.186×10^{-4}	171.2
10.010	5.435×10^{-2}	12.8	3.186×10^{-4}	170.6
10.109	6.702×10^{-2}	10.3	4.001×10^{-4}	167.5
10.310	1.002×10^{-1}	6.9	6.356×10^{-4}	157.6
10.311	1.009×10^{-1}	6.9	6.371×10^{-4}	158.3
10.510	1.610×10^{-1}	4.3	1.007×10^{-3}	159.8

† Stopped stirrer pH.

* $[OH^-] = \frac{10^{pH - 13.622}}{0.7670}$ (37°C and I = 0.1 mol l^{-1}).

Table 5.5 Data for Separation of k_E and k_{EH^+} for the Alkaline Hydrolysis of 2-AE Me.

$T = (37.10 \pm 0.05)°C$

$I = 0.1$ mol l^{-1}

pH†	$[H^+]^*$ (mol l^{-1})	$(K_a^T + H^+)$ (mol l^{-1})	$\frac{k_{obs}}{[OH^-]}$ (l mol^{-1} min^{-1})	$\frac{k_{obs}}{[OH^-]}(K_a^T + [H^+])$ (min^{-1})
8.013	1.265×10^{-8}	5.943×10^{-8}	1306.5	7.764×10^{-5}
8.208	8.076×10^{-9}	5.485×10^{-8}	946.5	5.192×10^{-5}
8.210	8.039×10^{-9}	5.481×10^{-8}	954.8	5.234×10^{-5}
8.411	5.061×10^{-9}	5.183×10^{-8}	698.8	3.622×10^{-5}
8.610	3.200×10^{-9}	4.997×10^{-8}	498.5	2.491×10^{-5}
8.611	3.193×10^{-9}	4.997×10^{-8}	495.6	2.476×10^{-5}
8.809	2.024×10^{-9}	4.880×10^{-8}	385.6	1.882×10^{-5}
9.009	1.277×10^{-9}	4.805×10^{-8}	298.5	1.434×10^{-5}
9.010	1.274×10^{-9}	4.805×10^{-8}	302.2	1.452×10^{-5}
9.208	8.076×10^{-10}	4.758×10^{-8}	221.5	1.054×10^{-5}
9.208	8.076×10^{-10}	4.758×10^{-8}	227.9	1.084×10^{-5}
9.409	5.084×10^{-10}	4.728×10^{-8}	200.1	9.461×10^{-6}
9.810	2.019×10^{-10}	4.698×10^{-8}	174.8	8.211×10^{-6}
10.010	1.274×10^{-10}	4.690×10^{-8}	171.2	8.029×10^{-6}
10.010	1.274×10^{-10}	4.690×10^{-8}	170.6	8.001×10^{-6}
10.109	1.014×10^{-10}	4.687×10^{-8}	167.5	7.852×10^{-6}
10.310	6.386×10^{-11}	4.684×10^{-8}	157.6	7.382×10^{-6}
10.311	6.371×10^{-11}	4.684×10^{-8}	158.3	7.414×10^{-6}
10.510	4.029×10^{-11}	4.681×10^{-8}	159.8	7.481×10^{-6}

Using $K_a^T = 4.677 \times 10^{-8}$; $pK_a^T = 7.33$ (37°C and I = 0.1 mol l^{-1}) (Table A1.11).

† Stopped stirrer pH.

* $[H^+] = \frac{10^{-pH}}{0.7670}$ (37°C and I = 0.1 mol l^{-1}).

Figure 5.3 Separation of k_E and k_{EH^+} for Alkaline Hydrolysis of 2-AE Me

$T = (37.10 \pm 0.05)°C$

$I = 0.1$ mol l^{-1}

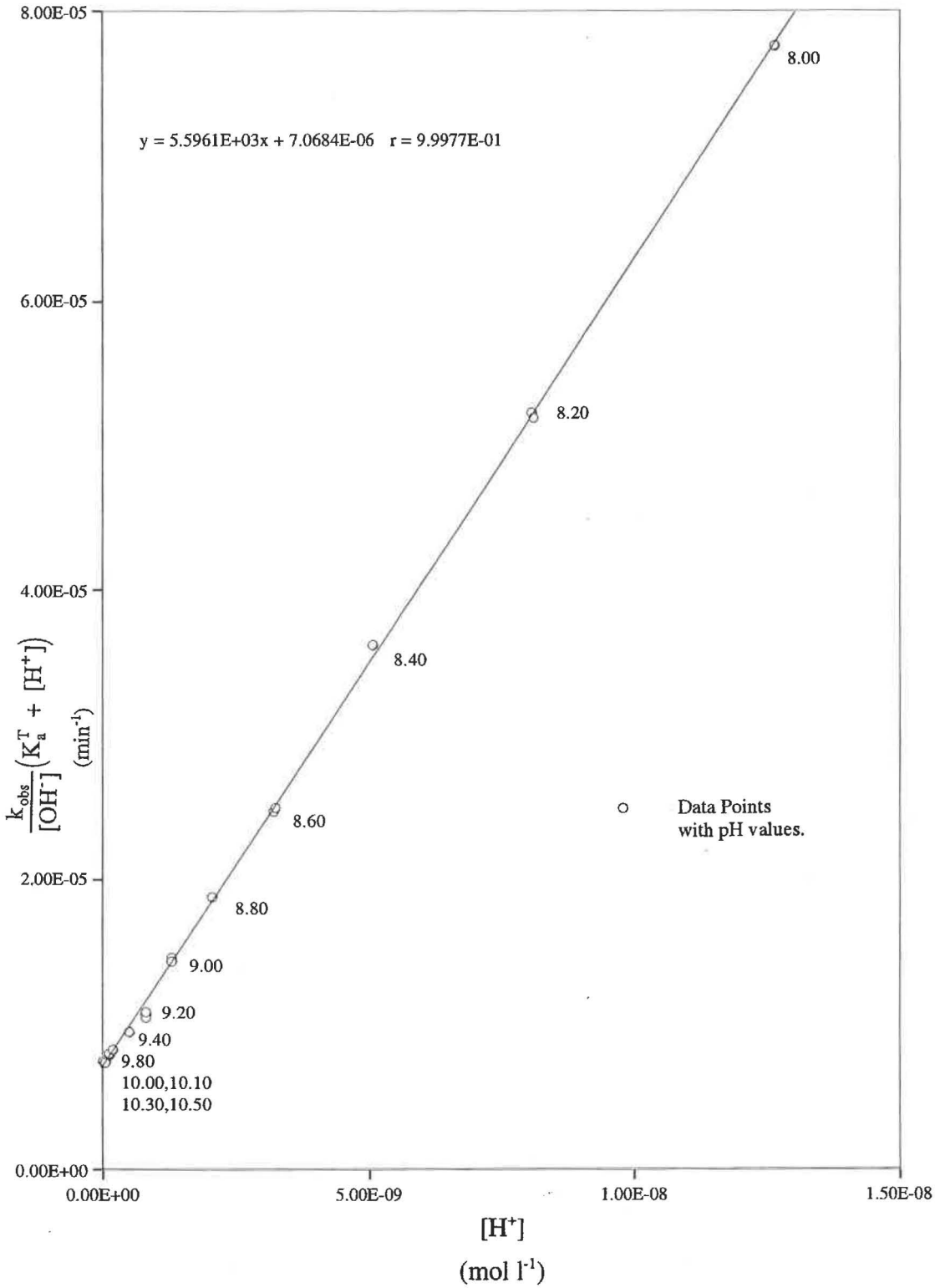

The errors for 2-AE Me at 37.1 °C and I = 0.1 mol l^{-1}, were calculated (see A5.3(a)), resulting in:

k_{EH^+} = (5600 ± 390) l mol^{-1} min^{-1} and k_E = (151 ± 3) l mol^{-1} min^{-1}.

These errors probably represent the maximum range of the true error. Consequently, the error for k_E was estimated to be ~ 2.5% and k_{EH^+} ~7.5% for all Group 1 esters. It was assumed that these errors are the same across all temperatures.

Tables for the effect of pH on the value of $k_{obs}/[OH^-]$, the data needed for the separation of k_{EH^+} and k_E and the resulting graphs for the remaining Group 1 amino acid esters are in Appendix 3. The rate constant separation graphs for Group 1 esters show estimated error bars (y-axis, ± 4.6%, x-axis, ± 2.3%), but the lines of maximum and minimum slopes have been omitted, for clarity.

Table 5.11 summarises the values of k_{EH^+}, k_E and k_L for all the amino acid esters studied in this thesis at 25°C and I = 0.1 mol^{-1}.

5.3(b) Group 2, Moderately Hydrolysing Esters

Included in this group were 4-AB Me, 4-AB Et, 4-MAB Me, 4-MAB Et, 4-A-3-MB Me, 4-A-3,3-DMB Me and Glu-5-Me. Detailed results are given for the typical case of 4-AB Me, where $(k_E + k_L)$ and k_{EH^+} need to be evaluated.

4-AB Me

The E form of this ester undergoes intramolecular aminolysis (Scheme 5.1), so that "k_E" is in fact k_E+ k_L, but it is assumed that k_E is negligibly small (estimated as ~ 9.1 l mol^{-1} min^{-1})[1] cf. k_{EH^+}. Determination of k_{obs} values for 4-AB Me presents some problems, since the intramolecular aminolysis reaction has been shown to be subject to general base catalysis. Consequently, "self-catalysis" can occur, since the E form of the ester is a fairly strong base (pK_b^T ~ 4.17 cf. 2-AE Me, pK_b^T ~ 6.32 at 25°C). Such "self-catalysis" has been observed at $[ester]_T$ = 10^{-2} mol l^{-1}, but does not occur at $[ester]_T \leq 1 \times 10^{-3}$ mol l^{-1}.[7] It can be checked for since it produces Guggenheim plots that are non-linear due to a small second order term in E, $k_2[E]^2$, in addition to the $k_E[E][OH^-]$ and $k_{EH^+}[EH^+][OH^-]$ terms. All Guggenheim plots for 4-AB Me

passed the "satisfactorily linear" criterion ($r > 0.995$), with a < 3% trend in k_{obs} with change in Δt from 1 to 3 half-lives. Therefore, it was unlikely that "self-catalysis" had occurred. Low $[ester]_T$ values of 1×10^{-3} mol l^{-1} were used to measure k_{obs} for all Group 2 amino acid esters. This was regardless of the fact that the V_∞ values became smaller at higher pH's since the increasing percentage of intramolecular catalysis consumes no OH^- overall (Scheme 5.1). Fortunately, this fall was insufficient to significantly reduce the accuracy of the kinetic plots.

Table 5.6 shows the effect of pH on the value of $k_{obs}/[OH^-]$ for 4-AB Me, at 25°C and I = 0.1 mol^{-1}). In contrast to 2-AE Me the value of $k_{obs}/[OH^-]$ increases with pH. This is typical of reactions that undergo intramolecular aminolysis. The rapidly increasing hydrolysis rates with increasing pH limited the maximum run pH to ~10.1, which is only just above the ester.HCl pK_a^T. The data needed for the separation of k_{EH^+} and k_E is displayed in Table 5.7. This data was used to construct the separation plot for 4-AB Me, at 25°C and I = 0.1 mol l^{-1} (Figure 5.4).

As it can be seen from Figure 5.4, the value of r = 0.9962, indicates good linearity. The values for k_{EH^+} and k_E were determined from Figure 5.4 using equ. 5.7. This produced the following results:

$$k_E = 1580.0 \text{ l mol}^{-1} \text{ min}^{-1} \cong k_L \qquad k_{EH^+} = 131.8 \text{ l mol}^{-1} \text{ min}^{-1}$$

The error was estimated to be ~4% for k_E (k_L) and ~10% for k_{EH^+}. (Appendix 5, Section A5.3(b)). Therefore,

$$k_L = (1580 \pm 60) \text{ l mol}^{-1} \text{ min}^{-1} \quad \text{and} \quad k_{EH^+} = (132 \pm 13) \text{ l mol}^{-1} \text{ min}^{-1}$$

These errors probably represent the maximum range of the true error. The same errors were applied to all Group 2 esters. It was assumed that these errors are the same across all temperatures.

Tables for the effect of pH on the value of $k_{obs}/[OH^-]$, the data needed for the separation of k_{EH^+} and k_E, and the separation graphs for the remaining Group 2 esters can be found in Appendix 3. The separation graphs show estimated error bars (y-axis ± 4.6%, x-axis ± 2.3%), but the lines of maximum and minimum slopes have been omitted.

Table 5.6 Effect of pH on the Value of $k_{obs}/[OH^-]$ for 4-AB Me

$T = (25.00 \pm 0.05)°C$

$I = 0.1$ mol l^{-1}

pH†	k_{obs} (min^{-1})	$t_{1/2}$ (min)	$[OH^-]$* (mol l^{-1})	$\frac{k_{obs}}{[OH^-]}$ (l mol^{-1} min^{-1})
9.099	5.147×10^{-3}	134.7	1.641×10^{-5}	313.6
9.198	7.256×10^{-3}	95.5	2.061×10^{-5}	352.0
9.201	7.304×10^{-3}	94.9	2.076×10^{-5}	351.9
9.300	1.055×10^{-2}	65.7	2.607×10^{-5}	404.7
9.398	1.465×10^{-2}	47.3	3.267×10^{-5}	448.5
9.401	1.479×10^{-2}	46.8	3.289×10^{-5}	449.8
9.498	2.105×10^{-2}	32.9	4.113×10^{-5}	511.8
9.501	2.149×10^{-2}	32.3	4.142×10^{-5}	518.9
9.503	2.159×10^{-2}	32.1	4.161×10^{-5}	519.0
9.596	3.016×10^{-2}	23.0	5.154×10^{-5}	585.2
9.603	3.079×10^{-2}	22.5	5.238×10^{-5}	587.8
9.701	4.419×10^{-2}	15.6	6.564×10^{-5}	673.2
9.704	4.462×10^{-2}	15.5	6.609×10^{-5}	675.2
9.802	6.209×10^{-2}	11.2	8.282×10^{-5}	749.6
9.802	6.212×10^{-2}	11.2	8.282×10^{-5}	750.0
9.901	8.377×10^{-2}	8.3	1.040×10^{-4}	805.3
9.902	8.452×10^{-2}	8.2	1.043×10^{-4}	810.6
10.003	1.177×10^{-1}	5.9	1.316×10^{-4}	894.2
10.004	1.184×10^{-1}	5.9	1.319×10^{-4}	897.8
10.102	1.632×10^{-1}	4.2	1.652×10^{-4}	987.2

† Stopped stirrer pH.

*$[OH^-] = \frac{10^{pH - 13.9965}}{0.7715}$ (25 °C and I = 0.1 mol l^{-1}).

Table 5.7 Data for Separation of k_E and k_{EH^+} for the Alkaline Hydrolysis 4-AB Me

$T = (25.00 \pm 0.05)°C$

$I = 0.1$ mol l^{-1}

pH†	$[H^+]^*$ (mol l^{-1})	$(K_a^T + H^+)$ (mol l^{-1})	$\frac{k_{obs}}{[OH^-]}$ (l mol^{-1} min^{-1})	$\frac{k_{obs}}{[OH^-]}(K_a^T + [H^+])$ (min^{-1})
9.099	1.032×10^{-9}	1.180×10^{-9}	313.6	3.700×10^{-7}
9.198	8.216×10^{-10}	9.695×10^{-10}	352.0	3.413×10^{-7}
9.201	8.160×10^{-10}	9.639×10^{-10}	351.9	3.391×10^{-7}
9.300	6.496×10^{-10}	7.975×10^{-10}	404.7	3.228×10^{-7}
9.398	5.184×10^{-10}	6.663×10^{-10}	448.3	2.987×10^{-7}
9.401	5.148×10^{-10}	6.627×10^{-10}	449.8	2.981×10^{-7}
9.498	4.118×10^{-10}	5.597×10^{-10}	511.8	2.865×10^{-7}
9.501	4.089×10^{-10}	5.568×10^{-10}	518.9	2.890×10^{-7}
9.503	4.071×10^{-10}	5.550×10^{-10}	519.0	2.880×10^{-7}
9.596	3.286×10^{-10}	4.765×10^{-10}	585.2	2.789×10^{-7}
9.603	3.233×10^{-10}	4.713×10^{-10}	587.8	$2.770. \times 10^{-7}$
9.701	2.580×10^{-10}	4.059×10^{-10}	673.2	2.733×10^{-7}
9.704	2.563×10^{-10}	4.042×10^{-10}	675.2	2.729×10^{-7}
9.802	2.045×10^{-10}	3.524×10^{-10}	747.2	2.633×10^{-7}
9.802	2.031×10^{-10}	3.510×10^{-10}	749.0	2.629×10^{-7}
9.901	1.628×10^{-10}	3.107×10^{-10}	805.3	2.502×10^{-7}
9.902	1.624×10^{-10}	3.103×10^{-10}	810.6	2.516×10^{-7}
10.003	1.287×10^{-10}	2.766×10^{-10}	894.2	2.474×10^{-7}
10.004	1.284×10^{-10}	2.763×10^{-10}	897.8	2.481×10^{-7}
10.102	1.024×10^{-10}	2.503×10^{-10}	987.2	2.472×10^{-7}

Using $K_a^T = 1.479 \times 10^{-10}$; $pK_a^T = 9.83$ (25°C and I = 0.1 mol l^{-1}). (Table 4.9).

† Stopped stirrer pH.

* $[H^+] = \frac{10^{-pH}}{0.7715}$ (25°C and I = 0.1 mol l^{-1}).

Figure 5.4 Separation of k_E and k_{EH^+} for Alkaline Hydrolysis of 4-AB Me

$T = (25.00 \pm 0.05)°C$

$I = 0.1$ mol l^{-1}

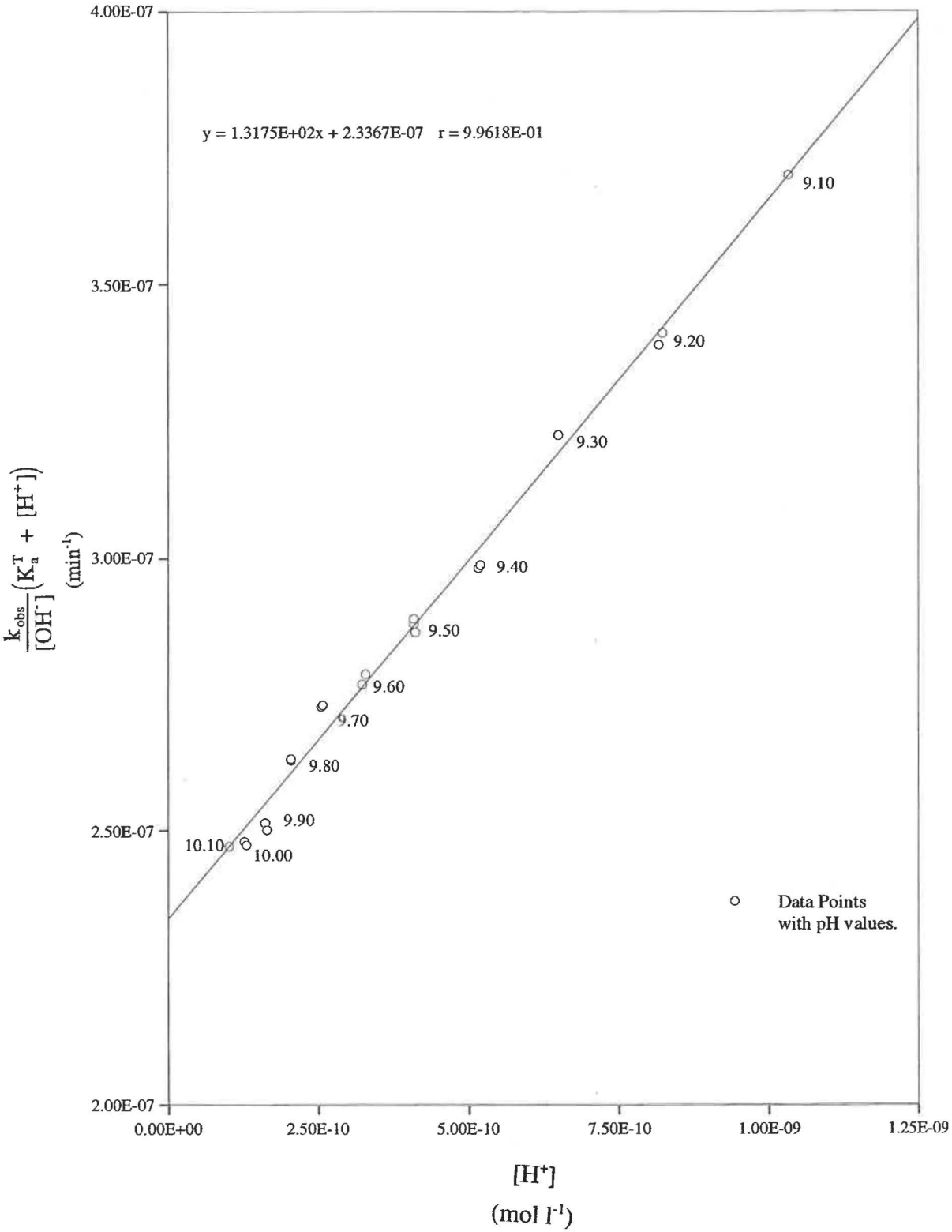

5.3(c) Group 3, Rapidly Hydrolysing Esters

Only two esters, 5-APe Me and 5-APe Et were in this group.

5-APe Me

The kinetics of the alkaline hydrolysis of this ester are complicated by its very rapid rate of lactamisation. Consequently, it was only possible to investigate the kinetics at low pH's (8.4 – 9.3 at 25 °C). The upper pH limit was slightly less than the pK_a^T (10.15 at 25 °C) but this was sufficient for an accurate graphical separation of the rate constants. No evidence was found for "self-catalysis" at this $[ester]_T = 1 \times 10^{-3}$ mol l^{-1}, since all Guggenheim plots were linear (i.e. $r > 0.995$).

Table 5.8 shows the effect of pH on the value of $k_{obs}/[OH^-]$, and Table 5.9 contains the data needed for the separation of k_{EH^+} and $k_E(k_L)$ for 5-APe Me, at 25°C and I = 0.1 mol l^{-1}. The graphical separation (Figure 5.5) shows good linearity, with r = 0.9948. The resulting values for k_{EH^+} and k_E (using equ. 5.7) are:

$$k_E = 36380 \text{ l mol}^{-1} \text{ min}^{-1} \cong k_L \quad \text{and} \quad k_{EH^+} = 545 \text{ l mol}^{-1} \text{ min}^{-1}$$

The error was estimated to be ~8% for k_E (k_L) and ~13% for k_{EH^+} (Appendix 5, Section A5.3(c)). Therefore,

$$k_L = (36380 \pm 3640) \text{ l mol}^{-1} \text{ min}^{-1} \quad \text{and} \quad k_{EH^+} = (545 \pm 71) \text{ l mol}^{-1} \text{ min}^{-1}$$

Again, these errors probably represent the maximum range of the true error. The same errors were applied to 5-APe Et. It was assumed that these errors are the same across all temperatures.

Quite clearly, a major limitation in the accuracy of the separation of k_{EH^+} and $k_E(k_L)$ for 5-APe Me is the limited accuracy of its pK_a^T. Great care was taken in obtaining the best possible value for 5-APe Me (see p.103), but there still remains the possibility that the pK_a^T is low because of rapid hydrolysis at the pH's required for the pK_a^T.

Table 5.8 Effect of pH on the Value of $k_{obs}/[OH^-]$ for 5-APe Me

$T = (25.00 \pm 0.05)°C$

$I = 0.1$ mol l^{-1}

pH†	k_{obs} (min^{-1})	$t_{1/2}$ (min)	$[OH^-]^*$ (mol l^{-1})	$\frac{k_{obs}}{[OH^-]}$ (l mol^{-1} min^{-1})
8.405	3.387×10^{-3}	204.7	3.320×10^{-6}	1020
8.495	4.718×10^{-3}	146.9	4.085×10^{-6}	1155
8.598	6.964×10^{-3}	99.5	5.178×10^{-6}	1345
8.600	6.945×10^{-3}	99.8	5.202×10^{-6}	1335
8.704	1.015×10^{-2}	68.3	6.609×10^{-6}	1535
8.706	1.013×10^{-2}	68.4	6.640×10^{-6}	1526
8.800	1.404×10^{-2}	49.4	8.244×10^{-6}	1715
8.802	1.414×10^{-2}	49.0	8.283×10^{-6}	1695
8.804	1.415×10^{-2}	49.0	8.321×10^{-6}	1700
8.898	2.071×10^{-2}	33.5	1.033×10^{-5}	1995
8.903	2.090×10^{-2}	32.7	1.045×10^{-5}	2005
8.904	2.090×10^{-2}	33.2	1.048×10^{-5}	2030
8.999	3.129×10^{-2}	22.2	1.304×10^{-5}	2400
9.002	3.131×10^{-2}	22.1	1.313×10^{-5}	2385
9.104	4.806×10^{-2}	14.4	1.660×10^{-5}	2895
9.105	4.718×10^{-2}	14.7	1.664×10^{-5}	2835
9.200	7.114×10^{-2}	9.7	2.071×10^{-5}	3435
9.201	7.234×10^{-2}	9.6	2.076×10^{-5}	3485
9.296	1.058×10^{-2}	6.6	2.583×10^{-5}	4095
9.301	1.078×10^{-2}	6.4	2.613×10^{-5}	4125

† Stopped stirrer pH.

$^*[OH^-] = \frac{10^{pH - 13.9965}}{0.7715}$ (25°C and I = 0.1 mol l^{-1}).

Table 5.9 Data for Separation of k_E and k_{EH+} for the Alkaline Hydrolysis 5-APe Me

$T = (25.00 \pm 0.05)°C$

$I = 0.1$ mol l^{-1}

pH†	$[H^+]^*$ (mol l^{-1})	$(K_a^T + H^+)$ (mol l^{-1})	$\frac{k_{obs}}{[OH^-]}$ (l mol^{-1} min^{-1})	$\frac{k_{obs}}{[OH^-]}(K_a^T + [H^+])$ (min^{-1})
8.405	5.101×10^{-9}	5.172×10^{-9}	1020	5.275×10^{-6}
8.495	4.146×10^{-9}	4.217×10^{-9}	1155	4.871×10^{-6}
8.598	3.271×10^{-9}	3.342×10^{-9}	1345	4.495×10^{-6}
8.600	3.256×10^{-9}	3.327×10^{-9}	1335	4.441×10^{-6}
8.704	2.563×10^{-9}	2.633×10^{-9}	1535	4.042×10^{-6}
8.706	2.551×10^{-9}	2.622×10^{-9}	1526	4.000×10^{-6}
8.800	2.054×10^{-9}	2.125×10^{-9}	1715	3.645×10^{-6}
8.802	2.045×10^{-9}	2.116×10^{-9}	1695	3.586×10^{-6}
8.804	2.035×10^{-9}	2.106×10^{-9}	1700	3.581×10^{-6}
8.898	1.639×10^{-9}	1.710×10^{-9}	1995	3.367×10^{-6}
8.903	1.621×10^{-9}	1.691×10^{-9}	2005	3.429×10^{-6}
8.904	1.617×10^{-9}	1.688×10^{-9}	2030	3.433×10^{-6}
8.999	1.299×10^{-9}	1.370×10^{-9}	2400	3.288×10^{-6}
9.002	1.290×10^{-9}	1.361×10^{-9}	2385	3.246×10^{-6}
9.104	1.020×10^{-9}	1.091×10^{-9}	2895	3.158×10^{-6}
9.105	1.018×10^{-9}	1.089×10^{-9}	2835	3.086×10^{-6}
9.200	8.178×10^{-10}	8.886×10^{-10}	3435	3.052×10^{-6}
9.201	8.160×10^{-10}	8.867×10^{-10}	3485	3.090×10^{-6}
9.296	6.556×10^{-10}	7.189×10^{-10}	4095	2.966×10^{-6}
9.301	6.481×10^{-10}	7.264×10^{-10}	4125	2.975×10^{-6}

Using $K_a^T = 7.079 \times 10^{-11}$; $pK_a^T = 10.15$ (25°C and I = 0.1 mol l^{-1}), (Table 4.7).

† Stopped stirrer pH.

* $[H^+] = \frac{10^{-pH}}{0.7715}$ (25°C and I = 0.1 mol l^{-1}).

Figure 5.5 Separation of k_E and k_{EH^+} for Alkaline Hydrolysis of 5-APe Me

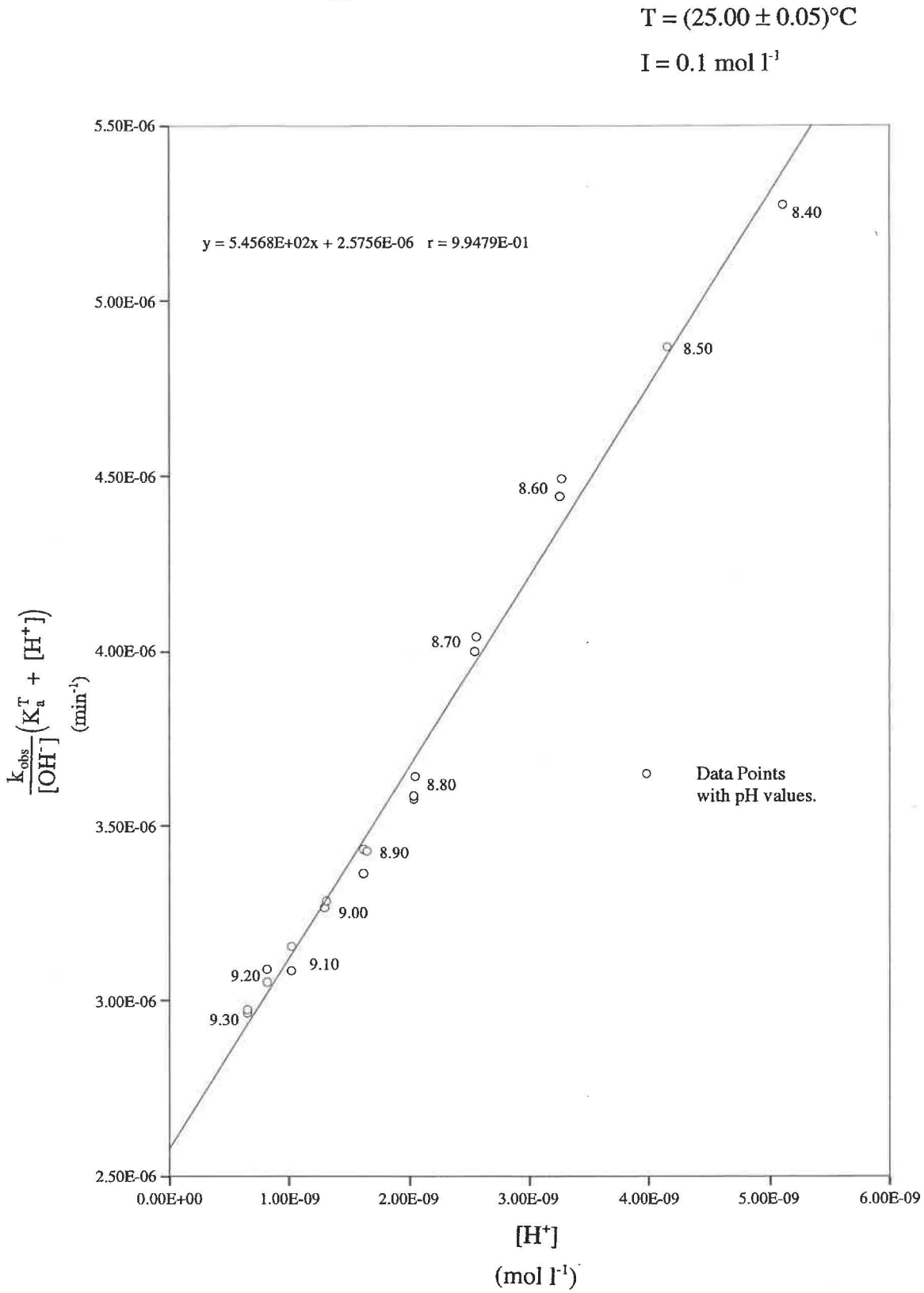

Table 5.10 shows the effect of raising the pK_a^T of 5-APe Me.HCl, at 25°C, from the experimental value of 10.15, to 10.20, 10.25 and 10.30, on the values of the rate constants, k_{EH^+} and $k_E(k_L)$.

Table 5.10 Effect of Changing pK_a^T on the Values of k_{EH^+} and k_E for 5-APe Me

pK_a^T	K_a^T	k_{EH^+} $l\ mol^{-1}\ min^{-1}$	y-axis intercept	$k_E\ (k_L)$ $l\ mol^{-1}\ min^{-1}$
10.15	7.079×10^{-11}	545.6	2.5756×10^{-6}	36380
10.20	6.310×10^{-11}	551.2	2.5465×10^{-6}	40360
10.25	5.623×10^{-11}	555.7	2.5223×10^{-6}	44855
10.30	5.012×10^{-11}	559.8	2.5003×10^{-6}	49885

These small changes in the pK_a^T values had no effect on the linearity of the graphical separation plots (all $r > 0.995$). As can be seen from Table 5.10, increasing the value of the pK_a^T from 10.15 to 10.30 produces only a small increase (~ 3 %) in the value of k_{EH^+}, but there is a dramatic rise in the value of $k_E(k_L)$ (~ 40 %). It seems unlikely that the value of pK_a^T was lowered by 0.15, but the sensitivity of the k_L value to changes in pK_a^T must be remembered in discussions of relative k_L values. This effect emphasizes the importance of putting a lot of effort into determining the best possible value for pK_a^T.

5.3(d) Esters of 2-Pyrrolidone-5-carboxylic Acid

Only P-5-CA Me and P-5-CA Et were in this group, and they differ from the ω-amino acid esters in that they exist only in an E form. Consequently, their kinetics are not complicated by the presence of a pH-dependent equilibrium. These esters undergo alkaline hydrolysis via pathway 2, Scheme 5.1; hence $k_{obs}/[OH^-] = k_E$ should remain constant, as the pH is varied.

P-5-CA Me

A 0.01 mol l^{-1} stock solution of this ester was prepared since it was an oil (see 2.1(f)) and it was difficult to weigh out accurately 1×10^{-4} moles. To minimise hydrolysis, the stock solution was refrigerated when not in use. The reaction solution for P-5-CA Me consisted of:

10.00 ml of 0.01 mol l^{-1} P-5-CA Me stock solution

80.00 ml DW

10.00 ml 1.0 mol l^{-1} KCl

Since the ester was present as a free base, no alkali was needed for neutralisation. Total volume = 100.00 ml, $[Ester]_T = 10^{-3}$ mol^{-1}, I = 0.1 mol l^{-1}. A summary of the results for this ester are in Appendix 3, and the k_E value is in Table 5.11

P-5-CA Et

This ester was weighed out as it was a solid, but it was only slightly soluble in H_2O, so it was initially dissolved in 5 ml of ethanol before being added to the reaction mixture. This consisted of:

10^{-4} moles P-5-CA Et

5.00 ml CH_3CH_2OH

85.00 ml DW

10.00 ml 1.0 mol l^{-1} KCl

Since the reaction solution was not 100% H_2O, pH $\neq -\log_{10}\{H^+\}$ (see 3.7) and values of $[OH^-]$ are approximate only. A summary of the results for this ester are in Appendix 3 and k_E is in Table 5.11.

5.4 Temperature Dependence of Rate Constants

5.4(a) Introduction

The reasons for studying the effect of temperature on the value of k_{EH^+}, and k_E or k_L for a particular compound were discussed previously (Section 5.1).

Accuracy checks on the equipment (see 3.2) and the experimental technique (see 5.3(a)) at 37.1°C and 50.2°C, were carried out weekly, using the rate constant for the alkaline hydrolysis of Ser Me. A GK2401B combination electrode was used and runs were done at pH = 10.3, (37.1°C) and pH = 9.3 (50.2°C). The results are summarised in Appendix 3, Tables A3.30 and A3.58, respectively.

Table 5.11 Summary of Rate Constants for Some ω-Monoamino Acid Esters and Related Compounds.

$T = (25.00 \pm 0.05)°C$

$I = 0.1$ mol l^{-1}

Ester	k_{EH^+} $l\ mol^{-1}\ min^{-1}$		k_E $l\ mol^{-1}\ min^{-1}$		k_L $l\ mol^{-1}\ min^{-1}$	
	Thesis Value	Lit. Values	Thesis Value	Lit. Values	Thesis Value	Lit. Values
Ser Me	-	-	58.8 ± 0.5	60[3] 59.3[1] 57.8[4] 58.9[5] 59.4[6]	-	-
2-AE Me*	-	2424[6] 1700[3] 2330[8]	-	72.2[6] 77.7[3] 74.4[7] 65.9[8]	-	-
3-AP Me†	-	412[9] 385[6] 383[7]	-	8.1[9] 8.2[6] 10.5[7]	-	-
4-AB Me	132 ± 13	125[9] 102[7]	~ 9	-	1580 ± 60	1758[9] 1671[7]
4-MAB Me	111 ± 11	-	~ 9	-	8610 ± 345	-
4-DMAB Me	-	265[6]	-	10.3[6]	-	-
4-A-3-MB Me	126 ± 13	-	~ 9	-	3400 ± 140	-
4-A-3,3-DMB Me	247 ± 25	-	~ 9	-	9390 ± 380	-
5-APe Me.	545 ± 71	5580[7]	~ 9	-	36380 ± 2910	28260[7]
Glu-5-Me	137 ± 14	-	~ 9	-	700 ± 28	-
Glu DMe**	2922 ± 220	-	~ 80***	-	~ 40***	122[3]

* Not studied at this temperature in this thesis.

† Not studied in this thesis.

** Value of rate constant for k_L is a combination of $k_E + k_L$.

*** see p.207 $k_L^A + k_{OH}^A = 121$ (see Scheme 5.2)

(Table 5.11 cont. next page)

$T = (25.00 \pm 0.05)°C$

$I = 0.1$ mol l^{-1}

Ester	k_{EH^+} l mol^{-1} min^{-1}		k_E l mol^{-1} min^{-1}		k_L l mol^{-1} min^{-1}	
	Thesis Value	Lit. Values	Thesis Value	Lit. Values	Thesis Value	Lit. Values
6-AH Me†	-	-	-	9.6[7]	-	-
4-AB Et	69.7 ± 7	-	~ 6	-	520 ± 21	530[10]§
4-MAB Et	75 ± 8	-	~ 6	-	2500 ± 100	-
4-DMAB Et	167 ± 13	-	6.9 ± 0.2	-	-	-
5-APe Et	89.4 ± 12	-	~ 6	-	11255 ± 900	13000[10]§
6-AH Et	14.6 ± 1.0	-	6.2 ± 0.2	-	-	-
2-AE Bz.	3326 ± 250	-	90 ± 2	-	-	-
3-AP Bz.	612 ± 46	-	14.0 ± 0.4	-	-	-
4-AB Bz	159 ± 16	-	~ 14	-	1843 ± 74	-
P-5-CA Me††	-	-	958 ± 10	960[11]	-	-
P-5-CA Et††	-	-	259 ± 7	-	-	-
CH_3COOCH_3	-	-		9.1[12]	-	-
$CH_3COOC_2H_5$	-	-		6.7[12]	-	-

* Not studied at this temperature in this thesis.

† Not studied in this thesis.

§ Literature value at T = 25°C and I = 0.2 mol l^{-1}

†† Error represents reproducibility.

5.4(b) Experimental

The same experimental procedure was used as at 25°C, with allowance being made for the expansion of water. The increase in temperature results in a decrease in the value of pK_a^T for the $-NH_3^+$ group by ~ 0.3 pK_a^T units per 12°C rise (see 4.4(b)). This is counterbalanced by an increase in rate constants of ~2 times per 12°C rise. Consequently, little modification was required to the pH-Stat procedures outlined at 25°C, except that $k_{obs}/[OH^-]$ values needed to be measured at progressively lower pH's with increased temperature.

Temperature dependence studies were performed on selected amino acids only. Those chosen were where no literature value existed but the effect of temperature was needed to help establish the nature of the intramolecular reaction mechanism, or where there was conflict within the literature results. The compounds studied were: Ser Me, 2-AE Me, 3-AP Bz, 4-AB Me, 4-AB Et, 4-AB Bz, 4-MAB Me, 4-MAB Et, 4-DMAB Me, 4-DMAB Et, 4-A-3-MB Me, 4-A-3,3-DMB Me, 5-APe Me and 5-APe Et.

Table 5.12 summarises the effect of temperature on the value of the rate constants for these amino acid esters along with the available literature values. Individual tables for the effect pH on the value of the $k_{obs}/[OH^-]$, data needed for the separation of k_E or k_L and k_{EH^+}, and the separation plots are in Appendix 3.

5.4(c) Thermodynamic Activation Parameters.

Introduction

Values for the Transition State Theory standard Gibbs Free Energy of activation ($\Delta G^{\ddagger}$), standard Enthalpy of Activation ($\Delta H^{\ddagger}$), standard Entropy of Activation, ($\Delta S^{\ddagger}$), and the Arrhenius Theory Energy of Activation (E_a) and Pre-exponential factor (A), for the amino acid esters were determined as follows:

$\Delta H^{\ddagger}$ and $\Delta S^{\ddagger}$ were evaluated from the temperature dependence of k_{EH^+} and k_E or k_L, using the following equations (a more detailed derivation of these is in Appendix A3.2):

Table 5.12 Temperature Dependence of k_E and k_{EH^+} of Selected Amino Acid Ester Hydrochlorides. [§]

$I = 0.1$ mol l^{-1}

Amino Acid Ester		25.0°C	37.1°C	50.2°C
Ser Me	k_E	58.8 ± 0.5	121 ± 2	268 ± 4
		59.3[9]	124.8[9]	271.1[9]
2-AE Me	k_E	72.2 ± 1.2[6]	151 ± 3	323 ± 6
		77.7[3]	145 [3]	285[3]
	k_{EH^+}	2420 ± 210[6]	5596 ± 448	11670 ± 934
2-AP Me	k_E	66.4	132.9	249.5
	k_{EH^+}	4815	9216	19471
3-AP Me*	k_E	8.1	22.3	56.9
	k_{EH^+}	412.1	933.3	2167
3-AP Bz	k_E	14.1 ± 0.3	28.8 ± 0.6	61.2 ± 1.2
	k_{EH^+}	612 ± 49	1419 ± 114	3247 ± 260
4-AB Me*	k_E	1580 ± 60	2470 ± 110	4020 ± 160
		1758[9]	2613[9]	4069[9]
		1674[7]	2868[9]	†
	k_{EH^+}	132 ± 13	205 ± 21	323 ± 33
		125[9]	216[9]	396[9]
4-AB Et*	k_E	520 ± 20	770 ± 30	1147 ± 46
	k_{EH^+}	69.7 ± 7.0	137 ± 14	276 ± 28
4-AB Bz*	k_E	1840 ± 70	2780 ± 110	4230 ± 170
	k_{EH^+}	159 ± 16	288 ± 29	520 ± 50
4-MAB Me*	k_E	8610 ± 345	11500 ± 460	15760 ± 630
	k_{EH^+}	111 ± 11	312 ± 31	850 ± 85

[§]All rate constants in 1 mol^{-1} min^{-1}.

*Ester underwent intramolecular aminolysis, $\therefore k_E$ is a combination of $k_E + k_L$

†Rate constant not determined at 50°C.

(Table 5.12 cont. next page)

Amino Acid Ester		25.0°C	37.1°C	50.2°C
4-MAB Et*	k_E	2500 ± 100	3570 ± 140	5320 ± 210
	k_{EH^+}	75.2 ± 7.5	210 ± 20	570 ± 60
4-DMAB Me	k_E	10.3 ± 0.2[6]	17.7 ± 0.4	30.3 ± 0.6
	k_{EH^+}	265 ± 23[6]	530 ± 40	1090 ± 40
4-DMAB Et	k_E	5.8 ± 0.1	9.2 ± 0.1	18.9 ± 0.4
	k_{EH^+}	168 ± 13	369 ± 30	669 ± 54
4-A-3-MB Me*	k_E	3400 ± 140	4920 ± 200	7460 ± 300
	k_{EH^+}	126 ± 13	216± 22	352 ± 35
4-A-3,3-DMB Me*	k_E	9390 ± 380	15520 ± 620	25900 ± 1000
	k_{EH^+}	247 ± 25	393 ± 39	630 ± 60
5-APe Me*	k_E	36380 ± 2550 28260[7]	47925 ± 3835 30340[7]	61800 ± 4900 †
	k_{EH^+}	545 ± 71	660 ± 90	760 ± 110
5-APe Et*	k_E	11300 ± 900	15900 ± 1300	21200 ± 1700
	k_{EH^+}	89.4 ± 12	119± 15	158± 21

§All rate constants in 1 mol^{-1} min^{-1}.

* Ester underwent intramolecular aminolysis, $\therefore$ k_E is a combination of $k_E + k_L$.

† Rate constant not determined at 50°C.

Transition State Theory Parameters

$\Delta H^{\ddagger}$

Rearranging equ. A3.15 (Appendix A79) gives:

$$-\frac{\Delta H^{\ddagger}}{R} = \left(\frac{\Delta \ln(k_2/T)}{\Delta(1/T)}\right) \qquad \ldots.(5.11)$$

For the same reasons outlined in Chapter 4, $\Delta H^{\ddagger}$ is best evaluated by calculation rather than graphically. This involves averaging three $\Delta H^{\ddagger}$ values which can be calculated using equ. 5.10 and taking the three pairs of the three $\ln(k_2/T)$ and $1/T$ values, with $R = 8.3145$ J K^{-1} mol^{-1}:

25.0 and 37.1 °C: $\Delta H^{\ddagger} = -8.3145\,\Delta \ln(k_2/T)/1.3081 \times 10^{-4}$ J mol^{-1} ....(5.11 (a))

25.0 and 50.2 °C: $\Delta H^{\ddagger} = -8.3145\,\Delta \ln(k_2/T)/2.6139 \times 10^{-4}$ J mol^{-1} ....(5.11 (b))

37.1 and 50.2 °C: $\Delta H^{\ddagger} = -8.3145\,\Delta \ln(k_2/T)/1.3058 \times 10^{-4}$ J mol^{-1} ....(5.11 (c))

where, $k_2 \equiv k_E$, k_L or k_{EH^+} in l mol^{-1} s^{-1}

T is in K

In general, there was excellent agreement between the three calculated values, which indicated that the $\ln(k_2/T)$ vs. $1/T$ plots would have shown good linearity, e.g. for Ser Me, the three values of $\Delta H^{\ddagger}$ were 43.25, 48.10 and 45.70 kJ mol^{-1} with the mean = (45.7 ± 2.3) kJ mol^{-1}

$\Delta S^{\ddagger}$

This was calculated by rearranging equ. A3.15, Appendix 3, which gives:

$$\Delta S^{\ddagger}_{298.15} = 8.3145 \cdot (\ln(k_2/298.15)) + \frac{\Delta H^{\ddagger}}{298.15} - 197.55 \text{ J K}^{-1} \text{ mol}^{-1} \qquad \ldots.(5.12)$$

with (k_2/T) in l mol^{-1} s^{-1} and $\Delta H^{\ddagger}$ in J mol^{-1}.

For Ser Me, $\Delta S^{\ddagger}_{298} = -92.0$ J K^{-1} mol^{-1} = $\Delta S^{\ddagger}_{310}$ = $\Delta S^{\ddagger}_{323}$. Any variation in $\Delta S^{\ddagger}$ indicates non-linearity of the $\ln(k_2/T)$ vs. $1/T$ plot.

$\Delta G^{\ddagger}$

From equ. A3.11, Appendix 3, at 298.15 K, this was given by:

$$\Delta G^{\ddagger}_{298} = \Delta H^{\ddagger} - 298.15 \cdot \Delta S^{\ddagger}_{298} \text{ kJ mol}^{-1},$$

with $\Delta H^{\ddagger}$ in kJ mol^{-1} and $\Delta S^{\ddagger}_{298}$ J K^{-1} mol^{-1}.

For Ser Me, $\Delta G^{\ddagger}_{298} = 73.1$ kJ mol^{-1}.

Table 5.13 summarises the $\Delta G^{\ddagger}_{298}$, $\Delta H^{\ddagger}$, and $\Delta S^{\ddagger}_{298}$ values for all the monoamino acid esters.

Arrhenius Parameters

E_a and A were included for completeness, and their values were calculated from the effect of temperature on $\ln k_2$ using equ. A3.18, Appendix 3. Hence,

$$\left(\frac{\Delta \ln k_2}{\Delta(1/T)}\right) = \frac{E_a}{R} \qquad \ldots.(5.13)$$

As before, E_a was best evaluated as the average of the three E_a values which can be calculated using equ. 5.13 by taking the three pairs of the three $\ln k_2$ and 1/T values, with k_2 expressed in l mol^{-1} s^{-1} and T in K.

E_a:

25.0 and 37.1 °C: $E_a = -8.3145\,\Delta \ln k_2 / 1.3081 \times 10^{-4}$ kJ mol^{-1} ....(5.13(a))

25.0 and 50.2 °C: $E_a = -8.3145\,\Delta \ln k_2 / 2.6139 \times 10^{-4}$ kJ mol^{-1} ....(5.13(b))

37.1 and 50.2 °C: $E_a = -8.3145\,\Delta \ln k_2 / 1.3058 \times 10^{-4}$ kJ mol^{-1} ....(5.13(c)),

with k_2 in l mol^{-1} s^{-1}.

For Ser Me, there was good agreement between the three values, with the mean E_a = (48.3 $\pm$ 2.4) kJ mol^{-1}

A:

lnA was calculated at 298 K by rearranging equ. A3.18, Appendix 3:

$$\ln A = \ln k_2(298.15) + \frac{E_a}{298.15 \cdot R} \text{ l mol}^{-1} \text{ s}^{-1} \quad \ldots.(5.14),$$

with k_2 in l mol^{-1} s^{-1}, E_a in J mol^{-1} and R in J K^{-1} mol^{-1}.

For Ser Me this gave $\ln A = 19.432$ $\therefore$ $A = (2.75 \pm 0.06) \times 10^8$ l mol^{-1} s^{-1}

Table 5.14 summarises the E_a, ln A and A values for all the monoamino acid esters.

Table 5.13 Thermodynamic Activation Parameters for Some Selected Amino Acid Esters

$I = 0.1$ mo l l^{-1}

Amino Acid Ester		$\Delta G^{\ddagger}_{298}$ * kJ mol^{-1}	$\Delta H^{\ddagger}$ kJ mol^{-1}	$\Delta S^{\ddagger}_{298}$ J K^{-1} mol^{-1}	$298 \cdot \Delta S^{\ddagger}_{298}$ kJ mol^{-1}
Ser Me	k_E	73.1	45.7 ± 2.3	-92.0	-27.4
Lit Value[9]		73.0	46.0	-90.4	-27.0
2-AE Me	k_E	72.5	45.1 ± 0.8	-92.0	-27.4
Lit. Value[3]		74.6	39.7	-117.2	-34.9
	k_{EH^+}	63.8	47.4 ± 3.3	-54.9	-16.4
2-AP Me[9]	k_E	72.5	39.7	-110.0	-32.8
	k_{EH^+}	62.1	42.3	-66.5	-19.8
2-AB Me[9]	k_E	75.4	40.2	-118.0	-35.2
	k_{EH^+}	63.6	44.8	-63.2	-18.8
3-AP Me[9]	k_E	77.9	59.8	-60.7	-18.1
	k_{EH^+}	68.1	50.6	-59.0	-17.5
3-AP Bz	k_E	76.6	44.1 ± 1.3	-109.1	-32.5
	k_{EH^+}	67.3	50.5 ± 0.4	-56.2	-16.8
4-AB Me	$k_E^{\dagger}$	64.9	27.1 ± 1.2	-126.9	-37.8
Lit. Value[9]		64.5	24.3	-134.7	-40.2
[7]		64.8	22.8	-141.0	-42.0
	k_{EH^+}	71.1	27.0 ± 1.1	-148.0	-44.1
Lit Value[9]		71.0	34.3	-123.0	-36.7
4-AB Et	$k_E^{\dagger}$	67.7	22.6 ± 0.1	-151.2	-45.1
	k_{EH^+}	72.7	41.2 ± 0.8	-105.5	-31.5
4-AB Bz	$k_E^{\dagger}$	64.5	23.8 ± 0.2	-136.5	-40.7
	k_{EH^+}	70.6	35.2 ± 0.1	-118.7	-35.4

(Table 5.13 cont. next page)

I = 0.1 mol l^{-1}

Amino Acid Ester		$\Delta G^{\ddagger}_{298}$ kJ mol^{-1}	$\Delta H^{\ddagger}$ kJ mol^{-1}	$\Delta S^{\ddagger}_{298}$ J K^{-1} mol^{-1}	$298 \cdot \Delta S^{\ddagger}_{298}$ kJ mol^{-1}
4-MAB Me	k_E†	60.8	16.7 ± 0.8	-147.8	-44.1
	k_{EH^+}	71.5	61.9 ± 0.7	-32.1	-9.6
4-MAB Et	k_E†	63.8	21.4 ± 1.3	-142.1	-42.4
	k_{EH^+}	72.5	61.9 ± 0.7	-35.4	-10.6
4-DMAB Me	k_E	77.5	31.8 ± 0.2	-153.1	-45.7
	k_{EH^+}	69.4	42.4 ± 0.7	-90.5	-27.0
4-DMAB Et	k_E	78.9	35.0 ± 8.2	-147.4	-43.9
	k_{EH^+}	70.5	41.4 ± 6.1	- 97.6	-29.1
4-A-3-MB Me	k_E†	63.0	22.4 ± 1.4	-136.2	-40.6
	k_{EH^+}	71.2	30.1 ± 1.6	-137.7	-41.1
4-A-3, 3-DMB Me	k_E†	60.5	29.8 ± 0.3	-103.1	-30.7
	k_{EH^+}	69.6	27.4 ± 0.4	-141.4	-42.2
5-APe Me	k_E†	57.2	14.3 ± 0.7	-143.8	-42.9
Lit Value[7]		57.9	2.1	-187	-55.8
	k_{EH^+}	67.5	7.8 ± 1.6	-200.2	-59.7
5-APe Et	k_E†	60.0	17.4 ± 1.7	-142.8	-42.6
	k_{EH^+}	72.0	15.5 ± 0.1	-189.5	-56.5

*Note this has been calculated from: $\Delta G^{\ddagger}_{298} = \Delta H^{\ddagger} - 298.15 \cdot \Delta S^{\ddagger}_{298}$

These values are in some cases slightly different from those calculated from $\Delta G^{\ddagger}_{298} = -298.15R\left(\ln\left(h/k_B\right) + \ln\left(k_2/298.15\right)\right) = -2478.97\left(-23.76 + \ln\left(k_2/298.15\right)\right)$, (where k_2 is expressed in l mol^{-1} s^{-1}), because of rounding.

† Ester underwent intramolecular aminolysis, $\therefore$ k_E is a combination of $k_E + k_L$.

Table 5.14 Arrhenius Parameters for Some Selected Amino Acid Esters

$I = 0.1$ mol l^{-1}

Amino Acid Ester		E_a kJ mol^{-1}	lnA	A l mol^{-1} s^{-1}
Ser Me	k_E	48.25± 2.38	19.432 ± 0.020	(2.75 ± 0.06) x 10^8
2-AE Me	k_E	47.75 ± 0.82	19.429 ± 0.09	(2.75 ± 0.06) x 10^8
	k_{EH^+}	50.04 ± 3.24	23.900 ± 0.034	(2.40 ± 0.08) x 10^{10}
3-AP Bz	k_E	46.69 ± 1.30	17.381 ± 0.014	(3.54 ± 0.05) x 10^7
	k_{EH^+}	53.08 ± 0.37	23.736 ± 0.002	(2.03 ± 0.00) x 10^{10}
4-AB Me	k_E	29.67 ± 1.27	15.231 ± 0.013	(4.12 ± 0.05) x 10^6
	k_{EH^+}	29.57 ± 1.12	12.703 ± 0.012	(3.29 ± 0.04) x 10^5
4-AB Et*	k_E	25.16 ± 0.03	12.310 ± 0.000	(2.22 ± 0.00) x 10^5
	k_{EH^+}	43.77 ± 0.82	17.804 ± 0.009	(5.40 ± 0.05) x 10^7
4-AB Bz*	k_E	26.42 ± 0.26	14.081 ± 0.003	(1.31 ± 0.01) x 10^6
	k_{EH^+}	37.81 ± 0.05	16.228 ± 0.001	(1.12 ± 0.01) x 10^7
4-MAB Me*	k_E	19.23 ± 0.83	12.720 ± 0.009	(3.34 ± 0.03) x 10^5
	k_{EH^+}	64.47 ± 0.65	26.636 ± 0.007	(3.70 ± 0.02) x 10^{11}
4-MAB Et*	k_E	24.01 ± 1.37	13.408 ± 0.014	(6.64 ± 0.11) x 10^5
	k_{EH^+}	64.48 ± 0.43	26.239 ± 0.005	(2.49 ± 0.01) x 10^{11}
4-DMAB Me	k_E	34.33 ± 0.11	12.088 ± 0.001	(1.78 ± 0.00) x 10^5
	k_{EH^+}	44.96 ± 0.90	19.617 ± 0.009	(3.31 ± 0.03) x 10^8
4-DMAB Et	k_E	37.57 ± 8.27	12.776 ± 0.087	(3.54 ± 0.32) x 10^5
	k_{EH^+}	43.77 ± 0.82	17.804 ± 0.009	(5.40 ± 0.05) x 10^7

*

(Table 5.14 cont. next page)

$I = 0.1$ mol l^{-1}

Amino Acid Ester		E_a kJ mol^{-1}	lnA	A l mol^{-1} s^{-1}
4-A-3-MB Me	k_E	25.02 ± 1.44	14.123 ± 0.015	(1.36 ± 0.02) x 10^6
	k_{EH^+}	26.77 ± 1.58	13.932 ± 1.63	(1.12 ± 0.02) x 10^6
4-A-3, 3-DMB Me	k_E	32.34 ± 0.30	18.095 ± 0.004	(7.22 ± 0.02) x 10^7
	k_{EH^+}	29.93 ± 0.42	13.488 ± 0.004	(7.21 ± 0.02) x 10^5
5-APe Me	k_E	16.83 ± 0.69	13.200 ± 0.007	(5.40 ± 0.04) x 10^5
	k_{EH^+}	10.41 ± 1.52	6.417 ± 0.016	(6.12 ± 0.10) x 10^2
5-APe Et	k_E	20.00 ± 1.67	13.315 ± 0.017	(6.06 ± 0.11) x 10^5
	k_{EH^+}	18.11 ± 0.06	7.706 ± 0.001	(2.22 ± 0.00) x 10^3

* Ester underwent intramolecular aminolysis, $\therefore k_E$ is a combination of $k_E + k_L$.

5.5 Discussion

5.5(a) Literature Comparison

k_E Values. As can be seen from Tables 5.11 and 5.12, the k_E results obtained in this study generally show good agreement with the available literature values within the error limits.

The greatest disagreements are the values of k_E (= k_L) for 5-APe Me. These differences of 25-50% are far larger than measurement errors and suggest a systematic error. The common source of systematic errors in pH-Stat studies is incorrect pH values; however, considerable care was taken throughout the current investigations to ensure that pH values were correct (see p. 161-162). Another possible source of systematic errors in the present pH-Stat studies is the value of pK_a^T used to separate k_L and k_{EH^+}. However, as has been discussed (p. 180 and 184), raising an hydrolysis affected pK_a^T **increases** k_L (Table 5.10), which makes the disagreement with the literature even larger. Since the literature values for k_L of 5-APe Me were determined by Stopped Flow, it must be concluded that there was probably some systematic error in the method (see 3.1(a), p.78).

k_{EH^+} Values. These generally show much greater disagreements than for the k_E values. This is particularly the case for 2-AE Me at 25°C and I = 0.1 mol l^{-1} (Table 5.11). The most likely reason for this is the different sizes of the pH range used to measure k_{obs} and separate k_E and k_{EH^+}. The pK_a^T is low (7.67 for 2-AE Me at 25°C), so k_{obs} values must be measured at low pH's (ideally below 7.67) in order to achieve a significant contribution from the hydrolysis of EH^+. At these low pH's the reaction is inconveniently slow and care must be taken to check for electrode drift over the long reaction times involved. The practical minimum reaction pH for 2-AE Me at 25°C was found to be ~ 8.8 ($t_{1/2}$ ~ 300 min.) and the maximum pH ~ 11.2 ($t_{1/2}$ ~ 6 min.).[6] Such large pH ranges, and measurements at low pH's as close as possible to the pK_a^T, yield the most accurate possible separation of the rate constants. This approach used in ref. 6 was also used in the present studies and so these results are the most accurate.

The other major disagreement with the literature is the result for 5-APe Me. The literature value is ~10 times the value obtained in this thesis (Table 5.11) and this

presumably relates to the probable systematic errors associated with the Stopped Flow investigation mentioned in the discussion of k_E values.

5.5(b) Substituent Effects

Information about the nature of a reaction mechanism can be gained by examining the effect of systematic structural changes on the value of the rate constant. These substituent effects arise from a variety of energy changes that contribute to $\Delta H^{\ddagger}$ and/or $\Delta S^{\ddagger}$ and hence to $\Delta G^{\ddagger}$ and the value of k (Appendix 3, equ. A3.15). The origin of these energy changes on substitution includes the following factors:

- Electronic effect changes: These are mainly ± **I** in aliphatic systems, and they contribute to changes in $\Delta H^{\ddagger}$. This effect is quantified by the Taft equation:[13]

$$\log_{10}\left(\frac{k}{k_o}\right) = \sigma^*\rho^*$$

- Bond changes: nett number and energy of bonds in the reactants and TS: The balance between bond breaking and bond formation in going from the reactant to the TS usually contributes to a change in $\Delta H^{\ddagger}$.

- Changes in nett solvation: The change in the extent of solvation in going from the reactants to the TS can be greatly affected by substitution, particularly for reactions involving ions in water. This will produce a change in both $\Delta H^{\ddagger}$ (via bond energy changes) and $\Delta S^{\ddagger}$ (due to a change in disorder).

- Electrostatic effects: Replacement of a neutral group by a charged group, e.g. $-NH_2$ by $-NH_3^+$, will produce major changes in $\Delta H^{\ddagger}$ and $\Delta S^{\ddagger}$ via changes in the solvation and bond energies in the reactants and TS. Changes in H-bonding (both intramolecular and intermolecular) can be a major contributor to this effect.

Clearly, to gain the best understanding of a reaction mechanism from studies on substituent effects, it is very important to determine values for $\Delta H^{\ddagger}$ and $\Delta S^{\ddagger}$, i.e. the temperature dependence of the rate constants must be established. Studies at a single temperature yield information about only a small part of the total change in energy –

classically, this small part is the contribution of inductive effects to the rate constant. Because such contributions are only a part of the total picture, conclusions drawn from single temperature studies are necessarily superficial and may be quite wrong.

The effect of substitution on the values of the rate constants will be discussed in two parts depending on the reaction mechanism involved: the $B_{Ac}2$ mechanism (paths 1 and 2, Scheme 5.1), or the OH^- assisted intramolecular nucleophilic aminolysis (path 3, Scheme 5.1).

(i) $B_{Ac}2$ mechanism

(1) ω-Amino Acid Esters; k_E Trends

It has been proposed that the alkaline hydrolysis of both the E and EH^+ forms of the methyl and ethyl esters of ω-amino acids, $H_2N(CH_2)_nCOOR'$ (where n = 1, 2 and 5) follow the $B_{AC}2$ type mechanism. It can be inferred that the analogous benzyl and the various C- and N- methylated derivatives also follow this mechanism. The rds is the first step, which involves attack of OH^- on the electron deficient carbonyl C of the ester,[14] i.e. for the E form:

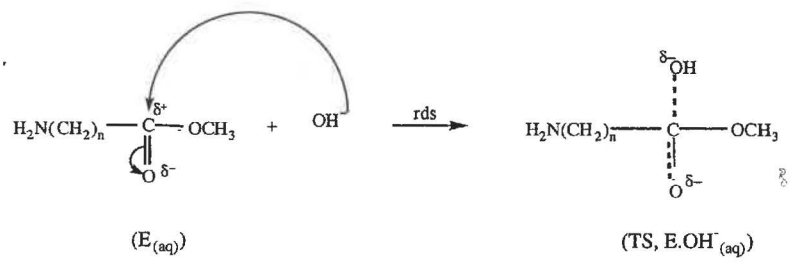

$(E_{(aq)})$ $(TS, E.OH^-_{(aq)})$

Scheme 5.3 Rate Determining Step in $B_{Ac}2$ Hydrolysis of E Form of ω-Amino Acid Methyl Esters.

Hence trends in k_E and k_{EH^+} with changes in structure (Tables 5.11 and 5.12) need to be examined to test this proposed mechanism. The available data (this thesis and literature results) is limited; much work remains to be done particularly regarding temperature dependence studies of the rate constants, so some of the conclusions drawn are necessarily tentative.

Considering only the straight chain, ω-amino acid methyl esters that belong to the homologous series, $H_2N(CH_2)_nCOOCH_3$ (n = 1, 2 and 5), the reference compound is CH_3COOCH_3. For ease of comparison, Table 5.15, summarises the values of k_E (from

Tables 5.11 and 5.12) and $\Delta H^{\ddagger}$, $\Delta S^{\ddagger}$ (from Table 5.13) for 2-AE Me, 3-AP Me, and CH_3COOCH_3. No temperature dependence studies have been made for 6-AH Me. Because of the limited data available for the series, data is also included for 2-AP Me and 2-AB Me (to assess factors which affect the values of the kinetic parameters for 2-AE Me), and for 4-DMAB Me (to help estimate values for 4-AB Me in the absence of lactamisation).

Table 5.15 Summary of k_E, $\Delta G^{\ddagger}$, $\Delta H^{\ddagger}$, $\Delta S^{\ddagger}$ and $T\Delta S^{\ddagger}$ Values for $B_{Ac}2$ Alkaline Hydrolysis of the E form of Some ω-Amino Acid Methyl Esters and Related Compounds.

Ester	k_E (298 K)	$\Delta G^{\ddagger}_{298}$ kJ mol^{-1}	$\Delta H^{\ddagger}$ kJ mol^{-1}	$\Delta S^{\ddagger}_{298}$ J K^{-1} mol^{-1}	$298 \cdot \Delta S^{\ddagger}_{298}$ kJ mol^{-1}
2-AE Me	72.2[6]	72.5*	45.1*	-92.0*	-27.4*
2-AP Me [9]	66.4	72.5	39.7	-110.0	-32.8
2-AB Me [9]	23.3	75.3	40.1	-118.0	-35.2
3-AP Me [9]	8.1	77.9	59.8	-60.7	-18.1
4-DMAB Me	10.3[6]	77.5*	31.8*	-153.1*	-45.7*
CH_3COOCH_3[12]	9.1	79.3	41.8	-125.9	-37.5
6-AH Me [7]	9.6	-	-	-	-

*This thesis.

Inductive Effect Explanation

Commonly, arguments based on inductive effects are used to explain why rate constants change with substitution; if one of the methyl group H's of the reference compound is replaced by $-NH_2$, the indirect –I effect of this group ($\sigma^* = +0.62$)[15] decreases the electron density at the carbonyl carbon and so facilitates the $B_{Ac}2$ rds (Scheme 5.3). Hence, k_E for 2-AE Me ($H_2NCH_2COOCH_3$) is predicted to be larger than for CH_3COOCH_3. This is correct (Table 5.15) with the two k_E values being 72.2 and 9.1 l mol^{-1} min^{-1} at 25°C.

However, inductive effects also predict that as the $-NH_2$ group is withdrawn from the carbonyl carbon, the indirect –I effect should rapidly decrease initially, followed by a slower decrease and the changes in k_E should follow this pattern. This prediction is only partly true. Table 5.15 shows that k_E decreases rapidly from 2-AE Me (n = 1,

k_E = 72.2 l mol^{-1} min^{-1} at 25°C) to 3-AP Me (n = 2, k_E = 8.2 l mol^{-1} min^{-1}). Lactamisation prevents the determination of k_E values for 4-AB Me (n = 3) and 5-APe Me (n = 4). However, for 6-AH Me (n = 5), k_E = 9.6 l mol^{-1} min^{-1} which is larger than for 3-AP Me! Clearly, the inductive effect argument is failing and the reasons for this are outlined in 5.5(b). Despite the limitations of inductive effect arguments, a value of k_E for 4-AB Me and 5-APe Me can be fairly confidently estimated as ~ 9 l mol^{-1} min^{-1}, which is insignificant compared to the k_L values.

Similar arguments apply to the more limited data for the corresponding Et and Bz ester series in Table 5.11.

Another failure of inductive effect arguments comes from the observed changes in k_E on alkylation at C-2 in 2-AE Me (2-AP Me and 2-AB Me). Replacement of one H by CH_3 produces little change (77.2 to 66.4 l mol^{-1} $min.^{-1}$), but replacement by CH_3CH_2 produces a large decrease to 23.3 l mol^{-1} $min.^{-1}$. Both groups are very weak +**I** (σ^* = 0.00 and -0.10) and so would be expected to have no effect on the reaction rate.

The failure of the inductive effect arguments emphasises the need for a more complete discussion involving all the energy terms that contribute to the changes in rate constants on substitution. This discussion must involve considering the signs and magnitudes of the $\Delta H^{\ddagger}$ and $\Delta S^{\ddagger}$ values.

$\Delta H^{\ddagger}$ and $\Delta S^{\ddagger}$ Explanation

$\Delta H^{\ddagger}$ is defined (from Scheme 5.3) by:

$$\Delta H^{\ddagger}(E) = H^{\circ}(TS, E{\cdot}OH^{-}_{(aq)}) - H^{\circ}(E_{(aq)}) - H^{\circ}(OH^{-})_{(aq)} \qquad \ldots.(5.15)$$

with a parallel definition for $\Delta S^{\ddagger}$ (equ. 5.15(a)).

There are a large number of factors (see 5.5(b)) which contribute to each of the terms on the right hand side of equations 5.15 and 5.15(a). In the following discussion, attempts will be made to identify the major factors which are responsible for the observed values of $\Delta H^{\ddagger}$ and $\Delta S^{\ddagger}$, and for changes in these values with changes in structure. Undoubtedly, there will be delicate balances – small differences between large numbers – the results of which will have profound effects on the reaction rates.

Experimental Errors

These must be estimated before any conclusions can be drawn from the changes in a given term in Table 5.15 with changes in structure. Calculations based on the error estimates for the rate constants and the range of the three calculated $\Delta H^{\ddagger}$ values (p. 191), show that the absolute error in $\Delta H^{\ddagger}$ is typically 1 (range ~ 0.7 - 2.2) kJ mol^{-1} while that in $\Delta S^{\ddagger}$ is ~ 4 (range 3 – 6) J K^{-1} mol^{-1}. Hence, differences between $\Delta H^{\ddagger}$ values, $\delta\Delta H^{\ddagger}$, of $< \sim 2$ kJ mol^{-1}, and between $\Delta S^{\ddagger}$ values, $\delta\Delta S^{\ddagger}$, of $< \sim 8$ J K^{-1} mol^{-1} are insignificant.

$\Delta H^{\ddagger}$ values for all the esters are large and positive (+30 to +60 kJ mol^{-1}). This means that the enthalpy of the $TS_{(aq)}$ is much larger than the sum of the enthalpies of $E_{(aq)}$ and $OH^-_{(aq)}$. The endothermic partial breaking of the strong carbonyl bond contributes a large positive term to $\Delta H^{\ddagger}$ but this is partly offset by the negative contribution from the partial formation of the carbonyl C to OH^- bond. There are additional bonding changes associated with alterations in the degree of hydration. The $B_{Ac}2$ TS is extremely polar (implied by the large negative $\Delta S^{\ddagger}$, see below). Consequently, there is a nett increase in hydration and the weak bonds involved in this will contribute another negative term to $\Delta H^{\ddagger}$. Overall, $\Delta H^{\ddagger}$ is large and positive due to the dominance of the bond breaking required to form the TS.

$\Delta S^{\ddagger}$ values are all large and negative (-60 to -150 J K^{-1} mol^{-1}). This large nett decrease in disorder on forming the TS reflects the highly polar nature of the $B_{Ac}2$ TS and the consequent huge increase in solvation. A smaller negative contribution to $\Delta S^{\ddagger}$ comes from the increase in order associated with a bimolecular reaction. Support for the importance of solvation effects comes from the difference in $\Delta S^{\ddagger}$ values for 2-AE Me (-92.0 J K^{-1} mol^{-1}) and CH_3COOCH_3 (-125.9 J K^{-1} mol^{-1}). Introduction of the **–I** amino group increases the polarisation of the carbonyl group in the reactant, thereby increasing the solvation, decreasing $S°(E_{(aq)})$ and raising $\Delta S^{\ddagger}$. The size of this effect in the TS is much smaller (i.e. $S°(TS_{(aq)})$ is decreased less) because of the presence of the OH^-, and so overall, $\Delta S^{\ddagger}$ is raised (equ. 5.15(a)). $\Delta H^{\ddagger}$ is also raised because of this increased solvation ($H°(E_{(aq)})$ decreases), equ. 5.15.

Note that solvation changes associated with the OH^- reactant have been ignored; it has been assumed that they will be constant throughout all the discussion.

Trends in $\Delta H^{\ddagger}$ and $\Delta S^{\ddagger}$ with Structure

(a) Amino Group

The difficulty in discussing the reasons for any changes in $\Delta H^{\ddagger}$ and $\Delta S^{\ddagger}$ as the $-NH_2$ group is moved along the C-chain (2-AE Me to 6-AH Me) is the limited data available (Table 5.15). Ideally, some "best" values for the parameters for each position should be calculated. However, only the 2-position has been investigated for more than one ester and the values of the three sets of parameters are surprisingly variable. The reasons for this illustrate the complex interactions of the many terms that make up the overall values for $\Delta H^{\ddagger}$ and $\Delta S^{\ddagger}$. 2-AE Me and 2-AP Me have significantly different, but compensating, $\Delta H^{\ddagger}$ and $\Delta S^{\ddagger}$ values so their k_E values are almost identical. 2-AB Me hydrolyses more slowly, mainly because of a more negative $\Delta S^{\ddagger}$. There is a steady decrease in $\Delta S^{\ddagger}$ on alkylation (2-AE to 2-AP to 2-AB Me). A similar phenomenon is observed in carboxylic acid esters and has been ascribed to steric effects.[16] Increased steric crowding at the "6-position" decreases the reaction rate mainly via a decrease in $\Delta S^{\ddagger}$ (the Newmann "rule of 6" involving addition to an unsaturated function; note that in this, numbering starts from the carbonyl-O and ends on terminal H's).[16] However, Taft[17] has stated that increases in steric hindrance in the TS generally produce an increase in $\Delta H^{\ddagger}$ as well as a decrease in $\Delta S^{\ddagger}$. In the present case, stepwise alkylation at the 2-position of 2-AE Me does produce a decrease in $\Delta S^{\ddagger}$ but $\Delta H^{\ddagger}$ **decreases** to 2-AP Me with no significant change to 2-AB Me. The major contributor to the fall in $\Delta S^{\ddagger}$ is presumably the "rule of 6" steric effect, since changes in other contributing terms (particularly solvation) are expected to be small with alkyl substitution. Apparently, the expected steric effect increase in $\Delta H^{\ddagger}$ is overbalanced by a decrease in another term. One possible source of this may be the weak **+I** effect of alkylation at the amino-C which decreases the polarisation of the carbonyl group produced by the $-NH_2$. The resulting decreased solvation in the reactant will increase $H^{\circ}(E_{(aq)})$. In the TS, polarisation effects are dominated by the partly bonded OH^- and the partly broken carbonyl bond which swamp changes produced by alkylation. Consequently, $H^{\circ}(TS, E{\cdot}OH^-_{(aq)})$ is unchanged and $\Delta H^{\ddagger}$ falls on alkylation, (equ. 5.15). This decreased solvation would also contribute an increase to $S^{\circ}(E_{(aq)})$ and assist the fall in $\Delta S^{\ddagger}$ (equ. 5.15(a)) associated with the steric effect.

Because of the unexpectedly large changes produced by alkylation at the 2-position, it is impossible to improve the quality of the parameters (Table 5.15) by averaging them for all the 2-amino acid esters. Consequently, the best comparison for assessing the effect of withdrawing the $-NH_2$ group to the 3-position is between 2-AE Me and 3-AP Me. This withdrawal produces a decrease in k_E which is usually explained in terms of a decreased **–I** effect of the $-NH_2$ group reducing the positive charge on the carbonyl C and hence decreasing the ease of OH^- attack. However, this explanation is clearly superficial because there are large increases in opposing effects - an increase in $\Delta H^{\ddagger}$ (~ 15 kJ mol^{-1}) and an increase in $\Delta S^{\ddagger}$ (~ 31 J K^{-1} mol^{-1}; T. $\Delta S^{\ddagger}$ ~ 9 kJ mol^{-1}). The increase in $\Delta H^{\ddagger}$ dominates, resulting in a decrease in k_E. The large $\Delta S^{\ddagger}$ change suggests a major role is being played by solvation effects. Removal of the $-NH_2$ group must be raising $S^{\circ}(TS, E{\cdot}OH^-_{(aq)})$ and/or lowering $S^{\circ}(E_{(aq)})$ (equ. 5.15(a)).

Raising $S^{\circ}(TS, E{\cdot}OH^-_{(aq)})$ requires decreased solvation in the TS. This is expected because the decrease in **–I** effect from the $-NH_2$ will reduce the polarisation at what was originally the carbonyl C. An alternative, or additional, explanation is that the increased chain length may allow intramolecular H-bonding to produce a 6-membered ring between an amino-H and the partly negatively charged O of the original carbonyl bond, which would again lead to decreased solvation. This is less likely because of the small ring size; 8-membered rings involving H-bonding are preferred.

Lowering $S^{\circ}(E_{(aq)})$ requires increased solvation; the reverse will in fact occur as removal of the $-NH_2$ will decrease its polarisation effect on the carbonyl group, releasing H_2O's. This negative contribution to $\Delta S^{\ddagger}$ must be outweighed by the positive term from the decreased solvation in the TS, so the overall value (equ. 5.15(a)) is positive.

This nett decrease in solvation will contribute to an increase in $\Delta H^{\ddagger}$. Further increases will come from the reduced **–I** effect of the NH_2 which both decreases the polarisation of the carbonyl group ($E_{(aq)}$ is more stable, $H^{\circ}(E_{(aq)})$ is lower) and also decreases the ease of OH^- attack with a weakening of the C---OH^- bond in the TS, which raises its enthalpy. Hence (equ. 5.15), overall there is a large increase in $\Delta H^{\ddagger}$.

The change in k_E (and its $\Delta H^{\ddagger}$, $\Delta S^{\ddagger}$) in going from the 3- to the 4- and 5-positions cannot be determined because of lactamisation. However, 4-DMAB Me gives some indication of the 4-position parameters (see (b) 4-DMAB Me below).

No $\Delta H^{\ddagger}$ and $\Delta S^{\ddagger}$ data is available for the 6-position.

(b) 4-DMAB Me

It was hoped that the k_E value for this compound would give an indication of the change in going from the 3- to the 4-position in the absence of lactamisation. With the k_E experimental error being ~ 2.5% (p.175), the result at 25°C (10.3 ± 0.3) is significantly larger than that for 3-AP Me (8.1 ± 0.2), but the values for 6-AH Me (9.6 ± 0.3)[7] and CH_3COOCH_3 (9.1, no error)[12] are also higher. It can be concluded that removal of the $-NH_2$ group beyond the 2-position reduces k_E to between 8 and 10 l mol^{-1} min^{-1}, with variations that cannot be explained by inductive effects. However, as can be seen from the $\Delta H^{\ddagger}$ and $\Delta S^{\ddagger}$ values, N-dimethylation has introduced some effects that would be absent in 4-AB Me with no lactamisation. The smallness of the change in k_E masks a large decrease in $\Delta H^{\ddagger}$ (28.0 kJ mol^{-1}) but the rate increase resulting from this is almost entirely cancelled out by a large fall in $\Delta S^{\ddagger}$ (~ 90 J K^{-1} mol^{-1}) ($T.\Delta S^{\ddagger}$ = 27.6 kJ mol^{-1}). The origin of this large change in $\Delta S^{\ddagger}$ is most likely solvation changes. N-dimethylation must be lowering $S°(TS, E{\cdot}OH^-_{(aq)})$ and/or raising $S°(E_{(aq)})$ (equ. 5.15(a)). One source of an increase in $S°(E_{(aq)})$ is the reduction in the **–I** effect of the $-NH_2$ group with its removal from the 3- to 4- position, and the replacement of the two H's by CH_3's. The major effect is the attenuation of the inductive effect with increased distance, but in addition, the **+I** effect of the two methyl groups will push electron density onto the amino-N. Both effects will reduce the polarisation of the carbonyl group and release bound H_2O in the reactant. These effects will be insignificant in the TS where solvation is dominated by the partly bonded OH^-, resulting overall in a decrease in $\Delta S^{\ddagger}$. Another consequence of this effect will be a fall in $\Delta H^{\ddagger}$ via the increase in $H°(E_{(aq)})$ and little change in $H°(TS, E{\cdot}OH^-_{(aq)})$ (equ. 5.15).

These changes in $\Delta H^{\ddagger}$ and $\Delta S^{\ddagger}$ also suggest that intramolecular H-bonding in the TS, between an amino-H and the partly negatively charged O of the original carbonyl bond, is not a factor where small (7-membered) rings are involved. N-dimethylation would prevent such bonding, leading to an increase in $S°(TS, E{\cdot}OH^-_{(aq)})$ and an increase in $\Delta S^{\ddagger}$ (and $\Delta H^{\ddagger}$), which is the opposite of what is observed.

(c) Ester/Leaving Group

The only data available for k_E is replacing methyl by benzyl (3-AP Me to 3-AP Bz, Table 5.13). This substitution results in little change in reactivity ($\Delta G^{\ddagger}$ decreases 1 kJ mol^{-1}). While this is predicted for the $B_{Ac}2$ mechanism from simple inductive effect considerations (the small increase in **-I** effect from the change in σ^* values ($-CH_3$, 0.00; $-CH_2C_6H_5$, +0.27[15] leads to little change in the electron density at the carbonyl carbon and the ease of OH^- attack will almost be unchanged), the small change in $\Delta G^{\ddagger}$ hides large decreases in both $\Delta H^{\ddagger}$ and $\Delta S^{\ddagger}$ (by 16 kJ mol^{-1} and 48 J K^{-1} mol^{-1} respectively). Several effects will contribute to these changes, but the large magnitudes of the overall change suggests that the terms arising from solvation effects are important.

One effect will be electronic; there is a small increase in the **-I** effect from $-CH_3$ to $-CH_2C_6H_5$ with the increase in the σ^* value. This will slightly lower the electron density on the carbonyl-C, assist rds attack by OH^- ($B_{Ac}2$ mechanism) and hence contribute to a small decrease in $\Delta H^{\ddagger}$. Also, the increase in **-I** effect strengthens the polarisation of the carbonyl group with a consequent increase in the solvation of the reactant ($S°(E_{(aq)})$ decreases). However in the TS, solvation is dominated by the developing negative charge on the oxygen and will be larger than for the reactant's carbonyl group. Consequently, the change in **-I** effect will have less effect and so there is only a slight decrease in $S°(TS, E{\cdot}OH^-_{(aq)})$. This contributes to an increase in $\Delta S^{\ddagger}$ and hence a rise in $\Delta H^{\ddagger}$ because of the smaller decrease in solvent bonding in the reactants as compared to the TS; $H°(E_{(aq)})$ rises much less than $H°(TS, E{\cdot}OH^-_{(aq)})$. Overall, the balance are the observed decreases in $\Delta H^{\ddagger}$ and $\Delta S^{\ddagger}$.

Another effect will be steric; substitution of $-CH_3$ by $-CH_2C_6H_5$ involves an increase in steric size. Since the $B_{Ac}2$ rds involves an increase in steric crowding at the carbonyl-C reaction centre (sp^3 change to sp^2/sp^3 hybridisation), the substitution will raise $H°(TS, E{\cdot}OH^-_{(aq)})$ more than $H°(E_{(aq)})$ and contribute to a rise in $\Delta H^{\ddagger}$. The increased steric crowding in the TS may also make it slightly less solvated. This would further raise both $H°(TS, E{\cdot}OH^-_{(aq)})$ and $S°(TS, E{\cdot}OH^-_{(aq)})$ with relatively small changes in the corresponding reactant terms and so contribute rises to both $\Delta H^{\ddagger}$ and $\Delta S^{\ddagger}$.

However, with the limited data, further work is needed to confirm this apparent effect of a bulky ester group on the parameters for amino acid ester $B_{Ac}2$ alkaline hydrolysis.

(2) Other k_E Values

An attempt was made to measure these for Glu DMe and Glu-5-Me as they are derivatives of 4-AB Me. The effect of substitution at C4 by $-COOCH_3$ and $-COO^-$ can be checked against the predictions of the $B_{Ac}2$ mechanism. Glu-5-Me is formed from Glu DMe but there is a parallel intramolecular aminolysis reaction to P-5-CA Me which then also hydrolyses (Scheme 5.2, p. 153), so this reaction was also investigated. Rate constants were measured only at 25°C, so the discussion is of limited value because the absence of $\Delta H^{\ddagger}$ and $\Delta S^{\ddagger}$.

Glu DMe

The complications in the alkaline hydrolysis of Glu DMe (a pair of parallel reactions which are both followed by consecutive reaction(s)) result in the value of "k_E" for Glu DMe being a combination of rate constants. However, because the subsequent reactions are either much faster (lactamisation (intramolecular aminolysis) of Glu-5-Me and dangling ester group hydrolysis of P-5-CA Me) or much slower (alkaline hydrolysis of Glu-5-Me), the measured k_E is approximately the sum of the two rate constants for the lactamisation and simple alkaline hydrolysis reactions, $k_L^A + k_{OH^-}^A$, respectively (Scheme 5.2, p. 153). This sum is 121 l mol^{-1} min^{-1} at 25°C (Table 5.11, p. 186) and, unlike the lactamisation reactions of 4-AB Me and 5-APe Me, the rate constant for lactamisation must be small and appears to be similar to that expected for the simple alkaline hydrolysis, $k_{OH^-}^A$. The latter can be estimated by considering Glu DMe to be part of the ester series $H_2N(CHR)COOCH_3$, where R = $-CH_2CH_2COOCH_3$. Substituting the polar substituent constant σ^* for R ($\sigma^* = +0.26$)[15] into the established Taft relationship[9] for the alkaline hydrolysis of α-amino acid methyl esters at 25°C; $\log(k_E/k_E^\circ) = 0.65\sigma^*$ (k_E° is the rate constant for 2-AP Me, 66.4 l mol^{-1} min^{-1}) yields $k_{OH^-}^A = 98$ l mol^{-1} min^{-1} and hence $k_L^A = 23$ l mol^{-1} min^{-1}. The estimate of the value for $k_{OH^-}^A$ appears slightly high, presumably because of the dominant, interferring, –I effect from the $-NH_2$ ($\sigma^* = +0.62$)[15] also attached to C-2

which makes the σ^* ($-CH_2CH_2COOCH_3$) value of +0.26 too large. A more realistic estimate for $k^A_{OH^-}$ would be that it is slightly larger than k_E for 2-AE Me, i.e. ~ 80 l mol^{-1} min^{-1} which makes k^A_L ~ 40 l mol^{-1} min^{-1}. This slow rate of lactamisation reflects the deactivation of the $-NH_2$ group by the adjacent electron withdrawing methoxycarbonyl.

Glu-5-Me

Lactamisation also complicates the alkaline hydrolysis of the E form of this ester, but here it must be fast since the overall rate constant is 700 l mol^{-1} min^{-1} (Table 5.11) and so this is the dominant reaction pathway. The ester's structure can be regarded as a 4–COO^- substituted 4-AB Me. Hence, the moderate **+I** effect from the carboxylate group (σ^* = -1.06)[15] will have little influence on the $-COOCH_3$ (because of attenuation by the three intervening C's) and so $k^C_{OH^-}$ will be small and similar to k_E for 4-AB Me (~ 9 l mol^{-1} min^{-1}). Consequently, the lactamisation rate constant is ~ 700 l mol^{-1} min^{-1}.

P-5-CA Me

This is the product from the lactamisation of Glu DMe (Scheme 5.2). k_E for the dangling ester group of P-5-CA Me is 958 l mol^{-1} min^{-1} (Table 5.11).This large value cannot be explained simply in terms of the inductive effect of a pyrrolidone group β to an ester group. While no σ^* value is available for pyrrolidone, it is expected to be similar to that for $-CH_2CONH_2$ (σ^* = +0.31)[15] and less than that for $-NH_2$ (σ^* = +0.62).[15] Hence, inductive effects would predict that, since the introduction of an $-NH_2$ group increases the k_E for CH_3COOCH_3 by ~ 8 times, the pyrrolidone group should increase it by a smaller factor and not the observed 100 times. The source of this large increase cannot be the change in steric crowding by the bulky pyrrolidone group as the reactant sp^2 hybridised C goes to the TS sp^2/sp^3 hybridised C, since this change will increase the steric strain and slow the rate. Changes in solvation are most likely to be involved, but in the absence of $\Delta H^‡$ and $\Delta S^‡$ data, no firm conclusions can be drawn. Studies on the ethyl ester showed that k_E was decreased by ~ 3.7 times (to 259 l mol^{-1} min^{-1}), a much larger decrease than the usual factor of ~ 2 times observed

in going from the methyl to the ethyl ester in simple $B_{Ac}2$ hydrolysis.[18] Again this suggests unusual effects which need further investigation.

(3) ω-Amino Acid Esters; k_{EH^+} Trends

Like the E forms, the EH^+ forms of the methyl and ethyl esters of ω-amino acids are believed to undergo alkaline hydrolysis by the $B_{Ac}2$ mechanism. The rds is analogous to Scheme 5.3. However, unlike the E forms, the predictions of this mechanism can be more thoroughly tested because there are no gaps in the data since intramolecular aminolysis cannot occur.

For the straight chain ω-amino acid methyl esters that belong to the homologous series, $^+NH_3(CH_2)_nCOOCH_3$ (n = 1, 2...5), the available kinetic data (from Tables 5.11, 5.12 and 5.13) is summarised in Table 5.16, for ease of comparison.

Table 5.16 Summary of k_{EH^+}, $\Delta G^{\ddagger}$, $\Delta H^{\ddagger}$, $\Delta S^{\ddagger}$ and $T\Delta S^{\ddagger}$ Values for $B_{Ac}2$ Alkaline Hydrolysis of the EH^+ Form of Some ω-Amino Acid Methyl Esters.

Amino Acid Ester	k_{EH^+} (298 K)	$\Delta G^{\ddagger}_{298}$ kJ mol^{-1}	$\Delta H^{\ddagger}$ kJ mol^{-1}	$\Delta S^{\ddagger}_{298}$ J K^{-1} mol^{-1}	$298 \cdot \Delta S^{\ddagger}_{298}$ kJ mol^{-1}
2-AE Me	2424[6]	63.8*	47.5*	-54.9*	-16.4*
3-AP Me[9]	412.1	68.1	50.6	-59.0	-17.5
4-AB Me*	132	71.1	27.0	-148.0	-44.1
5-APe Me*	545	67.6	7.8	-200.2	-59.7
5-APe Et*	89.4	72.0	15.5	-189.5	-56.5

*This thesis.

Inductive Effect Explanation

As can be seen, the value of k_{EH^+} decreases rapidly from 2-AE Me (n = 1) to 3-AP Me (n = 2), with a further, but much smaller, decrease to 4-AB Me (n = 3). This agrees with inductive effect predictions based on the $B_{Ac}2$ mechanism: as the strongly electron withdrawing $-NH_3^+$ group ($\sigma^* = +3.76$)[15] is withdrawn from the carbonyl carbon, the indirect **–I** effect it experiences decreases almost exponentially. Hence, there is a parallel decrease in the ease of nucleophilic attack by OH^-.

However, at n = 4 (5-APe Me) there is an increase in k_{EH^+} of ~ 4 times. This cannot be explained simply by inductive effects. The same conclusion applies to the relationship between k_{EH^+} for the 5-APe Me and Et esters – they differ by a factor of ~ 6 times instead of the expected ~ 2 times.[18] A more complete understanding of the factors controlling these trends can be found from the $\Delta H^{\ddagger}$ and $\Delta S^{\ddagger}$ values.

$\Delta H^{\ddagger}$ and $\Delta S^{\ddagger}$ Explanation

$\Delta H^{\ddagger}$ is defined (from Scheme 5.2) by:

$$\Delta H^{\ddagger}(EH^+) = H^{\circ}(TS, EH^+\cdot OH^-_{(aq)}) - H^{\circ}(EH^+_{(aq)}) - H^{\circ}(OH^-)_{(aq)} \quad ....(5.16)$$

with a parallel definition for $\Delta S^{\ddagger}$ (equ. 5.16(a)).

As before (p. 202), the following discussion will try to identify the major factors that control the values of each of the terms on the right hand sides of equations 5.16 and 5.16(a). Whether the differences in $\Delta H^{\ddagger}$ (or $\Delta S^{\ddagger}$) values for different compounds are significant is controlled by the experimental error limits which are the same as before (p. 203).

$\Delta H^{\ddagger}$ for 2-AE Me and 3-AP Me, like those for their k_E values (Table 5.15), are both large and positive. The reason for this is the same balance between bond breaking and formation discussed on p. 203, but this is modified by the presence of H^+. The ionic EH^+ is more solvated than the dipolar E. In the TS this charge is neutralised by OH^- which makes TS, $EH^+\cdot OH^-_{(aq)}$, less polar (and hence less solvated) than TS, $E\cdot OH^-_{(aq)}$. Consequently, $H^{\circ}(EH^+_{(aq)})$ is lowered cf. $H^{\circ}(E_{(aq)})$ while $H^{\circ}(TS, EH^+\cdot OH^-_{(aq)})$ is raised cf. $H^{\circ}(TS, E\cdot OH^-_{(aq)})$. Overall, $\Delta H^{\ddagger}$ values (equ. 5.16) are expected to be more positive than for the corresponding E form, when a comparison is possible (2-AE Me and 3-AP Me). This is correct, with $\Delta H^{\ddagger}$ for the EH^+ forms of 2-AE Me and 3-AP Me being larger (by 2.3 and 10.9 kJ mol^{-1}, respectively) than for their E forms.

However, 4-AB Me and the 5-APe esters have anomalously low $\Delta H^{\ddagger}$ values (~+27 and +8, +16 kJ mol^{-1}), although no direct comparison with E values is possible. This is discussed under the heading of trends with structure below.

$\Delta S^{\ddagger}$ values are all large and negative (-55 to -200 J K^{-1} mol^{-1}) and, as for the E form, this is mainly due to the high degree of solvation in the TS with the modifications due to the presence of H^+ outlined in the $\Delta H^{\ddagger}$ discussion above. Charge neutralisation on

forming the TS results in desolvation, i.e. $S°(TS, EH^+ \cdot OH^-_{(aq)})$ is raised, and the positive charge on EH^+ will make it more hydrated, i.e. $S°(EH^+_{(aq)})$ is lowered, compared to E. Overall, $\Delta S^‡$ values (equ. 5.16(b)) are expected to be more positive than for the corresponding E form, when a comparison is possible (2-AE Me and 3-AP Me). This is true for 2-AE Me ($\Delta S^‡$ increases from –92 to –55 J K^{-1} mol^{-1}) where the two charges in the TS are close. As the chain length increases, charge neutralisation becomes almost insignificant and consequently for 3-AP Me there is only a small increase in the $\Delta S^‡$ value (from -61 and –59 J K^{-1} mol^{-1}) in going from E to EH^+. No comparison between E and EH^+ can be made for 4-AB Me and 5-APe Me because of lactamisation. Their $\Delta S^‡$ values are much more negative (-148 to -200 J K^{-1} mol^{-1}) and this is accompanied by much smaller $\Delta H^‡$ values. This suggests additional factor(s) are involved. The reasons for these trends with structure are discussed in the next section.

Trends in $\Delta H^‡$ and $\Delta S^‡$ with Structure

(a) Ammonium Group

As this is moved from the 2- to the 3-position, $\Delta H^‡$ increases (by ~ 3 kJ mol^{-1}) and this is reinforced by a small decrease in $T.\Delta S^‡$ of ~ 1 kJ mol^{-1}. Combined, these produce a large fall in the reaction rate. This originates in the greatly reduced **–I** effect of the $–NH_3^+$ which lowers $H°(EH^+_{(aq)})$ (more stable because of decreased carbonyl polarisation) and raises $H°(TS, EH^+ \cdot OH^-_{(aq)})$ (C---OH^- bond is weaker); both terms contribute an increase to $\Delta H^‡$. The small decrease in $T.\Delta S^‡$ indicates a nett increase in order, presumably due to changes in solvation. Removal of the ammonium group will decrease its polarisation of the carbonyl group and release H_2O's (raising $S°(EH^+_{(aq)})$) but this negative contribution to $\Delta S^‡$ is not quite balanced by the positive contribution from decreased solvation in the TS (raised $S°(TS, EH^+ \cdot OH^-_{(aq)})$. This is the reverse of the entropy balance seen in the E form (p. 205) for the reasons discussed under the $\Delta S^‡$ heading above.

Removal of the ammonium group to the 4-position produces large decreases in both $\Delta H^‡$ (~ -25 kJ mol^{-1}) and $\Delta S^‡$ (~ -91 J K^{-1} mol^{-1}). However, these changes almost cancel each other; the $\Delta S^‡$ fall just dominates which results in a small rise in $\Delta G^‡$ (~ +3 kJ mol^{-1}) and a three-fold fall in k_{EH^+}. This rate constant decrease is sensible in terms of inductive effects, but again, **the inductive effect explanation hides most of**

the reasons for the change. The large fall in $\Delta S^{\ddagger}$ probably indicates a major difference in solvation effects accompanying the increased chain length and the shift of the ammonium group from the 3- to the 4-position. This shift must be lowering $S°(TS, EH^{+}\cdot OH^{-}_{(aq)})$ and/or raising $S°(EH^{+}_{(aq)})$ (equ. 5.16(a)).

Raising $S°(EH^{+}_{(aq)})$ requires decreased solvation; this would occur as removal of the $-NH_3^+$ will decrease its polarisation effect on the carbonyl group (releasing H_2O's), but the effect will be small as most of the attenuation of such indirect **–I** effects occurs in the 2- to 3-shift. Clearly, another type of interaction must be involved if $S°(EH^{+}_{(aq)})$ is to be greatly raised. A likely possibility is intramolecular H-bonding between the ammonium and carbonyl groups. Such bonding has been discussed in relation to its catalysis of ester hydrolysis via the withdrawal of electrons from the carbonyl C and hence increased ease of OH^- attack (ref. 9 and refs therein). A comparison was made between the alkaline hydrolysis rate constants for the two series $^{+}NH_3(CH_2)_nCOOCH_3$ and $(CH_3)_3N^{+}(CH_2)_nCOOCH_3$ (wherein no intramolecular H-bonding is possible), for n = 1, 2 and 3, at one temperature (25°C). Taking into account the different indirect **–I** effects of the two ammonium groups, the results suggested that H-bonding catalysis was insignificant for n = 1, 2 and 3 (5-, 6- and 7-membered rings, respectively). The validity of this conclusion is limited by the absence of temperature dependence studies for the quaternary ammonium esters, since there may be other factors hidden in the values of the rate constants ($\Delta G^{\ddagger}$). However, this conclusion is supported by the $\Delta H°$ and $\Delta S°$ data (but hidden in the $\Delta G°$ data) for the pK_a^T's of the amino acid ester hydrochlorides (p. 127 – 133). This data gives evidence for intramolecular H-bonding only at n = 4 (EH^+ form of 5-APe Me; 8-membered ring). Despite this, it may be that solvation effects are more sensitive to intramolecular H-bonding than these other effects. (A difference in sensitivities between phenomena such as pK_a^T's and rate constants is to be expected, since pK_a^T relate to equilibria (i.e. $\Delta G^{\circ} = \Sigma G^{\circ}_{products} - \Sigma G^{\circ}_{reactants}$), whereas rate constants relate to the kinetics of a reaction (i.e. $\Delta G^{\ddagger} = G^{\ddagger}_{TS.} - \Sigma G^{\circ}_{reactants}$). There is no reason why the rds for the $B_{Ac}2$ reaction for EH^+ form of 4-AB Me should have the same sensitivity to intramolecular H-bonding as its $-NH_3^+$ dissociation). Hence, the $\Delta S^{\ddagger}$ value may be affected also at n = 3 by such intramolecular H-bonding. For n = 3 and 4, this will result in 7- and 8-membered rings in EH^+ (Scheme 5.4):

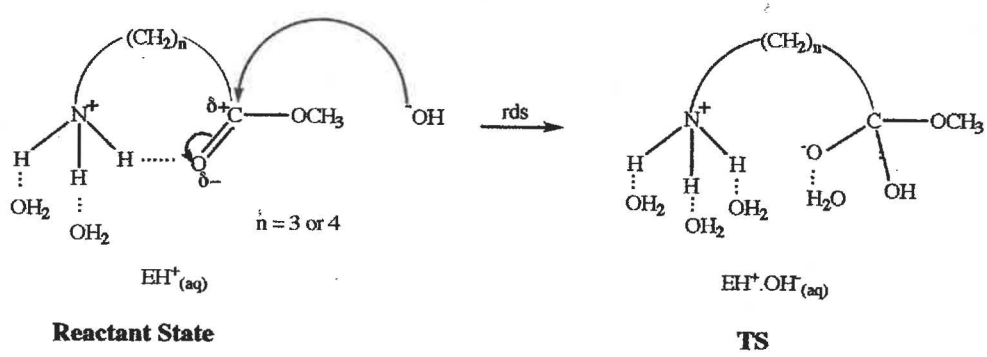

Scheme 5.4 Intramolecular H-bonding in the EH^+ Form of 4-AB Me and 5-APe Me.

Such H-bonding will considerably decrease the solvation in EH^+ (greatly increase $S°(EH^+_{(aq)})$ and so contribute a major decrease to $\Delta S^‡$), but this will be partly balanced by a resulting decrease in the internal freedom of EH^+.

The question then is what happens in the TS as the chain length is increased to n = 4, i.e. what happens to the value of $S°(TS, EH^+{\cdot}OH^-_{(aq)})$? This must either stay almost unchanged or decrease so that when combined with the increase in $S°(EH^+_{(aq)})$, there is the observed large decrease in $\Delta S^‡$. This implies that little if any intramolecular H-bonding occurs in the TS, (Scheme 5.4). Such bonding will raise $S°(TS, EH^+{\cdot}OH^-_{(aq)})$, cancel out the rise in $S°(EH^+_{(aq)})$ and make $\Delta S^‡$ more positive than is observed. The reason for the lack of significant intramolecular H-bonding in the TS must be due to the presence of OH^-. The resulting negative charge centre presumably forms strong intermolecular H-bonds to many water molecules rather than an intramolecular bond to an ammonium H. Combined with the hydration of a free ammonium group, this results in a heavily solvated TS for all n values (increased separation results in less charge neutralisation and hence increased solvation, see top of p. 212). The outcome is a large decrease in $\Delta S^‡$ in going from 3-AP Me to 4-AB Me. There is a further but slightly smaller decrease in going to 5-APe Me which suggests that intramolecular H-bonding in EH^+ is even more important for n = 4.

These changes in solvation will contribute to decreases in $\Delta H^‡$ for n = 3 and 4. $H°(EH^+_{(aq)})$ is raised due to the decreased solvation/bonding in EH^+ and there may be a fall in $H°(TS, EH^+{\cdot}OH^-_{(aq)})$ with increased solvation in the TS. Both factors decrease $\Delta H^‡$ from ~ 50 kJ mol^{-1} for 2-AE Me and 3-AP Me, to ~ 27 kJ mol^{-1} for 4-AB Me with a further large fall to ~ 8 kJ mol^{-1} for 5-APe Me. This latter change suggests that the decreased solvation accompanying intramolecular H-bonding in the EH^+ form of 5-APe Me has raised its enthalpy up to almost that of the TS; this would result in an

extremely rapid reaction were it not balanced by a large fall in $\Delta S^{\ddagger}$. Overall, at 25°C the k_{EH^+} value is about 10 times that expected from inductive effects (Table 5.16, 2-AE Me, 2420; 3-AP Me, 412; 4-AB Me, 132; 5-APe Me, 545 l mol^{-1} min^{-1} at 25°C). **Again, the importance of dividing $\Delta G^{\ddagger}$ (k_{EH^+}) into its $\Delta H^{\ddagger}$ and $\Delta S^{\ddagger}$ components is clear if the reasons for trends in rate constants with structural changes are to be understood.** Delicate balances between large opposing effects associated with solvation changes can tip the balance between $\Delta H^{\ddagger}$ and $\Delta S^{\ddagger}$ and result in "odd" changes in rate constants. To further emphasize this, the results for 5-APe Et (Table 5.16) are "unexpected". The much lower rate constant (89.4 l mol^{-1} min^{-1} at 25°C) than the methyl ester is due to a large rise in $\Delta H^{\ddagger}$ counterbalanced by a small rise in $\Delta S^{\ddagger}$. Similar "odd" behaviour was also seen for the pK_a^T of 5-APe Et (p. 131). From this viewpoint, the simplest explanation is that there is no intramolecular H-bonding in the EH^+ form of 5-APe Et. From a kinetic viewpoint, there is evidence for a small amount of intramolecular H-bonding: both the $\Delta H^{\ddagger}$ and $\Delta S^{\ddagger}$ are low but lie between the values for 4-AB Me and 5-APe Me. Additional kinetic support comes from the corresponding diamino acid ester, 2,5-DAPe Me (p. 132). The abnormally fast hydrolysis rate of the EH^+ form (2-NH_2, 5-NH_3^+) suggests catalysis by intramolecular H-bonding, but no temperature dependence studies have been made. $\Delta G^{\ddagger}$, $\Delta H^{\ddagger}$, $\Delta S^{\ddagger}$ and $T\Delta S^{\ddagger}$ data is available for some other diamino acid methyl ester EH^+ (ω-NH_3^+) forms, Table 5.17:

Table 5.17 Changes in k_{EH^+}, $\Delta G^{\ddagger}$, $\Delta H^{\ddagger}$, $\Delta S^{\ddagger}$ and $T\Delta S^{\ddagger}$ for the EH^+ Form (ω-NH_3^+) of Some α, ω-Diamino Acid Esters.

Amino Acid Ester	k_{EH^+} (298 K)	$\Delta G^{\ddagger}_{298}$ kJ mol^{-1}	$\Delta H^{\ddagger}$ kJ mol^{-1}	$\Delta S^{\ddagger}_{298}$ J K^{-1} mol^{-1}	$298 \cdot \Delta S^{\ddagger}_{298}$ kJ mol^{-1}
2,3-DAP Me[1]	3440	62.9	45.6	-58.2	-17.4
2,4-DAB Me[1]	24800	58.1	30.6	-92.1	-27.5
2,5-DAPe Me[7]	155400*	-	-	-	-
2,6-DAH Me[1]	73	72.6	36.4	-121.3	-36.2

*Temperature dependence studies not performed on the EH^+ form of this ester.

The decrease in $\Delta H^{\ddagger}$ from 2,3-DAP Me to 2,4 DAB Me (~15 kJ mol^{-1}) parallels that from 3-AP Me and 4-AB Me (~24 kJ mol^{-1}), with a similar relationship for $\Delta S^{\ddagger}$ (~ 34 and ~ 91 J K^{-1} mol^{-1}).

Clearly, more work needs to be done on the effects of substitution at the ester group before firm conclusions can be drawn regarding its solvation effects.

(b) N-methylation

Changes in the value of the rate constant on stepwise N-methylation of the protonated forms of the ω-amino acid esters should help assess the importance of intramolecular H-bonding assistance in the $B_{Ac}2$ mechanism, since such bonding will cease on complete methylation. For the derivatives of 2-AE Me and 3-AP Me, data is limited to a single temperature and so, in the absence of $\Delta H^{\ddagger}$ and $\Delta S^{\ddagger}$ values, any conclusions must be tentative. Such data is available for the derivatives of 4-AB Me and this will be discussed later. No data is available for 5-APe Me derivatives. The results from Table 5.11 and the literature at 25°C are summarised in Table 5.18:

Table 5.18 Effect of N-methylation on the Value of "k_{EH^+}" (l mol^{-1} min^{-1} at 25°C, I = 0.1 mol l^{-1}) for the Alkaline Hydrolysis of ω-Monoamino Acid Esters, $R(CH_2)_nCOOCH_3$.

R	n = 1	n = 2	n = 3
$-NH_3^+$	2424[6] (2-AE Me)	385[6] (3-AP Me)	132* (4-AB Me)
$-N(CH_3)H_2^+$	-	-	111[6] (4-MAB Me)
$-N(CH_3)_2H^+$	1236[19]	2730[19]	265[6] (4-DMAB Me)
$-N(CH_3)_3^+$	4764[19]	330[19]	60[19]

[8] This thesis

Simple inductive effect considerations predict that progressive replacement of the nitrogen-H's by +I CH_3 groups should decrease both the positive charge at N and the indirect –I effect of the group. Hence, the value of "k_{EH^+}" should decrease down the Table. This is clearly incorrect and other factors must be involved. The most important of these is probably solvation and the associated possible intramolecular H-bonding.

For n = 1, N-methylation results in "k_{EH^+}" for the trimethylammonium compound (wherein no intramolecular H-bonding is possible) being almost the same as for the other compounds. It was concluded[19] that, from a kinetic viewpoint, intramolecular H-bonding (which would involve a 5-membered ring) was insignificant in the whole series. The same conclusion can be drawn for n = 2 regarding a lack of any assistance in the hydrolysis of 3-AP Me (6-membered ring). However, the dimethylammonium compound hydrolyses 7-8 times faster than the other members of this series. It was concluded[19] that intramolecular H-bonding was forced on this molecule because it reduced the steric interaction between the two N-methyl groups and the adjacent pair of methylenes. At n = 3, there is a small fall in the rate constant on removal of all the N-H's. This suggests some intramolecular H-bonding in the other members of the series (again, larger at R = $-N(CH_3)_2H^+$ for steric reasons, as for n = 2) and this is supported by the large fall in $\Delta S^{\ddagger}$ (k_{EH^+}) on going from 3-AP Me to 4-AB Me (p. 212).

Hopefully, $\Delta H^{\ddagger}$ and $\Delta S^{\ddagger}$ values should help to more clearly define the reasons for these trends. These parameters are available for the 4-AB esters except for the N-trimethyl compounds (Table 5.19 ex. Tables 5.12 and 5.13):

Table 5.19 Effect of N-methylation on the Value of "k_{EH^+}", $\Delta G^{\ddagger}$, $\Delta H^{\ddagger}$, $\Delta S^{\ddagger}$ and $T\Delta S^{\ddagger}$ for the Methyl and Ethyl Esters of 4-AB and Some N-methylated Derivatives.

Amino Acid Methyl Ester	"k_{EH^+}" l mol^{-1} min^{-1}			$\Delta G^{\ddagger}_{298}$ kJ mol^{-1}	$\Delta H^{\ddagger}$ kJ mol^{-1}	$\Delta S^{\ddagger}_{298}$ J K^{-1} mol^{-1}	$298 \cdot \Delta S^{\ddagger}_{298}$ kJ mol^{-1}
	25°C	37°C	50°C				
4-AB Me	132	205	323	71.1	27.0	-148.0	-44.1
4-MAB Me	111	312	850	71.5	61.9	-32.1	-9.6
4-DMAB Me	265[6]	530*	1089*	69.4	42.4	-90.5	-27.0
4-AB Et	69.7	137	276	72.7	41.2	-105.5	-31.5
4-MAB Et	75.2	209	571	72.5	61.9	-35.4	-10.6
4-DMAB Et	168	369	669	70.5	41.4	- 97.6	-29.1

*This thesis.

Single N-methylation (4-AB to 4-MAB) produces a large rise (35 to 40 kJ mol^{-1}) in $\Delta H^{\ddagger}$ for both esters. This decrease in the rate constant is almost balanced by the increase associated with large increases in $\Delta S^{\ddagger}$ (70 to 116 J K^{-1} mol^{-1}) (T. $\Delta S^{\ddagger}$ increases by 22 to 35 kJ mol^{-1}). Again, small changes in the rate constant ($\Delta G^{\ddagger}$) hide large underlying effects. The large increases in $\Delta S^{\ddagger}$ suggest major changes in solvation on single N-methylation. Considering Scheme 5.4 for the EH^{+} form of 4-AB Me (p. 214), decreasing the number of N-H's by replacing one with an $N\text{-}CH_3$ will decrease the extent of intramolecular H-bonding, hence allowing more hydration in "EH^{+}". This will decrease $S°(EH^{+}_{(aq)})$ with little change in S°(TS, $EH^{+}\cdot OH^{-}_{(aq)}$) (TS lacks intramolecular H-bonding so $\Delta S^{\ddagger}$ will increase. Accompanying this will be an increase in $\Delta H^{\ddagger}$ due to the increased nett bonding in "EH^{+}".

However, this is reversed on dimethylation where the steric interactions discussed above favour some intramolecular H-bonding. This expected intermediate level of intramolecular H-bonding is supported by the $\Delta H^{\ddagger}$ and $\Delta S^{\ddagger}$ values which lie between those of the non-methylated (4-AB) and singly methylated (4-MAB) esters. The falls in both $\Delta H^{\ddagger}$ and $\Delta S^{\ddagger}$ in going from 4-MAB to 4-DMAB are delicately balanced in favour of the fall in $\Delta H^{\ddagger}$. Consequently, both of the dimethylated (4-DMAB) esters hydrolyse slightly more rapidly than their mono- and non-methylated analogues.

(c) C-methylation

It was hoped that the kinetic effects of stepwise methylation at C-3 of 4-AB Me would further help in understanding the importance of factors such as intramolecular H-bonding in controlling the rate constants for the $B_{Ac}2$ hydrolysis of the EH^{+} form of amino acid esters. Any conclusions must be preliminary since the data is limited; it is taken from Tables 5.12 and 5.13 and is summarised in Table 5.20:

Table 5.20 Effect of C-methylation on the Value of "k_{EH^+}", $\Delta G^{\ddagger}$, $\Delta H^{\ddagger}$, $\Delta S^{\ddagger}$ and $T\Delta S^{\ddagger}$ for the Methyl Ester of 4-AB and Some C-methylated Derivatives.

Amino Acid Methyl Ester	"k_{EH^+}" l mol^{-1} min^{-1}			$\Delta G^{\ddagger}_{298}$ kJ mol^{-1}	$\Delta H^{\ddagger}$ kJ mol^{-1}	$\Delta S^{\ddagger}_{298}$ J K^{-1} mol^{-1}	$298.\Delta S^{\ddagger}_{298}$ kJ mol^{-1}
	25°C	37°C	50°C				
4-AB Me	132	205	323	71.1	27.0	-148.0	-44.1
4-A-3-MB Me	126	216	352	71.2	30.1	-137.7	-41.1
4-A-3,3-DMB Me	247	393	633	69.6	27.4	-141.4	-42.2

*This thesis.

Mono-methylation at C-3 produces little change in "k_{EH^+}"at all three temperatures but, again **little change in $\Delta G^{\ddagger}$ hides significant changes in $\Delta S^{\ddagger}$ and $\Delta H^{\ddagger}$.** It has previously been concluded that there is some intramolecular H-bonding in the EH^+ form of 4-AB Me. This appears to be disrupted by the introduction of a methyl group at C-3 because there is an increase in $\Delta S^{\ddagger}$ that is most likely due to a decrease in $S°(EH^+_{(aq)})$, i.e. an increase in solvation in EH^+. (The value of $S°(TS, EH^+\cdot OH^-_{(aq)})$ is dominated by the presence of two charge centres and is unlikely to be affected by the small C-methylation change; there appears to be no intramolecular H-bonding in any of the three TS's). Disruption of intramolecular H-bonding is probably associated with the steric effect of the bulky methyl group which forces the ion to adopt conformations that are unfavourable to interactions between the ammonium and carbonyl groups. $\Delta H^{\ddagger}$ increases slightly which reflects the dominance of increased hydration in EH^+ (decrease in $H°(EH^+_{(aq)})$) over decreased intramolecular H-bonding (increase in $H°(EH^+_{(aq)})$), with $H°(TS, EH^+\cdot OH^-_{(aq)})$ presumably almost constant.

However, di-methylation results in approximately a two-fold increase in the rate constant which originates from a fall in $\Delta H^{\ddagger}$ (~3 kJ mol^{-1}) partly balanced by a fall in $\Delta S^{\ddagger}$, with values back towards those for 4-AB Me. This suggests a return to some intramolecular H-bonding and supports the conclusions from the pK_a^T studies (p. 138). The two gem-methyl groups sterically force a gauche conformation on the EH^+ form of 4-A-3,3-DMB Me resulting in a 7-membered intramolecular H-bond. Consequently, EH^+ is now less solvated, $S°(E_{(aq)})$ is raised and $\Delta S^{\ddagger}$ decreases as does

$\Delta H^{\ddagger}$, which is the reverse of the argument for the changes from 4-AB Me to 4-A-3-MB Me.

(d) Ester/Leaving Group

Data on the effect of changing the nature of the ester group on the value of k_{EH^+} is limited, but it is more extensive than for k_E. The results (ex. Tables 5.12 and 5.13) are summarised in Table 5.21:

Table 5.21 Effect of Varying the Leaving Group on the Values of k_{EH^+}, $\Delta G^{\ddagger}$, $\Delta H^{\ddagger}$, $\Delta S^{\ddagger}$ and $T\Delta S^{\ddagger}$ for Some Esters.

Amino Acid Ester	k_{EH^+} $l\ mol^{-1}\ min^{-1}$ (298 K)	$\Delta G^{\ddagger}_{298}$ $kJ\ mol^{-1}$	$\Delta H^{\ddagger}$ $kJ\ mol^{-1}$	$\Delta S^{\ddagger}_{298}$ $J\ K^{-1}\ mol^{-1}$	$298 \cdot \Delta S^{\ddagger}_{298}$ $kJ\ mol^{-1}$
4-AB Me	132	71.1	27.0	-148.0	-44.1
4-AB Et	69.7	72.7	41.2	-105.5	-31.5
4-AB Bz	159	70.6	35.2	-118.7	-35.4
4-MAB Me	111	71.5	61.9	-32.1	-9.6
4-MAB Et	75.2	72.5	61.9	-35.4	-10.6
4-DMAB Me	265	69.4	42.4	-90.5	-27.0
4-DMAB Et	168	70.5	41.4	-97.6	-29.1
5-APe Me	545	67.5	7.8	-200.2	-59.7
5-APe Et	89.4	72.0	15.5	-189.5	-56.5

As for the k_E discussion (p. 207), simple inductive effect considerations based on the $B_{Ac}2$ mechanism predict that the kinetic effects of the ester group changes in Table 5.21 will be small since there is little change in σ^* values ($-CH_3$ = 0.00, $-C_2H_5$ = -0.10, $-CH_2C_6H_5$ = +0.27).[15] Hence, there will be little change in the electron density at the carbonyl carbon and the ease of OH^- attack will be almost unchanged. However, Tables 5.12 and 5.21 show significant variations in k_{EH^+} values at all 3 temperatures.

For 4-AB, the ethyl ester is only about half as reactive as the methyl ester. This is commonly observed[18] for k_E but unexpected for k_{EH^+} where the positive charge effect

should outweigh the effect of minor changes in σ^* values for the ester group. Also, the pK_a^T data (p. 139) shows no difference between the two esters. Again, kinetics is apparently a more searching test for what are presumably changes in solvation effects since there are rises in both $\Delta H^{\ddagger}$ and $\Delta S^{\ddagger}$ in going from 4-AB Me to 4-AB Et. Such changes are characteristic of decreases in the extent of intramolecular H-bonding (see N-methylation discussion p. 216). In the present case the changes are relatively small, and probably result from minor changes in both electronic and steric effects; replacing $-CH_3$ by $-C_2H_5$ slightly increases electron withdrawl from the carbonyl C which increases polarisation in the carbonyl bond and strengthens intramolecular H-bonding to an ammonium-H. This substitution also increases the steric bulk of the ester group, which increases steric crowding at the sp^2 hybridised carbonyl C and this decreases the ease of intramolecular H-bonding; the balance is apparently a decrease.

The changes in $\Delta H^{\ddagger}$ and $\Delta S^{\ddagger}$ are reversed in going from the ethyl to the benzyl ester. The latter hydrolyses ~ 2 times faster than the ethyl ester and ~ 1.3 times faster than the methyl ester. While the $\Delta H^{\ddagger}$ and $\Delta S^{\ddagger}$ values both decrease back towards those for the methyl ester, the decrease in $\Delta H^{\ddagger}$ is larger and is responsible for the benzyl ester being more reactive than its ethyl analogue. It is the most reactive of the three esters because of its combination of intermediate $\Delta H^{\ddagger}$ value and high $\Delta S^{\ddagger}$.

The reasons for these changes appear complex. If as before, **intramolecular H-bonding** is dominant, replacing $-C_2H_5$ by $-CH_2C_6H_5$ will decrease electron dwithdrawl and increase steric bulk. The balance is small but if it is a decrease intramolecular H-bonding, as before, it will contribute falls in $\Delta H^{\ddagger}$ and $\Delta S^{\ddagger}$ which is in fact observed. Clearly, other consequences from the changes in electronic and steric effects may be important. These have been discussed previously for the 3-AP Me to 3-AP Bz change (p. 207) wherein intramolecular H-bonding is absent. **Electronic** effects also alter the ease of OH^- attack (small decrease in $\Delta H^{\ddagger}$) and the polarisation of the carbonyl group (solvation changes give significant changes to both $\Delta H^{\ddagger}$ and $\Delta S^{\ddagger}$). **Steric** effects alter the steric crowding at the reaction centre with possible solvation changes (increases in both $\Delta H^{\ddagger}$ and $\Delta S^{\ddagger}$). It was concluded that the dominant effect was solvation changes arising from the change in carbonyl group polarisation. This results in small decreases in $\Delta H^{\ddagger}$ and $\Delta S^{\ddagger}$ and, in the present case, combine with the falls in both terms from intramolecular H-bonding, produces the observed moderate fall in $\Delta H^{\ddagger}$ and slight fall in $\Delta S^{\ddagger}$. Apparently, the consequences of

carbonyl group solvation changes are hidden by those due to intramolecular H-bonding. There appears to be a delicate balance between these two opposing effects which can be tipped by small structural changes.

For 4-MAB, going from the Me to the Et ester produces a smaller decrease in k_{EH^+} than for the 4-AB esters. This is accompanied by no change in $\Delta H^{\ddagger}$ and a small decrease in $\Delta S^{\ddagger}$. Lack of the rise in both these terms, which is characteristic of a decrease in intramolecular H-bonding, as seen for 4-AB Me to Et, suggests that this is not the dominant feature. This agrees with the conclusion that there is much less intramolecular H-bonding in 4-MAB esters than in the corresponding 4-AB esters (see p. 217). Hence, there can be little decrease in this bonding and this will contribute only small increases to $\Delta H^{\ddagger}$ and $\Delta S^{\ddagger}$. Overriding this must be small decreases in both terms. The origin of other factors which contribute to changes in $\Delta H^{\ddagger}$ and $\Delta S^{\ddagger}$ have been discussed (p. 207 with a summary in 4-AB above). The balance between these produces decreases in $\Delta H^{\ddagger}$ and $\Delta S^{\ddagger}$. which, in this case, must be small to result in the observed overall changes. These small decreases (Me to Et) contrast with the large ones suggested for Me to Bz (3-AP) and Et to Bz (4-AB) changes, presumably because of differences in the changes in **+I** and steric effects. Again, a very delicate balance appears to exist, this time between small effects.

For 4-DMAB, the level of intramolecular H-bonding is intermediate between that for 4-AB (moderate) and 4-MAB (low) (p. 218). Replacement of $-CH_3$ by $-C_2H_5$ will thus contribute small increases to both $\Delta H^{\ddagger}$ and $\Delta S^{\ddagger}$ (via a small decrease in intramolecular H-bonding/increased solvation in EH^+) and small decreases to both terms via decreased solvation in EH^+ due to the increased electron donation and steric effects. The latter effects apparently dominate with overall, small falls in both $\Delta H^{\ddagger}$ and $\Delta S^{\ddagger}$. At first sight, this is surprising in view of the increase in H-bonding over the 4-MAB esters. However, the result undoubtedly reflects the delicate balance between these two opposing effects.

For 5-APe, the decrease in k_{EH^+} in going from the methyl to the ethyl ester is more dramatic (6 times cf. 1.5 to 1.9 times for the other esters). This is due to a large rise in $\Delta H^{\ddagger}$ ($\sim$ 8 kJ mol^{-1}), partly balanced by a smaller rise in T. $\Delta S^{\ddagger}$ ($\sim$ 3 kJ mol^{-1}). There is

considerable intramolecular H-bonding in the methyl ester but only a small amount in the ethyl ester (p. 213, 214). As before, this large decrease in such bonding produces big increases in both $\Delta H^{\ddagger}$ and $\Delta S^{\ddagger}$.

The reasons for the changes deduced in the extents of intramolecular H-bonding with the various structural changes outlined above involve the competition between this and intermolecular solvation to achieve energy minimisation. Minor structural changes appear to be able to tilt the preference in one direction or the other, within the need for at least a 7-membered ring size for intramolecular H-bonding.

(4) Other k_{EH^+} Values

As for the k_E values (p. 207), an attempt was made to measure k_{EH^+} for Glu DMe and Glu-5-Me. They are derivatives of 4-AB Me and the effect of C4 substitution by $-COOCH_3$ and $-COO^-$ can be checked against the predictions of the $B_{Ac}2$ mechanism applied to EH^+. The problem is the complexity of the reaction system, although it is simpler than that for the E form (Scheme 5.2, p. 153) because lactamisation is blocked by protonation. No temperature dependence of the overall rate constants was done, so the discussion is limited by the absence of $\Delta H^{\ddagger}$ and $\Delta S^{\ddagger}$ values.

Glu DMe

The EH^+ form of Glu DMe hydrolyses in two parallel pathways since both the 1-$COOCH_3$ and 5-$COOCH_3$ groups can undergo alkaline hydrolysis. The products are Glu-5-Me and Glu-1-Me, respectively. The overall value of k_{EH^+} is 2922 l mol^{-1} min^{-1} at 25°C (Table 5.11) which is a combination of the k_{EH^+} values for the two pathways. These cannot be separated experimentally using the ratio of the two product concentrations since both hydrolyse further. An estimate can be made assuming that the **–I** effect experienced by the 5-$COOCH_3$ group from the 1-$COOCH_3$ will be negligible, since it is attenuated by the intervening three C's. Therefore, the k_{EH^+} for the pathway to Glu-1-Me should be similar to that for 4-AB Me, 132 l mol^{-1} min^{-1}. Hence, the value of k_{EH^+} for the pathway to Glu-5-Me is ~ 2800 l mol^{-1} min^{-1}.

This estimate can be compared to the k_{EH^+} values for α-amino acid esters, since hydrolysis of the 1-ester group of Glu DMe parallels ester hydrolysis in α-amino acid esters, and it belongs to the series, $RCH(NH_3^+)COOCH_3$, with R = $-(CH_2)_2COOCH_3$ (Table 5.22):

Table 5.22 Comparison of k_{EH^+} Values for Some α-Amino Acid Methyl Esters, $RCH(NH_3^+)COOCH_3$.

Ester	2-AH Me	2-APe	2-AB Me	2-AP Me	2-AE Me
R	$-(CH_2)_3CH_3$	$-(CH_2)_2CH_3$	$-CH_2CH_3$	$-CH_3$	-H
$\sigma^{*(15)}$	-0.25	-0.12	-0.10	0.00	+0.49
k_{EH^+} (298 K)	2450[9]	2410[9]	2670[9]	4820[9]	2420[6]

The estimated value of k_{EH^+} for Glu DMe of ~2800 l mol^{-1} min^{-1} agrees well with the values for other α-amino acid esters, ignoring the anomalously large k_{EH^+} value for 2-AP Me. This agreement is consistent with the inductive effects expected from the $B_{Ac}2$ mechanism because there is little variation in σ^* values (Table 5.22).

The EH^+ form of Glu-5-Me, $^-OOCCH_2(NH_3^+)(CH_2)_2COOCH_3$, is unique among the ω-amino acid esters studied because it is a zwitterion. Based on the $B_{Ac}2$ mechanism, this overall neutral charge might be expected to make it react only very slowly with OH^-. However, it reacts quite rapidly and its rate constant (k_{EH^+} = 137 l mol^{-1} min^{-1}, Table 5.11, p.186) is similar to that for 4-AB Me (132 l mol^{-1} min^{-1}). This suggests assistance, possibly from intramolecular H-bonding between the $-NH_3^+$ and carbonyl oxygen of the $-COOCH_3$, via a 7-membered ring. The relevant $\Delta H^‡$ and $\Delta S^‡$ values are required before any firm conclusions can be drawn.

(5) Literature

For amino acid ester alkaline hydrolysis, no previous work appears to have been done on the temperature dependence of changes in the rate constant produced by structural changes in the ester group. The most relevant reference[20] relates only to k_E and is restricted to carboxylic acid esters, CH_3COOR'. Here, the effects of changes in R' from methyl to ethyl and then a range of branched chain alkyl groups, were studied. Deviations from a Taft plot ($\log_{10}(k/k_\circ)$ vs. σ^*) with chain branching were ascribed to steric effects since the polar (±I) effects of all the groups are similar. The effect of groups depended on the substitution position: methyl substitution in the α-position of the R' fragment of the ester produced an increase in $\Delta H^‡$ of ~ 5.4 kJ mol^{-1} cf. an increase of ~ 4.2 kJ mol^{-1} for substitution in the β-position. Accompanying these changes were increases in $\Delta S^‡$ of ~ 11.3 J K^{-1} mol^{-1} and ~ 9.6 J K^{-1} mol^{-1}, respectively. However, it is difficult to relate these conclusions to the present results

partly because they were done in mixed solvent (70% aq. acetone), but mainly because of the absence of an amino group. Its associated solvation effects have been shown to play such a dominant role in controlling the value of $\Delta S^{\ddagger}$, and hence $\Delta H^{\ddagger}$ and the value of the rate constant.

(ii) Intramolecular Aminolysis Mechanism

Intramolecular aminolysis in the alkaline hydrolysis of the E forms of the amino acid esters is characterised by fast reaction rates, the formation of a lactam and no overall consumption of OH^-. The kinetics are second order overall, first order in both E and OH^-. The values of k_L, separated from k_E as discussed in the text, and the values of $\Delta H^{\ddagger}$ and $\Delta S^{\ddagger}$ (where available), ex. Tables 5.11, 5.12 and 5.13, are summarised in Table 5.23:

Table 5.23 Values of k_L, and $\Delta G^{\ddagger}$, $\Delta H^{\ddagger}$, $\Delta S^{\ddagger}$, $T\Delta S^{\ddagger}$ for Esters Undergoing Intramolecular Aminolysis.

Amino Acid Ester	k_L l mol^{-1} min^{-1}			$\Delta G^{\ddagger}_{298}$ kJ mol^{-1}	$\Delta H^{\ddagger}$ kJ mol^{-1}	$\Delta S^{\ddagger}_{298}$ J K^{-1} mol^{-1}	$298.\Delta S^{\ddagger}_{298}$ kJ mol^{-1}
	25°C	37°C	50°C				
4-AB Me	1580	2470	4020	64.9	27.1	-126.9	-37.8
4-MAB Me	8610	11500	15760	60.8	16.7	-147.8	-44.1
4-A-3-MB Me	3400	4920	7460	63.0	22.4	-136.2	-40.6
4-A-3,3-DMB Me	9390	15520	25900	60.5	29.8	-103.1	-30.7
Glu-5-Me	700	-	-	-	-	-	-
Glu DMe	40	-	-	-	-	-	-
5-APe Me	36380	47900	61800	57.2	14.3	-143.8	-42.9
4-AB Et	520	770	1150	67.7	22.6	-151.2	-45.1
4-MAB Et	2500	3570	5320	63.8	21.4	-142.1	-42.4
5-APe Et	11300	15900	21200	60.0	17.4	-142.8	-42.6
4-AB Bz	1840	2780	4230	64.5	23.8	-136.5	-40.7

The rate constants are generally at least 50 and up to 3000 times larger than for the E forms undergoing $B_{Ac}2$ hydrolysis (Table 5.15, p. 201), and this is reflected in 10 to 20 kJ mol^{-1} smaller $\Delta G^{\ddagger}$ values. These large decreases in $\Delta G^{\ddagger}$ arise from large decreases in $\Delta H^{\ddagger}$ which are usually slightly countered by small decreases in $\Delta S^{\ddagger}$. The large negative values for $\Delta S^{\ddagger}$ suggest that the lactamisation TS is highly solvated, like the $B_{Ac}2$ TS, but is even more ordered presumably because of partial ring closure and the consequent loss of internal freedom.

N- and C-methyl substitution produce minor increases in these rate constants for the 4-AB esters:

N-methylation produces an increase of ~ 5 times. For the methyl ester, this is via a decrease in $\Delta H^{\ddagger}$ moderated by a decrease in $\Delta S^{\ddagger}$ whereas with the ethyl ester, the increase is due to both a decrease in $\Delta H^{\ddagger}$ and an increase in $\Delta S^{\ddagger}$.

C-3 mono-methylation increases the rate constant ~ 2 times due to a decrease in $\Delta H^{\ddagger}$ which is about half cancelled by a decrease in $\Delta S^{\ddagger}$. In contrast, the **C-3 dimethylation**, increase of ~ 6 times is driven by a large rise in $\Delta S^{\ddagger}$ partly cancelled by a rise in $\Delta H^{\ddagger}$.

Changes in the **ester/leaving group** produce a variety of effects on rate constants:

4-AB Me to Et results in a 3-fold fall with a large decrease in $\Delta S^{\ddagger}$ outweighing the $\Delta H^{\ddagger}$ fall.

4-AB Me to Bz produces little change but there are balancing moderate falls in both $\Delta H^{\ddagger}$ and $\Delta S^{\ddagger}$.

The **size of the ring** being closed has a dramatic effect; 6-membered ring closure (5-APe esters) has a rate constant ~ 23 times that for the 5-membered (4-AB esters) at 25°C, but this has fallen to 15 – 18 times at 50°C.

All these observations must be accommodated in any proposed reaction mechanism. There are a large number of possibilities which fit these experimental facts, but four mechanisms are considered to be the most likely, i.e. appear to be the most chemically sensible. Details of these will be given, followed by checks to show that they are consistent with the observed kinetics; checks on the other facts will follow later:

Mechanism 1

This involves an initial equilibrium in which the ester carbonyl group is subjected to nucleophilic attack by the $-NH_2$ group, resulting in the formation of an unstable zwitterionic lactam intermediate, X. This is similar to the intermolecular aminolysis mechanism in Scheme 1.16, p. 23. The second step is a rate determining OH^- catalysed deprotonation of the $-^+NH_2R$ group and the anionic intermediate formed rapidly breaks down, expelling the alkoxide leaving group which rapidly reacts with H_2O forming the parent alcohol and OH^-, Scheme 5.5:

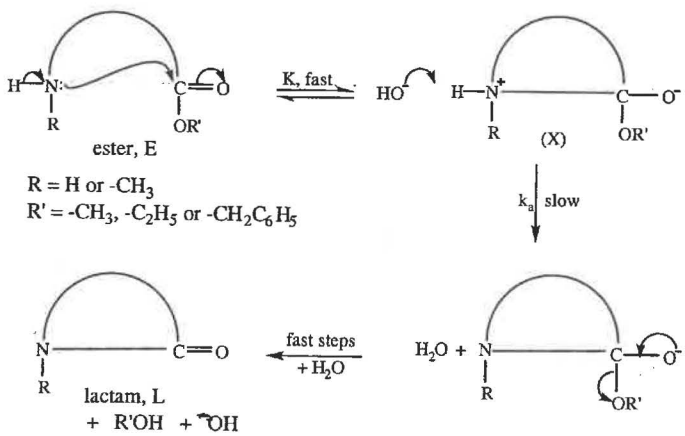

Scheme 5.5 Mechanism 1 for the Intramolecular Aminolysis of ω-Amino Acid Esters.

The rds of Scheme 5.5 yields:

$$\frac{d[L]}{dt} = k_a[X][OH^-]$$, where L is the lactam product and X is the zwitterionic lactam intermediate

But,

$$K = \frac{[X]}{[E]}, \quad \therefore [X] = K \cdot [E]$$

Also the stoichiometry is: $E + H_2O \rightarrow L + CH_3OH$

Hence,

$$-\frac{d[E]}{dt} = \frac{d[L]}{dt} = k_a \cdot K[E][OH^-]$$
$$= k_2[E][OH^-]$$

Mechanism 2

Again, the initial step is an equilibrium involving the formation of a zwitterionic intermediate, X, but this is followed by rapid internal proton transfer from the $-^{+}NH_2R$ to the $-O^{-}$ group. The resulting –OH group of the neutral intermediate, Y, formed then undergoes rate determining OH^{-} catalysed deprotonation. This produces an anionic intermediate which decomposes in several fast steps to form the products, Scheme 5.6:

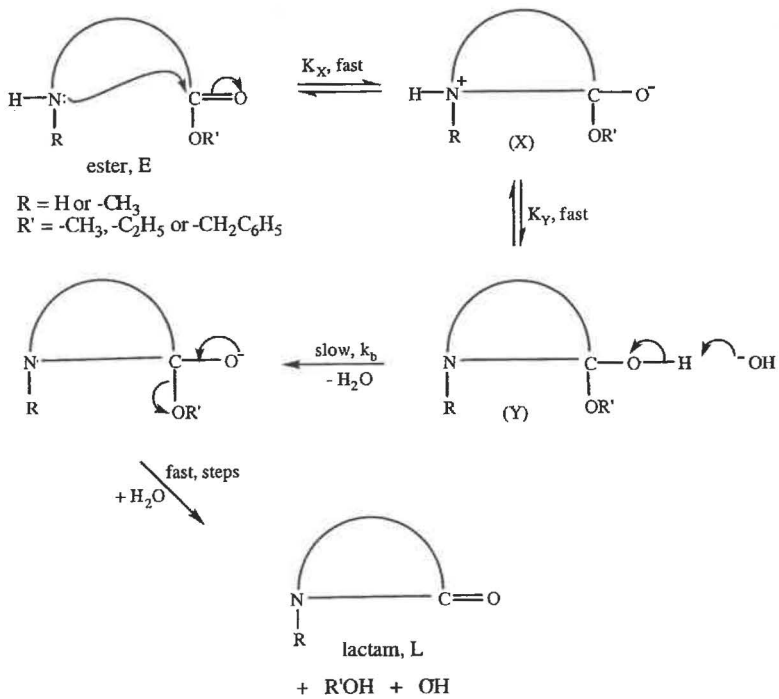

Scheme 5.6 Mechanism 2 for the Intramolecular Aminolysis of ω-Amino Acid Esters.

The rds of Scheme 5.6 gives:

$$\frac{d[L]}{dt} = k_b[Y][OH^-]$$

But,

$$K_X \cdot K_Y = \frac{[Y]}{[E]}, \quad \therefore \quad [Y] = K_X \cdot K_Y[E]$$

Hence, since the stoichiometry is as in Mechanism 1, it follows that:

$$-\frac{d[E]}{dt} = \frac{d[L]}{dt} = k_b \cdot K_X \cdot K_Y[E][OH^-]$$
$$= k_2[E][OH^-]$$

Mechanism 3

An initial equilibrium step involves rapid deprotonation of the $-NH_2$ group by OH^-. The resulting $-NH^-$ group then subjects the ester carbonyl-C to a rate determining nucleophilic attack and the resulting anionic lactam intermediate rapidly breaks down with the explusion of the alkoxide group, Scheme 5.7:

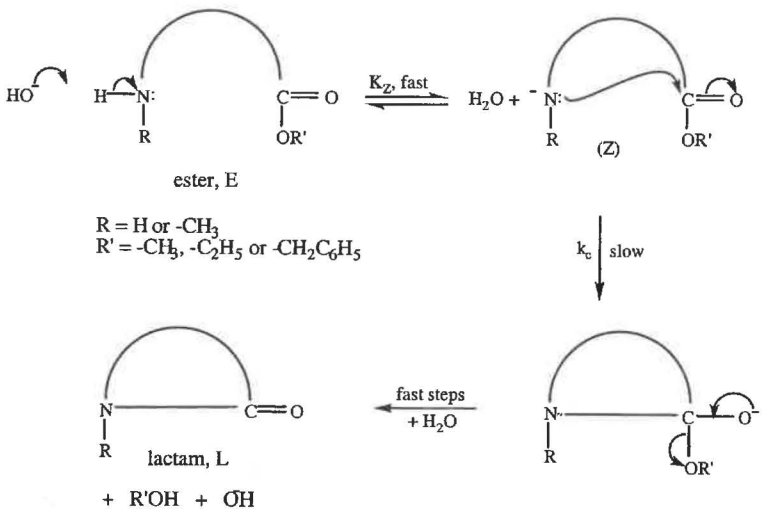

Scheme 5.7 Mechanism 3 for the Intramolecular Aminolysis of ω-Amino Acid Esters.

The rds of Scheme 5.7 gives:

$$\frac{d[L]}{dt} = k_c[Z]$$

But,

$$K_Z = \frac{[Z]}{[E][OH^-]} \quad \therefore \quad [Z] = K_Z \cdot [E][OH^-],$$

Hence, since the stoichiometry is as in Mechanism 1, it follows that:

$$-\frac{d[E]}{dt} = \frac{d[L]}{dt} = k_c \cdot K_Z[E][OH^-]$$
$$= k_2[E][OH^-]$$

Mechanism 4

This assumes no equilibria. The first step is rate determining and involves synchronous OH^- deprotonation of the $-NH_2$ group and intramolecular nucleophilic attack on the carbonyl-C by the resulting $-NH^-$. The anionic intermediate formed rapidly decomposes to the lactam product by ejecting the alkoxide. This picks up a proton from a water molecule, regenerating OH^- and forming the parent alcohol, Scheme 5.8:

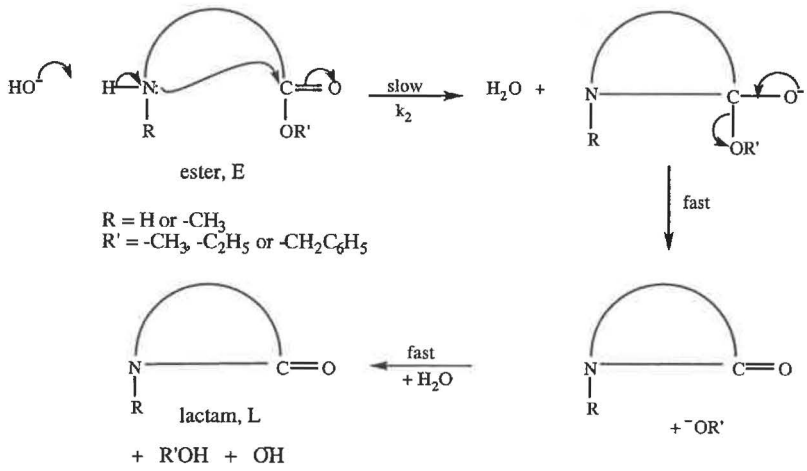

Scheme 5.8 Mechanism 4 for the Intramolecular Aminolysis of ω-Amino Acid Esters.

Since the first step is rate determining, the rate equation is:

$$-\frac{d[E]}{dt} = k_2[E][OH^-]$$

Hence, the four proposed mechanisms are consistent with the experimentally observed kinetics and are kinetically indistinguishable, with $k_2 = k_aK$, $k_bK_XK_Y$, k_cK_Z and simply k_2, for mechanisms 1, 2, 3 and 4, respectively.

Despite the differences in the terms contributing towards the k_2 value, distinguishing between the mechanisms will be difficult because the terms are interrelated due to the close similarity of the mechanisms. In each case the rds involves the formation of the same anionic intermediate which is related, either directly or indirectly via equilibria, to the reactant ester plus hydroxide.

However, some of the proposed mechanisms appear less likely because of evidence from related reaction mechanisms and knowledge about the relative reactivities of species:

Mechanism 1 (Scheme 5.5) has an rds involving proton transfer from a zwitterion intermediate to a OH^-, producing an anionic intermediate. Satterthwaite and Jencks,[21] concluded that, while proton transfer from an amine or zwitterionic species to a GB, such as hydrazine, is unfavourable, proton transfer from a zwitterion to OH^- is favoured. However, proton transfers between oxygen and nitrogen atoms are usually very fast. Their rates are usually diffusion controlled with rate constants ranging from $10^{10} - 10^{11}$ l mol^{-1} s^{-1} at 25°C, e.g. for $NH_4^+ + OH^- \rightarrow NH_3 + H_2O$, $k_2 = 3.4 \times 10^{10}$ l mol^{-1} s^{-1} and for imidazole-$H^+ + OH^- \rightarrow$ imidazole + H_2O, $k_2 = 2.5 \times 10^{10}$ l mol^{-1} s^{-1}.[22] Therefore, it appears unlikely that the proton transfer between a zwitterion and OH^- could be rate determining and this mechanism is rejected.

Mechanism 2 (Scheme 5.6) has the breakdown of a neutral tetrahedral intermediate via OH^- attack, as the rds. The anionic intermediate formed (required for the cleavage of the poor leaving group), rapidly forms the products in several steps. Gutherie[23] studied the kinetics of the breakdown, in basic solutions, of a series of neutral tetrahedral intermediates with various alkoxide leaving groups, similar to the type involved in Scheme 5.6. It was found that the activation energies were low; therefore such tetrahedral species are short lived and their breakdown is unlikely to be rate determining. Hence, mechanism 2 should be rejected.

Mechanism 3 (Scheme 5.7) involves the formation of an intermediate species Z which contains an $-NR^-$ group. While this species can be pictured to undergo rate determining intramolecular aminolysis, it will react rapidly with water to regenerate the ester reactant. Consequently, K_Z and [Z] will be very small and it seems unlikely that this pathway would make a significant contribution to the reaction.

In contrast to the above, **Mechanism 4** (Scheme 5.8) has an initial rds which involves hydroxide assisted INC by the amino group. This concerted step is followed by rapid expulsion of alkoxide from the anionic intermediate and formation of the products.

Essentially, this is the mechanism proposed by Martin et al.[10] in their studies on the intramolecular aminolysis of amino acid esters in boric acid – borate buffers. They found that at low buffer concentrations, the reaction involved rate determining OH^- and GB catalysed formation of a tetrahedral intermediate. Breakdown of this intermediate became the rds at high buffer concentrations.

Support for a concerted mechanism also comes from Satterthwaite and Jencks[21] who state that for ester aminolysis, a "concerted mechanism can become the more favoured path for catalysis if strong bases, such as the hydroxide ion" are used.

While this mechanism is the least complicated of the four, and it avoids the formation of an unstable zwitterion ion intermediate, the question remains as to whether it is supported by all the remaining experimental observations:

(1) $\Delta H^{\ddagger}$ and $\Delta S^{\ddagger}$ Values

Mechanism 4 appears to be consistent with the observed ranges for $\Delta H^{\ddagger}$ and $\Delta S^{\ddagger}$ for 4-AB Me/Et and 5-APe Me/Et (Table 5.23). It predicts that the TS of the rds will be highly solvated and this, combined with partial or complete ring closure, leads to large negative $\Delta S^{\ddagger}$ values, as observed. These are slightly more negative than for the corresponding $B_{Ac}2$ reactions but this rate slowing effect is greatly outweighed by much smaller $\Delta H^{\ddagger}$ values which reflect the large nett increase in bonding (solvation plus lactamisation). Note that similar conclusions can also be drawn for the other three mechanisms.

Trends in $\Delta H^{\ddagger}$ and $\Delta S^{\ddagger}$ with Structure

(a) N-methylation

It was hoped that the changes in $\Delta H^{\ddagger}$ and $\Delta S^{\ddagger}$ (and hence in the rate constant) with this substitution for the 4-AB esters might help identify the most likely mechanism.

N-dimethylation (4-DMAB esters), as expected, blocks intramolecular aminolysis because of the lack of an N-H bond and results in relatively slow (presumably $B_{Ac}2$) reactions with no lactam formation.

N-methylation (4-MAB esters) produces rate constant increases of ~ 5 times for both esters. However, these increases have different origins; for the methyl ester, $\Delta H^{\ddagger}$ decreases (by ~ 10 ± 2 kJ mol^{-1}) but this is countered by a decrease in $\Delta S^{\ddagger}$ (by ~ 21 ± 4 J K^{-1} mol^{-1}, T. $\Delta S^{\ddagger}$ ~ 6 ± 2 kJ mol^{-1}) (Table 5.23; error estimates, see p. 203, are:

$\delta\Delta H^{\ddagger}$ ~ 2 kJ mol^{-1}, $\delta\Delta S^{\ddagger}$ ~ 8 J K^{-1} mol^{-1} and $\delta(T.\ \Delta S^{\ddagger})$ ~ 2 kJ mol^{-1} and will be the same throughout the following discussion, but will be omitted for brevity unless they make the δ-value insignificant). With the ethyl ester, the $\Delta H^{\ddagger}$ fall is insignificantly small (~ 1 kJ mol^{-1}), but this is reinforced by a rise in $\Delta S^{\ddagger}$ (by ~ 9 J K^{-1} mol^{-1}, $T.\ \Delta S^{\ddagger}$ ~ 3 kJ mol^{-1}) so this is the main contributor to the rate constant increase.

$\Delta H^{\ddagger}$ decreases are consistent with the replacement of -H by the **+I** $-CH_3$ group increasing the nucleophilicity of the N and hence increasing the ease of its attack on the carbonyl-C ($E_{(aq)}$ is more reactive so $H°(E_{(aq)})$ increases thus lowering $\Delta H^{\ddagger}$, equ. 5.15, p. 202 applied to lactamisation Mechanism 4).

$\Delta S^{\ddagger}$ changes are, however, significant and indicate that the inductive effect argument is too simplistic. Solvation changes are the most likely source of the $\Delta S^{\ddagger}$ differences; these presumably relate to intermolecular effects since there is no evidence for intramolecular H-bonding in the E form. It appears that there are several opposing phenomena since $\Delta S^{\ddagger}$ changes in opposite directions for the closely related pairs of methyl and ethyl esters. Since the electronic effects of the methyl and ethyl groups are very similar, the source of any difference in the solvation change in going from the reactant to the TS may lie in differences in steric effects.

For the **methyl ester**, the ~ 21 J K^{-1} mol^{-1} decrease in $\Delta S^{\ddagger}$ on N-methylation indicates this structural change increases the order in the TS. This may be due to the **+I** effect of the $-CH_3$ group being transmitted across the ring forming N···C bond, hence increasing the negative charge on the what was originally the carbonyl-O and increasing its intermolecular H-bonding to H_2O. Consequently, $S°(TS,\ E{\cdot}OH^-_{(aq)})$ decreases with little change in $S°(E_{(aq)})$. This increased solvation in the TS will contribute a decrease to $H°(TS,\ E{\cdot}OH^-_{(aq)})$ and hence add to the decrease in $\Delta H^{\ddagger}$ associated with the **+I** effect of the $-CH_3$ group, Scheme 5.9:

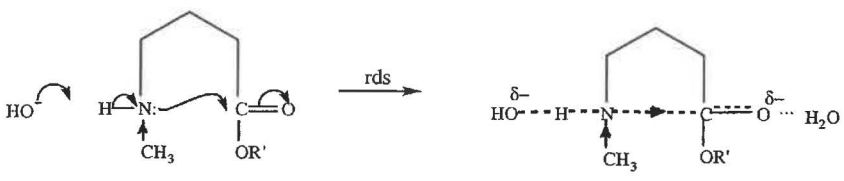

$(E_{(aq)})$

The +I effectof the N-CH_3 group increases the nuclephilicity of the attacking -N group.

$(TS.\ E.OH^-_{(aq)})$

The +I effectof the N-CH_3 group increases the electron density at the carbonyl-O gleading to increased solvation.

Scheme 5.9 Effect of N-methylation on Intramolecular Aminolysis of 4-AB Me.

In contrast, the **ethyl ester** $\Delta S^{\ddagger}$ increases on N-methylation which may be due to the bulkier ethyl group preventing the increased solvation of the methyl ester because of increased steric crowding as the carbonyl-C goes from sp^2 to sp^2/sp^3 in the TS. In addition, the slightly larger **+I** effect of the $-C_2H_5$ group may result in a weaker N---C bond in the TS than for the methyl ester, which would further raise $\Delta S^{\ddagger}$. Both factors will contribute increases to $\Delta H^{\ddagger}$ which will oppose the decrease due to the **+I** effect of the $N-CH_3$ group. The result is only a small change (decrease) in $\Delta H^{\ddagger}$ for the ethyl ester, as observed.

Once again, there appears to be a delicate balance between opposing effects, the balance of which controls the direction of change in $\Delta S^{\ddagger}$ on N-methylation and this contributes to the changes in $\Delta H^{\ddagger}$. These changes are hidden in the $\Delta G^{\ddagger}$ value.

The increased rate constants on N-methylation suggest that N-nucleophilic attack is involved in the rds. At first sight, this appears to support Mechanism 4 where the effect is **direct**: the rds is the first step and involves INC by amino assisted by OH^-. However, the effect could be **indirect** via increases in equilibrium or rate constants which contribute to k_2: in Mechanism 1, K increases ($k_2 = k_aK$), Mechanism 2, K_X increases ($k_2 = k_bK_XK_Y$) and in Mechanism 3, k_c increases ($k_2 = k_cK_Z$). So the result is also consistent with Mechanisms 1, 2 and 3.

(b) C-methylation

Examination of the effects of the stepwise replacement of H by CH_3 at C-3 in 4-AB Me may provide further help in understanding the nature of the intramolecular aminolysis mechanism. The question is do the kinetic effects of this substitution support Mechanism 4 rather than Mechanisms 1-3?

C-methylation will produce changes in inductive effects, but these are not expected to affect the electron densities at either the amino-N or carbonyl-C, and hence will not be responsible for any changes in the rate constants. However, rate constant changes are expected because the "gem-dimethyl effect" is well known as a sterically directing factor in ring closures.[25] Also, possible indirect changes in solvation need to be considered because of their importance in amino systems. Again, any conclusions are preliminary because of the limited data.

Monomethylation (4-A-3-MB Me) approximately doubles the value of k_L at all three temperatures while dimethylation (4-A-3,3-DMB Me) produces approximately six-fold increases. This steady increase in rate constant (steady decrease in $\Delta G^{\ddagger}$) with increased methylation is predicted by the gem-dimethyl effect. However, the trend hides very different changes in both $\Delta H^{\ddagger}$ and $\Delta S^{\ddagger}$ (Table 5.23, p. 225). The rate constant doubling is due to a 4.7 kJ mol^{-1} decrease in $\Delta H^{\ddagger}$ counterbalanced by a 9.3 J K^{-1} mol^{-1} decrease in $\Delta S^{\ddagger}$ (T. $\Delta S^{\ddagger}$ = 2.8 kJ mol^{-1}) whereas the six-fold increase arises from a large increase in $\Delta S^{\ddagger}$ (23.8 J K^{-1} mol^{-1} ; T. $\Delta S^{\ddagger}$ = 7.1 kJ mol^{-1}) which is partly countered by a rise in $\Delta H^{\ddagger}$ of 2.7 kJ mol^{-1} (barely significant within the estimated error limit of ±2 kJ mol^{-1}). These changes are in contrast to many of the previous substitution results ($\Delta H^{\ddagger}$ and $\Delta S^{\ddagger}$ moving in the same direction due to changes in solvation) which suggests other factors are involved possibly along with solvation effects.

There is some conflict in the literature regarding the origin of the gem-dimethyl (or dialkyl) effect.[25-29] One explanation is that "the substitution of alkyl groups for hydrogen pushes the reactive centres closer together by compressing the internal angle of the carbon chain"[29] (the Thorpe-Ingold effect[26]). Applied to the present case this explanation would be expected to reduce ring strain and hence decrease $\Delta H^{\ddagger}$ as well as increasing the chance of the two chain ends meeting, i.e. decrease $S^{o}(E_{(aq)})$ and hence raise $\Delta S^{\ddagger}$. Experimentally, both $\Delta H^{\ddagger}$ and $\Delta S^{\ddagger}$ change in opposite directions on stepwise C-methylation; both decrease in going from 4-AB Me to 4-A-3-MB Me but increase from 4-AB Me to 4-A-3,3-DMB Me. Clearly, this explanation is incorrect on its own. Attempts to find crystallographic evidence for compression of the internal bond angle on C-3-alkylation were unsuccessful because suitable crystals of either 4-A-3-MB Me or 4-A-3,3-DMB Me could not be grown. However, there is evidence that the gem-dialkyl effect can result in increased rate constants where bond angle spreading occurs,[27] so there is some doubt about the validity of the Thorpe-Ingold effect. Also, in another study of 5-membered ring closure involving some intramolecular Diels-Alder reactions, it was concluded that the source of gem-dialkyl substitution rate increases was not bond angle compression.[27]

Another explanation is the "Reactive Rotamer effect" which states that "the ring closure reaction proceeds at a greater rate on geminal (or alkyl) substitution because of the resultant decrease in unprofitable rotamer distribution".[28] Conformations with

widely separated reaction centres are unreactive, but increasing alkyl substitution can increase the population of folded conformations where the reaction centres are close enough (the reactive rotamers) for reaction to proceed. Such folded conformations will have an increased proportion of gauche bonds and an increased $H°(E_{(aq)})$ relative to the unfolded conformations. Since $H°(TS, E{\cdot}OH^-_{(aq)})$ is fixed, the result will be a decrease in $\Delta H^‡$. Bringing the reaction centres closer will decrease $S°(E_{(aq)})$ and this will contribute an increase to $\Delta S^‡$. These predictions are the same as for the Thorpe-Ingold effect and again are incorrect on their own for the present systems. In contrast, the Diels-Alder study[27] concluded that the observed rate constant increases could be explained by the Reactive Rotamer effect and originated solely in decreases in $\Delta H^‡$.

However, a theoretical study[29] has rejected both the Thorpe-Ingold and Reactive Rotamer effects in favour of a "Facilitated Transition State" hypothesis. This states that "increased steric hindrance reduces the overall activation energy by facilitating rotation through the transition state". This applies to the formation of 5-membered ring TS's, i.e. to "highly eclipsed" TS's and explains increases in rate constants as due to lowering of $\Delta H^‡$ via a "lowering of the barriers to conformational rotation along the reaction coordinate brought about by alkyl and gem-dialkyl substitution". Again, this explanation fails for the present systems where both $\Delta H^‡$ and $\Delta S^‡$ first decrease, then increase with increasing C-3 methylation. It also fails to discuss entropy changes which must be significant since C-alkylation must restrict conformer populations.

In the present case, the erratic changes in both $\Delta H^‡$ and $\Delta S^‡$ suggest several opposing factors. One factor will be restrictions in rotamer populations and freedom to rotate about single bonds which will affect both the enthalpy and entropy changes. Another factor that may be absent in previous studies (and certainly was absent in the gas phase theoretical calculations[29]) is solvation effects involving polar water molecules and polar amino and carbonyl groups.

Monomethylation (4-AB Me to 4-A-3-MB Me) may produce an overall increase in $S°(E_{(aq)})$ via rotamer population restriction (contributes a decrease; effect small?) and desolvation accompanying the increased proximity of the oppositely charged amino-N and carbonyl-C centres (contributes an increase; effect modest?). The overall balance of these two opposing effects is the observed small decrease in $\Delta S^‡$, assuming that $S°(TS, E{\cdot}OH^-_{(aq)})$ is unaffected by the methylation. Accompanying these two

effects will be changes in $H°(E_{(aq)})$. There will be an increase from rotamer population restriction and an increase from the reduced solvent bonding. Combining these terms will produce the observed small fall in $\Delta H^{\ddagger}$ (assuming $H°(TS, E{\cdot}OH^{-}_{(aq)})$ is constant), provided both terms are very small.

Dimethylation (4-AB Me to 4-A-3,3-DMB Me) may produce an overall decrease in $S°(E_{(aq)})$ via a much larger rotamer population restriction than for the monomethylation case (contributes a large decrease) which must outweigh desolvation effects (contribute an increase). This balance will result in a rise in $\Delta S^{\ddagger}$; experimentally, this rise is huge and suggests at least a greatly restricted rotamer population and more likely indicates a substantial ordering via a strong interaction between the amino-N and carbonyl-C. As before, rotamer restriction and desolvation will be accompanied by increases in $H°(E_{(aq)})$ which will contribute a large decrease to $\Delta H^{\ddagger}$. However, experimentally there is a small rise which suggests that at least one more factor is involved and this could be evidence for a strong amino-N to carbonyl-C interaction. Such "bonding" will substantially lower $H°(E_{(aq)})$ and so contribute a large enough increase to $\Delta H^{\ddagger}$ to just outweigh the decreases from the other two effects. There is support for an unusually high degree of order in the $E_{(aq)}$ form of 4-A-3,3-DMB Me from its pK_a^T results (p. 137). The deprotonation of $EH^{+}_{(aq)}$ is accompanied by an abnormally low $\Delta S°_{298}$ (large increase in order) (-41.6 J K^{-1} mol^{-1} cf. –8.7 and –4.1 for 4-AB Me and 4-A-3-MB Me, respectively). This was explained (p. 138) as possibly due to intramolecular H-bonding in EH^{+} causing extensive desolvation of this charged species, but intramolecular bonding in $E_{(aq)}$ (with relatively little desolvation as it is neutral) could be a contributing factor.

Clearly with the limited data, more investigations are needed, but it appears that amino acid ester systems in aqueous solvent show "unusual" gem-dimethyl effects.

(c) Ester/Leaving Group

Mechanisms 1-4 all involve ester group departure subsequent to the rds. If this is correct, then changing the leaving group should have little effect on the rate constant. However, since the results of such changes seemed unlikely to provide much discrimination between the four closely related preferred mechanisms, only a few

cases were examined: 4-AB (methyl, ethyl and benzyl esters), 4-MAB and 5-APe (methyl and ethyl esters). The results, ex. Table 5.23, are summarised in Table 5.24:

Table 5.24 Effect of Ester/Leaving Group Changes on the Values of k_L, $\Delta G^{\ddagger}$, $\Delta H^{\ddagger}$, $\Delta S^{\ddagger}$ and $T{\cdot}\Delta S^{\ddagger}$ for 4-AB, 4-MAB and 5-APe Esters.

Amino Acid Ester	k_L l mol^{-1} min^{-1}			$\Delta G^{\ddagger}_{298}$ kJ mol^{-1}	$\Delta H^{\ddagger}$ kJ mol^{-1} ± 1	$\Delta S^{\ddagger}_{298}$ J K^{-1} mol^{-1} ± 4	$298.\Delta S^{\ddagger}_{298}$ kJ mol^{-1} ± 2
	25°C	37°C	50°C				
4-AB Me	1580	2470	4020	64.9	27.1	-126.9	-37.8
4-AB Et	520	770	1150	67.7	22.6	-151.2	-45.1
4-AB Bz	1840	2780	4230	64.5	23.8	-136.5	-40.7
4-MAB Me	8610	11500	15760	60.8	16.7	-147.8	-44.1
4-MAB Et	2500	3570	5 320	63.8	21.4	-142.1	-42.4
5-APe Me	36380	47900	61800	57.2	14.3	-143.8	-42.9
5-APe Et	11300	15900	21200	60.0	17.4	-142.8	-42.6

As can be seen, changes in the ester/leaving group produce only small differences (which are sometimes insignificant within error limits) in the rate constants and component $\Delta H^{\ddagger}$ and $\Delta S^{\ddagger}$ values. While the structural changes are modest, this result probably indicates that the departure of the ester group and its accompanying bond breaking, is not the rds and also that this process does not contribute indirectly (via equilibrium constants or non-rds rate constants) to the value of k_L. This eliminates many mechanisms but is consistent with mechanisms 1-4 since they all involve leaving group departure subsequent to the rds.

The question remains whether the small changes observed originate from an effect (e.g. a solvation change) which is unique to just one of the four mechanisms.

There is some parallel between the $B_{Ac}2$ and the intramolecular aminolysis mechanisms 1-4; both involve rate determining nucleophilic attack at the ester carbonyl-C. Studies on the $B_{Ac}2$ hydrolysis of carboxylic acid esters have shown that

changes in the alcohol fragment produce modest changes in k_2, e.g. in CH_3COOR', for R' = CH_3: C_2H_5 : $CH(CH_3)_2$, the k_2 ratio is 1 : 0.601 : 0.146.[29] Later studies produced similar results[20] (see also p. 224) and all the decreasing values can be explained in terms of a combination of small increases in both steric crowding and +I effect (σ^*: $-CH_3$, 0.00; $-C_2H_5$, -0.10; $-CH(CH_3)_2$, -0.19).[15] Presumably, these will be two of the effects contributing to rate constant changes for the intramolecular aminolysis reactions. Additional effects will include solvation changes associated with the presence of the amino group, as seen previously.

4-AB Esters

At all temperatures, the relative reactivities of the Me : Et : Bz esters is ~ 3 : 1 : 3.6. The lower reactivity of the ethyl ester originates in a very low $\Delta S^{\ddagger}$ value, partly cancelled by a small $\Delta H^{\ddagger}$ value. In contrast, the methyl and benzyl esters have similar reactivities but this hides very different $\Delta H^{\ddagger}$ and $\Delta S^{\ddagger}$ values. This presumably indicates that there are several terms contributing to $\Delta H^{\ddagger}$ and to $\Delta S^{\ddagger}$ with, once again, a delicate balance resulting in the observed values. The effects of these terms will be examined in terms of the rds of the preferred mechanism 4 (Scheme 5.8).

One term will be inductive effects; the **+I** effect increases from $-CH_3$ ($\sigma^* = 0.00$)[15] to $-C_2H_5$ ($\sigma^* = -0.10$)[15]. This small increase in **+I** effect will raise the electron density on the carbonyl-C, hinder attack by the amino-N and hence contribute a small decrease to the rate constants via an increase in $\Delta H^{\ddagger}$. In addition, the weak polarisation of the carbonyl group will decrease significantly from $-CH_3$ to $-C_2H_5$ resulting in less hydration ($S°(E_{(aq)})$ increases). In the TS, hydration is dominated by the developing negative charge on the oxygen and will be larger than for the reactant's carbonyl group. Hence, it will be less affected by the changing **+I** effect, so $S°(TS, E{\cdot}OH^-_{(aq)})$ rises only slightly. This will contribute a decrease to $\Delta S^{\ddagger}$ and hence a decrease to $\Delta H^{\ddagger}$ (via increased $H°(E_{(aq)})$ with only a small increase in $H°(TS, E{\cdot}OH^-_{(aq)})$ from the methyl to the ethyl leaving groups.

Replacing the $-C_2H_5$ ($\sigma^* = -0.10$)[15] leaving group by $-CH_2C_6H_5$ ($\sigma^* = +0.27$)[15] results in a small increase in **–I** effect. This will slightly decrease the electron density on the carbonyl-C, assisting attack by the amino-N and hence contributing to an increase to the rate constant via a decrease in $\Delta H^{\ddagger}$. However, increased polarization of the carbonyl group will result in greater solvation, lowering $H°(E_{(aq)})$, raising $\Delta H^{\ddagger}$.

A second term will be steric effects; there is an increase in steric size across the series and since the rds (Scheme 5.8) involves an increase in steric crowding (conversion of the reaction centre carbonyl-C from sp^2 to sp^2/sp^3), the increase in $H°(TS, E{\cdot}OH^-_{(aq)})$ will be larger than the increase in $H°(E_{(aq)})$ and this will contribute an increase to $\Delta H^‡$. This increased steric crowding in the TS may also make it less solvated. This would further raise both $H°(TS, E{\cdot}OH^-_{(aq)})$ (i.e. raise $\Delta H^‡$) and $S°(TS, E{\cdot}OH^-_{(aq)})$ (i.e. raise $\Delta S^‡$).

A third term will be the solvation effects associated with the first and second terms, as discussed.

Overall:

$\Delta H^‡$ receives **increases** from:

- Decreasing σ^* values (increasing **+I** effects) which produce increasing carbonyl-C electron density.
- Increasing reactant solvation with increasing σ^* values.
- Increasing steric crowding in the TS (due to the change in carbonyl-C hybridisation) and decreased TS solvation.

A **decrease** arises from decreased reactant solvation with the decreasing σ^* values.

It is difficult to predict the balance between all of these small terms, but with the larger number producing increases, $\Delta H^‡$ might be expected to increase across the series. Experimentally (Table 5.24), this is true for the Et to Bz ester change (although the increase is within the estimated experimental error limits), but incorrect for the Me to Et change. The observed decrease of 4.5 kJ mol^{-1} suggests dominance by the reactant solvation decrease term which must outweigh the carbonyl-C electron density increase effect ; both are $\Delta\sigma^*$ related but the solvent effect is expected to be larger. The changes due to changes in steric effects appear insignificant suggesting that the steric difference between Me and Et is small in this reaction. The steric change from Et to Bz is much larger which makes its terms dominant, and producing a small increase in $\Delta H^‡$.

$\Delta S^‡$ receives a **decrease** from the decreasing reactant solvation (decreasing σ^* values) and an **increase** from decreasing solvation of the TS (increasing steric crowding). The $\Delta H^‡$ discussion concluded that the change in steric effect from Me to Et for this reaction was small. Hence, the change in σ^* dominates with a predicted decrease in

$\Delta S^{\ddagger}$, as observed (Table 5.24). The reverse occurs from Et to Bz with a predicted increase in $\Delta S^{\ddagger}$, as seen experimentally.

4-MAB Esters:

The relative reactivities of the Me : Et esters is ~ 3 : 1 at all temperatures (Table 5.24). As with the 4-AB case, the ethyl ester is less reactive but now for the opposite reasons: it has a higher $\Delta H^{\ddagger}$ value but a $\Delta S^{\ddagger}$ that is slightly larger (insignificantly so within estimated error limits) than for the Me ester. Clearly N-methylation has had a major effect on the terms which control the $\Delta H^{\ddagger}$ and $\Delta S^{\ddagger}$ values, but again this is hidden in the $\delta\Delta G^{\ddagger}$ which is the same (~ 3.1 kJ mol^{-1}) as for the 4-AB esters.

The terms that will contribute to the $\Delta H^{\ddagger}$ and $\Delta S^{\ddagger}$ values are the same as for the 4-AB esters with the addition of effects due to the presence of the N-methyl group. Its **+I** effect increases the electron density on the attacking N of the reactant and this will result in more electron density on the carbonyl-C of the TS. Superimposing these changes on the 4-AB ester discussion, from the methyl to the ethyl ester:

$\Delta H^{\ddagger}$ receives **increases** from:

- The decrease in σ^{*} value (carbonyl-C electron density increase; $\Delta H^{\ddagger}$ increase is probably slightly less than that for the 4-AB system because the methylated N's higher electron density reduces the effect of electron density changes at the carbonyl-C. Both $\Delta H^{\ddagger}$ values will be smaller because of the higher electron density on the methylated-N).
- The increase in steric crowding (carbonyl-C hybridisation change; N-methylation will increase the steric crowding at the TS carbonyl-C, so the change from Me to Et will be more important than for the 4-AB case, so the $\Delta H^{\ddagger}$ increase will be larger.
- The decrease in TS solvation due to the increased steric crowding (again N-methylation will make this larger).

$\Delta H^{\ddagger}$ receives a **decrease** from decreased reactant solvation with the decrease in σ^{*} value (decreased carbonyl group polarisation will be unaffected by methylation of the distant amino-N, so the $\Delta H^{\ddagger}$ decrease will be similar to the 4-AB case).

Again, the balance between these small terms is difficult to predict, but the larger number of terms producing increases, coupled with the increased importance of the

steric crowding term compared to the 4-AB case, suggests that overall, $\Delta H^{\ddagger}$ should increase. This is experimentally correct (Table 5.24) and is the reverse of the 4-AB result because N-methylation results in steric effects being more important than solvation changes.

$\Delta S^{\ddagger}$ receives a **decrease** from the decreasing reactant solvation that accompanies decreasing σ^{*} values and an **increase** from the decreasing solvation of the TS with increasing steric crowding. The dominance of steric crowding in this system predicts that $\Delta S^{\ddagger}$ should increase, as observed, although this change is insignificant within estimated error limits.

5-APe Esters:

Superficially, the results for these esters are similar to those for the 4-AB system - the methyl ester is about 3 times as reactive as the ethyl ester at all temperatures (Table 5.24). However, the reasons for this difference in reactivity are quite different. The higher reactivity of 4-AB Me is due to a much higher $\Delta S^{\ddagger}$ partly countered by a higher $\Delta H^{\ddagger}$ value whereas 5-APe Me is more reactive because of a lower $\Delta H^{\ddagger}$ with little change in $\Delta S^{\ddagger}$. Again, the importance in kinetics, of temperature dependence studies and the consequent examination of the contributors to $\Delta G^{\ddagger}$ (k_L), is clear. Doing this shows that the 5-APe Me results are suprisingly similar to those for the 4-MAB system. N-methylation of 4-AB esters produces similar results to increasing the ring size from 4 to 5. The causes of the often dramatic effects of changes in ring size on the kinetic parameters for these intramolecular reactions are discussed in the next section.

In conclusion, the observed leaving group effects can all be rationalised in terms of Mechanism 4. While the kinetic changes produced in going from Me to Et to Bz are small, there is nothing to indicate that one of the other mechanisms would be a better fit to the data.

(d) Ring Size

In Mechanisms 1-4, ring closure either precedes the rds (1 and 2) or is the rds (3 and 4) (see p. 226 – 230). Consequently, all four mechanisms predict that the ease of ring closure will have a significant effect on the rate constant, either indirectly (via the

value of equilibrium constants, Mechanisms 1 and 2) or directly (Mechanisms 3 and 4). The ease of ring closure will depend on the ring size. Experimentally, only 5- and 6-membered lactams are formed and the resulting rate constants (k_{L5} and k_{L6} from the esters of 4-AB and 5-APe, respectively) and their $\Delta H^{\ddagger}$ and $\Delta S^{\ddagger}$ values, will be examined to see if they are consistent with Mechanism 4 or better support one of the other mechanisms. Other ring sizes are not formed; 3- and 4-membered rings are too strained despite being entropically favoured (the chain ends are close), while 7-membered and larger rings while being less strained are entropically disfavoured because of the remoteness of their chain ends.

Table 5.24 (p. 238) shows that the size of the ring being closed has a dramatic effect on the value of the rate constant; 6-membered ring closure is much faster at all three temperatures. For the methyl esters (5-APe Me cf. 4-AB Me), k_{L6}/ k_{L5} = 23.0, 19.4 and 15.4 at 25°C, 37°C and 50°C, respectively, while for the corresponding ethyl esters, k_{L6}/ k_{L5} = 21.7, 20.6 and 18.4 at the three temperatures, respectively. These increases in rate constant with increasing ring size are due to falls in $\Delta H^{\ddagger}$ (12.8 kJ mol^{-1} for the methyl esters and 5.2 kJ mol^{-1} for the ethyl) which is partly cancelled by a fall in $T.\Delta S^{\ddagger}$ (5.1 kJ mol^{-1}) for the methyl ester but reinforced by a rise in $T.\Delta S^{\ddagger}$ (2.5 kJ mol^{1}) for the ethyl ester. Remarkably, this results in the falls in $\Delta G^{\ddagger}$ being the same (7.7 kJ mol^{-1}) for the two pairs of esters. These changes are all significant considering the experimental error limits (Table 5.24). As before, the origin of these changes will lie in contributions from several factors including electronic, steric and solvation effects. A comparison between the two methyl esters and between the two ethyl esters shows some differences in the effect of ring size:

4-AB Me and 5-APe Me

The large fall in $\Delta H^{\ddagger}$ responsible for the greater reactivity of 5-APe Me indicates a decrease in $H°(TS, E{\cdot}OH^{-}_{(aq)})$ and/or an increase in $H°(E_{(aq)})$ (equ. 5.15).

Inductive effect changes are one possible term contributing to the $\Delta H^{\ddagger}$ fall. The $-NH_2$ (σ^{*} = +0.62)[15] and $-COOCH_3$ (σ^{*} = +2.00)[15] groups exert **–I** effects on each other. Increase in chain length will decrease the extent of this interaction. This will raise the electron density on the amino-N (increasing its nucleophilicity and so produce an increased reaction rate via an increase in $H°(E_{(aq)})$) and also raise the electron density on the carbonyl-C of the methoxycarbonyl group (decreasing the

ease of nucleophilic attack and so produce a decreased reaction rate via a decrease in $H°(E_{(aq)})$). However, while the magnitudes of these two opposing changes will not be the same because of the different σ^* values, both will be very small, and probably negligible, because of attenuation of inductive effects by the intervening 3 or 4 methylenes.

Intramolecular H-bonding would change with increasing ring size but this also appears unimportant, since the pK_a^T studies (p. 127 – 133) yield no evidence for significant such bonding between the $-COOCH_3$ and $-NH_2$ groups in the E forms of both 4-AB Me and 5-APe Me.

Solvation changes have often been major contributors in previous discussions. Despite the lack of evidence for any H-bonding interaction, increasing chain length will increase the ease of approach of the $-COOCH_3$ and $-NH_2$ groups because decreasing bond angle strain outweighs entropy considerations (less chance of the chain ends meeting).[30] This increasing proximity (on average) of the two groups means that the carbonyl-$C^{\delta+}$ and amino-$N^{\delta-}$ can be close which will result in decreased solvation in the reactant and an increase in $S°(E_{(aq)})$. In the TS, solvation is dominated by the developing negative charge on what was originally the carbonyl oxygen. This solvation will be larger than for the reactant carbonyl group and little affected by changes in ring size. Consequently any change in $S°(TS,E{\cdot}OH^-_{(aq)})$ will be small (it may increase slightly) so, overall, $\Delta S^‡$ will receive a decrease (equ. 5.15(a)). Because of this decreasing reactant solvation change with increasing chain length, $H°(E_{(aq)})$ will increase, there will be little change in $H°(TS,E{\cdot}OH^-_{(aq)})$ and therefore a decrease is contributed to $\Delta H^‡$.

Ring strain in the partly closed ring of the TS will decrease as the ring size increases from 5- to 6-membered. The "envelope" shaped 5-membered rings involve some bond angle and eclipsing strain. Much of this is relieved in the 6-membered "chair" shaped ring.[30] Consequently, in going from a 5- to a 6-membered ring TS (4-AB Me to 5-APe Me), ring strain will contribute a decrease to $H°(TS,E{\cdot}OH^-_{(aq)})$, no change in $H°(E_{(aq)})$ and hence a decrease to $\Delta H^‡$.

Rotational freedom is lost on partial ring closure to the TS; this will be slightly larger for the longer chain 5-APe Me which results in a larger decrease in $S°(TS,E{\cdot}OH^-_{(aq)})$, and hence a fall in $\Delta S^‡$.

Steric crowding increases on formation of the TS since there is a change from sp^2 to sp^2/sp^3 hybridisation at the carbonyl-C reaction centre . Raising the size of the partly closed ring from 5 to 6 may slightly relieve this increase and so contribute a small decrease to $\Delta H^{\ddagger}$ via a decrease in of $H°(TS, E{\cdot}OH^-_{(aq)})$. Accompanying this relief would be a small increase in solvation in the TS, i.e. a decrease to $\Delta S^{\ddagger}$ due to a decrease in $S°(TS, E{\cdot}OH^-_{(aq)})$.

Overall, for $\mathbf{\Delta H^{\ddagger}}$, all the contributing terms (solvation, ring strain, steric crowding) produce decreases with the largest probably coming from the change in ring strain. The result is the observed large fall in $\Delta H^{\ddagger}$ in going from 4-AB Me to 5-APe Me.

For $\mathbf{\Delta S^{\ddagger}}$, the same contributing terms along with rotational freedom loss all produce decreases, but all appear to be small. Consequently, the $T.\Delta S^{\ddagger}$ fall (5.1 kJ mol^{-1}) is less than that for $\Delta H^{\ddagger}$ (12.8 kJ mol^{-1}). The balance of these opposing effects is a large nett decrease in $\Delta G^{\ddagger}$ (7.7 kJ mol^{-1}) and this results in a considerable increase in the rate constant.

4-AB Et and 5-APe Et

The 5-amino acid ester is again the more reactive with the same 7.7 kJ mol^{-1} decrease in $\Delta G^{\ddagger}$ seen for the pair of methyl esters. However, this equality hides a completely different source; now $\Delta H^{\ddagger}$ and $\Delta S^{\ddagger}$ work together instead of in opposition, with a small decrease in $\Delta H^{\ddagger}$ and a small increase in $\Delta S^{\ddagger}$.

These changes must arise from a combination of the same factors discussed for the methyl esters, superimposed on which will be the effect of replacing $-CH_3$ by $-C_2H_5$. The consequence of this substitution is a major change in the differences between the pairs of $\Delta S^{\ddagger}$ values. The value of $\Delta S^{\ddagger}$ **decreases** in going from 4-AB Me to 5-APe Me (by 16.9 J K^{-1} mol^{-1}) but **increases** (by 8.4 J K^{-1} mol^{-1}) from 4-AB Et to 5-APe Et. The large size of the change in the differences suggests they originate in solvation effects, although other factors may be minor contributors.

Solvation changes with increasing chain length for the methyl ester pair appear to be dominated by the proximity effect: increased reactant desolvation with increasing chain length contributes a large decrease to $\Delta S^{\ddagger}$. Replacing $-CH_3$ by $-C_2H_5$ increases both the electron density (increased **+I** effect) and the steric crowding at the carbonyl-C. Both of these changes will result in a decrease in solvation at the carbonyl-C (ignoring any proximity effect) and a decrease in the proximity effect. Consequently,

an increase in chain length no longer produces the increase in reactant desolvation seen for the methyl ester pair. This is reinforced by 4-AB Et having a very low $\Delta S^{\ddagger}$ due to low reactant solvation (p. 241). The delicate balance of factors that produce this appears to be reversed in going to 5-APe Et. Apparently, the increased chain length allows increased solvation possibly for conformational reasons. Consequently, the combination of the cancellation of the proximity effect (large $\Delta S^{\ddagger}$ decrease) and an increase in reactant solvation in going from 4-AB Et to 5-APe Et results in a positive contribution to $\Delta S^{\ddagger}$. There will be a corresponding increase contributed to $\Delta H^{\ddagger}$.

Rotational freedom loss on partial ring closure to the TS will be slightly larger for the longer chain 5-APe Et. However, the resulting fall in $\Delta S^{\ddagger}$ will probably be smaller than for the methyl ester pair because the bulkier Et group will restrict the freedom of rotation in both ethyl esters.

Ring strain will contribute a decrease to $\Delta H^{\ddagger}$ similar to that discussed for the methyl esters.

Steric crowding contributions to $\Delta H^{\ddagger}$ and $\Delta S^{\ddagger}$ are probably much the same as for methyl ester pair, i.e. a small decrease in both $\Delta H^{\ddagger}$ and $\Delta S^{\ddagger}$.

Overall, for $\mathbf{\Delta H^{\ddagger}}$, the balance of contributing terms (increase from solvation, decreases from ring strain and steric crowding) results in a much smaller fall in $\Delta H^{\ddagger}$ in going from 4-AB Et to 5-APe Et than for the methyl ester pair.

For $\mathbf{\Delta S^{\ddagger}}$, again there is a balance between the contributing terms but now the increase from solvation changes dominates the decreases from rotational entropy and steric crowding effects, so $\Delta S^{\ddagger}$ increases for the ethyl ester pair in contrast to the methyl esters. The combination of a small fall in $\Delta H^{\ddagger}$ and a rise in $\Delta S^{\ddagger}$ results in the observed increase in rate constant from 4-AB Et to 5-APe Et being similar to that for the methyl ester pair.

In conclusion, the effects of changing the ring size on the rate constants can be explained in terms of the preferred Mechanism 4. There is no evidence which suggests that one of the other three mechanisms discussed would better explain the observed results.

(2) Other k_L Values

Glu DMe and Glu-5-Me can be considered to be derivatives of 4-AB Me. The effect of substitution at C4 by $-COOCH_3$ and $-COO^-$ can be checked against the predictions of the intramolecular aminolysis mechanisms discussed previously (see p. 208). Rate constants were measured only at 25°C, so the discussion is of limited value because the absence of $\Delta H^{\ddagger}$ and $\Delta S^{\ddagger}$ values.

Glu DMe

The alkaline hydrolysis of Glu DMe is complicated by a pair of parallel reactions which are both followed by consecutive reaction(s). As a result, the measured value of "k_E" for Glu DMe is a combination of two rate constants – those for the lactamisation and simple alkaline hydrolysis reactions, $k_L^A + k_{OH^-}^A$, respectively (Scheme 5.2, p. 153). An estimated value for $k_L^A \sim 40$ l mol^{-1} min^{-1} was obtained (see discussion on p. 208). This slow rate of lactamisation reflects the deactivation of the $-NH_2$ group by the adjacent electron withdrawing methoxycarbonyl. As a result, at 25°C, 4-AB Me ($k_L = 1580$ l mol^{-1} l^{-1}) reacts almost 40 times faster than Glu DMe.

Glu-5-Me

Lactamisation also complicates the alkaline hydrolysis of the E form of this ester, but here it must be fast since the overall rate constant is 700 l mol^{-1} min^{-1} (Table 5.11) and so this is the dominant reaction pathway. The ester's structure can be regarded as a 4–COO^- substituted 4-AB Me. Hence, the moderate +I effect from the carboxylate group ($\sigma^* = -1.06$)[15] will have little influence on the $-COOCH_3$ (because of attenuation by the three intervening C's) and so $k_{OH^-}^C$ will be small and similar to k_E for 4-AB Me (~ 9 l mol^{-1} min^{-1}). Consequently, the lactamisation rate constant is ~ 700 l mol^{-1} min^{-1}.

In the case of Glu-5-Me, the value of k_L (25°C) is 700 l mol^{-1} min^{-1} (Table 5.11). However it is unlikely that inductive effects could be responsible for the fall in k_L, since the moderately electron donating $-COO^-$ group ($\sigma^* = -1.06$)[15] is attenuated from the γ-$COOCH_3$ group by the presence of 3 intervening $-CH_2$ groups. Instead it is likely that the reduced k_L value for Glu-5-Me is reduced due to an electrostatic effect, i.e. there will be an unfavourable reaction of two negatively charged ions, $E^- + OH^-$,

in the rds (Scheme 5.8), where a proton would be required to be removed from a negatively charged ester, i.e. an E^- species. However, because $\Delta H^{\ddagger}$ and $\Delta S^{\ddagger}$ are not available, no firm conclusions can be made.

In conclusion, these results can all be explained in terms of Mechanism 4 and there is no evidence which suggests that any of the other three mechanisms discussed would be a better fit to the data.

(3) Literature Results

The rate constants for the lactamisation of the corresponding α,ω-diamino acid methyl esters have also been investigated.[1,5,9] The $\Delta H^{\ddagger}$ and $\Delta S^{\ddagger}$ values for the intramolecular aminolysis reactions for the methyl esters of 2,4-diaminobutanoic acid 2,4-DAB (measured using pH-Stat) and 2,5-diaminopentanoic acid methyl 2,5-DAPe (measured using Stopped Flow) are summarised in Table 5.25:

Table 5.25 Summary of the Literature Values for k_L, $\Delta G^{\ddagger}$, $\Delta H^{\ddagger}$, $\Delta S^{\ddagger}$ and $T{\cdot}\Delta S^{\ddagger}$ for 2,4-DAB Me and 2,5-DAPe Me.

Amino Acid Ester	k_L (298 K)	$\Delta G^{\ddagger}_{298}$ kJ mol^{-1}	$\Delta H^{\ddagger}$ kJ mol^{-1}	$\Delta S^{\ddagger}_{298}$ J K^{-1} mol^{-1}	$298 \cdot \Delta S^{\ddagger}_{298}$ kJ mol^{-1}
2,4-DAB Me [1]	25300	58.1	29.5	-95.9	-28.6
[5]	25320	58.0	29.4	-95.9	-28.6
2,5-DAPe Me [9]	182640	53.0	1.4	-173.0	-51.6

As can be seen, there is clearly a greater preference for 6-membered ring closure. At 25°C, the ratio of reactivities for 2,4-DAB Me: 2,5-DAPe Me is 7.2:1. It is difficult to account for the lower reactivity of 2,4-DAB Me (apparently due to the anomalously small $\Delta H^{\ddagger}$ value for 2,5-DAPe Me) because this $\Delta H^{\ddagger}$ is probably low because of systematic problems with the Stopped Flow method that was used to measure the temperature dependence of the rate constants. This uncertainty in the $\Delta H^{\ddagger}$ and $\Delta S^{\ddagger}$ values means that there is little sense in discussing reasons for the greater reactivity of 2,5-DAPe Me cf. 2,4 DAB Me. Given this, it is more informative to try and account for the greater reactivity of the α,ω-diamino acid esters as compared to their analogous ω-monoamino acid esters.

Analysis of Tables 5.25 and 5.24 show that at 25°C, the ratio of the reactivities of 4-AB Me:2,4-DAB Me is 16 wheras that for 5-APe Me:2,5-DAPe Me is 5. Ignoring the 2,5-DAPe Me results, the greater reactivity of 2,4-DAB Me originates in a more positive $\Delta S^{\ddagger}$ value. This is 31 J K^{-1} mol^{-1} greater than for 4-AB Me. However, this $\Delta G^{\ddagger}$ decreasing effect is only partially balanced by a more positive $\Delta H^{\ddagger}$ value for 2,4-DAB Me of 2.4 kJ mol^{-1}. Both values lie outside the experimental error limits for $\Delta H^{\ddagger}$ and $\Delta S^{\ddagger}$ and therefore are significant.. Once again, these results presumably indicate that there are several terms contributing to $\Delta H^{\ddagger}$ and $\Delta S^{\ddagger}$, with a delicate balance determining the overall reactivity.

Inductive effects will account for some of these differences; 2,4-DAB Me can be considered to be a C-2 NH_2 ($\sigma^* = 0.62$)[15] substituted analogue of 4-AB Me. The moderate increase in **–I** effect will lower the electron density on the carbonyl C, which enhances nucleophilic attack by the amino-N, and this contributes to an increase in rate via a decrease in $\Delta H^{\ddagger}$ (due to an increase in $H°(E_{(aq)})$). However, the increased polarisation of the carbonyl group in the diamino acid ester will also result in increased hydration; $S°((E_{(aq)})$ decreases and therefore $\Delta S^{\ddagger}$ increases. As a result of this increased solvation of the reactant, $H°(E_{(aq)})$ will be lowered, hence raising $\Delta H^{\ddagger}$.

A second factor will be steric effects, since there will be an increase in steric bulk which accompanies NH_2-substitution at C-2. Since the rds of the preferred mechanism (Scheme 5.8) involves an increase in steric crowding, this increase in steric crowding will raise $H°(TS, E{\cdot}OH^-_{(aq)})$. This rise will be larger than the increase in $H°(E_{(aq)})$ and this will contribute to an increase to $\Delta H^{\ddagger}$(see p. 240). It is possible that the increased steric crowding in the TS will make it less solvated further raising both $H°(TS, E{\cdot}OH^-_{(aq)})$ (i.e. raising $\Delta H^{\ddagger}$) and $S°(TS, E{\cdot}OH^-_{(aq)})$ (i.e. increasing $\Delta S^{\ddagger}$).

A third term will involve the solvation factors that are associated with the first two terms. $\Delta H^{\ddagger}$ receives an increase from the decrease in TS solvation. The **–I** effect of the 2-NH_2 group withdraws electron density away from the developing negative charge on the oxygen. This decreased the solvation of the TS, raises both $H°(TS, E{\cdot}OH^-_{(aq)})$ (i.e. raises $\Delta H^{\ddagger}$) and $S°(TS, E{\cdot}OH^-_{(aq)})$ (i.e. raises $\Delta S^{\ddagger}$).

Quite clearly there is a delicate balance between the several factors that are responsible for the increase in reactivity seen when an -NH_2 group is substituted at the C-2 position of 4-AB Me. The dominant factor is solvation effects.

One possible complication that may exist in the comparison of the rates of 5- and 6-memembered lactamisation for the α,ω-diamino acid methyl esters is that an interaction may occur between the α–NH_2 group on the ω–NH_2 group involved in the ring closure. This may be different for the 5- and 6-membered ring closures. This potential problem can be avoided by assessing the relative rates of 5- and 6-membered ring closure where both reactions occur in a single compound, i.e. in 4,5-diaminopentanoic acid methyl ester, 4,5-DAPe Me.[4]

It would be anticipated that the –**I** electronic effects of the 4-NH_2 and 5-NH_2 groups on the –C=O group will be negligible, due to the attenuation of the three or four intervening methylene groups. The values of k_{L5} and k_{L6} were measured only at one temperature (25°C). Consequently, any explanation of the relative magnitudes of the k_L values will be limited. The ratio of k_{L6}/k_{L5} for 4,5-DAPe Me = 4.5 (25°C).[29] Again, 6-membered ring closure is significantly favoured. However, in the absence of any temperature dependence studies it is difficult to examine the underlying causes of the difference reactivities of 5- and 6-membered lactamisation.

References

1. R. W. Hay and P. J. Morris, *J. Chem. Perkin*, **1972**, 1021.
2. M. Caswell, R. K. Chaturvedi, S. M. Lane, B. Zvilichovsky and G. L. Schmir, *J. Org. Chem.*, **1981**, *46*, 1585.
3. R. W. Hay and L. J. Porter, *J. Chem. Soc. (B)*, **1967**, 1261.
4. K. H. Patterson, M Sc. Thesis, University of Waikato, **1985**.
5. G. J. Depree, M Sc. Thesis, University of Waikato, **1992**.
6. L. A. Kodikara, M Sc. Thesis, University of Waikato, **1996**.
7. J. A. Zender, M Sc. Thesis, University of Waikato, **1989**.
8. S. Clay, unpublished results.
9. R. W. Hay and P. J. Morris, *J. Chem. Soc. (B)*, **1970**, 1577.
10. R. B. Martin, A Purcell and R. I. Hedrick, *J. Am. Chem. Soc.*, **1964**, *86*, 2406.
11. T. Gillian, G. Mor, F. W. Pepper and S. G. Cohen, *Biorganic Chem*, **1976**, *6*, 329.
12. R. A. Fairclough and N. Hinshelwood, *J. Chem. Soc.*, 538, **1937**.
13. R. W. Taft, Steric Effects in Organic Chemistry, ed. M. S. Newman, John Wiley and Sons, New York, **1956**.
14. M. L. Bender, *J. Am. Chem. Soc.*, **1960**, *82* , 53.
15. D. D. Perrin, Dissociation Constants of Organic Bases in Aqueous Solution, Butterworths, London, **1969.**
16. M.S. Newman, Steric Effects in Organic Chemistry, Ed M.S. Newman, John Wiley, New York, **1956.**
17. R.W.Taft, Steric Effects in Organic Chemistry, Ed M.S. Newman, John Wiley, New York, **1956.**
18. R.W. Hay, L.J Porter and P.J. Morris, *Aust. J. Chem.*, **1966**, *19*, 1197.
19. G. Arksnes and P. Froyen, *Acta. Chem. Scand.*, **1966**, *20*, 1451.
20. R. W. A. Jones and J. A. R. Thomas, *J. Chem. Soc. (B)*, **1966**, 661.
21. A. C. Satterthwait and W. P. Jencks, *J. Am. Chem. Soc.*, **1974**, *96*, 7018.
22. JM. Eigen, *Angew. Int.*, **1964**, *3*, 1.
23. . P. Guthrie, *J. Am. Chem. Soc.*, **1974**, *96*, 3608.
24. B. Capon and S. P. M^{c}Manus, Neighbouring Group Participation, Vol. 1, Pleenium Press, New York, **1976**.
25. P. V. R. Schleyer, *J. Am. Chem. Soc.*, **1961**, *83*, 1368.
26. M. E. Jung and J. Gervay, *Tetrahedron Lett*, **1988**, *29*, 2429.

27. T. C. Bruice and U. K. Pandit, *J. Am. Chem. Soc.*, **1960**, *82,* 5858.

28. A. L. Parrill and D. P. Dolata, *Theochem*, **1996**, *370*, 187.

29. K. H. Patterson, G. J. Depree, J. A. Depree and P. J. Morris, *Tetrahedron Lett,* **1994**, *35*, 281.

Chapter Six

Conclusions

A major conclusion from the present studies is the importance of temperature dependence studies in gaining a complete understanding of the factors controlling both the thermodynamics and kinetics of chemical reactions.

For the thermodynamic aspect of the present studies, acid-base equilibria, the effect of temperature on pK_a^T yields values for $\Delta H°$ and $\Delta S°$ which provide a complete picture of the energy changes involved in the reaction. From this, inferences can be drawn regarding details of the reaction at the molecular level. Arguments based on single ideas such as inductive effects, often fail to explain observed trends in equilibrium constants with changes in structure because inductive effects are only one of the many energy terms that make up the total energy changes involved in $\Delta H°$ and $\Delta S°$. Solvation effects are often major contributors to both $\Delta H°$ and $\Delta S°$ for the amino acid ester hydrochloride dissociations in water, since ions and polar solvents are involved. The relationships: $\Delta G^\circ = \Delta H^\circ - T\Delta S^\circ = 2.3026RTpK_a^T$, are crucial to understanding the direction of pK_a^T changes produced by structural changes, e.g. the ammonium group dissociations for protonated amino acid esters generally have $\Delta H°$ values that are lower than for the analogous *n*-alkylammonium. The major contributors to $\Delta H°$ are inductive and solvation effects, but the latter is also a major contributor to $\Delta S°$. Ammonium dissociation usually results in increased solvation which produces a negative contribution to both $\Delta H°$ and $\Delta S°$. The nett $\Delta G°(pK_a^T)$, and hence a trend in these quantities, is often the result of a delicate balance between the two opposing terms, $\Delta H°$ and $\Delta S°$.

In the kinetic aspect of the current investigations, the effect of temperature on the rate constants yields values for $\Delta H^\ddagger$ and $\Delta S^\ddagger$. These give an insight into the reaction mechanism. Again, simple arguments based on inductive effects often fail to explain observed trends in rate constants with changes in structure, because inductive effects are only part of the energy balance that makes up $\Delta H^\ddagger$ and $\Delta S^\ddagger$. The equation:

$k = (RT/Nh)\exp(\Delta H^{\ddagger}/RT)\exp(\Delta S^{\ddagger}/R)$ is essential to understanding the effects of changes of $\Delta H^{\ddagger}$ and $\Delta S^{\ddagger}$, induced by structural changes, on the value of rate constants. Structural changes that produce a decrease in $\Delta H^{\ddagger}$ or an increase in $\Delta S^{\ddagger}$, will result in an increase in the rate constant. All of the kinetic data for each ester is consistent with a reaction scheme involving two parallel reactions, $E + OH^-$ and $EH^+ + OH^-$, with E and EH^+ being connected by a pH dependent equilibrium controlled by K_a^T for the ester concerned (see Scheme 5.1, p. 151). Values for the two rate constants, k_E and k_{EH^+}, can be found using plots of the type shown in Figure 5.3, p. 174. The $E + OH^-$ reaction involves intramolecular aminolysis for esters of 4-AB and 5-APe because 5- and 6-membered ring lactams are formed; k_E is replaced by a much larger k_L.

The mechanism for the simple alkaline hydrolysis reaction is $B_{Ac}2$. This is consistent with all the experimental evidence which includes the second order kinetics, the differences between k_{EH^+} and k_E values for a given ester, and trends in these rate constants with structural change. Explanations involve a number of factors contributing to changes in $\Delta H^{\ddagger}$ and $\Delta S^{\ddagger}$. There are often delicate balances between opposing effects, e.g. the value of k_{EH^+} decreases with increasing chain length due to changes in $\Delta H^{\ddagger}$ and $\Delta S^{\ddagger}$ associated with a declining **-I** effect of the ammonium group on the ester carbonyl C. However, at 5-APe Me, k_{EH^+} suddenly increases due to intramolecular H-bonding between the $-NH_3^+$ and carbonyl O; the resulting direct **-I** effect lowers both $\Delta H^{\ddagger}$ and T. $\Delta S^{\ddagger}$, with the balance tilted towards $\Delta H^{\ddagger}$, so $\Delta G^{\ddagger}$ is lowered.

Intramolecular catalysis by amino (lactamisation) is restricted to the E forms of the 4- and 5-amino acid esters, where stable 5- and 6-membered lactam rings can be formed. The simplest mechanism which fits all of the experimental results (see Scheme 5.7, p. 221) can be described as "OH^- assisted INC". It involves synchronous OH^- attack on the amino group as this group attacks the carbonyl C. The resulting tetrahedral intermediate then rapidly decomposes. The kinetics are second order and the experimental $\Delta S^{\ddagger}$ are all large and negative (~ -125 to -145 J K^{-1} mol^{-1}), in agreement with a bimolecular rds. This is unusual for INC reactions which are usually unimolecular with $\Delta S^{\ddagger}$ values near 0 J K^{-1} mol^{-1}. The mechanism is also consistent with the observed effects of structural changes on the rate constants, k_{L5} and k_{L6}, e.g. the rate determining ring closure is faster for the 6-membered case because of a lower $\Delta H^{\ddagger}$ associated with a less strained TS, so $k_{L6} > k_{L5}$. However,

again there are often delicate balances between changes in $\Delta H^{\ddagger}$ and $\Delta S^{\ddagger}$ produced by structural changes, e.g. single N-methylation in 4-AB Me increases k_{L5} due to a decrease in $\Delta H^{\ddagger}$. However, for the corresponding ethyl ester, this N-methylation increases k_{L5} via an increase in $\Delta S^{\ddagger}$. This difference in behaviour is due to slight differences in solvation effects which can change both $\Delta H^{\ddagger}$ and $\Delta S^{\ddagger}$. In both cases, the +I effect of the methyl group contributes to a decrease in $\Delta H^{\ddagger}$.

Similarly, the minor change in the ester group from 4-AB Me to 4-AB Et, produces a dramatic decrease in k_{L5} which is inexplicable in terms of simple inductive effects. In contrast, changing from 4-AB Me to 4-AB Bz results in a small increase in k_{L5}. Small changes in solvation appear to be involved which tilt the balance between $\Delta H^{\ddagger}$ and T. $\Delta S^{\ddagger}$ back and forth.

It is clear that solvation effects play a very important role in determining the effect of structural changes on both the equilibrium constants and the rate constants for reactions involving amino acid esters in aqueous solution.

Appendix 1

pK_a^T Values of Monoamino Acid Esters

A1.1 Calculation of pK_a^T Values of Monoamino Acid Ester Hydrochlorides.

The theory used for the calculation of pK_a^T for EH^+ is outlined below. The reaction mixture and conditions are given in Section 4.2.

Monoamino acid ester hydrochlorides, EH^+Cl^-, behave as monobasic acids in aqueous solution:

$$EH^+ + H_2O \rightleftharpoons E + H_3O^+ \qquad \text{....(A1.1)}$$

By definition, the thermodynamic dissociation constant

$$K_a^T = \frac{\{F\}\{H^+\}}{\{EH^+\}} = \frac{[E]\{H^+\}}{[EH^+]} \cdot \frac{y_\circ}{y_1} \qquad \text{....(A1.2)}$$

where, $y_\circ$ = activity coefficient of neutral species.

y_1 = activity coefficient of singly charged species.

Electroneutrality principle requires:

$$[EH^+] + [Na^+] + [H^+] = [OH^-] + [Cl^-] \qquad \text{....(A1.3)}$$

The concentration of the "total ester"

$$[E_T] = [E] + [EH^+] \qquad \text{....(A1.4)}$$

As the titration proceeds, the value of $[E_T]$ decreases due to dilution by the added NaOH solution. At any point in the titration:

$$[E_T] = \frac{W \cdot 10^3}{M(X + V_\circ)} \qquad \text{....(A1.5)}$$

where,

X = Volume of base added.

$V_\circ$ = Initial total volume.

M = Molecular weight of ester.

W = Weight of ester used.

Rearranging (A1.4), and then combining with (A1.3):

$$\begin{aligned}[E] &= [Cl^-] - [EH^+] \\ &= [Cl^-] - ([OH^-] + [Cl^-] - [Na^+] - [H^+]) \\ &= [Na^+] + [H^+] - [OH^-]\end{aligned}$$

$$[E] = \left(\frac{X}{X + V_\circ}\right) \cdot [base] + \frac{10^{-pH}}{y_1} - \frac{10^{-pK_a^W}}{y_1 \cdot 10^{-pH}} \qquad \text{....(A1.6)}$$

where [base] = concentration of NaOH titrant solution used.

Also from (A1.4) and (A1.5);

$$\begin{aligned}[EH^+] &= [E_T] - [E] \\ &= \frac{W \cdot 10^3}{M(X + V_\circ)} - [E]\end{aligned} \qquad \text{....(A1.7)}$$

Combining (A1.7) with (A1.6) gives:

$$[EH^+] = \frac{W \cdot 10^3}{M(X + V_\circ)} + \frac{10^{-pK_a^W}}{y_1 \cdot 10^{-pH}} - \left(\frac{X}{X + V_\circ}\right) \cdot [base] - \frac{10^{-pH}}{y_1} \qquad \text{....(A1.8)}$$

By definition

$$pK_a^T = -\log_{10} K_a^T \qquad \text{....(A1.9)}$$

Combining (A1.9) with (A1.2):

$$pK_a^T = -\log_{10}\left(\frac{[E]\{H^+\}\cdot y_\circ}{[EH^+]\cdot y_1}\right)$$

Substituting (A1.7) (assuming $y_\circ = 1$)

$$pK_a^T = -\log_{10}\left(\frac{\left(\frac{W\cdot 10^3}{M(X+V_\circ)} - [EH^+]\right)}{[EH^+]}\right) + pH + \log_{10} y_1 \qquad \ldots.(A1.10)$$

The pK_a^T value for Glu-5-Me, EH was determined in a similar manner to the EH^+Cl^-,, except that the equilibrium is now:

$$EH + H_2O \rightleftharpoons E^- + H_3O^+ \qquad \ldots.(A1.11)$$

$$K_a^T = \frac{\{H^+\}[E^-]}{[EH]}.\frac{y_1}{y_\circ} \qquad \ldots.(A1.12)$$

where, $y_\circ$ = activity coefficient of neutral species.

y_1 = activity coefficient of singly charged species.

Electroneutrality principle requires:

$$[E^-] + [OH^-] = [Na^+] + [H^+] \qquad \ldots.(A1.13)$$

The concentration of the "total ester"

$$[E_T] = [E^-] + [EH] \qquad \ldots.(A1.14)$$

As the titration proceeds, the value of $[E_T]$ decreases due to dilution by the added NaOH solution. At any point in the titration is given by (A1.15).

$$[E^-] = [Na^+] + [H^+] - [OH^-] \qquad \ldots.(A1.15)$$

$$[E^-] = \left(\frac{X}{X + V_\circ}\right)\cdot[\text{base}] + \frac{10^{-pH}}{y_1} - \frac{10^{-pK_a^W}}{y_1 \cdot 10^{-pH}} \quad \ldots.(A1.16)$$

Also from (A.14) and (A1.15);

$$[EH] = [E_T] - [E^-]$$

$$= \frac{W \cdot 10^3}{M(X + V_\circ)} - [E^-] \quad \ldots.(A.17)$$

Combining (A.17) with (A.16) gives:

$$[EH] = \frac{W \cdot 10^3}{M(X + V_\circ)} + \frac{10^{-pK_a^W}}{y_1 \cdot 10^{-pH}} - \left(\frac{X}{X + V_\circ}\right)\cdot[\text{base}] - \frac{10^{-pH}}{y_1} \quad \ldots.(A1.18)$$

By definition

$$pK_a^T = -\log_{10} K_a^T \quad \ldots.(A1.9)$$

Combining (A1.9) with (A.12):

$$pK_a^T = -\log_{10}\left(\frac{[E^-]\{H^+\}\cdot y_1}{[EH]\cdot y_\circ}\right)$$

Substituting (7) (assuming $y_\circ = 1$)

$$pK_a^T = -\log_{10}\left(\frac{\frac{W \cdot 10^3}{M(X+V_\circ)} - [EH^+]}{[EH^+]}\right) + pH - \log_{10} y_1 \quad \ldots.(A1.19)$$

	A	B	C	D	E	F	G	H	I
1	PKAESTER1								
2									
3									
4									
5		Variable	Value						
6		Intial Vol.	99.5						
7		y1	0.7715						
8		pKaW	13.9965						
9		NaOH Conc	0.1						
10		Moles Acid	0.0001	=1000*C10					
11									
12	Vol NaOH	pH	$[H^+]$	$[OH^-]$	$[Na^+]$	[E]	$[E_T]$	$[EH^+]$	pK_a^T
13			=10^-B13/C7	=(10^(B13-C8))/C7	=C9*A13/(A13+C6)	=E13+C13-D13	=D10/(A13+C6)	=G13-F13	=B13 + -LOG(F13/H13)+ LOG(C7)
14			=10^-B14/C7	=(10^(B14-C8))/C7	=C9*A14/(A14+C6)	=E14+C14-D14	=D10/(A14+C6)	=G14-F14	=B14 + -LOG(F14/H14)+ LOG(C7)
15			=10^-B15/C7	=(10^(B15-C8))/C7	=C9*A15/(A15+C6)	=E15+C15-D15	=D10/(A15+C6)	=G15-F15	=B15 + -LOG(F15/H15)+ LOG(C7)
16			=10^-B16/C7	=(10^(B16-C8))/C7	=C9*A16/(A16+C6)	=E16+C16-D16	=D10/(A16+C6)	=G16-F16	=B16 + -LOG(F16/H16)+ LOG(C7)
17			=10^-B17/C7	=(10^(B17-C8))/C7	=C9*A17/(A17+C6)	=E17+C17-D17	=D10/(A17+C6)	=G17-F17	=B17 + -LOG(F17/H17)+ LOG(C7)
18			=10^-B18/C7	=(10^(B18-C8))/C7	=C9*A18/(A18+C6)	=E18+C18-D18	=D10/(A18+C6)	=G18-F18	=B18 + -LOG(F18/H18)+ LOG(C7)
19			=10^-B19/C7	=(10^(B19-C8))/C7	=C9*A19/(A19+C6)	=E19+C19-D19	=D10/(A19+C6)	=G19-F19	=B19 + -LOG(F19/H19)+ LOG(C7)
20			=10^-B20/C7	=(10^(B20-C8))/C7	=C9*A20/(A20+C6)	=E20+C20-D20	=D10/(A20+C6)	=G20-F20	=B20 + -LOG(F20/H20)+ LOG(C7)
21			=10^-B21/C7	=(10^(B21-C8))/C7	=C9*A21/(A21+C6)	=E21+C21-D21	=D10/(A21+C6)	=G21-F21	=B21 + -LOG(F21/H21)+ LOG(C7)
22			=10^-B22/C7	=(10^(B22-C8))/C7	=C9*A22/(A22+C6)	=E22+C22-D22	=D10/(A22+C6)	=G22-F22	=B22 + -LOG(F22/H22)+ LOG(C7)
23			=10^-B23/C7	=(10^(B23-C8))/C7	=C9*A23/(A23+C6)	=E23+C23-D23	=D10/(A23+C6)	=G23-F23	=B23 + -LOG(F23/H23)+ LOG(C7)
24			=10^-B24/C7	=(10^(B24-C8))/C7	=C9*A24/(A24+C6)	=E24+C24-D24	=D10/(A24+C6)	=G24-F24	=B24 + -LOG(F24/H24)+ LOG(C7)
25			=10^-B25/C7	=(10^(B25-C8))/C7	=C9*A25/(A25+C6)	=E25+C25-D25	=D10/(A25+C6)	=G25-F25	=B25 + -LOG(F25/H25)+ LOG(C7)
26			=10^-B26/C7	=(10^(B26-C8))/C7	=C9*A26/(A26+C6)	=E26+C26-D26	=D10/(A26+C6)	=G26-F26	=B26 + -LOG(F26/H26)+ LOG(C7)

A1.2(b) PKAESTERS2

	A	B	C	D	E	F	G	H	I
1	PKAESTER2								
2									
3									
4									
5		Variable	Value						
6		Intial Vol.	99.5						
7		y1	0.7715						
8		pKaW	13.9965						
9		NaOH Conc	0.1						
10		Moles Ester	0.0001	=1000*C10					
11									
12	Vol NaOH	pH	$[H^+]$	$[OH^-]$	$[Na^+]$	$[E^-]$	$[E_T]$	[EH]	pK_a^T
13	0	5.7	=10^-B13/C7	=(10^(B13-C8))/C7	=C9*A13/(A13+C6)	=E13+C13-D13	=D10/(A13+C6)	=G13-F13	=B13 + -LOG(F13/H13)+ LOG(C7)
14	0.09	7.977	=10^-B14/C7	=(10^(B14-C8))/C7	=C9*A14/(A14+C6)	=E14+C14-D14	=D10/(A14+C6)	=G14-F14	=B14 + -LOG(F14/H14)+ LOG(C7)
15	0.19	8.415	=10^-B15/C7	=(10^(B15-C8))/C7	=C9*A15/(A15+C6)	=E15+C15-D15	=D10/(A15+C6)	=G15-F15	=B15 + -LOG(F15/H15)+ LOG(C7)
16	0.29	8.66	=10^-B16/C7	=(10^(B16-C8))/C7	=C9*A16/(A16+C6)	=E16+C16-D16	=D10/(A16+C6)	=G16-F16	=B16 + -LOG(F16/H16)+ LOG(C7)
17	0.39	8.859	=10^-B17/C7	=(10^(B17-C8))/C7	=C9*A17/(A17+C6)	=E17+C17-D17	=D10/(A17+C6)	=G17-F17	=B17 + -LOG(F17/H17)+ LOG(C7)
18	0.49	9.03	=10^-B18/C7	=(10^(B18-C8))/C7	=C9*A18/(A18+C6)	=E18+C18-D18	=D10/(A18+C6)	=G18-F18	=B18 + -LOG(F18/H18)+ LOG(C7)
19	0.59	9.189	=10^-B19/C7	=(10^(B19-C8))/C7	=C9*A19/(A19+C6)	=E19+C19-D19	=D10/(A19+C6)	=G19-F19	=B19 + -LOG(F19/H19)+ LOG(C7)
20	0.69	9.345	=10^-B20/C7	=(10^(B20-C8))/C7	=C9*A20/(A20+C6)	=E20+C20-D20	=D10/(A20+C6)	=G20-F20	=B20 + -LOG(F20/H20)+ LOG(C7)
21	0.79	9.507	=10^-B21/C7	=(10^(B21-C8))/C7	=C9*A21/(A21+C6)	=E21+C21-D21	=D10/(A21+C6)	=G21-F21	=B21 + -LOG(F21/H21)+ LOG(C7)
22	0.89	9.675	=10^-B22/C7	=(10^(B22-C8))/C7	=C9*A22/(A22+C6)	=E22+C22-D22	=D10/(A22+C6)	=G22-F22	=B22 + -LOG(F22/H22)+ LOG(C7)
23			=10^-B23/C7	=(10^(B23-C8))/C7	=C9*A23/(A23+C6)	=E23+C23-D23	=D10/(A23+C6)	=G23-F23	=B23 + -LOG(F23/H23)- LOG(C7)
24			=10^-B24/C7	=(10^(B24-C8))/C7	=C9*A24/(A24+C6)	=E24+C24-D24	=D10/(A24+C6)	=G24-F24	=B24 + -LOG(F24/H24)- LOG(C7)
25			=10^-B25/C7	=(10^(B25-C8))/C7	=C9*A25/(A25+C6)	=E25+C25-D25	=D10/(A25+C6)	=G25-F25	=B25 + -LOG(F25/H25)- LOG(C7)
26			=10^-B26/C7	=(10^(B26-C8))/C7	=C9*A26/(A26+C6)	=E26+C26-D26	=D10/(A26+C6)	=G26-F26	=B26 + -LOG(F26/H26)- LOG(C7)

A1.3 Summary Tables for Monoamino Acid Ester Hydrochlorides at 25.0°C

A1.3(a) Group 1, Monoamino Acid Esters

Section A1.3(a) contain tables that list typical pK_a^T titrations for monoamino acid ester hydrochlorides that underwent a slow rate of alkaline hydrolysis at 25.0°C and I = 0.1 mol l^{-1}.

Table A1.1 Determination of pK_a^T for 2-AE.Bz.HCl (1 x recryst.)

Test solution contained: 10^{-4} moles EH^+Cl^- 9.90 ml 1.0 mol l^{-1} KCl 89.60 ml DW			T = (25.00 ± 0.05)°C I = 0.1 mol l^{-1} $[ester]_{total} = 10^{-3}$ mol l^{-1}	
Vol. 0.1000 mol l^{-1} NaOH (ml)	Titration 1		Titration 2	
	pH	pK_a^T	pH	pK_a^T
0.000	5.329	-	5.362	-
0.050	6.312	(7.473)†	6.344	(7.505)†
0.100	6.652	(7.492)†	6.662	(7.503)†
0.200	7.022	7.511	7.030	7.520
0.300	7.268	7.524	7.272	7.527
0.400	7.463	7.527	7.467	7.531
0.500	7.641	7.529	7.644	7.532
0.600	7.813	7.526	7.819	7.532
0.700	8.002	7.524	8.009	7.531
0.800	8.222*	7.513	8.230*	7.521
0.900	8.522*	(7.476)†	8.531*	(7.485)†
Average pK_a^T =		7.522 ± 0.0.011		7.528 ± 0.008

Overall average pK_a^T = 7.52 ± 0.01

†Values in parentheses were excluded from the average.

* Hydrolysis noticeable.

Table A1.2 Determination of pK_a^T for 3-AP Bz.HCl (2 x recryst.)

Test solution contained: 10^{-4} moles EH^+Cl^- 9.90 ml 1.0 mol l^{-1} KCl 89.60 ml DW			$T = (25.00 \pm 0.05)°C$ $I = 0.1$ mol l^{-1} $[ester]_{total} = 10^{-3}$ mol l^{-1}	
Vol. 0.1000 mol l^{-1} NaOH (ml)	Titration 1		Titration 2	
	pH	pK_a^T	pH	pK_a^T
0.000	5.555	-	5.498	-
0.050	7.760	(8.933)†	7.720	(8.892)†
0.100	8.153	(9.004)†	8.136	(8.986)†
0.200	8.554	9.056	8.548	9.050
0.300	8.799	9.071	8.792	9.064
0.400	8.988	9.075	8.980	9.066
0.500	9.158	9.078	9.151	9.070
0.600	9.311	9.070	9.308	9.067
0.700	9.461	9.056	9.459	9.053
0.800	9.616*	(9.036)†	9.612*	(9.031)†
0.900	9.775*	(8.998)†	9.768*	(8.990)†
Average pK_a^T =		9.067 ± 0.011		9.062 ± 0.012

Overall average $pK_a^T = 9.06 \pm 0.01$

†Values in parentheses were excluded from the average.

* Hydrolysis occurs.

Table A1.3 Determination of pK_a^T for DMAB Et.HCl (2 x recryst.).

Test solution contained:			T = (25.00 ± 0.05)°C	
10^{-4} moles EH^+Cl^-			I = 0.1 mol l^{-1}	
9.90 ml 1.0 mol l^{-1} KCl			$[ester]_{total} = 10^{-3}$ mol l^{-1}	
89.60 ml DW				
Vol. 0.1000 mol l^{-1} NaOH (ml)	Titration 1		Titration 2	
	pH	pK_a^T	pH	pK_a^T
0.000	5.002	-	4.998	-
0.100	8.326	(9.180)†	8.292	(9.146)†
0.150	8.572	(9.220)†	8.550	(9.207)†
0.200	8.760	(9.267)†	8.738	(9.237)†
0.250	8.850	9.273	8.868	9.262
0.300	8.999	9.282	8.980	9.264
0.350	9.104	9.292	9.085	9.272
0.400	9.195	9.296	9.178	9.277
0.450	9.280	9.298	9.262	9.278
0.500	9.361	9.301	9.341	9.279
0.550	9.440	9.303	9.420	9.279
0.600	9.514	9.301	9.497	9.280
0.650	9.590	9.301	9.572	9.280
0.700	9.665	9.303	9.645	9.281
0.750	9.738	9.301	9.718	9.278
0.800	9.811	9.298	9.790	9.274
0.850	9.822*	(9.292)†	9.861*	(9.269)†
Average pK_a^T =		9.296 ± 0.023		9.276 ± 0.013

Overall average $pK_a^T = 9.29 \pm 0.02$

† Values in parentheses were excluded from the average.

* Hydrolysis occurs.

A1.3(b) Group 2, Moderately Hydrolysing Monoamino Acid Esters

Section A1.3(b) contain pK_a^T summary tables for Group 2, moderately hydrolysing amino acid esters, at 25°C and I = 0.1 mol l^{-1}.

Table A1.4 Determination of pK_a^T for 4-AB Et.HCl (3 x recryst.)

Test solution contained: 10^{-4} moles EH^+Cl^- 9.90 ml 1.0 mol l^{-1} KCl 89.60 ml DW			$T = (25.00 \pm 0.05)°C$ I = 0.1 mol l^{-1} $[ester]_{total} = 10^{-3}$ mol l^{-1}	
Vol. 0.1000 mol l^{-1} NaOH (ml)	Titration 1		Titration 2	
	pH	pK_a^T	pH	pK_a^T
0.000	4.992	-	4.880	-
0.100	8.828	(9.714)†	8.778	(9.659)†
0.150	9.094	(9.793)†	9.062	(9.756)†
0.200	9.270	(9.829)†	9.250	(9.805)†
0.250	9.414	9.860	9.409	9.855
0.300	9.513	9.861	9.511	9.855
0.350	9.605	9.866	9.596	9.855
0.400	9.685	9.867	9.678	9.858
0.450	9.757	9.866	9.751	9.858
0.500	9.825	9.866	9.819	9.858
0.550	9.889	9.866	9.881	9.958
0.600	9.948	9.864	9.945	9.956
0.650	10.006	9.864	10.001	9.956
0.700	10.060	9.861	10.053	9.855
0.750	10.113*	(9.860)†	10.104*	(9.852)†
Average pK_a^T =		9.864 ± 0.004		9.856 ± 0.002

Overall average pK_a^T = 9.86 ± 0.01

† Values in parentheses were excluded from the average.

*Hydrolysis occurs.

Table A1.5 Determination of pK_a^T for 4-AB Bz HCl (2 x recry.).

Test solution contained:			T = (25.00 ± 0.05)°C	
10^{-4} moles EH^+Cl^-			I = 0.1 mol l^{-1}	
9.90 ml 1.0 mol l^{-1} KCl			$[ester]_{total} = 10^{-3}$ mol l^{-1}	
89.60 ml DW				
Vol. 0.1000 mol l^{-1} NaOH (ml)	Titration 1§		Titration 2§§	
	pH	pK_a^T	pH	pK_a^T
0.040	6.475	-	6.510	-
0.100	8.589	(9.703)†	8.612	(9.729)†
0.150	8.923	(9.764)†	8.939	(9.782)†
0.200	9.130	9.793	9.145	9.811
0.250	9.276	9.803	9.290	9.820
0.300	9.390	9.805	9.405	9.822
0.350	9.486	9.803	9.503	9.823
0.400	9.570	9.800	9.588	9.822
0.450*	9.644	9.794	9.658	9.811
Average pK_a^T =		9.799 ± 0.006		9.818 ± 0.007

Overall average pK_a^T = 9.81 ± 0.02

§ pK_a^T values in Titration 1 calculated using a - 0.039 ml volume correction.

§§ pK_a^T values in Titration 2 calculated using a - 0.041 ml volume correction.

† Values in parentheses were excluded from the average.

* Hydrolysis occurs beyond 0.450 ml.

Table A1.6 Determination of the pK_a^T for 4-MAB Me.HCl (3 x recryst.)

Test solution contained: 10^{-4} moles EH^+Cl^- 9.90 ml 1.0 mol l^{-1} KCl 89.60 ml DW			T = (25.00 ± 0.05)°C I = 0.1 mol l^{-1} $[ester]_{total} = 10^{-3}$ mol l^{-1}	
Vol. 0.1000 mol l^{-1} NaOH (ml)	Titration 1		Titration 2	
	pH	pK_a^T	pH	pK_a^T
0.000	5.092	-	5.142	-
0.100	9.040	(9.958)†	9.012	(9.925)†
0.150	9.270	10.002	9.271	10.003
0.200	9.421	10.013	9.413	10.003
0.250	9.523	9.998	9.515	9.989
0.300	9.614	9.990	9.612	9.986
0.350	9.683*	(9.969)†	9.686*	(9.973)†
0.400	9.743*	(9.946)†	9.745*	(9.949)†
0.450	9.790*	(9.913)†	9.800*	(9.922)†
Average pK_a^T =		10.001 ± 0.012		9.995 ± 0.009

Overall average pK_a^T = 10.00 ± 0.01

† Values in parentheses were excluded from the average.

*Hydrolysis noticeable.

Table A1.7 Determination of the pK_a^T for 4-MAB Et.HCl (3 x recryst.)

Test solution contained: 10^{-4} moles EH^+Cl^- 9.90 ml 1.0 mol l^{-1} KCl 89.60 ml DW			$T = (25.00 \pm 0.05)°C$ $I = 0.1$ mol l^{-1} $[ester]_{total} = 10^{-3}$ mol l^{-1}	
Vol. 0.1000 mol l^{-1} NaOH (ml)	Titration 1		Titration 2	
	pH	pK_a^T	pH	pK_a^T
0.000	5.683	-	5.722	-
0.100	9.108	(10.037)†	9.109	(10.038)†
0.150	9.329	10.073	9.327	10.070
0.200	9.482	10.088	9.475	10.079
0.250	9.600	10.095	9.593	10.085
0.300	9.688	10.084	9.686	10.082
0.350	9.765	10.075	9.765	10.075
0.400	9.832*	(10.064)†	9.832*	(10.064)†
0.450	9.891*	((10.050)†	9.892*	(10.052)†
Average pK_a^T =		10.083 ± 0.012		10.078 ± 0.008

Overall average pK_a^T = 10.08 ± 0.01

† Values in parentheses were excluded from the average.

*Hydrolysis noticeable.

Table A1.8 Determination of the pK_a^T for 4-A-3-MB Me.HCl (3 x recryst.).

Test solution contained: 10^{-4} moles EH^+Cl^- 9.90 ml 1.0 mol l^{-1} KCl 89.60 ml DW			$T = (25.00 \pm 0.05)°C$ $I = 0.1$ mol l^{-1} $[ester]_{total} = 10^{-3}$ mol l^{-1}	
Vol. 0.1000 mol l^{-1} NaOH (ml)	Titration 1		Titration 2	
	pH	pK_a^T	pH	pK_a^T
0.000	5.510	-	5.699	-
0.100	8.535	(9.401)†	8.533	(9.399)†
0.150	8.770	(9.440)†	8.769	9.439
0.200	8.931	9.454	8.926	9.449
0.250	9.059	9.462	9.052	9.454
0.300	9.162	9.460	9.156	9.454
0.350	9.256	9.461	9.247	9.451
0.400	9.339	9.458	9.528	9.446
0.450	9.412	9.450	9.403	9.440
0.500	9.479*	(9.439)†	9.466*	(9.424)†
0.550	9.541*	(9.425)†	9.523*	(9.407)†
Average pK_a^T =		9.458 ± 0.008		9.449 ± 0.010

Overall average $pK_a^T = 9.45 \pm 0.01$

† Values in parentheses were excluded from the average.

*Hydrolysis noticeable.

Table A1.9 Determination of the pK_a^T for 4-A-3,3-DMB Me.HCl (3 x recryst.).

Test solution contained: 10^{-4} moles EH^+Cl^- 9.90 ml 1.0 mol l^{-1} KCl 89.60 ml DW			T = (25.00 ± 0.05)°C I = 0.1 mol l^{-1} $[ester]_{total} = 10^{-3}$ mol l^{-1}	
Vol. 0.1000 mol l^{-1} NaOH (ml)	Titration 1		Titration 2	
	pH	pK_a^T	pH	pK_a^T
0.000	4.700	-	4.707	-
0.100	8.188	(9.042)†	8.160	(9.013)†
0.150	8.500	(9.157)†	8.479	(9.136)†
0.200	8.703	9.219	8.695	9.216
0.250	8.832	99.220	8.829	9.218
0.300	8.949	9.232	8.933	9.220
0.350	9.051	9.239	9.041	9.228
0.400	9.141	9.241	9.129	9.228
0.450	9.218	9.235	9.210	9.226
0.500	9.291	9.227	9.281	9.216
0.550	9.359*	(9.216)†	9.344*	(9.204)†
0.600	9.436*	(9.205)†	9.410*	(9.187)†
Average pK_a^T =		9.230 ± 0.011		9.222 ± 0.006

Overall average pK_a^T = 9.23 ± 0.01

† Values in parentheses were excluded from the average.

*Hydrolysis noticeable.

A1.4 Summary Tables for Monoamino Acid Ester Hydrochlorides at 37.1°C

A1.4(a) Group 1, Amino Acid Esters

Section A1.4(a) contain pK_a^T summary tables for Group 1, slowly hydrolysing amino acid esters, at 37.1 °C and I = 0.1 mol l^{-1}. Due allowance was made for water expansion.

Table A1.10 Determination of pK_a^T for Ser Me.HCl (2 x recryst.)

Test solution contained: 10^{-4} moles EH^+Cl^- 9.90 ml 1.0 mol l^{-1} KCl 89.10 ml DW			$T = (37.10 \pm 0.05)°C$ $I = 0.1$ mol l^{-1} $[ester]_{total} = 10^{-3}$ mol l^{-1}	
Vol. 0.1000 mol l^{-1} NaOH (ml)	Titration 1		Titration 2	
	pH	pK_a^T	pH	pK_a^T
0.000	4.980	-	4.970	-
0.100	5.885	6.716	5.890	6.721
0.150	6.081	6.716	6.089	6.724
0.200	6.233	6.718	6.236	6.721
0.250	6.358	6.719	6.361	6.722
0.300	6.465	6.717	6.469	6.721
0.350	6.565	6.719	6.568	6.722
0.400	6.657	6.718	6.660	6.721
0.450	6.743	6.715	6.748	6.720
0.500	6.830	6.715	6.833	6.718
0.550	6.914*	(6.712)†	6.917*	(6.717)†
0.600	7.001*	(6.711)†	7.005*	(6.715)†
Average pK_a^T =		6.717 ± 0.002		6.721 ± 0.004

Overall average pK_a^T = 6.72 ± 0.01

* Hydrolysis noticeable.

†Values in parentheses were excluded from the average.

Table A1.11 Determination of pK_a^T for 2-AE Me.HCl (2 x recryst.)

Test solution contained: 10^{-4} moles EH^+Cl^- 9.90 ml 1.0 mol l^{-1} KCl 89.10 ml DW			$T = (37.10 \pm 0.05)°C$ $I = 0.1$ mol l^{-1} $[ester]_{total} = 10^{-3}$ mol l^{-1}	
Vol. 0.1000 mol l^{-1} NaOH (ml)	Titration 1		Titration 2	
	pH	pK_a^T	pH	pK_a^T
0.000	5.173	-	5.201	-
0.100	6.462	(7.299)†	6.463	(7.300)†
0.150	6.678	(7.316)†	6.675	(7.313)†
0.200	6.835	7.322	6.830	(7.317)†
0.250	6.963	7.325	6.958	7.320
0.300	7.076	7.330	7.070	7.324
0.350	7.177	7.332	7.170	7.325
0.400	7.270	7.332	7.262	7.324
0.450	7.358	7.332	7.352	7.326
0.500	7.445	7.332	7.440	7.327
0.550	7.531	7.331	7.527	7.327
0.600	7.620	7.332	7.615	7.326
0.650	7.710	7.330	7.706*	(7.322)
0.700	7.806	7.328	7.800*	(7.319)
0.750	7.910*	(7.324)†	7.905*	(7.317)†
0.800	8.028*	(7.320)†	8.025*	(7.311)†
Average pK_a^T =		7.329 ± 0.007		7.324 ± 0.004

Overall average $pK_a^T = 7.33 \pm 0.01$

† Values in parentheses were excluded from the average.

* Hydrolysis noticeable.

Table A1.12 Determination of pK_a^T for 3-AP Bz.HCl (2 x recryst.)

Test solution contained: 10^{-4} moles EH^+Cl^- 9.90 ml 1.0 mol l^{-1} KCl 89.10 ml DW			$T = (37.10 \pm 0.05)°C$ $I = 0.1$ mol l^{-1} $[ester]_{total} = 10^{-3}$ mol l^{-1}	
Vol. 0.1000 mol l^{-1} NaOH (ml)	Titration 1		Titration 2	
	pH	pK_a^T	pH	pK_a^T
0.000	5.358	-	5.358	-
0.050	7.087	(8.252)†	7.108	(8.274)†
0.100	7.712	(8.559)†	7.724	(8.571)†
0.150	7.988	(9.637)†	7.991	(8.640)†
0.200	8.175	8.675	8.178	8.678
0.250	8.303	8.680	8.306	8.683
0.300	8.414	8.684	8.415	8.685
0.350	8.511	8.684	8.513	8.686
0.400	8.599	8.683	8.602	8.686
0.450	8.684	8.683	8.686	8.685
0.500	8.764	8.681	8.766	8.683
0.550	8.840*	(8.676)†	8.844*	(8.680)†
0.600	8.910*	(8.665)†	8.912*	(8.667)†
Average pK_a^T =		8.681 ± 0.006		8.684 ± 0.006

Overall average pK_a^T = 8.69 ± 0.01

†Values in parentheses were excluded from the average.

* Hydrolysis occurs.

Table A1.13 Determination of pK_a^T for 4-DMAB MeHCl (2 x recryst.)

Test solution contained: 10^{-4} moles EH^+Cl^- 9.90 ml 1.0 mol l^{-1} KCl 89.10 ml DW			$T = (37.10 \pm 0.05)°C$ $I = 0.1$ mol l^{-1} $[ester]_{total} = 10^{-3}$ mol l^{-1}	
Vol. 0.1000 mol l^{-1} NaOH (ml)	Titration 1[§]		Titration 2[§§]	
	pH	pK_a^T	pH	pK_a^T
0.000	6.417	-	6.473	-
0.250	8.062	(9.061)	8.058	(9.090)
0.300	8.334	(9.091)	8.323	(9.101)
0.350	8.518	9.108	8.501	9.106
0.400	8.650	9.107	8.640	9.110
0.450	8.759	9.105	8.755	9.112
.500	8.852	9.099	8.855	9.113
0.550	8.950	9.109	8.945	9.113
0.600	9.031	9.108	9.027	9.113
0.650	9.109	9.108	9.105	9.114
0.700	9.182	9.106	9.180	9.112
0.750	9.254	9.106	9.241*	(9.099)
0.800	9.320	9.101	9.302*	(9.087)
0.850	9.380*	(9.089)	9.373*	(9.089)
Average pK_a^T =		9.106 ± 0.0067		9.112 ± 0.006

Overall average $pK_a^T = 9.10 \pm 0.01$

[§] Volume correction of – 0.175 ml used.

[§§] Volume correction of – 0.180 ml used.

[†] Values in parentheses were excluded from the average.

[*] Hydrolysis occurs.

Table A1.14 Determination of pK_a^T for 4-DMAB Et.HCl (2 x recryst.)

Test solution contained: 10^{-4} moles EH^+Cl^- 9.90 ml 1.0 mol l^{-1} KCl 89.10 ml DW			$T = (37.10 \pm 0.05)°C$ $I = 0.1$ mol l^{-1} $[ester]_{total} = 10^{-3}$ mol l^{-1}	
Vol. 0.1000 mol l^{-1} NaOH (ml)	Titration 1		Titration 2	
	pH	pK_a^T	pH	pK_a^T
0.000	5.562	-	5.449	-
0.100	8.100	(8.958)†	8.068	(8.925)†
0.150	8.335	(8.997)†	8.313	(8.973)†
0.200	8.496	(9.010)†	8.481	(8.994)†
0.250	8.627	9.020	8.613	9.005
0.300	8.732	9.020	8.722	9.009
0.350	8.828	9.023	8.822	9.016
0.400	8.912	9.020	8.910	9.018
0.450	8.992	9.018	8.990	9.016
0.500	9.073	9.022	9.070	9.019
0.550	9.148	9.023	9.145	9.019
0.600	9.219	9.020	9.215	9.015
0.650	9.288*	(9.016)†	9.285*	(9.013)†
0.700	9.355*	(9.011)†	9.718*	(9.007)†
Average pK_a^T =		9.021 ± 0.002		9.014 ± 0.009

Overall average $pK_a^T = 9.02 \pm 0.01$

† Values in parentheses were excluded from the average.

* Hydrolysis occurs.

A1.4(b) Group 2, Moderately Hydrolysing Amino Acid Esters

Section A1.4(b) contain pK_a^T summary tables for Group 2, moderately hydrolysing amino acid esters, at 37.1 °C and I = 0.1 mol l^{-1}.

Table A1.15 Determination of pK_a^T for 4-AB Me.HCl (2 x recryst.)

Test solution contained: 10^{-4} moles EH^+Cl^- 9.90 ml 1.0 mol l^{-1} KCl 89.10 ml DW		T = (37.10 ± 0.05)°C I = 0.1 mol l^{-1} $[ester]_{total} = 10^{-3}$ mol l^{-1}		
Vol. 0.1000 mol l^{-1} NaOH (ml)	Titration 1§		Titration 2§§	
	pH	pK_a^T	pH	pK_a^T
0.050	6.310	-	6.420	-
0.100	8.174	(9.362)†	8.199	(9.410)†
0.150	8.559	(9.445)†	8.559	9.455
0.200	8.770	9.466	8.761	9.463
0.250	8.915	9.469	8.905	9.463
0.300	9.029	9.467	9.019	9.461
0.350	9.120*	(9.457)†	9.104*	(9.442)†
0.400	9.203*	(9.451)†	9.187*	(9.436)†
0.450	9..280*	(9.448)†	9.255*	(9.421)†
Average pK_a^T =		9.467 ± 0.002		9.461 ± 0.006

Overall average pK_a^T = 9.46 ± 0.01

§ Volume correction of – 0.048 ml used.

§§ Volume correction of – 0.050 ml used.

† Values in parentheses were excluded from the average.

* Hydrolysis occurs.

Table A1.16 Determination of pK_a^T for 4-AB Et.HCl (3 x recryst.)

Test solution contained:			T = (37.10 ± 0.05)°C	
10^{-4} moles EH^+Cl^-			I = 0.1 mol l^{-1}	
9.90 ml 1.0 mol l^{-1} KCl			$[ester]_{total} = 10^{-3}$ mol l^{-1}	
89.10 ml DW				
Vol. 0.1000 mol l^{-1} NaOH (ml)	Titration 1		Titration 2	
	pH	pK_a^T	pH	pK_a^T
0.000	5.405	-	6.563	-
0.050	8.011	(9.204)†	8.055	(9.252)†
0.100	8.523	(9.414)†	8.527	(9.419)†
0.150	8.765	9.468	8.769	9.473
0.200	8.912	9.471	8.915	9.475
0.250	9.031	9.474	9.034	9.478
0.300	9.133	9.477	9.138	9.483
0.350	9.222	9.479	9.224	9.481
0.400	9.301	9.479	9.303	9.481
0.450	9.373	9.477	9.375	9.480
0.500	9.438*	(9.473)†	9.438*	(9.473)†
0.550	9.501*	(9.471)†	9.500*	(9.470)†
Average pK_a^T =		9.475 ± 0.007		9.478 ± 0.005

Overall average pK_a^T = 9.48 ± 0.01

† Values in parentheses were excluded from the average.

* Hydrolysis noticeable.

Table A1.17 Determination of pK_a^T for 4-AB Bz.HCl (3 x recryst.)

Test solution contained:			T = (37.10 ± 0.05)°C	
10^{-4} moles EH^+Cl^-			I = 0.1 mol l^{-1}	
9.90 ml 1.0 mol l^{-1} KCl			$[ester]_{total} = 10^{-3}$ mol l^{-1}	
89.10 ml DW				
Vol. 0.1000 mol l^{-1} NaOH (ml)	Titration 1§		Titration 2§§	
	pH	pK_a^T	pH	pK_a^T
0.040	5.982	-	5.935	-
0.100	8.164	(9.280)†	8.572	(9.333)†
0.150	8.572	(9.395)†	8.582	(9.395)†
0.200	8.762	9.410	8.762	9.410
0.250	8.902	9.416	8.902	9.416
0.300	9.015	9.417	9.014	9.417
0.350	9.109	9.415	9.109	9.415
0.400	9.187*	(9.405)†	9.187*	(9.405)†
0.450	9.258*	(9.396)†	9.258	(9.396)
Average pK_a^T =		9.415 ± 0.005		9.415 ± 0.005

Overall average pK_a^T = 9.42 ± 0.01

§ Volume correction of – 0.040 ml used.

§§ Volume correction of – 0.035 ml used.

† Values in parentheses were excluded from the average.

* Hydrolysis occurs.

Table A1.18 Determination of pK_a^T for 4-MAB Me.HCl (3 x recryst.)

Test solution contained:	T = (37.10 ± 0.05)°C
10^{-4} moles EH^+Cl^-	I = 0.1 mol l^{-1}
9.90 ml 1.0 mol l^{-1} KCl	$[ester]_{total} = 10^{-3}$ mol l^{-1}
89.10 ml DW	

Vol. 0.1000 mol l^{-1} NaOH (ml)	Titration 1[§]		Titration 2[§§]	
	pH	pK_a^T	pH	pK_a^T
0.000	6.312	-	6.276	-
0.080	8.005	(9.464)[†]	8.012	(9.529)[†]
0.090	8.314	9.732	8.281	9.730
0.100	8.405	9.729	8.384	9.737
0.120	8.546	9.727	8.529	9.735
0.140	8.656	9.728	8.644	9.739
0.160	8.746	9.731	8.731	9.732
0.180	8.820	9.730	8.810	9.731
0.200	8.881[*]	(9.724)[†]	8.864	(9.695)[†]
0.220	8.932[*]	(9.756)[†]	8.912	(9.695)[†]
Average pK_a^T =		9.730 ± 0.003		9.734 ± 0.005

Overall average pK_a^T = 9.73 ± 0.01

[§] Volume correction of – 0.047 ml used.

[§§] Volume correction of – 0.050 ml used.

[†] Values in parentheses were excluded from the average.

[*] Hydrolysis occurs.

Table A1.19 Determination of pK_a^T for 4-MAB Et.HCl (2 x recryst.)

Test solution contained: 10^{-4} moles EH^+Cl^- 9.90 ml 1.0 mol l^{-1} KCl 89.10 ml DW			$T = (37.10 \pm 0.05)°C$ $I = 0.1$ mol l^{-1} $[ester]_{total} = 10^{-3}$ mol l^{-1}	
Vol. 0.1000 mol l^{-1} NaOH (ml)	Titration 1		Titration 2	
	pH	pK_a^T	pH	pK_a^T
0.000	5.312	-	5.345	-
0.100	8.739	(9.669)†	8.742	(9.671)†
0.150	8.945	9.684	8.948	9.688
0.200	9.087	9.685	9.091	9.691
0.250	9.198	9.682	9.201	9.686
0.300	9.285	9.670	9.289	9.676
0.350	9.360*	(9.658)†	9.363*	(9.662)†
0.400	9.425*	(9.643)†	9.399*	(9.607)†
Average pK_a^T =		9.680 ± 0.010		9.685 ± 0.011

Overall average $pK_a^T = 9.68 \pm 0.01$

† Values in parentheses were excluded from the average.

* Hydrolysis noticeable.

Table A1.20 Determination of pK_a^T for 4-A-3-MB Me.HCl (2 x recryst.)

Test solution contained: 10^{-4} moles EH^+Cl^- 9.90 ml 1.0 mol l^{-1} KCl 89.10 ml DW			$T = (37.10 \pm 0.05)°C$ $I = 0.1$ mol l^{-1} $[ester]_{total} = 10^{-3}$ mol l^{-1}	
Vol. 0.1000 mol l^{-1} NaOH (ml)	Titration 1		Titration 2	
	pH	pK_a^T	pH	pK_a^T
0.000	5.466	-	5.424	-
0.100	8.195	(9.058)†	8.154	(9.015)†
0.150	8.408	9.074	8.398	9.063
0.200	8.561	9.079	8.558	9.076
0.250	8.684	9.082	8.678	9.075
0.300	8.782	9.075	8.778	9.070
0.350	8.864*	(9.023)†	8.861*	(9.059)†
Average pK_a^T =		9.078 ± 0.0.005		9 .071 ± 0.008

Overall average $pK_a^T = 9.08 \pm 0.01$

† Values in parentheses were excluded from the average.

* Hydrolysis noticeable.

Table A1.21 Determination of pK_a^T for 4-A-3,3-DMB Me.HCl (2 x recryst.)

Test solution contained: 10^{-4} moles EH^+Cl^- 9.90 ml 1.0 mol l^{-1} KCl 89.10 ml DW			$T = (37.10 \pm 0.05)°C$ $I = 0.1$ mol l^{-1} $[ester]_{total} = 10^{-3}$ mol l^{-1}	
Vol. 0.1000 mol l^{-1} NaOH (ml)	Titration 1		Titration 2	
	pH	pK_a^T	pH	pK_a^T
0.000	6.212	-	6.207	-
0.050	7.702	(8.880)†	7.695	(8.874)†
0.100	8.101	8.959	8.098	8.956
0.150	8.304	8.964	8.299	8.959
0.200	8.454	8.965	8.448	8.959
0.250	8.574	8.966	8.570	8.958
0.300	8.676	8.960	8.674	8.958
0.350	8.774	(8.956)†	8.764*	(8.953)†
Average pK_a^T =		8.963 ± 0.004		8.958 ± 0.002

Overall average $pK_a^T = 8.96 \pm 0.01$

† Values in parentheses were excluded from the average.

* Hydrolysis noticeable.

A1.4(c) Group 3, Rapidly Hydrolysing monoamino Acid Esters

Section A1.4(c) contain pK_a^T summary tables for Group 3, rapidly hydrolysing amino acid esters, at 37.1 °C and I = 0.1 mol l^{-1}.

Table A1.22 Determination of pK_a^T for 5 5-APe Et.HCl (2 x recryst.)

Test solution contained: 10^{-4} moles EH^+Cl^- 9.90 ml 1.0 mol l^{-1} KCl 89.10 ml DW			T = (37.10 ± 0.05)°C I = 0.1 mol l^{-1} $[ester]_{total} = 10^{-3}$ mol l^{-1}		
Vol. 0.1000 mol l^{-1} NaOH	Overall "Titration 1" pH	Overall "Titration 2" pH	Overall "Titration 3" pH	Averaged pH	pK_a^T
0.100	8.774	8.753	8.795	8.774 ± 0.021	(9.710)
0.110	8.830	8.842	8.854	8.842 ± 0.012	9.740
0.120	8.896	8.880	8.889	8.888 ± 0.009	9.747
0.130	8.920	8.898	8.909	8.909 ± 0.011	9.725
0.140	8.963	8.949	8.956	8.956 ± 0.007	9.740
0.150	8.981	8.971	8.991	8.981 ± 0.010	9.730
0.160	9.014	9.008	9.026	9.016 ± 0.009	9.735
0.170	9.056	9.038	9.070	9.054 ± 0.016	9.746
0.180	9.076	9.063	9.089	9.076 ± 0.012	9.738
				Averaged pK_a^T = 9.738 ± 0.013	

Overall average pK_a^T = 9.74 ± 0.02

† Values in parentheses were excluded from the average.

*Alkaline hydrolysis occurred beyond 0.190 ml.

Table A1.23 Determination of pK_a^T for 5-APe Me.HCl (2 x recryst.)

Test solution contained:					T = (37.10 ± 0.05)°C	
10^{-4} moles EH^+Cl^-					I = 0.1 mol l^{-1}	
9.90 ml 1.0 mol l^{-1} KCl					$[ester]_{total}$ = 10^{-3} mol l^{-1}	
89.10 ml DW						
Vol 0.1000 mol l^{-1} NaOH	Overall "Titration 1"		Overall "Titration 2"		Overall "Titration 3"	
	pH	pK_a^T	pH	pK_a^T	pH	pK_a^T
0.000	6.35	-	6.53	-	6.58	-
0.040	8.368	9.723	8.360	9.713	8.360	9.713
0.050	8.460	9.713	8.458	9.711	8.460	9.713
0.060	8.532	9.701	8.530	9.698	8.533	9.702
0.070	8.634*	(9.688)†	8.624*	(9.675)†	8.598	9.696
Averaged pK_a^T Values =		9.712 ± 0.011		9.707 ± 0.009		9.706 ± 0.010

Overall average pK_a^T = 9.71 ± 0.02

† Values in parentheses were excluded from the average.

* Hydrolysis noticeable.

A1.5 Summary Tables for Monoamino Acid Ester Hydrochlorides at 50.2°C

A1.5(a) Group 1, Slowly Hydrolsing Monoamino Acid Esters

Section A1.5(a) contain pK_a^T summary tables for Group 1, slowly hydrolysing amino acid esters, at 50.2°C and I = 0.1 mol l^{-1}. Due allowance was made for water expansion

Table A1.24 Determination of pK_a^T pK_a^T for Ser Me.HCl (2 x recryst.)

Test solution contained: 10^{-4} moles EH^+Cl^- 9.90 ml 1.0 mol l^{-1} KCl 88.70 ml DW			$T = (50.20 \pm 0.10)°C$ $I = 0.1$ mol l^{-1} $[ester]_{total} = 10^{-3}$ mol l^{-1}	
Vol. 0.1000 mol l^{-1} NaOH (ml)	Titration 1		Titration 2	
	pH	pK_a^T	pH	pK_a^T
0.000	4.810	-	4.801	-
0.100	5.615	(6.436)†	5.595	(6.415)†
0.150	5.799	(6.427)†	5.790	(6.418)†
0.200	5.945	6.425	5.932	6.412
0.250	6.065	6.422	6.055	6.412
0.300	6.177	6.425	6.165	6.413
0.350	6.271	6.421	6.260	6.410
0.400	6.364	6.421	6.352	6.409
0.450	6.451	6.420	6.440	6.409
0.500	6.539	6.421	6.525	6.407
0.550	6.625	6.420	6.612*	(6.407)†
0.600	6.625*	(6.416)†	6.701*	(6.407)†
0.650	6.625*	(6.413)	6.789*	(6.403)†
Average pK_a^T =		6.422± 0.002		6.410 ± 0.003

Overall average pK_a^T = 6.42 ± 0.01

†Values in parentheses were excluded from the average.

* Hydrolysis noticeable.

Table A1.25 Determination of for 2-AE Me.HCl (2 x recryst.)

Test solution contained: 10^{-4} moles EH^+Cl^- 9.90 ml 1.0 mol l^{-1} KCl 88.70 ml DW			$T = (50.20 \pm 0.10)°C$ $I = 0.1$ mol l^{-1} $[ester]_{total} = 10^{-3}$ mol l^{-1}	
Vol. 0.1000 mol l^{-1} NaOH (ml)	Titration 1		Titration 2	
	pH	pK_a^T	pH	pK_a^T
0.000	5.082	-	5.079	-
0.100	6.187	7.019	6.180	(7.012)†
0.150	6.388	7.022	6.378	(7.012)†
0.200	6.535	7.019	6.532	7.016
0.250	6.662	7.021	6.661	7.020
0.300	6.770	7.020	6.769	7.019
0.350	6.867	7.019	6.769	7.020
0.400	6.960	7.019	6.868	7.020
0.450	7.046*	(7.016)†	6.961	7.018
0.500	7.130*	(7.014)†	7.048	7.019
0.550	7.210*	(7.007)†	7.135*	(7.010)†
0.600	7.297*	(7.006)†	7.213*	(7.011)†
Average pK_a^T =		7.020 ± 0.002		7.019 ± 0.003

Overall average $pK_a^T = 7.02 \pm 0.01$

† Values in parentheses were excluded from the average.

* Hydrolysis noticeable.

Table A1.26 Determination of pK_a^T for 3-AP Bz.HCl (2 x recryst.)

Test solution contained:	$T = (50.20 \pm 0.10)°C$
10^{-4} moles EH^+Cl^-	$I = 0.1$ mol l^{-1}
9.90 ml 1.0 mol l^{-1} KCl	$[ester]_{total} = 10^{-3}$ mol l^{-1}
88.70 ml DW	

Vol. 0.1000 mol l^{-1} NaOH (ml)	Titration 1		Titration 2	
	pH	pK_a^T	pH	pK_a^T
0.000	5.598	-	5.440	-
0.100	7.672	(8.305)†	7.468	(8.314)†
0.150	7.829	(8.319)†	7.692	8.339
0.200	7.829	8.326	7.845	8.343
0.250	7.952	8.326	7.968	8.343
0.300	8.058	8.325	8.072	8.340
0.350	8.158	8.329	8.166	8.337
0.400	8.249	8.330	8.253	8.335
0.450	8.335	8.332	8.330*	(8.326)†
0.500	8.417	8.332	8.402	(8.316)†
0.550	8.494	8.328	8.474*	(8.307)†
0.600	8.494*	(8.325)†	8.542*	(8.293)†
Average pK_a^T =		8.329 ± 0.003		8.340 ± 0.005

Overall average pK_a^T = 8.34 ± 0.01

† Values in parentheses were excluded from the average.

* Hydrolysis noticeable.

Table A1.27 Determination of for 4-DMAB MeHCl (2 x recryst.)

Test solution contained: 10^{-4} moles EH^+Cl^- 9.90 ml 1.0 mol l^{-1} KCl 88.70 ml DW		T = (50.20 ± 0.10)°C I = 0.1 mol l^{-1} $[ester]_{total} = 10^{-3}$ mol l^{-1}		
Vol. 0.1000 mol l^{-1} NaOH (ml)	Titration 1[§]		Titration 2[§§]	
	pH	pK_a^T	pH	pK_a^T
0.000	6.417	-	6.473	-
0.250	7.678	(8.824)[†]	7.718	(8.867)[†]
0.300	8.000	(8.846)[†]	8.021	8.869
0.350	8.198	8.855	8.216	8.875
0.400	8.347	8.861	8.362	8.875
0.450	8.468	8.865	8.474	8.878
0.500	8.572	8.868	8.576	8.872
0.550	8.661	8.866	8.661	8.873
0.600	8.743	8.865	8.749	8.870
0.650	8.819	8.863	8.818[*]	(8.867)[†]
0.700	8.890	8.861	8.882[*]	(8.862)[†]
0.750	8.955[*]	(8.854)[†]	8.951[*]	(8.851)[†]
0.800	9.020[*]	(8.851)[†]	9.013[*]	(8.849)[†]
0.850	9.084[*]	(8.848)[†]	9.073[*]	(9.102)[†]
Average pK_a^T =	8.863 ± 0.005		8.873± 0.005	

Overall average pK_a^T = 8.87 ± 0.01

[§] Volume correction of – 0.175 ml used.

[§§] Volume correction of – 0.180 ml used.

[†] Values in parentheses were excluded from the average.

[*] Hydrolysis occurs.

Table A1.28 Determination of pK_a^T for for 4-DMAB Et.HCl (2 x recryst.)

Test solution contained:			T = (50.20 ± 0.10)°C	
10^{-4} moles EH^+Cl^-			I = 0.1 mol l^{-1}	
9.90 ml 1.0 mol l^{-1} KCl			$[ester]_{total} = 10^{-3}$ mol l^{-1}	
88.70 ml DW				
Vol. 0.1000 mol l^{-1} NaOH (ml)	Titration 1		Titration 2	
	pH	pK_a^T	pH	pK_a^T
0.000	5.565	-	5.535	-
0.100	7.857	(8.718)†	7.870	(8.764)†
0.150	8.080	(8.745)†	8.098	8.772
0.200	8.238	8.756	8.252	8.779
0.250	8.361	8.759	8.379	8.777
0.300	8.466	8.760	8.481	8.781
0.350	8.559	8.760	8.577	8.780
0.400	8.641	8.757	8.661	8.777
0.450	8.716	8.753	8.738	8.772
0.500	8.790	8.750	8.809*	(8.766)†
0.550	8.862*	(8.748)†	8.877*	(8.760)†
0.600	8.931*	(8.746)†	8.942*	(8.750)†
0.650	8.999*	(8.744)†	9.003*	(8.747)†
Average pK_a^T =		8.756 ± 0.006		8.777 ± 0.005

Overall average pK_a^T = 8.76 ± 0.01

† Values in parentheses were excluded from the average.

* Hydrolysis occurs.

A1.5(b) Group 2, Moderately Hydrolysing Amino Acid Esters

Section A1.5(b) contain pK_a^T summary tables for Group 2, moderately hydrolysing amino acid esters, at 50.2 °C and I = 0.1 mol l^{-1}.

Table A1.29 Determination of pK_a^T of pK_a^T for 4-AB Me.HCl (2 x recryst.)

Test solution contained: 10^{-4} moles EH^+Cl^- 9.90 ml 1.0 mol l^{-1} KCl 88.70 ml DW			$T = (50.20 \pm 0.10)°C$ $I = 0.1$ mol l^{-1} $[ester]_{total} = 10^{-3}$ mol l^{-1}	
Vol. 0.1000 mol l^{-1} NaOH (ml)	Titration 1[§]		Titration 2[§§]	
	pH	pK_a^T	pH	pK_a^T
0.100	7.902	(9.069)[†]	7.879	(9.043)[†]
0.150	8.223	9.094	8.211	9.080
0.200	8.411	9.094	8.402	9.083
0.250	8.550	9.092	8.547	9.088
0.300	8.664	9.090	8.660	9.086
0.350	8.750[*]	(9.076)[†]	8.750[*]	(9.075)[†]
0.400	8.830[*]	(9.067)[†]	8.830[*]	(9.066)[†]
0.450	8.900[*]	(9.055)[†]	8.894[*]	(9.047)[†]
Average pK_a^T =		9.093 ± 0.003		9.084 ± 0.004

Overall average pK_a^T = 9.09 ± 0.01

[§] Volume correction of – 0.045 ml used.

[§§] Volume correction of – 0.045 ml used.

[†] Values in parentheses were excluded from the average.

[*] Hydrolysis occurs.

Table A1.30 Determination of pK_a^T for 4-AB Et.HCl (3 x recryst.)

Test solution contained: 10^{-4} moles EH^+Cl^- 9.90 ml 1.0 mol l^{-1} KCl 88.70 ml DW			$T = (50.20 \pm 0.10)°C$ $I = 0.1$ mol l^{-1} $[ester]_{total} = 10^{-3}$ mol l^{-1}	
Vol. 0.1000 mol l^{-1} NaOH (ml)	Titration 1		Titration 2	
	pH	pK_a^T	pH	pK_a^T
0.000	5.179	-	5.362	-
0.100	8.178	(9.069)†	8.170	(9.060)†
0.150	8.398	9.096	8.391	(9.089)†
0.200	8.547	9.101	8.542	9.097
0.250	8.662	9.101	8.660	9.099
0.300	8.762	9.102	8.762	9.102
0.350	8.849	9.100	8.849	9.100
0.400	8.922*	(9.089)†	8.927	9.098
0.450	8.982*	(9.074)†	8.999	9.097
0.500	9.049*	(9.072)†	9.063*	(9.091)†
Average pK_a^T =		9.100 ± 0.004		9.099 ± 0.003

Overall average $pK_a^T = 9.10 \pm 0.01$

† Values in parentheses were excluded from the average.

* Hydrolysis noticeable.

Table A1.31 Determination of pK_a^T for 4-AB Bz.HCl (3 x recryst.)

Test solution contained: 10^{-4} moles EH^+Cl^- 9.90 ml 1.0 mol l^{-1} KCl 88.70 ml DW			$T = (50.20 \pm 0.10)°C$ $I = 0.1$ mol l^{-1} $[ester]_{total} = 10^{-3}$ mol l^{-1}	
Vol. 0.1000 mol l^{-1} NaOH (ml)	Titration 1[§]		Titration 2[§§]	
	pH	pK_a^T	pH	pK_a^T
0.040	4.790	-	4.785	-
0.100	7.899	(8.981)[†]	7.875	(8.995)[†]
0.150	8.218	(9.039)[†]	8.190	9.031
0.200	8.409	9.056	8.373	9.032
0.250	8.551	9.064	8.516	9.038
0.300	8.662	9.064	8.630	9.038
0.350	8.751	9.055	8.720[*]	(9.029)[†]
0.400	8.827[*]	(9.043)[†]	8.793[*]	(9.012)[†]
0.450	8.892[*]	(9.026)[†]	8.859[*]	(8.995)[†]
Average pK_a^T =		9.060 ± 0.005		9.035 ± 0.004

Overall average $pK_a^T = 9.05 \pm 0.02$

[§] Volume correction of – 0.035 ml used.

[§§] Volume correction of – 0.040 ml used.

[†] Values in parentheses were excluded from the average.

[*] Hydrolysis occurs.

Table A1.32 Determination of pK_a^T for 4-MAB Me.HCl (3 x recryst.)

Test solution contained: 10^{-4} moles EH^+Cl^- 9.90 ml 1.0 mol l^{-1} KCl 88.70 ml DW		$T = (50.20 \pm 0.10)°C$ $I = 0.1$ mol l^{-1} $[ester]_{total} = 10^{-3}$ mol l^{-1}		
Vol. 0.1000 mol l^{-1} NaOH (ml)	Titration 1[§]		Titration 2[§§]	
	pH	pK_a^T	pH	pK_a^T
0.000	6.212	-	6.276	-
0.100	8.149	(9.412)[†]	8.145	(9.407)[†]
0.120	8.335	9.456	8.331	9.451
0.140	8.448	9.454	8.445	9.450
0.160	8.544	9.458	8.543	9.457
0.180	8.620	9.455	8.617	9.451
0.200	8.689	9.457	8.685	9.452
0.220	8.742	9.448	8.740	9.445
0.240	8.786[*]	(9.434)[†]	8.789	(9.438)[†]
Average pK_a^T =		9.455 ± 0.007		9.451 ± 0.006

Overall average $pK_a^T = 9.45 \pm 0.01$

[§] Volume correction of – 0.050 ml used.

[§§] Volume correction of – 0.050 ml used.

[†] Values in parentheses were excluded from the average.

[*] Hydrolysis occurs.

Table A1.33 Determination of the pK_a^T for 4-MAB Et.HCl (2 x recryst.)

Test solution contained:	$T = (50.20 \pm 0.10)°C$
10^{-4} moles EH^+Cl^-	$I = 0.1$ mol l^{-1}
9.90 ml 1.0 mol l^{-1} KCl	$[ester]_{total} = 10^{-3}$ mol l^{-1}
88.70 ml DW	

Vol. 0.1000 mol l^{-1} NaOH (ml)	Titration 1		Titration 2	
	pH	pK_a^T	pH	pK_a^T
0.000	5.078	-	4.958	-
0.100	8.327	(9.242)†	8.311	(9.223)†
0.150	8.572	9.306	8.569	9.300
0.200	8.722	9.315	8.715	9.308
0.250	8.837	9.315	8.830	9.310
0.300	8.839	9.307	8.920	9.301
0.350	8.924*	(9.295)†	8.992*	(9.285)†
0.400	8.999*	(9.277)†	9.053	(9.264)†
Average pK_a^T =		9.311 ± 0.005		9.305 ± 0.005

Overall average $pK_a^T = 9.30 \pm 0.01$

*† Values in parentheses were excluded from the average.

* Hydrolysis noticeable.

Table A1.34 Determination of the pK_a^T for 4-A-3-MB Me.HCl (2 x recryst.)

Test solution contained: 10^{-4} moles EH^+Cl^- 9.90 ml 1.0 mol l^{-1} KCl 88.70 ml DW			$T = (50.20 \pm 0.10)°C$ $I = 0.1$ mol l^{-1} $[ester]_{total} = 10^{-3}$ mol l^{-1}	
Vol. 0.1000 mol l^{-1} NaOH (ml)	Titration 1		Titration 2	
	pH	pK_a^T	pH	pK_a^T
0.000	5.512	-	5.581	-
0.100	7.860	(8.722)†	7.832	(8.692)†
0.150	8.071	8.736	8.059	(8.723)†
0.200	8.222	8.739	8.220	8.737
0.250	8.336	8.732	8.340	8.736
0.300	8.433*	(8.724)†	8.441	8.733
0.350	8.525*	(8.723)†	8.528	8.726
0.400	8.592*	(8.702)†	8.605*	(8.716)†
Average pK_a^T =		8.736 ± 0.004		8.733 ± 0.007

Overall average $pK_a^T = 8.73 \pm 0.01$

† Values in parentheses were excluded from the average.

* Hydrolysis noticeable.

Table A1.35 Determination of the pK_a^T pK_a^T for 4-A-3,3-DMB Me.HCl (2 x recryst.)

Test solution contained: 10^{-4} moles EH^+Cl^- 9.90 ml 1.0 mol l^{-1} KCl 88.70 ml DW			$T = (50.20 \pm 0.10)°C$ $I = 0.1$ mol l^{-1} $[ester]_{total} = 10^{-3}$ mol l^{-1}	
Vol. 0.1000 mol l^{-1} NaOH (ml)	Titration 1		Titration 2	
	pH	pK_a^T	pH	pK_a^T
0.000	5.405	-	5.428	-
0.050	7.806	(8.664)†	7.799	(8.657)†
0.100	8.018	8.679	8.012	8.673
0.150	8.169	8.682	8.163	8.676
0.200	8.290	8.682	8.283	8.675
0.250	8.390	8.677	8.385	8.672
0.300	8.464*	(8.655)†	8.457*	(8.648)†
0.350	8.545	(8.649)†	8.534*	(8.637)†
Average pK_a^T =		8.680 ± 0.003		8.674 ± 0.002

Overall average pK_a^T = 8.68 ± 0.01

† Values in parentheses were excluded from the average.

* Hydrolysis noticeable.

A1.5(c) Group 3 Rapidly Hydrolysing Monoamino Acid Esters

Section A1.4(c) contain pK_a^T summary tables for Group 3, rapidly hydrolysing monoamino acid esters, at 50.2 °C and I = 0.1 mol l^{-1}.

Table A1.36 Determination of the pK_a^T for 5 5-APe Et.HCl (2 x recryst.)

Test solution contained: 10^{-4} moles EH^+Cl^- 9.90 ml 1.0 mol l^{-1} KCl 88.70 ml DW			T = (50.20 ± 0.10)°C I = 0.1 mol l^{-1} $[ester]_{total} = 10^{-3}$ mol l^{-1}	
Vol. 0.1000 mol l^{-1} NaOH (ml)	Titration 1[§]		Titration 2[§§]	
	pH	pK_a^T	pH	pK_a^T
0.000	4.900	-	4.904	-
0.050	7.836	(9.344)[†]	7.829	(9.355)[†]
0.060	7.988	(9.364)[†]	8.000	9.393
0.070	8.102	9.376	8.114	9.403
0.080	8.187	9.376	8.203	9.406
0.090	8.254	9.369	8.279	9.409
0.100	8.314	9.366	8.338	9.404
Average pK_a^T =		9.372 ± 0.0.004		9.403 ± 0.010

Overall average pK_a^T = 9.39 ± 0.02

[§] Volume correction of – 0.022 ml used.

[§§] Volume correction of – 0.023 ml used.

[†] Values in parentheses were excluded from the average.

[*] Hydrolysis occurs.

Table A1.37 Determination of pK_a^T for 5-APe Me.HCl (2 x recryst.)

Test solution contained: 10^{-4} moles EH^+Cl^- 9.90 ml 1.0 mol l^{-1} KCl 88.70 ml DW			T = (50.20 ± 0.10)°C I = 0.1 mol l^{-1} $[ester]_{total} = 10^{-3}$ mol l^{-1}			
Vol 0.1000 mol l^{-1} NaOH	Overall "Titration 1"		Overall "Titration 2"		Overall "Titration 3"	
	pH	pK_a^T	pH	pK_a^T	pH	pK_a^T
0.000	6.198	-	5.852	-	6.268	-
0.030	7.786	(9.247)†	7.792	(9.254)†	7.848	9.321
0.035	7.883	9.281	7.883	9.281	7.915	9.319
0.040	7.934	9.271	7.931	9.267	7.966	9.309
0.045	7.995	9.281	7.991	9.276	8.020	9.311
Averaged pK_a^T Values =		9.277 ± 0.006		9.275 ± 0.008		9.315 ± 0.006

Overall average pK_a^T = 9.30 ± 0.02

† Values in parentheses were excluded from the average.

* Hydrolysis occured beyond 0.050 ml.

Appendix 2

pK_a^T Values of Monoamino Acids

A2.1Calculation of pK_a^T Values of Monoamino Acids

A2.1(a) Introduction

The theory used for the calculation of pK_a^T for AH is outlined below. The reaction mixture and conditions are given in Section 4.3.

A2.1(b) Zwitterions

Monoamino acid ester hydrochlorides, AH, behave as monobasic acids in aqueous solution:

$$AH \rightleftharpoons A^- + H^+$$

By definition the thermodynamic dissociation constant

$$K_a^T = \frac{\{A^-\}\{H^+\}}{\{AH\}} = \frac{[A^-]\{H^+\}}{[AH]} \cdot \frac{y_1}{y_\circ} \qquad \ldots.(A2.1)$$

Where, $y_\circ$ = activity coefficient of neutral species.

y_1 = activity coefficient of singly charged species.

Electroneutrlity principle requires:

$$[Na^+] + [H^+] = [OH^-] + [A^-] \qquad \ldots.(A2.2)$$

The concentration of the "total acid"

$$[A_T] = [AH] + [A^-] \qquad \ldots.(A2.3)$$

As the titration proceeds, the value of $[A_T]$ decreases due to dilution by the added NaOH solution. At any point in the titration:

$$[A_T] = \frac{W \cdot 10^3}{M(X + V_\circ)} \qquad \ldots.(A2.4)$$

where,

X = Volume of base added.

$V_\circ$ = Initial total volume.

M = Molecular weight of acid.

W = Weight of acid used.

Rearranging (A2.3), and then combining with (A2.2):

$$[A^-] = [Na^+] + [H^+] - [OH^-]$$

$$[A^-] = \left(\frac{X}{X + V_\circ}\right) \cdot [base] + \frac{10^{-pH}}{y_1} - \frac{10^{-pK_a^W}}{y_1 \cdot 10^{-pH}} \qquad \ldots.(A2.5)$$

where [base] = concentration of NaOH titrant solution used.

Also from (A2.3) and A2.4);

$$[AH] = [A_T] - [A^-]$$

$$= \frac{W \cdot 10^3}{M(X + V_\circ)} - [A^-] \qquad \ldots.(A2.6)$$

Combining (A2.6) with (A2.5) gives:

$$[AH] = \frac{W \cdot 10^3}{M(X + V_\circ)} + \frac{10^{-pK_a^W}}{y_1 \cdot 10^{-pH}} - \left(\frac{X}{X + V_\circ}\right) \cdot [base] - \frac{10^{-pH}}{y_1} \qquad \ldots.(A2.7)$$

By definition

$$pK_a^T = -\log_{10} K_a^T \qquad \ldots.(A2.8)$$

Combining (A2.8) with (A2.1):

$$pK_a^T = -\log_{10}\left(\frac{[A^-]\{H^+\} \cdot y_1}{[AH] \cdot y_\circ}\right)$$

Substituting (A2.6) (assuming $y_o = 1$)

$$pK_a^T = -\log_{10}\left(\frac{\frac{W \cdot 10^3}{M(X+V_o)} - [AH]}{[AH]}\right) + pH - \log_{10} y_1 \qquad \ldots.(A2.9)$$

A2.1(c) Monoamino Acid Hydrochlorides

The pK_a^T for $AH_2^+Cl^-$ is outlined below. The reaction mixture and conditions are given in Section 4.3. These compounds behave as dibasic acids in aqueous solution: The dissociation of the carboxylate group is defined by;

$$AH_2^+ \rightleftharpoons AH + H^+$$

The dissociation of the amino group is defined by;

$$AH \rightleftharpoons A^- + H^+$$

This gives the thermodynamic dissociation constant shown in A2.1:

$$K_a^T = \frac{\{A^-\}\{H^+\}}{\{AH\}} = \frac{[A^-]\{H^+\}}{[AH]} \cdot \frac{y_1}{y_o} \qquad \ldots.(A2.1)$$

Hence equation A2.1 can be used to calculate the pK_a^T of $AH_2^+Cl^-$. The reaction mixture and conditions are given in Section 4.3.

A2.1(d) Monoamino Dicarboxylic Acids

The dissociation of the γ-carboxylate group is defined by;

$$AH_2 \rightleftharpoons AH^- + H^+$$

The dissociation of the amino group is defined by;

$$AH^- \rightleftharpoons A^{2-} + H^+$$

By definition the thermodynamic dissociation constant

$$K_a^T = \frac{\{A^{2-}\}\{H^+\}}{\{AH^-\}} = \frac{[A^{2-}]\{H^+\}}{[AH^-]} \cdot \frac{y_2}{y_1} \qquad \text{....(A2.10)}$$

where, y_1 = activity coefficient of singly species.

y_2 = activity coefficient of doubly charged species.

Electroneutrlity principle requires:

$$[Na^+] + [H^+] = [OH^-] + [AH^-] + 2[A^{2-}] \qquad \text{....(A2.11)}$$

The concentration of the "total acid", assuming $[AH_2]$ to be negligible

$$[A_T] = [AH^-] + [A^{2-}] \qquad \text{....(A2.12)}$$

As the titration proceeds, the value of $[A_T]$ decreases due to dilution by the added NaOH solution. At any point in the titration is given by (A2.4)

Rearranging (A2.11) generates,

$$2[A^{2-}] = [Na^+] + [H^+] - [OH^-] - [AH^-] \qquad \text{....(A2.13)}$$

Rearranging (A2.12) and combining (A2.13)

$$[A^{2-}] = \left(\frac{X}{X + V_\circ}\right) \cdot [\text{base}] + \frac{10^{-pH}}{y_1} - \frac{10^{-pK_a^W}}{y_1 \cdot 10^{-pH}} - [A_T] \qquad \text{....(A2.14)}$$

where [base] = concentration of NaOH titrant solution used.

Also from (A2.12) and (A2.4);

$$[AH^-] = [A_T] - [A^{2-}]$$

$$= \frac{W \cdot 10^3}{M(X + V_\circ)} - [A^{2-}] \qquad \text{....(A2.15)}$$

Combining (A2.15) with (A2.14) gives:

$$[AH^-] = 2\cdot\left(\frac{W\cdot 10^3}{M(X + V_\circ)}\right) + \frac{10^{-pK_a^W}}{y_1\cdot 10^{-pH}} - \left(\frac{X}{X + V_\circ}\right)\cdot[\text{base}] - \frac{10^{-pH}}{y_1} \quad \ldots.(A2.16)$$

By definition

$$pK_a^T = -\log_{10}K_a^T \quad \ldots.(A2.8)$$

Combining (A2.8) with (A2.10):

$$pK_a^T = -\log_{10}\left(\frac{[A^{2-}]\{H^+\}\cdot y_2}{[AH^-]\cdot y_1}\right)$$

Substituting (A2.6) (assuming $y_\circ = 1$)

$$pK_a^T = -\log_{10}\left(\frac{\frac{W\cdot 10^3}{M(X+V_\circ)} - [AH^-]}{[AH^-]}\right) + pH - \log_{10}y_2 + \log_{10}y_1 \quad \ldots.(A2.17)$$

	A	B	C	D	E	F	G	H	I
1	PKAACIDS1								
2									
3									
4									
5		Variable	Value						
6		Intial Vol.	99.5						
7		y_I	0.7715						
8		pKaW	13.9965						
9		NaOH Conc	0.1						
10		Moles Acid	0.0001	=1000*C10					
11									
12	Vol NaOH	pH	$[H^+]$	$[OH^-]$	$[Na^+]$	$[A^-]$	$[A_T]$	[AH]	pKaT
13		5.682	=10^-B13/C7	=(10^(B13-C8))/C7	=C9*A13/(A13+C6)	=E13+C13-D13	=D10/(A13+C6)	=G13-F13	=B13 + -LOG(F13/H13)- LOG(C7)
14			=10^-B14/C7	=(10^(B14-C8))/C7	=C9*A14/(A14+C6)	=E14+C14-D14	=D10/(A14+C6)	=G14-F14	=B14 + -LOG(F14/H14)- LOG(C7)
15			=10^-B15/C7	=(10^(B15-C8))/C7	=C9*A15/(A15+C6)	=E15+C15-D15	=D10/(A15+C6)	=G15-F15	=B15 + -LOG(F15/H15)- LOG(C7)
16			=10^-B16/C7	=(10^(B16-C8))/C7	=C9*A16/(A16+C6)	=E16+C16-D16	=D10/(A16+C6)	=G16-F16	=B16 + -LOG(F16/H16)- LOG(C7)
17			=10^-B17/C7	=(10^(B17-C8))/C7	=C9*A17/(A17+C6)	=E17+C17-D17	=D10/(A17+C6)	=G17-F17	=B17 + -LOG(F17/H17)- LOG(C7)
18			=10^-B18/C7	=(10^(B18-C8))/C7	=C9*A18/(A18+C6)	=E18+C18-D18	=D10/(A18+C6)	=G18-F18	=B18 + -LOG(F18/H18)- LOG(C7)
19			=10^-B19/C7	=(10^(B19-C8))/C7	=C9*A19/(A19+C6)	=E19+C19-D19	=D10/(A19+C6)	=G19-F19	=B19 + -LOG(F19/H19)- LOG(C7)
20			=10^-B20/C7	=(10^(B20-C8))/C7	=C9*A20/(A20+C6)	=E20+C20-D20	=D10/(A20+C6)	=G20-F20	=B20 + -LOG(F20/H20)- LOG(C7)
21			=10^-B21/C7	=(10^(B21-C8))/C7	=C9*A21/(A21+C6)	=E21+C21-D21	=D10/(A21+C6)	=G21-F21	=B21 + -LOG(F21/H21)- LOG(C7)
22			=10^-B22/C7	=(10^(B22-C8))/C7	=C9*A22/(A22+C6)	=E22+C22-D22	=D10/(A22+C6)	=G22-F22	=B22 + -LOG(F22/H22)- LOG(C7)
23			=10^-B23/C7	=(10^(B23-C8))/C7	=C9*A23/(A23+C6)	=E23+C23-D23	=D10/(A23+C6)	=G23-F23	=B23 + -LOG(F23/H23)- LOG(C7)
24			=10^-B24/C7	=(10^(B24-C8))/C7	=C9*A24/(A24+C6)	=E24+C24-D24	=D10/(A24+C6)	=G24-F24	=B24 + -LOG(F24/H24)- LOG(C7)
25			=10^-B25/C7	=(10^(B25-C8))/C7	=C9*A25/(A25+C6)	=E25+C25-D25	=D10/(A25+C6)	=G25-F25	=B25 + -LOG(F25/H25)- LOG(C7)
26			=10^-B26/C7	=(10^(B26-C8))/C7	=C9*A26/(A26+C6)	=E26+C26-D26	=D10/(A26+C6)	=G26-F26	=B26 + -LOG(F26/H26)- LOG(C7)

A2.2(b) PKAACIDS2

	A	B	C	D	E	F	G	H	I
1	PKAACIDS2								
2									
3									
4									
5		Variable	Value						
6		Intial Vol.	98.5						
7		y_1	0.7715						
8		y_2	0.3545						
9		pKaW	13.9965						
10		NaOH Conc	0.1						
11		Moles Acid	0.0001	=1000*C11					
12									
13	Vol NaOH	pH	$[H^+]$	$[OH^-]$	$[Na^+]$	$[A^{2-}]$	$[A_T]$	[AH]	pKaT
14	1	6.953	=10^-B14/C7	=(10^(B14-C9))/C7	=C10*A14/(A14+C6)	=E14+C14-D14-G14	=D11/(A14+C6)	=G14-F14	=B14 + -LOG(F14/H14)+ LOG(C7)-I
15	1.1	8.678	=10^-B15/C7	=(10^(B15-C9))/C7	=C10*A15/(A15+C6)	=E15+C15-D15-G15	=D11/(A15+C6)	=G15-F15	=B15 + -LOG(F15/H15)+ LOG(C7)-I
16	1.2	9.036	=10^-B16/C7	=(10^(B16-C9))/C7	=C10*A16/(A16+C6)	=E16+C16-D16-G16	=D11/(A16+C6)	=G16-F16	=B16 + -LOG(F16/H16)+ LOG(C7)-I
17	1.3	9.266	=10^-B17/C7	=(10^(B17-C9))/C7	=C10*A17/(A17+C6)	=E17+C17-D17-G17	=D11/(A17+C6)	=G17-F17	=B17 + -LOG(F17/H17)+ LOG(C7)-I
18	1.4	9.441	=10^-B18/C7	=(10^(B18-C9))/C7	=C10*A18/(A18+C6)	=E18+C18-D18-G18	=D11/(A18+C6)	=G18-F18	=B18 + -LOG(F18/H18)+ LOG(C7)-I
19	1.5	9.595	=10^-B19/C7	=(10^(B19-C9))/C7	=C10*A19/(A19+C6)	=E19+C19-D19-G19	=D11/(A19+C6)	=G19-F19	=B19 + -LOG(F19/H19)+ LOG(C7)-I
20	1.6	9.73	=10^-B20/C7	=(10^(B20-C9))/C7	=C10*A20/(A20+C6)	=E20+C20-D20-G20	=D11/(A20+C6)	=G20-F20	=B20 + -LOG(F20/H20)+ LOG(C7)-I
21	1.7	9.858	=10^-B21/C7	=(10^(B21-C9))/C7	=C10*A21/(A21+C6)	=E21+C21-D21-G21	=D11/(A21+C6)	=G21-F21	=B21 + -LOG(F21/H21)+ LOG(C7)-I
22	1.8	9.981	=10^-B22/C7	=(10^(B22-C9))/C7	=C10*A22/(A22+C6)	=E22+C22-D22-G22	=D11/(A22+C6)	=G22-F22	=B22 + -LOG(F22/H22)+ LOG(C7)-I
23			=10^-B23/C7	=(10^(B23-C9))/C7	=C10*A23/(A23+C6)	=E23+C23-D23-G23	=D11/(A23+C6)	=G23-F23	=B23 + -LOG(F23/H23)+ LOG(C7)-I
24			=10^-B24/C7	=(10^(B24-C9))/C7	=C10*A24/(A24+C6)	=E24+C24-D24-G24	=D11/(A24+C6)	=G24-F24	=B24 + -LOG(F24/H24)+ LOG(C7)-I
25			=10^-B25/C7	=(10^(B25-C9))/C7	=C10*A25/(A25+C6)	=E25+C25-D25-G25	=D11/(A25+C6)	=G25-F25	=B25 + -LOG(F25/H25)+ LOG(C7)-I
26			=10^-B26/C7	=(10^(B26-C9))/C7	=C10*A26/(A26+C6)	=E26+C26-D26-G26	=D11/(A26+C6)	=G26-F26	=B26 + -LOG(F26/H26)+ LOG(C7)-I
27			=10^-B27/C7	=(10^(B27-C9))/C7	=C10*A27/(A27+C6)	=E27+C27-D27-G27	=D11/(A27+C6)	=G27-F27	=B27 + -LOG(F27/H27)+ LOG(C7)-I

A2.3 Summary Tables for Monoamino Acids at 25.0 °C

Section A2.3 contain pK_a^T summary tables for amino acids studied in their zwitterion (AH), or monoamino acid hydrochloride ($AH_2^+Cl^-$) and monoamino dicarboxylic acid (AH_2) form, at 25.0°C and I = 0.1 mol l^{-1}.

Table A2.1 Determination of pK_a^T for 2-AE (1 x recryst.).

Test solution contained: 10^{-4} moles AH 9.95 ml 1.0 mol l^{-1} KCl 89.55 ml DW			T = (25.00 ± 0.05)°C I = 0.1 mol l^{-1} $[acid]_{total} = 10^{-3}$ mol l^{-1}	
Vol. 0.1000 mol l^{-1} NaOH (ml)	Titration 1		Titration 2	
	pH	pK_a^T	pH	pK_a^T
0.000	5.682	-	5.655	-
0.050	8.215	(9.626)†	8.200	(9.611)†
0.100	8.622	(9.716)†	8.609	(9.702)†
0.150	8.849	(9.747)†	8.842	(9.740)†
0.200	9.016	(9.768)†	9.013	(9.765)†
0.250	9.146	9.779	9.144	9.777
0.300	9.256	9.786	9.253	9.783
0.350	9.353	9.792	9.350	9.788
0.400	9.439	9.794	9.437	9.791
0.450	9.520	9.797	9.516	9.792
0.500	9.596	9.799	9.591	9.792
0.550	9.668	9.800	9.660	9.790
0.600	9.735	9.777	9.729	9.790
0.650	9.800	9.795	9.793	9.785
0.700	9.866	9.796	9.859	9.786
0.750	9.928	9.793	9.920	9.781
0.800	9.989	9.790	9.981	9.777
0.850	10.053	9.794	10.049	9.787
0.900	10.118	9.803	10.109	9.787
Average pK_a^T =		9.795 ± 0.009		9.786 ± 0.009*

Overall average pK_a^T = 9.79 ± 0.01

† Values in parentheses were excluded from the average.

Table A2.2 Determination of pK_a^T for 3-AP (2 x recryst.).

Test solution contained: 10^{-4} moles AH 9.95 ml 1.0 mol l^{-1} KCl 89.55 ml DW			$T = (25.00 \pm 0.05)°C$ $I = 0.1$ mol l^{-1} $[acid]_{total} = 10^{-3}$ mol l^{-1}	
Vol. 0.1000 mol l^{-1} NaOH (ml)	Titration 1		Titration 2	
	pH	pK_a^T	pH	pK_a^T
0.000	6.022	-	6.158	-
0.050	8.649	(10.097)†	8.687	(10.140)†
0.100	9.055	(10.198)†	9.071	(10.217)†
0.150	9.278	(10.235)†	9.284	(10.242)†
0.200	9.434	(10.252)†	9.440	(10.260)†
0.250	9.556	10.262	9.559	10.266
0.300	9.658	10.270	9.658	10.270
0.350	9.741	10.268	9.744	10.272
0.400	9.819	10.271	9.820	10.273
0.450	9.888	10.271	9.892	10.277
0.500	9.951	10.270	9.956	10.278
0.550	10.018	10.282	10.014	10.276
0.600	10.074	10.283	10.074	10.283
0.650	10.129	10.287	10.128	10.285
0.700	10.179	10.288	10.180	10.289
0.750	10.226	10.287	10.226	10.287
0.800	10.270	10.285	10.272	10.289
0.850	10.312	10.283	10.312	10.283
0.900	10.353	10.282	10.353	10.282
0.950	10.394	10.285	10.392	10.280
Average pK_a^T =		10.278± 0.016*		10.279 ± 0.013*

Overall average $pK_a^T = 10.28 \pm 0.01$.

† Values in parentheses were excluded from the average.

Table A2.3 Determination of pK_a^T for 4-AB (3 x recryst.) $[acid]_{total} = 1 \times 10^{-3}$ mol l^{-1}.

Test solution contained: 10^{-4} moles AH 9.95 ml 1.0 mol l^{-1} KCl 89.55 ml DW			$T = (25.00 \pm 0.05)°C$ $I = 0.1$ mol l^{-1} $[acid]_{total} = 10^{-3}$ mol l^{-1}	
Vol. 0.1000 mol l^{-1} NaOH (ml)	Titration 1		Titration 2	
	pH	pK_a^T	pH	pK_a^T
0.000	6.225	-	6.251	-
0.050	8.800	(10.273)†	8.809	(10.284)†
0.100	9.237	(10.425)†	9.252	(10.445)†
0.150	9.470	(10.484)†	9.480	(10.498)†
0.200	9.625	(10.508)†	9.632	(10.518)†
0.250	9.743	(10.520)†	9.752	(10.534)†
0.300	9.842	10.532	9.847	10.539
0.350	9.925	10.538	9.930	10.546
0.400	9.999	10.544	10.002	10.549
0.450	10.063	10.546	10.3068	10.554
0.500	10.132	10.566	10.135	10.572
0.550	10.197	10.590	10.189	10.574
0.600	10.245	10.589	10.240	10.579
0.650	10.290	10.588	10.286	10.580
0.700	10.332	10.587	10.331	10.585
0.750	10.372	10.587	10.372	10.587
0.800	10.414	10.596	10.411	10.589
0.850	10.452	10.602	10.449	10.594
0.900	10.489	10.609	10.485	10.599
40.950	10.521	10.609	10.520	10.606
Average pK_a^T =		10.577± 0.035*		10.575 ± 0.036*

Overall average $pK_a^T = 10.58 \pm 0.04$

† Values in parentheses were excluded from the average.

Table A2.4 Determination of pK_a^T for 4-AB (3 x recryst.) $[acid]_{total} = 5 \times 10^{-3}$ mol l^{-1}.

Test solution contained:			T = (25.00 ± 0.05)°C	
5×10^{-4} moles AH			I = 0.1 mol l^{-1}	
9.75 ml 1.0 mol l^{-1} KCl			$[acid]_{total} = 5 \times 10^{-3}$ mol l^{-1}	
87.75 ml DW				
Vol. 0.1000 mol l^{-1} NaOH (ml)	Titration 1		Titration 2	
	pH	pK_a^T	pH	pK_a^T
0.000	6.588	-	6.564	-
0.250	9.122	(10.545)	9.127	(10.551)
0.500	9.470	(10.574)	9.474	(10.579)
0.750	9.673	(10.582)	9.680	10.589
1.000	9.822	(10.585)	9.828	10.591
1.250	9.942	10.586	9.948	10.593
1.500	10.052	10.595	10.057	10.601
1.750	10.146	10.599	10.150	10.603
2.000	10.230	10.600	10.231	10.602
2.250	10.308	10.602	10.309	10.603
2.500	10.382	10.605	10.386	10.610
2.750	10.451	10.605	10.452	10.607
3.000	10.519	10.609	10.518	10.607
3.250	10.582	10.609	10.581	10.607
3.500	10.645	10.611	10.645	10.611
3.750	10.704	10.611	10.705	10.613
4.000	10.762	10.612	10.762	10.612
4.250	10.820	10.617	10.819	10.615
4.500	10.873	10.616	10.873	10.616
4.750	10.926	10.618	10.927	10.620
Average pK_a^T =		10.278± 0.01		10.279 ± 0.013*

Overall average $pK_a^T = 10.60 \pm 0.02$

† Values in parentheses were excluded from the average.

Table A2.5 Determination of pK_a^T for 6-AH (2 x recryst.), using $[acid]_{total} = 5 \times 10^{-3}$ mol l^{-1} and $[acid]_{total} = 10^{-2}$ mol l^{-1}.

Test solution contained:	Test solution contained:	T = (25.00 ± 0.05)°C
$[acid]_{total} = 5 \times 10^{-3}$ mol l^{-1}	$[acid]_{total} = 1 \times 10^{-2}$ mol l^{-1}	I = 0.1 mol l^{-1}
5×10^{-4} moles AH	10^{-3} moles AH	
9.75 ml 1.0 mol l^{-1} KCl	9.50 ml 1.0 mol l^{-1} KCl	
87.75 ml DW	85.50 ml DW	

Vol. 0.1000 mol l^{-1} NaOH (ml) $[Acid]_{total}$ (mol l^{-1})		Titration 1 $[acid]_{total} = 5 \times 10^{-3}$ mol l^{-1}		Titration 2 $[acid]_{total} = 1 \times 10^{-2}$ mol l^{-1}	
5×10^{-3}	1×10^{-2}	pH	pK_a^T	pH	pK_a^T
0.000§	0.000§§	6.716	-	6.987	-
0.250	0.500	9.401	(10.855)†	9.482	(10.907)†
0.500	1.000	9.759	(10.902)†	9.821	(10.928)†
0.750	1.500	9.964	(10.916)†	10.022	(10.933)†
1.000	2.000	10.119	(10.932)†	10.179	(10.945)†
1.250	2.500	10.239	10.940	10.300	10.948
1.500	3.000	10.337	10.941	10.402	10.949
1.750	3.500	10.422	10.942	10.492	10.949
2.000	4.000	10.501	10.946	10.576	10.952
2.250	4.500	10.572	10.948	10.652	10.953
2.500	5.000	10.638	10.951	10.724	10.954
2.750	5.500	10.698	10.952	10.790	10.953
3.000	6.000	10.753	10.951	10.853	10.951
3.250	6.500	10.808	10.954	10.916	10.953
3.500	7.000	10.858	10.954	10.976	10.954
3.750	7.500	10.906	10.954	11.036	10.959
4.000	8.000	10.950	10.952	11.094	(10.964)
4.250	8.500	10.998	(10.961)†	11.150	(10.970)†
4.500	9.000	11.004	(10.972)†	11.201	(10.971)†
Average pK_a^T =			10.949 ± 0.009		10.952 ± 0.007

Overall average $pK_a^T = 10.95 \pm 0.01$

† Values in parentheses were excluded from the average.

Table A2.6 Determination of pK_a^T for 5-APe.HCl (1 x recryst.).

Test solution contained:			$T = (25.00 \pm 0.05)°C$	
10^{-4} moles $AH_2^+Cl^-$			$I = 0.1$ mol l^{-1}	
9.85 ml 1.0 mol l^{-1} KCl			$[acid]_{total} = 10^{-3}$ mol l^{-1}	
88.65 ml DW				
Vol. 0.1000 mol l^{-1} NaOH (ml)	Titration 1[§]		Titration 2[§§]	
	pH	pK_a^T	pH	pK_a^T
0.000	3.758	-	3.754	-
0.100	3.875	-	3.872	-
0.200	4.002	-	4.000	-
0.300	4.136	-	4.138	-
0.400	4.274	-	4.278	-
0.500	4.420	-	4.427	-
0.600	4.581	-	4.590	-
0.700	4.766	-	4.782	-
0.800	5.003	-	5.035	-
0.900	5.389	-	5.466	-
0.920	5.513	-	5.622	-
0.940	5.671	-	5.822	-
0.960	5.882	-	6.154	-
0.980	6.243	-	6.915	-
0.990	6.495	-	7.650	-
1.000	6.901	-	8.302	-
1.010	7.652	-	8.618	-
1.020	8.258	-	8.820	-
1.040	8.800	-	9.080	-
1.060	9.062	-	9.243	-
1.080	9.232	-	9.366	-
1.100	9.358	(10.648)[†]	9.468	(10.692)[†]
1.200	9.733	(10.705)[†]	9.789	10.728
1.300	9.944	10.723	9.982	10.739
1.400	10.103	10.749	10.132	10.762
1.500	10.222	10.757	10.245	10.767
1.600	10.321	10.765	10.340	10.772
1.700	10.404	10.766	10.421	10.775
1.800	10.478	10.770	10.492	10.775
1.900	10.544	10.774	10.555	10.774
Average pK_a^T =		10.758± 0.035*		10.762 ± 0.034

Overall average $pK_a^T = 10.76 \pm 0.04$

[§] Volume correction of – 0.035 ml used. [§§] Volume correction of – 0.040 ml used.

[†] Values in parentheses were excluded from the average.

Figure A2.1 Titration Curve for pK_a^T for 5-APe.HCl (2 x recryst.), Titration 1.

$T = (25.00 \pm 0.05)°C$

$I = 0.1$ mol l^{-1}

$[acid]_{total} = 10^{-3}$ mol l^{-1}

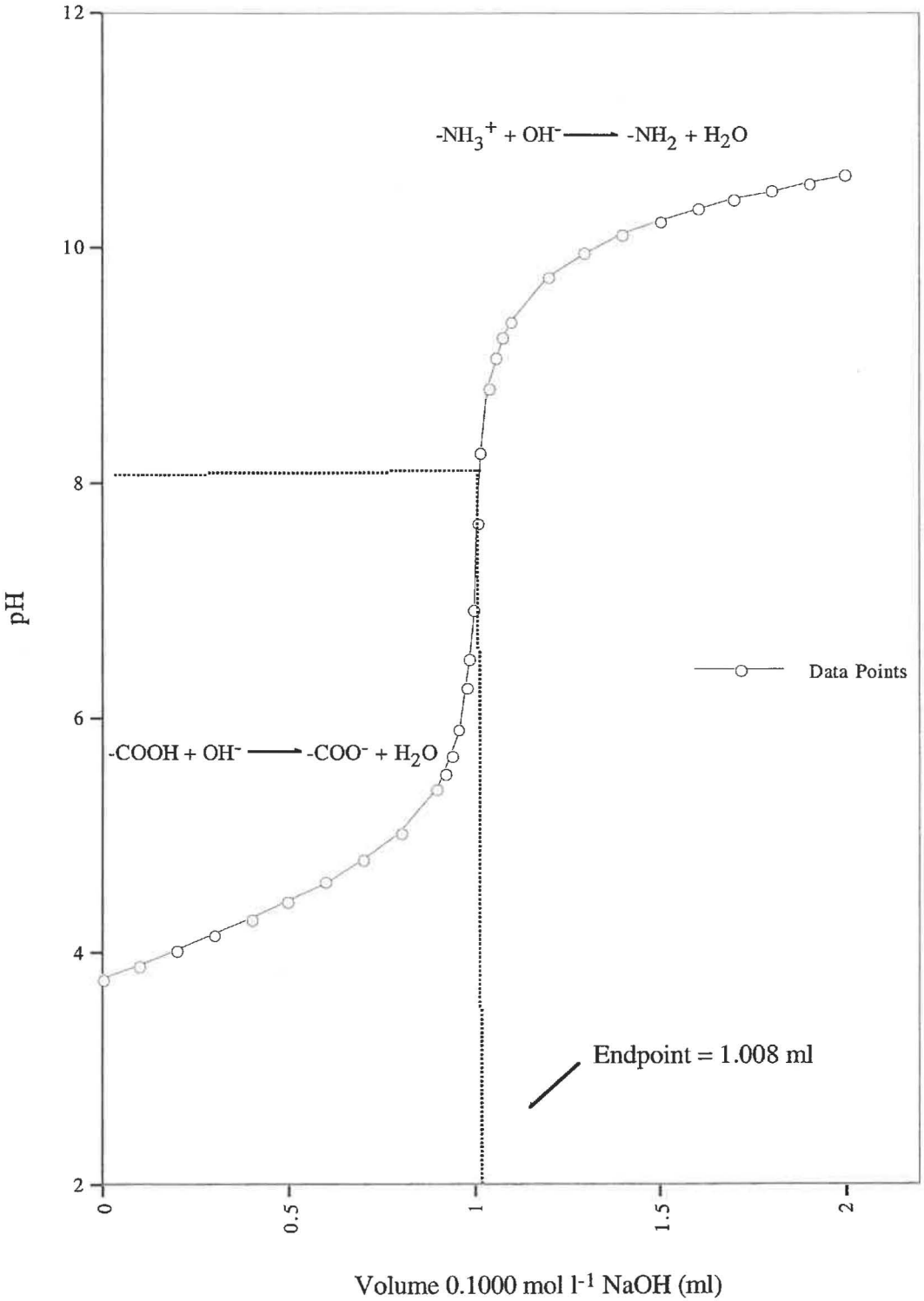

Table A2.7 Determination of pK_a^T for -A-3-MB HCl (2 x recry.).

Test solution contained: 10^{-4} moles $AH_2^+Cl^-/AH$ 9.93 ml 1.0 mol l^{-1} KCl 88.82 ml DW			$T = (25.00 \pm 0.05)°C$ $I = 0.1$ mol l^{-1} $[acid]_{total} = 10^{-3}$ mol l^{-1}	
Vol. 0.1000 mol l^{-1} NaOH (ml)	Titration 1[§]		Titration 2[§§]	
	pH	pK_a^T	pH	pK_a^T
0.000	3.701	-	3.693	-
0.100	3.816	-	3.812	-
0.200	3.952	-	3.949	-
0.300	4.107	-	4.109	-
0.400	4.260	-	4.295	-
0.500	4.490	-	4.535	-
0.600	4.833	-	4.905	-
0.650	5.103	-	5.262	-
0.670	5.268	-	5.485	-
0.690	5.493	-	5.870	-
0.710	5.853	-	6.480	-
0.720	6.110	-	6.770	-
0.730	6.461	-	7.080	-
0.740	6.925	-	7.380	-
0.750	7.365	-	7.640	-
0.760	7.640	-	7.840	-
0.770	7.850	-	7.990	-
0.780	7.991	-	8.118	-
0.790	8.115	-	8.220	-
0.810	8.298	-	8.378	-
0.830	8.439	-	8.495	-
0.850	8.548	(9.589)[†]	8.598	
0.900	8.754	(9.611)[†]	8.787	(9.512)[†]
1.000	9.034	9.633	9.060	9.623
1.100	9.242	9.648	9.268	9.638
1.200	9.413	9.654	9.439	9.649
1.300	9.568	9.660	9.591	9.653
1.400	9.703	9.650	9.730	9.649
1.500	9.830	(9.593)[†]	9.854	(9.626)[†]
Average pK_a^T =		9.649 ± 0.01		9.642 ± 0.019

Overall average $pK_a^T = 9.65 \pm 0.02$

[§] Volume correction of + 0.010 ml used.

[§§] Volume correction of + 0.020 ml used.

[†] Values in parentheses were excluded from the average.

Figure A2.1 Titration Curve for pK_a^T for 4-A-3-MB (2 x recryst.), Titration 1.

$T = (25.00 \pm 0.05)°C$

$I = 0.1$ mol l^{-1}

$[acid]_{total} = 10^{-3}$ mol l^{-1}

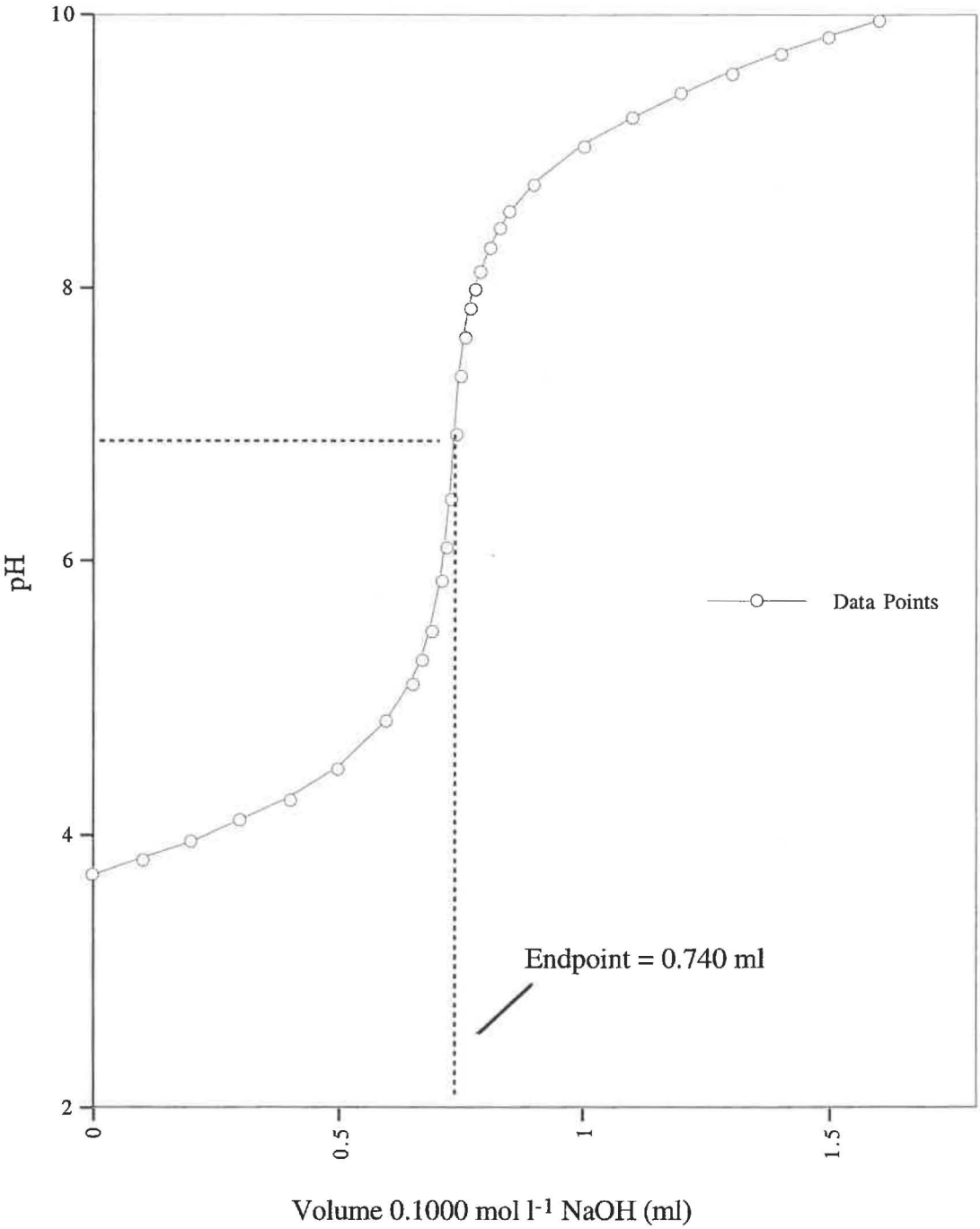

Table A2.8 Determination of pK_a^T for 4-A-3, 3-DMB HCl (2 x recry.).

Test solution contained:			T = (25.00 ± 0.05)°C	
10^{-4} moles $AH_2^+Cl^-$			I = 0.1 mol l^{-1}	
9.85 ml 1.0 mol l^{-1} KCl			$[acid]_{total} = 10^{-3}$ mol l^{-1}	
88.65 ml DW				
Vol. 0.1000 mol l^{-1} NaOH (ml)	Titration 1§		Titration 2§§	
	pH	pK_a^T	pH	pK_a^T
0.000	3.595	-	3.598	-
0.100	3.680	-	3.680	-
0.300	3.872	-	3.872	-
0.500	4.111	-	4.110	-
0.600	4.258	-	4.252	-
0.700	4.432	-	4.425	-
0.800	4.670	-	4.659	-
0.900	5.081	-	5.047	-
0.950	5.544	-	5.475	-
0.960	5.710	-	5.623	-
0.970	5.950	-	5.840	-
0.980	6.282	-	6.142	-
0.990	6.855	-	6.780	-
1.000	7.692	-	7.682	-
1.010	8.210	-	8.234	-
1.020	8.488	-	8.491	-
1.030	8.669	-	8.679	-
1.040	8.798	-	8.800	-
1.050	8.894	-	8.908	-
1.100	9.231	(10.399)†	9.240	(10.399)†
1.200	9.578	10.432	9.587	10.437
1.300	9.792	10.449	9.798	10.453
1.400	9.950	10.459	9.955	10.462
1.500	10.085	10.478	10.089	10.481
1.600	10.195	10.487	10.198	10.489
1.700	10.291	10.496	10.292	10.494
1.800	10.378	(10.508)†	10.379	(10.507)†
Average pK_a^T =		10.467± 0.035		10.469 ± 0.033

Overall average pK_a^T = 10.47 ± 0.03

§ Volume correction of + 0.005 ml used. §§ Volume correction of + 0.005 ml used.

†Values in parentheses were excluded from the average.

Table A2.9 Determination of pK_a^T for Glu (2 x recry.)

Test solution contained: 10^{-4} moles AH_2 9.80 ml 1.0 mol l^{-1} KCl 88.90 ml DW			$T = (25.00 \pm 0.05)°C$ $I = 0.1$ mol l^{-1} $[acid]_{total} = 10^{-3}$ mol l^{-1}	
Vol. 0.1000 mol l^{-1} NaOH (ml)	Titration 1		Titration 2	
	pH	pK_a^T	pH	pK_a^T
0.000	3.762	-	3.769	-
0.300	4.099	-	4.102	-
0.500	4.361	-	4.364	-
0.700	4.691	-	4.695	-
0.800	4.919	-	4.922	-
0.900	5.292	-	5.288	-
0.920	5.402	-	5.401	-
0.940	5.555	-	5.549	-
0.960	5.760	-	5.745	-
0.980	6.113	-	6.062	-
0.990	6.410	-	6.292	-
1.000	6.953	-	6.800	-
1.010	7.514	-	7.350	-
1.020	7.852	-	7.755	-
1.040	8.218	-	8.163	-
1.060	8.422	-	8.390	-
1.080	8.562	-	8.542	-
1.100	8.678	(10.001)†	8.661	(9.983)†
1.200	9.036	10.015	9.030	10.009
1.300	9.266	10.023	9.260	10.016
1.400	9.441	10.021	9.440	10.020
1.500	9.595	10.022	9.594	10.021
1.600	9.730	10.016	9.730	10.016
1.700	9.858	10.010	9.858	10.010
1.800	9.981	10.002	9.980	10.001
Average pK_a^T =		10.016 ± 0.014		10.013 ± 0.012

Overall average pK_a^T = 10.01 ± 0.01

† Values in parentheses were excluded from the average.

A2.4 Monoamino Acids at 37.1°C

Section A2.4 contain pK_a^T summary tables for amino acids studied in their zwitterion (AH), or monoamino acid hydrochloride ($AH_2^+Cl^-$) forms, at 37.1°C and $I = 0.1$ mol l^{-1}. Due allowance was made for water expansion.

Table A2.10 Determination of pK_a^T for 2-AE (1 x recryst.)

Test solution contained: 10^{-4} moles AH 9.95 ml 1.0 mol l^{-1} KCl 89.05 ml DW			$T = (37.10 \pm 0.05)$°C $I = 0.1$ mol l^{-1} $[acid]_{total} = 10^{-3}$ mol l^{-1}	
Vol. 0.1000 mol l^{-1} NaOH (ml)	Titration 1		Titration 2	
	pH	pK_a^T	pH	pK_a^T
0.000	5.950	-	6.158	-
0.050	8.003	(9.426)†	7.998	(9.421)†
0.100	8.370	(9.476)†	8.367	(9.472)†
0.150	8.580	(9.490)†	8.578	(9.488)†
0.200	8.731	9.495	8.730	(9.494)†
0.250	8.851	9.496	8.850	9.495
0.300	8.955	9.498	8.953	9.496
0.350	9.050	9.502	9.051	9.503
0.400	9.137	9.507	9.133	9.502
0.450	9.213	9.506	9.211	9.503
0.500	9.285	9.505	9.283	9.502
0.550	9.353	9.503	9.352	9.502
0.600	9.420	9.504	9.419	9.503
0.650	9.486	9.506	9.485	9.505
0.700	9.545	9.501	9.545	9.501
0.750	9.607	9.503	9.610	9.507
0.800	9.662	9.496	9.667	9.504
0.850	9.719	9.494	9.723	9.501
Average pK_a^T =		9.501± 0.00 7*		9.502 ± 0.007*

Overall average $pK_a^T = 9.50 \pm 0.01$

† Values in parentheses were excluded from the average.

Table A2.11 Determination of pK_a^T for 5-APe.HCl (2 x recryst.)

Test solution contained:			T = (37.10 ± 0.05)°C	
10^{-4} moles $AH_2^+Cl^-$			I = 0.1 mol l^{-1}	
9.85 ml 1.0 mol l^{-1} KCl			$[acid]_{total} = 10^{-3}$ mol l^{-1}	
88.12 ml DW				
Vol. 0.1000 mol l^{-1} NaOH (ml)	Titration 1§		Titration 2§§	
	pH	pK_a^T	pH	pK_a^T
0.000	3.793	-	3.788	-
0.900*	5.442		5.434	
0.920	5.572	-	5.562	-
0.940	5.740	-	5.733	-
.950	5.842	-	5.839	-
.960	5.982	-	5.970	-
0.970	6.169	-	6.134	-
0.980	6.418		6.368	-
0.990	6.825		6.725	-
0.995	7.090	-	7.008	-
1.000	7.500	-	7.419	-
1.005	7.892	-	7.824	-
1.010	8.210	-	8.101	-
1.015	8.369	-	8.280	-
1.020	8.480	-	8.420	-
1.030	8.645		8.598	
1.050	8.862	-	8.827	-
1.100	9.170	(10.487)	9.150	(10.490)
1.200	9.492	10.521	9.472	10.508
1.300	9.682	10.532	9.670	10.527
1.400	9.820	10.539	9.809	10.527
1.500	9.928	10.541	9.919	10.531
1.600	10.018	10.543	10.008	10.528
1.700	10.096	10.547	10.086	10.529
1.800	10.167	10.558	10.158	10.541
1.900	10.232	(10.569)	10.222	(10.551)
Average pK_a^T =		10.540 ± 0.019*		10.527 ± 0.019*

Overall average $pK_a^T = 10.58 \pm 0.02$

§ No volume correction used. §§ Volume correction of – 0.010 ml used.

*Volumes prior to 0.900 ml were neglected.

† Values in parentheses were excluded from the average.

Table A2.12 Determination of pK_a^T for 4-MAB.HCl (2 x recry.)

Test solution contained:			T = (37.10 ± 0.05)°C	
$10.589\ 10^{-4}$ moles $AH_2^+Cl^-$			I = 0.1 mol l^{-1}	
9.85 ml 1.0 mol l^{-1} KCl			$[acid]_{total} = 10^{-3}$ mol l^{-1}	
88.12 ml DW				
Vol. 0.1000 mol l^{-1} NaOH (ml)	Titration 1§		Titration 2§§	
	pH	pK_a^T	pH	pK_a^T
0.000	3.670	-	3.682	-
0.900	5.136	-	5.160	-
0.920	5247	-	5.265	-
0.940	5.358	-	5.414	-
.960	5.573	-	5.601	-
0.970	5.703	-	5.719	-
0.980	5.858	-	5.860	-
0.990	6.103		6.061	-
0.995	6.270		6.182	-
1.000	6.487	-	6.330	-
1.005	6.770	-	6.502	-
1.010	7.230	-	6.711	-
1.015	7.718	-	7.028	-
1.020	8.069	-	7.411	-
1.025	8.236	-	7.871	-
1.030	8.432		8.130	
1.035	-		8.468	
1.050	8.755	-	8.628	-
1.100	9.140	(10.472)†	9.080	(10.495)†
1.200	9.492	(10.544)†	9.458	(10.548)†
1.300	9.692	10.570	9.668	10.570
1.400	9.835	10.588	9.811	10.574
1.500	9.945	10.596	9.921	10.572
1.600	10.032	10.591	10.016	10.582
1.700	10.108	10.591	10.096	10.588
1.800	10.176	10.595	10.163	10.585
1.900	10.248	(10.638)†	10.227	(10.596)†
Average pK_a^T =		10.589 ±0.019*		10.579 ±0.009*

Overall average $pK_a^T = 10.58 \pm 0.02$

§ No volume correction used. §§ Volume correction of – 0.010 ml used.

* Volumes prior to 0.900 ml were neglected.

† Values in parentheses were excluded from the average.

Table A2.13 Determination of pK_a^T for 4-DMAB.HCl (2 x recryst.)

Test solution contained: 10^{-4} moles $AH_2^+Cl^-$ 9.85 ml 1.0 mol l^{-1} KCl 88.12 ml DW			$T = (37.10 \pm 0.05)°C$ $I = 0.1$ mol l^{-1} $[acid]_{total} = 10^{-3}$ mol l^{-1}	
Vol. 0.1000 mol l^{-1} NaOH (ml)	Titration 1[§]		Titration 2[§§]	
	pH	pK_a^T	pH	pK_a^T
0.000	3.650	-	3.633	-
0.900*	5.095	-	4.933	-
0.920	5.191	-	5.003	-
0.940	5.328	-	5.095	-
.960	5.408	-	5.190	-
0.970	5.508	-	5.203	-
0.980	5.628	-	5.268	-
0.990	5.770		5.343	-
0.995	5.971		5.432	-
1.000	6.108	-	5.540	-
1.005	6.235	-	5.600	-
1.010	6.420	-	5.662	-
1.015	6.620	-	5.748	-
1.020	6.955	-	5.845	-
1.025	7.242	-	5.953	-
1.030	7.525		6.082	
1.035	7.902		6.250	
1.050	8.187	-	7.082	-
1.100	8.625	9.884	8.380	(9.904)†
1.200	9.009	9.883	8.901	9.880
1.300	9.235	9.883	9.165	9.883
1.400	9.404	9.885	9.348	9.883
1.500	9.542	9.885	9.493	9.881
1.600	9.662	9.887	9.619	9.882
1.700	9.768	9.888	9.726	9.878
1.800	9.862	9.885	9.825	9.877
1.900	9.951	9.889	9.918	9.882
Average pK_a^T =		9.885± 0.004*		9.881 ± 0.004*

Overall average $pK_a^T = 9.89 \pm 0.01$

[§] Volume correction of –0.020 ml used.

[§§] Volume correction of – 0.055 ml used.

* Volumes prior to 0.900 ml were neglected.

† Values in parentheses were excluded from the average.

Table A2.14 Determination of pK_a^T for 4-A-3-MB.HCl (2 x recryst.)

Test solution contained: 10^{-4} moles $AH_2^+Cl^-$/AH 9.93 ml 1.0 mol l^{-1} KCl 88.30 ml DW			$T = (37.10 \pm 0.05)°C$ $I = 0.1$ mol l^{-1} $[acid]_{total} = 10^{-3}$ mol l^{-1}	
Vol. 0.1000 mol l^{-1} NaOH (ml)	Titration 1§		Titration 2§§	
	pH	pK_a^T	pH	pK_a^T
0.000	3.719	-	3.712	-
0.600*	4.808	-	4.819	-
0.650	5.049	-	5.088	-
0.670	5.188	-	5.238	-
0.690	5.378	-	5.448	-
0.710	5.675	-	5.795	-
0.715	5.785	-	-	-
0.720	5.890	-	6.069	-
0.725	6.025	-	6.229	-
0.730	6.175	-	6.435	-
0.735	6.380	-	6.683	-
0.740	6.618	-	6.908	-
0.745	6.838	-	7.103	-
0.750	7.030	-	7.270	-
0.755	7.208	-	-	-
0.760	7.338	-	7.501	-
0.780	7.702	-	-	-
0.800	7.901	-	7.958	-
0.850	8.212	(9.258)†	8.245	(9.270)†
0.950	8.561	9.282	8.584	9.293
1.050	8.791	9.293	8.809	9.303
1.150	8.975	9.302	8.991	9.310
1.250	9.137	9.309	9.150	9.316
1.350	9.279	9.306	9.291	9.312
1.450	9.412	9.297	9.422	9.301
1.550	9.533	(9.273)†	9.656	(9.278)†
Average pK_a^T =		9.298 ± 0.016		9.306 ± 0.013*

Overall average $pK_a^T = 9.89 \pm 0.01$

§ Volume correction of +0.010 ml used.

§§ Volume correction of +0.015 ml used.

* Volumes prior to 0.600 ml were neglected.

† Values in parentheses were excluded from the average.

Table A2.15 Determination of pK_a^T for 4-A-3,3-DMB.HCl (2 x recryst.)

Test solution contained:			T = (37.10 ± 0.05)°C	
10^{-4} moles $AH_2^+Cl^-$			I = 0.1 mol l^{-1}	
9.85 ml 1.0 mol l^{-1} KCl			$[acid]_{total} = 10^{-3}$ mol l^{-1}	
88.12 ml DW				
Vol. 0.1000 mol l^{-1} NaOH (ml)	Titration 1[§]		Titration 2[§§]	
	pH	pK_a^T	pH	pK_a^T
0.000	3.593	-	3.588	-
0.900*	5.102	-	5.018	-
0.920	5.249	-	5.139	-
0.940	5.472	-	5.308	-
0.950	5.642	-	5.418	-
0.960	5.850	-	5.555	-
0.970	6.155	-	5.725	-
0.980	6.680	-	5.945	-
0.985	7.120	-	-	-
0.990	7.518	-	6.282	-
0.995	7.793	-	6.522	-
1.000	7.993	-	6.828	-
1.005	8.132	-	7.240	-
1.010	8.246	-	7.605	-
1.015	8.329	-	7.852	-
1.020	8.403	-	8.039	-
1.030	-	-	8.275	-
1.050	8.707	-	8.544	-
1.100	8.979	(10.124)†	8.892	(10.125)†
1.200	9.295	10.151	9.247	10.150
1.300	9.492	10.161	9.458	10.160
1.400	9.642	10.170	9.613	10.166
1.500	9.762	10.175	9.736	10.168
1.600	9.862	10.175	9.841	10.171
1.700	9.951	10.177	9.932	10.173
1.800	10.035	(10.191)†	10.018	(10.186)†
Average pK_a^T =		10.168± 0.017*		10.165 ± 0.015*

Overall average pK_a^T = 10.17 ± 0.02

[§] Volume correction of +0.015 ml used. [§§] Volume correction of +0.005 ml used.

* Volumes prior to 0.900 ml were neglected.

† Values in parentheses were excluded from the average.

A2.5 Summary Tables for Monoamino Acids at 50.2 °C

Section A2.5 contain pK_a^T summary tables for amino acids studied in their zwitterion (AH), or monoamino acid hydrochloride ($AH_2^+Cl^-$) forms, at 50.2°C and I = 0.1 mol l^{-1}. Due allowance was made for water expansion.

Table A2.16 Determination of pK_a^T for 2-AE (1 x recryst.)

Test solution contained:			T = (50.20 ± 0.10)°C	
10^{-4} moles AH			I = 0.1 mol l^{-1}	
9.95 ml 1.0 mol l^{-1} KCl			$[acid]_{total} = 10^{-3}$ mol l^{-1}	
88.53 ml DW				
Vol. 0.1000 mol l^{-1} NaOH (ml)	Titration 1		Titration 2	
	pH	pK_a^T	pH	pK_a^T
0.000	6.012	-	6.062	-
0.050	7.691	(9.121)†	7.715	(9.147)†
0.100	8.075	(9.190)†	8.080	(9.196)†
0.150	8.290	(9.211)†	8.291	(9.212)†
0.200	8.442	(9.218)†	8.444	(9.221)†
0.250	8.567	9.226	8.567	9.226
0.300	8.669	9.227	8.669	9.227
0.350	8.760	9.228	8.759	9.227
0.400	8.841	9.228	8.840	9.227
0.450	8.916	9.227	8.917	9.228
0.500	8.989	9.230	8.989	9.230
0.550	9.059	9.234	9.060	9.235
0.600	9.123	9.234	9.127	9.239
0.650	9.189	9.240	9.187	9.237
0.700	9.248	9.239	9.249	9.241
0.750	9.307	9.242	9.306	9.241
0.800	9.363	9.243	9.360	9.238
0.850	9.418	(9.246)†	9.418	(9.246)†
Average pK_a^T =		9.233 ± 0.010*		9.233 ± 0.008*

Overall average $pK_a^T = 9.50 \pm 0.01$

† Values in parentheses were excluded from the average.

Table A2.17 Determination of pK_a^T for 5-APe.HCl (2 x recryst.)

Test solution contained:			$T = (50.20 \pm 0.10)°C$	
10^{-4} moles $AH_2^+Cl^-$			$I = 0.1$ mol l^{-1}	
9.85 ml 1.0 mol l^{-1} KCl			$[acid]_{total} = 10^{-3}$ mol l^{-1}	
87.63 ml DW				
Vol. 0.1000 mol l^{-1} NaOH (ml)	Titration 1§		Titration 2§§	
	pH	pK_a^T	pH	pK_a^T
0.000	3.784	-	3.773	-
0.900*	5.399	-	5.385	-
0.920	5.513	-	5.489	-
0.940	5.655	-	5.632	-
.950	5.745	-	5.717	-
.960	5.852	-	5.811	-
0.970	5.988	-	5.928	-
0.980	6.150		6.075	-
0.990	6.372		6.272	-
0.995	6.535	-	6.405	-
1.000	6.725	-	6.575	-
1.005	6.955	-	6.755	-
1.010	7.288	-	6.981	-
1.015	7.578	-	7.288	-
1.020	7.788	-	7.605	-
1.030	8.081		7.955	
1.040	8.221		8.165	
1.050	8.379	-	8.308	-
1.100	8.745	(10.140)	8.713	(10.128)
1.200	9.096	10.166	9.079	(10.156)
1.300	9.298	10.174	9.285	10.168
1.400	9.438	10.177	9.432	10.178
1.500	9.928	10.181	9.545	10.181
1.600	9.550	10.182	9.642	10.193
1.700	9.642	10.184	9.723	10.200
1.800	9.721	10.183	9.796	10.213
1.900	9.852	(10.189)	9.861	(10.227)
Average pK_a^T =		10.178 ± 0.012		10.189 ± 0.024*

Overall average $pK_a^T = 10.19 \pm 0.02$

§ Volume correction of – 0.010 ml used. §§ Volume correction of – 0.015 ml used.

*Volumes prior to 0.900 ml were neglected.

† Values in parentheses were excluded from the average.

Table A2.18 Determination of pK_a^T for 4-MAB.HCl (2 x recryst.)

Test solution contained: 10^{-4} moles $AH_2^+Cl^-$ 9.85 ml 1.0 mol l^{-1} KCl 87.63 ml DW			$T = (50.20 \pm 0.10)°C$ $I = 0.1$ mol l^{-1} $[acid]_{total} = 10^{-3}$ mol l^{-1}	
Vol. 0.1000 mol l^{-1} NaOH (ml)	Titration 1[§]		Titration 2[§§]	
	pH	pK_a^T	pH	pK_a^T
0.000	3.660	-	3.652	-
0.900*	5.118	-	5.150	-
0.920	5.229	-	5.265	-
0.940	5.382	-	5.419	-
.960	5.592	-	5.635	-
0.970	5.731	-	5.775	-
0.980	5.907	-	5.945	-
0.990	6.169		6.153	-
0.995	6.355		6.290	-
1.000	6.582	-	6.421	-
1.005	6.865	-	6.631	-
1.010	7.249	-	6.842	-
1.015	7.618	-	7.155	-
1.020	7.842	-	7.462	-
1.025	7.914	-	7.725	-
1.030	8.143		7.906	
1.040	-		8.146	
1.050	8.451	-	8.318	-
1.100	8.818	(10.285)†	8.750	(10.198)†
1.200	9.157	10.296	9.121	(10.242)†
1.300	9.348	10.291	9.324	(10.254)†
1.400	9.486	10.293	9.472	10.275
1.500	9.596	10.299	9.584	10.280
1.600	9.687	10.306	9.675	10.283
1.700	9.763	10.307	9.752	10.284
1.800	9.830	10.311	9.820	10.286
1.900	9.892	(10.323)†	9.881	(10.294)†
Average pK_a^T =		10.300 ± 0.011*		10.281 ± 0.006*

Overall average $pK_a^T = 10.29 \pm 0.02$

[§] Volume correction of –0.010 ml used. [§§] Volume correction of –0.015 ml used.

* Volumes prior to 0.900 ml were neglected.

† Values in parentheses were excluded from the average.

Table A2.19 Determination of pK_a^T for 4-DMAB.HCl (2 x recryst.)

Test solution contained: 10^{-4} moles $AH_2^+Cl^-$ 9.85 ml 1.0 mol l^{-1} KCl 87.63 ml DW			$T = (50.20 \pm 0.10)°C$ $I = 0.1$ mol l^{-1} $[acid]_{total} = 10^{-3}$ mol l^{-1}	
Vol. 0.1000 mol l^{-1} NaOH (ml)	Titration 1[§]		Titration 2[§§]	
	pH	pK_a^T	pH	pK_a^T
0.000	3.635	-	3.643	-
0.900*	5.087	-	5.087	-
0.920	5.199	-	5.195	-
0.940	5.345	-	5.334	-
.960	5.541	-	5.521	-
0.970	5.682	-	5.648	-
0.980	5.855	-	5.803	-
0.990	6.121		6.011	-
0.995	6.293		6.142	-
1.000	6.545	-	6.302	-
1.005	6.851	-	6.491	-
1.010	7.125	-	6.721	-
1.015	7.363	-	6.992	-
1.020	7.555	-	7.281	-
1.025	7.694	-	7.463	-
1.030	7.791		7.633	
1.040	7.962		7.832	
1.050	8.075	-	7.981	-
1.100	8.433	(9.639)†	8.393	(9.620)†
1.200	8.778	(9.643)†	8.770	(9.649)†
1.300	8.994	9.650	8.991	9.660
1.400	9.158	9.662	9.155	9.668
1.500	9.285	9.660	9.285	9.669
1.600	9.399	9.667	9.400	9.678
1.700	9.499	9.673	9.499	9.682
1.800	9.588	9.679	9.589	9.690
1.900	9.668	(9.683)†	9.672	(9.702)†
Average pK_a^T =		9.665± 0.015*		9.674 ± 0.014*

Overall average $pK_a^T = 9.67 \pm 0.01$

[§] Volume correction of –0.005 ml used. [§§] Volume correction of –0.010 ml used.

* Volumes prior to 0.900 ml were neglected.

† Values in parentheses were excluded from the average.

Table A2.20 Determination of pK_a^T for 4-A-3-MB.HCl (2 x recryst.)

Test solution contained:	$T = (50.20 \pm 0.10)°C$
10^{-4} moles $AH_2^+Cl^-$/AH	$I = 0.1$ mol l^{-1}
9.93 ml 1.0 mol l^{-1} KCl	$[acid]_{total} = 10^{-3}$ mol l^{-1}
87.82 ml DW	

Vol. 0.1000 mol l^{-1} NaOH (ml)	Titration 1§		Titration 2§§	
	pH	pK_a^T	pH	pK_a^T
0.000	3.688	-	3.709	-
0.600*	4.731	-	4.732	-
0.650	4.943	-	4.930	-
0.670	5.062	-	5.037	-
0.690	5.209	-	5.173	-
0.710	5.296	-	5.343	-
0.715	5.403	-	-	-
0.720	5.538	-	5.455	-
0.725	5.617	-	5.535	-
0.730	5.697	-	5.601	-
0.735	5.791	-	-	-
0.740	5.908	-	5.767	-
0.745	6.031	-	5.890	-
0.750	6.203	-	6.031	-
0.755	6.352	-	6.165	-
0.760	6.499	-	6.312	-
0.780	7.052	-	6.938	-
0.800	7.349	-	7.301	-
0.850	7.750	(8.868)†	7.714	(8.830)†
0.950	8.146	(8.908)†	8.145	(8.907)†
1.050	8.398	8.934	8.398	8.933
1.150	8.591	8.946	8.592	8.947
1.250	8.754	8.952	8.756	8.954
1.350	8.899	8.951	8.900	8.952
1.450	9.037	8.949	9.038	8.950
1.550	9.162	(8.932)†	9.161	8.931
Average pK_a^T =		8.946 ± 0.012*		8.945 ± 0.014*

Overall average $pK_a^T = 8.95 \pm 0.01$

§ Volume correction of -0.005 ml used.

§§ Volume correction of -0.005 ml used.

* Volumes prior to 0.600 ml were neglected.

† Values in parentheses were excluded from the average.

Table A2.21 Determination of pK_a^T for 4-A-3,3-DMB.HCl (2 x recryst.)

Test solution contained:			T = (50.20 ± 0.10)°C	
10^{-4} moles $AH_2^+Cl^-$			I = 0.1 mol l^{-1}	
9.85 ml 1.0 mol l^{-1} KCl			$[acid]_{total} = 10^{-3}$ mol l^{-1}	
87.63 ml DW				
Vol. 0.1000 mol l^{-1} NaOH (ml)	Titration 1§		Titration 2§§	
	pH	pK_a^T	pH	pK_a^T
0.000	3.587	-	3.605	-
0.900*	5.102	-	5.132	-
0.920	5.249	-	5.279	-
0.940	5.362	-	5.382	-
0.950	5.414	-	5.433	-
0.960	5.556	-	5.575	-
0.970	5.703	-	5.725	-
0.980	5.879	-	5.899	-
0.985	6.119	-	6.139	-
0.990	6.345	-	6.365	-
0.995	6.584	-	6.603	-
1.000	6.705	-	6.728	-
1.005	7.045	-	7.069	-
1.010	7.345	-	7.365	-
1.015	7.582	-	7.601	-
1.020	7.743	-	7.762	-
1.030	7.971	-	7.993	-
1.050	8.335	-	8.339	-
1.100	8.639	9.856	8.644	9.863
1.200	8.952	9.856	8.956	9.862
1.300	9.148	9.857	9.152	9.864
1.400	9.297	9.864	9.301	9.870
1.500	9.419	9.872	9.422	9.878
1.600	9.520	9.876	9.522	9.880
1.700	9.602	9.866	9.604	9.870
1.800	9.688	(9.877)†	9.692	(9.897)†
Average pK_a^T =		9.864± 0.01*		9.867 ± 0.013*

Overall average pK_a^T = 9.86 ± 0.02

§ Volume correction of -0.005 ml used. §§ Volume correction of -0.005 ml used.

* Volumes prior to 0.900 ml were neglected.

† Values in parentheses were excluded from the average.

Appendix 3

Methods of Data Analysis and Kinetic Results

A3.1 Introduction

A3.1(a) General

All reactions studied were pseudo first order at constant pH i.e. the reaction probably involves a rate determining step of the type:

$$\therefore \text{ rate, } v = \frac{d[A]}{dt} = k_{obs}[A] \qquad \text{....(A3.1)}$$

where k_{obs} = observed rate constant

Separating the variables and integrating between limits:

$$\text{or} \qquad \int_{[A]_0}^{[A]} \frac{d[A]}{[A]} = -k_{obs}[A] \qquad \text{....(A3.2)}$$

Gives:

$$\ln \frac{[A]}{[A]_0} = -k_{obs} \cdot t \qquad \text{....(A3.3)}$$

Rearranging (3):

$$\log_{10} \frac{[A]}{[A]_0} = -\frac{k_{obs} \cdot t}{2.303} \qquad \text{....(A3.4)}$$

$$\therefore [A] = [A]_0 e^{-k_{obs} \cdot t} \qquad \text{....(A3.5)}$$

where, $[A]_0$ = concentration of A at t= 0.

[A] = concentration of A at a given time t.

For a first order reaction, therefore, a plot of ln [A] (or $\log_{10}$ [A]) vs. t is linear, and the rate constant, k_{obs}, can be obtained from the slope.

k_{obs} has the dimensions time^{-1}, the unit used in this thesis was min^{-1}.

The half-life is defined to be the time required for the reactant concentration to decay to half of its initial value.

Substituting $[A] = [A]_0 / 2$ when $t = t_{1/2}$ into (A3.3):

$$t_{1/2} = \frac{\ln 2}{k_{obs}} = \frac{0.6931}{k_{obs}} \quad \text{....(A3.6)}$$

A3.1(b) Infinity Method

General

This method is a well established method for evaluating first order rate constants. It can be shown from equation (A3.5) that:

$$\frac{[A]}{[A_0]} = \frac{V_t - V_\infty}{V_0 - V_\infty} = \frac{V_\infty - V_t}{V_\infty - V_0} \quad \text{....(A3.7)}$$

where, V_0 is the volume at time $t = 0$, V_∞ is the volume at $t = \infty$, and V_t is the volume at time t.

Combining equations (A3.4) and (A3.7) gives:

$$\log_{10} (V_\infty - V_t) = -\frac{k_{obs} \cdot t}{2.303} + \log_{10}(V_\infty - V_0) \quad \text{....(A3.8)}$$

A linear plot for $\log_{10}(V_\infty - V_t)$ vs. t (over ~ 2-3 reaction half-lives) confirms that the reaction is first-order. From the slope of the line the rate constant can be calculated. All calculations were made by hand.

A3.1(c) Guggenheim Method

General

The Guggenheim method was used to evaluate k_{obs} for each of the reactions studied.[1] The method for the determination of k_{obs} by E. A. Guggenheim eliminates the need for an infinity value. This saves time for long reactions and avoids the cumulative error and the dependence on a single reading.

1. E. A. Guggenheim, *Phil. Mag.*, **1926**, *1*, 538.

Guggenheim's equation is:

$$\log_{10}(\lambda_1 - \lambda_1') = \frac{-k_{obs} \cdot t}{2.303} + \log_{10}[(\lambda_\infty - \lambda_0)(1 - e^{-k_{obs} \cdot \Delta t})] \quad \text{....(A3.9)}$$

where λ_1 is a measurement of a physical property at time t1 and λ_1' is a measurement of that same physical property at $t + \Delta t$, where Δt is a constant time interval, generally between 1 and 2 reaction half-lives. Equation (A3.9) is a straight line, whose slope yields the value of k_{obs}.

A spreadsheet program, GUGG was written and run on Microsoft™ Excel® (Version 98 for Macintosh).

The program calculates and outputs $\log_{10}(\lambda_1' - \lambda_1)$ vs. time (t) values, for each volume (λ_1) and time (t) (readings taken during the reaction. To operate this, an appropriate Δt value is initially chosen (~ 2 half-lives). Based on this, the data can then be separated into two equivalent sets (i.e. for values at time t and at time $t+\Delta t$). These are then entered in each of the respective cells of the spreadsheet .The values generated by the program are subsequently used to construct the plot needed to determine the rate constant. To produce the best plots it is recommended that each set contains ~ 15 data points. Too few values lead to plots that are inaccurate, while too many can cause cluttering of the graph.

A3.1(d) GUGG

	A	B	C	D	E	F
1	Time	Volume (V1)	Time	Volume (V2)	V2-V1	LOG10(V2-V1)
2					=D2-B2	=LOG10(E2)
3					=D3-B3	=LOG10(E3)
4					=D4-B4	=LOG10(E4)
5					=D5-B5	=LOG10(E5)
6					=D6-B6	=LOG10(E6)
7					=D7-B7	=LOG10(E7)
8					=D8-B8	=LOG10(E8)
9					=D9-B9	=LOG10(E9)
10					=D10-B10	=LOG10(E10)
11					=D11-B11	=LOG10(E11)
12					=D12-B12	=LOG10(E12)
13					=D13-B13	=LOG10(E13)
14					=D14-B14	=LOG10(E14)
15					=D15-B15	=LOG10(E15)
16					=D16-B16	=LOG10(E16)
17					=D17-B17	=LOG10(E17)
18					=D18-B18	=LOG10(E18)
19					=D19-B19	=LOG10(E19)
20					=D20-B20	=LOG10(E20)
21					=D21-B21	=LOG10(E21)
22					=D22-B22	=LOG10(E22)

A3.2 The Effect of Temperature on Reaction Rate

A3.2(a) Transition State Theory

The relationship between rate constant and temperature can be expressed by equation A3.10

$$k_2 = \left(\frac{k_B T}{h}\right) K^{\ddagger} \qquad \text{....(A3.10)}$$

(Assuming, the transmission coefficient, $K = 1$)

Where;

k_2 = Second order rate constant

k_B = Boltzmann constant

h = Planck constant

$K^{\ddagger}$ = Equilibrium constant for the formation of the transition state.

Since the thermodynamic equilibrium is assumed to exist between the transition state, we can define the free energy ($\Delta G^{\ddagger}$), enthalpy ($\Delta H^{\ddagger}$) and entropy ($\Delta S^{\ddagger}$) of activation for such a reaction in terms of the equilibrium constant ($K^{\ddagger}$) in the usual manner.

Thus

$$\Delta G^{\ddagger} = \Delta H^{\ddagger} - T\Delta S^{\ddagger} = -RT\ln K^{\ddagger} \qquad \text{....(A3.11)}$$

and

$$\frac{-\Delta H^{\ddagger}}{R} = \frac{d\ln K^{\ddagger}}{d\left(1/T\right)} \qquad \text{....(A.3.12)}$$

where R = Gas constant

Rearranging A3.11 and combination with A3.10 gives

$$k_2 = \frac{k_B T}{h}\left(e^{-\frac{\Delta G^{\ddagger}}{RT}}\right) \qquad \text{....(A3.13)}$$

Thus

$$\ln\left(\frac{h}{k_B}\right) + \ln\left(\frac{k_2}{T}\right) = -\frac{\Delta G^{\ddagger}}{RT} \qquad \ldots.(A3.14)$$

It follows that

$$\ln\left(\frac{k_2}{T}\right) = -\frac{\Delta H^{\ddagger}}{RT} + \left(\frac{\Delta S^{\ddagger}}{R} + \ln\left(\frac{k_B}{h}\right)\right) \qquad \ldots.(A3.15)$$

Therefore, a plot of $\ln\left(\frac{k_2}{T}\right)$ versus $\frac{1}{T}$ yields a slope that is equal to $\frac{-\Delta H^{\ddagger}}{R}$ and an intercept of $\left(\frac{\Delta S^{\ddagger}}{R} + \ln\left(\frac{k_B}{h}\right)\right)$ or $\left(\frac{\Delta S^{\ddagger}}{R} + 23.76\right)$.

A3.2(b) Arrhenius Parameters

It is useful to be able to relate the values of $\Delta H^{\ddagger}$ and $\Delta S^{\ddagger}$ to the Arrhenius parameters, activation energy, E_a and pre exponential factor, A. This can be achieved according to the following procedure

According to the Arrhenius Equation

$$k_2 = Ae^{-\frac{E_a}{RT}} \qquad \ldots.(A3.16)$$

$$\therefore \qquad \ln k_2 = \ln A - \frac{E_a}{RT} \qquad \ldots.(A3.17)$$

The slope of the plot of $\ln k_2$ vs. $\frac{1}{T}$ gives

$$\frac{d\ln k_2}{d\left(\frac{1}{T}\right)} = -\frac{E_a}{R} \qquad \ldots.(A3.18)$$

From equation A3.10

$$\frac{d\ln K^{\ddagger}}{d\left(1/T\right)} = \frac{d\ln k_2}{d\left(1/T\right)} + \frac{d\ln\left(1/T\right)}{d\left(1/T\right)} \qquad \ldots.(A3.19)$$

Combination of A3.12 and A3.18 into A3.19, with rearrangement, gives

Combination of A3.12 and A3.18 into A3.19, with rearrangement, gives

$$E_a = \Delta H^{\ddagger} + RT \qquad \ldots.(A3.20)$$

Re-arranging A3.14 gives

$$\Delta G^{\ddagger} = -RT\ln k_2 + RT\ln\left(\frac{k_B T}{h}\right) \qquad \ldots.(A3.21)$$

Substitution of A3.11 and A3.17 into A3.21gives

$$\Delta H^{\ddagger} - T\Delta S^{\ddagger} = -RT\left(\ln A - \frac{E_a}{RT}\right) + RT\ln\left(\frac{k_B T}{h}\right) \qquad \ldots.(A3.22)$$

Placing A3.20 into A3.22 gives:

$$E_a - RT - T\Delta S^{\ddagger} = -RT\ln A + E_a + RT\ln\left(\frac{k_B T}{h}\right) \qquad \ldots.(A3.23)$$

Rearranging A3.23 gives

$$\Delta S^{\ddagger} = R\left(\ln A - \ln\left(\frac{k_B T}{h}\right) - 1\right) \qquad \ldots.(A3.24)$$

At 298 K, A3.24 rearranges to give

$$\ln A = \left(\frac{\Delta S^{\ddagger}}{8.3145} + 30.45\right) \qquad \ldots.(A3.25)$$

A3.3 Summary of Kinetics for Amino Acid Esters

A3.3(a) Results for Amino Acid Esters at25°C

Section A3.3(b) contain tables that list the effect of pH on the value of $k_{obs}/[OH^-]$, data needed for the separation of k_E and k_{EH^+} and the corresponding pH/rate profiles for the various amino acid ester studied at 25.0°C and I = 0.1 mol l^{-1}.

Table A3.1 Summary of $k_{obs}/[OH^-]$ for Ser Me at at pH =11.000

T = (25.00 ± 0.05)°C

I = 0.1 mol l^{-1}

pH†	k_{obs} (min^{-1})	$t_{1/2}$ (min)	$[OH^-]^*$ (mol l^{-1})	$\frac{k_{obs}}{[OH^-]}$ (l mol^{-1} min^{-1})
11.007	7.848×10^{-2}	8.8	1.328×10^{-3}	59.1
11.008	7.826×10^{-2}	8.9	1.331×10^{-3}	58.8
11.007	7.808×10^{-2}	8.9	1.328×10^{-3}	58.8
11.006	7.764×10^{-2}	8.9	1.325×10^{-3}	58.6
11.008	7.866×10^{-2}	8.8	1.331×10^{-3}	59.1
11.009	7.897×10^{-2}	8.8	1.334×10^{-3}	59.2
11.005	7.746×10^{-2}	8.9	1.322×10^{-3}	58.6
11.008	7.773×10^{-2}	8.9	1.331×10^{-3}	58.4
11.009	7.831×10^{-2}	8.9	1.334×10^{-3}	58.7
11.008	7.799×10^{-2}	8.9	1.331×10^{-3}	58.6
11.006	7.830×10^{-2}	8.9	1.325×10^{-3}	59.1
11.007	7.861×10^{-2}	8.8	1.328×10^{-3}	59.2
11.006	7.856×10^{-2}	8.8	1.325×10^{-3}	59.3
11.010	7.916×10^{-2}	8.8	1.337×10^{-3}	59.2
11.005	7.706×10^{-2}	9.0	1.322×10^{-3}	58.3
11.006	7.750×10^{-2}	8.9	1.325×10^{-3}	58.5
11.007	7.755×10^{-2}	8.9	1.328×10^{-3}	58.4

Overall $k_{obs}/[OH^-]$ = (58.8 ± 0.5) l mol^{-1} min^{-1}

†Stopped Stirrer pH, $^*[OH^-] = \frac{10^{pH\ -\ 13.9965}}{0.7715}$ (25°C and I = 0.1 mol l^{-1}).

Table A3.2 Effect of pH on the Value of $k_{obs}/[OH^-]$ for 2-AE Bz

$T = (25.00 \pm 0.05)°C$

$I = 0.1$ mol l^{-1}

pH†	k_{obs} (min^{-1})	$t_{1/2}$ (min)	$[OH^-]^*$ (mol l^{-1})	$\frac{k_{obs}}{[OH^-]}$ (l mol^{-1} min^{-1})
8.905	2.814×10^{-3}	246.3	1.050×10^{-5}	268.0
8.906	2.788×10^{-3}	248.6	1.052×10^{-5}	265.0
9.104	3.403×10^{-3}	203.7	1.660×10^{-5}	205.0
9.106	3.319×10^{-3}	208.8	1.668×10^{-5}	199.0
9.304	4.183×10^{-3}	165.7	2.631×10^{-5}	159.0
9.306	4.255×10^{-3}	162.9	2.643×10^{-5}	161.0
9.504	5.442×10^{-3}	127.4	4.170×10^{-5}	130.5
9.505	5.526×10^{-3}	125.4	4.180×10^{-5}	132.2
9.705	7.652×10^{-3}	90.6	6.625×10^{-5}	115.5
9.706	7.543×10^{-3}	91.9	6.640×10^{-5}	113.6
10.105	1.632×10^{-2}	42.5	1.664×10^{-4}	98.1
10.106	1.628×10^{-2}	42.6	1.664×10^{-4}	97.6
10.306	2.576×10^{-2}	27.0	2.643×10^{-4}	97.2
10.307	2.597×10^{-2}	26.7	2.650×10^{-4}	98.0
10.507	4.031×10^{-2}	17.2	4.199×10^{-4}	96.0
10.508	4.062×10^{-2}	17.1	4.209×10^{-4}	96.5
10.707	6.409×10^{-2}	10.8	6.656×10^{-4}	96.3
10.708	6.410×10^{-2}	10.8	6.671×10^{-4}	96.1
10.808	8.045×10^{-2}	8.6	8.398×10^{-4}	95.9
10.808	8.053×10^{-2}	8.6	8.398×10^{-4}	95.8
10.908	1.004×10^{-1}	6.9	1.057×10^{-3}	95.0
10.908	1.002×10^{-1}	6.9	1.057×10^{-3}	94.8

†Stopped Stirrer pH, $^*[OH^-] = \frac{10^{pH\ -\ 13.9965}}{0.7715}$ (25°C and I = 0.1 mol l^{-1}).

Table A3.3 Data for Separation of k_E and k_{EH^+} for the Alkaline Hydrolysis of 2-AE Bz

$T = (25.00 \pm 0.05)°C$

$I = 0.1$ mol l^{-1}

pH†	$[H^+]$ (mol l^{-1})	$(K_a^T + H^+)$ (mol l^{-1})	$\frac{k_{obs}}{[OH^-]}$ (l mol^{-1} min^{-1})	$\frac{k_{obs}}{[OH^-]}(K_a^T + [H^+])$ (min^{-1})
8.905	1.613×10^{-9}	3.181×10^{-8}	268.0	8.526×10^{-6}
8.906	1.609×10^{-9}	3.181×10^{-8}	265.0	8.429×10^{-6}
9.104	1.020×10^{-9}	3.122×10^{-8}	205.0	6.400×10^{-6}
9.106	1.015×10^{-9}	3.122×10^{-8}	199.0	6.212×10^{-6}
9.304	6.437×10^{-10}	3.084×10^{-8}	159.0	4.904×10^{-6}
9.306	6.407×10^{-10}	3.084×10^{-8}	161.0	4.965×10^{-6}
9.504	4.061×10^{-10}	3.061×10^{-8}	130.5	3.994×10^{-6}
9.505	4.052×10^{-10}	3.061×10^{-8}	132.2	4.046×10^{-6}
9.705	2.557×10^{-10}	3.046×10^{-8}	115.5	3.518×10^{-6}
9.706	2.551×10^{-10}	3.046×10^{-8}	113.6	3.460×10^{-6}
10.105	1.018×10^{-10}	3.030×10^{-8}	98.1	2.973×10^{-6}
10.106	1.016×10^{-10}	3.030×10^{-8}	97.6	2.957×10^{-6}
10.306	6.407×10^{-11}	3.026×10^{-8}	97.2	2.952×10^{-6}
10.307	6.392×10^{-11}	3.026×10^{-8}	98.0	2.966×10^{-6}
10.507	4.033×10^{-11}	3.024×10^{-8}	96.0	2.903×10^{-6}
10.508	4.024×10^{-11}	3.024×10^{-8}	96.5	2.918×10^{-6}
10.707	2.545×10^{-11}	3.023×10^{-8}	96.3	2.911×10^{-6}
10.708	2.539×10^{-11}	3.023×10^{-8}	96.1	2.905×10^{-6}
10.808	2.017×10^{-11}	3.022×10^{-8}	95.9	2.898×10^{-6}
10.808	2.017×10^{-11}	3.022×10^{-8}	95.8	2.895×10^{-6}
10.908	1.602×10^{-11}	3.022×10^{-8}	95.0	2.871×10^{-6}
10.908	1.602×10^{-11}	3.022×10^{-8}	94.8	2.864×10^{-6}

Using $K_a^T = 3.020 \times 10^{-8}$; $pK_a^T = 7.52$ (25°C and I = 0.1 mol l^{-1}), (Table A1.1).

†Stopped Stirrer pH. $[H^+] = \frac{10^{-pH}}{0.7715}$ (25°C and I = 0.1 mol l^{-1}).

Figure A3.1 Separation of k_E and k_{EH^+} for Alkaline Hydrolysis of 2-AE Bz

$T = (25.00 \pm 0.05)°C$

$I = 0.1$ mol l^{-1}

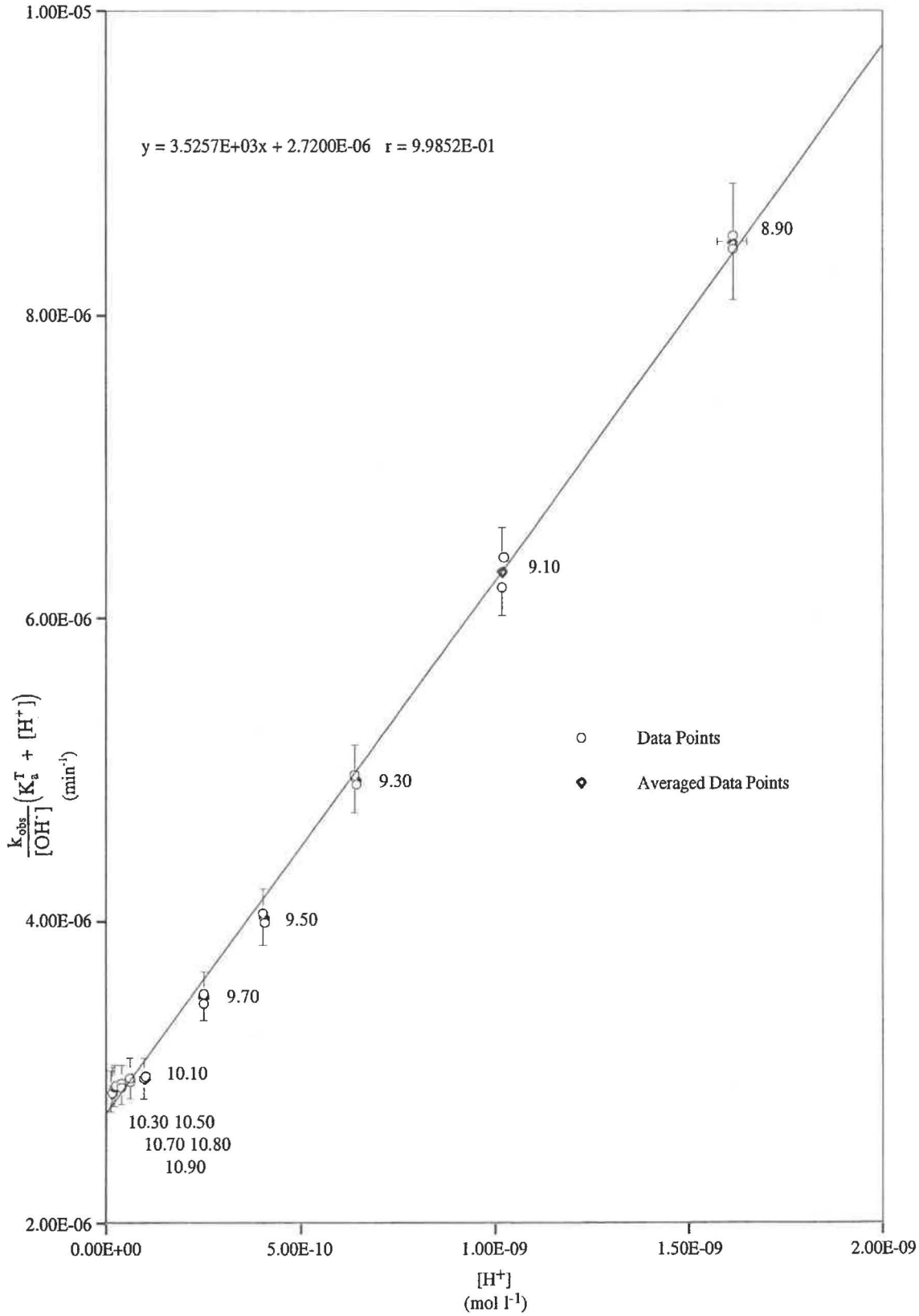

Table A3.4 Effect of pH on the Value of $k_{obs}/[OH^-]$ for 3-AP Bz

$T = (25.00 \pm 0.05)°C$

$I = 0.1$ mol l^{-1}

pH†	k_{obs} (min^{-1})	$t_{1/2}$ (min)	$[OH^-]^*$ (mol l^{-1})	$\frac{k_{obs}}{[OH^-]}$ (l mol^{-1} min^{-1})
9.207	6.356×10^{-3}	109.1	2.105×10^{-5}	302.0
9.406	7.684×10^{-3}	90.2	3.328×10^{-5}	230.9
9.406	7.548×10^{-3}	91.8	3.328×10^{-5}	226.8
9.606	9.647×10^{-3}	71.9	5.274×10^{-5}	182.9
9.606	9.303×10^{-3}	74.5	5.274×10^{-5}	176.4
9.706	1.010×10^{-2}	68.7	6.640×10^{-5}	152.0
9.806	1.100×10^{-3}	63.0	8.359×10^{-5}	131.6
9.807	1.093×10^{-3}	63.4	8.378×10^{-5}	130.5
9.907	1.155×10^{-3}	60.0	1.055×10^{-4}	109.5
9.908	1.162×10^{-3}	59.6	1.057×10^{-4}	110.0
10.006	1.235×10^{-2}	56.1	1.325×10^{-4}	93.2
10.008	1.224×10^{-2}	56.6	1.331×10^{-4}	92.0
10.206	1.338×10^{-2}	51.8	2.099×10^{-4}	63.7
10.207	1.282×10^{-2}	54.1	2.105×10^{-4}	60.9
10.307	1.393×10^{-2}	49.7	2.650×10^{-4}	52.6
10.406	1.527×10^{-2}	45.4	3.328×10^{-4}	45.9
10.406	1.518×10^{-2}	45.7	3.328×10^{-4}	45.6
10.608	1.748×10^{-2}	39.8	5.298×10^{-4}	32.9
10.808	2.209×10^{-2}	31.4	8.398×10^{-4}	26.3
10.908	2.389×10^{-2}	29.0	1.057×10^{-3}	22.6
10.908	2.367×10^{-2}	29.2	1.057×10^{-3}	22.4
11.006	2.848×10^{-2}	24.3	1.325×10^{-3}	21.5

†Stopped Stirrer pH, $^*[OH^-] = \frac{10^{pH - 13.9965}}{0.7715}$ (25°C and I = 0.1 mol l^{-1}).

Table A3.5 Data for Separation of k_E and k_{EH+} for Alkaline Hydrolysis of 3-AP Bz

$T = (25.00 \pm 0.05)°C$

$I = 0.1$ mol l^{-1}

pH†	$[H^+]$ (mol l^{-1})	$(K_a^T + H^+)$ (mol l^{-1})	$\frac{k_{obs}}{[OH^-]}$ (l mol^{-1} min^{-1})	$\frac{k_{obs}}{[OH^-]}(K_a^T + [H^+])$ (min^{-1})
9.207	8.048×10^{-10}	1.676×10^{-9}	302.0	5.061×10^{-7}
9.406	5.089×10^{-10}	1.380×10^{-9}	230.9	3.186×10^{-7}
9.406	5.089×10^{-10}	1.380×10^{-9}	226.8	3.130×10^{-7}
9.606	3.211×10^{-10}	1.192×10^{-9}	182.9	2.180×10^{-7}
9.606	3.211×10^{-10}	1.192×10^{-9}	176.4	2.103×10^{-7}
9.706	2.551×10^{-10}	1.126×10^{-9}	152.0	1.712×10^{-7}
9.806	2.026×10^{-10}	1.074×10^{-9}	131.6	1.413×10^{-7}
9.807	2.021×10^{-10}	1.073×10^{-9}	130.5	1.400×10^{-7}
9.907	1.606×10^{-10}	1.032×10^{-9}	109.5	1.129×10^{-7}
9.908	1.602×10^{-10}	1.031×10^{-9}	110.0	1.135×10^{-7}
10.006	1.278×10^{-10}	9.988×10^{-10}	93.2	9.303×10^{-8}
10.008	1.273×10^{-10}	9.982×10^{-10}	92.0	9.189×10^{-8}
10.206	8.066×10^{-11}	9.516×10^{-10}	63.7	6.062×10^{-8}
10.207	8.048×10^{-11}	9.514×10^{-10}	60.9	5.794×10^{-8}
10.307	6.392×10^{-11}	9.349×10^{-10}	52.6	4.918×10^{-8}
10.406	5.089×10^{-11}	9.219×10^{-10}	45.9	4.231×10^{-8}
10.406	5.089×10^{-11}	9.219×10^{-10}	45.6	4.204×10^{-8}
10.608	3.196×10^{-11}	9.029×10^{-10}	32.9	2.971×10^{-8}
10.808	2.017×10^{-11}	8.911×10^{-10}	26.3	2.344×10^{-8}
10.908	1.602×10^{-11}	8.870×10^{-10}	22.6	2.005×10^{-8}
10.908	1.602×10^{-11}	8.870×10^{-10}	22.4	1.987×10^{-8}
11.006	1.278×10^{-11}	8.837×10^{-10}	21.5	1.900×10^{-8}

Using $K_a^T = 8.710 \times 10^{-10}$; $pK_a^T = 9.06$ (25°C and I = 0.1 mol l^{-1}), (Table A1.2).

†Stopped Stirrer pH. $[H^+] = \frac{10^{-pH}}{0.7715}$ (at 25.0 °C and I = 0.1 mol l^{-1}).

Figure A3.2 Separation of k_E and k_{EH^+} for Alkaline Hydrolysis of 3-AP Bz

$T = (25.00 \pm 0.05)°C$

$I = 0.1$ mol l^{-1}

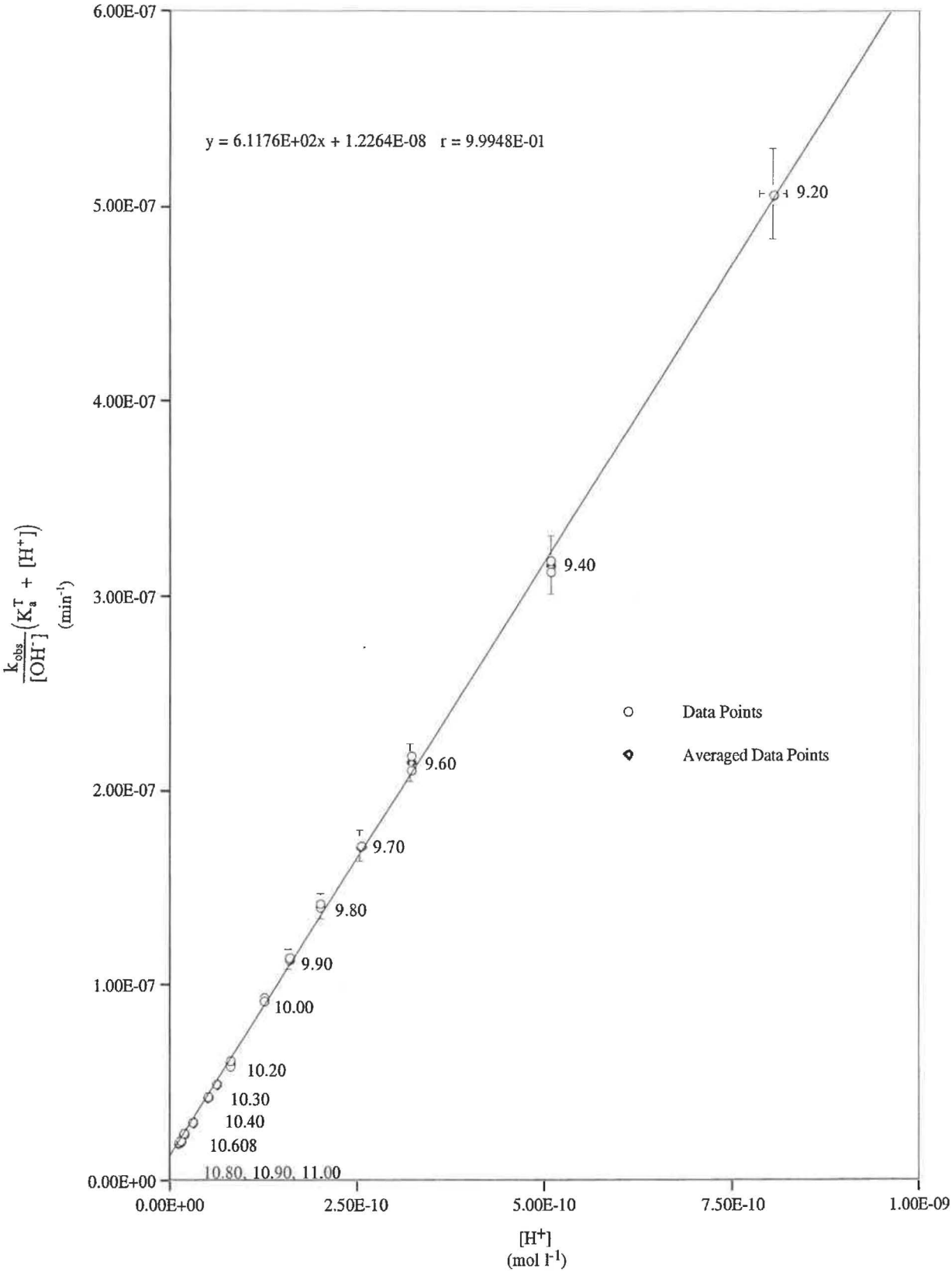

Table A3.6 Effect of pH on the Value of $k_{obs}/[OH^-]$ for 4-DMAB Et.

$T = (25.00 \pm 0.05)°C$

$I = 0.1$ mol l^{-1}

pH†	k_{obs} (min^{-1})	$t_{1/2}$ (min)	$[OH^-]^*$ (mol l^{-1})	$\frac{k_{obs}}{[OH^-]}$ (l mol^{-1} min^{-1})
10.103	5.383×10^{-3}	128.8	1.656×10^{-4}	32.5
10.304	6.631×10^{-3}	104.5	2.631×10^{-4}	25.2
10.503	7.656×10^{-3}	90.5	4.161×10^{-4}	18.4
10.704	8.989×10^{-3}	77.1	6.609×10^{-4}	13.6
10.903	1.139×10^{-2}	60.8	1.045×10^{-3}	10.9
10.904	1.152×10^{-2}	60.2	1.048×10^{-3}	11.0
11.003	1.197×10^{-2}	57.9	1.316×10^{-3}	9.1
11.006	1.219×10^{-2}	56.9	1.325×10^{-3}	9.2

†Stopped Stirrer pH, $^*[OH^-] = \frac{10^{pH\ -\ 13.9965}}{0.7715}$, (25°C and I = 0.1 mol l^{-1}).

Table A3.7 Data for Separation of k_E and k_{EH+} for the Alkaline Hydrolysis 4-DMAB Et

$T = (25.00 \pm 0.05)°C$

$I = 0.1$ mol l^{-1}

pH†	$[H^+]$ (mol l^{-1})	$(K_a^T + H^+)$ (mol l^{-1})	$\frac{k_{obs}}{[OH^-]}$ (l mol^{-1} min^{-1})	$\frac{k_{obs}}{[OH^-]}(K_a^T + [H^+])$ (min^{-1})
10.103	5.101×10^{-9}	5.172×10^{-9}	32.5	5.948×10^{-6}
10.304	3.271×10^{-9}	3.342×10^{-9}	25.2	4.678×10^{-6}
10.503	3.256×10^{-9}	3.327×10^{-9}	18.4	4.657×10^{-6}
10.704	2.563×10^{-9}	2.633×10^{-9}	13.6	4.161×10^{-6}
10.903	2.551×10^{-9}	2.622×10^{-9}	10.9	4.155×10^{-6}
10.904	2.054×10^{-9}	2.125×10^{-9}	11.0	3.676×10^{-6}
11.003	2.045×10^{-9}	2.116×10^{-9}	9.1	3.671×10^{-6}
11.006	2.035×10^{-9}	2.106×10^{-9}	9.2	3.633×10^{-6}

Using $K_a^T = 5.129 \times 10^{-10}$; $pK_a^T = 9.29$ (25°C and I = 0.1 mol l^{-1}), (Table A1.3).

†Stopped Stirrer pH, $[H^+] = \frac{10^{-pH}}{0.7715}$ (25°C and I = 0.1 mol l^{-1}).

Figure A3.3 Separation of k_E and k_{EH^+} for Alkaline Hydrolysis of 4-DMAB Et

$T = (25.00 \pm 0.05)°C$

$I = 0.1$ mol l^{-1}

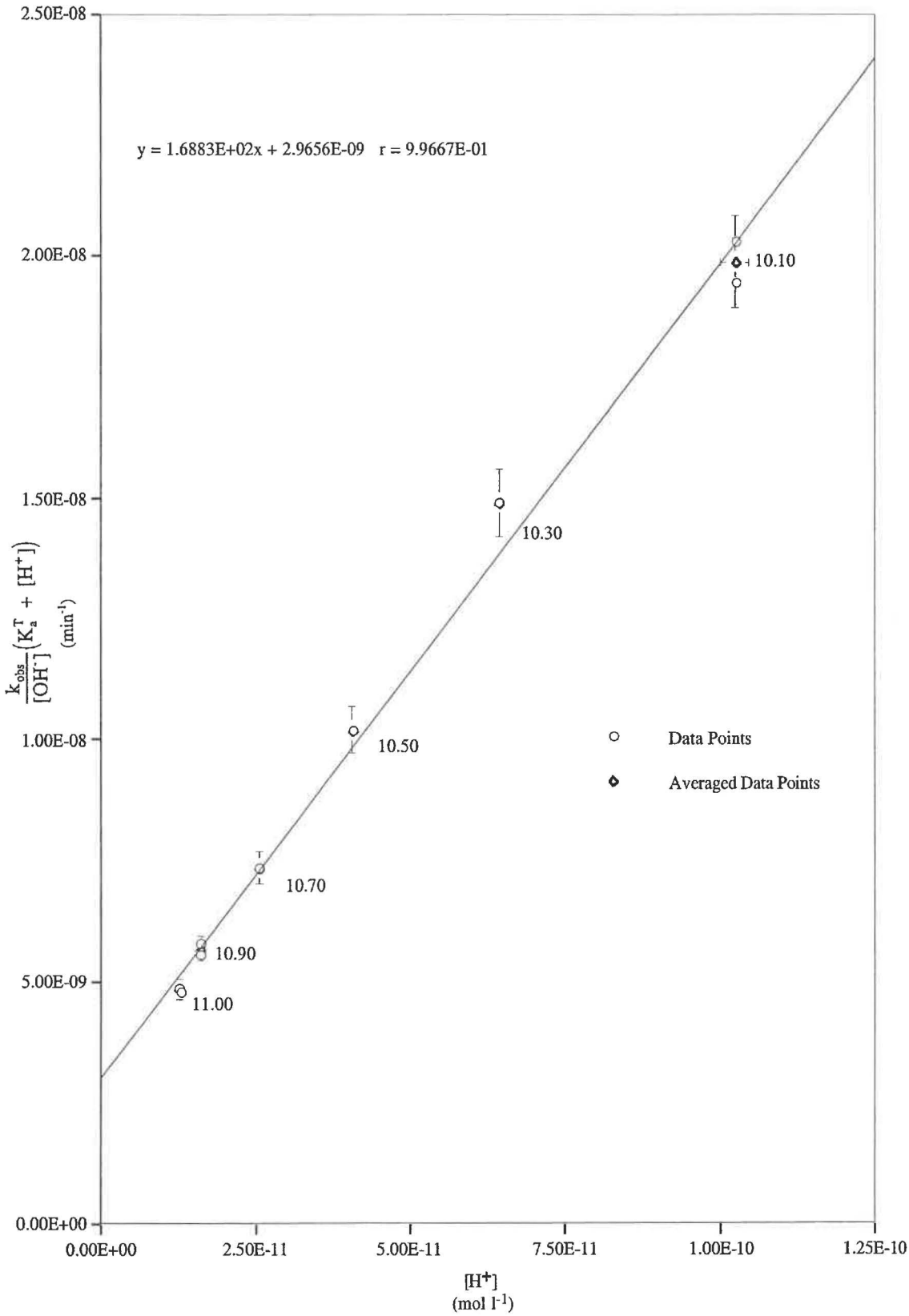

Table A3.8 Effect of pH on the Value of $k_{obs}/[OH^-]$ for Glu DMe.

$T = (25.00 \pm 0.05)°C$

$I = 0.1$ mol l^{-1}

pH†	k_{obs} (min^{-1})	$t_{1/2}$ (min)	$[OH^-]^*$ (mol l^{-1})	$\frac{k_{obs}}{[OH^-]}$ (1 mol^{-1} min^{-1})
8.603	1.100×10^{-3}	629.8	5.238×10^{-6}	210.1
8.804	1.532×10^{-3}	452.8	8.321×10^{-6}	184.2
9.003	2.104×10^{-3}	329.4	1.316×10^{-5}	159.9
9.203	3.086×10^{-3}	224.6	2.085×10^{-5}	148.0
9.205	3.046×10^{-3}	228.0	2.095×10^{-5}	145.1
9.303	3.646×10^{-3}	190.1	2.625×10^{-5}	138.9
9.305	3.689×10^{-3}	187.8	2.637×10^{-5}	139.9
9.599	6.797×10^{-3}	102.0	5.189×10^{-5}	131.0
9.600	6.866×10^{-3}	101.0	5.202×10^{-5}	132.0
9.800	1.047×10^{-2}	66.2	8.244×10^{-5}	127.1
9.803	1.073×10^{-2}	64.6	8.302×10^{-5}	129.2
9.995	1.631×10^{-2}	42.6	1.292×10^{-4}	126.2
10.204	2.589×10^{-2}	26.8	2.090×10^{-4}	123.9
10.303	3.260×10^{-2}	21.3	2.625×10^{-4}	124.2
10.601	6.257×10^{-2}	11.1	5.214×10^{-4}	120.0
10.604	6.363×10^{-2}	10.9	5.250×10^{-4}	121.2
10.803	9.987×10^{-2}	7.0	8.302×10^{-4}	120.3
10.803	9.995×10^{-2}	7.0	8.302×10^{-4}	119.8
10.903	1.256×10^{-1}	5.5	1.045×10^{-3}	120.1
10.905	1.258×10^{-1}	5.5	1.050×10^{-3}	119.8
11.002	1.580×10^{-1}	4.4	1.313×10^{-3}	120.2

†Stopped Stirrer pH, $^*[OH^-] = \frac{10^{pH - 13.9965}}{0.7715}$ (25°C and I = 0.1 mol l^{-1}).

Table A3.9 Data for Separation of k_E and k_{EH^+} for the Alkaline Hydrolysis of Glu DMe

$T = (25.00 \pm 0.05)°C$

$I = 0.1$ mol l^{-1}

pH†	$[H^+]$ (mol l^{-1})	$(K_a^T + H^+)$ (mol l^{-1})	$\frac{k_{obs}}{[OH^-]}$ (l mol^{-1} min^{-1})	$\frac{k_{obs}}{[OH^-]}(K_a^T + [H^+])$ (min^{-1})
8.603	3.233×10^{-9}	9.656×10^{-8}	210.1	2.028×10^{-6}
8.804	2.036×10^{-9}	9.536×10^{-8}	184.2	1.755×10^{-6}
9.003	1.287×10^{-9}	9.461×10^{-8}	159.9	1.513×10^{-6}
9.203	8.122×10^{-10}	9.414×10^{-8}	148.0	1.393×10^{-6}
9.205	8.084×10^{-10}	9.413×10^{-8}	145.1	1.365×10^{-6}
9.303	6.451×10^{-10}	9.397×10^{-8}	138.9	1.297×10^{-6}
9.305	6.421×10^{-10}	9.396×10^{-8}	139.9	1.316×10^{-6}
9.599	3.263×10^{-10}	9.365×10^{-8}	131.0	1.236×10^{-6}
9.600	3.256×10^{-10}	9.365×10^{-8}	132.0	1.227×10^{-6}
9.800	2.054×10^{-10}	9.353×10^{-8}	127.1	1.207×10^{-6}
9.803	2.040×10^{-10}	9.353×10^{-8}	129.2	$1.188. \times 10^{-6}$
9.995	1.311×10^{-10}	9.346×10^{-9}	126.2	1.178×10^{-6}
10.204	8.103×10^{-11}	9.341×10^{-8}	123.9	1.158×10^{-6}
10.303	6.451×10^{-11}	9.339×10^{-8}	124.2	1.158×10^{-6}
10.601	3.248×10^{-11}	9.336×10^{-8}	120.0	1.120×10^{-6}
10.604	3.226×10^{-11}	9.336×10^{-8}	121.2	1.139×10^{-6}
10.803	2.040×10^{-11}	9.334×10^{-8}	120.3	1.120×10^{-6}
10.803	2.040×10^{-11}	9.334×10^{-8}	119.8	1.110×10^{-6}
10.903	1.620×10^{-11}	9.334×10^{-8}	120.1	1.111×10^{-6}
10.905	1.613×10^{-11}	9.334×10^{-8}	119.8	1.120×10^{-6}
11.002	1.290×10^{-11}	9.333×10^{-8}	120.2	1.120×10^{-6}

†Using $K_a^T = 9.333 \times 10^{-8}$; $pK_a^T = 7.03$ (25°C and I = 0.1 mol l^{-1}), (Table 4.4).

†Stopped Stirrer pH. $[H^+] = \frac{10^{-pH}}{0.7715}$ (25°C and I = 0.1 mol l^{-1}).

Figure A3.4 Separation of k_E and k_{EH^+} for Alkaline Hydrolysis of Glu DMe

$T = (25.00 \pm 0.05)°C$

$I = 0.1$ mol l^{-1}

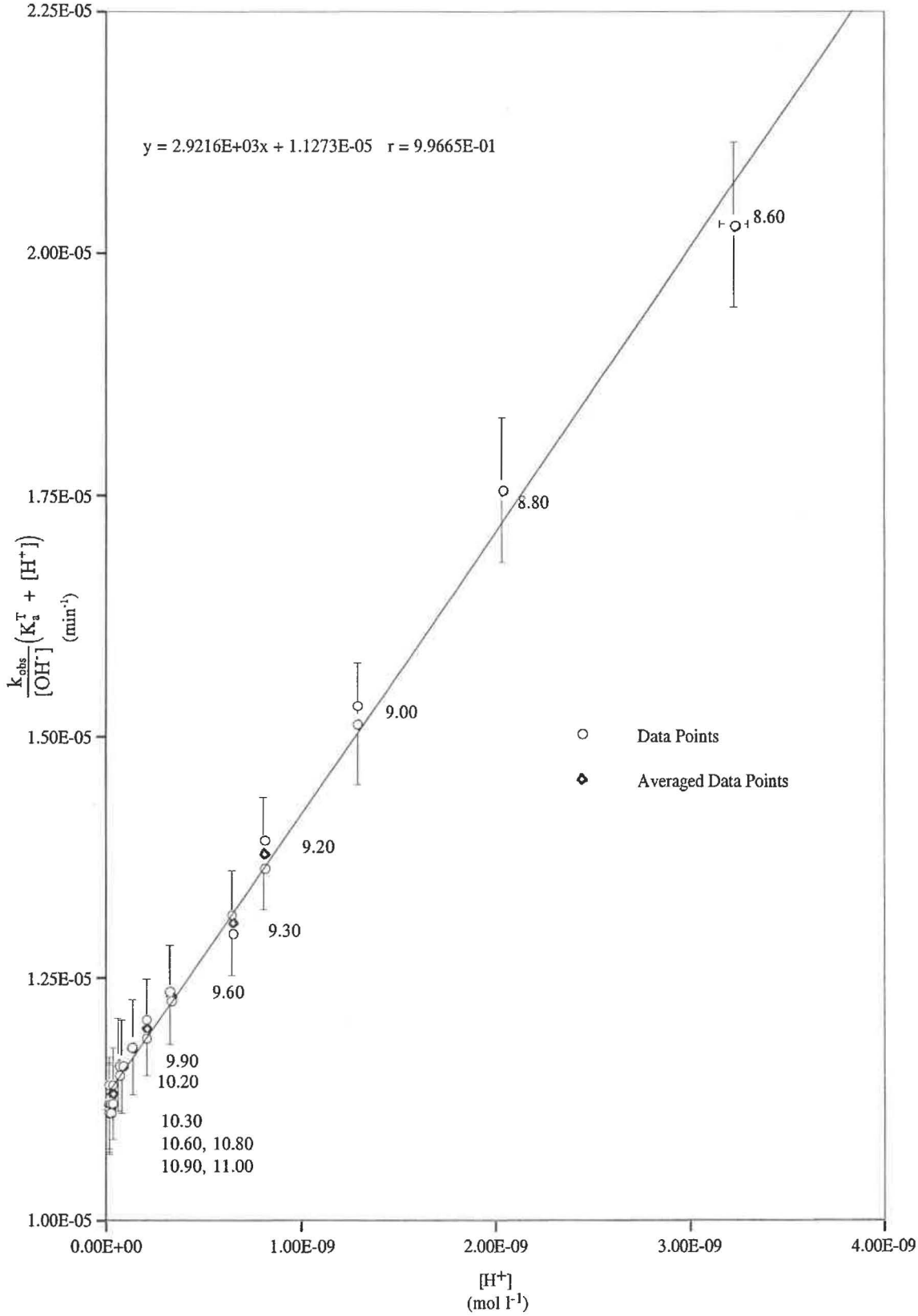

Table A3.10 Effect of pH on the Value of $k_{obs}/[OH^-]$ for 6-AH Et

$T = (25.00 \pm 0.05)°C$

$I = 0.1$ mol l^{-1}

pH†	k_{obs} (min^{-1})	$t_{1/2}$ (min)	$[OH^-]^*$ (mol l^{-1})	$\frac{k_{obs}}{[OH^-]}$ (l mol^{-1} min^{-1})
10.203	2.544×10^{-3}	274.1	2.085×10^{-4}	12.2
810.204	2.529×10^{-3}	274.1	2.090×10^{-4}	12.1
10.305	3.117×10^{-3}	222.8	2.637×10^{-4}	11.8
10.306	3.092×10^{-3}	224.2	2.643×10^{-4}	11.7
10.405	3.752×10^{-3}	184.8	3.320×10^{-4}	11.3
10.406	3.694×10^{-3}	187.6	3.328×10^{-4}	11.1
10.504	4.504×10^{-3}	153.9	4.170×10^{-4}	10.8
10.505	4.556×10^{-3}	152.1	4.180×10^{-4}	10.9
10.605	5.472×10^{-3}	126.7	5.262×10^{-4}	10.4
10.606	5.538×10^{-3}	125.2	5.274×10^{-4}	10.5
10.706	6.574×10^{-3}	105.4	6.640×10^{-4}	9.9
10.707	6.655×10^{-3}	104.2	6.655×10^{-4}	10.0
10.806	7.857×10^{-3}	88.2	8.359×10^{-4}	9.4
10.807	8.043×10^{-3}	86.2	8.378×10^{-4}	9.6
10.907	9.275×10^{-3}	74.7	1.054×10^{-3}	8.8
10.908	9.407×10^{-3}	73.7	1.057×10^{-3}	8.9
11.008	1.091×10^{-2}	63.5	1.331×10^{-3}	8.2
11.009	1.147×10^{-2}	60.4	1.334×10^{-3}	8.6
11.109	1.309×10^{-2}	52.9	1.679×10^{-3}	7.8
11.110	1.346×10^{-2}	51.5	1.683×10^{-3}	8.0

†Stopped Stirrer pH, $^*[OH^-] = \frac{10^{pH - 13.9965}}{0.7715}$ (25°C and I = 0.1 mol l^{-1}).

Table A3.11 Data for Separation of k_E and k_{EH^+} for the Alkaline Hydrolysis of 6-AH Et

$T = (25.00 \pm 0.05)°C$

$I = 0.1$ mol l^{-1}

pH†	$[H^+]$ (mol l^{-1})	$(K_a^T + H^+)$ (mol l^{-1})	$\frac{k_{obs}}{[OH^-]}$ (l mol^{-1} min^{-1})	$\frac{k_{obs}}{[OH^-]}(K_a^T + [H^+])$ (min^{-1})
10.203	8.122×10^{-11}	1.136×10^{-10}	12.2	1.386×10^{-9}
10.204	8.103×10^{-11}	1.134×10^{-10}	12.1	1.372×10^{-9}
10.305	6.422×10^{-11}	9.658×10^{-11}	11.8	1.140×10^{-9}
10.306	6.407×10^{-11}	9.643×10^{-11}	11.7	1.128×10^{-9}
10.405	5.101×10^{-11}	8.337×10^{-11}	11.3	9.421×10^{-10}
10.406	5.089×10^{-11}	8.325×10^{-11}	11.1	9.241×10^{-10}
10.504	4.061×10^{-11}	7.297×10^{-11}	10.8	7.811×10^{-10}
10.505	4.052×10^{-11}	7.288×10^{-11}	10.9	7.944×10^{-10}
10.605	3.219×10^{-11}	6.454×10^{-11}	10.4	6.713×10^{-10}
10.606	3.211×10^{-11}	6.447×10^{-11}	10.5	6.769×10^{-10}
10.706	2.551×10^{-11}	5.787×10^{-11}	10.0	5.729×10^{-10}
10.707	2.545×10^{-11}	5.781×10^{-11}	9.9	5.781×10^{-10}
10.806	2.026×10^{-11}	5.262×10^{-11}	9.4	4.946×10^{-10}
10.807	2.022×10^{-11}	5.257×10^{-11}	9.6	5.047×10^{-10}
10.907	1.606×10^{-11}	4.842×10^{-11}	8.8	4.261×10^{-10}
10.908	1.602×10^{-11}	4.838×10^{-11}	9.0	4.354×10^{-10}
11.008	1.273×10^{-11}	4.509×10^{-11}	8.2	3.697×10^{-10}
11.009	1.270×10^{-11}	4.506×10^{-11}	8.6	3.875×10^{-10}
11.109	1.009×10^{-11}	4.244×10^{-11}	7.8	3.311×10^{-10}
11.110	1.006×10^{-11}	4.242×10^{-11}	8.0	3.394×10^{-10}

Using $K_a^T = 3.236 \times 10^{-11}$; $pK_a^T = 10.49$ (25°C and I = 0.1 mol l^{-1}), (Table 4.3).

†Stopped Stirrer pH. $[H^+] = \frac{10^{-pH}}{0.7715}$ (25°C and I = 0.1 mol l^{-1}).

Figure A3.5 Separation of k_E and k_{EH^+} for Alkaline Hydrolysis of 6-AH Et

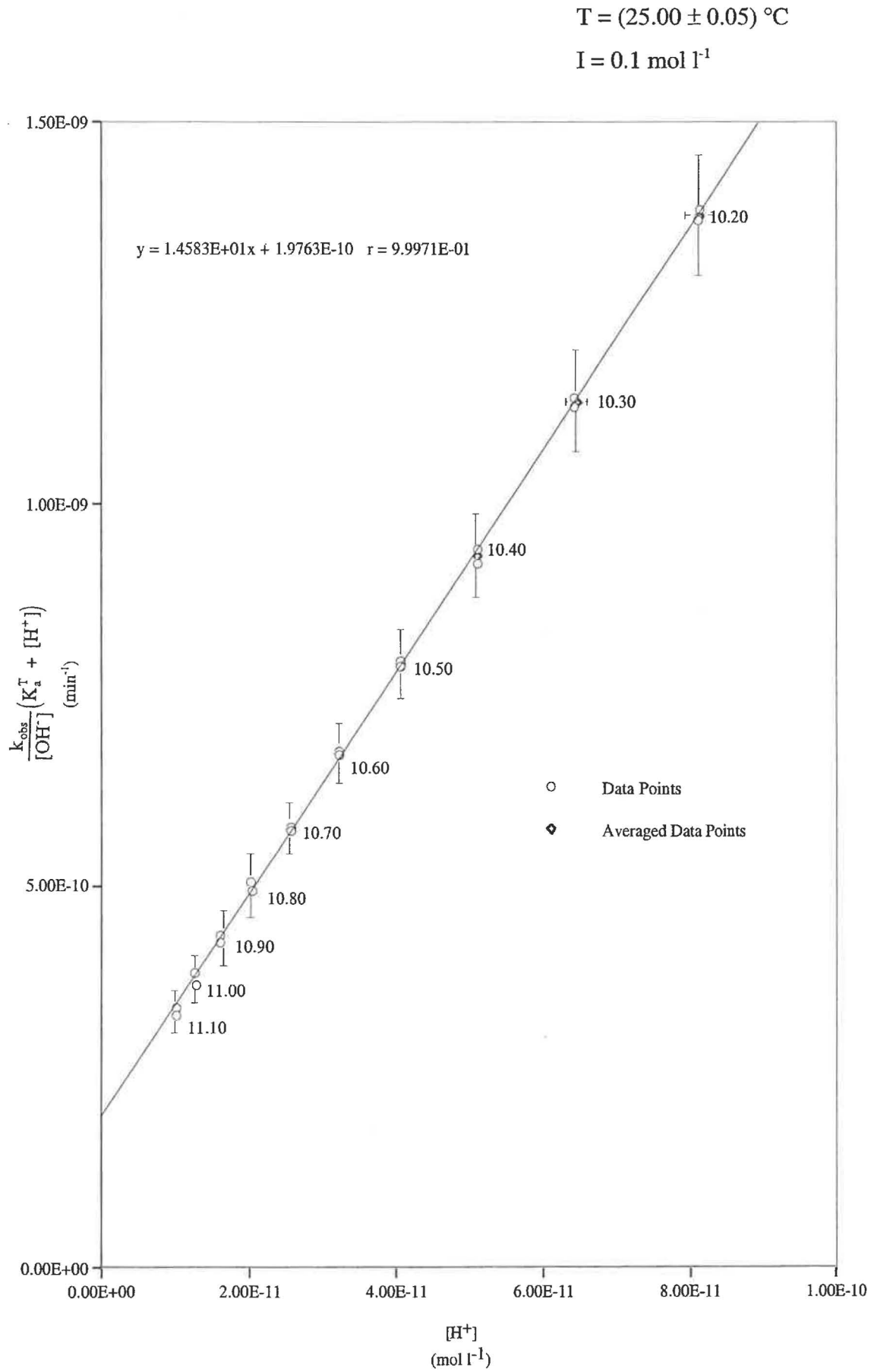

Table A3.12 Effect of pH on the Value of $k_{obs}/[OH^-]$ for 4-AB Et.

$T = (25.00 \pm 0.05)°C$

$I = 0.1$ mol l^{-1}

pH†	k_{obs} (min^{-1})	$t_{1/2}$ (min)	$[OH^-]^*$ (mol l^{-1})	$\frac{k_{obs}}{[OH^-]}$ (l mol^{-1} min^{-1})
9.298	3.854×10^{-3}	179.9	2.595×10^{-5}	148.5
9.299	3.852×10^{-3}	180.0	2.601×10^{-5}	148.1
9.398	5.391×10^{-3}	126.4	3.267×10^{-5}	166.0
9.403	5.486×10^{-3}	126.3	3.305×10^{-5}	165.0
9.489	7.252×10^{-3}	95.6	4.029×10^{-5}	180.0
9.490	7.289×10^{-3}	95.1	4.038×10^{-5}	180.5
9.590	1.022×10^{-2}	67.2	5.084×10^{-5}	202.6
9.590	1.022×10^{-2}	67.2	5.084×10^{-5}	202.6
9.700	1.490×10^{-2}	46.5	6.545×10^{-5}	227.5
9.701	1.493×10^{-2}	46.2	6.564×10^{-5}	227.5
9.800	2.053×10^{-2}	33.8	8.245×10^{-5}	249.0
9.801	2.082×10^{-2}	33.3	8.264×10^{-5}	252.0
9.900	2.823×10^{-2}	24.6	1.038×10^{-4}	272.6
9.902	2.847×10^{-2}	24.3	1.043×10^{-4}	273.0
9.999	3.898×10^{-2}	18.0	1.304×10^{-4}	299.0
10.002	3.979×10^{-2}	17.5	1.313×10^{-4}	303.0
10.100	5.412×10^{-2}	12.8	1.645×10^{-4}	329.0
10.102	5.437×10^{-2}	12.7	1.653×10^{-4}	329.0
10.201	7.452×10^{-2}	9.3	2.076×10^{-4}	359.0

†Stopped Stirrer pH, $^*[OH^-] = \frac{10^{pH\ -\ 13.9965}}{0.7715}$ (25°C and I = 0.1 mol l^{-1}).

Table A3.13 Data for Separation of k_E and k_{EH+} for the Alkaline Hydrolysis of 4-AB Et

$T = (25.00 \pm 0.05)°C$

$I = 0.1$ mol l^{-1}

pH†	$[H^+]$ (mol l^{-1})	$(K_a^T + H^+)$ (l mol^{-1} min^{-1})	$\frac{k_{obs}}{[OH^-]}$ (l mol^{-1} min^{-1})	$\frac{k_{obs}}{[OH^-]}(K_a^T + [H^+])$ (min^{-1})
9.298	6.526×10^{-10}	7.907×10^{-10}	148.5	1.174×10^{-7}
9.299	6.511×10^{-10}	7.892×10^{-10}	148.1	1.168×10^{-7}
9.398	5.125×10^{-10}	6.505×10^{-10}	166.0	1.080×10^{-7}
9.403	5.184×10^{-10}	6.564×10^{-10}	165.0	1.083×10^{-7}
9.489	4.204×10^{-10}	5.584×10^{-10}	180.0	1.005×10^{-7}
9.490	4.194×10^{-10}	5.575×10^{-10}	180.5	1.006×10^{-7}
9.590	3.332×10^{-10}	4.712×10^{-10}	202.6	9.547×10^{-8}
9.590	3.332×10^{-10}	4.712×10^{-10}	202.6	9.547×10^{-8}
9.700	2.580×10^{-10}	3.967×10^{-10}	227.5	9.024×10^{-8}
9.701	2.586×10^{-10}	3.961×10^{-10}	227.5	9.010×10^{-8}
9.800	2.054×10^{-10}	3.345×10^{-10}	249.0	8.552×10^{-8}
9.801	2.050×10^{-10}	3.430×10^{-10}	252.0	8.644×10^{-8}
9.900	1.632×10^{-10}	3.012×10^{-10}	272.6	8.211×10^{-8}
9.902	1.624×10^{-10}	3.005×10^{-10}	273.0	8.203×10^{-8}
9.999	1.299×10^{-10}	2.680×10^{-10}	299.0	8.012×10^{-8}
10.002	1.290×10^{-10}	2.671×10^{-10}	303.0	8.092×10^{-8}
10.100	1.030×10^{-10}	2.410×10^{-10}	329.0	7.929×10^{-8}
10.102	1.025×10^{-10}	2.405×10^{-10}	329.0	7.913×10^{-8}
10.201	8.160×10^{-11}	2.196×10^{-10}	359.0	7.885×10^{-8}

Using $K_a^T = 1.380 \times 10^{-10}$; $pK_a^T = 9.86$ (25°C and I = 0.1 mol l^{-1}), (Table A1.4).

†Stopped Stirrer pH. $[H^+] = \frac{10^{-pH}}{0.7715}$ (at 25.0 °C and I = 0.1 mol l^{-1}).

Figure A3.6 Separation of k_E and k_{EH^+} for Alkaline Hydrolysis of 4-AB Et

$T = (25.00 \pm 0.05)°C$

$I = 0.1 \text{ mol } l^{-1}$

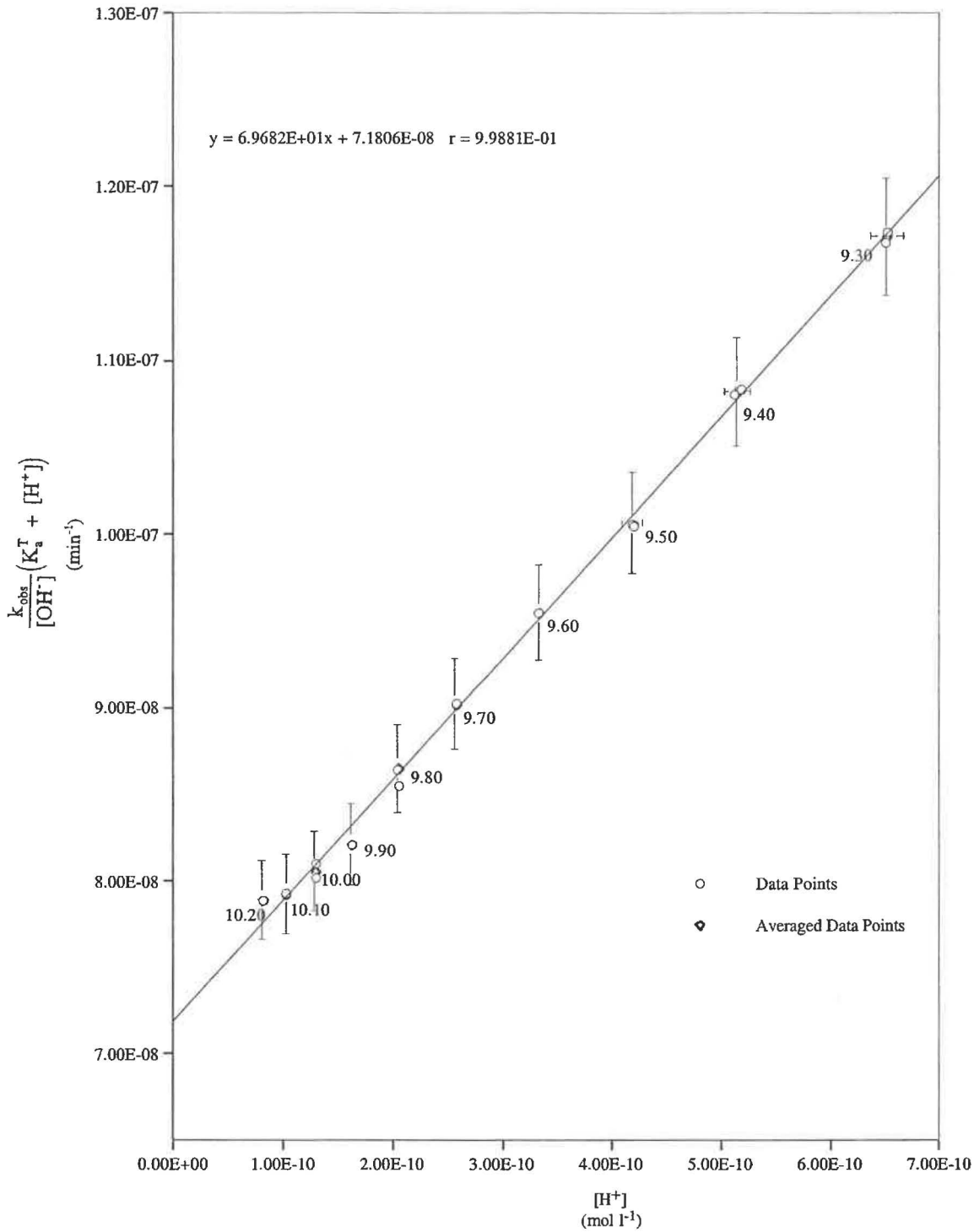

Table A3.14 Effect of pH on the Value of $k_{obs}/[OH^-]$ for 4-AB Bz

$T = (25.00 \pm 0.05)°C$

$I = 0.1$ mol l^{-1}

pH†	k_{obs} (min^{-1})	$t_{1/2}$ (min)	$[OH^-]^*$ (mol l^{-1})	$\frac{k_{obs}}{[OH^-]}$ (l mol^{-1} min^{-1})
9.102	6.195×10^{-3}	111.9	1.653×10^{-5}	374.8
9.202	8.900×10^{-3}	77.9	2.080×10^{-5}	427.9
9.203	8.992×10^{-3}	77.1	2.085×10^{-5}	431.2
9.303	1.272×10^{-3}	54.5	2.625×10^{-5}	484.5
9.303	1.270×10^{-3}	54.6	2.625×10^{-5}	483.9
9.400	1.813×10^{-2}	38.2	3.282×10^{-5}	552.3
9.403	1.828×10^{-3}	37.9	3.305×10^{-5}	553.2
9.503	2.631×10^{-3}	26.3	4.161×10^{-5}	632.4
9.505	2.640×10^{-3}	26.3	4.186×10^{-5}	631.6
9.604	3.750×10^{-3}	18.5	5.250×10^{-5}	714.2
9.605	3.765×10^{-2}	18.4	5.262×10^{-5}	715.4
9.705	5.230×10^{-2}	13.3	6.624×10^{-5}	789.5
9.706	5.250×10^{-2}	13.2	6.640×10^{-5}	790.6
9.805	7.415×10^{-2}	9.3	8.340×10^{-5}	889.1
9.806	7.440×10^{-2}	9.3	8.359×10^{-5}	890.0
9.808	7.463×10^{-2}	9.3	8.398×10^{-5}	888.7
9.905	1.012×10^{-1}	6.8	1.050×10^{-4}	964.1
9.907	1.016×10^{-1}	6.8	1.055×10^{-4}	963.3
10.003	1.429×10^{-1}	4.8	1.316×10^{-4}	1086.3
10.004	1.414×10^{-1}	4.8	1.319×10^{-4}	1072.3

†Stopped Stirrer pH, * $[OH^-] = \frac{10^{pH \,-\, 13.9965}}{0.7715}$ (25°C and I = 0.1 mol l^{-1}).

Table A3.15 Data for Separation of k_E and k_{EH^+} for the Alkaline Hydrolysis of 4-AB Bz

$T = (25.00 \pm 0.05)°C$

$I = 0.1$ mol l^{-1}

pH†	$[H^+]$ (mol l^{-1})	$(K_a^T + H^+)$ (mol l^{-1})	$\frac{k_{obs}}{[OH^-]}$ (l mol^{-1} min^{-1})	$\frac{k_{obs}}{[OH^-]}(K_a^T + [H^+])$ (min^{-1})
9.102	1.025×10^{-9}	1.180×10^{-9}	374.8	4.422×10^{-7}
9.202	8.141×10^{-10}	9.690×10^{-10}	427.9	4.146×10^{-7}
9.203	8.122×10^{-10}	9.671×10^{-10}	431.2	4.170×10^{-7}
9.303	6.452×10^{-10}	8.000×10^{-10}	484.5	3.876×10^{-7}
9.303	6.452×10^{-10}	8.000×10^{-10}	483.9	3.871×10^{-7}
9.400	5.160×10^{-10}	6.709×10^{-10}	552.3	3.705×10^{-7}
9.403	5.125×10^{-10}	6.673×10^{-10}	553.2	3.692×10^{-7}
9.503	4.071×10^{-10}	5.619×10^{-10}	632.4	3.554×10^{-7}
9.505	4.052×10^{-10}	5.601×10^{-10}	631.6	3.537×10^{-7}
9.604	3.226×10^{-10}	4.775×10^{-10}	714.2	3.410×10^{-7}
9.605	3.219×10^{-10}	4.767×10^{-10}	715.4	3.411×10^{-7}
9.705	2.557×10^{-10}	4.105×10^{-10}	789.5	3.241×10^{-7}
9.706	2.551×10^{-10}	4.100×10^{-10}	790.6	3.241×10^{-7}
9.805	2.031×10^{-10}	3.580×10^{-10}	889.1	3.183×10^{-7}
9.806	2.026×10^{-10}	3.575×10^{-10}	890.0	3.182×10^{-7}
9.808	2.017×10^{-10}	3.566×10^{-10}	888.7	3.169×10^{-7}
9.905	1.613×10^{-10}	3.162×10^{-10}	964.1	3.048×10^{-7}
9.907	1.606×10^{-10}	3.155×10^{-10}	963.3	3.039×10^{-7}
10.003	1.287×10^{-10}	2.836×10^{-10}	1086.3	3.081×10^{-7}
10.004	1.284×10^{-10}	2.833×10^{-10}	1072.3	3.038×10^{-7}

Using $K_a^T = 1.549 \times 10^{-10}$; $pK_a^T = 9.81$ (25°C and I = 0.1 mol l^{-1}), (Table A1.5).

†Stopped Stirrer pH. $[H^+] = \frac{10^{-pH}}{0.7715}$ (at 25.0 °C and I = 0.1 mol l^{-1}).

Figure A3.7 Separation of k_E and k_{EH^+} for Alkaline Hydrolysis of 4-AB Bz

$T = (25.00 \pm 0.05)°C$

$I = 0.1 \text{ mol } l^{-1}$

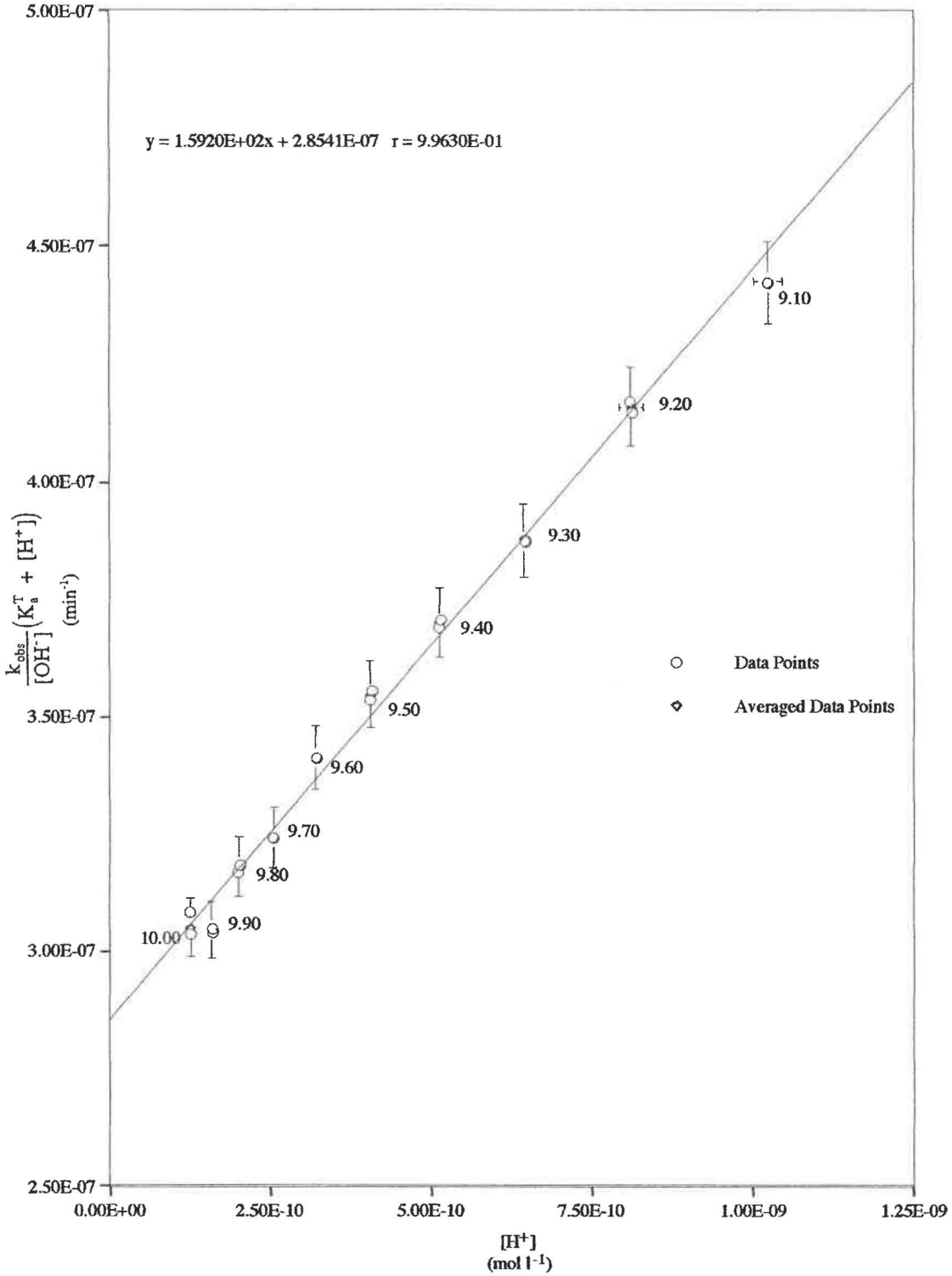

Table A3.16 Effect of pH on the Value of $k_{obs}/[OH^-]$ for 4-MAB Me

$T = (25.00 \pm 0.05)°C$

$I = 0.1$ mol l^{-1}

pH†	k_{obs} (min^{-1})	$t_{1/2}$ (min)	$[OH^-]^*$ (mol l^{-1})	$\frac{k_{obs}}{[OH^-]}$ (l mol^{-1} min^{-1})
8.704	2.841×10^{-3}	244.0	6.609×10^{-6}	429.5
8.706	2.866×10^{-3}	241.9	6.640×10^{-6}	431.6
8.800	4.171×10^{-3}	166.2	8.245×10^{-6}	505.8
8.806	4.268×10^{-3}	162.4	8.359×10^{-6}	510.6
8.900	6.230×10^{-3}	111.3	1.038×10^{-5}	600.2
8.902	6.269×10^{-3}	110.6	1.043×10^{-5}	601.2
9.003	9.536×10^{-3}	72.7	1.316×10^{-5}	724.8
9.005	9.518×10^{-3}	72.8	1.322×10^{-5}	720.1
9.102	1.430×10^{-2}	48.5	1.653×10^{-5}	865.2
9.102	1.431×10^{-2}	48.2	1.653×10^{-5}	869.8
9.200	2.154×10^{-2}	32.2	2.071×10^{-5}	1040.2
9.201	2.165×10^{-2}	32.0	2.076×10^{-5}	1042.8
9.302	3.269×10^{-2}	21.2	2.619×10^{-5}	1248.3
9.303	3.294×10^{-2}	21.0	2.625×10^{-5}	1254.9
9.399	4.885×10^{-2}	14.2	3.275×10^{-5}	1491.8
9.402	4.909×10^{-2}	14.1	3.297×10^{-5}	1489.0
9.501	7.375×10^{-2}	9.4	4.142×10^{-5}	1780.6
9.503	7.450×10^{-2}	9.3	4.151×10^{-5}	1794.9
9.504	7.457×10^{-2}	9.3	4.170×10^{-5}	1788.3

†Stopped Stirrer pH, $^*[OH^-] = \frac{10^{pH - 13.9965}}{0.7715}$ (25°C and I = 0.1 $moll^{-1}$).

Table A3.17 Data for Separation of k_E and k_{EH^+} for the Alkaline Hydrolysis of 4-MAB Me

$T = (25.00 \pm 0.05)°C$

$I = 0.1$ mol l^{-1}

pH†	$[H^+]$ (mol l^{-1})	$(K_a^T + H^+)$ (mol l^{-1})	$\frac{k_{obs}}{[OH^-]}$ (l mol^{-1} min^{-1})	$\frac{k_{obs}}{[OH^-]}(K_a^T + [H^+])$ (min^{-1})
8.704	2.586×10^{-9}	2.686×10^{-9}	429.5	1.154×10^{-6}
8.706	2.551×10^{-9}	2.651×10^{-9}	431.6	1.144×10^{-6}
8.800	2.054×10^{-9}	2.154×10^{-9}	505.8	1.089×10^{-6}
8.806	2.026×10^{-9}	2.128×10^{-9}	510.6	1.086×10^{-6}
8.900	1.632×10^{-9}	1.732×10^{-9}	600.2	1.040×10^{-6}
8.902	1.624×10^{-9}	1.724×10^{-9}	601.2	1.038×10^{-6}
9.003	1.287×10^{-9}	1.387×10^{-9}	724.8	1.006×10^{-6}
9.005	1.281×10^{-9}	1.381×10^{-9}	720.1	9.946×10^{-7}
9.102	1.025×10^{-9}	. 1.125×10^{-9}	865.2	9.730×10^{-7}
9.102	1.025×10^{-9}	1.125×10^{-9}	869.8	9.786×10^{-7}
9.200	8.178×10^{-10}	9.178×10^{-10}	1040.2	9.545×10^{-7}
9.201	8.160×10^{-10}	9.160×10^{-10}	1042.8	9.552×10^{-7}
9.302	6.466×10^{-10}	7.466×10^{-10}	1248.3	9.319×10^{-7}
9.303	$6.452x\ 10^{-10}$	7.452×10^{-10}	1254.9	9.352×10^{-7}
9.399	5.172×10^{-10}	6.172×10^{-10}	1491.8	9.209×10^{-7}
9.402	5.137×10^{-10}	6.136×10^{-10}	1489.0	9.137×10^{-7}
9.501	4.089×10^{-10}	5.089×10^{-10}	1780.6	9.062×10^{-7}
9.503	4.071×10^{-10}	5.071×10^{-10}	1794.9	9.102×10^{-7}
9.504	4.061×10^{-10}	5.061×10^{-10}	1788.3	9.051×10^{-7}

Using $K_a^T = 1.000 \times 10^{-10}$; $pK_a^T = 10.00$ (25°C and I = 0.1 mol l^{-1}), (See Table A1.6).

†Stopped Stirrer pH. $[H^+] = \frac{10^{-pH}}{0.7715}$ (at 25°C and I = 0.1 mol l^{-1}).

Figure A3.8 Separation of k_E and k_{EH^+} for Alkaline Hydrolysis of 4-MAB Me

$T = (25.00 \pm 0.05)°C$

$I = 0.1$ mol l^{-1}

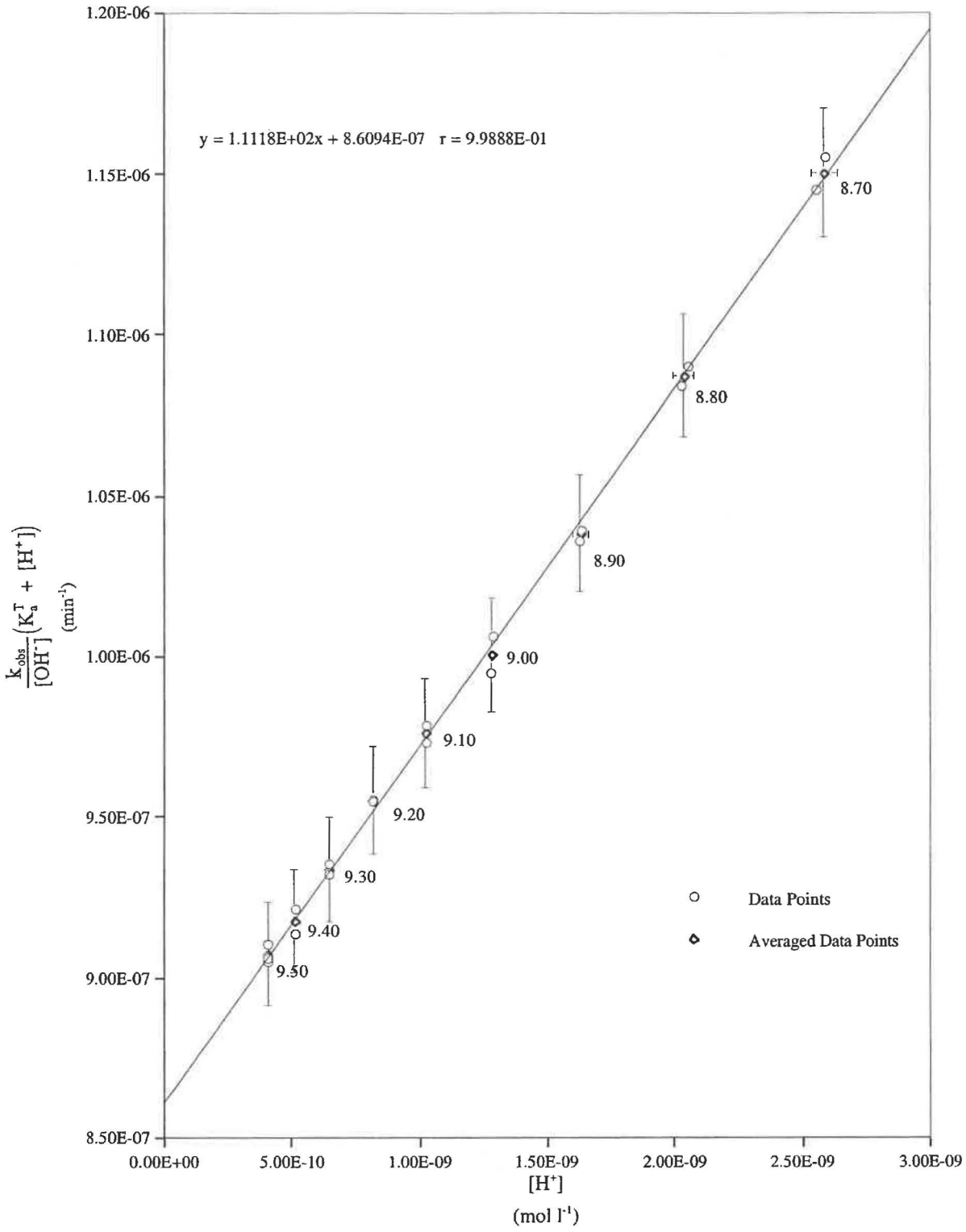

Table A3.18 Effect of pH on the Value of $k_{obs}/[OH^-]$ for 4-MAB Et

$T = (25.00 \pm 0.05)°C$

$I = 0.1$ mol l^{-1}

pH†	k_{obs} (min^{-1})	$t_{1/2}$ (min)	$[OH^-]^*$ (mol l^{-1})	$\frac{k_{obs}}{[OH^-]}$ (l mol^{-1} min^{-1})
9.005	2.951×10^{-3}	235.0	1.322×10^{-5}	223.2
9.102	4.233×10^{-3}	163.7	1.653×10^{-5}	256.1
9.198	6.078×10^{-3}	114.0	2.061×10^{-5}	294.9
9.202	6.302×10^{-3}	110.0	2.080×10^{-5}	303.0
9.301	6.200×10^{-3}	75.3	2.613×10^{-5}	352.1
9.402	1.372×10^{-2}	50.5	3.297×10^{-5}	416.1
9.404	1.372×10^{-2}	50.5	3.313×10^{-5}	414.2
9.503	2.039×10^{-2}	34.0	4.161×10^{-5}	489.9
9.504	2.044×10^{-2}	33.9	4.170×10^{-5}	490.1
9.601	2.962×10^{-2}	23.4	5.214×10^{-5}	568.0
9.602	2.999×10^{-2}	23.1	5.226×10^{-5}	574.0
9.699	4.358×10^{-2}	15.9	6.533×10^{-5}	667.1
9.703	4.450×10^{-2}	15.6	6.594×10^{-5}	674.9
9.795	6.236×10^{-2}	11.1	8.150×10^{-5}	765.1
9.798	6.249×10^{-2}	11.1	8.201×10^{-5}	762.0
9.803	6.488×10^{-2}	10.7	8.302×10^{-5}	781.5
9.900	9.250×10^{-2}	7.5	1.058×10^{-4}	891.2
9.905	9.393×10^{-2}	7.4	1.050×10^{-4}	894.6
10.000	1.333×10^{-1}	5.2	1.307×10^{-4}	1019.7

†Stopped Stirrer pH, $^*[OH^-] = \frac{10^{pH\ -\ 13.9965}}{0.7715}$ (25°C and I = 0.1 mol l^{-1}).

Table A3.19 Data for Separation of k_E and k_{EH^+} for the Alkaline Hydrolysis of 4-MAB Et

$T = (25.00 \pm 0.05)°C$

$I = 0.1$ mol l^{-1}

pH†	$[H^+]$ (mol l^{-1})	$(K_a^T + H^+)$ (mol l^{-1})	$\frac{k_{obs}}{[OH^-]}$ (l mol^{-1} min^{-1})	$\frac{k_{obs}}{[OH^-]}(K_a^T + [H^+])$ (min^{-1})
9.005	1.281×10^{-9}	1.365×10^{-9}	223.2	3.047×10^{-7}
9.102	1.025×10^{-9}	1.108×10^{-9}	256.1	2.838×10^{-7}
9.198	8.216×10^{-10}	9.048×10^{-10}	294.9	2.668×10^{-7}
9.202	8.141×10^{-10}	8.973×10^{-10}	303.0	2.719×10^{-7}
9.301	6.481×10^{-10}	7.313×10^{-10}	352.1	2.575×10^{-7}
9.402	5.137×10^{-10}	5.945×10^{-10}	416.1	2.474×10^{-7}
9.404	5.113×10^{-10}	5.968×10^{-10}	414.2	2.472×10^{-7}
9.503	4.071×10^{-10}	4.902×10^{-10}	489.9	2.402×10^{-7}
9.504	4.061×10^{-10}	4.893×10^{-10}	490.1	2.398×10^{-7}
9.601	3.248×10^{-10}	4.080×10^{-10}	568.0	2.317×10^{-7}
9.602	3.241×10^{-10}	4.073×10^{-10}	574.0	2.338×10^{-7}
9.699	2.592×10^{-10}	3.424×10^{-10}	667.1	2.284×10^{-7}
9.703	2.568×10^{-10}	3.400×10^{-10}	674.9	2.282×10^{-7}
9.795	2.078×10^{-10}	2.910×10^{-10}	765.1	2.292×10^{-7}
9.798	2.064×10^{-10}	2.896×10^{-10}	762.0	2.206×10^{-7}
9.803	2.040×10^{-10}	2.872×10^{-10}	781.5	2.244×10^{-7}
9.900	1.632×10^{-10}	2.464×10^{-10}	891.2	2.195×10^{-7}
9.905	1.613×10^{-10}	2.445×10^{-10}	894.6	2.187×10^{-7}
10.000	1.296×10^{-10}	2.128×10^{-10}	1019.7	2.170×10^{-7}

Using $K_a^T = 8.318 \times 10^{-11}$; $pK_a^T = 10.08$ (25°C and I = 0.1 mol l^{-1}), (Table A1.7).

†Stopped Stirrer pH. $[H^+] = \frac{10^{-pH}}{0.7715}$ (25°C and I = 0.1 mol l^{-1}).

Figure A3.9 Separation of k_E and k_{EH^+} for Alkaline Hydrolysis of 4-MAB Et

$T = (25.00 \pm 0.05)°C$

$I = 0.1$ mol l^{-1}

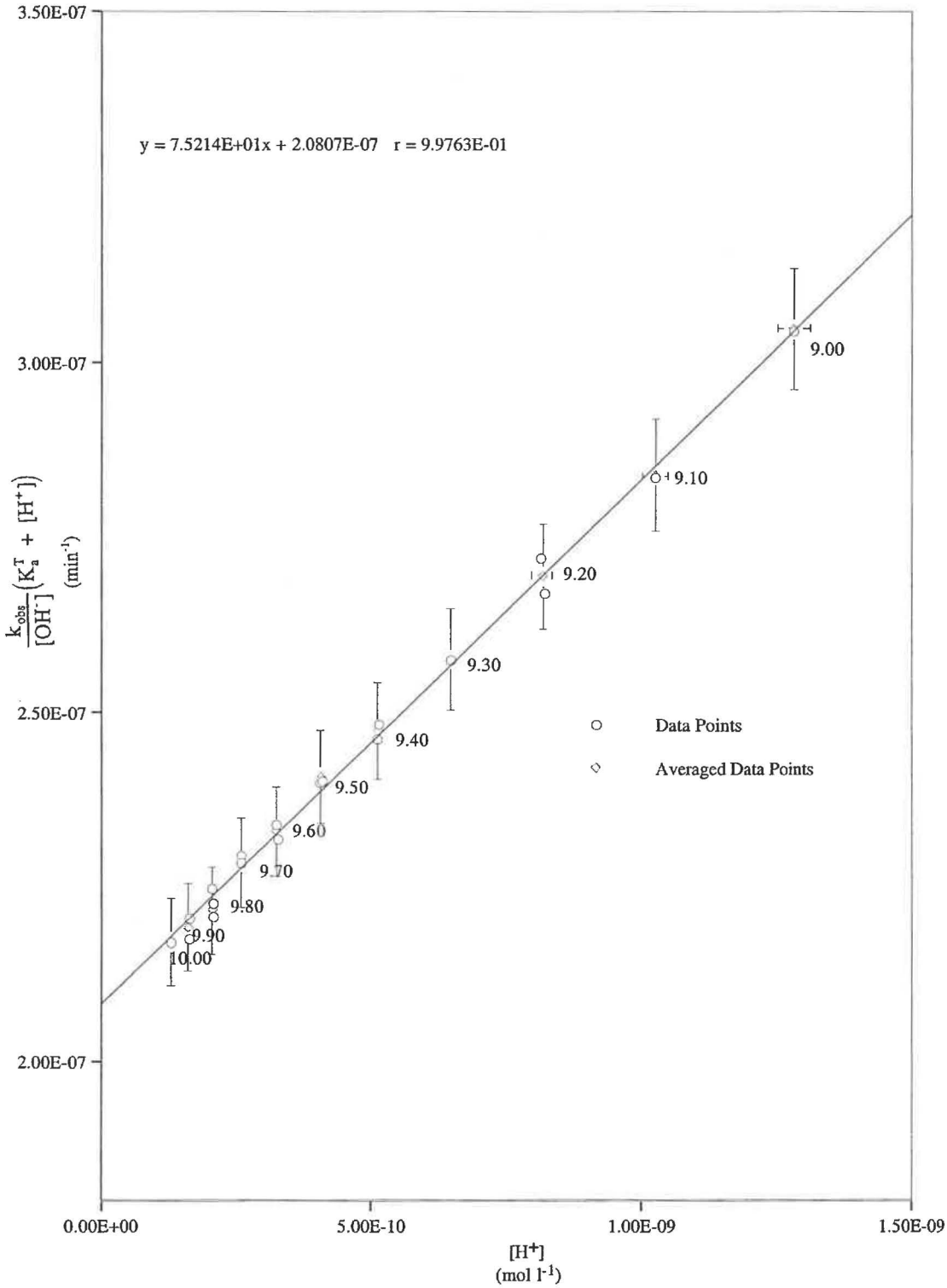

Table A3.20 Effect of pH on the Value of $k_{obs}/[OH^-]$ for 4-A-3-MB Me

$T = (25.00 \pm 0.05)°C$

$I = 0.1$ mol l^{-1}

pH†	k_{obs} (min^{-1})	$t_{1/2}$ (min)	$[OH^-]^*$ (mol l^{-1})	$\frac{k_{obs}}{[OH^-]}$ (l mol^{-1} min^{-1})
8.800	4.996×10^{-3}	138.8	8.244×10^{-6}	606.1
8.801	4.993×10^{-3}	138.7	8.264×10^{-6}	604.3
8.898	7.298×10^{-3}	95.0	1.033×10^{-5}	706.5
8.901	8.003×10^{-3}	86.6	1.119×10^{-5}	715.2
8.990	1.048×10^{-2}	66.2	1.277×10^{-5}	820.3
8.993	1.057×10^{-2}	65.5	1.286×10^{-5}	822.5
9.102	1.602×10^{-2}	43.3	1.652×10^{-5}	970.0
9.103	1.600×10^{-2}	43.3	1.656×10^{-5}	966.4
9.202	2.328×10^{-2}	29.8	2.080×10^{-5}	1119.6
9.202	2.339×10^{-2}	29.6	2.080×10^{-5}	1124.8
9.300	3.337×10^{-2}	20.8	2.607×10^{-5}	1280.2
9.302	3.366×10^{-2}	20.6	2.619×10^{-5}	1285.1
9.403	4.858×10^{-2}	14.3	3.305×10^{-5}	1470.0
9.405	4.865×10^{-2}	14.3	3.320×10^{-5}	1465.6
9.502	6.813×10^{-2}	10.2	4.151×10^{-5}	1641.2
9.504	6.813×10^{-2}	10.2	4.170×10^{-5}	1645.0
9.601	9.534×10^{-2}	7.3	5.214×10^{-5}	1828.6
9.603	9.595×10^{-2}	7.2	5.238×10^{-5}	1831.8

†Stopped Stirrer pH, $^*[OH^-] = \frac{10^{pH\ -\ 13.9965}}{0.7715}$ (25°C and I = 0.1 mol l^{-1}).

Table A3.21 Data for Separation of k_E and k_{EH+} for the Alkaline Hydrolysis of 4-A-3MB Me

$T = (25.00 \pm 0.05)°C$

$I = 0.1$ mol l^{-1}

pH†	$[H^+]$ (mol l^{-1})	$(K_a^T + H^+)$ (mol l^{-1})	$\frac{k_{obs}}{[OH^-]}$ (l mol^{-1} min^{-1})	$\frac{k_{obs}}{[OH^-]}(K_a^T + [H^+])$ (min^{-1})
8.800	2.054×10^{-9}	2.409×10^{-9}	606.1	1.460×10^{-6}
8.801	2.050×10^{-9}	2.404×10^{-9}	604.3	1.453×10^{-6}
8.898	1.639×10^{-9}	1.994×10^{-9}	706.5	1.409×10^{-6}
8.901	1.628×10^{-9}	1.983×10^{-9}	715..2	1.418×10^{-6}
8.999	1.326×10^{-9}	1.681×10^{-9}	820.3	1.379×10^{-6}
8.993	1.317×10^{-9}	1.672×10^{-9}	822.5	1.375×10^{-6}
9.102	1.025×10^{-9}	1.380×10^{-9}	970.0	1.338×10^{-6}
9.103	1.023×10^{-9}	1.377×10^{-9}	966.4	1.331×10^{-6}
9.202	8.141×10^{-10}	1.169×10^{-9}	1119.6	1.309×10^{-6}
9.202	8.141×10^{-10}	1.169×10^{-9}	1124.8	1.315×10^{-6}
9.300	6.496×10^{-10}	1.004×10^{-9}	1280.2	1.286×10^{-6}
9.302	6.466×10^{-10}	1.001×10^{-9}	1285.1	1.287×10^{-6}
9.403	5.125×10^{-10}	8.672×10^{-10}	1470.0	1.275×10^{-6}
9.405	5.101×10^{-10}	8.649×10^{-10}	1465.6	1.267×10^{-6}
9.502	4.080×10^{-10}	7.628×10^{-10}	1641.2	1.252×10^{-6}
9.506	4.061×10^{-10}	7.609×10^{-10}	1645.0	1.252×10^{-6}
9.601	3.248×10^{-10}	6.796×10^{-10}	1828.6	1.243×10^{-6}
9.603	3.233×10^{-10}	6.782×10^{-10}	1831.8	1.242×10^{-6}

Using $K_a^T = 3.548 \times 10^{-10}$; $pK_a^T = 9.45$ (25°C and I = 0.1 mol l^{-1}), (Table A1.8).

†Stopped Stirrer pH. $[H^+] = \frac{10^{-pH}}{0.7715}$ (25°C and I = 0.1 mol l^{-1}).

Graph 3.10 Separation of k_E and k_{EH^+} for Alkaline Hydrolysis of 4-A-3-MB Me

$T = (25.00 \pm 0.05)°C$

$I = 0.1 \text{ mol } l^{-1}$

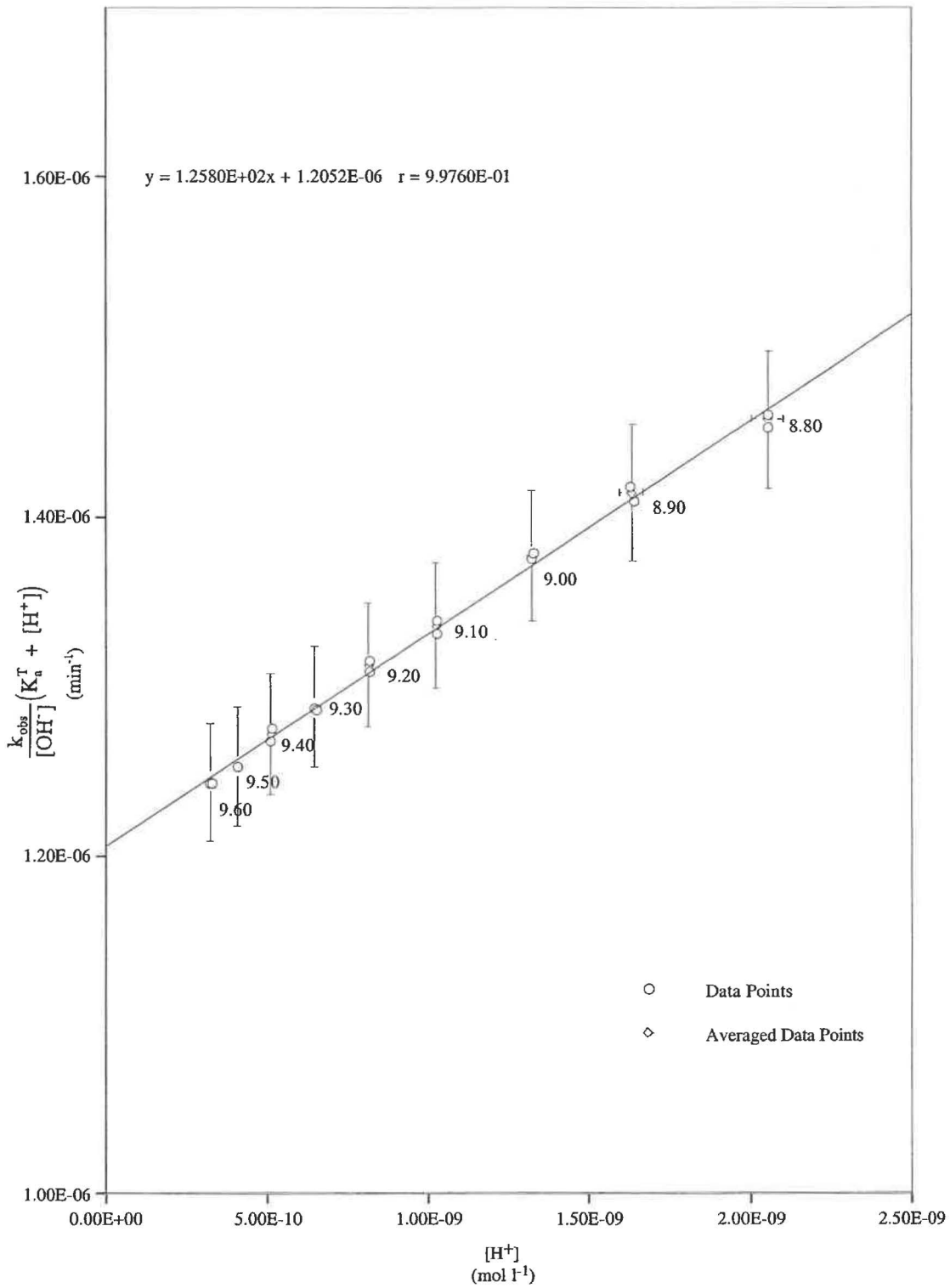

Table A3.22 Effect of pH on the Value of $k_{obs}/[OH^-]$ for 4-A-3,3-DMB Me

$T = (25.00 \pm 0.05)°C$

$I = 0.1$ mol l^{-1}

pH†	k_{obs} (min^{-1})	$t_{1/2}$ (min)	$[OH^-]^*$ (mol l^{-1})	$\frac{k_{obs}}{[OH^-]}$ (l mol^{-1} min^{-1})
8.402	3.891×10^{-3}	178.1	3.297×10^{-6}	1180.2
8.403	3.918×10^{-3}	176.9	3.305×10^{-6}	1185.4
8.501	5.820×10^{-3}	119.1	4.142×10^{-6}	1405.2
8.503	5.859×10^{-3}	118.3	4.161×10^{-6}	1408.1
8.600	8.634×10^{-3}	80.2	5.202×10^{-6}	1659.8
8.602	8.623×10^{-3}	80.4	5.226×10^{-6}	1650.1
8.699	1.261×10^{-2}	56.0	6.534×10^{-6}	1930.0
8.703	1.291×10^{-2}	53.6	6.594×10^{-6}	1958.2
8.799	1.867×10^{-2}	37.1	8.226×10^{-6}	2270.0
8.800	1.876×10^{-2}	36.9	8.244×10^{-6}	2276.1
8.802	1.891×10^{-2}	36.7	8.283×10^{-6}	283.2
8.899	2.758×10^{-2}	25.1	1.035×10^{-5}	2665.0
8.902	2.780×10^{-2}	24.9	1.042×10^{-5}	2668.2
8.998	4.033×10^{-2}	17.2	1.301×10^{-5}	3100.0
9.002	4.070×10^{-2}	17.0	1.313×10^{-5}	3100.4
9.104	5.976×10^{-2}	11.6	1.660×10^{-5}	3600.2
9.106	6.001×10^{-2}	11.5	1.668×10^{-5}	3603.1
9.196	8.300×10^{-2}	8.4	2.052×10^{-5}	4050.2
9.201	8.472×10^{-2}	8.2	2.076×10^{-5}	4081.1

†Stopped Stirrer pH, $^*[OH^-] = \frac{10^{pH - 13.9965}}{0.7715}$ (25°C and I = 0.1 mol l^{-1}).

Table A3.23 Data for Separation of k_E and k_{EH+} for the Alkaline Hydrolysis of 4-A-3, 3-DMB Me

$T = (25.00 \pm 0.05)°C$

$I = 0.1$ mol l^{-1}

pH†	$[H^+]$ (mol l^{-1})	$(K_a^T + H^+)$ (mol l^{-1})	$\frac{k_{obs}}{[OH^-]}$ (l mol^{-1} min^{-1})	$\frac{k_{obs}}{[OH^-]}(K_a^T + [H^+])$ (min^{-1})
8.402	5.136×10^{-9}	5.725×10^{-9}	1180.2	6.756×10^{-6}
8.403	5.125×10^{-9}	5.713×10^{-9}	1185.4	6.770×10^{-6}
8.501	1.089×10^{-9}	4.678×10^{-9}	1405.2	6.573×10^{-6}
8.503	1.071×10^{-9}	4.660×10^{-9}	1408.1	6.561×10^{-6}
8.600	3.256×10^{-9}	3.845×10^{-9}	1659.8	6.344×10^{-6}
8.602	3.240×10^{-9}	3.830×10^{-9}	1650.1	6.357×10^{-6}
8.699	2.592×10^{-9}	3.181×10^{-9}	1930.0	6.139×10^{-6}
8.703	2.568×10^{-9}	3.157×10^{-9}	1958.2	6.188×10^{-6}
8.798	2.063×10^{-9}	2.652×10^{-9}	2270.0	6.020×10^{-6}
8.799	2.059×10^{-9}	2.648×10^{-9}	2276.1	6.027×10^{-6}
8.802	2.045×10^{-9}	2.634×10^{-9}	2283.2	6.013×10^{-6}
8.899	1.636×10^{-9}	2.224×10^{-9}	2665.0	5.928×10^{-6}
8.902	1.624×10^{-9}	2.213×10^{-9}	2668.2	5.904×10^{-6}
8.998	1.302×10^{-9}	1.891×10^{-9}	3100.0	5.862×10^{-6}
9.002	1.290×10^{-9}	1.879×10^{-9}	3100.4	5.825×10^{-6}
9.104	1.020×10^{-9}	1.609×10^{-9}	3600.2	5.792×10^{-6}
9.106	1.015×10^{-9}	1.604×10^{-9}	3603.1	5.776×10^{-6}
9.196	8.254×10^{-10}	1.414×10^{-9}	4050.2	5.721×10^{-6}
9.201	8.160×10^{-10}	1.405×10^{-9}	4081.1	5.732×10^{-6}

Using $K_a^T = 5.888 \times 10^{-10}$; $pK_a^T = 9.23$ (25°C and I = 0.1 mol l^{-1}), (Table A1.9,).

†Stopped Stirrer pH. $[H^+] = \frac{10^{-pH}}{0.7715}$ (25°C and I = 0.1 mol l^{-1}).

Figure A3.11 Separation of k_E and k_{EH^+} for Alkaline Hydrolysis of 4-A-3, 3-DMB Me

$T = (25.00 \pm 0.05)°C$

$I = 0.1$ mol l^{-1}

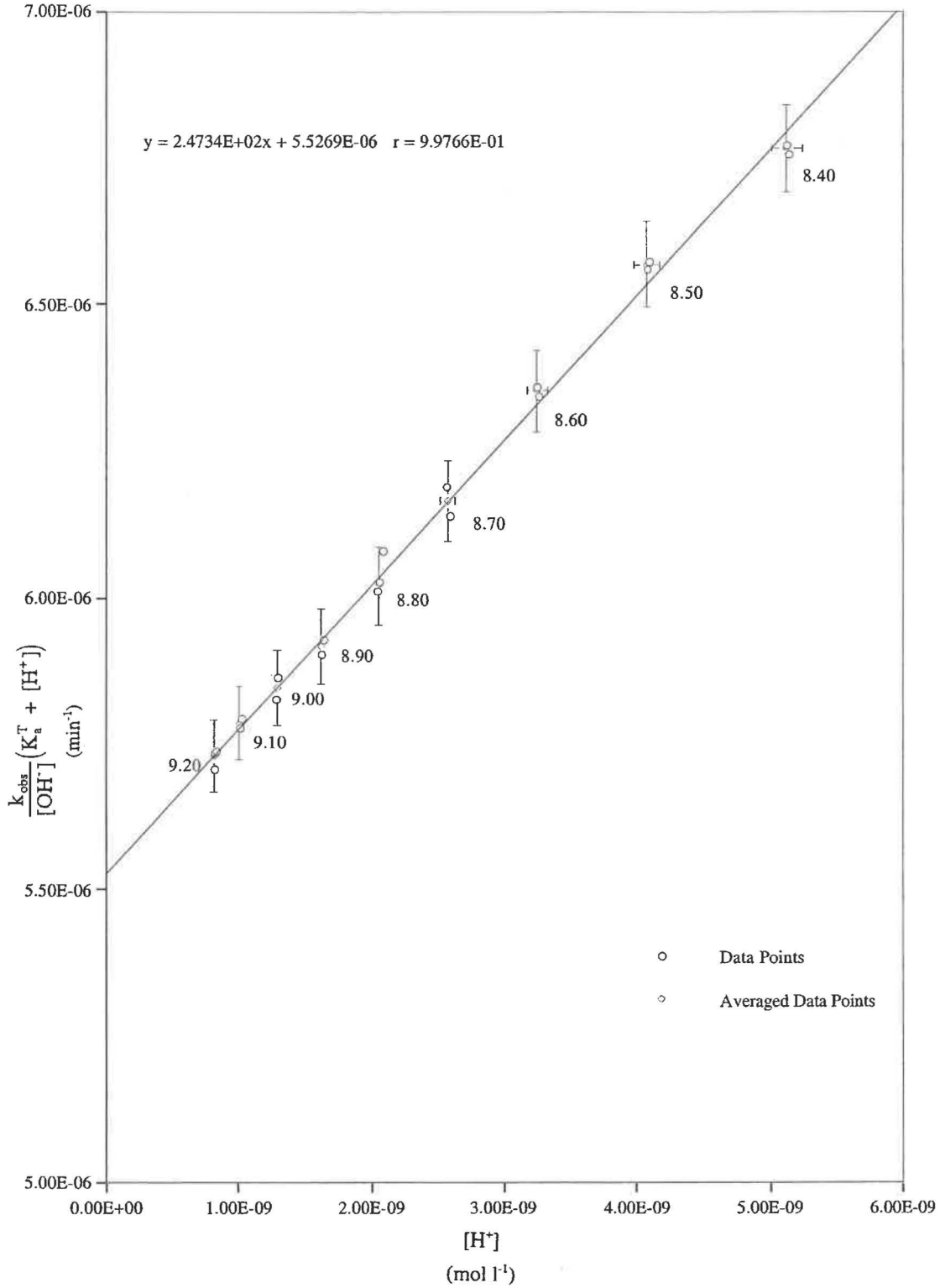

Table A3.24 Effect of the pH on the Value of $k_{obs}/[OH^-]$ for Glu-5-Me

$T = (25.00 \pm 0.05)°C$

$I = 0.1$ mol l^{-1}

pH†	k_{obs} (min^{-1})	$t_{1/2}$ (min)	$[OH^-]^*$ (mol l^{-1})	$\frac{k_{obs}}{[OH^-]}$ (l mol^{-1} min^{-1})
8.701	2.035×10^{-3}	340.5	6.564×10^{-6}	310.1
8.800	2.805×10^{-3}	247.1	8.244×10^{-6}	340.2
8.901	3.796×10^{-3}	182.5	1.040×10^{-5}	365.2
9.000	5.124×10^{-3}	132.9	1.307×10^{-5}	398.9
9.101	7.028×10^{-3}	98.6	1.649×10^{-5}	426.2
9.102	7.076×10^{-3}	98.0	1.653×10^{-5}	428.1
9.201	9.346×10^{-3}	74.2	2.076×10^{-5}	450.2
9.203	9.495×10^{-3}	73.0	2.085×10^{-5}	455.4
9.300	1.259×10^{-2}	55.0	2.607×10^{-5}	483.3
9.302	1.260×10^{-2}	55.0	2.619×10^{-5}	484.0
9.403	1.709×10^{-2}	40.6	3.305×10^{-5}	517.2
9.404	1.723×10^{-2}	40.3	3.313×10^{-5}	520.1
9.504	1.292×10^{-2}	30.2	4.170×10^{-5}	549.8
9.600	3.017×10^{-2}	23.0	5.202×10^{-5}	580.0
9.602	3.035×10^{-2}	22.8	5.226×10^{-5}	580.8
9.700	3.932×10^{-2}	17.6	6.549×10^{-5}	600.4
9.804	5.158×10^{-2}	13.4	8.321×10^{-5}	619.9
9.806	5.209×10^{-2}	13.3	8.359×10^{-5}	623.2
9.903	6.636×10^{-2}	10.4	1.045×10^{-4}	635.0
10.004	8.571×10^{-2}	8.1	1.319×10^{-4}	649.9

†Stopped Stirrer pH, $^*[OH^-] = \frac{10^{pH - 13.9965}}{0.7715}$ (25 °C and I = 0.1 mol l^{-1}).

Table A3.25 Data for Separation of k_E and k_{EH+} for the Alkaline Hydrolysis Glu-5- Me

$T = (25.00 \pm 0.05)°C$

$I = 0.1$ mol l^{-1}

pH†	$[H^+]$ (mol l^{-1})	$(K_a^T + H^+)$ (mol l^{-1})	$\frac{k_{obs}}{[OH^-]}$ (l mol^{-1} min^{-1})	$\frac{k_{obs}}{[OH^-]}(K_a^T + [H^+])$ (min^{-1})
8.701	2.586×10^{-9}	3.457×10^{-9}	310.1	1.148×10^{-6}
8.800	2.054×10^{-9}	2.925×10^{-9}	340.2	1.081×10^{-6}
8.901	1.632×10^{-9}	2.503×10^{-9}	365.0	1.004×10^{-6}
9.000	1.296×10^{-9}	2.167×10^{-9}	398.9	9.646×10^{-7}
9.101	1.030×10^{-9}	1.910×10^{-9}	426.2	9.160×10^{-7}
9.102	1.025×10^{-9}	1.895×10^{-9}	428.1	9.191×10^{-7}
9.201	8.160×10^{-10}	1.687×10^{-9}	450.2	8.843×10^{-7}
9.203	8.122×10^{-10}	1.683×10^{-9}	455.4	8.863×10^{-7}
9.300	6.496×10^{-10}	1.521×10^{-9}	483.3	8.612×10^{-7}
9.302	6.466×10^{-10}	1.518×10^{-9}	484.0	8.583×10^{-7}
9.403	5.125×10^{-10}	1.383×10^{-9}	517.2	$8.454. \times 10^{-7}$
9.404	5.113×10^{-10}	1.382×10^{-9}	520.1	8.495×10^{-7}
9.504	4.061×10^{-10}	1.277×10^{-9}	549.8	8.402×10^{-7}
9.600	3.256×10^{-10}	1.197×10^{-9}	580.0	8.396×10^{-7}
9.602	3.240×10^{-10}	1.195×10^{-9}	580.8	8.399×10^{-7}
9.700	2.586×10^{-10}	1.130×10^{-9}	600.4	8.289×10^{-7}
9.804	2.035×10^{-10}	1.075×10^{-9}	619.9	8.217×10^{-7}
9.806	2.026×10^{-10}	1.074×10^{-9}	623.2	8.255×10^{-7}
9.903	1.621×10^{-10}	1.033×10^{-9}	635.0	8.154×10^{-7}
10.004	1.284×10^{-10}	9.993×10^{-10}	649.9	8.127×10^{-7}

Using $K_a^T = 1.122 \times 10^{-9}$; $pK_a^T = 8.95$ (25°C and I = 0.1 mol l^{-1}), (Table 4.5).

†Stopped Stirrer pH. $[H^+] = \frac{10^{-pH}}{0.7715}$ (25°C and I = 0.1 mol l^{-1}).

Figure A3.12 Separation of k_E and k_{EH^+} for Alkaline Hydrolysis of Glu-5-Me

$T = (25.00 \pm 0.05)°C$

$I = 0.1$ mol l^{-1}

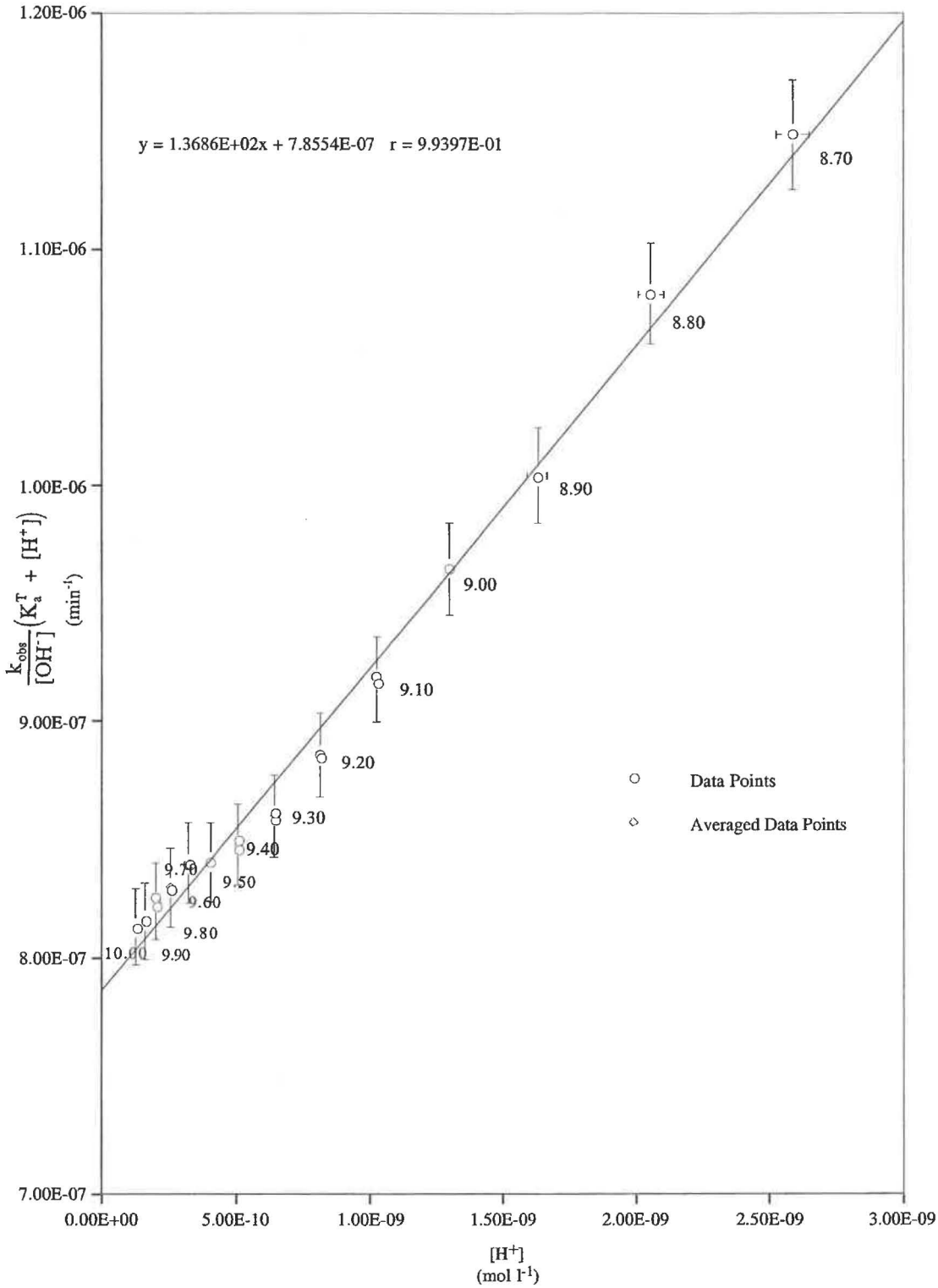

Table A3.26 Effect of pH on the Value of $k_{obs}/[OH^-]$ for 5-Pe Et.

$T = (25.00 \pm 0.05)°C$

$I = 0.1$ mol l^{-1}

pH†	k_{obs} (min^{-1})	$t_{1/2}$ (min)	$[OH^-]^*$ (mol l^{-1})	$\frac{k_{obs}}{[OH^-]}$ (l mol^{-1} min^{-1})
8.698	2.738×10^{-3}	253.2	6.519×10^{-6}	420.0
8.699	2.757×10^{-3}	251.4	6.534×10^{-6}	422.0
8.802	4.199×10^{-3}	165.1	8.283×10^{-6}	506.9
8.803	4.266×10^{-3}	164.0	8.302×10^{-6}	509.0
8.899	6.265×10^{-3}	110.6	1.036×10^{-5}	604.7
8.901	6.325×10^{-3}	109.6	1.040×10^{-5}	608.2
9.002	9.648×10^{-3}	71.8	1.313×10^{-5}	734.8
9.003	9.736×10^{-3}	71.2	1.316×10^{-5}	739.8
9.103	1.487×10^{-2}	46.6	1.656×10^{-5}	898.0
9.104	1.494×10^{-2}	46.4	1.660×10^{-5}	900.0
9.199	2.231×10^{-2}	31.1	2.066×10^{-5}	1079.9
9.200	2.230×10^{-2}	31.1	2.071×10^{-5}	1076.8
9.300	3.389×10^{-2}	20.5	2.607×10^{-5}	1300.0
9.301	3.410×10^{-2}	20.3	2.613×10^{-5}	1305.0
9.402	5.210×10^{-2}	13.3	3.297×10^{-5}	1580.2
9.403	5.238×10^{-2}	13.2	3.305×10^{-5}	1584.9
9.501	7.889×10^{-2}	8.8	4.142×10^{-5}	1904.6
9.502	7.949×10^{-2}	8.7	4.151×10^{-5}	1915.0

†Stopped Stirrer pH, $^*[OH^-] = \frac{10^{pH - 13.9965}}{0.7715}$ (25°C and I = 0.1 mol l^{-1}).

Table A3.27 Data for Separation of k_E and k_{EH^+} for the Alkaline Hydrolysis of 5-APe Et

$T = (25.00 \pm 0.05)°C$

$I = 0.1$ mol l^{-1}

pH†	$[H^+]$ (mol l^{-1})	$(K_a^T + H^+)$ (mol l^{-1})	$\frac{k_{obs}}{[OH^-]}$ (l mol^{-1} min^{-1})	$\frac{k_{obs}}{[OH^-]}(K_a^T + [H^+])$ (min^{-1})
8.698	2.598×10^{-9}	2.678×10^{-9}	420.0	$1.125\ 10^{-6}$
8.699	2.592×10^{-9}	2.672×10^{-9}	422.0	1.125×10^{-6}
8.802	2.045×10^{-9}	2.124×10^{-9}	506.9	1.081×10^{-6}
8.803	2.040×10^{-9}	2.120×10^{-9}	509.0	$1.081x\ 10^{-6}$
8.899	1.636×10^{-9}	1.715×10^{-9}	604.7	1.038×10^{-6}
8.901	1.628×10^{-9}	1.707×10^{-9}	608.2	1.038×10^{-6}
9.002	1.290×10^{-9}	1.370×10^{-9}	734.8	$1.011x\ 10^{-6}$
9.003	1.287×10^{-9}	1.367×10^{-9}	739.8	1.007×10^{-6}
9.103	1.023×10^{-9}	1.102×10^{-9}	898.0	9.917×10^{-7}
9.104	1.020×10^{-9}	1.100×10^{-9}	900.0	9.896×10^{-7}
9.199	8.197×10^{-9}	8.992×10^{-9}	1079.9	9.711×10^{-7}
9.200	8.178×10^{-10}	8.973×10^{-10}	1076.8	$9.664x\ 10^{-7}$
9.300	6.496×10^{-10}	7.291×10^{-10}	1300.0	9.478×10^{-7}
9.301	6.481×10^{-10}	7.276×10^{-10}	1305.0	9.495×10^{-7}
9.402	5.136×10^{-10}	5.931×10^{-10}	1580.2	9.371×10^{-7}
9.402	5.136×10^{-10}	5.931×10^{-10}	1584.9	9.400×10^{-7}
9.501	4.089×10^{-10}	4.884×10^{-10}	1904.6	9.304×10^{-7}
9.502	4.080×10^{-10}	4.874×10^{-10}	1915.0	9.334×10^{-7}

†Using $K_a^T = 7.943 \times 10^{-11}$; $pK_a^T = 10.10$ (25°C and I = 0.1 mol l^{-1}), (Table 4.8).

†Stopped Stirrer pH. $[H^+] = \frac{10^{-pH}}{0.7715}$ (25°C and I = 0.1 mol l^{-1}).

Figure A3.13 Separation of k_E and k_{EH^+} for Alkaline Hydrolysis of 5-APe Et

$T = (25.00 \pm 0.05)°C$

$I = 0.1$ mol l^{-1}

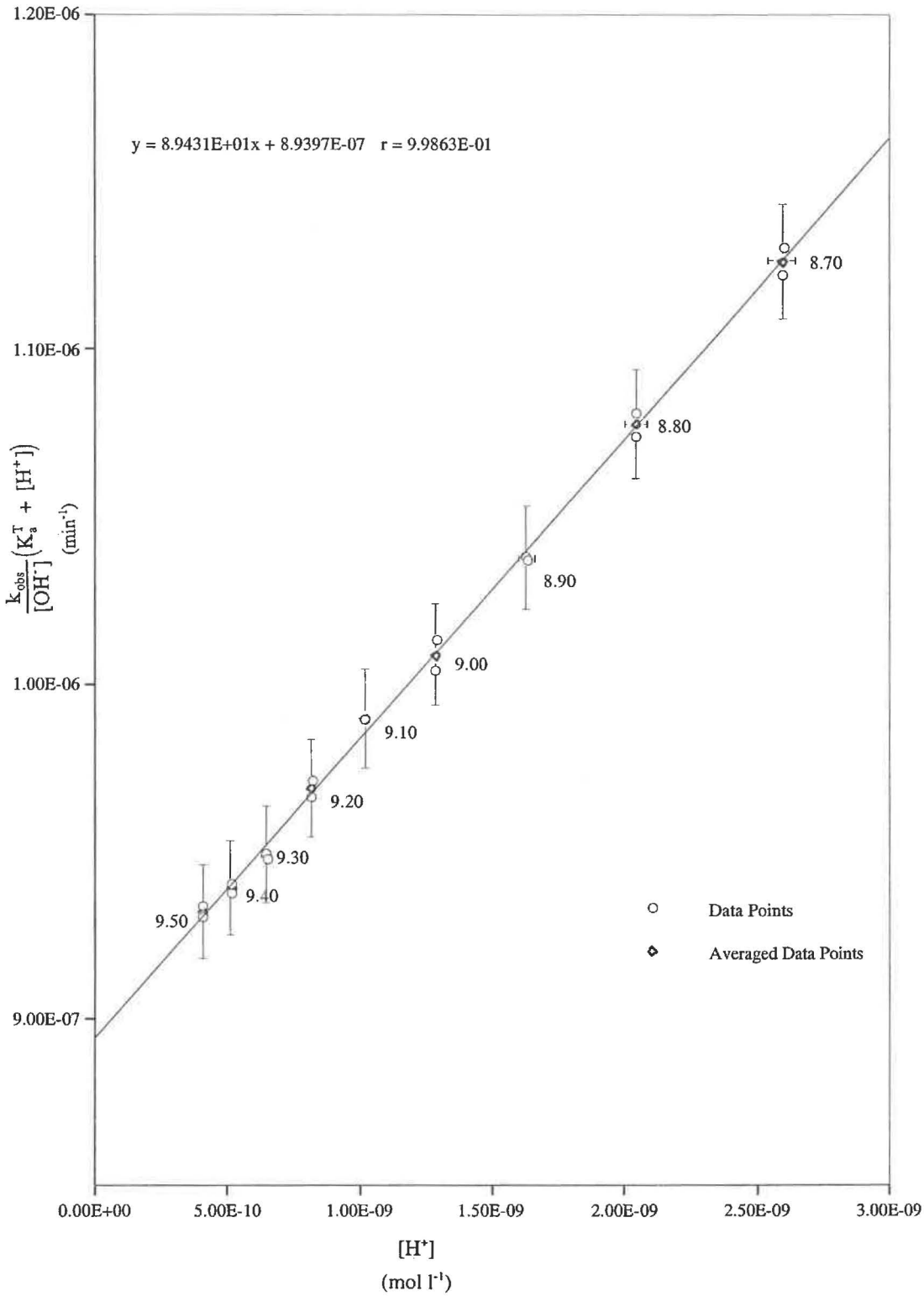

Table A3.28 Effect of pH on the Value of $k_{obs}/[OH^-]$ for P-5-CA Me

$T = (25.00 \pm 0.05)°C$

$I = 0.1$ mol l^{-1}

pH†	k_{obs} (min^{-1})	$t_{1/2}$ (min)	$[OH^-]^*$ (mol l^{-1})	$\frac{k_{obs}}{[OH^-]}$ (l mol^{-1} min^{-1})
9.201	1.966×10^{-2}	35.3	2.076×10^{-5}	947.5
9.203	1.989×10^{-2}	34.9	2.085×10^{-5}	953.6
9.401	3.160×10^{-2}	21.9	3.290×10^{-5}	960.5
9.403	3.166×10^{-2}	21.9	3.305×10^{-5}	957.9
9.603	5.041×10^{-2}	13.8	5.238×10^{-5}	962.3
9.604	5.062×10^{-2}	13.7	5.250×10^{-5}	964.2
9.804	7.933×10^{-2}	8.7	8.321×10^{-5}	953.4
9.805	8.041×10^{-2}	8.6	8.340×10^{-5}	964.2
10.003	1.265×10^{-1}	5.5	1.316×10^{-4}	961.2
10.005	1.261×10^{-1}	5.5	1.322×10^{-4}	954.3
10.203	1.994×10^{-1}	3.5	2.085×10^{-4}	956.3
10.205	2.002×10^{-1}	3.5	2.095×10^{-4}	955.6

†Stopped Stirrer pH, $^*[OH^-] = \frac{10^{pH - 13.9965}}{0.7715}$ (25°C and I = 0.1 mol l^{-1}),

Table A3.29 Effect of pH on the Value of $k_{obs}/[OH^-]$ for P-5-CA Et.[§]

$T = (25.00 \pm 0.05)°C$

$I = 0.1$ mol l^{-1}

pH[†]	k_{obs} (min^{-1})	$t_{1/2}$ (min)	$[OH^-]^*$ (mol l^{-1})	$\frac{k_{obs}}{[OH^-]}$ (l mol^{-1} min^{-1})
9.601	1.315×10^{-2}	52.7	5.214×10^{-5}	252.3
9.602	1.334×10^{-2}	52.0	5.226×10^{-5}	255.3
9.802	2.202×10^{-2}	31.5	8.283×10^{-5}	265.8
9.804	2.224×10^{-2}	31.2	8.321×10^{-5}	267.3
10.001	3.412×10^{-2}	20.3	1.310×10^{-4}	260.5
10.003	3.333×10^{-2}	20.8	1.316×10^{-4}	253.2
10.201	5.326×10^{-1}	13.0	2.076×10^{-4}	256.6
10.203	5.386×10^{-1}	12.9	2.085×10^{-4}	258.3

[§](90% H_3O: 10%EtOH (v/v).

[†]Stopped Stirrer pH, $^*[OH^-] = \frac{10^{-pH\ -\ 13.9965}}{0.7715}$ (25°C and I = 0.1 mol l^{-1}).

*Approximation, since test solutions were not 100% aqueous.

A3.3(b) Summary of Kinetic Tables for Amino Acid Esters at 37.1°C

Section A3.3(b) contain tables that list the effect of pH on the value of $k_{obs}/[OH^-]$, data needed for the separation of k_E and k_{EH^+} and the corresponding pH/rate profiles for the various amino acid ester studied at 37.1°C and I = 0.1 mol l^{-1}.

Table A3.30 Summary of $k_{obs}/[OH^-]$ for Ser Me

T = (37.10 ± 0.05)°C

I = 0.1 mol l^{-1}

pH†	k_{obs} (min^{-1})	$t_{1/2}$ (min)	$[OH^-]^*$ (mol l^{-1})	$\frac{k_{obs}}{[OH^-]}$ (l mol^{-1} min^{-1})
10.310	7.684×10^{-2}	9.0	6.356×10^{-4}	120.9
10.310	7.819×10^{-2}	8.9	6.356×10^{-4}	123.0
10.309	7.633×10^{-2}	9.1	6.342×10^{-4}	120.4
10.309	7.668×10^{-2}	9.0	6.342×10^{-4}	120.9
10.310	7.782×10^{-2}	8.9	6.356×10^{-4}	122.4
10.308	7.731×10^{-2}	9.0	6.327×10^{-4}	122.2
10.311	7.910×10^{-2}	8.8	6.371×10^{-4}	123.4
10.309	7.816×10^{-2}	8.9	6.342×10^{-4}	123.2
10.308	7.585×10^{-2}	9.1	6.327×10^{-4}	119.9
10.309	7.786×10^{-2}	8.9	6.342×10^{-4}	122.7
10.307	7.545×10^{-2}	9.2	6.313×10^{-4}	119.5
10.307	7.614×10^{-2}	9.1	6.313×10^{-4}	120.6
10.308	$7.649x\ 10^{-2}$	9.1	6.327×10^{-4}	120.9
10.306	7.597×10^{-2}	9.1	6.298×10^{-4}	120.6
10.307	7.581×10^{-2}	9.1	6.313×10^{-4}	120.1
10.310	7.697×10^{-2}	9.0	6.356×10^{-4}	121.1
10.309	7.642×10^{-2}	9.1	6.342×10^{-4}	120.5

Overall $k_{obs}/[OH^-]$ = (121 ± 2) l mol^{-1} min^{-1}

†Stopped Stirrer pH, $^*[OH^-] = \frac{10^{pH\ -\ 13.622}}{0.7670}$ (37°C and I = 0.1 mol l^{-1}).

Table A3.31 Effect of pH on the Value of $k_{obs}/[OH^-]$ for 3-AP Bz

$T = (37.10 \pm 0.05)°C$

$I = 0.1$ mol l^{-1}

pH†	k_{obs} (min^{-1})	$t_{1/2}$ (min)	$[OH^-]^*$ (mol l^{-1})	$\frac{k_{obs}}{[OH^-]}$ (l mol^{-1} min^{-1})
8.701	1.278×10^{-2}	54.2	1.564×10^{-5}	817.0
8.909	1.560×10^{-2}	44.4	2.525×10^{-5}	617.9
9.108	1.957×10^{-2}	35.4	3.992×10^{-5}	490.3
9.109	1.926×10^{-2}	36.0	4.001×10^{-5}	481.3
9.307	2.228×10^{-2}	31.1	6.313×10^{-5}	352.9
9.510	2.659×10^{-2}	26.1	1.007×10^{-4}	263.9
9.709	2.901×10^{-2}	23.9	1.593×10^{-4}	182.1
9.910	3.095×10^{-2}	22.4	2.530×10^{-4}	122.3
9.910	3.272×10^{-2}	21.2	2.530×10^{-4}	129.3
10.109	4.049×10^{-2}	17.1	4.001×10^{-4}	101.2
10.110	4.103×10^{-2}	16.9	4.011×10^{-4}	102.3
10.208	4.739×10^{-2}	14.6	5.026×10^{-4}	94.3
10.308	4.587×10^{-2}	15.1	$6.327x\ 10^{-4}$	72.5
10.310	4.322×10^{-2}	16.0	6.356×10^{-4}	68.0
10.408	4.962×10^{-2}	14.0	7.965×10^{-4}	62.3
10.410	5.057×10^{-2}	13.7	8.002×10^{-4}	63.2
10.510	5.682×10^{-2}	12.2	1.007×10^{-3}	56.4
10.511	5.675×10^{-2}	12.2	1.010×10^{-3}	56.2
10.610	6.874×10^{-2}	10.1	1.268×10^{-3}	54.2
10.611	7.030×10^{-2}	9.9	1.271×10^{-3}	55.3

†Stopped Stirrer pH, $^*[OH^-] = \frac{10^{pH\ -\ 13.622}}{0.7670}$ (37°C and I = 0.1 mol l^{-1}).

Table A3.32 Data for Separation of k_E and k_{EH^+} for the Alkaline Hydrolysis of 3-AP Bz

$T = (37.10 \pm 0.05)°C$

$I = 0.1$ mol l^{-1}

pH†	$[H^+]$ (mol l^{-1})	$(K_a^T + H^+)$ (mol l^{-1})	$\frac{k_{obs}}{[OH^-]}$ (l mol^{-1} min^{-1})	$\frac{k_{obs}}{[OH^-]}(K_a^T + [H^+])$ (min^{-1})
8.707	2.560×10^{-9}	4.602×10^{-9}	817.0	3.759×10^{-6}
8.909	1.608×10^{-9}	3.649×10^{-9}	617.9	2.255×10^{-6}
9.108	1.017×10^{-9}	3.058×10^{-9}	490.3	1.500×10^{-6}
9.109	1.014×10^{-9}	3.056×10^{-9}	481.3	1.471×10^{-6}
9.307	6.430×10^{-10}	2.685×10^{-9}	352.9	9.474×10^{-7}
9.510	4.029×10^{-10}	2.445×10^{-9}	263.9	6.451×10^{-7}
9.709	2.548×10^{-10}	2.297×10^{-9}	182.1	4.182×10^{-7}
9.910	1.604×10^{-10}	2.202×10^{-9}	122.3	2.693×10^{-7}
9.910	1.604×10^{-10}	2.202×10^{-9}	129.3	2.847×10^{-7}
10.109	1.014×10^{-10}	2.143×10^{-9}	101.2	2.169×10^{-7}
10.110	1.012×10^{-10}	2.143×10^{-9}	102.3	2.192×10^{-7}
10.208	8.076×10^{-11}	2.122×10^{-9}	94.3	2.002×10^{-7}
10.308	6.415×10^{-11}	2.106×10^{-9}	72.5	1.527×10^{-7}
10.310	6.386×10^{-11}	2.106×10^{-9}	68.0	1.432×10^{-7}
10.408	5.096×10^{-11}	2.093×10^{-9}	62.3	1.304×10^{-7}
10.410	5.072×10^{-11}	2.092×10^{-9}	63.2	1.322×10^{-7}
10.510	4.029×10^{-11}	2.082×10^{-9}	56.4	1.174×10^{-7}
10.511	4.020×10^{-11}	2.082×10^{-9}	56.2	1.170×10^{-7}
10.610	3.200×10^{-11}	2.074×10^{-9}	54.2	1.124×10^{-7}
10.611	3.193×10^{-11}	2.074×10^{-9}	55.3	1.147×10^{-8}

Using $K_a^T = 2.042 \times 10^{-9}$; $pK_a^T = 8.69$ (37°C and I = 0.1 mol l^{-1}), (Table A1.12).

†Stopped Stirrer pH. $[H^+] = \frac{10^{-pH}}{0.7670}$ (37°C and I = 0.1 mol l^{-1}).

Figure A3.14 Separation of k_E and k_{EH^+} for Alkaline Hydrolysis of 3-AP Bz

$T = (37.10 \pm 0.05)°C$

$I = 0.1$ mol l^{-1}

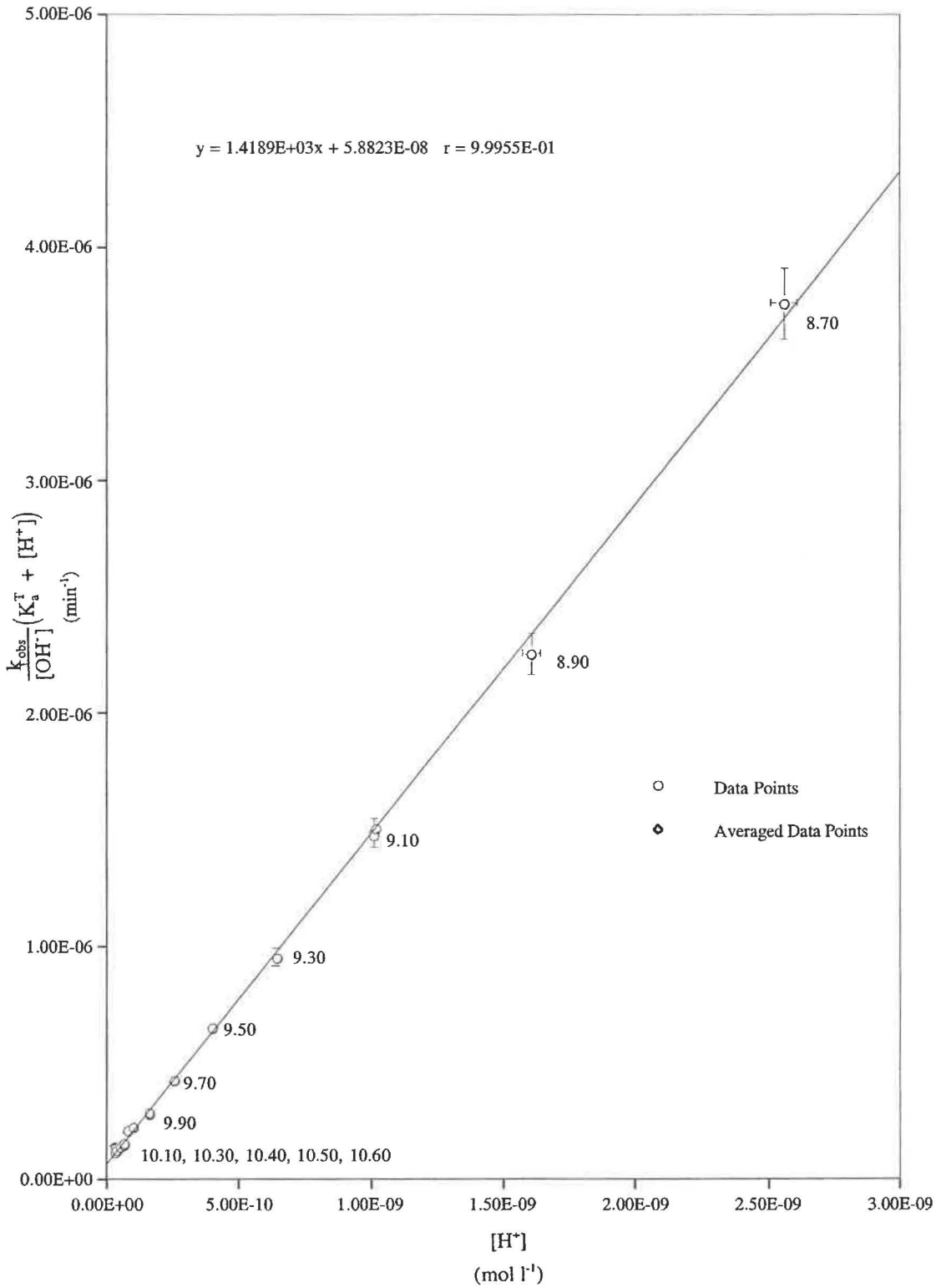

Table A3.33 Effect of pH on the Value of $k_{obs}/[OH^-]$ for 4-DMAB Me.

$T = (37.10 \pm 0.05)°C$

$I = 0.1$ mol l^{-1}

pH†	k_{obs} (min^{-1})	$t_{1/2}$ (min)	$[OH^-]^*$ (mol l^{-1})	$\frac{k_{obs}}{[OH^-]}$ (1 mol^{-1} min^{-1})
10.005	2.806×10^{-2}	24.7	3.149×10^{-4}	89.1
10.006	2.803×10^{-2}	24.7	3.156×10^{-4}	88.8
10.304	3.567×10^{-2}	19.4	6.269×10^{-4}	56.9
10.501	4.302×10^{-2}	16.1	9.867×10^{-4}	43.6
10.502	4.282×10^{-2}	16.2	9.890×10^{-4}	43.3
10.703	5.232×10^{-2}	13.2	1.571×10^{-3}	33.3
10.806	5.995×10^{-2}	11.6	1.992×10^{-3}	30.1
10.807	6.029×10^{-2}	11.5	1.996×10^{-3}	30.2

†Stopped Stirrer pH, $^*[OH^-] = \frac{10^{pH\ -\ 13.622}}{0.7670}$, (37°C and I = 0.1 mol l^{-1}).

Table A3.34 Data for Separation of k_E and k_{EH^+} for the Alkaline Hydrolysis 4-DMAB Me.

$T = (37.10 \pm 0.05)°C$

$I = 0.1$ mol l^{-1}

pH†	$[H^+]$ (mol l^{-1})	$(K_a^T + H^+)$ (mol l^{-1})	$\frac{k_{obs}}{[OH^-]}$ (1 mol^{-1} min^{-1})	$\frac{k_{obs}}{[OH^-]}(K_a^T + [H^+])$ (min^{-1})
10.005	1.289×10^{-10}	9.232×10^{-10}	89.1	8.226×10^{-8}
10.006	1.286×10^{-10}	9.229×10^{-10}	88.8	8.196×10^{-8}
10.304	6.474×10^{-11}	8.591×10^{-10}	56.9	4.888×10^{-8}
10.501	4.113×10^{-11}	8.355×10^{-10}	43.6	3.643×10^{-8}
10.502	4.104×10^{-11}	8.354×10^{-10}	43.3	3.617×10^{-8}
10.703	2.583×10^{-11}	8.202×10^{-10}	33.3	2.731×10^{-8}
10.806	2.038×10^{-11}	8.147×10^{-10}	30.1	2.452×10^{-8}
10.807	2.033×10^{-11}	8.147×10^{-10}	30.2	2.460×10^{-8}

Using $K_a^T = 7.943 \times 10^{-10}$; $pK_a^T = 9.10$ (37.1°C and I = 0.1 mol l^{-1}), (Table A1.13).

†Stopped Stirrer pH, $[H^+] = \frac{10^{-pH}}{0.7670}$ (37°C and I = 0.1 mol l^{-1})

Figure A3.15 Separation of k_E and k_{EH^+} for Alkaline Hydrolysis of 4-DMAB Me

$T = (37.10 \pm 0.05)°C$

$I = 0.1$ mol l^{-1}

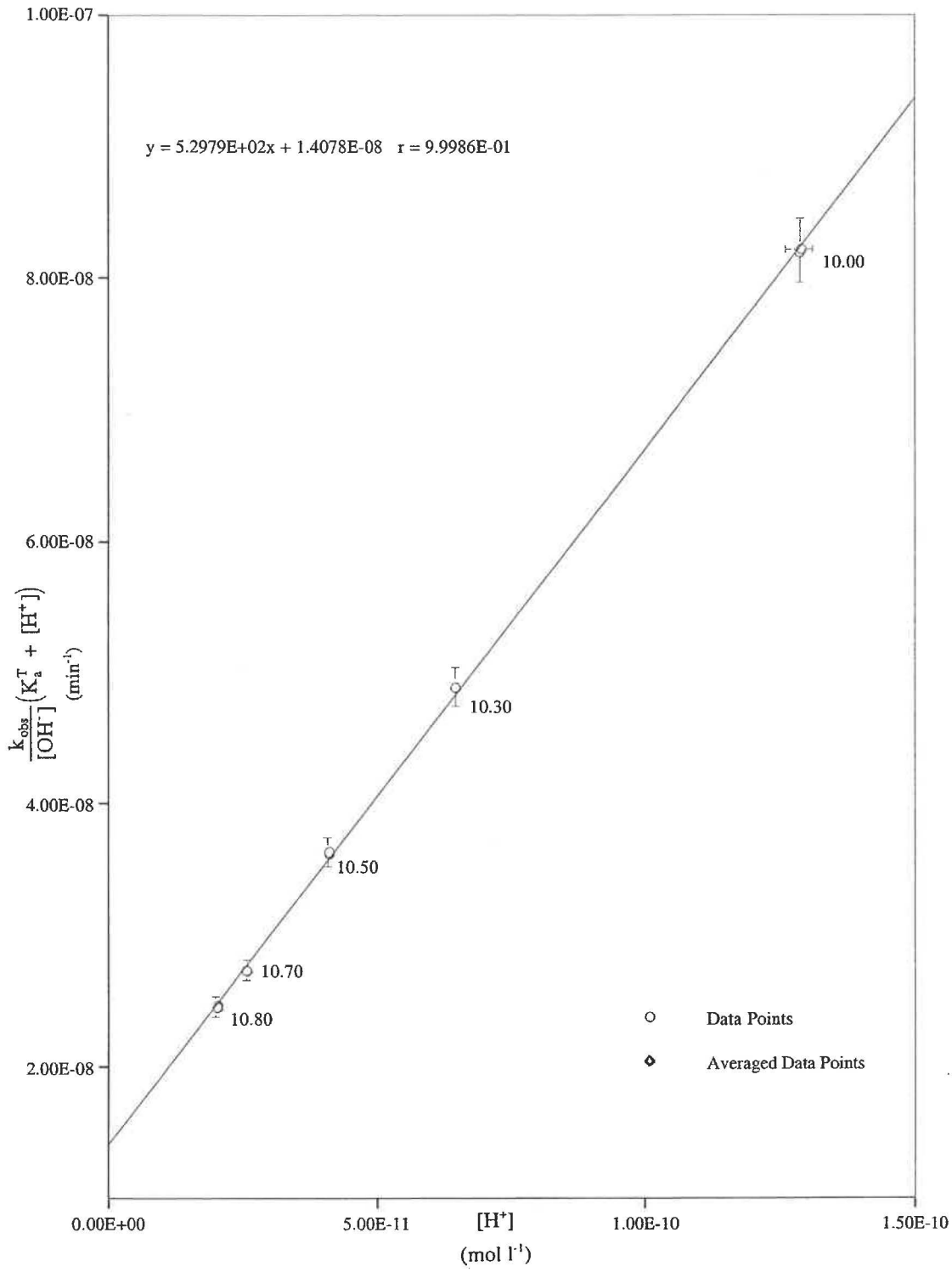

Table A3.35 Effect of pH on the Value of $k_{obs}/[OH^-]$ for 4-DMAB Et

$T = (37.10 \pm 0.05)°C$

$I = 0.1$ mol l^{-1}

pH†	k_{obs} (min^{-1})	$t_{1/2}$ (min)	$[OH^-]^*$ (mol l^{-1})	$\frac{k_{obs}}{[OH^-]}$ (l mol^{-1} min^{-1})
10.006	1.626×10^{-2}	42.6	3.156×10^{-4}	51.5
10.204	1.828×10^{-2}	37.9	4.980×10^{-4}	36.7
10.205	1.912×10^{-2}	36.3	4.991×10^{-4}	38.3
10.405	2.254×10^{-2}	30.7	7.911×10^{-4}	28.5
10.605	2.708×10^{-2}	25.6	1.254×10^{-3}	21.6
10.606	2.702×10^{-2}	25.7	1.257×10^{-3}	21.5
10.806	3.147×10^{-2}	22.0	1.992×10^{-3}	15.8
10.807	3.174×10^{-2}	21.8	1.996×10^{-3}	15.9

†Stopped Stirrer pH, $^*[OH^-] = \frac{10^{pH\ -\ 13.622}}{0.7670}$, (37°C and I = 0.1 mol l^{-1})

Table A3.36 Data for Separation of k_E and k_{EH^+} for the Alkaline Hydrolysis of 4-DMAB Et

$T = (37.10 \pm 0.05)°C$

$I = 0.1$ mol l^{-1}

pH†	$[H^+]$ (mol l^{-1})	$(K_a^T + H^+)$ (mol l^{-1})	$\frac{k_{obs}}{[OH^-]}$ (l mol^{-1} min^{-1})	$\frac{k_{obs}}{[OH^-]}(K_a^T + [H^+])$ (min^{-1})
10.006	1.286×10^{-10}	1.084×10^{-9}	51.5	5.580×10^{-8}
10.204	8.151×10^{-11}	1.037×10^{-9}	36.7	3.804×10^{-8}
10.205	8.132×10^{-11}	1.036×10^{-9}	38.3	3.969×10^{-8}
10.405	5.131×10^{-11}	1.006×10^{-9}	28.5	2.868×10^{-8}
10.605	3.237×10^{-11}	9.874×10^{-10}	21.6	2.133×10^{-8}
10.606	3.230×10^{-11}	9.873×10^{-10}	21.5	2.123×10^{-8}
10.806	2.038×10^{-11}	9.754×10^{-10}	15.8	1.541×10^{-8}
10.807	2.033×10^{-11}	9.753×10^{-10}	15.9	1.551×10^{-8}

Using $K_a^T = 9.549 \times 10^{-10}$; $pK_a^T = 9.02$ (37°C and I = 0.1 mol l^{-1}), (Table A1.14).

†Stopped Stirrer pH, $[H^+] = \frac{10^{-pH}}{0.7670}$ (37°C and I = 0.1 mol l^{-1}

Figure A3.16 Separation of k_E and k_{EH^+} for Alkaline Hydrolysis of 4-DMAB Et

$T = (37.10 \pm 0.05)°C$

$I = 0.1$ mol l^{-1}

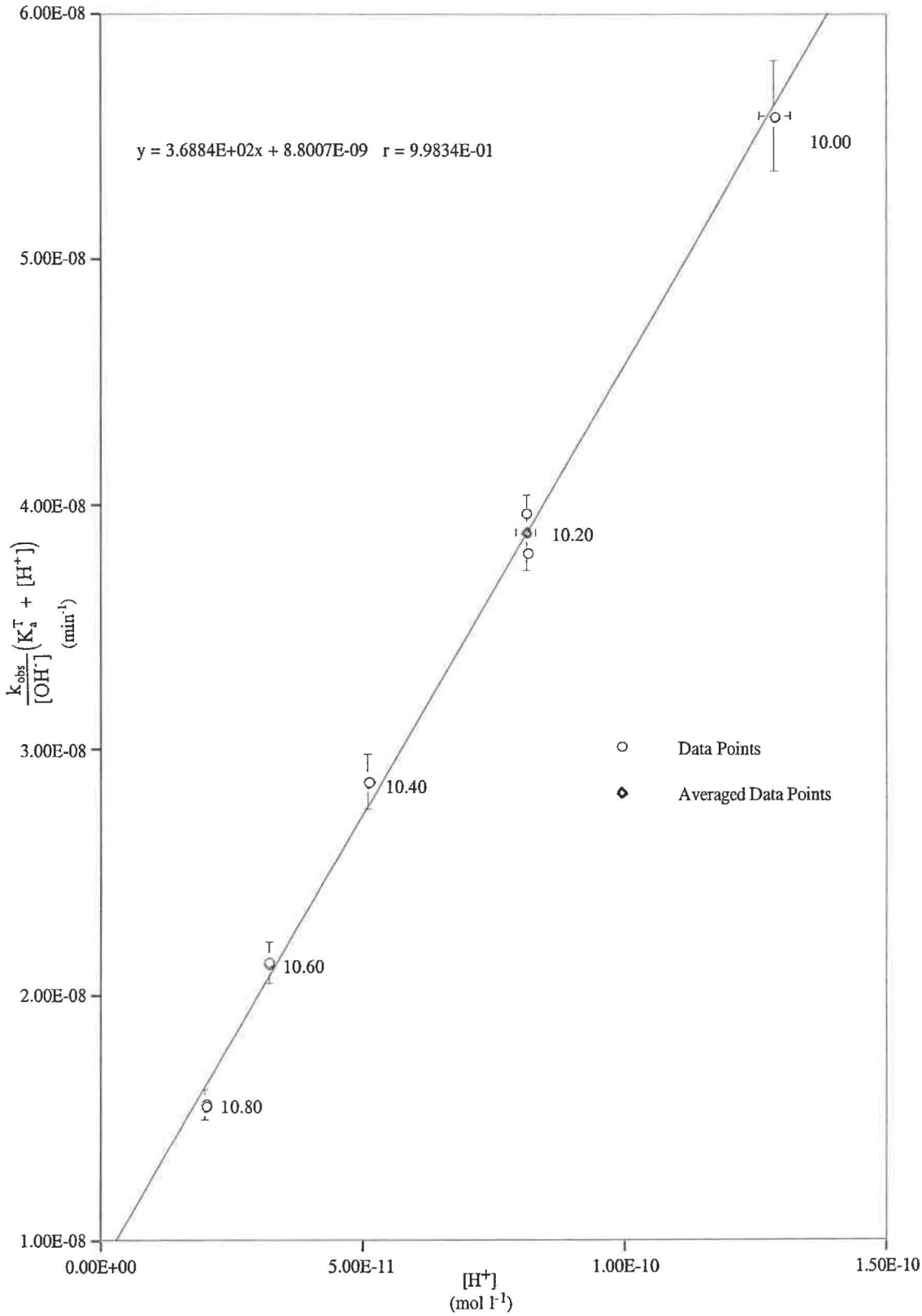

Table A3.37 Effect of pH on the Value of $k_{obs}/[OH^-]$ for 4-AB Me

$T = (37.10 \pm 0.05)°C$

$I = 0.1$ mol l^{-1}

pH†	k_{obs} (min^{-1})	$t_{1/2}$ (min)	$[OH^-]^*$ (mol l^{-1})	$\frac{k_{obs}}{[OH^-]}$ (l mol^{-1} min^{-1})
8.701	7.425×10^{-3}	93.3	1.564×10^{-5}	474.8
8.801	1.026×10^{-2}	67.6	1.969×10^{-5}	521.2
8.803	1.036×10^{-2}	66.9	1.978×10^{-5}	523.9
8.902	1.498×10^{-2}	46.3	2.484×10^{-5}	602.8
8.904	1.533×10^{-2}	45.2	2.496×10^{-5}	614.4
9.002	2.159×10^{-2}	32.1	3.128×10^{-5}	690.2
9.003	2.148×10^{-2}	32.3	3.135×10^{-5}	685.1
9.101	3.097×10^{-2}	22.4	3.928×10^{-5}	788.3
9.102	3.081×10^{-2}	22.5	3.937×10^{-5}	782.5
9.202	4.289×10^{-2}	16.2	4.957×10^{-5}	865.2
9.203	4.399×10^{-2}	15.8	4.968×10^{-5}	885.4
9.303	6.178×10^{-2}	11.2	5.255×10^{-5}	987.7
9.304	6.218×10^{-2}	11.1	6.269×10^{-5}	991.9
9.405	8.738×10^{-2}	7.9	7.911×10^{-5}	1104.6
9.406	8.791×10^{-2}	7.9	7.929×10^{-5}	1108.7
9.507	1.244×10^{-1}	5.6	1.000×10^{-4}	1243.6
9.508	1.270×10^{-1}	5.5	1.003×10^{-4}	1266.3

†Stopped Stirrer pH, $^*[OH^-] = \frac{10^{pH - 13.622}}{0.7670}$ (37°C and I = 0.1 mol l^{-1}).

Table A3.38 Data for Separation of k_E and k_{EH+} for the Alkaline Hydrolysis of 4-AB Me

$T = (37.10 \pm 0.05)°C$

$I = 0.1$ mol l^{-1}

pH†	$[H^+]$ (mol l^{-1})	$(K_a^T + H^+)$ (mol l^{-1})	$\frac{k_{obs}}{[OH^-]}$ (l mol^{-1} min^{-1})	$\frac{k_{obs}}{[OH^-]}(K_a^T + [H^+])$ (min^{-1})
8.701	2.595×10^{-9}	2.942×10^{-9}	474.8	3.700×10^{-7}
8.801	2.062×10^{-9}	2.408×10^{-9}	521.2	3.413×10^{-7}
8.803	2.052×10^{-9}	2.399×10^{-9}	523.9	3.391×10^{-7}
8.902	1.634×10^{-9}	1.981×10^{-9}	602.8	3.228×10^{-7}
8.904	1.626×10^{-9}	1.973×10^{-9}	614.4	2.987×10^{-7}
9.002	1.298×10^{-9}	1.645×10^{-9}	690.2	2.981×10^{-7}
9.003	1.295×10^{-9}	1.642×10^{-9}	685.1	2.865×10^{-7}
9.101	1.033×10^{-9}	1.380×10^{-9}	788.3	2.890×10^{-7}
9.102	1.031×10^{-9}	1.378×10^{-9}	782.5	2.880×10^{-7}
9.202	8.189×10^{-10}	1.166×10^{-9}	865.2	2.789×10^{-7}
9.203	8.170×10^{-10}	1.164×10^{-9}	885.4	$2.770. \times 10^{-7}$
9.303	6.489×10^{-10}	9.957×10^{-10}	987.7	2.733×10^{-7}
9.304	6.474×10^{-10}	9.942×10^{-10}	991.9	2.729×10^{-7}
9.405	5.131×10^{-10}	8.598×10^{-10}	1104.6	2.633×10^{-7}
9.406	5.119×10^{-10}	8.587×10^{-10}	1108.7	2.629×10^{-7}
9.507	4.057×10^{-10}	7.524×10^{-10}	1243.6	2.502×10^{-7}
9.508	4.048×10^{-10}	7.515×10^{-10}	1266.3	2.516×10^{-7}

Using $K_a^T = 3.467 \times 10^{-10}$; $pK_a^T = 9.46$ (37°C and I = 0.1 mol l^{-1}), (Table A1.15).

†Stopped Stirrer pH. $[H^+] = \frac{10^{-pH}}{0.7670}$ (37°C and I = 0.1 mol l^{-1}).

Figure A3.17 Separation of k_E and k_{EH^+} for Alkaline Hydrolysis of 4-AB Me

$T = (37.10 \pm 0.05)°C$

$I = 0.1$ mol l^{-1}

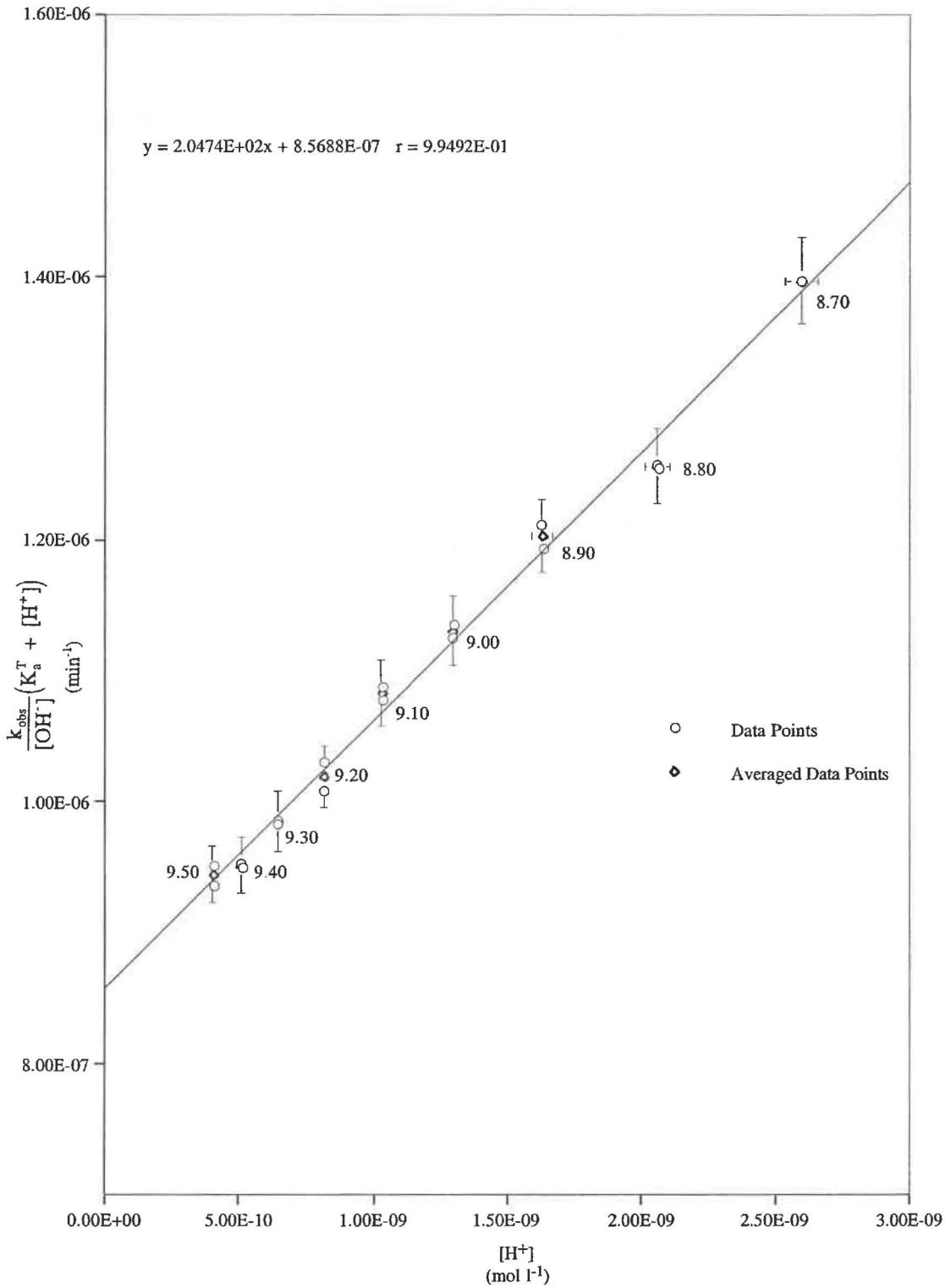

Table A3.39 Effect of pH on the Value of $k_{obs}/[OH^-]$ for 4-AB Et

$T = (37.10 \pm 0.05)°C$

$I = 0.1$ mol l^{-1}

pH†	k_{obs} (min^{-1})	$t_{1/2}$ (min)	$[OH^-]^*$ (mol l^{-1})	$\frac{k_{obs}}{[OH^-]}$ (l mol^{-1} min^{-1})
8.802	4.446×10^{-3}	155.9	1.973×10^{-5}	225.3
9.002	8.250×10^{-3}	84.0	3.128×10^{-5}	263.8
9.003	8.351×10^{-3}	83.0	3.135×10^{-5}	266.4
9.202	1.598×10^{-2}	43.4	4.957×10^{-5}	322.3
9.203	1.599×10^{-2}	43.4	4.968×10^{-5}	321.8
9.301	2.213×10^{-2}	31.3	6.226×10^{-5}	355.5
9.401	3.051×10^{-2}	22.7	7.838×10^{-5}	389.2
9.402	3.073×10^{-2}	22.6	7.856×10^{-5}	391.2
9.502	4.244×10^{-2}	16.3	9.890×10^{-5}	429.1
9.601	5.668×10^{-2}	12.2	1.242×10^{-4}	456.3
9.602	5.742×10^{-2}	12.1	1.245×10^{-4}	461.2
9.701	7.643×10^{-2}	9.1	1.564×10^{-4}	488.7
9.801	1.019×10^{-1}	6.8	1.969×10^{-4}	517.7
9.802	1.017×10^{-1}	6.8	1.973×10^{-4}	515.6

†Stopped Stirrer pH, $^*[OH^-] = \frac{10^{pH - 13.622}}{0.7670}$ (37°C and I = 0.1 mol l^{-1}).

Table A3.40 Data for Separation of k_E and k_{EH^+} for the Alkaline Hydrolysis of 4-AB Et

$T = (37.10 \pm 0.05)°C$

$I = 0.1$ mol l^{-1}

pH†	$[H^+]$ (mol l^{-1})	$(K_a^T + H^+)$ (mol l^{-1})	$\frac{k_{obs}}{[OH^-]}$ (l mol^{-1} min^{-1})	$\frac{k_{obs}}{[OH^-]}(K_a^T + [H^+])$ (min^{-1})
8.802	2.057×10^{-9}	2.388×10^{-9}	225.3	5.380×10^{-7}
9.002	1.298×10^{-9}	1.629×10^{-9}	263.8	4.297×10^{-7}
9.003	1.295×10^{-9}	1.626×10^{-9}	266.4	4.331×10^{-7}
9.202	8.189×10^{-10}	1.150×10^{-9}	322.3	3.706×10^{-7}
9.203	8.170×10^{-10}	1.148×10^{-9}	321.8	3.695×10^{-7}
9.301	6.519×10^{-10}	9.831×10^{-10}	355.5	3.495×10^{-7}
9.401	5.179×10^{-10}	8.490×10^{-10}	389.2	3.304×10^{-7}
9.402	5.167×10^{-10}	8.478×10^{-10}	391.2	3.317×10^{-7}
9.502	4.104×10^{-10}	7.415×10^{-10}	429.1	3.182×10^{-7}
9.601	3.267×10^{-10}	6.579×10^{-10}	456.3	3.002×10^{-7}
9.602	3.260×10^{-10}	6.571×10^{-10}	461.2	$3.031. \times 10^{-7}$
9.701	2.595×10^{-10}	5.907×10^{-10}	488.7	2.887×10^{-7}
9.801	2.062×10^{-10}	5.373×10^{-10}	517.7	2.782×10^{-7}
9.802	2.0571×10^{-10}	5.368×10^{-10}	515.6	2.768×10^{-7}

Using $K_a^T = 3.311 \times 10^{-10}$; $pK_a^T = 9.48$ (37°C and I = 0.1 mol l^{-1}), (Table A1.16).

† Stopped Stirrer pH. $[H^+] = \frac{10^{-pH}}{0.7670}$ (37°C and I = 0.1 mol l^{-1}).

Figure 3.18 Separation of k_E and k_{EH^+} for Alkaline Hydrolysis of 4-AB Et

$T = (37.10 \pm 0.05)°C$

$I = 0.1 \text{ mol } l^{-1}$

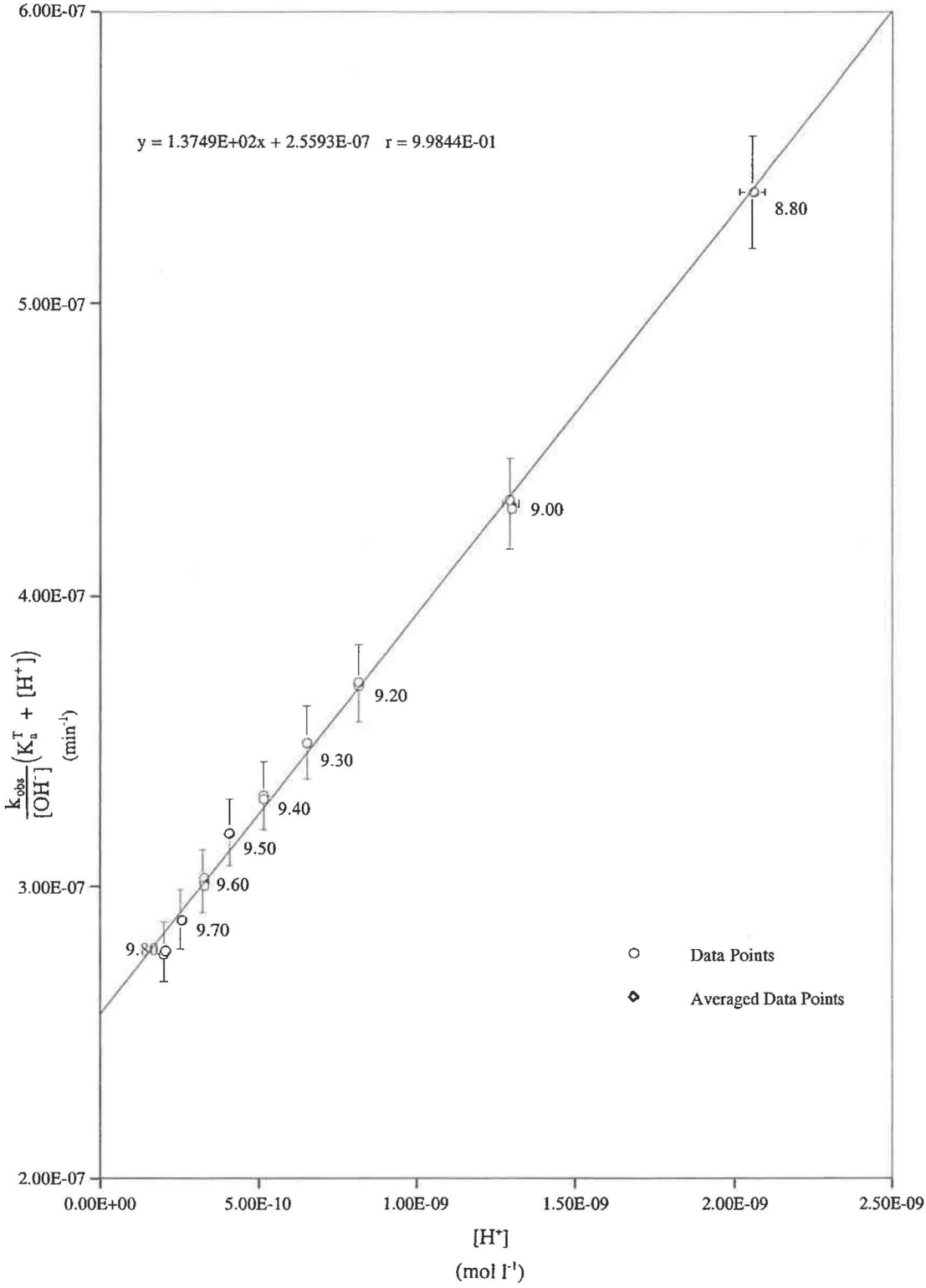

Table A3.41 Effect of pH on the Value of $k_{obs}/[OH^-]$ for 4-AB Bz

$T = (37.10 \pm 0.05)°C$

$I = 0.1$ mol l^{-1}

pH†	k_{obs} (min^{-1})	$t_{1/2}$ (min)	$[OH^-]^*$ (mol l^{-1})	$\frac{k_{obs}}{[OH^-]}$ (l mol^{-1} min^{-1})
8.606	6.856×10^{-3}	101.1	1.257×10^{-5}	545.6
8.708	9.634×10^{-3}	71.9	1.589×10^{-5}	606.2
8.804	1.357×10^{-2}	51.1	1.982×10^{-5}	684.4
8.805	1.348×10^{-2}	51.4	1.987×10^{-5}	678.5
8.905	1.917×10^{-2}	36.2	2.502×10^{-5}	766.2
9.005	2.751×10^{-2}	25.2	3.149×10^{-5}	873.5
9.006	2.742×10^{-2}	25.3	3.156×10^{-5}	868.6
9.106	3.888×10^{-2}	17.8	3.974×10^{-5}	978.5
9.204	5.410×10^{-2}	12.8	4.980×10^{-5}	1086.5
9.205	5.369×10^{-2}	12.9	4.991×10^{-5}	1075.6
9.308	7.721×10^{-2}	9.0	6.327×10^{-5}	1220.3
9.310	7.713×10^{-2}	9.0	6.356×10^{-5}	1213.5
9.409	1.066×10^{-1}	6.5	7.984×10^{-5}	1335.6
9.409	1.062×10^{-1}	6.5	7.984×10^{-5}	1330.2
9.505	1.479×10^{-1}	4.7	9.959×10^{-5}	1485.6
9.605	2.038×10^{-1}	3.4	1.254×10^{-4}	1625.3

†Stopped Stirrer pH, $^*[OH^-] = \frac{10^{pH - 13.622}}{0.7670}$ (37°C and I = 0.1 mol l^{-1}).

Table 5.42 Data for Separation of k_E and k_{EH+} for the Alkaline Hydrolysis of 4-AB Bz

$T = (37.10 \pm 0.05)°C$

$I = 0.1$ mol l^{-1}

pH†	$[H^+]$ (mol l^{-1})	$(K_a^T + H^+)$ (mol l^{-1})	$\frac{k_{obs}}{[OH^-]}$ (l mol^{-1} min^{-1})	$\frac{k_{obs}}{[OH^-]}(K_a^T + [H^+])$ (min^{-1})
8.606	3.230×10^{-9}	3.610×10^{-9}	545.6	1.970×10^{-6}
8.708	2.554×10^{-9}	2.934×10^{-9}	606.2	1.779×10^{-6}
8.804	2.047×10^{-9}	2.428×10^{-9}	684.4	1.661×10^{-6}
8.805	2.043×10^{-9}	2.423×10^{-9}	678.5	1.644×10^{-6}
8.905	1.623×10^{-9}	2.003×10^{-9}	766.2	1.535×10^{-6}
9.005	1.289×10^{-9}	1.669×10^{-9}	873.5	1.458×10^{-6}
9.006	1.286×10^{-9}	1.666×10^{-9}	868.6	1.447×10^{-6}
9.106	1.021×10^{-9}	1.402×10^{-9}	978.5	1.371×10^{-6}
9.204	8.151×10^{-10}	1.195×10^{-9}	1086.5	1.299×10^{-6}
9.205	8.132×10^{-10}	1.193×10^{-9}	1075.6	1.284×10^{-6}
9.308	6.415×10^{-10}	1.022×10^{-9}	1220.3	$1.247. \times 10^{-6}$
9.310	6.386×10^{-10}	1.019×10^{-9}	1213.5	1.236×10^{-6}
9.409	5.084×10^{-10}	8.886×10^{-10}	1335.6	1.187×10^{-6}
9.409	5.084×10^{-10}	8.886×10^{-10}	1330.2	1.182×10^{-6}
9.505	4.076×10^{-10}	7.878×10^{-10}	1485.6	1.170×10^{-6}
9.605	3.237×10^{-10}	7.039×10^{-10}	1625.3	1.144×10^{-6}

Using $K_a^T = 3.802 \times 10^{-10}$; $pK_a^T = 9.42$ (37°C and I = 0.1 mol l^{-1}), (Table A1.17).

†Stopped Stirrer pH. $[H^+] = \frac{10^{-pH}}{0.7670}$ (37°C and I = 0.1 mol l^{-1}).

Figure A3.19 Separation of k_E and k_{EH^+} for Alkaline Hydrolysis of 4-AB Bz

$T = (37.10 \pm 0.05)°C$

$I = 0.1 \text{ mol } l^{-1}$

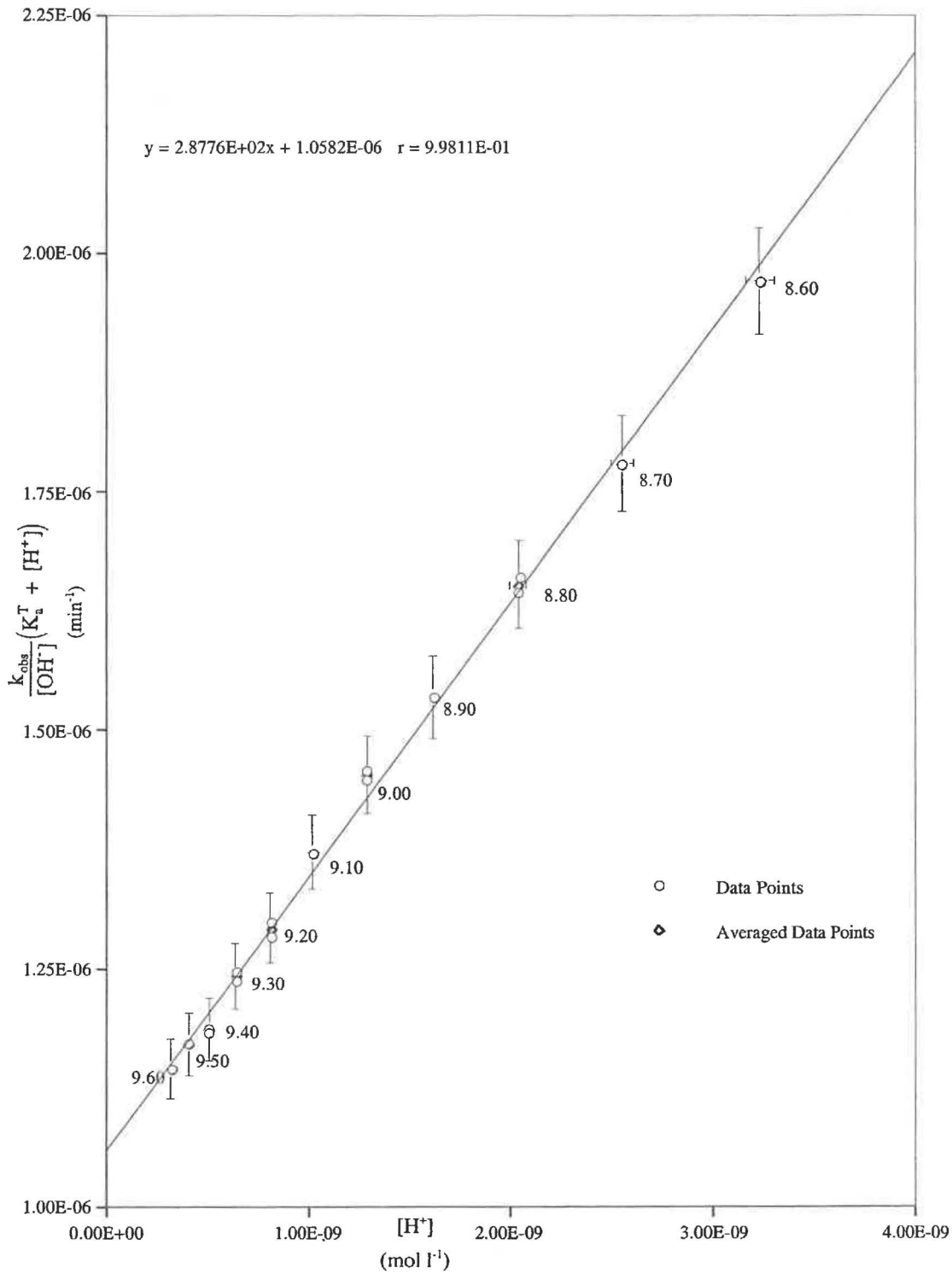

Table A3.43 Effect of pH on the Value of $k_{obs}/[OH^-]$ for 4-MAB Me

$T = (37.10 \pm 0.05)°C$

$I = 0.1$ mol l^{-1}

pH†	k_{obs} (min^{-1})	$t_{1/2}$ (min)	$[OH^-]^*$ (mol l^{-1})	$\frac{k_{obs}}{[OH^-]}$ (l mol^{-1} min^{-1})
8.402	5.486×10^{-3}	126.4	7.856×10^{-6}	698.3
8.501	7.869×10^{-3}	88.1	9.867×10^{-6}	797.5
8.502	7.935×10^{-3}	87.4	9.890×10^{-6}	802.3
8.601	1.134×10^{-2}	61.1	1.242×10^{-5}	913.2
8.602	1.139×10^{-2}	60.9	1.245×10^{-5}	914.6
8.703	1.674×10^{-2}	41.4	1.571×10^{-5}	1065.3
8.704	1.672×10^{-2}	41.5	1.575×10^{-5}	1061.9
8.803	2.501×10^{-2}	27.7	1.978×10^{-5}	1264.5
8.804	2.501×10^{-2}	27.7	1.982×10^{-5}	1261.4
8.903	3.583×10^{-2}	19.3	2.490×10^{-5}	1438.9
8.903	3.548×10^{-2}	19.5	2.490×10^{-5}	1424.7
9.003	5.438×10^{-2}	12.7	3.135×10^{-5}	1734.6
9.004	5.471×10^{-2}	12.7	3.142×10^{-5}	1741.2
9.102	7.959×10^{-2}	8.7	3.937×10^{-5}	2021.3
9.104	7.969×10^{-2}	8.7	3.956×10^{-5}	2014.6

†Stopped Stirrer pH, $^*[OH^-] = \frac{10^{pH - 13.622}}{0.7670}$ (37°C and I = 0.1 mol l^{-1}).

Table A3.44 Data for Separation of k_E and k_{EH^+} for the Alkaline Hydrolysis of 4-MAB Me

$T = (37.10 \pm 0.05)°C$

$I = 0.1$ mol l^{-1}

pH†	$[H^+]$ (mol l^{-1})	$(K_a^T + H^+)$ (mol l^{-1})	$\frac{k_{obs}}{[OH^-]}$ (l mol^{-1} min^{-1})	$\frac{k_{obs}}{[OH^-]}(K_a^T + [H^+])$ (min^{-1})
8.402	5.167×10^{-9}	5.353×10^{-9}	698.3	3.738×10^{-6}
8.501	4.113×10^{-9}	4.300×10^{-9}	797.5	3.429×10^{-6}
8.502	4.104×10^{-9}	4.290×10^{-9}	802.3	3.442×10^{-6}
8.601	3.267×10^{-9}	3.454×10^{-9}	913.2	3.154×10^{-6}
8.602	3.260×10^{-9}	3.446×10^{-9}	914.6	3.152×10^{-6}
8.703	2.583×10^{-9}	2.770×10^{-9}	1065.3	2.951×10^{-6}
8.704	2.578×10^{-9}	2.764×10^{-9}	1061.9	2.935×10^{-6}
8.803	2.052×10^{-9}	2.238×10^{-9}	1264.5	2.830×10^{-6}
8.804	2.047×10^{-9}	2.234×10^{-9}	1261.4	2.817×10^{-6}
8.903	1.630×10^{-9}	1.816×10^{-9}	1438.9	2.613×10^{-6}
8.903	1.630×10^{-9}	1.816×10^{-9}	1424.7	2.588×10^{-6}
9.003	1.295×10^{-9}	1.481×10^{-9}	1734.6	2.569×10^{-6}
9.004	1.292×10^{-9}	1.478×10^{-9}	1741.2	2.574×10^{-6}
9.102	1.031×10^{-10}	1.217×10^{-9}	2021.3	2.460×10^{-6}
9.104	1.026×10^{-10}	1.212×10^{-9}	2014.6	2.442×10^{-6}

Using $K_a^T = 1.862 \times 10^{-10}$; $pK_a^T = 9.73$ (37°C and I = 0.1 mol l^{-1}), (Table A1.18).

†Stopped Stirrer pH. $[H^+] = \frac{10^{-pH}}{0.7670}$ (37°C and I = 0.1 mol l^{-1}).

Figure A3.20 Separation of k_E and k_{EH^+} for Alkaline Hydrolysis of 4-MAB Me

$T = (37.10 \pm 0.05)°C$

$I = 0.1$ mol l^{-1}

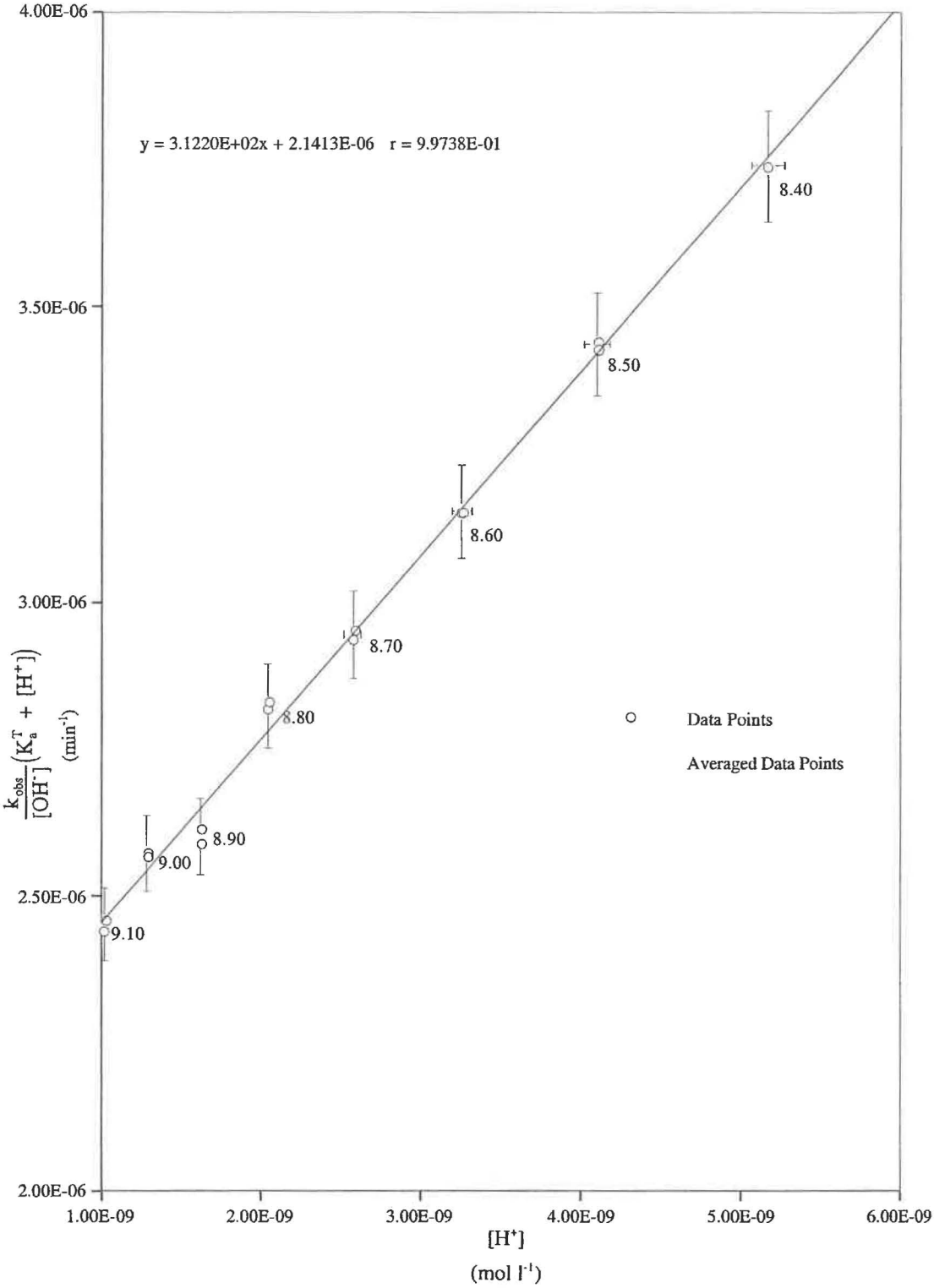

Table A3.45 Effect of pH on the Value of $k_{obs}/[OH^-]$ for 4-MAB Et

$T = (37.10 \pm 0.05)°C$

$I = 0.1$ mol l^{-1}

pH†	k_{obs} (min^{-1})	$t_{1/2}$ (min)	$[OH^-]^*$ (mol l^{-1})	$\frac{k_{obs}}{[OH^-]}$ (l mol^{-1} min^{-1})
8.704	7.343×10^{-3}	94.4	1.575×10^{-5}	466.3
8.705	7.398×10^{-3}	93.7	1.578×10^{-5}	468.7
8.805	1.018×10^{-2}	68.1	1.987×10^{-5}	512.2
8.905	1.479×10^{-2}	46.9	2.502×10^{-5}	591.4
8.906	1.478×10^{-2}	46.9	2.507×10^{-5}	589.3
9.004	2.131×10^{-2}	32.5	3.142×10^{-5}	678.3
9.100	3.062×10^{-2}	22.6	3.919×10^{-5}	781.2
9.103	3.061×10^{-2}	22.6	3.946×10^{-5}	775.6
9.201	4.457×10^{-2}	15.6	4.945×10^{-5}	901.2
9.204	4.525×10^{-2}	15.3	4.980×10^{-5}	908.6
9.303	6.401×10^{-2}	10.8	6.255×10^{-5}	1023.4
9.303	6.453×10^{-2}	10.7	6.255×10^{-5}	1031.7
9.406	9.539×10^{-2}	7.3	7.929×10^{-5}	1203.1
9.406	9.501×10^{-2}	7.3	7.929×10^{-5}	1198.3
9.505	1.351×10^{-1}	5.1	9.959×10^{-5}	1356.4

†Stopped Stirrer pH, $^*[OH^-] = \frac{10^{pH - 13.622}}{0.7670}$ (37°C and I = 0.1 mol l^{-1}).

Table A3.46 Data for Separation of k_E and k_{EH+} for the Alkaline Hydrolysis of 4-MAB Et

$T = (37.10 \pm 0.05)°C$

$I = 0.1$ mol l^{-1}

pH†	$[H^+]$ (mol l^{-1})	$(K_a^T + H^+)$ (mol l^{-1})	$\frac{k_{obs}}{[OH^-]}$ (l mol^{-1} min^{-1})	$\frac{k_{obs}}{[OH^-]}(K_a^T + [H^+])$ (min^{-1})
8.704	2.578×10^{-9}	2.787×10^{-9}	466.3	1.300×10^{-6}
8.705	2.572×10^{-9}	2.781×10^{-9}	468.7	1.303×10^{-6}
8.805	2.043×10^{-9}	2.252×10^{-9}	512.2	1.153×10^{-6}
8.905	1.623×10^{-9}	1.832×10^{-9}	591.4	1.083×10^{-6}
8.906	1619×10^{-9}	1.828×10^{-9}	589.3	1.077×10^{-6}
9.004	1.292×10^{-9}	1.501×10^{-9}	678.3	1.018×10^{-6}
9.100	1036×10^{-9}	1.449×10^{-9}	781.2	1.132×10^{-6}
9.103	1.029×10^{-9}	1.238×10^{-9}	775.6	9.601×10^{-7}
9.201	8.207×10^{-10}	1.030×10^{-9}	901.2	9.279×10^{-7}
9.204	8.151×10^{-10}	1.024×10^{-9}	908.6	9.304×10^{-7}
9.303	6.489×10^{-10}	8.578×10^{-10}	1023.4	$8.778. \times 10^{-7}$
9.303	6.489×10^{-10}	8.578×10^{-10}	1031.7	8.850×10^{-7}
9.406	5.119×10^{-10}	7.208×10^{-10}	1203.1	8.672×10^{-7}
9.406	5.119×10^{-10}	7.208×10^{-10}	1198.3	8.637×10^{-7}
9.505	4.076×10^{-10}	6.165×10^{-10}	1356.4	8.362×10^{-7}

Using $K_a^T = 2.089 \times 10^{-10}$; $pK_a^T = 9.68$ (37°C and I = 0.1 mol l^{-1}), (Table A1.19).

†Stopped Stirrer pH. $[H^+] = \frac{10^{-pH}}{0.7670}$ (37°C and I = 0.1 mol l^{-1}).

Figure A3.21 Separation of k_E and k_{EH^+} for Alkaline Hydrolysis of 4-MAB Et

$T = (37.10 \pm 0.05)°C$

$I = 0.1$ mol l^{-1}

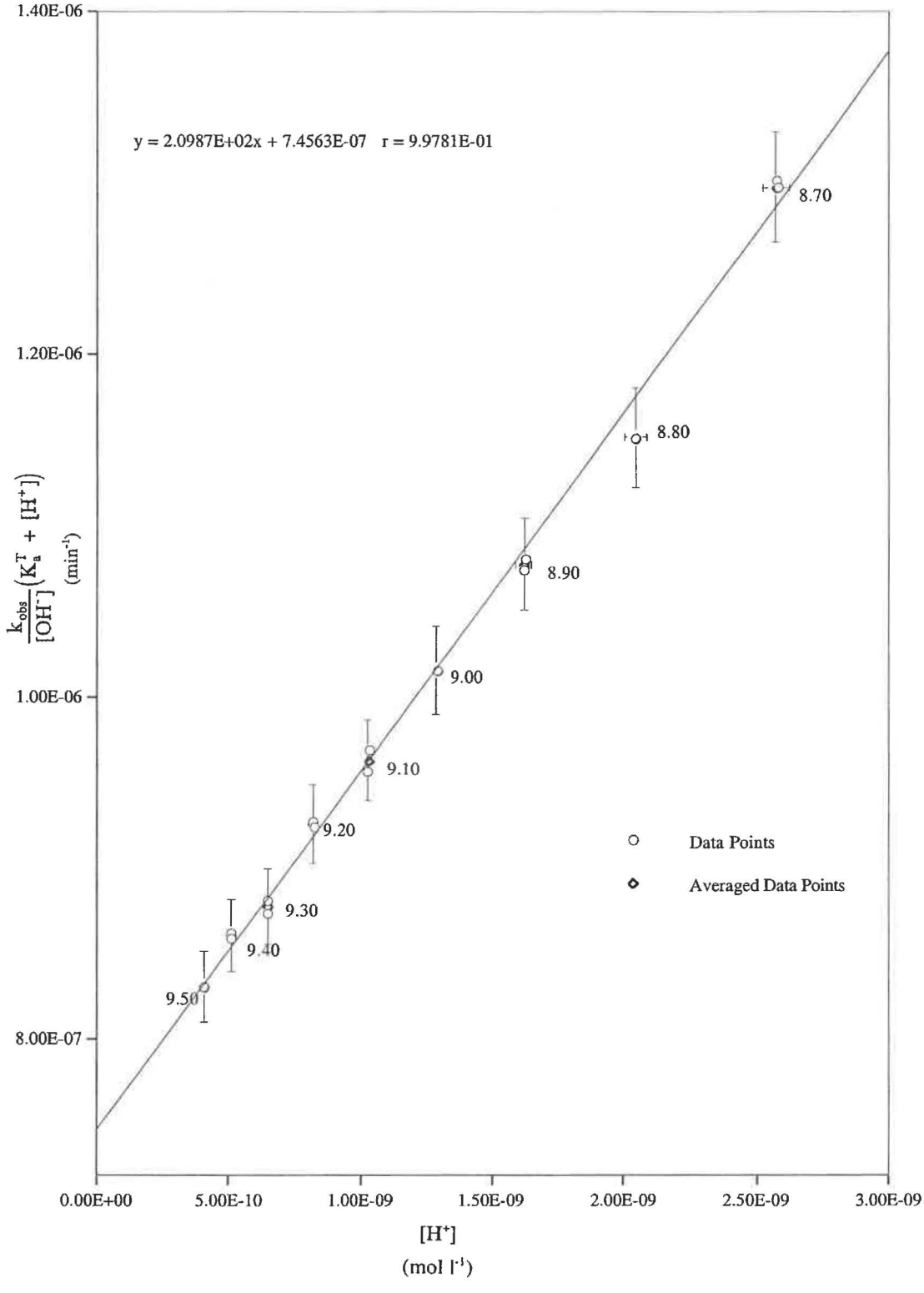

Table A3.47 Effect of the pH on the Value of $k_{obs}/[OH^-]$ for 4-A-3-MB Me

$T = (37.10 \pm 0.05)°C$

$I = 0.1$ mol l^{-1}

pH†	k_{obs} (min^{-1})	$t_{1/2}$ (min)	$[OH^-]^*$ (mol l^{-1})	$\frac{k_{obs}}{[OH^-]}$ (l mol^{-1} min^{-1})
8.202	3.178×10^{-3}	218.1	4.957×10^{-6}	641.1
8.403	6.867×10^{-3}	100.9	7.874×10^{-6}	872.1
8.404	6.944×10^{-3}	99.8	7.892×10^{-6}	879.8
8.603	1.487×10^{-2}	46.6	1.248×10^{-5}	1191.2
8.604	1.503×10^{-2}	46.1	1.251×10^{-5}	1201.3
8.703	2.125×10^{-2}	32.6	1.571×10^{-5}	1352.3
8.803	3.127×10^{-2}	22.2	1.978×10^{-5}	1581.2
8.804	3.103×10^{-2}	22.3	1.982×10^{-5}	1565.2
8.902	4.499×10^{-2}	15.4	2.484×10^{-5}	1811.0
9.000	6.305×10^{-2}	11.0	3.113×10^{-5}	2025.3
9.001	6.370×10^{-2}	10.9	3.120×10^{-5}	2041.3
9.100	9.018×10^{-2}	7.7	3.919×10^{-5}	2301.0
9.106	9.183×10^{-2}	7.5	3.974×10^{-5}	2311.0

† Stopped Stirrer pH, $^*[OH^-] = \frac{10^{pH - 13.622}}{0.7670}$ (37°C and I = 0.1 mol l^{-1}).

Table A3.48 Data for Separation of k_E and k_{EH+} for the Alkaline Hydrolysis of 4-A-3MB Me

$T = (37.10 \pm 0.05)°C$

$I = 0.1$ mol l^{-1}

pH†	$[H^+]$ (mol l^{-1})	$(K_a^T + H^+)$ (mol l^{-1})	$\frac{k_{obs}}{[OH^-]}$ (l mol^{-1} min^{-1})	$\frac{k_{obs}}{[OH^-]}(K_a^T + [H^+])$ (min^{-1})
8.202	8.189×10^{-9}	9.020×10^{-9}	641.1	5.783×10^{-6}
8.403	5.155×10^{-9}	5.986×10^{-9}	872.1	5.221×10^{-6}
8.404	5.143×10^{-9}	5.975×10^{-9}	879.8	5.256×10^{-6}
8.603	3.252×10^{-9}	4.084×10^{-9}	1191.2	4.865×10^{-6}
8.604	3.245×10^{-9}	4.077×10^{-9}	1201.3	4.897×10^{-6}
8.703	2.583×10^{-9}	3.415×10^{-9}	1352.3	4.618×10^{-6}
8.803	2.052×10^{-9}	2.884×10^{-9}	1581.2	4.560×10^{-6}
8.804	2.047×10^{-9}	2.879×10^{-9}	1565.2	4.506×10^{-6}
8.902	1.634×10^{-9}	2.466×10^{-9}	1811.0	4.465×10^{-6}
9.000	1.304×10^{-9}	2.136×10^{-9}	2025.3	4.325×10^{-6}
9.001	1.301×10^{-9}	2.133×10^{-9}	2041.3	4.353×10^{-6}
9.100	1.036×10^{-9}	1.867×10^{-9}	2301.0	4.297×10^{-6}
9.106	1.021×10^{-9}	1.853×10^{-9}	2311.0	4.283×10^{-6}

Using $K_a^T = 8.318 \times 10^{-10}$; $pK_a^T = 9.08$ (37°C and I = 0.1 mol l^{-1}), (Table A1.20).

†Stopped Stirrer pH. $[H^+] = \frac{10^{-pH}}{0.7670}$ (37 °C and I = 0.1 mol l^{-1}).

Figure A3.22 Separation of k_E and k_{EH^+} for Alkaline Hydrolysis of 4-A-3-MB Me

$T = (37.10 \pm 0.05)°C$

$I = 0.1$ mol l^{-1}

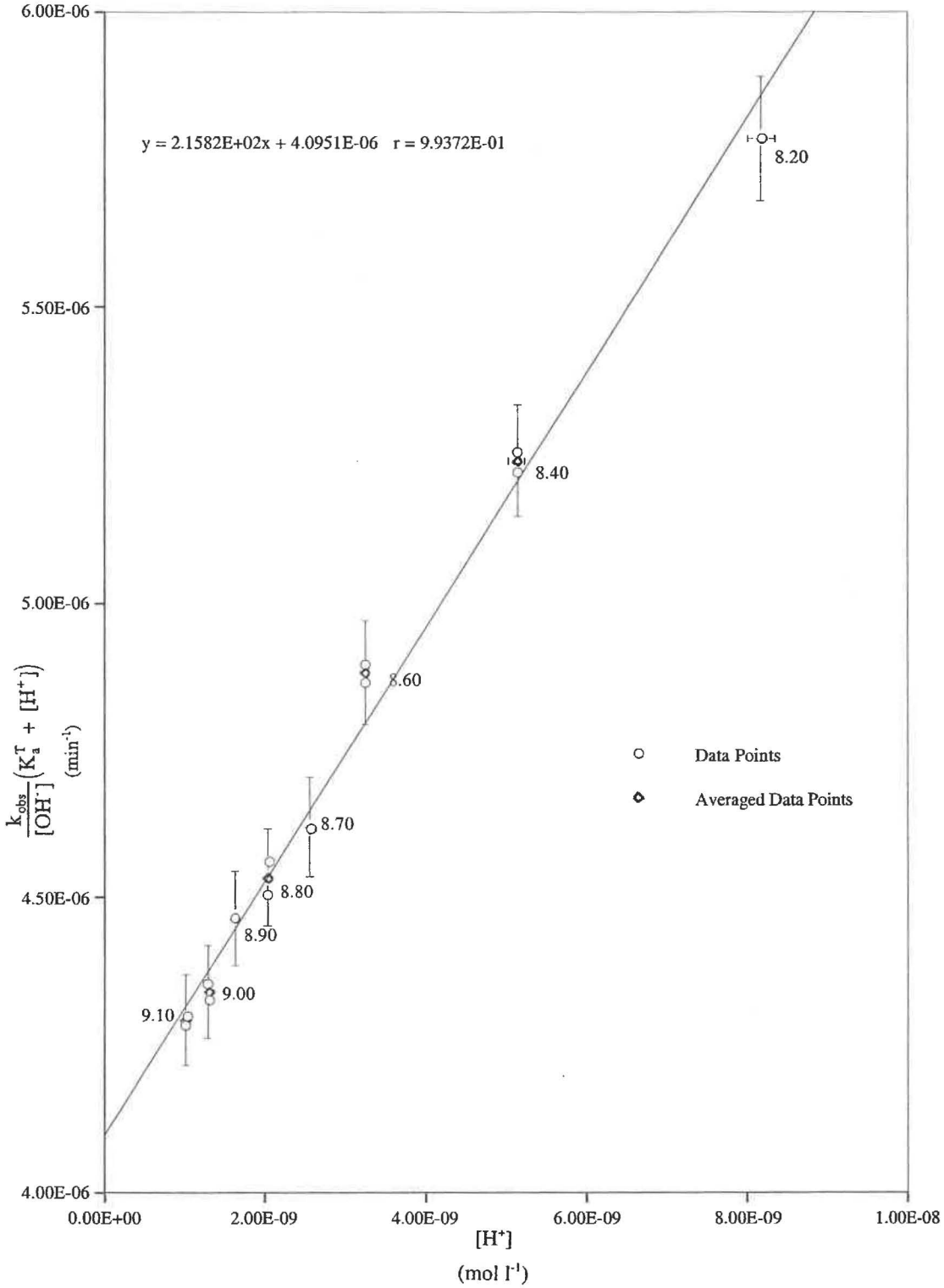

Table A3.49 Effect of pH on the Value of $k_{obs}/[OH^-]$ for 4-A-3,3-DMB Me

$T = (37.10 \pm 0.05)°C$

$I = 0.1$ mol l^{-1}

pH†	k_{obs} (min^{-1})	$t_{1/2}$ (min)	$[OH^-]^*$ (mol l^{-1})	$\frac{k_{obs}}{[OH^-]}$ (l mol^{-1} min^{-1})
8.006	4.962×10^{-3}	139.7	3.156×10^{-6}	1572.3
8.201	1.082×10^{-2}	64.0	4.945×10^{-6}	2188.3
8.202	1.079×10^{-2}	64.2	4.957×10^{-6}	2177.4
8.402	2.416×10^{-2}	28.7	7.856×10^{-6}	3075.4
8.503	3.585×10^{-2}	19.3	9.913×10^{-6}	3616.6
8.507	3.591×10^{-2}	19.3	1.000×10^{-5}	3589.8
8.603	5.257×10^{-2}	13.2	1.248×10^{-5}	4212.3
8.804	1.127×10^{-1}	6.1	1.982×10^{-5}	5685.2
8.804	1.126×10^{-1}	6.2	1.982×10^{-5}	5681.4
8.904	1.602×10^{-1}	4.3	2.496×10^{-5}	6418.5
8.904	1.608×10^{-1}	4.3	2.496×10^{-5}	6441.1

†Stopped Stirrer pH, $^*[OH^-] = \frac{10^{pH - 13.622}}{0.7670}$ (37°C and I = 0.1 mol l^{-1}).

Table A3.50 Data for Separation of k_E and k_{EH+} for the Alkaline Hydrolysis of 4-A-3, 3-DMB Me

$T = (37.10 \pm 0.05)°C$

$I = 0.1$ mol l^{-1}

pH†	$[H^+]$ (mol l^{-1})	$(K_a^T + H^+)$ (mol l^{-1})	$\frac{k_{obs}}{[OH^-]}$ (l mol^{-1} min^{-1})	$\frac{k_{obs}}{[OH^-]}(K_a^T + [H^+])$ (min^{-1})
8.006	1.286×10^{-8}	1.396×10^{-8}	1572.3	2.194×10^{-5}
8.201	8.207×10^{-9}	9.304×10^{-9}	2188.3	2.036×10^{-5}
8.202	8.189×10^{-9}	9.285×10^{-9}	2177.4	2.022×10^{-5}
8.402	5.167×10^{-9}	6.263×10^{-9}	3075.4	1.926×10^{-5}
8.503	4.095×10^{-9}	5.191×10^{-9}	3616.6	1.877×10^{-5}
8.507	4.057×10^{-9}	5.153×10^{-9}	3589.8	1.850×10^{-5}
8.603	3.252×10^{-9}	4.349×10^{-9}	4212.3	1.832×10^{-5}
8.804	2.047×10^{-9}	3.144×10^{-9}	5685.2	1.787×10^{-5}
8.804	2.047×10^{-9}	3.144×10^{-9}	5681.4	1.786×10^{-5}
8.904	1.626×10^{-9}	2.723×10^{-9}	6418.5	1.748×10^{-5}
8.904	1.626×10^{-9}	2.723×10^{-9}	6441.1	1.754×10^{-5}

Using $K_a^T = 1.096 \times 10^{-9}$; $pK_a^T = 8.96$ (37°C and I = 0.1 mol l^{-1}), (Table A1.21).

†Stopped Stirrer pH. $[H^+] = \frac{10^{-pH}}{0.7670}$ (37°C and I = 0.1 mol l^{-1}).

Figure A3.23 Separation of k_E and k_{EH^+} for Alkaline Hydrolysis of 4-A-3, 3-DMB Me

$T = (37.10 \pm 0.05)°C$

$I = 0.1$ mol l^{-1}

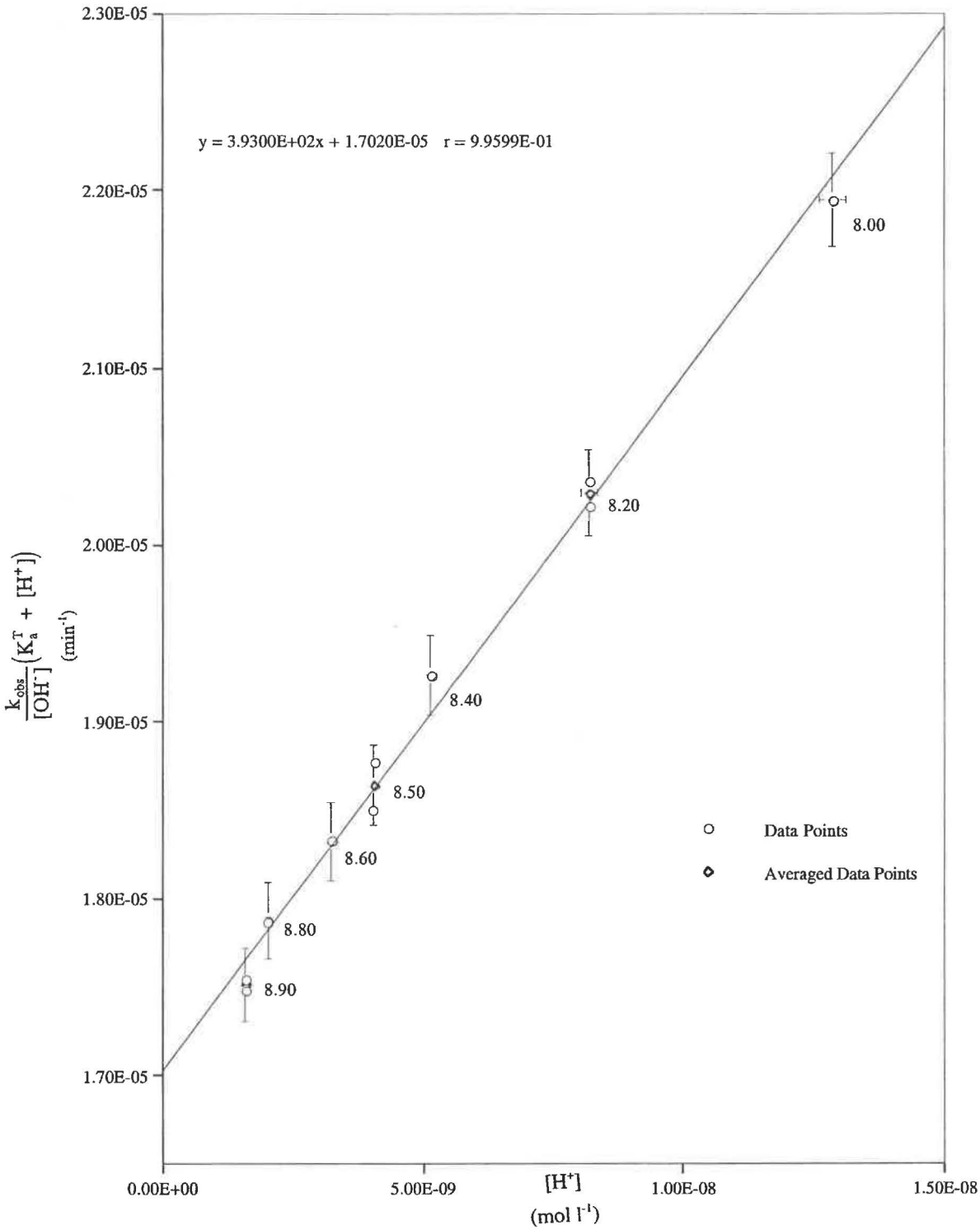

Table A3.51 Effect of pH on the Value of $k_{obs}/[OH^-]$ for 5-APe Et

$T = (37.10 \pm 0.05)°C$

$I = 0.1$ mol l^{-1}

pH†	k_{obs} (min^{-1})	$t_{1/2}$ (min)	$[OH^-]^*$ (mol l^{-1})	$\frac{k_{obs}}{[OH^-]}$ (l mol^{-1} min^{-1})
8.305	3.426×10^{-3}	202.3	6.284×10^{-6}	545.3
8.402	5.158×10^{-3}	134.4	7.856×10^{-6}	656.5
8.501	7.851×10^{-3}	88.3	9.867×10^{-6}	795.6
8.501	7.788×10^{-3}	89.0	9.867×10^{-6}	789.3
8.602	1.184×10^{-2}	58.5	1.245×10^{-5}	951.2
8.701	1.803×10^{-2}	38.4	1.564×10^{-5}	1153.2
8.801	2.771×10^{-2}	25.0	1.969×10^{-5}	1407.2
8.903	4.268×10^{-2}	16.2	2.490×10^{-5}	1713.9
8.905	4.318×10^{-2}	16.1	2.502×10^{-5}	1726.3
9.005	6.471×10^{-2}	10.7	3.149×10^{-5}	2054.7
9.005	6.504×10^{-2}	10.7	3.149×10^{-5}	2065.4
9.105	9.815×10^{-2}	7.1	3.965×10^{-5}	2475.6
9.105	9.788×10^{-2}	7.1	3.965×10^{-5}	2468.9

†Stopped Stirrer pH, $^*[OH^-] = \frac{10^{-pH\ -\ 13.622}}{0.7670}$ (37°C and I = 0.1 mol l^{-1}).

Table A3.52 Data for Separation of k_E and k_{EH+} for the Alkaline Hydrolysis of 5-APe Et

$T = (37.10 \pm 0.05)°C$

$I = 0.1$ mol l^{-1}

pH†	$[H^+]$ (mol l^{-1})	$(K_a^T + H^+)$ (mol l^{-1})	$\frac{k_{obs}}{[OH^-]}$ (l mol^{-1} min^{-1})	$\frac{k_{obs}}{[OH^-]}(K_a^T + [H^+])$ (min^{-1})
8.305	6.460×10^{-9}	6.641×10^{-9}	545.3	3.621×10^{-6}
8.402	5.167×10^{-9}	5.348×10^{-9}	656.3	3.511×10^{-6}
8.501	4.113×10^{-9}	4.295×10^{-9}	795.6	3.417×10^{-6}
8.501	4.113×10^{-9}	4.295×10^{-9}	789.3	3.390×10^{-6}
8.602	3.260×10^{-9}	3.441×10^{-9}	951.2	3.274×10^{-6}
8.701	2.595×10^{-9}	2.777×10^{-9}	1153.2	3.203×10^{-6}
8.801	2.062×10^{-9}	2.244×10^{-9}	1407.2	3.157×10^{-6}
8.903	1.630×10^{-9}	1.812×10^{-9}	1713.9	3.106×10^{-6}
8.905	1.623×10^{-9}	1.804×10^{-9}	1726.3	3.115×10^{-6}
9.005	1.289×10^{-9}	1.471×10^{-9}	2054.7	3.022×10^{-6}
9.005	1.289×10^{-9}	1.471×10^{-9}	2065.4	$3.038. \times 10^{-6}$
9.105	1.024×10^{-9}	1.206×10^{-9}	2475.6	2.985×10^{-6}
9.105	1.024×10^{-9}	1.206×10^{-9}	2468.9	2.977×10^{-6}

Using $K_a^T = 1.820 \times 10^{-10}$; $pK_a^T = 9.74$ (37°C and I = 0.1 mol l^{-1}), (Table A1.22).

†Stopped Stirrer pH. $[H^+] = \frac{10^{-pH}}{0.7670}$ (37°C and I = 0.1 mol l^{-1}).

Figure A3.24 Separation of k_E and k_{EH^+} for Alkaline Hydrolysis of 5-APe Et

$T = (37.10 \pm 0.05)°C$

$I = 0.1$ mol l^{-1}

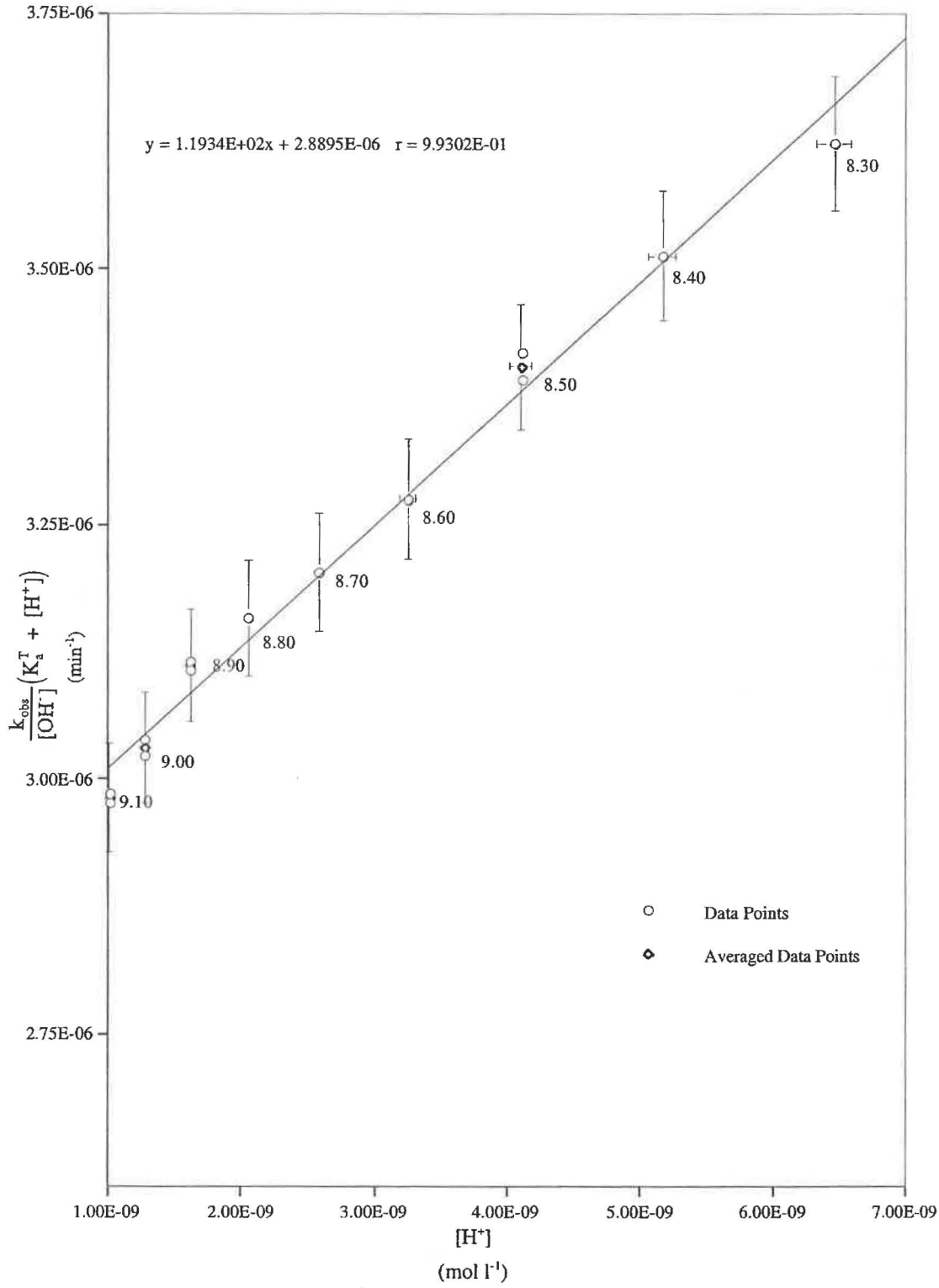

Table A3.53 Effect of pH on the Value of $k_{obs}/[OH^-]$ for 5-APe Me.

$T = (37.10 \pm 0.05)°C$

$I = 0.1$ mol l^{-1}

pH†	k_{obs} (min^{-1})	$t_{1/2}$ (min)	$[OH^-]^*$ (mol l^{-1})	$\frac{k_{obs}}{[OH^-]}$ (l mol^{-1} min^{-1})
8.202	8.666×10^{-3}	80.0	4.957×10^{-6}	1748.2
8.299	1.247×10^{-2}	55.6	6.197×10^{-6}	2012.3
8.303	1.267×10^{-2}	54.7	6.255×10^{-6}	2025.3
8.404	1.893×10^{-2}	36.6	7.892×10^{-6}	2398.1
8.503	2.812×10^{-2}	24.7	9.913×10^{-6}	2836.5
8.504	2.838×10^{-2}	24.4	9.936×10^{-6}	2856.3
8.604	4.251×10^{-2}	16.3	1.251×10^{-5}	3398.2
8.606	4.233×10^{-2}	16.4	1.257×10^{-5}	3368.9
8.701	6.324×10^{-2}	11.1	1.564×10^{-5}	3986.3
8.702	6.201×10^{-2}	11.2	1.567×10^{-5}	3956.2
8.801	9.186×10^{-2}	7.5	1.969×10^{-5}	4665.8
8.802	9.124×10^{-2}	7.6	1.973×10^{-5}	4623.5

†Stopped Stirrer pH, $^*[OH^-] = \frac{10^{pH - 13.9965}}{0.7670}$ (37°C and I = 0.1 mol l^{-1}).

Table A3.54 Data for Separation of k_E and k_{EH+} for the Alkaline Hydrolysis 5-APe Me

$T = (37.10 \pm 0.05)°C$

$I = 0.1$ mol l^{-1}

pH†	$[H^+]$ (mol l^{-1})	$(K_a^T + H^+)$ (mol l^{-1})	$\frac{k_{obs}}{[OH^-]}$ (l mol^{-1} min^{-1})	$\frac{k_{obs}}{[OH^-]}(K_a^T + [H^+])$ (min^{-1})
8.202	8.189×10^{-9}	8.383×10^{-9}	1748.2	1.466×10^{-5}
8.299	6.549×10^{-9}	6.744×10^{-9}	2012.3	1.357×10^{-5}
8.303	6.489×10^{-9}	6.684×10^{-9}	2025.3	1.354×10^{-5}
8.404	5.143×10^{-9}	5.338×10^{-9}	2398.1	1.280×10^{-5}
8.503	4.095×10^{-9}	4.290×10^{-9}	2836.5	1.217×10^{-5}
8.504	4.085×10^{-9}	4.280×10^{-9}	2856.3	1.223×10^{-5}
8.604	3.245×10^{-9}	3.440×10^{-9}	3398.2	1.169×10^{-5}
8.606	3.230×10^{-9}	3.425×10^{-9}	3368.9	1.154×10^{-5}
8.701	2.595×10^{-9}	2.790×10^{-9}	3986.3	1.112×10^{-5}
8.702	2.589×10^{-9}	2.784×10^{-9}	3956.2	1.102×10^{-5}
8.801	2.062×10^{-9}	2.257×10^{-9}	4665.8	1.053×10^{-5}
8.802	2.057×10^{-9}	2.252×10^{-9}	4623.5	1.041×10^{-5}

Using $K_a^T = 1.950 \times 10^{-10}$; $pK_a^T = 9.71$ (37.°C and I = 0.1 mol l^{-1}), (Table A1.23).

†Stopped Stirrer pH. $[H^+] = \frac{10^{-pH}}{0.7670}$ (37°C and I = 0.1 mol l^{-1}).

Figure A3.25 Separation of k_E and k_{EH^+} for Alkaline Hydrolysis of 5-APe Me

$T = (37.10 \pm 0.05)°C$

$I = 0.1$ mol l^{-1}

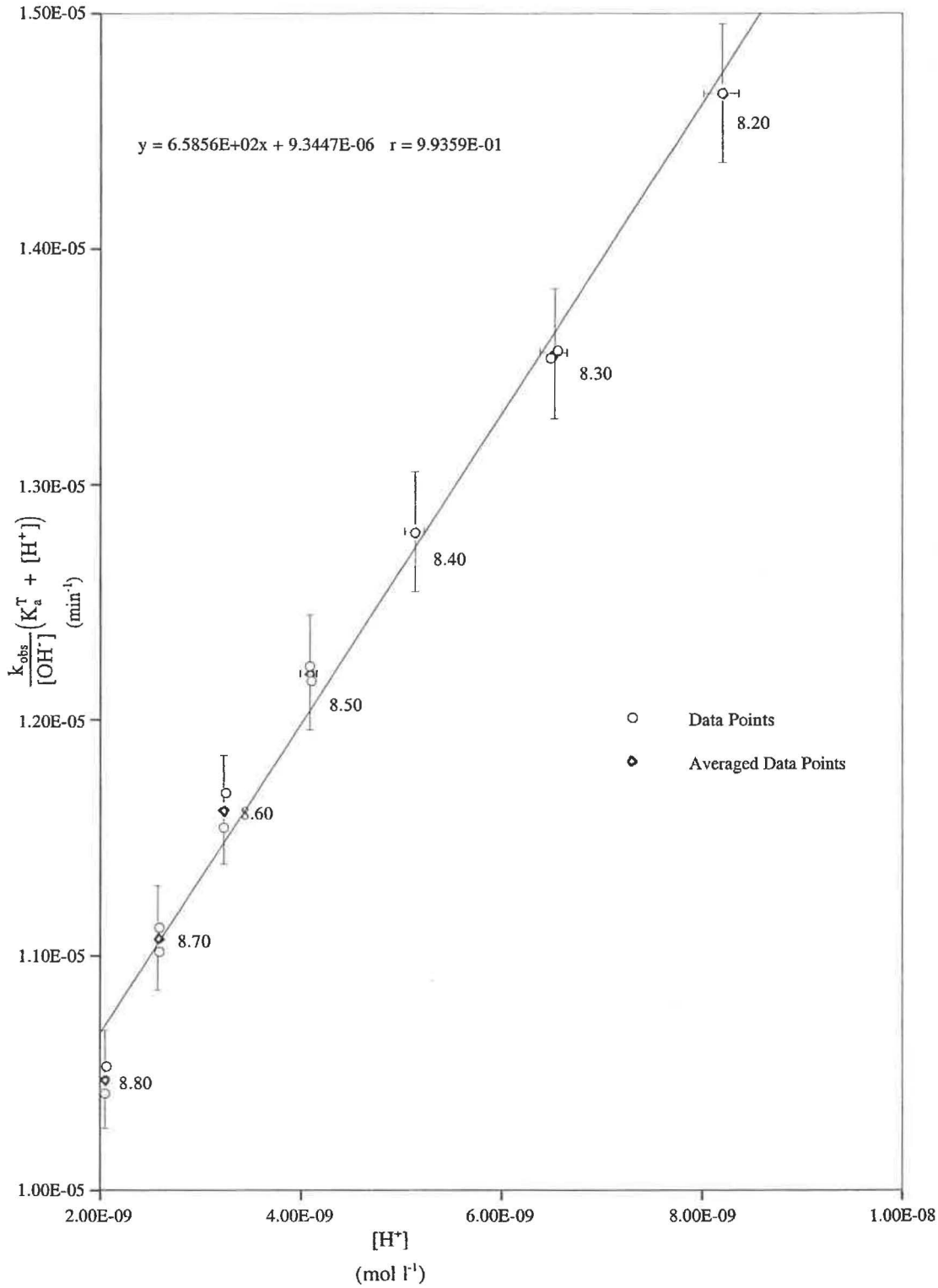

A3.3(c) Summary of Kinetic Tables for Amino Acid Esters at 50.2°C

Section A3.3(c) contain tables that list the effect of pH on the value of $k_{obs}/[OH^-]$, data needed for the separation of k_E and k_{EH^+} and the corresponding pH/rate profiles for the various amino acid ester studied 50.2°C and I = 0.1 mol l^{-1}.

Table A3.55 Summary of $k_{obs}/[OH^-]$ for Ser Me

$T = (50.20 \pm 0.10)°C$

$I = 0.1$ mol l^{-1}

pH†	k_{obs} (min^{-1})	$t_{1/2}$ (min)	$[OH^-]^*$ (mol l^{-1})	$\frac{k_{obs}}{[OH^-]}$ (l mol^{-1} min^{-1})
9.609	7.773×10^{-2}	8.9	2.922×10^{-4}	266.0
9.611	7.964×10^{-2}	8.7	2.935×10^{-4}	271.3
9.611	7.988×10^{-2}	8.7	2.935×10^{-4}	272.2
9.611	7.843×10^{-2}	8.8	2.928×10^{-4}	267.8
9.609	7.879×10^{-2}	8.8	2.922×10^{-4}	269.7
9.609	7.740×10^{-2}	8.9	2.922×10^{-4}	266.0
9.610	7.904×10^{-2}	8.8	2.928×10^{-4}	265.0
9.610	7.762×10^{-2}	8.9	2.928×10^{-4}	265.0
9.609	7.857×10^{-2}	8.8	2.922×10^{-4}	268.9
9.612	7.925×10^{-2}	8.7	2.942×10^{-4}	268.9
9.608	7.805×10^{-2}	8.9	2.915×10^{-4}	267.7
9.609	7.784×10^{-2}	8.9	2.922×10^{-4}	266.4
9.610	7.885×10^{-2}	8.8	2.928×10^{-4}	269.2
9.609	7.837×10^{-2}	8.8	2.922×10^{-4}	268.2

Overall $\frac{k_{obs}}{[OH^-]} = (268 \pm 4)$ l mol^{-1} min^{-1}

†Stopped Stirrer pH, $^*[OH^-] = \frac{10^{pH - 13.2617}}{0.7615}$ (50°C and I = 0.1 mol l^{-1}).

Table A3.56 Effect of pH on the Value of $k_{obs}/[OH^-]$ for 2-AE Me

$T = (50.2 \pm 0.10)°C$

$I = 0.1$ mol l^{-1}

pH†	k_{obs} (min^{-1})	$t_{1/2}$ (min)	$[OH^-]^*$ (mol l^{-1})	$\frac{k_{obs}}{[OH^-]}$ (l mol^{-1} min^{-1})
7.711	1.018×10^{-2}	68.1	3.695×10^{-6}	2755.1
7.911	1.127×10^{-2}	61.5	5.856×10^{-6}	1924.5
8.110	1.290×10^{-2}	53.7	9.282×10^{-6}	1374.7
8.111	1.276×10^{-2}	54.3	9.260×10^{-6}	1378.0
8.311	1.589×10^{-2}	43.6	1.471×10^{-5}	1080.2
8.508	1.797×10^{-2}	38.6	2.315×10^{-5}	776.2
8.509	1.852×10^{-2}	37.4	2.321×10^{-5}	797.9
8.711	2.243×10^{-2}	30.9	3.695×10^{-5}	607.0
8.901	2.833×10^{-2}	24.5	5.723×10^{-5}	495.0
8.906	2.924×10^{-2}	23.7	5.789×10^{-5}	505.1
9.105	3.836×10^{-2}	18.1	9.154×10^{-5}	419.1
9.304	5.891×10^{-2}	11.8	1.448×10^{-4}	406.8
9.306	5.948×10^{-2}	11.7	1.454×10^{-4}	409.1
9.505	8.692×10^{-2}	8.0	2.299×10^{-4}	378.1
9.506	8.920×10^{-2}	7.8	2.305×10^{-4}	387.0
9.705	1.374×10^{-1}	5.0	3.644×10^{-4}	377.1
9.806	1.646×10^{-1}	4.2	4.599×10^{-4}	357.9
9.807	1.659×10^{-1}	4.2	4.609×10^{-4}	359.9

†Stopped Stirrer pH, $^*[OH^-] = \frac{10^{pH - 13.2617}}{0.7615}$ (50°C and I = 0.1 mol l^{-1}).

Table A3.57 Data for Separation of k_E and k_{EH^+} for the Alkaline Hydrolysis of 2-AE Me

$T = (50.2 \pm 0.10)°C$

$I = 0.1$ mol l^{-1}

pH†	$[H^+]$ (mol l^{-1})	$(K_a^T + H^+)$ (mol l^{-1})	$\frac{k_{obs}}{[OH^-]}$ (l mol^{-1} min^{-1})	$\frac{k_{obs}}{[OH^-]}(K_a^T + [H^+])$ (min^{-1})
7.711	2.555×10^{-8}	1.210×10^{-7}	2755.1	3.334×10^{-4}
7.911	1.612×10^{-8}	1.116×10^{-7}	1924.5	2.149×10^{-4}
8.110	1.017×10^{-8}	1.057×10^{-7}	1374.7	1.469×10^{-4}
8.111	1.019×10^{-8}	1.057×10^{-7}	1378.0	1.456×10^{-4}
8.311	6.417×10^{-9}	1.019×10^{-7}	1080.2	1.101×10^{-4}
8.508	4.077×10^{-9}	9.958×10^{-8}	776.2	7.727×10^{-5}
8.509	4.068×10^{-9}	9.957×10^{-8}	797.9	7.945×10^{-5}
8.711	2.555×10^{-9}	9.805×10^{-8}	607.0	5.952×10^{-5}
8.901	1.649×10^{-9}	9.715×10^{-8}	495.0	4.809×10^{-5}
8.906	1.631×10^{-9}	9.713×10^{-8}	505.1	4.905×10^{-5}
9.105	1.031×10^{-9}	9.653×10^{-8}	419.1	4.045×10^{-5}
9.304	6.521×10^{-10}	9.615×10^{-8}	406.8	3.913×10^{-6}
9.306	6.491×10^{-10}	9.615×10^{-8}	409.1	3.932×10^{-6}
9.505	4.105×10^{-10}	9.591×10^{-8}	378.1	3.625×10^{-6}
9.506	4.096×10^{-10}	9.591×10^{-8}	387.0	3.712×10^{-6}
9.705	2.590×10^{-10}	9.576×10^{-8}	377.1	3.610×10^{-6}
9.806	2.053×10^{-10}	9.570×10^{-8}	357.9	3.426×10^{-6}
9.807	2.048×10^{-11}	9.570×10^{-8}	359.9	3.445×10^{-6}

Using $K_a^T = 9.550 \times 10^{-8}$; $pK_a^T = 7.02$ (50°C and I = 0.1 mol l^{-1}), (Table A1.25).

†Stopped Stirrer pH. $[H^+] = \frac{10^{-pH}}{0.7615}$ (50°C and I = 0.1 mol l^{-1}).

Figure A3.26 Separation of k_E and k_{EH^+} for Alkaline Hydrolysis of 2-AE Me

$T = (50.20 \pm 0.10)°C$

$I = 0.1$ mol l^{-1}

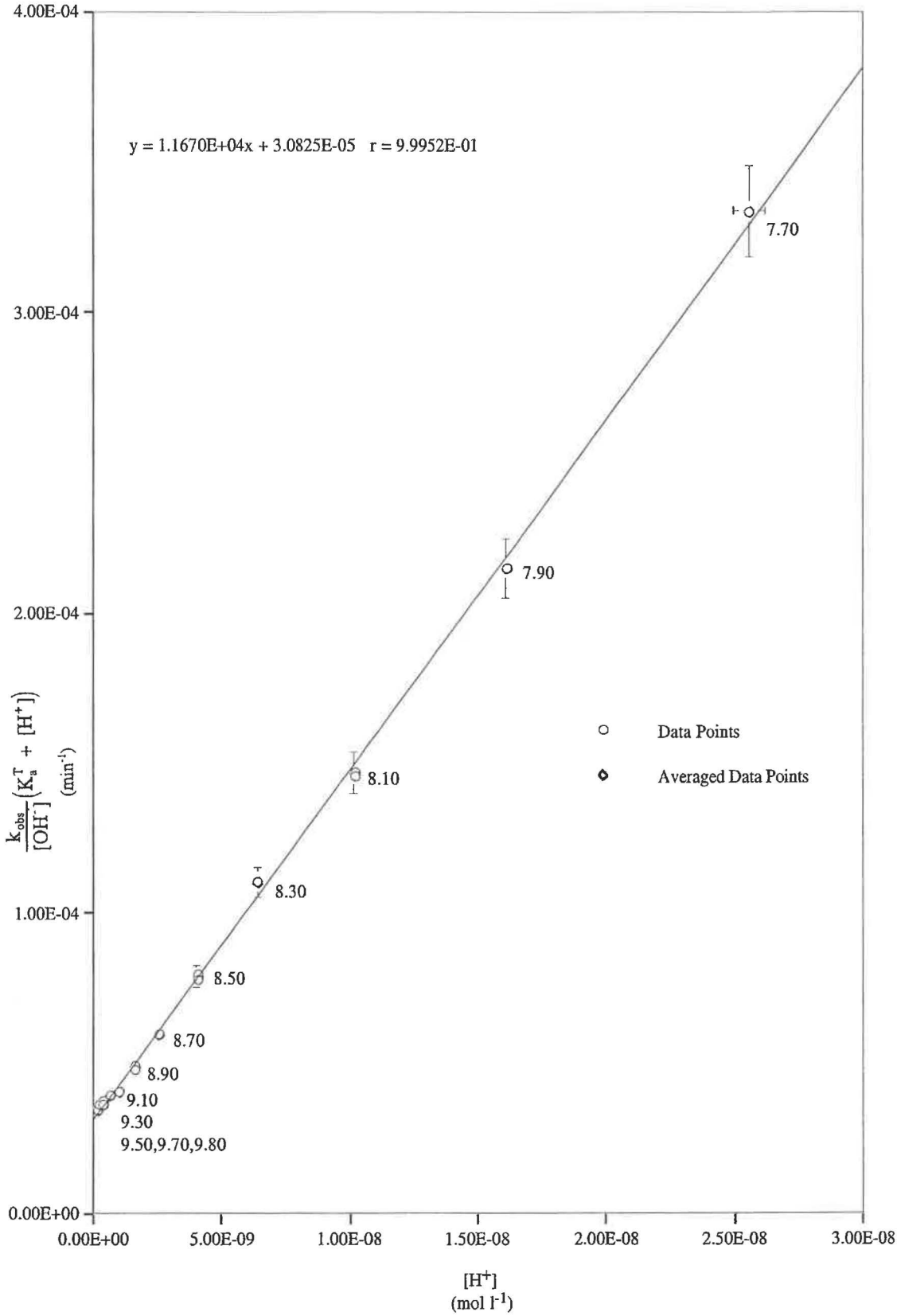

Table A3.58 Effect of the pH on the Value of $k_{obs}/[OH^-]$ for 3-AP Bz

$T = (50.20 \pm 0.10)°C$

$I = 0.1$ mol l^{-1}

pH†	k_{obs} (min^{-1})	$t_{1/2}$ (min)	$[OH^-]^*$ (mol l^{-1})	$\frac{k_{obs}}{[OH^-]}$ (l mol^{-1} min^{-1})
8.203	2.396×10^{-2}	28.9	1.147×10^{-5}	2088.8
8.403	3.299×10^{-2}	21.0	1.818×10^{-5}	1814.5
8.403	3.195×10^{-2}	21.7	1.818×10^{-5}	1757.2
8.604	3.943×10^{-2}	17.6	2.888×10^{-5}	1365.2
8.804	4.677×10^{-2}	14.8	4.578×10^{-5}	1021.7
8.804	4.963×10^{-2}	14.0	4.578×10^{-5}	1084.3
9.002	4.996×10^{-2}	13.9	7.222×10^{-5}	691.8
9.204	6.104×10^{-2}	11.4	1.150×10^{-4}	530.9
9.205	6.455×10^{-2}	10.7	1.52×10^{-4}	560.1
9.405	7.676×10^{-2}	9.0	1.827×10^{-4}	420.3
9.608	8.637×10^{-2}	8.0	2.915×10^{-4}	296.3
9.609	8.733×10^{-2}	7.9	2.922×10^{-4}	298.9
9.708	9.622×10^{-2}	7.2	3.670×10^{-4}	262.2
9.808	8.732×10^{-2}	7.9	4.620×10^{-4}	189.0
9.809	8.756×10^{-2}	7.9	4.631×10^{-4}	189.1
10.011	9.179×10^{-2}	7.6	7.373×10^{-4}	124.5
10.011	9.186×10^{-2}	7.5	7.373×10^{-3}	124.6

†Stopped Stirrer pH, $^*[OH^-] = \frac{10^{pH - 13.2617}}{0.7615}$ (50°C and I = 0.1 mol l^{-1}).

Table A3.59 Data for Separation of k_E and k_{EH^+} for the Alkaline Hydrolysis of 3-AP Bz

$T = (50.20 \pm 0.10)°C$

$I = 0.1$ mol l^{-1}

pH†	$[H^+]$ (mol l^{-1})	$(K_a^T + H^+)$ (mol l^{-1})	$\frac{k_{obs}}{[OH^-]}$ (l mol^{-1} min^{-1})	$\frac{k_{obs}}{[OH^-]}(K_a^T + [H^+])$ (min^{-1})
8.203	8.229×10^{-9}	1.280×10^{-8}	2088.8	2.674×10^{-5}
8.403	5.192×10^{-9}	9.763×10^{-9}	1814.5	1.771×10^{-5}
8.403	5.192×10^{-9}	9.763×10^{-9}	1757.2	1.716×10^{-5}
8.604	3.268×10^{-9}	7.839×10^{-9}	1365.2	1.070×10^{-5}
8.804	2.062×10^{-9}	6.633×10^{-9}	1021.7	6.777×10^{-6}
8.804	2.062×10^{-9}	6.633×10^{-9}	1084.3	7.192×10^{-6}
9.002	1.307×10^{-9}	5.878×10^{-9}	691.8	4.066×10^{-6}
9.204	8.210×10^{-10}	5.392×10^{-9}	530.9	2.863×10^{-6}
9.205	8.191×10^{-10}	5.390×10^{-9}	560.1	3.019×10^{-6}
9.405	5.168×10^{-10}	5.088×10^{-9}	420.3	2.138×10^{-6}
9.608	3.238×10^{-10}	4.895×10^{-9}	296.3	1.450×10^{-6}
9.609	3.231×10^{-10}	4.894×10^{-9}	298.9	1.463×10^{-6}
9.708	2.572×10^{-10}	4.828×10^{-9}	262.2	1.266×10^{-6}
9.808	2.043×10^{-10}	4.775×10^{-9}	189.0	9.025×10^{-7}
9.809	2.039×10^{-10}	4.775×10^{-9}	189.1	9.029×10^{-7}
10.011	1.280×10^{-10}	4.699×10^{-9}	124.5	5.850×10^{-7}
10.011	1.280×10^{-10}	4.699×10^{-9}	124.6	5.855×10^{-7}

Using $K_a^T = 4.571 \times 10^{-9}$; $pK_a^T = 8.34$ (50°C and I = 0.1 mol l^{-1}), (Table A1.26).

†Stopped Stirrer pH. $[H^+] = \frac{10^{-pH}}{0.7615}$ (50°C and I = 0.1 mol l^{-1}).

Figure A3.27 Separation of k_E and k_{EH^+} for Alkaline Hydrolysis of 3-AP Bz

$T = (50.20 \pm 0.10)°C$

$I = 0.1$ mol l^{-1}

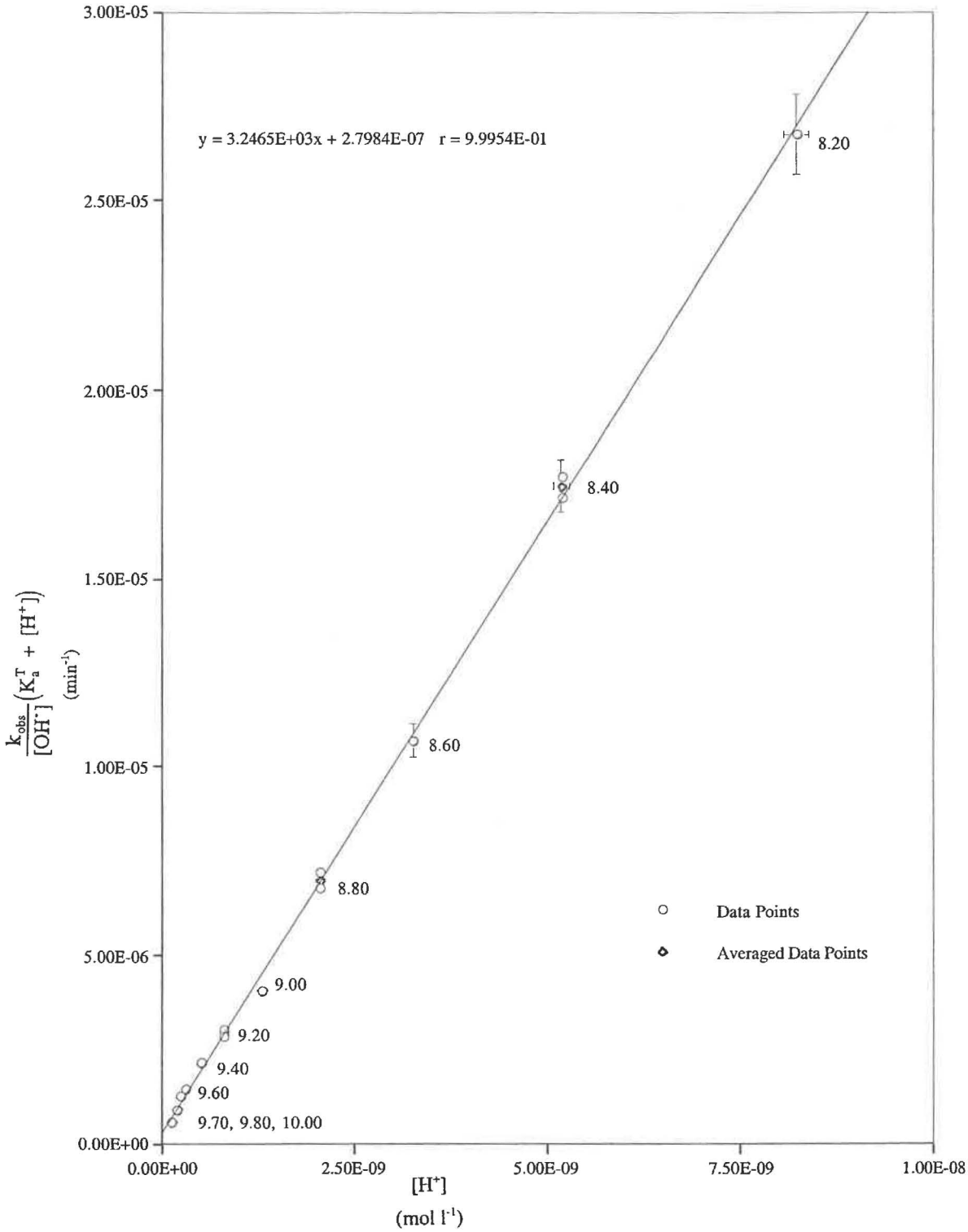

Table A3.60 Effect of pH on the Value of $k_{obs}/[OH^-]$ for 4-DMAB Me.

$T = (50.20 \pm 0.10)°C$

$I = 0.1$ mol l^{-1}

pH†	k_{obs} (min^{-1})	$t_{1/2}$ (min)	$[OH^-]^*$ (mol l^{-1})	$\frac{k_{obs}}{[OH^-]}$ (l mol^{-1} min^{-1})
8.708	2.654×10^{-2}	26.1	3.670×10^{-5}	723.2
8.911	3.603×10^{-2}	19.2	5.856×10^{-5}	615.2
9.009	4.068×10^{-2}	17.0	7.339×10^{-5}	554.3
9.310	5.072×10^{-2}	13.7	1.468×10^{-4}	345.6
9.311	5.247×10^{-2}	13.2	1.471×10^{-4}	356.7
9.511	6.377×10^{-2}	10.9	2.331×10^{-4}	273.5
9.711	6.869×10^{-2}	10.1	3.695×10^{-4}	185.9
9.911	8.650×10^{-2}	8.0	5.856×10^{-4}	147.7
10.110	1.080×10^{-1}	6.4	9.260×10^{-4}	116.6
10.209	1.151×10^{-1}	6.0	1.163×10^{-3}	99.0
10.210	1.073×10^{-1}	6.5	1.166×10^{-3}	92.0
10.309	1.415×10^{-1}	4.9	1.464×10^{-3}	96.6

†Stopped Stirrer pH, $^*[OH^-] = \frac{10^{pH\ -\ 13.2617}}{0.7615}$, (50°C and I = 0.1 mol l^{-1}).

Table A3.61 Data for Separation of k_E and k_{EH^+} for the Alkaline Hydrolysis 4-DMAB Me.

$T = (50.20 \pm 0.05)°C$

$I = 0.1$ mol l^{-1}

pH†	$[H^+]$ (mol l^{-1})	$(K_a^T + H^+)$ (mol l^{-1})	$\frac{k_{obs}}{[OH^-]}$ (l mol^{-1} min^{-1})	$\frac{k_{obs}}{[OH^-]}(K_a^T + [H^+])$ (min^{-1})
8.708	2.572×10^{-9}	3.921×10^{-9}	723.2	2.836×10^{-6}
8.911	1.612×10^{-9}	2.961×10^{-9}	615.2	1.822×10^{-6}
9.009	1.286×10^{-9}	2.635×10^{-9}	554.3	1.461×10^{-6}
9.310	6.432×10^{-10}	1.992×10^{-9}	345.6	6.885×10^{-7}
9.311	6.417×10^{-10}	1.991×10^{-9}	356.7	7.101×10^{-7}
9.511	4.049×10^{-10}	1.754×10^{-9}	273.5	4.797×10^{-7}
9.711	2.555×10^{-10}	1.604×10^{-9}	185.9	2.983×10^{-7}
9.911	1.612×10^{-10}	1.510×10^{-9}	147.7	2.230×10^{-7}
10.110	1.019×10^{-10}	1.451×10^{-9}	116.6	1.692×10^{-7}
10.209	8.116×10^{-11}	1.430×10^{-9}	99.0	1.416×10^{-7}
10.210	8.097×10^{-11}	1.430×10^{-9}	92.0	1.316×10^{-7}
10.309	6.447×10^{-11}	1.413×10^{-9}	96.6	1.365×10^{-7}

Using $K_a^T = 1.349 \times 10^{-9}$; $pK_a^T = 8.87$ (50°C and I = 0.1 mol l^{-1}), (Table A1.27).

†Stopped Stirrer pH, $[H^+] = \frac{10^{-pH}}{0.7615}$ (50°C and I = 0.1 mol l^{-1}).

Figure A3.28 Separation of k_E and k_{EH^+} for Alkaline Hydrolysis of 4-DMAB Me

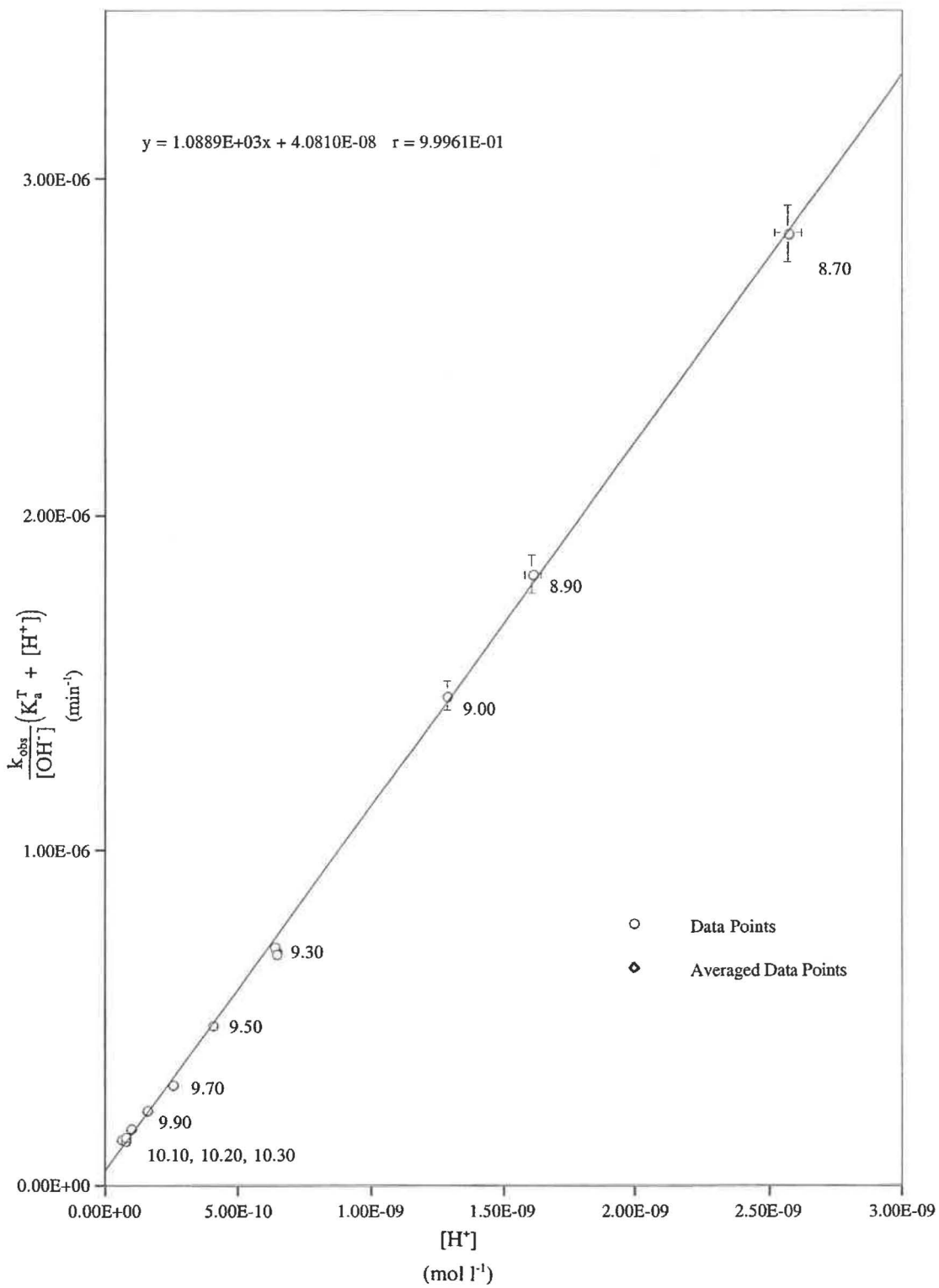

Table A3.62 Effect of pH on the Value of $k_{obs}/[OH^-]$ for 4-DMAB Et

$T = (50.20 \pm 0.10)°C$

$I = 0.1$ mol l^{-1}

pH†	k_{obs} (min^{-1})	$t_{1/2}$ (min)	$[OH^-]^*$ (mol l^{-1})	$\frac{k_{obs}}{[OH^-]}$ (l mol^{-1} min^{-1})
9.106	2.437×10^{-2}	28.4	9.176×10^{-5}	265.6
9.306	2.664×10^{-2}	26.0	1.454×10^{-4}	183.2
9.506	3.347×10^{-2}	20.7	2.305×10^{-4}	145.2
9.707	4.035×10^{-2}	17.2	3.661×10^{-4}	110.2
9.908	4.542×10^{-2}	15.3	5.816×10^{-4}	78.1
10.108	3.853×10^{-2}	18.0	9.218×10^{-4}	41.8
10.211	5.714×10^{-2}	12.1	1.169×10^{-3}	48.9
10.212	5.938×10^{-2}	11.7	1.171×10^{-3}	50.7
10.310	6.737×10^{-2}	10.3	1.468×10^{-3}	45.9

†Stopped Stirrer pH, $^*[OH^-] = \frac{10^{pH\ -\ 13.2617}}{0.7615}$, (50°C and I = 0.1 mol l^{-1}).

Table A3.63 Data for Separation of k_E and k_{EH+} for the Alkaline Hydrolysis of 4-DMAB Et

$T = (50.20 \pm 0.10)°C$

$I = 0.1$ mol l^{-1}

pH†	$[H^+]$ (mol l^{-1})	$(K_a^T + H^+)$ (mol l^{-1})	$\frac{k_{obs}}{[OH^-]}$ (l mol^{-1} min^{-1})	$\frac{k_{obs}}{[OH^-]}(K_a^T + [H^+])$ (min^{-1})
9.106	1.029×10^{-9}	2.767×10^{-9}	265.6	7.348×10^{-7}
9.306	6.491×10^{-10}	2.387×10^{-9}	183.2	4.373×10^{-7}
9.506	4.096×10^{-10}	2.147×10^{-9}	145.2	3.118×10^{-7}
9.707	2.578×10^{-10}	1.996×10^{-9}	110.2	2.199×10^{-7}
9.908	1.623×10^{-10}	1.900×10^{-9}	78.1	1.484×10^{-7}
10.108	1.024×10^{-10}	1.840×10^{-9}	41.8	7.692×10^{-8}
10.211	8.078×10^{-11}	1.819×10^{-10}	48.9	8.893×10^{-8}
10.212	8.060×10^{-11}	1.818×10^{-10}	50.7	9.219×10^{-8}
10.310	6.432×10^{-11}	1.802×10^{-10}	45.9	8.272×10^{-8}

Using $K_a^T = 1.738 \times 10^{-9}$; $pK_a^T = 8.76$ (50°C and I = 0.1 mol l^{-1}), (Table A1.28).

†Stopped Stirrer pH, $[H^+] = \frac{10^{-pH}}{0.7615}$ (50°C and I = 0.1 mol l^{-1}).

Figure A3.29 Separation of k_E and k_{EH^+} for Alkaline Hydrolysis of 4-DMAB Et

$T = (50.20 \pm 0.10)°C$

$I = 0.1$ mol l^{-1}

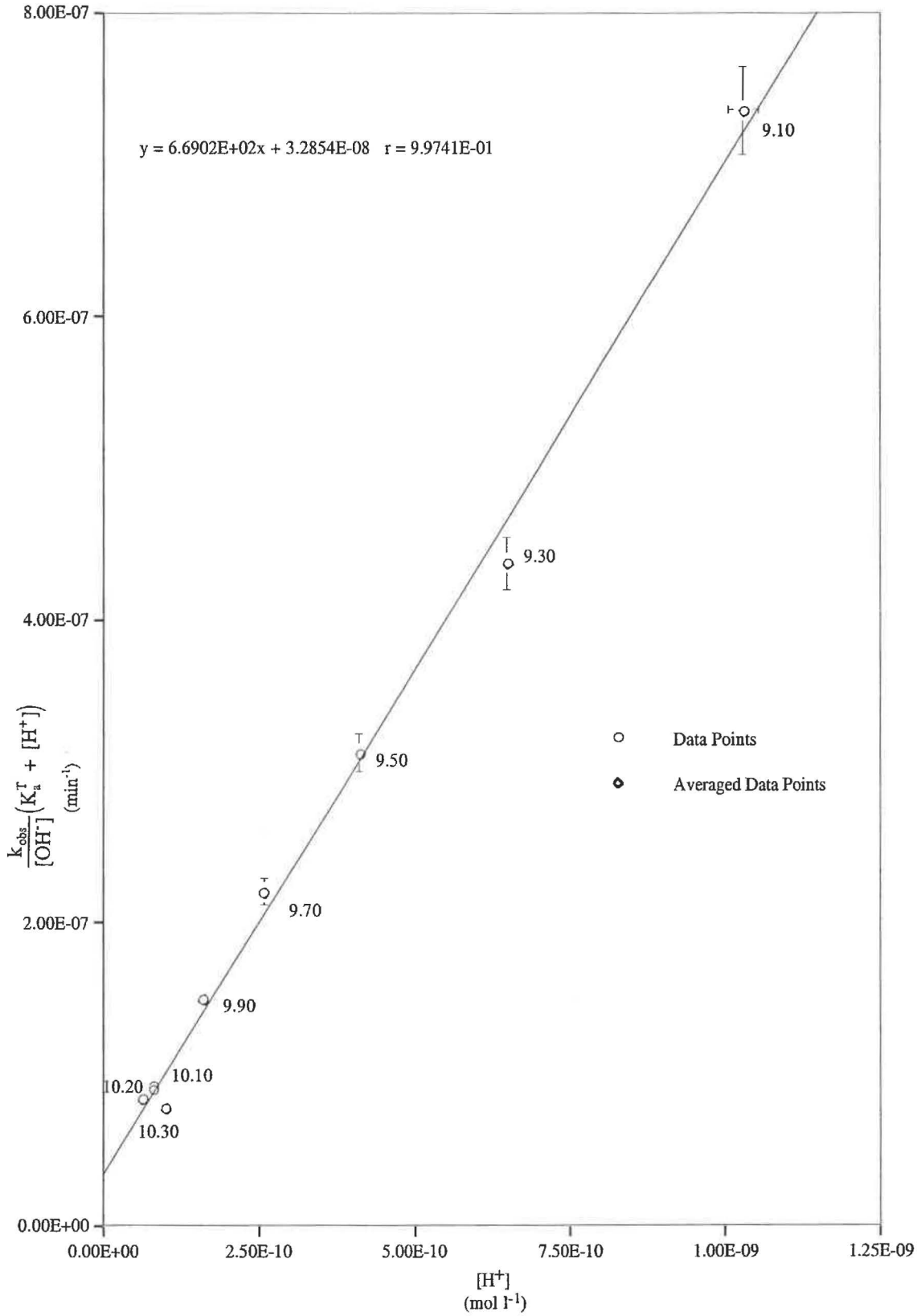

Table A3.64 Effect of pH on the Value of $k_{obs}/[OH^-]$ for 4-AB Me

$T = (50.20 \pm 0.10)°C$

$I = 0.1$ mol l^{-1}

pH†	k_{obs} (min^{-1})	$t_{1/2}$ (min)	$[OH^-]^*$ (mol l^{-1})	$\frac{k_{obs}}{[OH^-]}$ (l mol^{-1} min^{-1})
8.006	3.932×10^{-3}	176.3	7.288×10^{-6}	539.5
8.103	5.488×10^{-3}	126.3	9.112×10^{-6}	602.3
8.103	5.478×10^{-3}	126.5	9.112×10^{-6}	601.2
8.206	7.766×10^{-3}	89.3	1.155×10^{-5}	672.3
8.304	1.076×10^{-2}	64.4	1.448×10^{-5}	743.5
8.304	1.073×10^{-2}	64.6	1.448×10^{-5}	741.2
8.406	1.542×10^{-2}	44.9	1.831×10^{-5}	842.5
8.503	2.180×10^{-2}	31.8	2.289×10^{-5}	952.6
8.504	2.182×10^{-2}	31.8	2.294×10^{-5}	951.2
8.604	3.098×10^{-2}	22.4	2.888×10^{-5}	1072.8
8.706	4.415×10^{-2}	15.7	3.653×10^{-5}	1208.7
8.807	6.448×10^{-2}	10.8	4.609×10^{-5}	1398.7
8.907	8.711×10^{-2}	8.0	5.803×10^{-5}	1501.2
8.907	8.756×10^{-2}	7.9	5.803×10^{-5}	1508.9

†Stopped Stirrer pH, $^*[OH^-] = \frac{10^{pH - 13.2617}}{0.7615}$ (50°C and I = 0.1 mol l^{-1}).

Table A3.65 Data for Separation of k_E and k_{EH+} for the Alkaline Hydrolysis 4-AB Me

$T = (50.20 \pm 0.10)°C$

$I = 0.1$ mol l^{-1}

pH†	$[H^+]$ (mol l^{-1})	$(K_a^T + H^+)$ (mol l^{-1})	$\frac{k_{obs}}{[OH^-]}$ (l mol^{-1} min^{-1})	$\frac{k_{obs}}{[OH^-]}(K_a^T + [H^+])$ (min^{-1})
8.006	1.295×10^{-8}	1.376×10^{-8}	539.5	7.426×10^{-6}
8.103	1.036×10^{-8}	1.117×10^{-8}	602.3	6.729×10^{-6}
8.103	1.036×10^{-8}	1.117×10^{-8}	601.2	6.717×10^{-6}
8.206	8.172×10^{-9}	8.985×10^{-9}	672.3	6.041×10^{-6}
8.304	6.521×10^{-9}	7.334×10^{-9}	743.5	5.453×10^{-6}
8.304	6.521×10^{-9}	7.334×10^{-9}	741.2	5.436×10^{-6}
8.406	5.156×10^{-9}	5.969×10^{-9}	842.5	5.029×10^{-6}
8.503	4.124×10^{-9}	4.937×10^{-9}	952.6	4.703×10^{-6}
8.504	4.115×10^{-9}	4.927×10^{-9}	951.2	4.687×10^{-6}
8.604	3.268×10^{-9}	4.081×10^{-9}	1072.8	4.378×10^{-6}
8.706	2.584×10^{-9}	3.397×10^{-9}	1208.7	$4.106. \times 10^{-6}$
8.807	2.048×10^{-9}	2.861×10^{-9}	1398.7	4.002×10^{-6}
8.907	1.627×10^{-9}	2.440×10^{-9}	1501.2	3.662×10^{-6}
8.907	1.627×10^{-9}	2.440×10^{-9}	1508.9	3.681×10^{-6}

Using $K_a^T = 8.128 \times 10^{-10}$; $pK_a^T = 9.09$ (50°C and I = 0.1 mol l^{-1}), (Table A1.29).

†Stopped Stirrer pH. $[H^+] = \frac{10^{-pH}}{0.7615}$ (50°C and I = 0.1 mol l^{-1}).

Figure A3.30 Separation of k_E and k_{EH^+} for Alkaline Hydrolysis of 4-AB Me

$T = (50.20 \pm 0.10)°C$

$I = 0.1 \text{ mol } l^{-1}$

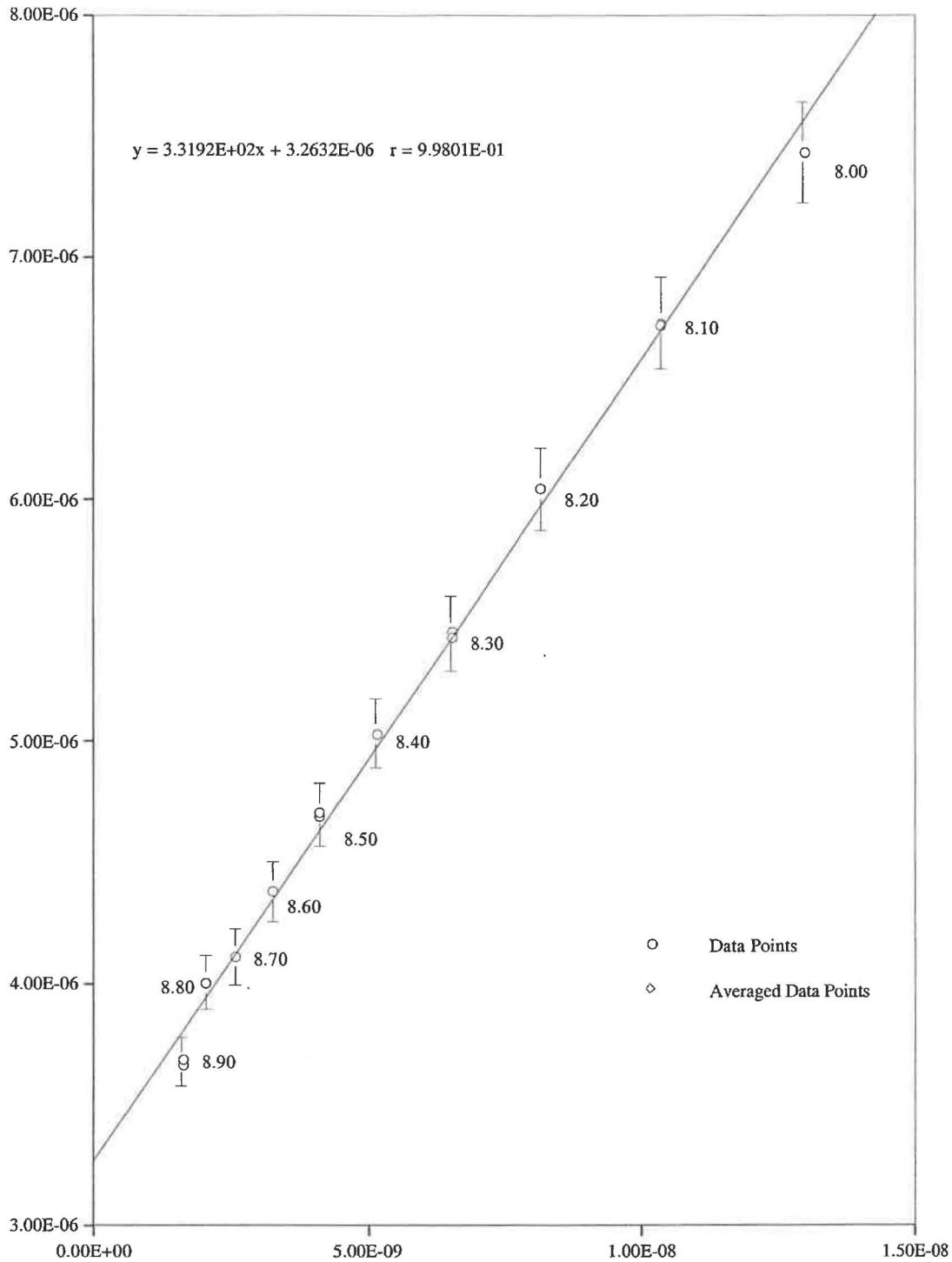

Table A3.66 Effect of pH on the Value of $k_{obs}/[OH^-]$ for 4-AB Et

$T = (50.20 \pm 0.10)°C$

$I = 0.1$ mol l^{-1}

pH†	k_{obs} (min^{-1})	$t_{1/2}$ (min)	$[OH^-]^*$ (mol l^{-1})	$\frac{k_{obs}}{[OH^-]}$ (l mol^{-1} min^{-1})
8.305	5.402×10^{-3}	128.3	1.451×10^{-5}	372.3
8.405	7.219×10^{-3}	96.0	1.827×10^{-5}	395.2
8.407	7.292×10^{-3}	95.1	1.835×10^{-5}	397.4
8.507	9.525×10^{-3}	72.8	2.310×10^{-5}	412.3
8.608	1.295×10^{-2}	53.5	2.915×10^{-5}	444.4
8.608	1.307×10^{-2}	53.0	2.915×10^{-5}	448.3
8.707	1.720×10^{-2}	40.3	3.661×10^{-5}	469.8
8.806	2.328×10^{-2}	29.8	4.599×10^{-5}	506.3
8.806	2.340×10^{-2}	29.6	4.599×10^{-5}	508.9
8.906	3.178×10^{-2}	21.8	5.789×10^{-5}	548.9
9.006	4.425×10^{-2}	15.7	7.288×10^{-5}	607.2
9.006	4.444×10^{-2}	15.6	7.288×10^{-5}	609.8
9.105	6.132×10^{-2}	11.3	9.154×10^{-5}	669.8
9.207	8.466×10^{-2}	8.2	1.158×10^{-4}	731.2
9.208	8.469×10^{-2}	8.2	1.160×10^{-4}	729.8

†Stopped Stirrer pH, $^*[OH^-] = \frac{10^{pH - 13.2617}}{0.7615}$ (50°C and I = 0.1 mol l^{-1}).

Table A3.67 Data for Separation of k_E and k_{EH^+} for the Alkaline Hydrolysis of 4-AB Et

$T = (50.20 \pm 0.10)°C$

$I = 0.1$ mol l^{-1}

pH†	$[H^+]$ (mol l^{-1})	$(K_a^T + H^+)$ (mol l^{-1})	$\frac{k_{obs}}{[OH^-]}$ (l mol^{-1} min^{-1})	$\frac{k_{obs}}{[OH^-]}(K_a^T + [H^+])$ (min^{-1})
8.305	6.506×10^{-9}	7.300×10^{-9}	372.3	2.718×10^{-6}
8.405	5.168×10^{-9}	5.962×10^{-9}	395.2	2.356×10^{-6}
8.407	5.144×10^{-9}	5.938×10^{-9}	397.4	2.360×10^{-6}
8.507	4.086×10^{-9}	4.880×10^{-9}	412.3	2.012×10^{-6}
8.608	3.238×10^{-9}	4.032×10^{-9}	444.4	1.792×10^{-6}
8.608	3.238×10^{-9}	4.032×10^{-9}	448.3	1.808×10^{-6}
8.707	2.578×10^{-9}	3.372×10^{-9}	469.8	1.584×10^{-6}
8.806	2.053×10^{-9}	2.847×10^{-9}	506.3	1.442×10^{-6}
8.806	2.053×10^{-9}	2.847×10^{-9}	508.9	1.449×10^{-6}
8.906	1.631×10^{-9}	2.425×10^{-9}	548.9	1.331×10^{-6}
9.006	1.295×10^{-9}	2.089×10^{-9}	607.2	$1.269. \times 10^{-6}$
9.006	1.295×10^{-9}	2.089×10^{-9}	609.8	1.274×10^{-6}
9.105	1.031×10^{-9}	1.825×10^{-9}	669.8	1.223×10^{-6}
9.207	8.153×10^{-10}	1.608×10^{-9}	731.2	1.176×10^{-6}
9.208	8.134×10^{-10}	1.608×10^{-9}	729.8	1.173×10^{-6}

Using $K_a^T = 7.943 \times 10^{-10}$; $pK_a^T = 9.10$ (50°C and I = 0.1 mol l^{-1}), (Table A1.30).

†Stopped Stirrer pH. $[H^+] = \frac{10^{-pH}}{0.7615}$ (50 °C and I = 0.1 mol l^{-1}).

Figure A3.31 Separation of k_E and k_{EH^+} for Alkaline Hydrolysis of 4-AB Et

$T = (50.20 \pm 0.10)°C$

$I = 0.1$ mol l^{-1}

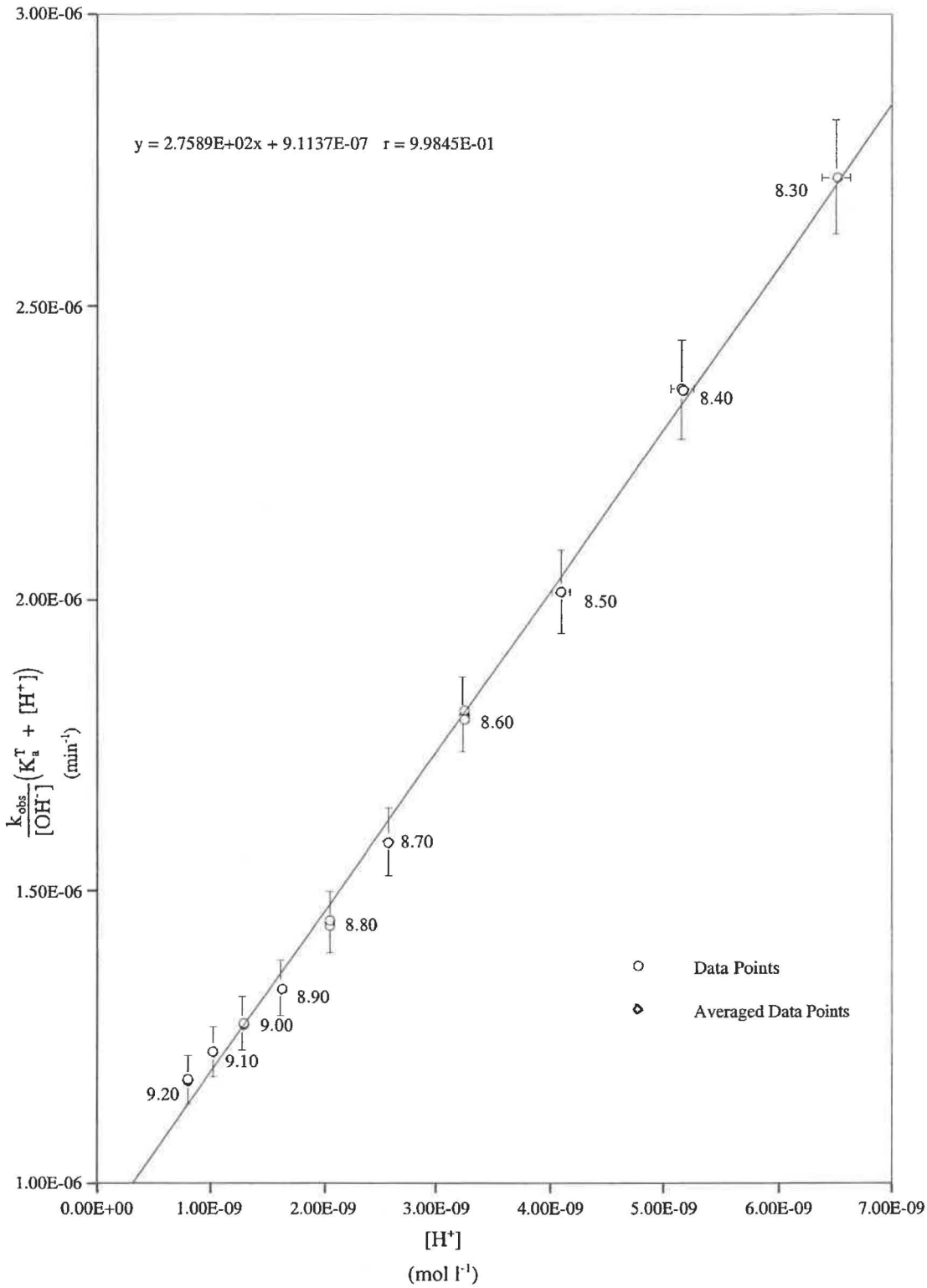

Table A3.68 Effect of pH on the Value of $k_{obs}/[OH^-]$ for 4-AB Bz

$T = (50.20 \pm 0.10)°C$

$I = 0.1$ mol l^{-1}

pH†	k_{obs} (min^{-1})	$t_{1/2}$ (min)	$[OH^-]^*$ (mol l^{-1})	$\frac{k_{obs}}{[OH^-]}$ (l mol^{-1} min^{-1})
8.105	7.427×10^{-3}	93.3	9.176×10^{-6}	813.2
8.106	7.462×10^{-3}	92.9	9.154×10^{-6}	811.3
8.205	1.025×10^{-2}	67.6	1.152×10^{-5}	889.5
8.306	1.383×10^{-2}	50.1	1.454×10^{-5}	951.3
8.406	1.975×10^{-2}	35.1	1.831×10^{-5}	1078.6
8.406	1.980×10^{-2}	35.0	1.831×10^{-5}	1081.3
8.506	2.822×10^{-2}	24.6	2.305×10^{-5}	1224.3
8.606	3.925×10^{-2}	17.7	2.902×10^{-5}	1352.6
8.606	3.910×10^{-2}	17.7	2.902×10^{-5}	1347.6
8.708	5.353×10^{-2}	12.9	3.670×10^{-5}	1458.6
8.810	7.437×10^{-2}	9.3	4.641×10^{-5}	1602.3
8.810	7.473×10^{-2}	9.3	4.641×10^{-5}	1610.2
8.908	1.048×10^{-1}	6.6	5.816×10^{-5}	1802.3
9.006	1.477×10^{-1}	4.7	7.288×10^{-5}	2026.3

†Stopped Stirrer pH, $^*[OH^-] = \frac{10^{pH\ -\ 13.2617}}{0.7615}$ (50°C and I = 0.1 mol l^{-1}).

Table A3.71 Data for Separation of k_E and k_{EH+} for the Alkaline Hydrolysis of 4-AB Bz

$T = (50.20 \pm 0.10)°C$

$I = 0.1$ mol l^{-1}

pH†	$[H^+]$ (mol l^{-1})	$(K_a^T + H^+)$ (mol l^{-1})	$\frac{k_{obs}}{[OH^-]}$ (l mol^{-1} min^{-1})	$\frac{k_{obs}}{[OH^-]}(K_a^T + [H^+])$ (min^{-1})
8.105	1.029×10^{-8}	1.118×10^{-8}	811.3	9.089×10^{-6}
8.106	1.031×10^{-8}	1.120×10^{-8}	813.2	9.091×10^{-6}
8.205	8.191×10^{-9}	9.082×10^{-9}	889.5	8.079×10^{-6}
8.306	6.491×10^{-9}	7.383×10^{-9}	951.3	7.023×10^{-6}
8.406	5.156×10^{-9}	6.047×10^{-9}	1078.6	6.523×10^{-6}
8.406	5.156×10^{-9}	6.047×10^{-9}	1081.3	6.539×10^{-6}
8.506	4.096×10^{-9}	4.987×10^{-9}	1224.5	6.107×10^{-6}
8.606	3.253×10^{-9}	4.145×10^{-9}	1352.6	5.606×10^{-6}
8.606	3.253×10^{-9}	4.145×10^{-9}	1347.6	5.585×10^{-6}
8.708	2.572×10^{-9}	3.464×10^{-9}	1458.6	5.052×10^{-6}
8.810	2.034×10^{-9}	2.925×10^{-9}	1602.3	$4.687. \times 10^{-6}$
8.810	2.034×10^{-9}	2.925×10^{-9}	1610.2	4.710×10^{-6}
8.908	1.623×10^{-9}	2.514×10^{-9}	1802.3	4.532×10^{-6}
9.006	1.295×10^{-9}	2.186×10^{-9}	2026.3	4.430×10^{-6}

Using $K_a^T = 8.913 \times 10^{-10}$; $pK_a^T = 9.05$ (50°C and I = 0.1 mol l^{-1}), Table A1.31).

†Stopped Stirrer pH. $[H^+] = \frac{10^{-pH}}{0.7615}$ (50°C and I = 0.1 mol l^{-1}).

Figure A3.32 Separation of k_E and k_{EH^+} for Alkaline Hydrolysis of 4-AB Bz

$T = (50.20 \pm 0.10)°C$

$I = 0.1$ mol l^{-1}

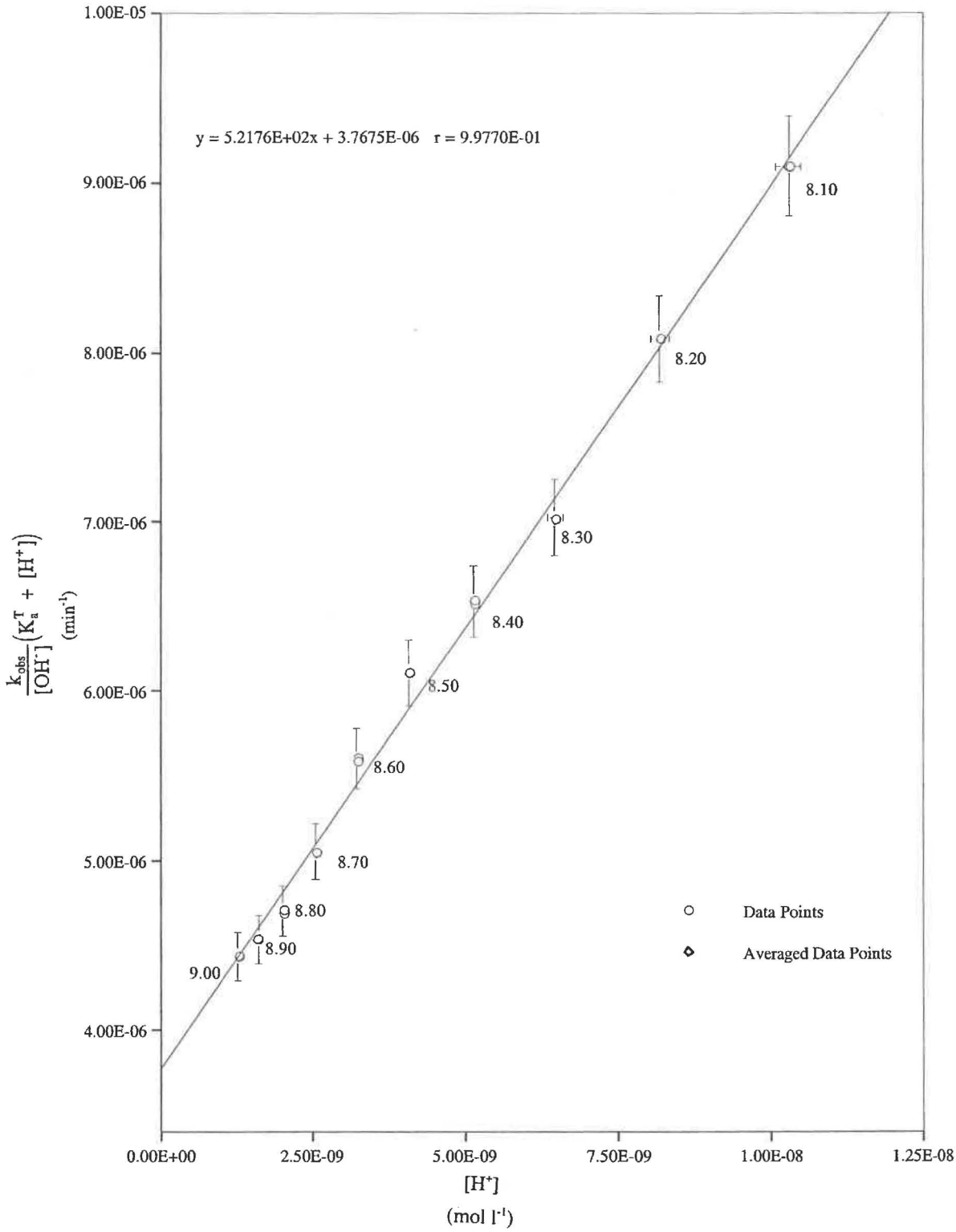

Table A3.70 Effect of pH on the Value of $k_{obs}/[OH^-]$ for 4-MAB Me

$T = (50.20 \pm 0.10)°C$

$I = 0.1$ mol l^{-1}

pH†	k_{obs} (min^{-1})	$t_{1/2}$ (min)	$[OH^-]$* (mol l^{-1})	$\frac{k_{obs}}{[OH^-]}$ (l mol^{-1} min^{-1})
7.808	5.031×10^{-3}	137.8	4.620×10^{-6}	1088.9
7.903	6.604×10^{-3}	105.0	5.750×10^{-6}	1148.7
7.903	6.651×10^{-3}	104.2	5.750×10^{-6}	1156.8
8.001	9.139×10^{-3}	75.8	7.205×10^{-6}	1268.5
8.103	1.256×10^{-2}	55.2	9.112×10^{-6}	1378.8
8.104	1.253×10^{-2}	55.3	9.133×10^{-6}	1372.2
8.204	1.736×10^{-2}	39.9	1.150×10^{-5}	1509.7
8.303	2.381×10^{-2}	29.1	1.144×10^{-5}	1648.8
8.304	2.398×10^{-2}	28.9	1.448×10^{-5}	1656.6
8.404	3.313×10^{-2}	20.9	1.822×10^{-5}	1818.2
8.503	4.526×10^{-2}	15.3	2.289×10^{-5}	1977.4
8.503	4.519×10^{-2}	15.3	2.289×10^{-5}	1974.5
8.603	6.525×10^{-2}	10.6	2.882×10^{-5}	2264.5
8.703	9.295×10^{-2}	7.5	3.628×10^{-5}	2562.3
8.703	9.273×10^{-2}	7.5	3.628×10^{-5}	2556.2

†Stopped Stirrer pH, $^*[OH^-] = \frac{10^{pH\ -\ 13.2617}}{0.7615}$ (50°C and I = 0.1 mol l^{-1}).

Table A3.71 Data for Separation of k_E and k_{EH+} for the Alkaline Hydrolysis of 4-MAB Me

$T = (50.20 \pm 0.10)°C$

$I = 0.1$ mol l^{-1}

pH†	$[H^+]$ (mol l^{-1})	$(K_a^T + H^+)$ (mol l^{-1})	$\frac{k_{obs}}{[OH^-]}$ (l mol^{-1} min^{-1})	$\frac{k_{obs}}{[OH^-]}(K_a^T + [H^+])$ (min^{-1})
7.808	2.043×10^{-8}	2.079×10^{-8}	1088.9	2.264×10^{-5}
7.903	1.642×10^{-8}	1.677×10^{-8}	1148.7	1.927×10^{-5}
7.903	1.642×10^{-8}	1.677×10^{-8}	1156.8	1.940×10^{-5}
8.001	1.310×10^{-8}	1.346×10^{-8}	1268.5	1.707×10^{-5}
8.103	1.036×10^{-8}	1.071×10^{-8}	1378.8	1.477×10^{-5}
8.104	1.034×10^{-8}	1.069×10^{-8}	1372.2	1.467×10^{-5}
8.204	8.210×10^{-9}	8.565×10^{-9}	1509.7	1.293×10^{-5}
8.303	6.536×10^{-9}	6.891×10^{-9}	1648.8	1.136×10^{-5}
8.304	6.521×10^{-9}	6.876×10^{-9}	1656.6	1.139×10^{-5}
8.404	5.180×10^{-9}	5.535×10^{-9}	1818.2	1.006×10^{-5}
8.503	4.124×10^{-9}	4.479×10^{-9}	1977.2	8.857×10^{-6}
8.503	4.124×10^{-9}	4.479×10^{-9}	1974.5	8.844×10^{-6}
8.603	3.276×10^{-9}	3.631×10^{-9}	2264.5	8.222×10^{-6}
8.703	2.602×10^{-9}	2.957×10^{-9}	2562.3	7.577×10^{-6}
8.703	2.602×10^{-9}	2.957×10^{-9}	2556.2	7.559×10^{-6}

Using $K_a^T = 3.548 \times 10^{-10}$; $pK_a^T = 9.45$ (50°C and I = 0.1 mol l^{-1}), (Table A1.32).

†Stopped Stirrer pH. $[H^+] = \frac{10^{-pH}}{0.7615}$ (50°C and I = 0.1 mol l^{-1}).

Figure A3.33 Separation of k_E and k_{EH^+} for Alkaline Hydrolysis of 4-MAB Me

$T = (50.20 \pm 0.10)°C$

$I = 0.1$ mol l^{-1}

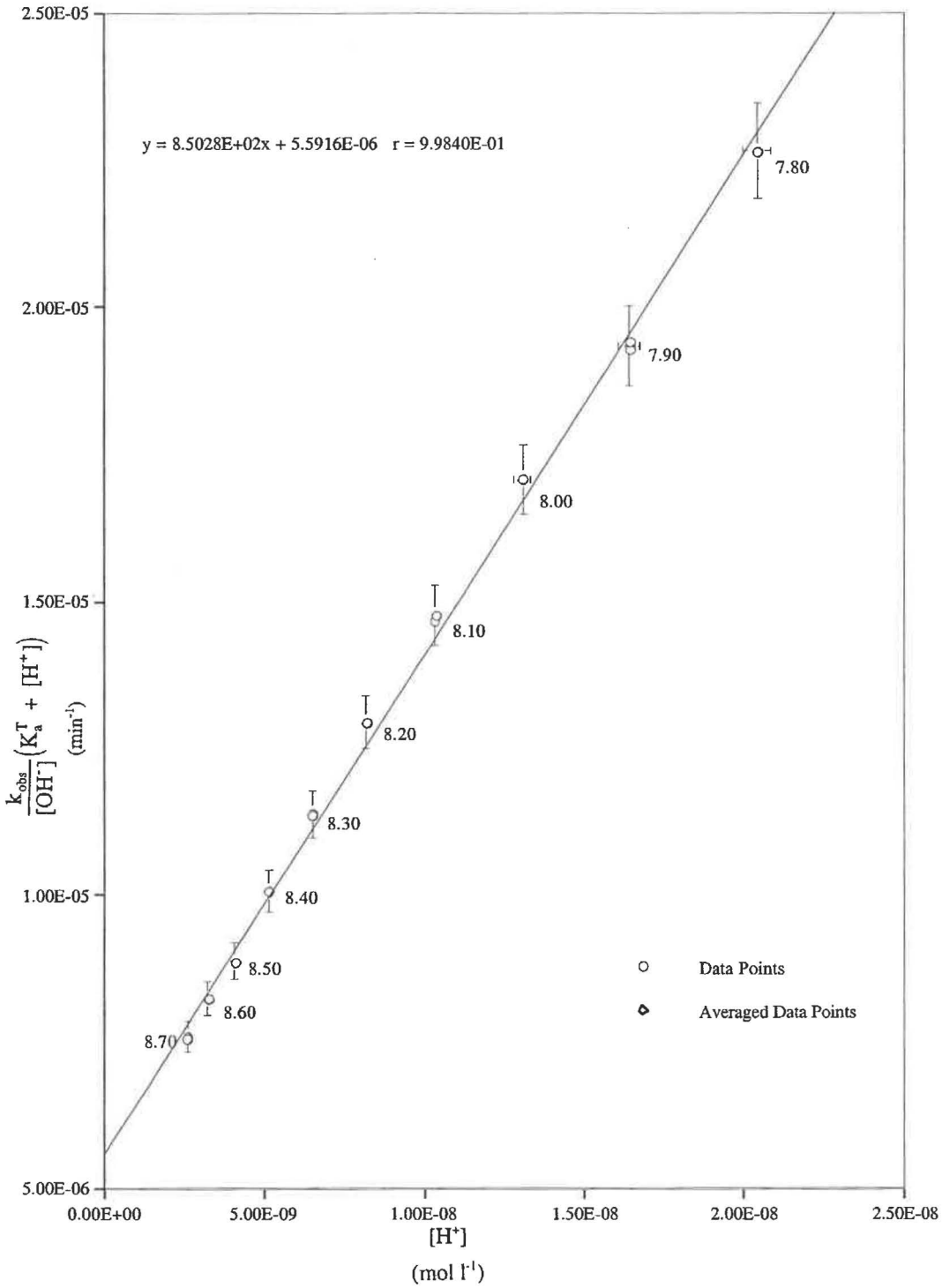

Table A3.72 Effect of pH on the Value of $k_{obs}/[OH^-]$ for 4-MAB Et

$T = (50.20 \pm 0.10)°C$

$I = 0.1$ mol l^{-1}

pH†	k_{obs} (min^{-1})	$t_{1/2}$ (min)	$[OH^-]^*$ (mol l^{-1})	$\frac{k_{obs}}{[OH^-]}$ (l mol^{-1} min^{-1})
8.206	5.906×10^{-3}	117.4	1.155×10^{-5}	511.3
8.304	8.318×10^{-3}	83.3	1.448×10^{-5}	574.6
8.405	1.163×10^{-3}	59.6	1.827×10^{-5}	636.5
8.405	1.162×10^{-2}	59.6	1.827×10^{-5}	636.2
8.505	1.722×10^{-2}	40.2	2.299×10^{-5}	749.0
8.604	2.430×10^{-2}	28.5	2.888×10^{-5}	841.3
8.605	2.464×10^{-2}	28.1	2.895×10^{-5}	851.3
8.707	3.527×10^{-2}	19.7	3.661×10^{-5}	963.2
8.907	7.924×10^{-2}	8.7	5.803×10^{-5}	1365.6
9.006	1.140×10^{-1}	6.1	7.288×10^{-5}	1564.2
9.007	1.154×10^{-2}	6.0	7.305×10^{-5}	1580.3
9.104	1.614×10^{-2}	4.3	9.133×10^{-5}	1767.5
9.105	1.641×10^{-2}	4.2	9.154×10^{-5}	1792.3

†Stopped Stirrer pH, $^*[OH^-] = \frac{10^{pH - 13.2617}}{0.7615}$ (50°C and I = 0.1 mol l^{-1}).

Table A3.73 Data for Separation of k_E and k_{EH^+} for the Alkaline Hydrolysis of 4-MAB Et

$T = (50.20 \pm 0.10)°C$

$I = 0.1$ mol l^{-1}

pH†	$[H^+]$ (mol l^{-1})	$(K_a^T + H^+)$ (mol l^{-1})	$\frac{k_{obs}}{[OH^-]}$ (l mol^{-1} min^{-1})	$\frac{k_{obs}}{[OH^-]}(K_a^T + [H^+])$ (min^{-1})
8.206	8.172×10^{-9}	8.673×10^{-9}	866.6	7.516×10^{-6}
8.304	6.521×10^{-9}	7.022×10^{-9}	911.2	6.399×10^{-6}
8.405	5.168×10^{-9}	5.669×10^{-9}	971.2	5.506×10^{-6}
8.405	5.168×10^{-9}	5.669×10^{-9}	974.8	5.526×10^{-7}
8.505	4.105×10^{-9}	4.606×10^{-9}	1077.4	4.963×10^{-6}
8.604	3.268×10^{-9}	3.770×10^{-9}	1188.7	4.481×10^{-6}
8.605	3.261×10^{-9}	3.762×10^{-9}	1190.2	4.478×10^{-6}
8.707	2.578×10^{-9}	3.079×10^{-9}	1303.2	4.013×10^{-6}
8.907	1.627×10^{-9}	2.128×10^{-9}	1723.5	3.668×10^{-6}
9.006	1.295×10^{-9}	1.796×10^{-9}	1912.3	3.435×10^{-6}
9.007	1.292×10^{-9}	1.793×10^{-9}	1922.3	$3.447. \times 10^{-6}$
9.104	1.034×10^{-9}	1.535×10^{-9}	2171.3	$3.332. \times 10^{-6}$
9.105	1.031×10^{-9}	1.532×10^{-9}	2165.2	3.318×10^{-6}

Using $K_a^T = 5.012 \times 10^{-10}$; $pK_a^T = 9.30$ (50°C and I = 0.1 mol l^{-1}), (Table A1.33).

† Stopped Stirrer pH. $[H^+] = \frac{10^{-pH}}{0.7670}$ (at 50°C and I = 0.1 mol l^{-1}).

Figure A3.34 Separation of k_E and k_{EH^+} for Alkaline Hydrolysis of 4-MAB Et

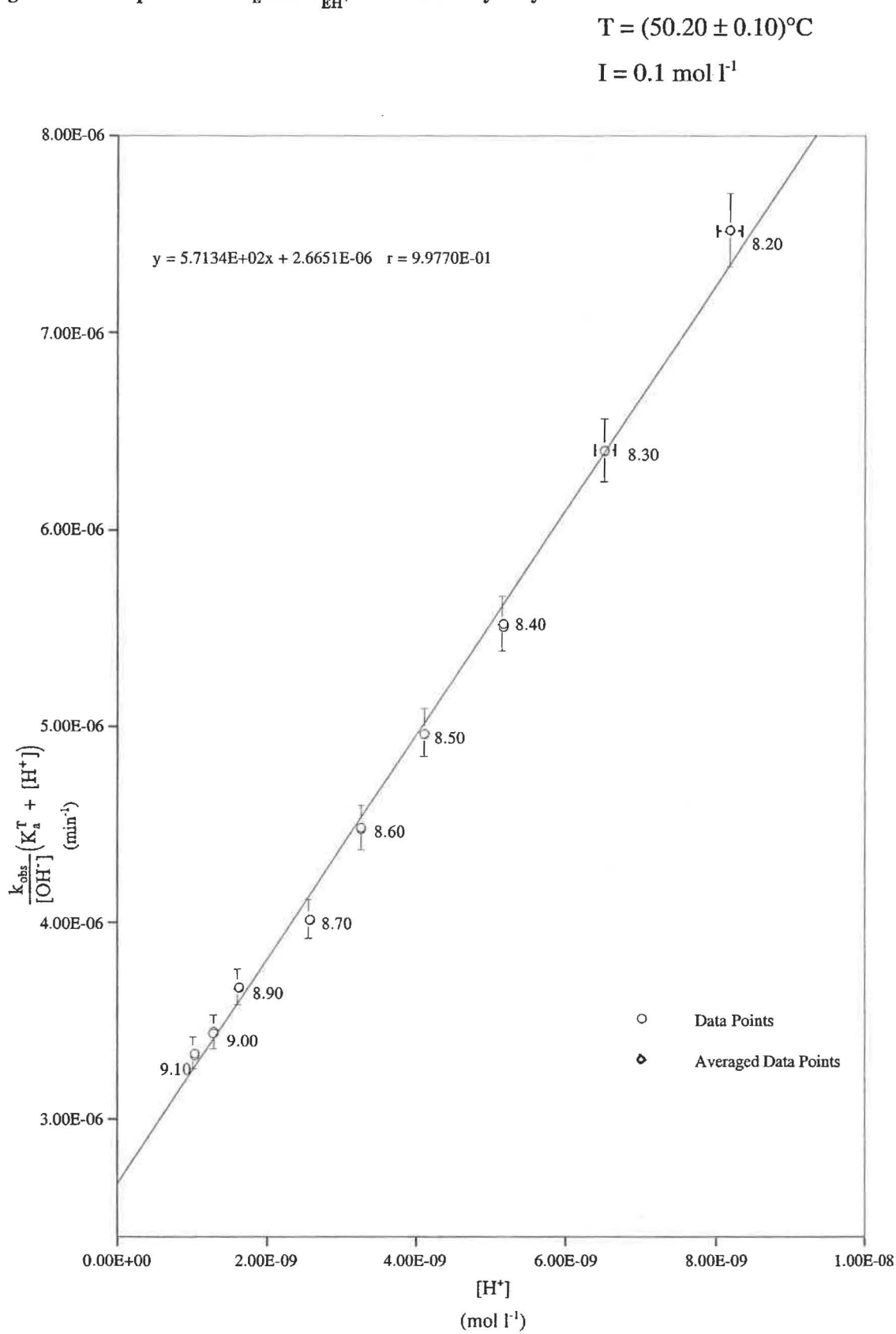

Table A3.74 Effect of the pH on the Value of $k_{obs}/[OH^-]$ for 4-A-3-MB Me

$T = (50.20 \pm 0.10)°C$

$I = 0.1$ mol l^{-1}

pH†	k_{obs} (min^{-1})	$t_{1/2}$ (min)	$[OH^-]^*$ (mol l^{-1})	$\frac{k_{obs}}{[OH^-]}$ (l mol^{-1} min^{-1})
7.805	4.343×10^{-3}	159.6	4.588×10^{-6}	946.5
7.904	6.268×10^{-3}	110.6	5.763×10^{-6}	1087.6
8.003	8.950×10^{-3}	77.4	7.238×10^{-6}	1236.5
8.004	8.732×10^{-3}	79.4	7.255×10^{-6}	1203.6
8.104	1.302×10^{-2}	53.2	9.133×10^{-6}	1425.6
8.203	1.913×10^{-2}	36.2	1.147×10^{-5}	1667.6
8.204	1.935×10^{-2}	35.8	1.150×10^{-5}	1682.5
8.303	2.810×10^{-2}	24.7	1.444×10^{-5}	1945.8
8.404	4.121×10^{-2}	16.8	1.822×10^{-5}	2261.3
8.404	4.155×10^{-2}	16.7	1.822×10^{-5}	2280.3
8.505	5.837×10^{-2}	11.9	2.299×10^{-5}	2538.6
8.604	8.314×10^{-2}	8.3	2.888×10^{-5}	2878.6
8.604	8.463×10^{-2}	8.2	2.888×10^{-5}	2930.2
8.708	1.224×10^{-1}	5.7	3.670×10^{-5}	3335.2

†Stopped Stirrer pH, $^*[OH^-] = \frac{10^{pH - 13.2617}}{0.7615}$ (50°C and I = 0.1 mol l^{-1}).

Table A3.75 Data for Separation of k_E and k_{EH^+} for the Alkaline Hydrolysis of 4-A-3MB Me.

$T = (50.20 \pm 0.10)°C$

$I = 0.1$ mol l^{-1}

pH†	$[H^+]$ (mol l^{-1})	$(K_a^T + H^+)$ (mol l^{-1})	$\frac{k_{obs}}{[OH^-]}$ (l mol^{-1} min^{-1})	$\frac{k_{obs}}{[OH^-]}(K_a^T + [H^+])$ (min^{-1})
7.805	2.057×10^{-8}	2.244×10^{-8}	946.5	2.124×10^{-5}
7.904	1.638×10^{-8}	1.824×10^{-8}	1087.6	1.984×10^{-5}
8.003	1.304×10^{-8}	1.490×10^{-8}	1236.5	1.843×10^{-5}
8.004	1.301×10^{-8}	1.487×10^{-8}	1203.6	1.790×10^{-5}
8.104	1.034×10^{-8}	1.220×10^{-8}	1425.6	1.739×10^{-5}
8.203	8.229×10^{-9}	1.009×10^{-8}	1667.6	1.683×10^{-5}
8.204	8.210×10^{-9}	1.007×10^{-8}	1682.5	1.695×10^{-5}
8.303	6.536×10^{-9}	8.398×10^{-9}	1945.8	1.634×10^{-5}
8.404	5.180×10^{-9}	7.042×10^{-9}	2261.3	1.592×10^{-5}
8.404	5.180×10^{-9}	7.042×10^{-9}	2280.3	1.606×10^{-5}
8.505	4.105×10^{-9}	5.967×10^{-9}	2538.6	1.515×10^{-5}
8.604	3.268×10^{-9}	5.130×10^{-9}	2878.6	1.477×10^{-5}
8.604	3.268×10^{-9}	5.130×10^{-9}	2930.2	1.503×10^{-5}
8.708	2.578×10^{-9}	4.434×10^{-9}	3335.2	1.479×10^{-5}

Using $K_a^T = 1.862 \times 10^{-9}$ $pK_a^T = 8.73$ (50°C and I = 0.1 mol l^{-1}), (Table A1.34).

†Stopped Stirrer pH. $[H^+] = \frac{10^{-pH}}{0.7615}$ (50°C and I = 0.1 mol l^{-1}).

Graph A3.35 Separation of k_E and k_{EH^+} for Alkaline Hydrolysis of 4-A-3-MB Me

$T = (50.20 \pm 0.10)°C$

$I = 0.1$ mol l^{-1}

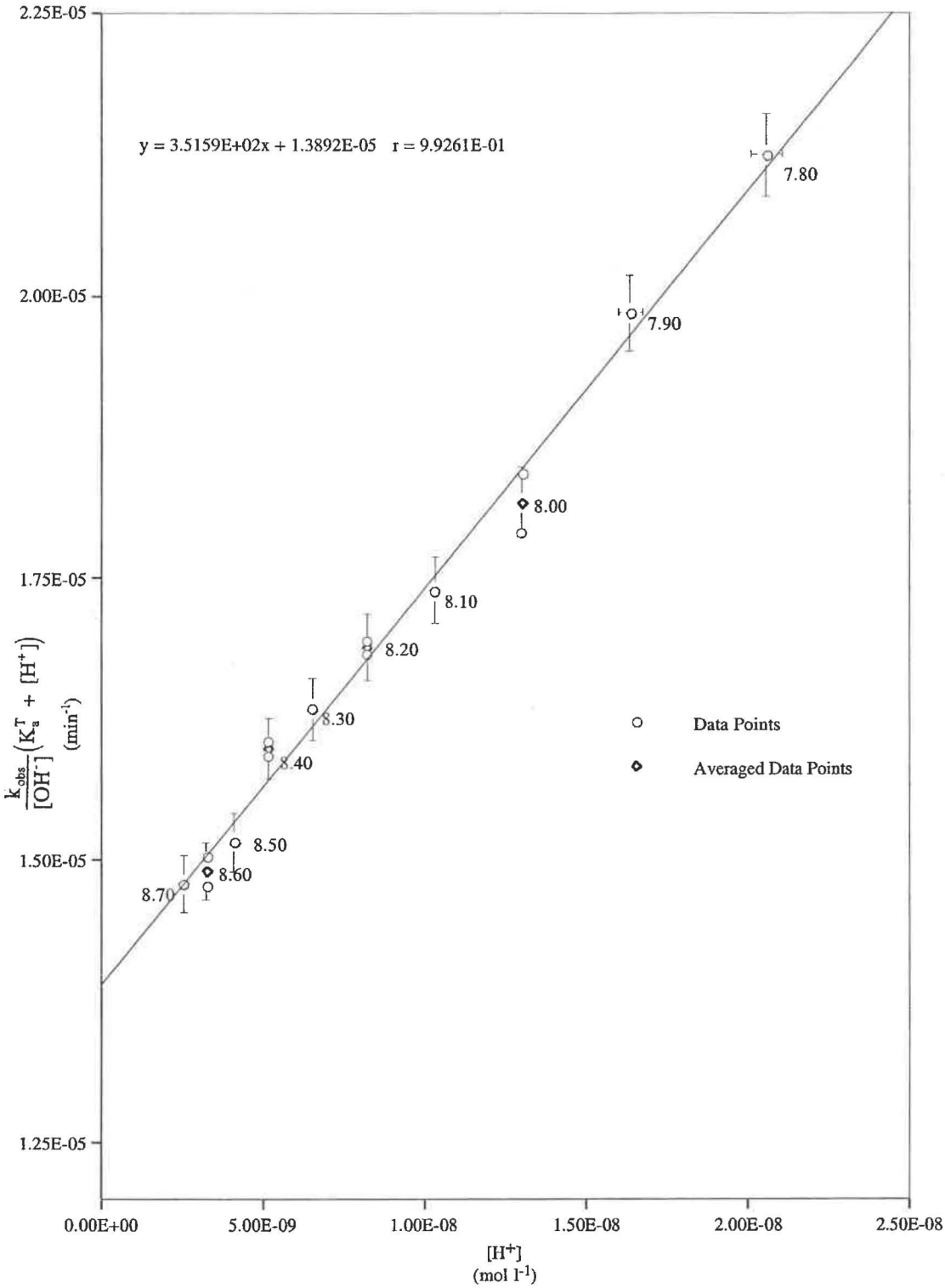

Table A3.76 Effect of pH on the Value of $k_{obs}/[OH^-]$ for 4-A-3,3-DMB Me

$T = (50.20 \pm 0.10)°C$

$I = 0.1$ mol l^{-1}

pH†	k_{obs} (min^{-1})	$t_{1/2}$ (min)	$[OH^-]^*$ (mol l^{-1})	$\frac{k_{obs}}{[OH^-]}$ (l mol^{-1} min^{-1})
7.508	4.345×10^{-3}	159.5	2.315×10^{-6}	1876.5
7.605	6.152×10^{-3}	112.7	2.895×10^{-6}	2125.3
7.606	6.251×10^{-3}	110.9	2.902×10^{-6}	2154.2
7.706	9.126×10^{-3}	76.0	3.653×10^{-6}	2498.3
7.803	1.368×10^{-2}	50.7	4.567×10^{-6}	2996.2
7.804	1.367×10^{-2}	50.7	4.578×10^{-6}	2987.4
7.903	2.022×10^{-2}	34.3	5.750×10^{-6}	3516.4
8.005	3.030×10^{-2}	22.9	7.272×10^{-6}	4166.3
8.005	3.021×10^{-2}	22.9	7.272×10^{-6}	4154.8
8.102	4.488×10^{-2}	15.4	9.091×10^{-6}	4936.2
8.203	6.570×10^{-2}	10.5	1.147×10^{-5}	5727.4
8.203	6.580×10^{-2}	10.5	1.147×10^{-5}	5735.4
8.305	9.829×10^{-2}	7.1	1.451×10^{-5}	6774.5
8.408	1.463×10^{-1}	4.7	1.839×10^{-5}	7956.2
8.409	1.463×10^{-1}	4.7	1.843×10^{-5}	7935.6
8.506	12.080×10^{-1}	3.3	2.305×10^{-5}	9025.6

†Stopped Stirrer pH, $^*[OH^-] = \frac{10^{pH - 13.2617}}{0.7615}$ (50°C and I = 0.1 mol l^{-1}).

Table A3.77 Data for Separation of k_E and k_{EH^+} for the Alkaline Hydrolysis of 4-A-3,3-DMB Me

$T = (50.20 \pm 0.10)°C$

$I = 0.1$ mol l^{-1}

pH†	$[H^+]$ (mol l^{-1})	$(K_a^T + H^+)$ (mol l^{-1})	$\frac{k_{obs}}{[OH^-]}$ (l mol^{-1} min^{-1})	$\frac{k_{obs}}{[OH^-]}(K_a^T + [H^+])$ (min^{-1})
7.508	4.077×10^{-8}	4.286×10^{-8}	1876.5	8.042×10^{-5}
7.605	3.261×10^{-8}	3.470×10^{-8}	2125.3	7.374×10^{-5}
7.606	3.253×10^{-8}	3.462×10^{-8}	2154.2	7.458×10^{-5}
7.706	2.584×10^{-8}	2.793×10^{-8}	2498.3	6.978×10^{-5}
7.803	2.067×10^{-8}	2.276×10^{-8}	2996.2	6.819×10^{-5}
7.804	2.062×10^{-8}	2.271×10^{-8}	2987.4	6.785×10^{-5}
7.903	1.642×10^{-8}	1.851×10^{-8}	3516.2	6.508×10^{-5}
8.005	1.298×10^{-8}	1.507×10^{-8}	4166.3	6.279×10^{-5}
8.005	1.298×10^{-8}	1.507×10^{-8}	4154.8	6.262×10^{-5}
8.102	1.038×10^{-8}	1.247×10^{-8}	4936.2	6.157×10^{-5}
8.203	8.229×10^{-9}	1.032×10^{-8}	5727.4	5.910×10^{-5}
8.203	8.229×10^{-9}	1.032×10^{-8}	5735.4	5.918×10^{-5}
8.305	6.506×10^{-9}	8.596×10^{-9}	6774.5	5.823×10^{-5}
8.408	5.133×10^{-9}	7.222×10^{-9}	7956.2	5.746×10^{-5}
8.409	5.121×10^{-9}	7.210×10^{-9}	7935.6	5.722×10^{-5}
8.506	4.096×10^{-9}	6.185×10^{-9}	9025.6	5.582×10^{-5}

Using $K_a^T = 2.089 \times 10^{-9}$; $pK_a^T = 8.68$ (50°C and I = 0.1 mol l^{-1}), (Table A1.35).

†Stopped Stirrer pH. $[H^+] = \frac{10^{-pH}}{0.7615}$ (50°C and I = 0.1 mol l^{-1}).

Figure A3.36 Separation of k_E and k_{EH^+} for Alkaline Hydrolysis of 4-A-3,3-DMB Me

$T = (50.20 \pm 0.10)°C$

$I = 0.1$ mol l^{-1}

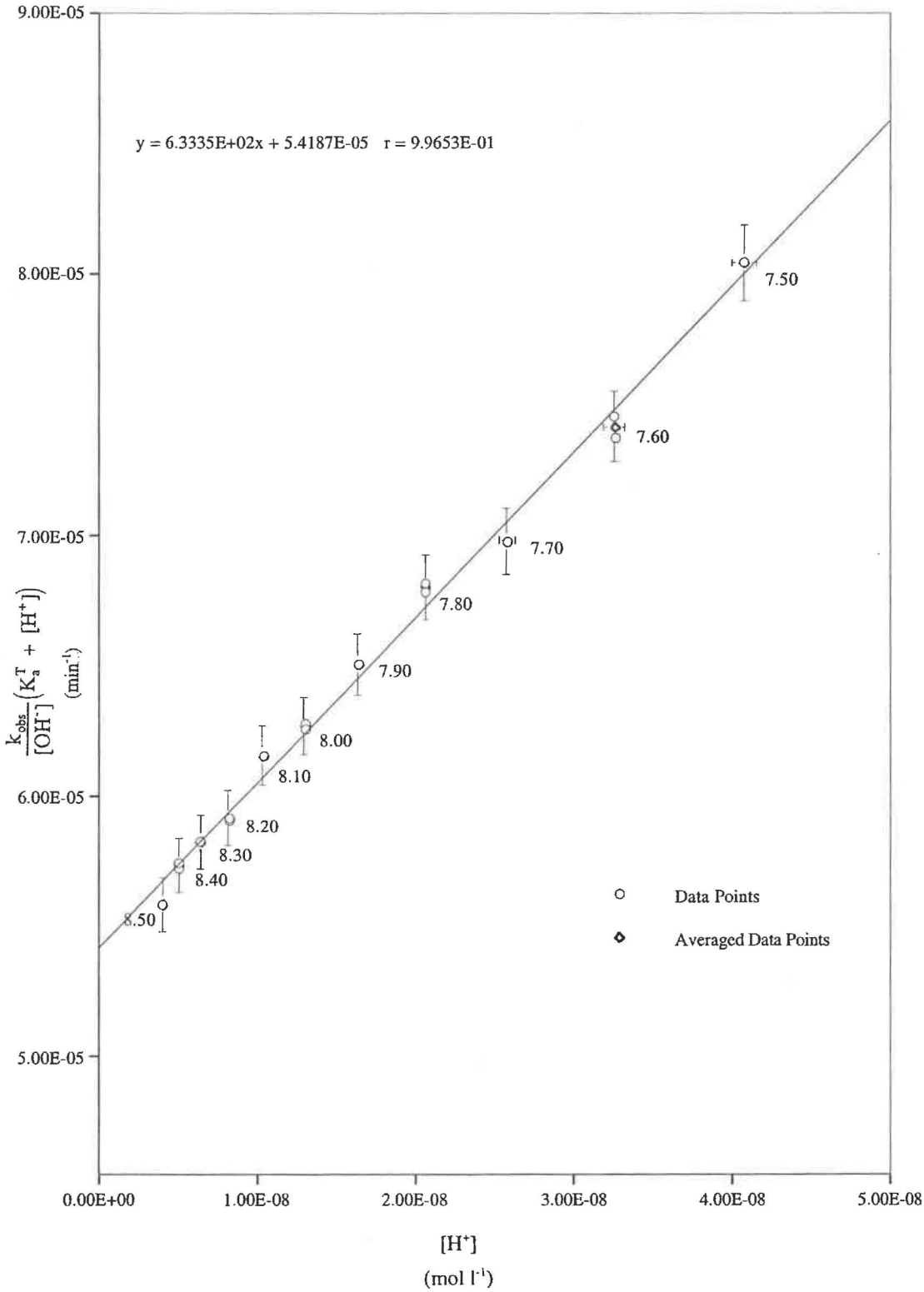

Table A3.78 Effect of the pH on the Value of $k_{obs}/[OH^-]$ for 5-APe Et

$T = (50.20 \pm 0.10)°C$

$I = 0.1$ mol l^{-1}

pH†	k_{obs} (min^{-1})	$t_{1/2}$ (min)	$[OH^-]^*$ (mol l^{-1})	$\frac{k_{obs}}{[OH^-]}$ (l mol^{-1} min^{-1})
8.005	5.814×10^{-3}	119.2	7.272×10^{-6}	799.6
8.102	8.633×10^{-3}	80.3	9.091×10^{-6}	949.6
8.204	1.319×10^{-2}	52.6	1.150×10^{-5}	1146.8
8.304	2.020×10^{-2}	34.3	1.448×10^{-5}	1395.8
8.404	3.100×10^{-2}	22.4	1.822×10^{-5}	1701.2
8.505	4.735×10^{-2}	14.6	2.299×10^{-5}	2059.2
8.604	7.210×10^{-2}	9.6	2.888×10^{-5}	2496.5
8.707	1.107×10^{-1}	6.3	3.661×10^{-5}	3023.6
8.805	1.663×10^{-1}	4.2	4.588×10^{-5}	3624.3
8.806	1.673×10^{-1}	4.1	4.599×10^{-5}	3638.3

†Stopped Stirrer pH, $^*[OH^-] = \frac{10^{-pH\ -\ 13.2617}}{0.7615}$ (50°C and I = 0.1 mol l^{-1}).

Table A3.79 Data for Separation of k_E and k_{EH^+} for the Alkaline Hydrolysis of 5-APe Et

$T = (50.20 \pm 0.05)°C$

$I = 0.1$ mol l^{-1}

pH†	$[H^+]$ (mol l^{-1})	$(K_a^T + H^+)$ (mol l^{-1})	$\frac{k_{obs}}{[OH^-]}$ (l mol^{-1} min^{-1})	$\frac{k_{obs}}{[OH^-]}(K_a^T + [H^+])$ (min^{-1})
8.005	1.298×10^{-8}	1.339×10^{-8}	799.6	1.071×10^{-5}
8.102	1.038×10^{-8}	1.079×10^{-8}	949.6	1.025×10^{-5}
8.204	8.210×10^{-9}	8.617×10^{-9}	1146.8	9.882×10^{-6}
8.304	6.521×10^{-9}	6.929×10^{-9}	1395.8	9.670×10^{-6}
8.404	5.180×10^{-9}	5.587×10^{-9}	1701.2	9.505×10^{-6}
8.505	4.105×10^{-9}	4.513×10^{-9}	2059.2	9.292×10^{-6}
8.604	3.268×10^{-9}	3.676×10^{-9}	2496.5	9.176×10^{-6}
8.707	2.578×10^{-9}	2.986×10^{-9}	3023.6	9.027×10^{-6}
8.805	2.057×10^{-9}	2.465×10^{-9}	3624.3	8.933×10^{-6}
8.806	2.053×10^{-9}	2.460×10^{-9}	3638.3	8.951×10^{-6}

Using $K_a^T = 4.074 \times 10^{-10}$; $pK_a^T = 9.39$ (50°C and I = 0.1 mol l^{-1}), (Table A1.36).

†Stopped Stirrer pH. $[H^+] = \frac{10^{-pH}}{0.7615}$ (50°C and I = 0.1 mol l^{-1}).

Figure A3.37 Separation of k_E and k_{EH^+} for Alkaline Hydrolysis of 5-APe Et

$T = (50.20 \pm 0.10)°C$

$I = 0.1$ mol l^{-1}

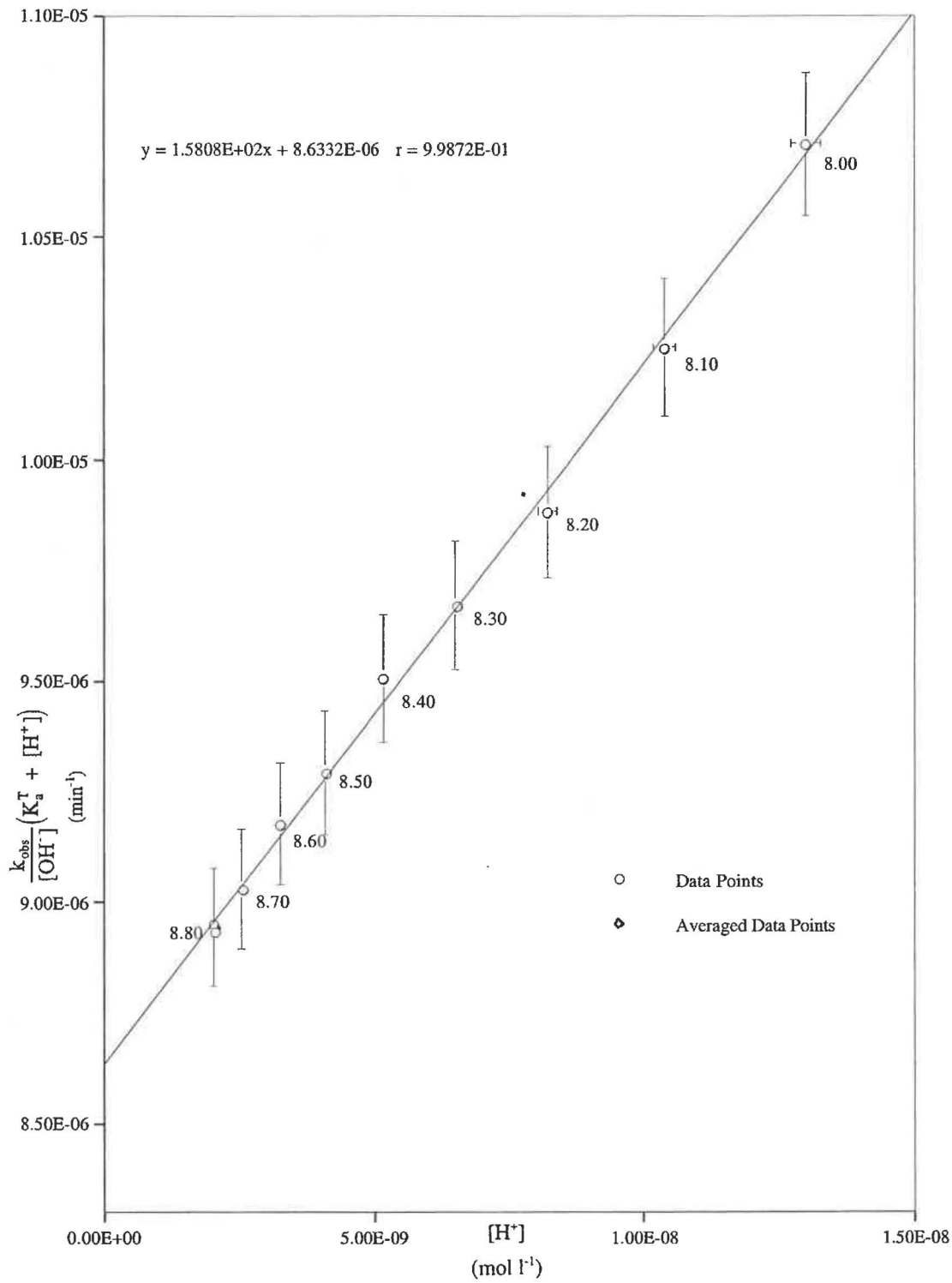

Table A3.80 Effect of the pH on the Value of $k_{obs}/[OH^-]$ for 5-APe Me.

$T = (50.20 \pm 0.10)°C$

$I = 0.1$ mol l^{-1}

pH†	k_{obs} (min^{-1})	$t_{1/2}$ (min)	$[OH^-]^*$ (mol l^{-1})	$\frac{k_{obs}}{[OH^-]}$ (l mol^{-1} min^{-1})
7.604	4.887×10^{-3}	141.8	2.888×10^{-6}	1692.3
7.703	6.938×10^{-3}	99.9	3.628×10^{-6}	1912.3
7.798	9.943×10^{-3}	69.7	4.515×10^{-6}	2202.3
7.805	1.004×10^{-2}	69.1	4.588×10^{-6}	2187.2
7.903	1.435×10^{-2}	48.3	5.750×10^{-6}	2495.6
8.001	2.170×10^{-2}	31.9	7.205×10^{-6}	3012.5
8.005	2.178×10^{-2}	31.8	7.272×10^{-6}	2995.9
8.100	3.238×10^{-2}	21.4	9.050×10^{-6}	3578.2
8.103	3.282×10^{-2}	21.1	9.112×10^{-6}	3601.2
8.202	4.849×10^{-2}	14.3	1.145×10^{-5}	4236.5
8.203	4.917×10^{-2}	14.1	1.147×10^{-5}	4286.5
8.302	7.208×10^{-2}	9.6	1.441×10^{-5}	5002.3
8.404	1.142×10^{-1}	6.1	1.822×10^{-5}	6265.4
8.408	1.149×10^{-1}	6.0	1.843×10^{-5}	6235.2

†Stopped Stirrer pH, $^*[OH^-] = \frac{10^{pH\ -\ 13.2617}}{0.7615}$ (50°C and I = 0.1 mol l^{-1}).

Table A3.81 Data for Separation of k_E and k_{EH+} for the Alkaline Hydrolysis 5-APe Me

$T = (50.20 \pm 0.10)°C$

$I = 0.1$ mol l^{-1}

pH†	$[H^+]$ (mol l^{-1})	$(K_a^T + H^+)$ (mol l^{-1})	$\frac{k_{obs}}{[OH^-]}$ (l mol^{-1} min^{-1})	$\frac{k_{obs}}{[OH^-]}(K_a^T + [H^+])$ (min^{-1})
7.604	3.268×10^{-8}	3.318×10^{-8}	1692.3	5.616×10^{-5}
7.703	2.602×10^{-8}	2.652×10^{-8}	1912.3	5.072×10^{-5}
7.798	2.091×10^{-8}	2.141×10^{-8}	2202.3	4.715×10^{-5}
7.805	2.057×10^{-8}	2.108×10^{-8}	2187.2	4.610×10^{-5}
7.903	1.642×10^{-8}	1.692×10^{-8}	2495.6	4.222×10^{-5}
8.001	1.310×10^{-8}	1.360×10^{-8}	3012.5	4.098×10^{-5}
8.005	1.298×10^{-8}	1.348×10^{-8}	2995.9	4.039×10^{-5}
8.100	1.043×10^{-8}	1.093×10^{-8}	3578.2	3.912×10^{-5}
8.103	1.036×10^{-8}	1.086×10^{-8}	3601.2	3.911×10^{-5}
8.202	8.248×10^{-9}	8.749×10^{-9}	4236.5	3.706×10^{-5}
8.203	8.229×10^{-9}	8.730×10^{-9}	4286.5	3.742×10^{-5}
8.302	6.551×10^{-9}	7.053×10^{-9}	5002.3	3.528×10^{-5}
8.404	5.180×10^{-9}	5.681×10^{-9}	6265.4	3.560×10^{-5}
8.409	5.121×10^{-9}	5.622×10^{-9}	6235.2	3.505×10^{-5}

Using $K_a^T = 5.012 \times 10^{-11}$; $pK_a^T = 9.30$ (50°C and I = 0.1 mol l^{-1}), (Table A1.37).

†Stopped Stirrer pH. $[H^+] = \frac{10^{-pH}}{0.7615}$ (50°C and I = 0.1 mol l^{-1}).

Figure A3.39 Separation of k_E and k_{EH^+} for Alkaline Hydrolysis of 5-APe Me

$T = (50.20 \pm 0.10)°C$

$I = 0.1$ mol l^{-1}

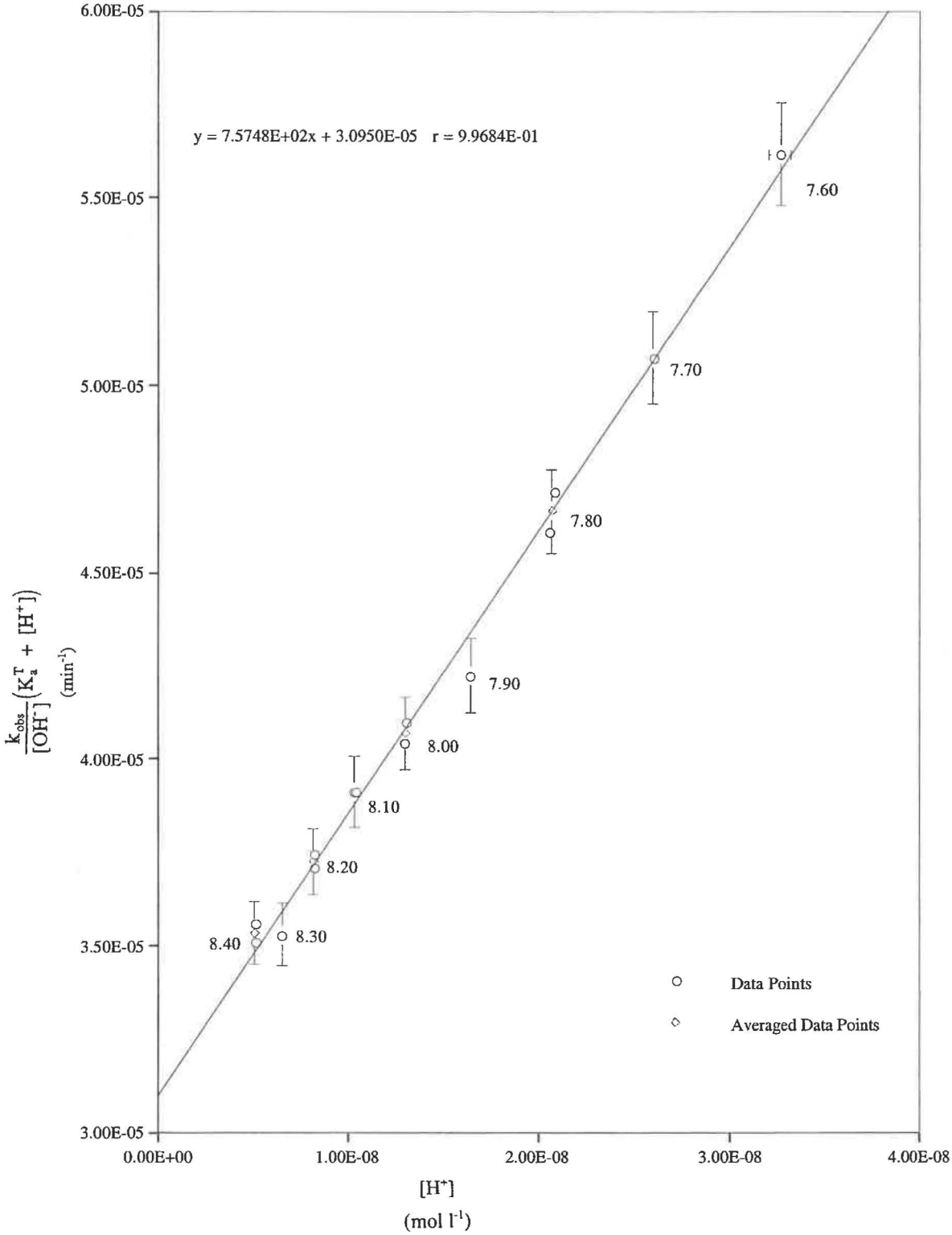

Appendix 4

Reaction Mixture Composition Calculations

% EH^+ and %E vs. pH

A4.1 General

A4.1(a) Calculation of the Relative % Composition of $[EH^+]$ and [E]

$$EH^+ \rightleftharpoons E + H^+ \qquad \text{....(A4.1)}$$

$$K_a^T = \frac{\{E\}\{H^+\}}{\{EH^+\}} = \frac{[E] \cdot y_0 \{H^+\}}{[EH^+] \cdot y_1} \qquad \text{....(A4.2)}$$

By definition: $$pK_a^T = -\log_{10} K_a^T \qquad \text{....(A4.3)}$$

$$pH = -\log_{10}\{H^+\} \qquad \text{....(A4.4)}$$

Rearranging (A4.2), and combining (A4.3) and (A4.4):

$$pK_a^T = pH + py_0 + py_1 - \log_{10}\frac{[E]}{[EH^+]} \qquad \text{....(A4.5)}$$

Rearranging (A4.5) gives:

$$-\log_{10}\frac{[E]}{[EH^+]} = pH - pK_a^T - py_1 \qquad \text{....(A4.6)}$$

$$\frac{[E]}{[EH^+]} = 10^{pH - pK_a^T - py_1} \qquad \text{....(A4.7)}$$

Therefore:

$$[EH^+]\% = \frac{[EH^+]}{[E] + [EH^+]} \times 100 \qquad \text{....(A4.8)}$$

Rearranging (A4.7), and then substituting into (A4.8):

$$= \frac{[EH^+]}{[EH^+] \cdot 10^{pH - pK_a^T - py_1}} \times 100 \qquad \text{....(A4.9)}$$

Rearranging (A4.9):

$$[EH^+] = \frac{100}{10^{pH - pK_a^T - py_1} + 1} \qquad \text{....(A4.10)}$$

To determine % [E]:

$$[E]\% = 100 - [EH^+] \qquad \text{....(A4.11)}$$

Combining (A4.10) with (A4.11):

$$= 100 - \frac{100}{10^{pH - pK_a^T - py_1} + 1} \qquad \text{....(A4.12)}$$

Hence it follows that:

$$[E]\% = \frac{100\,(10^{pH - pK_a^T - py_1})}{10^{pH - pK_a^T - py_1} + 1} \qquad \text{....(A4.13)}$$

From eqns. (A4.11) and (A4.13), a plot % species vs. pH graph can be constructed. This is illustrated for 2-AE Me at 25°C and 0.1 mol l^{-1} (using $pK_a^T = 7.67$, Table 4.9) in Figure A4.1:

Figure A4.1 Concentration % Species (EH^+ and E) vs. pH for 2-AE Me

$T = (50.20 \pm 0.10)°C$

$I = 0.1$ mol l^{-1}

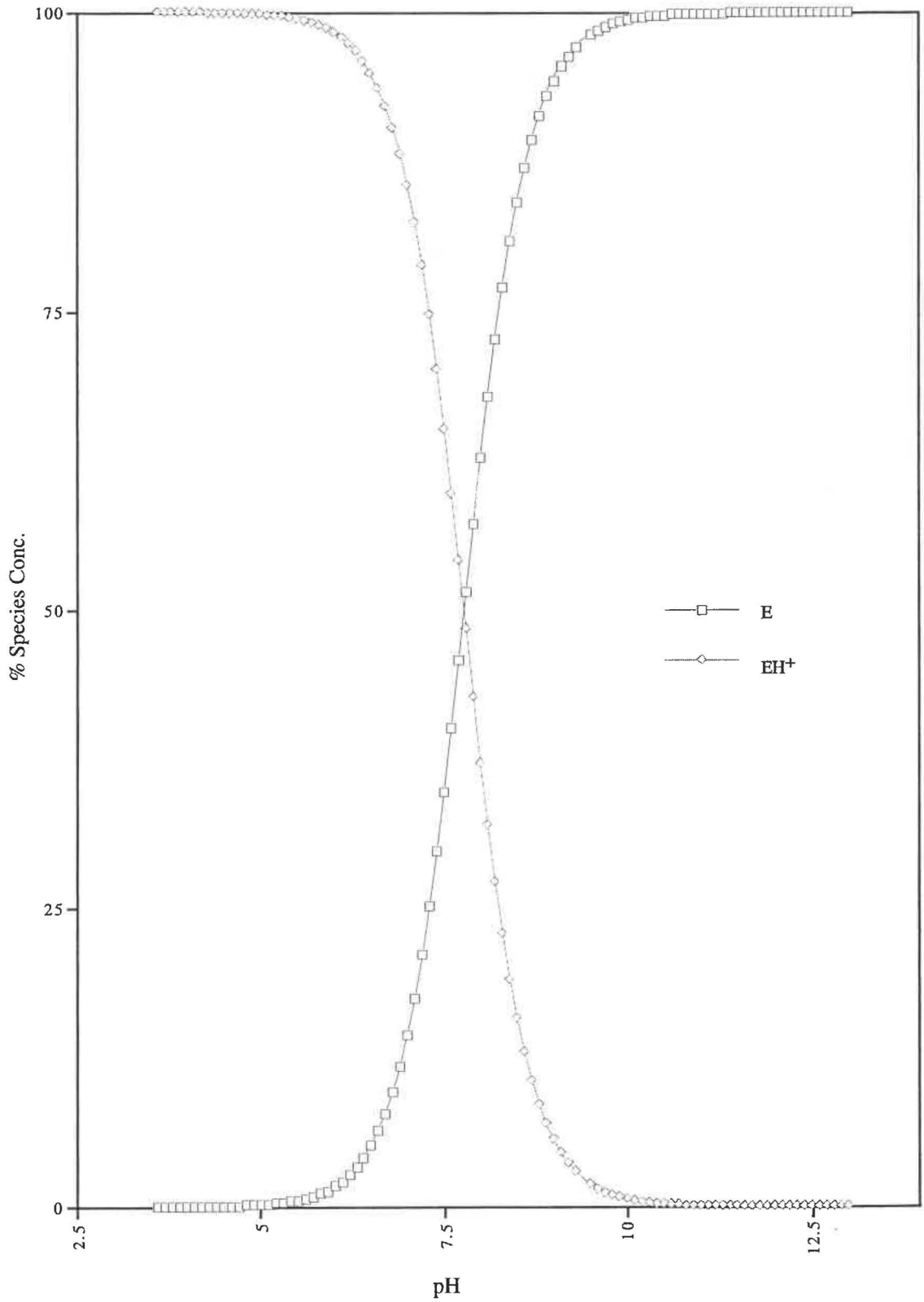

Appendix 5

Procedures for

Error Calculations

A5.1 Error Calculations for the Values of the Rate Constants

A5.1(a) Introduction

An integral part of any quantitative physico-chemical investigation is the estimation of possible sources of error, and the extent to which they effect the accuracy of the final result.

There is an uncertainty associated with pH measurement because the "stirrer effect" (see 3.2(c)) is unknown. Consequently, these readings involve a systematic error. Therefore it is not possible to use statistical methods of data analysis to estimate the overall error, because such methods assume the error in the measurement to be random. Instead the systematic errors for k_{EH^+} and $k_E(k_L)$ were estimated using a graphical method in this thesis.

A5.1(b) General Errors

For an expression where

$$c = a + b \qquad \text{....(A5.1)}$$

The absolute error in c, Δc is given by:

$$\Delta c = \Delta a + \Delta b \qquad \text{....(A5.2)}$$

where

Δa = absolute error in a

Δb = absolute error in b

And, for the expression

$$f = d \times e \qquad \text{....(A5.3)}$$

The absolute error in y, Δy is given by:

$$\frac{\Delta f}{f} = \frac{\Delta d}{d} + \frac{\Delta e}{e} \qquad \text{....(A5.4)}$$

Equations A5.2 and A5.4 were used to estimate the possible error in the separation of k_E and k_{EH^+}

A5.1(c) Estimation of Error for k_E and k_{EH^+}

These rate constants, were separated from the plot of $\frac{k_{obs}}{[OH^-]}(K_a^T + [H^+])$ vs. $[H^+]$ using eqn. 5.13 (Chapter 5). In general, this plot produces a slope (a) that is equivalent to k_{EH^+} and intercept, (b), equivalent to $k_E \cdot K_a^T$. Hence, the errors in k_E and k_{EH^+} can be estimated from the lines of maximum and minimum slope and intercept for the data points on the separation plot.

By definition the slope of maximum error in the line of best fit (a_1) passes through the apex of the positive error bar of the greatest y-axis data point (y) and the minimum extrema of the corresponding x-axis data point (x), passing through all other data points and eventually bisecting the base of the negative error of the smallest y-axis data point (y′) and maximum extrema of the corresponding x value (x'). The extrapolation of this line at the y-axis (i.e. $[H^+] = 0$) should yield the minimum error in the intercept (b_2).

Conversely, the slope of minimum error in the line of best fit (a_2), will pass through the base of the negative error bar of y and maximum x, passing through the apex of the positive error bar of y′ and minimum of x'. The line if extrapolated to the y-axis will give the maximum error in the intercept (b_1).

The gradients of the maximum and minimum error in the line of best fit can be obtained by eqn. (A5.5).

$$a_1 \text{ or } a_2 = \frac{(y \pm \Delta y) - (y' \mp \Delta y')}{(x \pm \Delta x) - (x' \mp \Delta x')} \qquad \text{....(A5.5)}$$

Where,

Δy = Absolute error of maximum y.

$\Delta y'$ = Absolute error of minimum y'.

Δx = Absolute error of maximum x.

$\Delta x'$ = Absolute error of minimum x'.

However, before the lines of maximum and minimum slope can be drawn, it is necessary to determine the total error in both the x- and y-directions. The source of error for the y-direction for the data points on the separation plot can be estimated from the overall error in the $k_{obs}/[OH^-](K_a^T + [H^+])$ term of eqn. 513, where:

The error for the terms in the parentheses consists of the absolute error ΔK_a^T (which is the overall error in the individual ester.HCl pK_a^T)) summed with the absolute error $\Delta[H^+]$ (i.e. the absolute error in pH meter reading). This error can be calculated using equation A5.2, i.e. $\Delta c = (\Delta[H^+] + \Delta K_a^T)$.

The error in the $k_{obs}/[OH^-]$ term was calculated from eqn. A5.4,
i.e. $\Delta f = \Delta k_{obs}/k_{obs}$ and $\Delta[OH^-]/[OH^-]$ ($[OH^-]$ and $[H^+]$ errors are identical).

Hence, the overall error in the y-direction obtained from the combination of the absolute errors terms in 1 and 2. The overall error in the x-axis is due to $\Delta[H^+]$.

Since the term 1 is dependent on the accuracy of the pK_a^T (i.e. K_a^T), overall errors were calculated for Group 1 (slowly hydrolysing esters), Group 2 (moderately hydrolysing esters) and Group 3 (rapidly hydrolysing esters) separately.

A5.2 Estimation of Errors

A5.2(a) Group 1, Slowly Hydrolysing Amino Acid Esters

2-AE Me is a typical example of Group 1 ester. using the data for this ester at 37.1°C, Chapter 5, 5.3(b), it is possible to estimate the absolute errors for the y-axis and x-axis terms.

Errors for x- and y-axis Terms

The estimated absolute error in $[OH^-]$ (and $[H^+]$) results from the ± 0.01 pH error in see 3.2(c). The error for the k_{obs} term was assumed to be 1% overall, since these values were obtained from Guggenheim plots that had excellent linearity (see Figures 5.1 and 5.2) and typically used between 15 – 20 points.

Hence, $\Delta[OH^-]/[OH^-] = 0.023$, or 2.3%, this gives an overall error of 3.3% for the $k_{obs}/[OH^-]$ component in the y-axis term.

Although, strictly this error should be calculated using $\frac{k_{obs} \pm \Delta k_{obs}}{[OH^-] \mp \Delta[OH^-]}$.

The absolute error in K_a^T, can be estimated from the pK_a^T value for 2-AE Me.HCl at 37.1°C and I = 0.1 mol l^{-1}, 7.33 ± 0.01(Table 4.11). This gave $K_a^T = (4.571 \pm 0.176) \times 10^{-8}$. $[H^+]$ will also be 2.3%. For the range of pH's studied for 2-AE Me, at 37°C (Table 5.5), the value of $K_a^T > [H^+]$.

The overall error for the terms in the parentheses (eqn. 5.13) was calculated for a selection of values (at high, mid-range and low $[H^+]$) form Table 5.5, for 2-AE Me. These calculations are summarised in Table A5.1.

Table A5.1 Estimation of the Absolute Error for the Parentheses Terms for 2-AE Me.

pH	$[H^+]$	$\Delta[H^+]$	$\left(K_a^T + [H^+]\right)$	$\Delta K_a^T + \Delta[H^+]^*$	$\left(\frac{\Delta K_a^T + \Delta[H^+]}{\left(K_a^T + [H^+]\right)}\right)$
8.013	1.265×10^{-8}	0.029×10^{-8}	5.943×10^{-8}	1.370×10^{-8}	0.023
9.208	8.076×10^{-10}	0.070×10^{-10}	4.758×10^{-8}	1.094×10^{-9}	0.023
10.510	4.029×10^{-11}	0.092×10^{-11}	4.681×10^{-8}	1.077×10^{-9}	0.023

*Using $\Delta K_a^T = 1.080 \times 10\text{-}^8$

Clearly, as it can be seen from Table A5.1, the error in K_a^T dominates the error in the parenthesis term. Therefore, this has an error of 2.3% for all data points.

Hence, overall error in the y-axis found by rearranging eqn. A5.4

$$\frac{\Delta y}{y} = \left(\frac{\Delta K_a^T + \Delta[H^+]}{\left(K_a^T + [H^+]\right)}\right) + \frac{\Delta[OH^-]}{[OH^-]} + \frac{\Delta k_{obs}}{k_{obs}} \qquad \text{(A5.6)}$$

This gave a total error of 5.6% in the y-axis. The total error in $[H^+]$ (x-axis) was found to be 2.3%.

The data from Table 5.6 was used to construct a separation plot of $k_{obs}/[OH^-]\left(K_a^T + [H^+]\right)$ vs. $[H^+]$ for 2-AE Me, using the procedure outlined in 5.3(b). Error bars were set with a ± 2.3% error for the x-coordinates and ± 5.6% for the y coordinates. To minimise potential clustering of error bars on the separation plot, data values for x- and y-coordinates at each pH were averaged (where possible), and error bars were then displayed for these averaged values. The maximum and minimum error lines were manually drawn, and extrapolated to the intercept of the y-axis.

The plot for 2-AE Me, at 37.1°C is shown in Figure A5.1.

The lines of maximum and minimum error were calculated using eqn. A5.5, using the averaged values for largest and smallest independent and dependent values in Table 5.6. This gave:

$$a_1 \text{ or } a_2 = \frac{(7.764 \pm 0.434) - (0.748 \mp 0.042)}{((1.265 \mp 0.029) \times 10^{-9}) - ((4.029 \pm 0.093) \times 10^{-11})} \times 10^{-6}$$

$$a_1 = 6273 \text{ l mol}^{-1} \text{ min}^{-1}, \quad a_2 = 5280 \text{ l mol}^{-1} \text{ min}^{-1}$$

The standard deviation of the slope (σ_a) is expressed by eqn. (A5.7):

$$\sigma_a \approx \frac{1}{4}(a_2 - a_1) \qquad \text{....(A5.7)}$$

The estimated absolute error in k_{EH^+} is provided by eqn. (A5.8):

$$k_{EH^+} = k_{EH^+} \pm 2\sigma_a \qquad \text{....(A5.8)}$$

The maximum and minimum intercepts were estimated from the y-axis of the separation plot displayed in Figure A5.1. Clearly, there is likely to be a certain degree of uncertainty in these values.

These were estimated to be $b_1 = 6.89 \times 10^{-6}$ and $b_2 = 7.25 \times 10^{-6}$

Figure A5.1 Separation of k_E and k_{EH^+} for Alkaline Hydrolysis of 2-AE Me

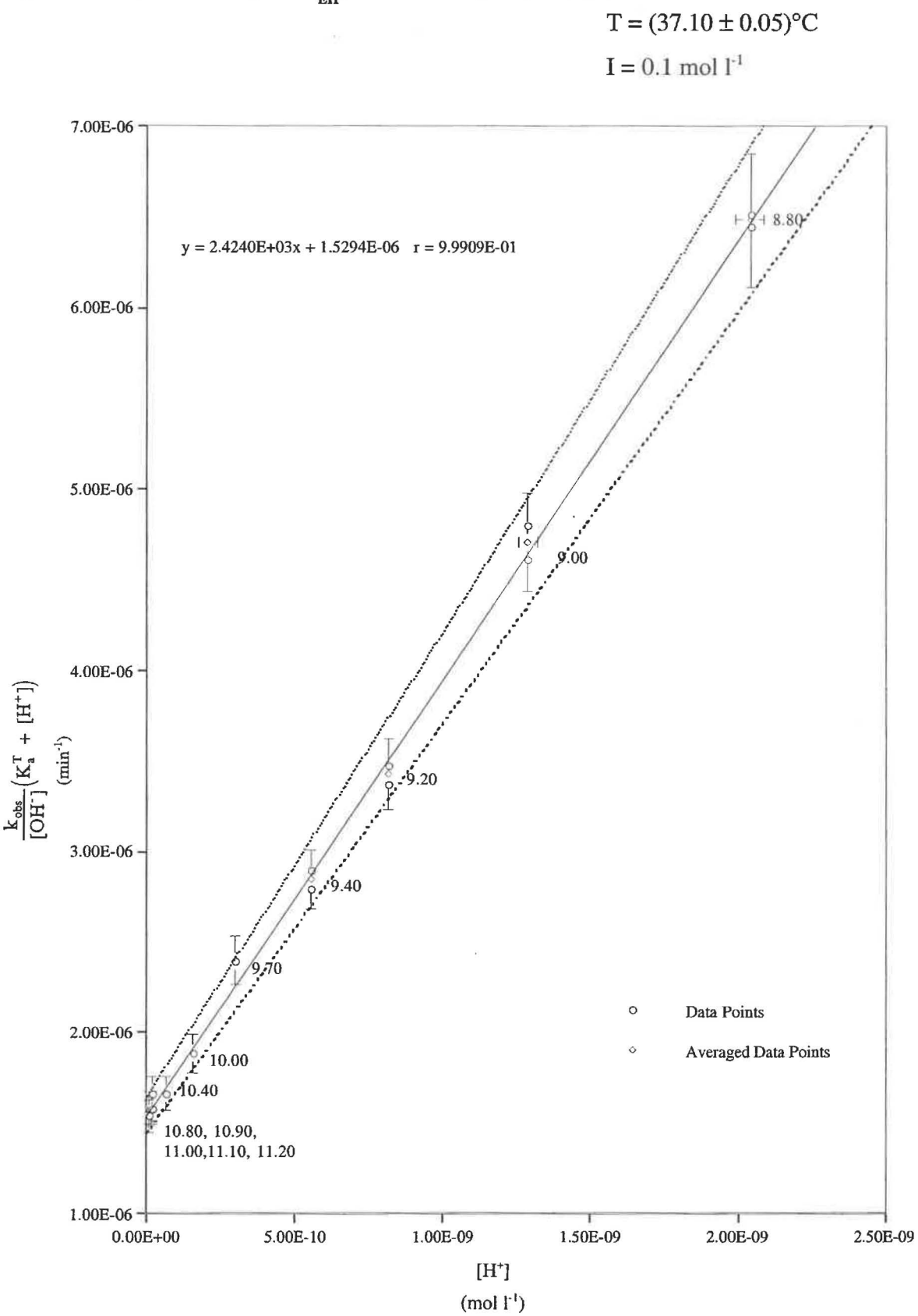

The standard deviation of the intercept (σ_b) is expressed by eqn. (A5.9):

$$\sigma_b = \frac{1}{4}(b_2 - b_1) \qquad \ldots.(A5.9)$$

The estimated error in the intercept is expressed eqn. (A5.10):

$$k_E \cdot K_a^T = b \pm 2\sigma_b \qquad \ldots.(A5.10)$$

$$\therefore \quad k_{EH^+} = (5596 \pm 497)\ l\ mol^{-1}\ min^{-1} \text{ and } k_E = (151 \pm 3)\ l\ mol^{-1}\ min^{-1}$$

Clearly, the error in k_{EH^+} is large ~9% and this probably an over-estimation of the true error. Such a large error in the slope of seems unlikely, since there is relatively little scatter of the data points in the pH/rate profile (Figure A5.1), which is evident from the value of $r > 0.995$.

Consequently, it was necessary to improve the estimate of the error for k_{EH^+}. Therefore, a better estimate of the error in pH could be ± 0.005. Since $K_a^T > [H^+]$, this modification will have a negligible effect on the total error for the parentheses terms, but will effect the total error in $k_{obs}/[OH^-]$, which becomes 2.2% (since $\Delta[OH^-] = 1.2\%$). Hence, the overall error in the y-axis becomes ± 4.5 %. The x-axis error ($[H^+]$) = ±1.2%. Figure A5.2 displays the separation plot for 2-AE Me, at 37.1°C using the recalculated values for the x and y-axis errors. Lines of maximum and minimum were drawn as previously outlined, and their values were calculated using eqn. A5.5. This produced the following:

$$a_1 \text{ or } a_2 = \frac{(7.764 \pm 0.349) - (0.748 \mp 0.033)}{((1.265 \mp 0.015) \times 10^{-9}) - ((4.029 \pm 0.048) \times 10^{-11})} \times 10^{-6}$$

$$a_1 = 5980\ l\ mol^{-1}\ min^{-1},\ a_2 = 5211\ l\ mol^{-1}\ min^{-1}$$

It should be noted that there is negligible change to the errors for the intercept value. Therefore, the errors gave:

$$k_{EH^+} = (5596 \pm 385)\ l\ mol^{-1}\ min^{-1} \text{ and } k_E = (151 \pm 3)\ l\ mol^{-1}\ min^{-1}$$

Figure A5.2 Separation of k_E and k_{EH^+} for Alkaline Hydrolysis of 2-AE Me (Modified)

$T = (37.10 \pm 0.05)$ °C

$I = 0.1$ mol l^{-1}

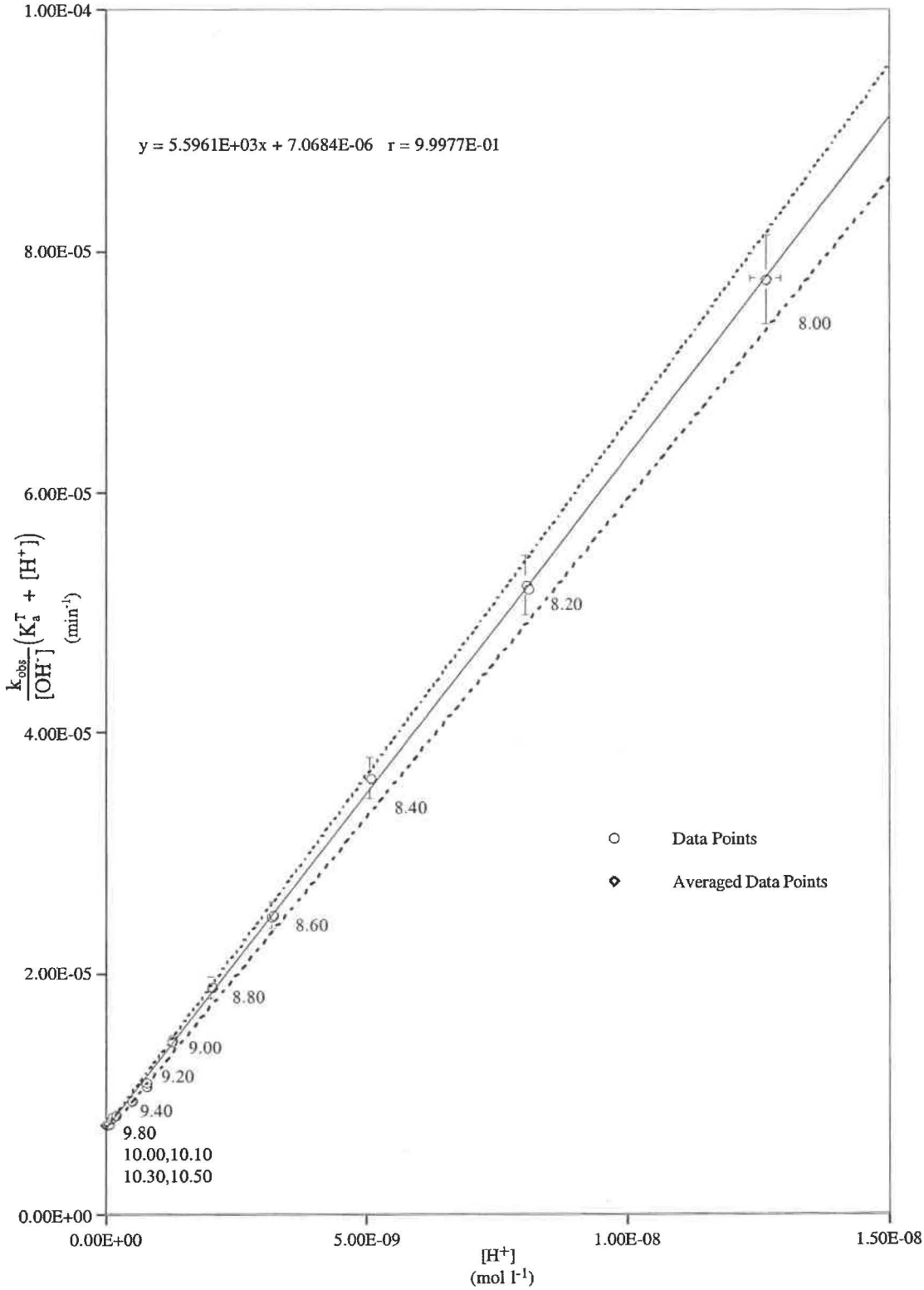

The overall error in k_{EH^+} is ~ 7%, which is probably a "more realistic" estimate of error for 2-AE Me. The magnitude of this value is probably due to the small % of the EH^+ form present at the pH's where the reaction rates were measured (since 2-AE Me.HCl $pK_a^T = 7.33$ at 37.1°C and I = 0.1 mol l^{-1}, Table A1..11). For Group 1 esters the errors for pK_a^T(or K_a^T) were found to be ± 0.01 or better, consequently have a small effect on the value of k_{EH^+}.

Interestingly, the error for k_E (~2.5 %) remained unchanged by the modification. This is probably an accurate estimation of the error since at high pH's were reaction rates were measured there is a large % of the E form present.

All Group 1 esters were assumed to have identical errors for k_{EH^+} and k_E.

A5.2(b) Group 2, Moderately Hydrolysing Amino Acid Esters

A procedure was used to calculate the errors for these esters as outlined in A5.2(a). 4-AB Me (see 5.3(c)) was used to estimate the error in k_{EH^+} and $k_E(k_L)$for a typical Group 2 ester. Table A5.2 displays the error calculations for the parentheses terms, where a selection of values (at high, mid-range and low $[H^+]$) were chosen from Table 5..7, where 4-AB Me.HCl, $pK_a^T = 9.83 \pm 0.01$, at 25°C , I = 0.1 mol l^{-1} (Table 4.9). Hence, $K_a^T = 1.480 \times 10^{-10}$. An estimated error of pH ± 0.005 was used in the calculations.

Table A5.2 Estimation of the Absolute Error for the Parentheses Terms for 4-AB Me.

pH	$[H^+]$	$\Delta[H^+]$	$(K_a^T + [H^+])$	$\Delta K_a^T + \Delta[H^+]$	$\left(\frac{\Delta K_a^T + \Delta[H^+]}{(K_a^T + [H^+])}\right)$
9.099	1.023×10^{-9}	0.012×10^{-9}	1.180×10^{-9}	1.540×10^{-11}	0.013
9.503	4.071×10^{-10}	0.047×10^{-10}	5.550×10^{-10}	8.100×10^{-12}	0.015
10.102	1.024×10^{-10}	0.012×10^{-10}	2.503×10^{-10}	5.800×10^{-12}	0.018

Using $\Delta K_a^T = 0.034 \times 10^{-10}$

For these esters, the error in $[H^+]$ has a more significant contribution to overall error for the parenthesis terms in the pH range where k_{obs} values were measured (cf. Group 1 esters). But, as it can be seen from Table A5.2 shows, the contribution K_a^T to the total error increases with pH, however rapid alkaline hydrolysis prevented k_{obs} values been measured at higher pH'. The overall error for the parenthesis terms was estimated to be ~ 2 %. The estimated overall error in y-axis for 4-AB Me was estimated to be ~4.5 %. For the x-axis error ($[H^+]$) ~ 1.2% .

Figure A5.3 displays the separation plot for 4-AB Me, using data from Table 5.7, and x- and y-error bars, where the line of best fit, maximum and minimum error were drawn by the methods outlined previously.

Eqn. A5.5 was used to calculate a_1 and a_2 for 4-AB Me:

$$a_1 \text{ or } a_2 = \frac{(3.700 \pm 0.135) - (2.491 \mp 0.054)}{((1.032 \mp 0.012) \times 10^{-9}) - ((1.025 \pm 0.012) \times 10^{-11})} \times 10^{-7}$$

$$a_1 = 148.3 \text{ l mol}^{-1} \text{ min}^{-1}, \; a_2 = 111.3 \text{ l mol}^{-1} \text{ min}^{-1}$$

The maximum and minimum error in the intercept were extrapolated from Figure A5.3

$$b_2 = 2.43 \times 10^{-7}, \; b_1 = 2.25 \times 10^{-7}$$

The error in the rate constants, k_{EH^+} and $(k_E + k_L)$ as $(\pm 2\sigma)$ gave:

$$k_{EH^+} = (131 \pm 19) \text{ l mol}^{-1} \text{ min}^{-1} \text{ and } (k_E + k_L) = (1580 \pm 60) \text{ l mol}^{-1} \text{ min}^{-1}$$

Clearly, the error in k_{EH^+} is large and is probably an over-estimation of the true error, (even using 4.3% error for the y-axis). An error of ~ 15% in the slope seems unlikely, because of the good linearity of the pH/rate profile plot (Figure A5.3), i.e. $r > 0.995$.

Figure A5.3 Separation of k_E and k_{EH^+} for Alkaline Hydrolysis of 4-AB Me

$T = (25.00 \pm 0.05)\ °C$

$I = 0.1\ mol\ l^{-1}$

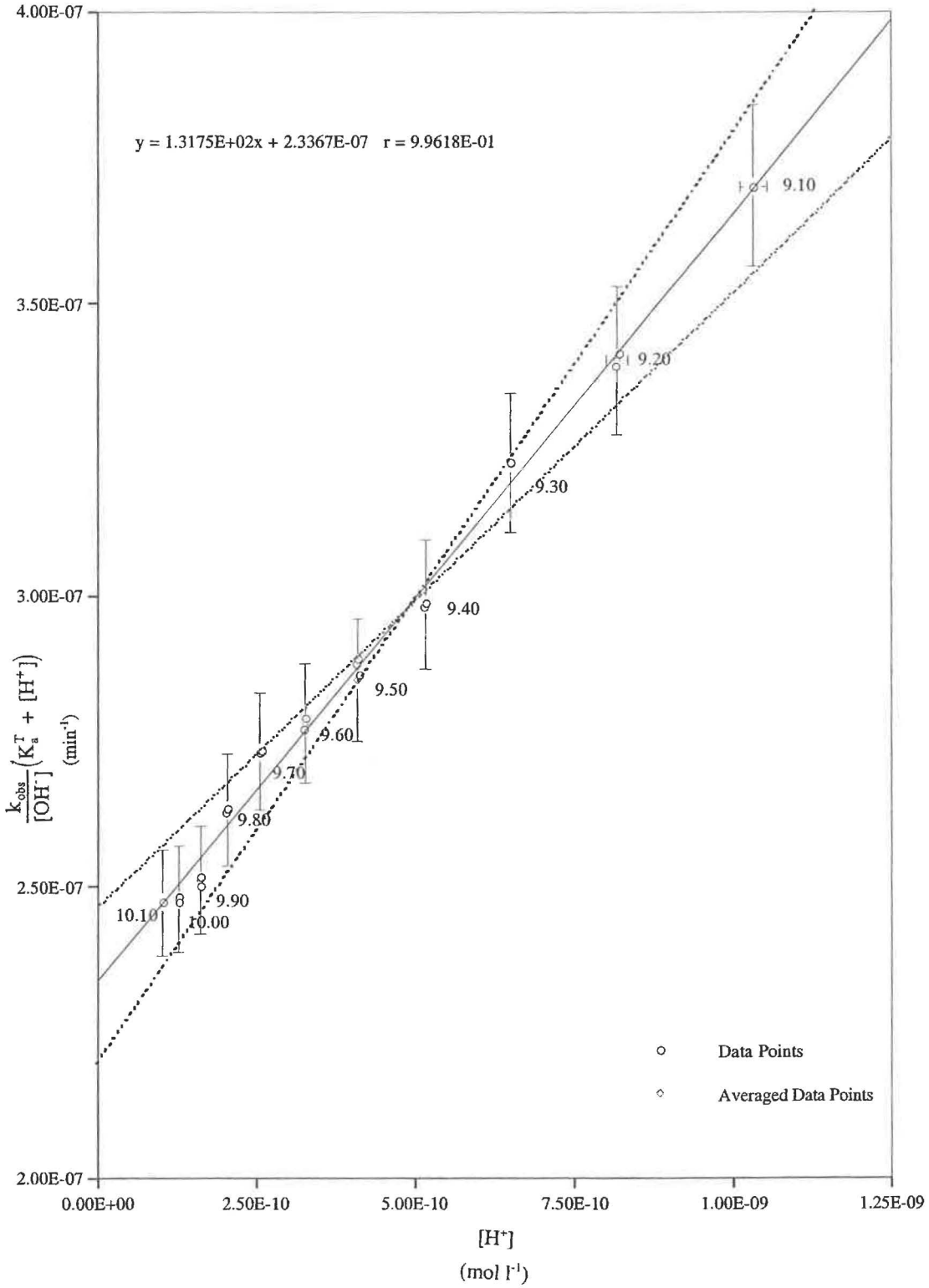

This large error results partly from the logarithmic nature of the pH/rate profile, and will be augmented by the shallowness of 4-AB Me slope (cf. Figure A5.2). Small changes in the y-direction in Figure A5.3, will produce large changes to the magnitude of gradient. This is probably a limitation of using a graphical method to estimate error.

Instead a better estimate for the error in k_{EH^+} for 4-AB Me, could be ~ 10%. This value is based on the error obtained for 2-AE Me (~7%), and takes into account. the greater % of EH^+ form of the 4-AB Me (cf. 2-AE Me) present in the pH range where reaction rates were monitored (which should produce a more accurate k_{EH^+} value) but be counterbalanced by faster rate of hydrolysis of 4-AB Me (and other Group 2 esters).

The error in the intercept (Figure A5.3), was found to be (1580 ± 60) l mol^{-1} min^{-1}, i.e. ~ 4%, this is probably a reasonable estimate in the true error of k_E (or k_L). Since, this error was found to be 2.5%, for 2-AE Me, the greater error for 4-AB Me is probably a reflection of the uncertainty in $k_E(k_L)$ associated with its faster rates of hydrolysis.

All Group 2 esters were assumed to have identical errors for k_{EH^+} and k_E (k_L).

A5.2(c) Group 3, Rapidly Hydrolysing Amino Acid Esters

Using the data from 5.3(d) errors were calculated for 5-APe Me using a similar procedure as in A5.2(a). Table A5.3 displays the error calculations for the parenthesis terms for 5-APe Me.HCl, $pK_a^T = 10.15 \pm 0.02$, at 25°C , I = 0.1 mol l^{-1} (Table 4.7). Hence, $K_a^T = 1.480 \times 10^{-10}$. Hence $K_a^T = 7.880 \times 10^{-11}$. Using error of pH ± 0.005.

Table A5.3 Estimation of the Absolute Error for the Parentheses Terms for 5-APe Me.

pH	$[H^+]$	$\Delta[H^+]$	$\left(K_a^T + [H^+]\right)$	$\Delta K_a^T + \Delta[H^+]$	$\left(\frac{\Delta K_a^T + \Delta[H^+]}{\left(K_a^T + [H^+]\right)}\right)$
8.405	5.101×10^{-9}	0.059×10^{-9}	5.172×10^{-9}	1.202×10^{-11}	0.012
8.903	1.621×10^{-9}	0.187×10^{-10}	1.691×10^{-9}	4.046×10^{-11}	0.013
9.301	6.481×10^{-10}	0.075×10^{-10}	7.189×10^{-10}	1.809×10^{-11}	0.015

Using $\Delta K_a^T = \pm 0.336 \times 10^{-11}$.

These calculations displayed in Table A5.3 differ to those for 2-AE Me (Table A5.1) because the error for the parenthesis terms are dominated by values of $[H^+] > K_a^T$ .for the range of pH's were k_{obs} were measured, and $[H^+]$ error is the major contributor to the overall error. This value was estimated to be 1.3 %.
The estimated error in y-axis (for 5-APe Me (was estimated to be 3.7 % for y-axis values. The error in the x-axis which is $[H^+]$ = 1.2%.

Figure A5.4 displays the separation plot for 5-APe Me, using data from Table 5.9, and x- and y-error bars, where the line of best fit, maximum and minimum error were drawn by the methods previously outlined.

Equ A5.5 was used to calculate a_1 and a_2 for 5-APe Me:

$$a_1 \text{ or } a_2 = \frac{(5.276 \pm 0.175) - (2.971 \mp 0.101)}{((5.101 \mp 0.059) \times 10^{-9}) - ((6.519 \pm 0.078) \times 10^{-10})} \times 10^{-6}$$

$$a_1 = 589 \text{ l mol}^{-1} \text{ min}^{-1}, \; a_2 = 449 \text{ l mol}^{-1} \text{ min}^{-1}$$

The maximum and minimum error in the intercept were extrapolated from Fig. A5.5:

$$b_2 = 2.82 \times 10^{-6}, \; b_1 = 2.46 \times 10^{-6}$$

The error in the rate constants, k_{EH^+} and $(k_E + k_L)$ as $(\pm 2\sigma)$ gives:

$$k_{EH^+} = (546 \pm 71) \text{ l mol}^{-1} \text{ min}^{-1} \text{ and } k_E + k_L = (36380 \pm 2550) \text{ l mol}^{-1} \text{ min}^{-1}$$

Interestingly the error in the pK_a^T for 5-APe Me.HCl (10.15 ± 0.02) makes little contribution to error in k_{EH^+} because, the error calculation for the terms in the parentheses is dominated by magnitude of $[H^+] > K_a^T$ in the pH range (8.4 – 9.5) where reaction rates were measured. Rapid alkaline hydrolysis prevented higher pH's from been investigated. The error in k_{EH^+} for 5-APe Me, ~ 13% seem to be reasonable based on the corresponding values for 4-AB Me (~ 10% for k_{EH^+} and ~ 4% for k_E). The uncertainty in the error is probably a reflection of its rapid rate of hydrolysis.

All Group 3 esters were assumed to have identical errors for k_{EH^+} and k_E (k_L).

Figure A5.4 Separation of k_E and k_{EH^+} for Alkaline Hydrolysis of 5-APe Me

$T = (25.00 \pm 0.05)\ °C$

$I = 0.1\ mol\ l^{-1}$